

---

# **QUANTIFYING THE RISK OF GEOTECHNICAL SITE INVESTIGATIONS**

**JASON SCOTT GOLDSWORTHY**

B.E. (Hons), M.I.E. (Aust)

Thesis submitted for the Degree of  
Doctor of Philosophy (PhD)



School of Civil and Environmental Engineering

**JANUARY 2006**

---



---

For my grandfather,  
***Kevin Marsh,***  
for his  
dedication  
and devotion

---





---

***"people know the price of everything  
and the value of nothing"***

Oscar Wilde (1854-1900)

---



## PREFACE

This thesis is the culmination of three and a half years work between July 2002 and January 2006. To the author's knowledge, all information and material obtained from other sources has been credited through citations and references. The following sections contain material for which the author claims originality.

### In Chapter 3:

- Development and implementation of a method to investigate the risk and reliability of foundation designs based on the results from a site investigation.

### In Chapter 4:

- Identification of a worst case scale of fluctuation (SOF) which is a function of the size of the averaging domain;
- Using a field translation technique to reduce aliasing or gridding when generating three-dimensional random fields based on a lognormal distribution; and
- Use of a depth constraint to reduce the contribution of small strains on settlement estimates.

### In Chapter 5:

- Measurement of the conservatism inherent in settlement prediction techniques for the analysis and design of a foundation on a soil with a spatially random elastic modulus; and
- Identification of an influence region within which an averaged elastic modulus value yields settlement estimates that accommodate soil variability.

**In Chapter 6:**

- Measurement of the effect of site investigations on the selection of design parameters;
- Analysis of the effect of site investigations on foundation design.

**In Chapter 7:**

- Reliability analysis of foundation designs based on the results from a site investigation in comparison with an optimal foundation design achieved using the complete knowledge of the soil;
- Use of an average design error to measure degree of under- and over-design of a foundation design based on the results from a site investigation;
- Recommendation of a single sampling location in a foundation system consisting of multiple footings; and
- Evaluation of the effect of measurement errors on the design of a foundation.

**In Chapter 8:**

- Risk assessment of a foundation designed on the basis of results from a site investigation;
- Identification of an optimal site investigation expenditure that yields a foundation design with lowest financial risk;
- Evaluation of the benefits of increased site investigation expenditure or sampling on the financial risk of a design;
- Identification of the most cost-effective types of site investigation tests.

**In Chapter 9:**

- Evaluation of the optimal site investigation strategy at three soil sites, where sufficient soil data has been made available for accurate characterisation of the soil variability.

The following publications have resulted from the research contained within this thesis:

**Goldsworthy, J S, Jaksa, M B, Kaggwa, G W S., Fenton, G A, Griffiths, D V and Poulos, H G (2005).** "Reliability of Site Investigations Using Different Reduction Techniques for Foundation Design," *9th International Conference on Structural Safety and Reliability*, Rome, Italy, pp. 901–908. (On CD.)

**Jaksa, M B, Goldsworthy, J S, Fenton, G A, Kaggwa, G W S, Griffiths, D V, Kuo, Y L and Poulos, H G (2005).** "Towards Reliable and Effective Site Investigations," *Geotechnique*, 55(2), pp. 109-121.

**Goldsworthy, J S, Jaksa, M B, Kaggwa, W S, Fenton, G A, Griffiths, D V and Poulos, H G (2004).** "Cost of Foundation Failures Due to Limited Site Investigations," *The International Conference on Structural and Foundation Failures*, Singapore, pp. 398-409.

**Goldsworthy, J S and Jaksa, M B (2004).** "Effect of Design Models and Test Numbers on the Design of Pad Foundations," *6th Australian Young Geotechnical Professionals Conference*, Gold Coast, Australia, pp. 74-79.

**Goldsworthy, J S, Jaksa, M B, Fenton, G A, Kaggwa, W S, Griffiths, D V, Poulos, H G and Kuo, Y L (2004).** "Influence of Site Investigations on the Design of Pad Footings," *9th Australia New Zealand Conference on Geomechanics*, Auckland, New Zealand, pp. 282-288.



## ABSTRACT

The site investigation phase plays a vital role in any foundation design where inadequate characterisation of the subsurface conditions may lead to either a significantly over designed foundation that is not cost-effective, or an under-designed foundation, which may result in foundation failure. As such, the scope of an investigation should be dependent on the conditions at the site and the importance of the structure. However, it is common for the expense dedicated to the site investigation to be a fraction of the total cost of the project, and is typically determined by budget and time constraints, and the experience and judgement of the geotechnical engineer. However, additional site investigation expenditure or sampling is expected to reduce the financial risk of the design by reducing the uncertainties in the geotechnical system and protecting against possible foundation failures.

This research has quantified the relative benefits of undertaking site investigations of increased and differing scope. This has been achieved by simulating the design process to yield a foundation design based on the results of a site investigation. Such a design has been compared to an optimal design that utilises the complete knowledge of the soil, which has only been possible due to the use of simulated soils. Comparisons between these two design types indicate the performance of the site investigation to accurately or adequately characterise the site conditions. Furthermore, the design based on the results of the site investigation have been analysed using the complete knowledge of the soil. This yields a probability of failure and, therefore, has been included in a risk analysis where the costs associated with the site investigation have been measured against the financial risk of the design. As such, potential savings in financial risk for increased site investigation expenditure have been subsequently identified.

A Monte Carlo analysis has been used in this research to incorporate the uncertainties in the foundation design process. Uncertainties have been included due to soil variability; sampling errors; measurement and transformation model errors; and errors related to the use of a simplified foundation response prediction method. The Monte Carlo analysis has

also provided the means to obtain results in a probabilistic framework to enable reliability and risk analyses. Computer code has been specifically developed with an aim to: generate a simulated soil that conforms to the variability of soil properties; simulate a site investigation to estimate data for a foundation design; simulate the design of a foundation and conduct a reliability and risk analysis of such a design.

Results indicate that there are significant benefits to be derived from increasing the scope of a site investigation in terms of the risk and reliability of the foundation design. However, it also appears that an optimal site investigation scope or expenditure exists where additional expenditure leads to a design with a higher financial risk due to the increased cost of the site investigation. The expected savings in terms of financial risk are significant when compared to the increased investigation cost. These results will assist geotechnical engineers in planning a site investigation in a more rational manner with knowledge of the associated risks.



## **STATEMENT OF ORIGINALITY**

This thesis contains no material which has been accepted for the award of any other degree or diploma in any university, or other tertiary institution and, to the best of my knowledge and belief, contains no material previously published or written by another person, except where due reference has been made in the text.

I give consent to this copy of my thesis, when deposited in the University Library, being made available for loan and photocopying.

Signed:



Date: 30 January 2006

■



## **ACKNOWLEDGMENTS**

This document encapsulates the last three and half years of research I have undertaken at the University of Adelaide, Australia. This period has been a special part of my life that I have thoroughly enjoyed and will always look back on with fond memories. This is direct result of the support, friendship and direction that several people have afforded me. First and foremost, I owe a great deal to my principal supervisor, Dr Mark Jaksa from the University of Adelaide. He has not only provided a great source of direction and support throughout this research, but has also become a close friend. For this I am forever indebted to him. I would also like to share my appreciation for the support of my co-supervisor, Dr William Kaggwa, also from the University of Adelaide. Although his involvement in this research has not been to the same extent as Dr Jaksa's, he has provided invaluable direction regarding the significance and application of results and the final structure of this document.

Acknowledgement is also made to the Australian Research Council who funded this research as part of Discovery Project Grant. Without their financial assistance, this research would not have been possible.

I would also like to acknowledge three additional people who have all been directly involved in this project: Professor Vaughan Griffiths, from the Colorado School of Mines, USA; Professor Harry Poulos, from Coffey Geosciences and the University of Sydney in Australia; and Professor Gordon Fenton, from Dalhousie University in Canada. Professor Poulos has given valuable direction regarding the foundation design process and the geotechnical engineering industry in general. Professor Griffiths graciously provided the three-dimensional finite element analysis code that has been used for the optimal design. Furthermore, he also provided invaluable direction regarding the prediction of footing settlements using finite element analyses. I would also specially like to thank Professor Fenton, who not only offered the use of his random field generator, which enabled the genera-

tion of a simulated soil, but also spent nearly 12 months at the University of Adelaide assisting with this research. Thus, his contribution and influence on this research should not be underestimated and I would like to offer my sincere gratitude for his time and assistance.

I have also been afforded some advice from Professor Fred Kulhawy, from Cornell University in USA, and Associate Professor Kok Kwang Phoon, from the National University of Singapore. Professor Kulhawy provided general direction in the early stages of this research, while Associate Professor Phoon has provided direction in the latter stages. For this I thank them both very much and appreciate their valuable time.

The wide range of results shown in this research has required the use of significant computing resources at the University of Adelaide. Therefore, it has been necessary to program, compile and build the computer code for execution on several different computing systems and two different platforms. I would like to thank four people in particular for the assistance they have given me in this capacity: Dr Stephen Carr, from the School of Civil and Environmental Engineering at the University of Adelaide, who has not only helped with the code generation, but also several other issues regarding software and computing; and Mr Paul Coddington, Patrick Fitzhenry and Grant Ward, who all provided assistance with building and running the computer code on a supercomputer managed by the South Australia Partnership for Advanced Computing (SAPAC) called Hydra. These people have gone beyond the call of duty to lend assistance regarding the intricacies of running computer code on a multi-processor system.

Finally, I would also like to thank my close friends and family who have supported me and helped me to enjoy this journey. I would especially like to thank my parents, Robyn and Tony Goldsworthy, who have always encouraged me to achieve my goals and afforded me unconditional support. I would also like to acknowledge my grandparents, Pat and Kevin Marsh, who have been an amazing source of support and encouragement, not only for these last few years. Last by no means least, I would like to thank my partner, Natalie Pearce, who has endured this journey with me, whilst always keeping a smile on her face. She is an amazing person who has ensured that I have kept on track and never lost sight of the final goal. For this I am eternally grateful.

Last of all, I would like to thank you, the reader, for spending the time in ploughing through this research, which I hold very dear. I hope you enjoy the read and find it enlightening in some way.

## CONTENTS

<i>Preface</i>	<i>i</i>
<i>Abstract</i>	<i>v</i>
<i>Statement of Originality</i>	<i>vii</i>
<i>Acknowledgments</i>	<i>ix</i>
<i>Contents</i>	<i>xi</i>
<i>List of Figures</i>	<i>xvii</i>
<i>List of Tables</i>	<i>xxxv</i>
<i>Notation</i>	<i>xxxix</i>
<b>Chapter 1 Introduction</b>	<b>1</b>
<b>1.1 Site Investigations</b>	<b>1</b>
<b>1.2 Aim and Scope of this Research</b>	<b>3</b>
<b>1.3 Layout of this Thesis</b>	<b>4</b>
<b>Chapter 2 Literature Review</b>	<b>7</b>
<b>2.1 Introduction</b>	<b>7</b>
<b>2.2 Foundation Design</b>	<b>7</b>
2.2.1 Site Characterisation	7
2.2.2 Shallow Foundations	13
2.2.3 Raft Foundations	25
2.2.4 Piled Foundations	26
2.2.5 Summary	26
<b>2.3 Uncertainties in Geotechnical Engineering</b>	<b>27</b>
2.3.1 Sources of Uncertainty for Soil Properties	27
2.3.2 Inherent Soil Variability	29
2.3.3 Statistical Uncertainty	39
2.3.4 Measurement Error	41
2.3.5 Transformation Model Uncertainty	43
<b>2.4 Geotechnical Design Incorporating Uncertainties</b>	<b>45</b>
<b>2.5 Summary</b>	<b>54</b>

<b>Chapter 3</b>	<b>Methodology Development</b>	<b>55</b>
<b>3.1</b>	<b>Introduction</b>	<b>55</b>
<b>3.2</b>	<b>Method Overview</b>	<b>55</b>
<b>3.3</b>	<b>Soil Simulation</b>	<b>57</b>
3.3.1	Target Distribution and Correlation Structure of Simulated Soil	57
3.3.2	Generating Random Fields	61
3.3.3	Transformation of the Generated Soil Properties	65
3.3.4	Effects of Local Averaging on Random Fields	66
3.3.5	Size of the Simulated Soil Site	67
<b>3.4</b>	<b>Site Investigation</b>	<b>67</b>
3.4.1	Patterns and Quantity of Sampling	68
3.4.2	Soil Parameter Reduction Techniques	71
3.4.3	Types of Soil Tests	73
<b>3.5</b>	<b>Foundation Design Methodology</b>	<b>77</b>
3.5.1	Pad Foundation Geometry	78
3.5.2	Requirement for an Alternative Foundation Type	79
<b>3.6</b>	<b>Pad Foundation Design</b>	<b>79</b>
3.6.1	Pad Foundation Design Criteria	80
3.6.2	Settlement Prediction Techniques	81
3.6.3	Determination of Rigid Footing Displacements	83
3.6.4	Procedure used to Account for Multiple Footing Interactions	85
3.6.5	Numerical Modelling of Footing Settlement	87
<b>3.7</b>	<b>Monte Carlo Analysis</b>	<b>96</b>
3.7.1	Nomenclature and Metrics	96
3.7.2	Number of Realisations	98
3.7.3	Optimisation of Computational Time	100
<b>3.8</b>	<b>Summary</b>	<b>107</b>
<b>Chapter 4</b>	<b>Verification of Methodology</b>	<b>109</b>
<b>4.1</b>	<b>Introduction</b>	<b>109</b>
<b>4.2</b>	<b>Verifying the Properties in the Simulated Soil</b>	<b>109</b>
4.2.1	Verifying the Target Distribution	109
4.2.2	Verifying the Correlation Structure	118
4.2.3	Investigation of Transformation Effects	122
<b>4.3</b>	<b>Verification of the Implementation of Settlement Prediction Techniques</b>	<b>125</b>
4.3.1	Comparing Simulation and Calculated Settlement Predictions	126
4.3.2	Calibration of 3DFEA to Measured Settlements	128
<b>4.4</b>	<b>Verification of Mean and Variability of Settlement Estimates</b>	<b>135</b>
<b>4.5</b>	<b>Summary</b>	<b>142</b>

<b>Chapter 5</b>	<b>Effect of Different Settlement Prediction Techniques on the Design and Analysis of a Pad Foundation</b>	<b>143</b>
<b>5.1</b>	<b>Introduction</b>	<b>143</b>
<b>5.2</b>	<b>Settlement Analyses</b>	<b>145</b>
5.2.1	Settlement Analysis on a Soil with Uniform Properties	145
5.2.2	Settlement Analysis on a Spatially Random Soil	151
5.2.3	Analysis Using an Influence Region of Properties	166
5.2.4	Summary	177
<b>5.3</b>	<b>Pad Foundation Design Using Different Settlement Prediction Techniques</b>	<b>178</b>
<b>5.4</b>	<b>Summary</b>	<b>195</b>
<b>Chapter 6</b>	<b>Effect of Site Investigations on Design Parameters and the Design of a Pad Foundation</b>	<b>197</b>
<b>6.1</b>	<b>Introduction</b>	<b>197</b>
<b>6.2</b>	<b>Effect of Site Investigation Scope on Design Parameters</b>	<b>198</b>
6.2.1	Soil Variability	198
6.2.2	Sampling Patterns and Reduction Techniques	202
6.2.3	Types of Soil Tests	211
6.2.4	Summary	213
<b>6.3</b>	<b>Effect of Site Investigation Scope on the Expected Pad Foundation Design</b>	<b>213</b>
6.3.1	Soil Variability	213
6.3.2	Sampling Patterns and Reduction Techniques	217
6.3.3	Types of Soil Tests	226
6.3.4	Settlement Prediction Techniques	234
6.3.5	Summary	236
<b>6.4</b>	<b>Effect of Site Investigation Scope on the Variability of a Pad Foundation Design</b>	<b>236</b>
6.4.1	Soil Variability	237
6.4.2	Sampling Patterns and Reduction Techniques	241
6.4.3	Types of Soil Tests	243
6.4.4	Settlement Prediction Techniques	246
<b>6.5</b>	<b>Summary</b>	<b>249</b>
<b>Chapter 7</b>	<b>Reliability Assessment of a Site Investigation in Terms of Foundation Design</b>	<b>251</b>
<b>7.1</b>	<b>Introduction</b>	<b>251</b>
<b>7.2</b>	<b>Effect of Site Investigation Scope on the Probability of Under- and Over-Design</b>	<b>252</b>
7.2.1	Soil Variability	252
7.2.2	Sampling Patterns and Reduction Techniques	260

7.2.3	Types of Soil Tests	265
7.2.4	Settlement Prediction Techniques	268
7.2.5	Summary	268
<b>7.3</b>	<b>Effect of Site Investigation Scope on the Design Error</b>	<b>270</b>
7.3.1	Soil Variability	271
7.3.2	Sampling Patterns and Reduction Techniques	276
7.3.3	Types of Soil Tests	280
7.3.4	Settlement Prediction Techniques	282
7.3.5	Analysis of a Single Pad Footing	284
7.3.6	Summary	285
<b>7.4</b>	<b>Reliability Assessment Due to Individual Sources of Uncertainty</b>	<b>286</b>
7.4.1	Statistical Uncertainty	286
7.4.2	Measurement Error	292
<b>7.5</b>	<b>Summary</b>	<b>297</b>
<b>Chapter 8 Risk Assessment of Site Investigations in Terms of Foundation Design</b>		<b>299</b>
<b>8.1</b>	<b>Introduction</b>	<b>299</b>
<b>8.2</b>	<b>Calculation of Total Foundation Cost</b>	<b>300</b>
8.2.1	Site Investigation and Construction Costs	300
8.2.2	Failure Costs	304
<b>8.3</b>	<b>Effect of Site Investigation Scope on the Total Foundation Cost</b>	<b>308</b>
8.3.1	Failure Analysis Using 3D FEA	309
8.3.2	Failure Analysis Using Schmertmann 2B-0.6	318
8.3.3	Variables Impacting the Effect of Site Investigation Scope on the Total Foundation Cost	320
8.3.4	Sensitivity of Rehabilitation Limits on the Total Foundation Cost	340
<b>8.4</b>	<b>Optimal Site Investigation Strategies</b>	<b>341</b>
<b>8.5</b>	<b>Expected Savings from Increased Site Investigation</b>	<b>349</b>
<b>8.6</b>	<b>Summary</b>	<b>351</b>
<b>Chapter 9 Analysis Using Specific Soil Data</b>		<b>353</b>
<b>9.1</b>	<b>Introduction</b>	<b>353</b>
<b>9.2</b>	<b>Site 1: Stiff-Overconsolidated Clay</b>	<b>354</b>
<b>9.3</b>	<b>Site 2: Sand Site at the Texas A&amp;M NGES</b>	<b>360</b>
<b>9.4</b>	<b>Site 3: Varved Clay</b>	<b>364</b>
<b>9.5</b>	<b>Summary</b>	<b>367</b>
<b>Chapter 10 Summary and Recommendations</b>		<b>369</b>
<b>10.1</b>	<b>Introduction</b>	<b>369</b>



---

<b>10.2 Summary</b>	<b>369</b>
<b>10.3 Limitations and Restrictions</b>	<b>379</b>
10.3.1 Soil Simulation	379
10.3.2 Simulated Site Investigation	380
10.3.3 Foundation Design	381
<b>10.4 Future Directions of Research</b>	<b>382</b>
10.4.1 Analysis Using More Complex Soil Models	382
10.4.2 Incorporating the Bearing Capacity of a Foundation	383
10.4.3 Investigating the Design of Other Types of Foundation Systems	383
10.4.4 Analysing More Complex Site Investigation Strategies	384
10.4.5 Refining the Element Size	384
10.4.6 Other Recommended Research	385
<b>10.5 Conclusion and Recommendations</b>	<b>386</b>
<b>References</b>	<b>387</b>
<b>Appendices</b>	<b>407</b>
Appendix A Settlement Analysis	409
Appendix B Average and Variance of Foundation Design Results	421
Appendix C Probabilities of Under- and Over-design and Probabilities of Obtaining an Optimal Design	437
Appendix D Average Design Error	459
Appendix E Foundation Design Costs	475



## LIST OF FIGURES

### Chapter 1 Introduction

### Chapter 2 Literature Review

Figure 2-1	Typical triaxial cell After Craig (Craig 1997)	9
Figure 2-2	Schematic of split spoon sampler in a standard penetration test After Bowles (1997)	9
Figure 2-3	Schematic of the cone penetrometer After Holtz and Kovacs (1981)	10
Figure 2-4	Schematic of the flat plate dilatometer After Marchetti (1980)	11
Figure 2-5	Herringbone sampling pattern After Ferguson (1992)	12
Figure 2-6	Four different sampling designs: (a) regular (square); (b) stratified random; (c) simple random and (d) stratified systematic unaligned After Ferguson (1992)	12
Figure 2-7	Schmertmann's strain influence triangles: (a) 2B-0.6 triangle from Schmertmann (1970) and (b) modified triangle from Schmertmann et al. (1978)	20
Figure 2-8	Result of the FEA of a clay slope After Griffiths and Fenton (2000)	22
Figure 2-9	Result of the FEA of the bearing capacity of a rigid strip footing After Griffiths et al. (2002a)	22
Figure 2-10	Effects of uncertainties on the estimate of a soil property After Kulhawy (1992)	28
Figure 2-11	Influence of measurement uncertainty and transformation model uncertainty After Phoon and Kulhawy (1999b)	44
Figure 2-12	(a) Normal and (b) log normal distributions After Baecher and Christian (2003)	50
Figure 2-13	Load, $F$ , and capacity or resistance, $R$ , distributions (normal) After Phoon et al. (1995)	51
Figure 2-14	(a) Probability density and (b) cumulative probability function of safety margin, $M$ , based on normal $F$ and $R$ After Phoon et al. (1995)	51
Figure 2-15	Cost-benefit analysis After Phoon et al. (1995)	54

### Chapter 3 Methodology Development

Figure 3-1	Simulation model flowchart	57
Figure 3-2	Elastic modulus values for a soil COV of 50% and SOF of (a) 1 m, (b) 2 m, (c) 4 m, (d) 8 m, (e) 16 m and (f) 32 m	58
Figure 3-3	LAS process illustrating a top-down approach After Fenton (1990)	62
Figure 3-4	Comparison of estimated and exact covariances across cell boundaries in Local Average Subdivision process After Fenton (1990)	63
Figure 3-5	Estimated covariance using LAS for 3-D isotropic field with scale of fluctuation (a) $\theta = 4$ (Averaged over 50 realisations) and (b) $\theta = 1/2$ (Averaged over 10 realisations) After Fenton (1990)	64
Figure 3-6	Relative size of site investigation area compared with total site area	68
Figure 3-7	Sampling patterns based on a regular grid (RG) pattern	69
Figure 3-8	Sampling patterns based on a stratified random (SR) pattern	69
Figure 3-9	Process of combining results from multiple samples into a reduced sample	71
Figure 3-10	Process of attributing test uncertainties	76
Figure 3-11	Comparison of test values with bias and random effects and actual soil properties	77
Figure 3-12	Process of increasing footing size	78
Figure 3-13	Threshold yielding an alternative foundation type (green – pad footing is suitable, red – requires an alternative foundation type)	79
Figure 3-14	Calculation of differential settlement between two adjacent footings	80
Figure 3-15	Janbu settlement equation coefficient $\mu_1$ for varying soil depth to footing width ratio	82
Figure 3-16	Distribution of settlements for a (a) rigid and (b) flexible loaded areas After Holtz (1991)	83
Figure 3-17	Settlement of a flexible footing	84
Figure 3-18	Settlement of a rigid footing	84
Figure 3-19	Overlay of settlement distribution of a flexible and rigid footing	84
Figure 3-20	Centroid of the settlement distribution of a flexible footing	85
Figure 3-21	Two adjacent footings with areas $A_1$ and $A_2$ , and applied loads, $P_1$ and $P_2$	86
Figure 3-22	Determination of (a) internal and (b) external radius of annulus	86
Figure 3-23	Schematic of shaded annulus	86
Figure 3-24	Determination of angle, $\alpha$	87
Figure 3-25	Effect of convergence tolerance on the (a) settlement estimate, (b) relative settlement error and (c) computational time using 3DFEA	90
Figure 3-26	Effect of increasing the number of elements beneath a footing on the accuracy of 3DFEA settlement estimates	92
Figure 3-27	Effect of the number of elements in the mesh (element size) on the accuracy and computational time of 3DFEA settlement estimates	94
Figure 3-28	Influence of boundary effects on the accuracy of 3DFEA settlement estimates	95

Figure 3-29	Notation of footing area or footing settlement	97
Figure 3-30	Pad foundation system used in analysis to determine suitable number of Monte Carlo realisations	99
Figure 3-31	Convergence rate of 9-pad system designed using 3DFEA and based on a soil COV of 50% and SOF of 8 m	100
Figure 3-32	Cross platform computational times	103
Figure 3-33	Typical steps in an MPI program	104
Figure 3-34	Effect of additional processors on the computational time and relative speed increase	106

## Chapter 4 Verification of Methodology

Figure 4-1	Frequency distributions of elastic modulus values from the simulated soil using LAS (based on soil properties at the surface)	111
Figure 4-2	Effect of target soil COV on the sample (a) mean and (b) standard deviation	113
Figure 4-3	Effect of target soil SOF on the sample (a) mean and (b) standard deviation	114
Figure 4-4	Sample standard deviation of the elastic modulus field for an increasing (a) element size and (b) target SOF	115
Figure 4-5	Sample standard deviation of elastic modulus field based on different element sizes	116
Figure 4-6	Correlation structure of simulated field using <i>dlavx3</i> and a (a) COV of 50% and a SOF of 1 m and (b) COV of 50% and a SOF of 16 m	119
Figure 4-7	Correlation structure of simulated field using <i>dlspvx3</i> and a (a) COV of 50% and a SOF of 1 m and (b) COV of 50% and a SOF of 16 m	120
Figure 4-8	Surface properties for a soil COV of 50% and a SOF of 1 m using (a) <i>dlavx3</i> and (b) <i>dlspvx3</i> variance functions	121
Figure 4-9	Surface properties for a soil COV of 50% and a SOF of 16 m using (a) <i>dlavx3</i> and (b) <i>dlspvx3</i> variance functions	121
Figure 4-10	Correlation structures generated by <i>dlavx3</i> function for (a) increasing target SOF and (b) increasing target COV	122
Figure 4-11	Sample element (a) mean and (b) standard deviation of elastic modulus values at the surface ( $z = 1$ ) from a simulated soil with a COV of 50% and a SOF of (i) 1 m, (ii) 4 m and (iii) 16 m	123
Figure 4-12	Sample element (a) mean and (b) standard deviation of elastic modulus values using <i>field translation</i> and a soil with a COV of 50% and a SOF of (i) 1 m, (ii) 4 m and (iii) 16 m	125
Figure 4-13	System of 9-pad footings	127
Figure 4-14	Comparison between group and individual settlement for each footing in the 9-pad foundation system	128
Figure 4-15	Comparison between measured settlement and 3DFEA settlement using a full depth analysis	130
Figure 4-16	Comparison between measured settlement and 3DFEA settlement using an analysis depth of (a) $2b$ , (b) $5b$ and (c) $8b$ , where $b$ is the least plan dimension of the footing	131

Figure 4-17	Comparison between 3DFEA settlement with varying depth analyses and other settlement prediction techniques for 9 the pad footing foundation system with widths equal to (a) 1.5 m, (b) 2.5 m and (c) 3.5 m	133
Figure 4-18	Comparison between settlement estimates of 3DFEA with full and 5b depth with common settlement prediction techniques of a single pad footing of varying width under (a) constant load and (b) constant pressure	135
Figure 4-19	Distance used to determine correlation, $\rho_{ij}$ , between two sample locations and between soil properties spaced in the vertical direction	137
Figure 4-20	Effect of increasing the sample separation distance on the average and standard deviation of settlement estimates using the adopted methodology and theoretical evaluation for a soil COV of 50% and SOF of (a) 1 m and (b) 16 m	138
Figure 4-21	Effect of increasing the sample separation distance on the average and standard deviation of settlement estimates using the adopted methodology and theoretical evaluation for a soil SOF of 4 m and COV of (a) 50% and (b) 100%	139
Figure 4-22	Effect of increasing the sample separation distance on the average settlement error using the adopted methodology and theoretical solution on a soil with an increasing elastic modulus (a) SOF (COV of 50%) and (b) COV (SOF of 4 m)	141

## Chapter 5 Effect of Different Settlement Prediction Techniques on the Design and Analysis of a Pad Foundation

Figure 5-1	Layout of (a) single, (b) 4-pad and (c) 9-pad system foundation system	144
Figure 5-2	Results of the settlement prediction techniques for a single pad footing for a soil with a uniform elastic modulus showing (a) absolute settlement and (b) relative to 3DFEA	146
Figure 5-3	Results of the settlement prediction techniques for each footing in the 4-pad system for a soil with a uniform elastic modulus showing (a) absolute settlement and (b) settlements relative to 3DFEA	149
Figure 5-4	Results for the corner, centre and remaining footings in the 9-pad system, for a soil with a uniform elastic modulus showing (a) absolute settlement and a (b) settlement error with 3DFEA	150
Figure 5-5	Settlement error relative to 3DFEA settlement for a single pad footing of varying size for a soil with a uniform elastic modulus	151
Figure 5-6	Frequency distribution of estimated settlement of a single pad footing, for a soil COV of 50% and SOF of 8 m	154
Figure 5-7	3DFEA settlement distribution with idealised lognormal distribution, for a soil COV of 50% and SOF of 4 m	155
Figure 5-8	Comparison of idealised settlement distributions, for a soil SOF of 4 m, with respect to the (a) 2:1, (b) Janbu, (c) Newmark, (d) Perloff, (e) Schmertmann Modified, (f) Schmertmann 2B-0.6, (g) Timoshenko and Goodier and (h) Westergaard settlement prediction techniques	156
Figure 5-9	Comparison of idealised settlement distributions, for a soil COV of 50%, with respect to the (a) 2:1, (b) Janbu, (c) Newmark, (d) Perloff, (e) Schmertmann Modified, (f) Schmermann 2B-0.6, (g) Timoshenko and Goodier and (h) Westergaard settlement prediction techniques	157

Figure 5-10	Effect of increasing the soil COV (SOF of 8 m) on the average settlement of a single pad footing using (a) 3DFEA and (b) the Schmertmann 2B-0.6 technique	158
Figure 5-11	Effect of increasing the soil SOF (COV of 50%) on the average settlement of a single pad footing using (a) 3DFEA and (b) the Schmertmann 2B-0.6 technique	159
Figure 5-12	Effect of increasing the soil COV (SOF of 8 m) on the COV of settlement of a single pad footing using (a) 3DFEA and (b) Schmertmann's 2B-0.6 relationship	161
Figure 5-13	Effect of increasing the soil SOF (COV of 50%) on the COV of settlement of a single pad footing using (a) 3DFEA and (b) Schmertmann's 2B-0.6 relationship	161
Figure 5-14	Average settlement error for an increasing soil (a) COV (SOF of 8 m) and (b) SOF (COV of 50%)	164
Figure 5-15	Pressure isobars shown for a square and strip footing After Bowles (1997)	167
Figure 5-16	Example of a site investigation programme consisting of 10 random borehole locations for a foundation system with 4 pad footings and their corresponding optimal influence region areas	168
Figure 5-17	Increasing influence areas from a (a) vertical line to a (d) comparatively large region	169
Figure 5-18	Effect of increasing the size of the influence region within which properties are averaged using (a) SA, (b) GA and (c) HA on the average settlement error of a single pad footing, for an increasing soil COV and SOF of 8 m	170
Figure 5-19	Effect of increasing the size of the influence region within which properties are averaged using (a) SA, (b) GA and (c) HA on the average settlement error of a single pad footing, for an increasing soil SOF and COV of 50%	171
Figure 5-20	Effect of increasing the influence region within which soil properties are averaged with the (a) SA and (b) GA on the average settlement error of a single pad footing of varying widths, for a soil COV of 50% and SOF of 8 m	175
Figure 5-21	Effect of increasing the influence region within which soil properties are averaged using the (a) SA and (b) GA on the average settlement error of a single pad footing using different prediction relationships, for a soil COV of 50% and SOF of 8 m	176
Figure 5-22	Effect of increasing the influence region within which soil properties are averaged using the (a) SA and (b) GA on the average settlement error of a single pad footing using different prediction relationships, for a soil COV of 100% and SOF of 8 mm	177
Figure 5-23	Difference between design area distributions using the Schmertmann 2B-0.6 prediction technique with a (i) 0.5 m and (ii) 0.05 m discretisation for a single pad footing, for a soil COV of 50% and SOF of (a) 1 m, (b) 4 m and (c) 16 m	179
Figure 5-24	Effect of increasing soil COV and SOF on the average total footing area of a system of 9-pad footings, designed using (a) 3DFEA and (b) the Schmertmann 2B-0.6 prediction technique	181
Figure 5-25	Effect of increasing soil COV and SOF on the COV total footing area of a system of 9-pad footings, designed using (a) 3DFEA and (b) the Schmertmann 2B-0.6 prediction technique	181

Figure 5-26	Footing number convention for the 9-pad system shown in 5-1(c)	183
Figure 5-27	Footing area (a) average and (b) COV for individual footings in the 9-pad system designed using 3DFEA and the Schmertmann's 2B-0.6 technique, for a COV of 50% and SOF of 8 m	185
Figure 5-28	Effect of increasing the horizontal to vertical SOF ratio (COV of 50%) on the (a) average and (b) COV total footing area, of the 9-pad system, designed using 3DFEA and Schmertmann 2B-0.6 technique	186
Figure 5-29	Effect of increasing the horizontal to vertical SOF ratio (COV of 50%) on the average total footing area, of the 9-pad system, designed using 3DFEA and Schmertmann 2B-0.6 technique	187
Figure 5-30	Effect of increasing soil COV and SOF on the probability of (a) under- and (b) over-design of a 9-pad system designed using the Schmertmann 2B-0.6 technique (SCH)	188
Figure 5-31	Effect of increasing soil (a) COV (SOF of 8 m) and (b) SOF (COV of 50%) on the probability of under-design of a 9-pad system, designed using each settlement prediction technique	189
Figure 5-32	Effect of increasing soil (a) COV (SOF of 8 m) and (b) SOF (COV of 50%) on the probability of over-design of a 9-pad system, designed using each settlement prediction technique	190
Figure 5-33	Effect of increasing soil COV and SOF on the average design error of a 9-pad system designed using the Schmertmann 2B-0.6 prediction technique	193
Figure 5-34	Effect of increasing soil (a) COV (SOF of 8 m) and (b) SOF (COV of 50%) on the average design error of a 9-pad system, designed using each settlement prediction technique	193

## **Chapter 6 Effect of Site Investigations on Design Parameters and the Design of a Pad Foundation**

Figure 6-1	Effect of increasing the soil (a) COV and (b) SOF on the sampled data and soil average	199
Figure 6-2	Effect of increasing the target soil (a) COV and (b) SOF on the sample data and soil standard deviation	201
Figure 6-3	Sampling locations based on the regular grid pattern Repeated from 3-7	202
Figure 6-4	Histogram of elastic modulus values resulting from a site investigation program consisting of sample locations arranged in a regular grid pattern for a soil COV of 50% and SOF of 8 m	203
Figure 6-5	Effect of using different reduction techniques on the estimate of soil properties based on a site investigation program consisting of sample locations arranged in a regular grid pattern for a soil COV of 50% and SOF of 8 m	206
Figure 6-6	Sample distributions of the (a) non-reduced sampled data and the reduced sample using the (b) SA, (c) GA, (d) HA, (e) MN and (f) 1Q from 5 sample locations, for a soil COV of 50% and SOF of 8 m	208
Figure 6-7	Sample distributions of the (a) non-reduced sampled data and the reduced sample using the (b) SA, (c) GA, (d) HA, (e) MN and (f) 1Q from 25 sample locations, for a soil COV of 50% and SOF of 8 m	208
Figure 6-8	Effect of increased sampling using different reduction techniques on the reduced sample average for a soil COV of 50% and SOF of 8 m	209



Figure 6-9	Effect of increased sampling using different reduction techniques on the reduced sample standard deviation for a soil COV of 50% and SOF of 8 m	209
Figure 6-10	Effect of including uncertainties on the design parameter (a) average and (b) standard deviation based on 1, 5 and 25 CPT samples, arranged in a RG for a soil COV of 50% and SOF of 8 m	212
Figure 6-11	Standard legend of results for Chapter 6, Chapter 7, Chapter 8 and Chapter 9	214
Figure 6-12	Sampling arrangements with the same number of sampling locations for the (a) RG and (b) SR	215
Figure 6-13	Effect of sampling on the mean total footing area, for an increasing soil (a) COV (SOF of 8 m) and (b) SOF (COV of 50%)	215
Figure 6-14	Effect of increasing the degree of anisotropy for a horizontal soil SOF, $\theta_h$ , of (a) 8 m, (b) 16 m and (c) 32 m on the average total footing area based on a site investigation	218
Figure 6-15	Effect of increased sampling on a site investigation of varying size, where samples are arranged in a (a) RG, (b) SR and (c) RN pattern and reduced using the SA for a soil COV of 50% and SOF of 8 m	220
Figure 6-16	Effect of sampling rate per 300 m <sup>2</sup> on a site investigation of varying size, where samples are arranged in a (a) RG, (b) SR and (c) RN pattern and reduced using the SA for a soil COV of 50% and SOF of 8 m	220
Figure 6-17	Effect of increased sampling with different sampling patterns on the average total footing area, for a soil COV of 50% and SOF of 8 m	221
Figure 6-18	Effect of sampling with different reduction techniques on the average total footing area, for a soil COV of 50% and SOF of 8 m, (a) including MN and (b) excluding MN	223
Figure 6-19	Effect of sampling with different reduction techniques on the average total footing area based on a (a) SR and (b) RN sampling pattern for a soil COV of 50% and SOF of 8 m	225
Figure 6-20	Effect of sampling on the average footing area of each footing in the 9-pad system for a soil COV of 50% and SOF of 8 m	227
Figure 6-21	Effect of sampling using different test types on the average total footing area of the 9-pad system for a soil SOF of 8 m and COV of (a) 20%, (b) 50% and (c) 100%	229
Figure 6-22	Effect of sampling using different test types on the average total footing area of the 9-pad system for a soil COV of 50% and SOF of (a) 1 m, (b) 8 m and (c) 32 m	229
Figure 6-23	Effect of sampling, including measurement and transformation model errors for the (a) SPT and (b) CPT on the average total footing area, for a soil COV of 50% and SOF of 4 m	231
Figure 6-24	Effect of sampling and the use of different settlement relationships on the average total footing area of the 9-pad system for a soil SOF of 8 m and COV of (a) 20%, (b) 50% and (c) 100%	235
Figure 6-25	Effect of sampling and the use of different settlement relationships on the average total footing area of the 9-pad system for a soil COV of 50% and SOF of (a) 1 m, (b) 8 m and (c) 32 m	235
Figure 6-26	Sample distributions of total footing area for the Schmertmann 2B-0.6 settlement relationship for a soil SOF of 8 m and COV of (a) 50% and (b) 100%	238

Figure 6-27	Effect of sampling on the COV of total footing area, for an increasing soil (a) COV (SOF of 8 m) and (b) SOF (COV of 50%)	239
Figure 6-28	Effect of sampling on the spread of total footing area using $\pm 1$ standard deviation from the average using Schmertmann 2B-0.6 and 3DFEA for a soil COV of 50% and SOF of 8 m	241
Figure 6-29	Effect of increased sampling with different sampling patterns on the COV of total footing area, for a soil COV of 50% and SOF of 8 m	242
Figure 6-30	Effect of sampling with different reduction techniques on the standard deviation of total footing area, for a soil COV of 50% and SOF of 8 m	243
Figure 6-31	Effect of sampling with different reduction techniques on the COV of total footing area, for a soil COV of 50% and SOF of 8 m	243
Figure 6-32	Effect of sampling with different test types on the COV of total footing area of the 9-pad system, for a soil SOF of 8 m and COV of (a) 20%, (b) 50% and (c) 100%	245
Figure 6-33	Effect of sampling with different test types on the COV of total footing area of the 9-pad system, for a soil COV of 50% and SOF of (a) 1 m, (b) 8 m and (c) 32 m	245
Figure 6-34	Effect of sampling and settlement technique on the COV total footing area of the 9-pad system, for a soil SOF of 8 m and COV of (a) 20%, (b) 50% and (c) 100%	247
Figure 6-35	Effect of sampling and settlement technique on the COV total footing area of the 9-pad system, for a soil COV of 50% and SOF of (a) 1 m, (b) 8 m and (c) 32 m	247

## **Chapter 7 Reliability Assessment of a Site Investigation in Terms of Foundation Design**

Figure 7-1	Effect of sampling on the probability of (a) under- and (b) over-design, for an increasing soil COV (SOF of 8 m)	253
Figure 7-2	Effect of sampling on the probability of (a) under- and (b) over-design, for an increasing soil SOF (COV of 50%)	254
Figure 7-3	Effect of sampling on the probability of obtaining the optimal design, for an increasing soil (a) COV (SOF of 8 m) and (b) SOF (COV of 50%)	257
Figure 7-4	Effect of sampling on the probability of under- and over-design, and probability of obtaining an optimal design, for each footing in the 9-pad system, based on a SI (RG, SA, CPT)	258
Figure 7-5	Effect of sampling on the probability of a requiring an alternative design for the 9-pad system for an increasing soil COV and SOF of 8 m	260
Figure 7-6	Effect of sampling with different sampling patterns on the probability of under- and over-design and the probability of obtaining an optimal, for a soil COV of 50% and SOF of 8 m	261
Figure 7-7	Effect of increased sampling with different reduction techniques on the probability of (a) under- and (b) over-design and (c) the probability of obtaining an optimal, for a soil COV of 50% and SOF of 8 m	263
Figure 7-8	Effect of sampling with different test types on the probability of (a) under- and (b) over-design and (c) the probability of obtaining an optimal design, for a soil COV of 50% and SOF of 8 m	266

Figure 7-9	Effect of sampling and the use of different settlement prediction techniques on the probability of (a) under- and (b) over-design and (c) the probability of obtaining an optimal, for a soil COV of 50% and SOF of 8 m	269
Figure 7-10	Effect of increased sampling on the average design error, for an increasing soil COV and SOF of (a) 1 m, (b) 4 m, (c) 8 m and (d) 32 m	272
Figure 7-11	Effect of increased sampling on the average design error, for an increasing soil SOF and COV of (a) 10%, (b) 20%, (c) 50% and (d) 100%	273
Figure 7-12	Effect of increased sampling on the average design error, for an increasing soil (a) COV (SOF of 8 m) and (b) SOF (COV of 50%)	274
Figure 7-13	Effect of increased sampling on the average total footing area, for an increasing soil SOF and COV of 50%	275
Figure 7-14	Effect of sampling on the average design error of each footing in the 9-pad system, based on a design using Sch2B and a SI (CPT, RG, SA) and an optimal design using 3DFEA and CK, for a soil COV of 50% and SOF of 8 m	277
Figure 7-15	Effect of sampling using different patterns on the average design error, for a soil COV of 50% and SOF of 8 m	278
Figure 7-16	Effect of sampling and different reduction techniques on the average design error, for a soil COV of 50% and SOF of 8 m	279
Figure 7-17	Effect of sampling and different test types using the (a) SA, (b) GA and (c) 1Q reduction techniques on average design error, for a soil COV of 50 % and SOF of 8 m	281
Figure 7-18	Effect of sampling and different settlement prediction techniques for the design based on a SI (CPT, RG, SA) on the average design error of the 9-pad system, for a soil SOF of 8 m and COV of (a) 20%, (b) 50% and (c) 100%	283
Figure 7-19	Effect of sampling and different settlement prediction techniques for the design based on a SI (CPT, RG, SA) on the average design error of the 9-pad system, for a soil COV of 50% and SOF of (a) 1 m, (b) 8 m and (c) 32 m	283
Figure 7-20	Effect of sampling on the average design error of a single pad footing, for an increasing soil (a) COV (SOF of 4 m) and (b) SOF (COV of 50%)	285
Figure 7-21	Sampling locations in the site area with respect to the system of 9-pad footings	287
Figure 7-22	Average design error of a single pad footing at sample locations, for a soil SOF of 4 m and COV of (a) 20% and (b) 100% (Note the change in scale of E[DE])	288
Figure 7-23	Average design error of a single pad footing at sample locations, for a soil COV of 50 % and SOF of (a) 1 m, (b) 4 m, (c) 16 m and (d) 100 m	289
Figure 7-24	Effect of increasing the sample-to-footing separation distance on the average design error of a single pad footing, for an increasing soil SOF and COV of 50%	290
Figure 7-25	Average design error of a 4-pad system at sample locations for a soil COV of 50% and SOF of (a) 1 m and (c) 16 m	291
Figure 7-26	Average design error of a 9-pad system at sample locations, for a soil COV of 50% and SOF of (a) 1 m and (c) 16 m	291

Figure 7-27	Effect of increasing the bias and random components of measurement error for the (a) SPT and (b) CPT, on the average design error, for a soil with a uniform elastic modulus	293
Figure 7-28	Effect of increasing the bias and random components of measurement error for the SPT, on the average design error, for a soil with a SOF of 4 m and COV of (a) 20%, (b) 50% and (c) 100%	294
Figure 7-29	Effect of increasing the bias and random components of measurement error for the SPT, on the average design error, for a soil with a COV of 50% and SOF of (a) 1 m, (b) 4 m and (c) 16 m	294
Figure 7-30	Effect of increasing the bias and random components of measurement error for the CPT, on the average design error, for a soil with a SOF of 4 m and COV of (a) 20%, (b) 50% and (c) 100%	294
Figure 7-31	Effect of increasing the bias and random components of measurement error for the CPT, on the average design error, for a soil with a COV of 50% and SOF of (a) 1 m, (b) 4 m and (c) 16 m	294
Figure 7-32	Effect of increasing the bias and random components of measurement error, based on a TT with a vertical sampling rate of (a) 1, (b) 2, (c) 4 and (d) 8 samples per borehole, for a soil COV of 50% and SOF of 4 m	296

## **Chapter 8 Risk Assessment of Site Investigations in Terms of Foundation Design**

Figure 8-1	Relationship between construction cost (excluding substructure) and number of storeys	301
Figure 8-2	Relationship of minor and major retrofit and demolish and rebuild for buildings of varying storeys	305
Figure 8-3	Criteria of damage based on angular distortion After Bjerrum (1963)	306
Figure 8-4	Rehabilitation cost ratio for buildings of varying numbers of storeys undergoing increasing (a) total and (b) differential settlement	308
Figure 8-5	Schematic of the 5-storey building with 9 columns transferring loads to the foundations	309
Figure 8-6	Effect of increased site investigation expenditure on the construction, failure and total cost based on 3DFEA, for a soil SOF of 8 m and COV of (a) 20%, (b) 50% and (c) 100%	311
Figure 8-7	Effect of increased site investigation expenditure on the construction, failure and total cost based on 3DFEA, for a soil COV of 50% and SOF of (a) 1 m, (b) 4 m and (c) 32 m	312
Figure 8-8	Effect of increased site investigation expenditure on the construction cost of the design	313
Figure 8-9	Sample distributions of construction, failure and total costs for foundation designs based on (a) 1, (b) 5 and (c) 25 sample locations, for a soil COV of 50% and SOF of 8 m	314
Figure 8-10	Sample distribution of maximum settlements of the foundation design analysed using complete knowledge, for a soil COV of 50% and SOF of 16 m	315
Figure 8-11	Effect of increased sampling on the number of occurrences of ‘true’ (a) total and (b) differential settlements, based on 3DFEA using CK, for a soil COV of 50% and SOF of 16 m	317

Figure 8-12	Effect of increasing the width of the plan area of the influence region on the mean settlement error of a single footing for different site conditions and footing widths, $b$ .	319
Figure 8-13	Effect of increased site investigation expenditure on the construction, failure and total cost, based on an influence region analysis, for a soil SOF of 8 m and COV of (a) 20%, (b) 50% and (c) 100%	321
Figure 8-14	Effect of increased site investigation expenditure on the construction, failure and total cost, based on an influence region analysis, for a soil COV of 50% and SOF of (a) 1 m, (b) 4 m and (c) 32 m	322
Figure 8-15	Effect of increased site investigation expenditure on the total cost, based on an influence region analysis, for an increasing soil (a) COV (SOF of 8 m) and (b) SOF (COV of 50%)	325
Figure 8-16	Effect of increased site investigation expenditure on the construction cost including and excluding site investigation costs, for an increasing soil COV and SOF of 8 m	326
Figure 8-17	Effect of increased site investigation expenditure with different reduction techniques on the total cost, based on an influence region analysis, for a soil COV of 50% and SOF of 8 m	327
Figure 8-18	Effect of increased site investigation expenditure with different reduction techniques on the construction cost, for a soil COV of 50% and SOF of 8 m	328
Figure 8-19	Effect of increased site investigation expenditure with different test types on the total cost of the foundation, based on an influence region analysis, for a soil COV of 50% and SOF of 8 m	329
Figure 8-20	Effect of increased site investigation expenditure with different settlement techniques on the total cost of the foundation, based on an influence region analysis, for a soil COV of 50% and SOF 8 m	331
Figure 8-21	Effect of increased site investigation expenditure with different settlement techniques on the total cost of the foundation, based on an influence region analysis, for a soil COV of 50% and SOF 8 m	331
Figure 8-22	Effect of increased site investigation expenditure using the (a) SA, (b) GA and (c) 1Q on the total cost of 3 different building sizes for a soil COV of 50% and SOF of 8 m	333
Figure 8-23	Effect of increased site investigation expenditure on the construction and failure costs of 3 different building sizes, for a soil COV of 50% and SOF of 8 m	335
Figure 8-24	Effect of increased site investigation expenditure on the 25-pad system showing (a) total costs for different reduction techniques and (b) all costs using only the 1Q, for a soil COV of 50% and SOF of 8 m	337
Figure 8-25	Effect of increased site investigation expenditure on the (a) total cost, (b) construction cost and (c) failure cost, for an increasing soil mean elastic modulus, a COV of 50% and SOF of 8 m	339
Figure 8-26	Effect of increased site investigation expenditure on the probability of requiring an alternative foundation type, for a soil with an increasing mean elastic modulus, a COV of 50% and SOF of 8 m	340
Figure 8-27	Effect of increased site investigation expenditure using the 1Q and the CPT, on the total cost, based on different rehabilitation limits, for a soil COV of 50% and SOF of 8 m	342

Figure 8-28	Effect of increased site investigation using the 1Q on the total cost, based on an influence region analysis, for an increasing soil (a) COV (SOF of 8 m) and (b) SOF (COV of 50%)	344
Figure 8-29	Effect of increased site investigation expenditure on the total cost for changing soil variability	345
Figure 8-30	Cost of the optimal site investigation for different reduction techniques and test types, for a soil COV of 50% and SOF of 8 m	345
Figure 8-31	Total costs results from the optimal site investigation for different reduction techniques and test types, for a soil COV of 50% and SOF of 8 m	346
Figure 8-32	Total cost savings for an increased site investigation cost using different test types, for a soil SOF of 8 m and COV of (a) 20%, (b) 50% and (c) 100%	350

## **Chapter 9 Analysis Using Specific Soil Data**

---

Figure 9-1	Schematic of the 3-storey building with 9 columns transferring loads to the foundations	354
Figure 9-2	Field testing layout for the Site 1 After Jaksa (1995)	355
Figure 9-3	Effect of increased site investigation expenditure on the total cost, using different reduction techniques, for Site 1	356
Figure 9-4	Effect of increased site investigation expenditure on the total cost, using different settlement prediction techniques, for Site 1	357
Figure 9-5	Effect of increased site investigation expenditure on the probability of requiring an alternative foundation design, using different settlement prediction techniques, for Site 1	359
Figure 9-6	Effect of increased site investigation expenditure on the construction cost, using different settlement prediction techniques, for Site 1	359
Figure 9-7	Effect of increased site investigation expenditure on the total cost, using different reduction techniques, for Site 2	362
Figure 9-8	Effect of increased site investigation expenditure on the probability of requiring an alternative foundation design, using different reduction techniques, for Site 2	362
Figure 9-9	Effect of increased site investigation expenditure on the total cost, using different settlement prediction techniques, for Site 2	363
Figure 9-10	Effect of increased site investigation expenditure on the probability of requiring an alternative foundation design, using different settlement prediction techniques, for Site 2	363
Figure 9-11	Effect of increased site investigation expenditure on the total cost, using different (a) reduction techniques and (b) test types, for Site 3	365
Figure 9-12	Effect of increased site investigation expenditure on the total cost, using different settlement prediction techniques, for Site 3	366
Figure 9-13	Effect of increased site investigation expenditure on the probability of requiring an alternative foundation design, using different settlement prediction techniques, for Site 3	367
Figure 9-14	Effect of increased site investigation expenditure on the construction cost, using different settlement prediction relationships, for Site 3	368

---

## Chapter 10 Summary and Recommendations

---

Figure 10-1	Using an influence region to determine which soil properties should be considered	372
Figure 10-2	General relationship between increased site investigation expenditure and total cost for different soil conditions	377

## Appendices

---

### Appendix A Settlement Analysis

Figure A-1	Settlement distributions of different settlement prediction techniques for a soil with a COV of 10% and SOF of 8 m	410
Figure A-2	Settlement distributions of different settlement prediction techniques for a soil with a COV of 20% and SOF of 8 m	411
Figure A-3	Settlement distributions of different settlement prediction techniques for a soil with a COV of 100% and SOF of 8 m	412
Figure A-4	Settlement distributions of different settlement prediction techniques for a soil with a COV of 50% and SOF of 1 m	413
Figure A-5	Settlement distributions of different settlement prediction techniques for a soil with a COV of 50% and SOF of 4 m	414
Figure A-6	Settlement distributions of different settlement prediction techniques for a soil with a COV of 50% and SOF of 16 m	415
Figure A-7	Effect of increasing the soil COV (SOF of 8 m) on the average settlement of a single pad footing using different prediction techniques	416
Figure A-8	Effect of increasing the soil COV (SOF of 8 m) on the settlement COV of a single pad footing using different prediction techniques	417
Figure A-9	Effect of increasing the soil SOF (COV of 50%) on the average settlement of a single pad footing using different prediction techniques	418
Figure A-10	Effect of increasing the soil SOF (COV of 50%) on the settlement COV of a single pad footing using different prediction techniques	419

### Appendix B Average and Variance of Foundation Design Results

Figure B-1	Effect of increasing the horizontal to vertical SOF ratio (COV of 50%) on the average total footing area, of the 9-pad system, designed using 3DFEA and different prediction techniques	422
Figure B-2	Effect of increasing the horizontal to vertical SOF ratio (COV of 50%) on the COV of total footing area, of the 9-pad system, designed using 3DFEA and different prediction techniques	423
Figure B-3	Effect of increased sampling using different reduction techniques on the average total footing area, for a soil SOF of 8 m and COV of (a) 20%, (b) 50% and (c) 100%	424
Figure B-4	Effect of increased sampling using different reduction techniques on the average total footing area, for a soil COV of 50% and SOF of (a) 1 m, (b) 4 m and (c) 32 m	425
Figure B-5	Effect of increased sampling and the inclusion of measurement and transformation model errors of the SPT on the average total footing area, for a soil SOF of 8 m and COV of (a) 20%, (b) 50% and (c) 100%	426

Figure B-6	Effect of increased sampling and the inclusion of measurement and transformation model errors of the SPT on the average total footing area, for a soil COV of 50% and SOF of (a) 1 m, (b) 4 m and (c) 16 m	427
Figure B-7	Effect of increased sampling and the inclusion of measurement and transformation model errors of the CPT on the average total footing area, for a soil SOF of 8 m and COV of (a) 20%, (b) 50% and (c) 100%	428
Figure B-8	Effect of increased sampling and the inclusion of measurement and transformation model errors of the CPT on the average total footing area, for a soil COV of 50% and SOF of (a) 1 m, (b) 4 m and (c) 16 m	429
Figure B-9	Effect of increased sampling and the inclusion of measurement and transformation model errors of the TT on the average total footing area, for a soil SOF of 8 m and COV of (a) 20%, (b) 50% and (c) 100%	430
Figure B-10	Effect of increased sampling and the inclusion of measurement and transformation model errors of the TT on the average total footing area, for a soil COV of 50% and SOF of (a) 1 m, (b) 4 m and (c) 16 m	431
Figure B-11	Effect of increased sampling and the inclusion of measurement and transformation model errors of the DMT on the average total footing area, for a soil SOF of 8 m and COV of (a) 20%, (b) 50% and (c) 100%	432
Figure B-12	Effect of increased sampling and the inclusion of measurement and transformation model errors of the DMT on the average total footing area, for a soil COV of 50% and SOF of (a) 1 m, (b) 4 m and (c) 16 m	433
Figure B-13	Effect of increased sampling using different reduction techniques on the COV of total footing area, for a soil SOF of 8 m and COV of (a) 20%, (b) 50% and (c) 100%	434
Figure B-14	Effect of increased sampling using different reduction techniques on the COV of total footing area, for a soil COV of 50% and SOF of (a) 1 m, (b) 4 m and (c) 32 m	435
<b>Appendix C Probabilities of Under- and Over-design and Probabilities of Obtaining an Optimal Design</b>		
Figure C-1	Effect of increased sampling on the probability of (a) under- and (b) over-design and (c) the probability of obtaining an optimal design, for a soil SOF of 1 m and varying COV	438
Figure C-2	Effect of increased sampling on the probability of (a) under- and (b) over-design and (c) the probability of obtaining an optimal design, for a soil SOF of 4 m and varying COV	439
Figure C-3	Effect of increased sampling on the probability of (a) under- and (b) over-design and (c) the probability of obtaining an optimal design, for a soil SOF of 32 m and varying COV	440
Figure C-4	Effect of increased sampling on the probability of (a) under- and (b) over-design and (c) the probability of obtaining an optimal design, for a soil COV of 10% and varying SOF	441
Figure C-5	Effect of increased sampling on the probability of (a) under- and (b) over-design and (c) the probability of obtaining an optimal design, for a soil COV of 20% and varying SOF	442
Figure C-6	Effect of increased sampling on the probability of (a) under- and (b) over-design and (c) the probability of obtaining an optimal design, for a soil COV of 100% and varying SOF	443



Figure C-7	Effect of increased sampling with different reduction techniques on the probability of (a) under- and (b) over-design and (c) the probability of obtaining an optimal design, for a soil COV of 20% and SOF of 8 m	444
Figure C-8	Effect of increased sampling with different reduction techniques on the probability of (a) under- and (b) over-design and (c) the probability of obtaining an optimal design, for a soil COV of 100% and SOF of 8 m	445
Figure C-9	Effect of increased sampling with different reduction techniques on the probability of (a) under- and (b) over-design and (c) the probability of obtaining an optimal design, for a soil COV of 50% and SOF of 1 m	446
Figure C-10	Effect of increased sampling with different reduction techniques on the probability of (a) under- and (b) over-design and (c) the probability of obtaining an optimal design, for a soil COV of 50% and SOF of 4 m	447
Figure C-11	Effect of increased sampling with different reduction techniques on the probability of (a) under- and (b) over-design and (c) the probability of obtaining an optimal design, for a soil COV of 50% and SOF of 32 m	448
Figure C-12	Effect of increased sampling with different test types on the probability of (a) under- and (b) over-design and (c) the probability of obtaining an optimal design, for a soil COV of 20% and SOF of 8 m	449
Figure C-13	Effect of increased sampling with different test types on the probability of (a) under- and (b) over-design and (c) the probability of obtaining an optimal design, for a soil COV of 100% and SOF of 8 m	450
Figure C-14	Effect of increased sampling with different test types on the probability of (a) under- and (b) over-design and (c) the probability of obtaining an optimal design, for a soil with a COV of 50% and a SOF of 1 m	451
Figure C-15	Effect of increased sampling with different test types on the probability of (a) under- and (b) over-design and (c) the probability of obtaining an optimal design, for a soil COV of 50% and SOF of 4 m	452
Figure C-16	Effect of increased sampling with different test types on the probability of (a) under- and (b) over-design and (c) the probability of obtaining an optimal design, for a soil COV of 50% and SOF of 32 m	453
Figure C-17	Effect of increased sampling and different prediction techniques on the probability of (a) under- and (b) over-design and (c) the probability of obtaining an optimal design, for a soil COV of 20% and SOF of 8 m	454
Figure C-18	Effect of increased sampling and different prediction techniques on the probability of (a) under- and (b) over-design and (c) the probability of obtaining an optimal design, for a soil COV of 100% and SOF of 8 m	455
Figure C-19	Effect of increased sampling and different prediction techniques on the probability of (a) under- and (b) over-design and (c) the probability of obtaining an optimal design, for a soil COV of 50% and SOF of 1 m	456
Figure C-20	Effect of increased sampling and different prediction techniques on the probability of (a) under- and (b) over-design and (c) the probability of obtaining an optimal design, for a soil COV of 50% and SOF of 4 m	457
Figure C-21	Effect of increased sampling and different prediction techniques on the probability of (a) under- and (b) over-design and (c) the probability of obtaining an optimal design, for a soil COV of 50% and SOF of 32 m	458

#### **Appendix D Average Design Error**

Figure D-1	Effect of increased sampling on the average design error for a soil with an increasing COV and a SOF of (a) 1 m, (b) 4 m and (c) 32 m	460
------------	---	-----

Figure D-2	Effect of increased sampling on the average design error for a soil with an increasing SOF and a COV of (a) 10%, (b) 20% and (c) 100%	461
Figure D-3	Effect of increased sampling with different reduction techniques on the average design error for a soil SOF of 8 m and a COV of (a) 10%, (b) 20% and (c) 100%	462
Figure D-4	Effect of increased sampling with different reduction techniques on the average design error for a soil with a COV of 50% and a SOF of (a) 1 m, (b) 4 m and (c) 32 m	463
Figure D-5	Effect of increased sampling with different test types and the SA on the average design error for a soil with a SOF of 8 m and a COV of (a) 10%, (b) 20% and (c) 100%	464
Figure D-6	Effect of increased sampling with different test types and the SA on the average design error for a soil with a COV of 50% and a COV of (a) 1 m, (b) 4 m and (c) 32 m	465
Figure D-7	Effect of increased sampling with different test types and the GA on the average design error for a soil with a SOF of 8 m and a COV of (a) 10%, (b) 20% and (c) 100%	466
Figure D-8	Effect of increased sampling with different test types and the GA on the average design error for a soil with a COV of 50% and a COV of (a) 1 m, (b) 4 m and (c) 32 m	467
Figure D-9	Effect of increased sampling with different test types and the 1Q on the average design error for a soil with a SOF of 8 m and a COV of (a) 10%, (b) 20% and (c) 100%	468
Figure D-10	Effect of increased sampling with different test types and the 1Q on the average design error for a soil with a COV of 50% and a COV of (a) 1 m, (b) 4 m and (c) 32 m	469
Figure D-11	Effect of increased sampling using the GA and different settlement prediction techniques on the average design error, for a soil SOF of 8 m and COV of (a) 20%, (b) 50% and (c) 100%	470
Figure D-12	Effect of increased sampling using the GA and different settlement prediction techniques on the average design error, for a soil COV of 50% and SOF of (a) 1 m, (b) 4 m and (c) 32 m	471
Figure D-13	Effect of increased sampling with different reduction techniques on the average design error of the single pad foundation system, for a soil SOF of 4 m and COV of (a) 20%, (b) 50% and (c) 100%	472
Figure D-14	Effect of increased sampling with different reduction techniques on the average design error of the single pad foundation system, for a soil COV of 50% and SOF of (a) 1 m, (b) 4 m and (c) 16 m	473
 <b>Appendix E Foundation Design Costs</b>		
Figure E-1	Effect of increased site investigation expenditure with different reduction techniques on the total cost, based on an influence region analysis, for a soil SOF of 8 m and COV of (a) 20%, (b) 50% and (c) 100%	476
Figure E-2	Effect of increased site investigation expenditure with different reduction techniques on the total cost, based on an influence region analysis, for a soil COV of 50% and SOF of (a) 1 m, (b) 4 m and (c) 32 m	477
Figure E-3	Effect of increased site investigation expenditure with different reduction techniques on the construction cost, for a soil SOF of 8 m and COV of (a) 20%, (b) 50% and (c) 100%	478

Figure E-4	Effect of increased site investigation expenditure with different reduction techniques on the construction cost, for a soil COV of 50% and SOF of (a) 1 m, (b) 4 m and (c) 32 m	479
Figure E-5	Effect of increased site investigation expenditure with different test types on the total cost, based on an influence region analysis, for a soil SOF of 8 m and COV of (a) 20%, (b) 50% and (c) 100%	480
Figure E-6	Effect of increased site investigation expenditure with different test types on the total cost, based on an influence region analysis, for a soil COV of 50% and SOF of (a) 1 m, (b) 4 m and (c) 32 m	481
Figure E-7	Effect of increased site investigation expenditure with different test types on the construction cost, for a soil SOF of 8 m and COV of (a) 20%, (b) 50% and (c) 100%	482
Figure E-8	Effect of increased site investigation expenditure with different test types on the construction cost, for a soil COV of 50% and SOF of (a) 1 m, (b) 4 m and (c) 32 m	483
Figure E-9	Effect of increased site investigation expenditure with different settlement prediction techniques on the total cost, based on an influence region analysis, for a soil SOF of 8 m and COV of (a) 20%, (b) 50% and (c) 100%	484
Figure E-10	Effect of increased site investigation expenditure with different settlement prediction techniques on the total cost, based on an influence region analysis, for a soil COV of 50% and SOF of (a) 1 m, (b) 4 m and (c) 32 m	485
Figure E-11	Effect of increased site investigation expenditure with different settlement prediction techniques on the construction cost, for a soil SOF of 8 m and COV of (a) 20%, (b) 50% and (c) 100%	486
Figure E-12	Effect of increased site investigation expenditure with different settlement prediction techniques on the construction cost, for a soil COV of 50% and SOF of (a) 1 m, (b) 4 m and (c) 32 m	487



## LIST OF TABLES

### Chapter 1 Introduction

### Chapter 2 Literature Review

Table 2-1	Recommendations for varying site investigation plans After Ferguson (1992)	12
Table 2-2	Suggested uses for bearing capacity equations After Bowles (1997)	15
Table 2-3	Relative importance of immediate, consolidation and secondary settlement for different soil types After Holtz (1991)	16
Table 2-4	Tolerable settlement of buildings in millimetres Recommended maximum values in parenthesis After Bowles (1997)	24
Table 2-5	Summary of Allowable Settlements for Different Buildings and Limiting Criteria After Sowers (1962)	24
Table 2-6	Inherent soil variability based on common test types After Phoon et al. (1995)	32
Table 2-7	Example scale of fluctuation values based of geotechnical properties After Phoon et al. (1995)	33
Table 2-8	Statistical properties from extensively tested sites	35
Table 2-9	Measurement errors of common in situ tests expressed as a coefficient of variation After Phoon and Kulhawy (1999a)	42
Table 2-10	Correlations between soil properties and test results for (a) cohesive and (b) non-cohesive soils After Phoon and Kulhawy (1999b)	46
Table 2-11	Design capacity example using several assumptions and equations After Kulhawy (1984)	47

### Chapter 3 Methodology Development

Table 3-1	Range of statistical properties used in soil simulation	59
Table 3-2	Sampling density based on 1 sample/300 m <sup>2</sup> compared with adopted sampling density for research methodology	70
Table 3-3	Vertical sampling frequencies for each test type (element size = 0.5 m × 0.5 m × 0.5 m)	74
Table 3-4	Uncertainties due to measurement and transformation model error for each test type	75

Table 3-5	Comparison of settlement prediction techniques adopted in the methodology, not including the numerical method	81
Table 3-6	Element and site sizes used to increase the number of elements beneath the footing	91
Table 3-7	Element size and number used to investigate the influence of	93
Table 3-8	Statistical properties obtained from Monte Carlo simulation to measure effectiveness of site investigation scope	98
Table 3-9	Code profiling results	101
Table 3-10	Benchmark results for various FORTRAN 77 and FORTRAN 90 compilers After Polyhedron Software (2004)	101
Table 3-11	Cross platform computational times for 1000 Monte Carlo realisations for a soil COV of 50% and SOF of 8 m	103
Table 3-12	Comparison of program run times for varying number of processors using Message Passing Interface (MPI)	105

#### **Chapter 4 Verification of Methodology**

---

Table 4-1	Goodness of fit statistics for simulated soil with a lognormal distribution	110
Table 4-2	Comparison between target and sample mean and standard deviation of simulated soils	112
Table 4-3	Verification of settlement estimates for single pad footing	126
Table 4-4	Settlement estimates for corner and central edge footings of the 9-pad system	127
Table 4-5	Measured settlements obtained from various literature sources including analysis parameters	129

#### **Chapter 5 Effect of Different Settlement Prediction Techniques on the Design and Analysis of a Pad Foundation**

---

Table 5-1	Comparison of settlement prediction technique coefficients based on a 1.5 m × 1.5 m footing for a soil with a uniform elastic modulus	148
Table 5-2	Results of the Chi-square goodness-of-fit test for settlement estimates with a lognormal distribution ( <i>p</i> value shown in parenthesis)	155
Table 5-3	Probability that prediction technique settlement is less than 3DFEA settlement	163

#### **Chapter 6 Effect of Site Investigations on Design Parameters and the Design of a Pad Foundation**

---

Table 6-1	Adopted uncertainties due to measurement and transformation model error for each test type investigated	228
-----------	---	-----

#### **Chapter 7 Reliability Assessment of a Site Investigation in Terms of Foundation Design**

---

Table 7-1	Range of uncertainties used in sensitivity analysis of test measurement error	292
-----------	---	-----

---

## **Chapter 8 Risk Assessment of Site Investigations in Terms of Foundation Design**

---

Table 8-1	Costs associated with different site investigation tests Adapted from Jaksa (2004)	300
Table 8-2	Building construction and substructure costs by number of storeys	301
Table 8-3	Description of failure severities and rehabilitation works	305
Table 8-4	Severity of cracking damage After Day (1999)	307
Table 8-5	Adopted settlement and differential settlement limits for failure severity or rehabilitation work category	307
Table 8-6	Pad footing loads for the three building sizes investigated	332
Table 8-7	Range of rehabilitation limits trailed in sensitivity analysis Differential settlements in parenthesis (m/m)	341
Table 8-8	Effect of site conditions and site investigation variables on costs	348

## **Chapter 9 Analysis Using Specific Soil Data**

---

Table 9-1	Summary of results from the South Parklands site Adapted from Jaksa (1995)	355
Table 9-2	Average statistical values of the cone tip resistance for each layer and overall depth at the Texas A&M University “Sand Site” Adapted from Akkaya and Vanmarcke (2003)	360
Table 9-3	Statistical properties of the varved clay site in New Liskeard, Canada	364

## **Chapter 10 Summary and Recommendations**

---

Table 10-1	Effect of site conditions and site investigation variables on costs	378
------------	---	-----





## NOTATION

1Q	1 <sup>st</sup> quartile selection
2:1	2:1 settlement prediction technique
3DFEA	Three dimensional finite element analysis
$A$	Area – subscripts used to denote object (e.g. footing, influence area)
$A_{opt}$	Optimal footing area designed using complete knowledge
$B$	Shape factor for settlement estimate
$a$	Shape factor for settlement estimate
$b$	Width or least plan dimension of the footing
$b_{infrac}$	Width of the influence region
$b'$	Effective width or least plan dimension of the footing
$C^*$	Variable representing correction factors, load and footing size
$C^{**}$	Variable representing strain influence factor and $C^*$
$C_1$	Footing embedment correction factor (Schmertmann)
$C_2$	Time correction factor (Schmertmann)
CK	Complete knowledge of the soil (all properties known)
COV	Coefficient of variation
Cov[.]	Covariance operator
CPT	Cone penetration test
$c$	Cohesion
$c_w$	Width of column
$D$	Depth of the compressible soil layer
$D_A$	Test parameter $A$ from DMT
$D_B$	Test parameter $B$ from DMT
$DE$	Design error
$d_e$	Footing embedment depth
DFT	Discrete Fourier transformation method

DMT	Marchetti flat plate dilatometer test
$D_r$	Relative density
$D_v$	Averaging domain
$d$	Thickness of footing for beam shear
$d_{om}$	Depth to top of reinforcing
$d_t$	Total thickness of footing
$E$	Elastic modulus
$E[.]$	Expectation operator
$E_{ave}$	Averaged elastic modulus value
$E_{COV}$	Coefficient of variation of elastic modulus field
$E_D$	Elastic modulus from DMT
$E_f$	Elastic modulus value taken directly from random field
$E_{PMT}$	Elastic modulus from PMT
$E_r$	Resultant elastic modulus value after effects of system uncertainty
$E_{SOF}$	Scale of Fluctuation of elastic modulus field (isotropic)
$e_i$	Proportion of element size in relation to total
$F$	Random variable representing load
FFT	Fast Fourier transformation
FORM	First order reliability method
FOS	Factor of safety
FOSM	First order second moment reliability method
$f'_c$	Yield strength of concrete
$f_{cv}$	Shear capacity of concrete
$f_i$	Proportion of number of samples in relation to number of elements
$f_s$	Sleeve friction from CPT
$G$	Shear strain modulus
GA	Geometric average
$H$	Depth of stress change
HA	Harmonic average
$H_b$	Height of structure of building
$h$	Difference between corner and middle settlements of a flexible footing
$I_1; I_2; I_F$	Shape factors
$I_2$	Inverse distance squared weighted
ID	Inversed distance weighted
$I_p$	Influence factor

$Ip_x, Ip_y$	Size of the site investigation in x- and y-directions
$I_z$	Strain influence factor
Jan	Janbu settlement prediction technique
$K_D$	From DMT
$k$	Bulk modulus
$k_s$	Modulus of subgrade reaction
$L$	Shape factor for settlement estimate
LAS	Local average subdivision
$LI$	Liquid index
$l$	Length or largest plan dimension of the footing
$M$	Shape factor for settlement estimate
MA	Moving average method
MN	Minimum value selection
$MOS$	Margin of safety
MPI	Message passing interface (parallel processing)
$m$	Random variable representing measurement error
$m_b$	Random variable representing bias component of measurement error
$m_F$	Mean of random variable representing load
$m_R$	Mean of random variable representing capacity
$m_r$	Random variable representing random component of measurement error
$N$	SPT blow count
$N_\gamma$	Bearing capacity factor
$N_0$	Shape factor for settlement estimate
$N_c$	Bearing capacity factor
New	Newmark settlement prediction technique
$N_q$	Bearing capacity factor
$n$	Number of samples to reduce
$n_f$	Number of footings in foundation system
$n_l$	Number of discretised layers
$n_r$	Number of realisations
$n_t$	Total population size
OCR	Over-consolidation ratio
$P$	Applied footing load
Per	Perloff settlement prediction technique

$PI$	Plastic index
PMT	Pressuremeter test
$p_f$	Probability of failure
$p_L$	Pressuremeter limit stress
$p_{od}$	Probability of over design
$p_{op}$	Probability of attaining an optimal design
$p_{ud}$	Probability of under design
$Q_{su}$	Side resistance
$Q_{tu}$	Tip resistance
$Q_u$	Available capacity
$Q_{ud}$	Design uplift capacity
$q$	Applied footing pressure
$q_a$	Allowable bearing capacity
$q_{a_{net}}$	Net allowable bearing capacity
$q_{av}$	Averaging pressure over the footing contact area
$q_c$	Cone tip resistance from CPT
$q_u$	Unconfined compression strength
$q_{ult}$	Ultimate bearing capacity
$q_z$	Stress at depth $z$
$q_z$	Stress in soil at depth $z$
$\Delta q$	Change in stress
$R$	Random variability representing capacity
RFEM	Random finite element method
RG	Regular grid sampling pattern
RN	Simple random arrangement of sample locations
$r_i$	Internal radius of annulus
$r_o$	External radius of annulus
$S$	Estimated footing settlement
SA	Standard arithmetic average
Sch2B	Schmertmann settlement prediction technique based on 2B-0.6 strain distribution
SchM	Schmertmann settlement prediction technique based on Modified strain distribution
$SE$	Settlement error
SFEM	Stochastic finite element method
SGS	Sequential Gaussian simulation

SI	Site investigation knowledge of the soil (based on sampling)
$SI_{opt}$	Optimal site investigation cost, based on yielding the lowest total cost
$SI_{opt}^*$	Optimal site investigation cost for the worst case SOF
SIS	Sequential indicator simulation
SOF	Scale of fluctuation (measure of correlation distance)
SOSM	Second-order second-moment reliability method
SPT	Standard penetration test
SR	Stratified random sampling pattern
$St_x, St_y$	Size of the site in x- and y-directions
$s_\gamma$	Bearing capacity correction factor for unit weight
$s_c$	Bearing capacity correction factor for cohesion
$s_i$	Distance separating the $i$ th sample location and the footing
$s_F$	Standard deviation of random variable representing load
$s_R$	Standard deviation of random variable representing capacity
$s_{tot}$	Total distance separating all sample locations and the footing
$s_u$	Undrained shear strength
$sv$	Random variable representing uncertainty due to spatial variability
$T$	Transformation model
T&G	Timoshenko and Goodier settlement prediction technique
TBM	Turning bands method
TBM	Turning bands method
TT	Triaxial test
$t(z)$	Trend value at depth $z$
$tm$	random variable representing transformation model error
$V$	Shape factor for settlement estimate
$V^*$	Applied shear load on footing
$V_1$	Shape factor for settlement estimate
$V_1^*; V_2^*$	Components of the applied shear load, $V^*$
VST	Vane shear test
Var[.]	Variance operator
$V_{u0}$	Punching shear capacity
$V_{uc}$	Beam shear capacity
$W$	Weight of shaft
$W_b$	Width of structure or building
Wst	Westergaard settlement prediction technique

$w(z)$	Fluctuating residual value at depth $z$
$w_L$	Water content at liquid limit
$w_n$	Natural water content
$w_p$	Water content at plastic limit
$X$	Random variable
$X_{\ln}$	Lognormal random variable
$x$	Individual property that conforms to $X$
$x_c$	X coordinate
$x_d$	Distance to parabolic centroid
$Y$	Random variable
$y_c$	Y coordinate
$Z$	Centre-to-centre spacing of two adjacent footings
$z$	Depth in soil layer
$\Delta z$	Soil layer thickness
$\alpha$	Shape factor for settlement estimate
$\beta$	Reliability index
$\beta_1$	Shape factor for beam shear capacity
$\beta_\tau$	Covariance at lag $\tau$
$\delta$	Footing settlement
$\delta_{1 2}$	Settlement of Footing 1 due to Footing 2
$\delta_{ann}$	Settlement of rigid annulus
$\delta_c$	Corner settlement of flexible footing
$\delta_m$	Centre settlement of flexible footing
$\delta_r$	Rigid footing settlement
$\varepsilon$	Strain
$\gamma$	Unit weight of soil
$\gamma'$	Effective unit weight of soil
$\gamma_d$	Dry unit weight of soil
$\gamma(D)$	Variance reduction based on an averaging domain of $D$
$\gamma_h$	Semivariogram value at distance $h$
$\eta_0$	Footing embedment correction factor
$\eta_1$	Layer depth correction factor
$\eta_a, \eta_b$	Fitted constants for the Janbu settlement relationship
$\kappa$	Deterministic coefficient representing settlement prediction technique coefficients and design criteria limits

$\lambda$	Differential settlement ratio $ \delta_1 - \delta_2 /Z$
$\mu_{\ln x}$	Sample mean of the logarithm of $x$
$\mu_x$	Sample mean of $x$
$\nu$	Poisson's ratio
$\theta$	Isotropic scale of fluctuation, SOF
$\theta_h$	Vertical scale of fluctuation, SOF
$\theta_v$	Vertical scale of fluctuation, SOF
$\theta_{wc}$	Worst case scale of fluctuation, SOF
$\rho_{min}$	Percentage of steel reinforcing
$\rho_\tau$	Correlation at lag $\tau$
$\sigma_e^2$	Variance due to equipment effects
$\sigma_{\ln x}$	Sample standard deviation of the logarithm of $x$
$\sigma_{\ln x}^2$	Sample variance of the logarithm of $x$
$\sigma_m^2$	Variance due to measurement error
$\sigma_n'$	Overburden pressure
$\sigma_{p/o}^2$	Variance due to procedural and operator effects
$\sigma_{sv}^2$	Variance due to spatial variability
$\sigma_T^2$	Variance due to all forms of uncertainty
$\sigma_{tm}^2$	Variance due to transformation model error
$\sigma_r^2$	Variance due to random test effects
$\sigma_x$	Sample standard deviation of $x$
$\sigma_x^2$	Sample variance of $x$
$\phi$	Angle of internal friction
$\phi_{red}$	Concrete strength reduction factor
$\tau$	Lag or separation distance vector = $\{\tau_x, \tau_y, \tau_z\}$
$\tau_x$	Lag or separation distance in the x-direction
$\tau_y$	Lag or separation distance in the y-direction
$\tau_z$	Lag or separation distance in the z-direction
$\omega$	Angle representing the rate of stress decrease
$\psi^\circ$	Angle in degrees used to proportion footing area in relation to annulus
$\psi^f$	Angle in radians used to proportion footing area in relation to annulus
$\xi_d$	Design parameter
$\xi_m$	Measured soil property
$\xi(z)$	In situ soil property at depth $z$





# Chapter 1 INTRODUCTION

## 1.1 SITE INVESTIGATIONS

---

In all forms of engineering, suitable information or data is required for a successful design. In structural engineering, such information is readily available and is typically well defined because materials like concrete and steel are manufactured to specific quality guidelines. However, geotechnical engineering is very different. Instead of manufactured materials, geotechnical engineers deal with materials that have generally been provided by nature. Therefore, the data or information collection about the ground conditions is vital to the accuracy and adequacy of the design. Furthermore, the available testing methods are prone to significant errors due to procedural, random and model effects.

The activity of estimating ground conditions has been termed a site characterisation and may consist of reconnaissance and investigative components. Generally, the investigation phase of such a characterisation yields specific information regarding usable properties of the site including the geology, strength and deformation characteristics. It is these results that are used to predict the response of the soil to applied loads. In the case of a foundation, the response may be the bearing capacity or the expected deformation. However, the results of the analysis are only as accurate as that of the estimated soil properties that have been obtained from a site investigation.

Temple and Stukhart (1987), the Institution of Civil Engineers (1991), Littlejohn et al. (1994) and Whyte (1995) indicated that one of the greatest sources of technical and financial risk in a building project is related to ground engineering. Furthermore, Osterberg (1989) indicated that inadequate subsurface exploration, and failure to appreciate or understand the in situ behaviour of soil, is one of the main reasons behind major and catastrophic failures of structures. Despite this, Clayton (2001) suggested that insufficient expenditure is afforded to ground investigation. The Site Investigation Steering Group (1993) sug-

gested that typical expenditure ranged between 0.1% and 0.3% of the project cost, yet, Jaksa (2000) noted that it may be as low as 0.025%. Others believed that site investigation expenditure for a foundation project is around 0.2% (Clayton et al. 1982). However, in all cases it appears that it is less than 1% (Peacock and Whyte 1988). Ideally, the National Research Council (1984) suggested that site investigation expenditure should be approximately 3% of the cost of the project. However, Littlejohn et al. (1994) believed that the scope of a site investigation should not be based on a percentage of total cost. Instead, the scope should take into account the uncertainty and inherent risk associated with the site.

Since site investigation expenditure is a small fraction of the project cost, an increase in scope that reduces the risk of a cost overrun or foundation failure, does not have a significant impact on the total cost (Clayton et al. 1982). However, the Site Investigation Steering Group (1993) believed that an improved site investigation may not necessarily incur an additional cost. Instead, they believed that current site investigation practices could be refined to yield designs with a lower risk of failure or cost overrun.

Because no two sites are the same, it is difficult to prescribe minimum guidelines regarding the scope of a site investigation. Codes from several countries provide open-ended recommendations like:

“the investigation shall evaluate the material properties and the volume of ground which will significantly effect the performance of ... the proposed works.” (Australian Standards AS1726, 1993)

Some independent research has also been conducted to measure the effectiveness of site investigation plans. Whitman (2000) suggested *search theory* as introduced by Baecher (1979) and Halim and Tang (1993) as a probabilistic method to measure the adequacy of a site investigation. Search theory provides a probabilistic estimate of the ability to find a flaw or defect in a soil deposit with reasonably known conditions. Parsons and Frost (2002) also used probabilistic methods to measure the *thoroughness* of site investigations. They used geostatistics and a GIS (Geographic Information System) to compare the ability of one sampling strategy to another to characterise a known soil. Tsai and Frost (1999) have also used thoroughness to examine the quality of site investigations in a similar framework. In a more specific account, Wiesner (1999) suggested that using vertical holes on a 50 m grid is common practice. However, Bowles (1997) suggested that the frequency and arrangement of sampling should be sufficient to investigate the site area that may be affected by the final design. This is very general and provides little quantitative assistance for the practitioner.

---

## 1.2 AIM AND SCOPE OF THIS RESEARCH

---

Baecher and Christian (2003) indicated there is definite scope for research measuring the effectiveness of site investigations. In fact, they suggested that many believe there is a solution to the problem of site characterisation waiting to be discovered. Furthermore, Clayton (2001) believed that a new risk-based method is required for ground investigations. Therefore, the primary aim of this research is to quantify the risk of a site investigation in terms of financial implications. This is achieved by investigating the impact of site investigation scope on the design of a foundation. More specifically, this research concentrates on the design of pad foundations, although, consideration is also made when a pad foundation is inappropriate. The scope of a site investigation is characterised in terms of:

- The number of samples;
- The arrangement of such sampling;
- The method to select characteristic values; and
- The test type.

Therefore, the general aims of this research are to provide answers to questions like:

- What are the benefits of increased sampling or testing?
- Do the results of say, 3 cone penetrations tests, yield a more efficient foundation design than 5 standard penetration tests?
- Is a conservative foundation design suitable in terms of financial risk?

The aims of this research are addressed in the following way:

- Use of a simulated soil, whereby the properties are known at all locations in detail. The soil simulation involves generating three-dimensional random fields by specifying the mean, standard deviation and scale of fluctuation;
- The use of a probabilistic framework enables comparisons to be made regarding the influences of each source of uncertainty on the foundation design. It should be noted that uncertainties with the applied foundation loads are not included in this research.

- The success of a particular site investigation, which represents limited knowledge of the site, is measured by comparing the resulting foundation design to that where complete knowledge is used; and
- Determination of project risk in terms of overall project costs as well as potential rehabilitation costs due to foundation failures. An optimal site investigation that minimises the costs is also determined.

The results of this research are essentially a series of conclusions regarding the effect of site investigations with varying scope on the design of a foundation system and the resulting total cost. Recommendations are also made as to how to reduce the total cost of the project, which also includes the costs associated with rehabilitation. It is expected that these recommendations will assist geotechnical engineers in making more rational decisions regarding the scope of a site investigation with a greater appreciation of the associated risks.

### **1.3 LAYOUT OF THIS THESIS**

---

Chapter 2 deals with a treatment of the literature regarding the current practice in geotechnical design and, more specifically, the design of a foundation and how it is affected by site investigations. The discussion includes treatment of reliability-based design principles and the uncertainties inherent in a geotechnical model. Discussions regarding the typical scope of a site investigation, as well as the procedures used to design a foundation, are also included.

The methodology that is adopted to measure the effectiveness of a site investigation is described in Chapter 3. This includes the procedures utilised to generate a simulated soil based on random field theory, the design of a foundation for settlement, based on complete knowledge of the soil, and the results of a simulated site investigation. The technique adopted to account for the uncertainties in the geotechnical model and the determination of probabilistic solutions suitable for a reliability and risk analysis, are also discussed in Chapter 3.

The verification procedure is presented in Chapter 4, where the implementation of the methodology described in Chapter 3 is examined for accuracy and validity. The verifications are undertaken to ensure that any conclusions resulting from the method are robust and appropriate.

The first results of the research are described in Chapter 5. In this chapter, the effects of different settlement prediction techniques on the analysis and design of a foundation are presented. Results also illustrate the sensitivity of inherent conservatism of the different settlement prediction techniques.

The results of the research dealing with site investigations are first presented in Chapter 6, where the influence of increased sampling on design parameters and foundation design are examined. The effect of a site investigation on the foundation design is demonstrated using distributions of footing area and measures of the average and standard deviation.

Chapter 7 deals with probabilistic comparisons between designs using data from a site investigation and an optimal design. In this chapter, the effect of site investigations is measured by the probability of under- and over-design, as well as an additional measure called the design error. Such results provide suitable means to compare the performance of one site investigation with another.

Further discussion regarding the performance of site investigations are contained in Chapter 8, where costs associated with the site investigation, construction, and possible foundation failure, are included into the analysis. This enables the site investigation expenditure to be measured against the total cost of the design or the financial risk.

Chapter 9 provides a discussion regarding whether the conclusions from Chapter 8 are applicable to specific soil conditions. In this case, the methodology is applied to three case studies, where extensive soil testing data allows the estimation of the statistical properties of the soil.

Final conclusions and recommendations are presented in Chapter 10, as well as the limitations and difficulties associated with the research and future directions.

Special note should also be made regarding the *specific conclusions*, which are included throughout this document. These have been highlighted and contained within shaded boxes. The aim of these specific conclusions is to emphasize conclusions that have been drawn from the discussion of the results prior. It is hoped that this will aid the reader in recognising the pertinent results.



## **Chapter 2 LITERATURE REVIEW**

### **2.1 INTRODUCTION**

---

To quantify the effectiveness of a site investigation it is important to consider the effects of such an investigation. In this research, a site investigation procedure has been implemented to facilitate the design of a foundation. This is a similar procedure to that used in practice. Therefore, it is necessary to evaluate the foundation design process starting from the analysis of the site to the design of the foundation. It is also important to recognise the uncertainties in such a design process. Therefore, information discussed in this chapter is a review of the current state of practice associated with foundation design. This includes foundation design methods, uncertainties in the geotechnical model, and the means to deal with such uncertainties.

### **2.2 FOUNDATION DESIGN**

---

Foundations are designed to meet specific design criteria (Chen and McCarron 1991). This is achieved by sizing the foundation based on the predicted response of the footing due to its applied loading. However, suitable knowledge of the underlying soil properties is paramount to any successful design. Such knowledge is typically attained from site characterisation. As such, the following sections discuss the major components of a foundation design including the site characterisation activities and the prediction of foundation response.

#### **2.2.1 Site Characterisation**

The purpose of site characterisation is to obtain a reasonable representation of the subsurface conditions (Lee et al. 1983, Lowe III and Zaccheo 1991, Bowles 1997). Characterisation refers to both reconnaissance and investigation, where the former relates to the review

of surrounding geology and the latter involves ground exploration through testing (Baecher and Christian 2003). Lee et al. (1983) further categorised investigative methods into *areal* and *local* explorations. Areal explorations are not concerned with obtaining specific soil properties, whereas local explorations are directed towards such properties. Areal explorations may also include drilling and sampling (Lowe III and Zaccheo 1991). Samples obtained from areal exploration techniques are usually undisturbed and are suitable for soil classification or laboratory tests. In situ geotechnical tests are examples of local explorations and provide results regarding physical and mechanical soil properties (Lee et al. 1983). Sample disturbance is common with local explorations, potentially affecting the accuracy of the resulting properties. Laboratory tests generally provide results that have a greater theoretical basis and are sometimes easier to incorporate into design relationships. However, such tests do not always accurately simulate the stresses and in situ soil conditions (Becker 2001).

Local explorative methods are more common in typical site investigations (Lee et al. 1983). Such methods include the standard penetration test, the cone penetration test and the dilatometer (Becker 2001). One of the most developed and most frequently used laboratory tests is the triaxial test, which uses samples obtained from local explorations (Lee et al. 1983). The triaxial test is the most common shear strength test that is suitable for most types of soils (Craig 1997). The test simulates the in-situ stresses using a cell pressure in a triaxial cell, as illustrated in Figure 2-1. Several parameters are measured due to an increasing axial load, including the increase in cell pressure, sample strain and increase in pore water pressure. Such measures provide a means to estimate soil properties such as the shear strength ( $s_u$ ) and elastic modulus ( $E$ ). One of the advantages of the triaxial test is the ability to control drainage conditions (Bowles 1997).

The standard penetration test (SPT) uses a split spoon sampler, as shown in Figure 2-2, which is driven into soil to a depth of 450 mm (Craig 1997). The standard penetration resistance number,  $N$ , is a measure of the number of blows required to drive the sampler 300 mm (Lee et al. 1983, Bowles 1997, Craig 1997, Becker 2001). The SPT has the unique advantage over other in situ or local explorative methods in that it produces a sample, from which other physical properties may be obtained (Becker 2001). Several empirical correlations exist relating the elastic modulus ( $E$ ), shear strength ( $s_u$ ), angle of friction ( $\phi$ ) and unconfined compression strength ( $q_u$ ) to the SPT  $N$  value (Bowles 1997). Similar correlations also exist between the SPT  $N$  value and the settlement of foundations or the required footing size to meet specific design criteria (Holtz 1991, Small 2001).



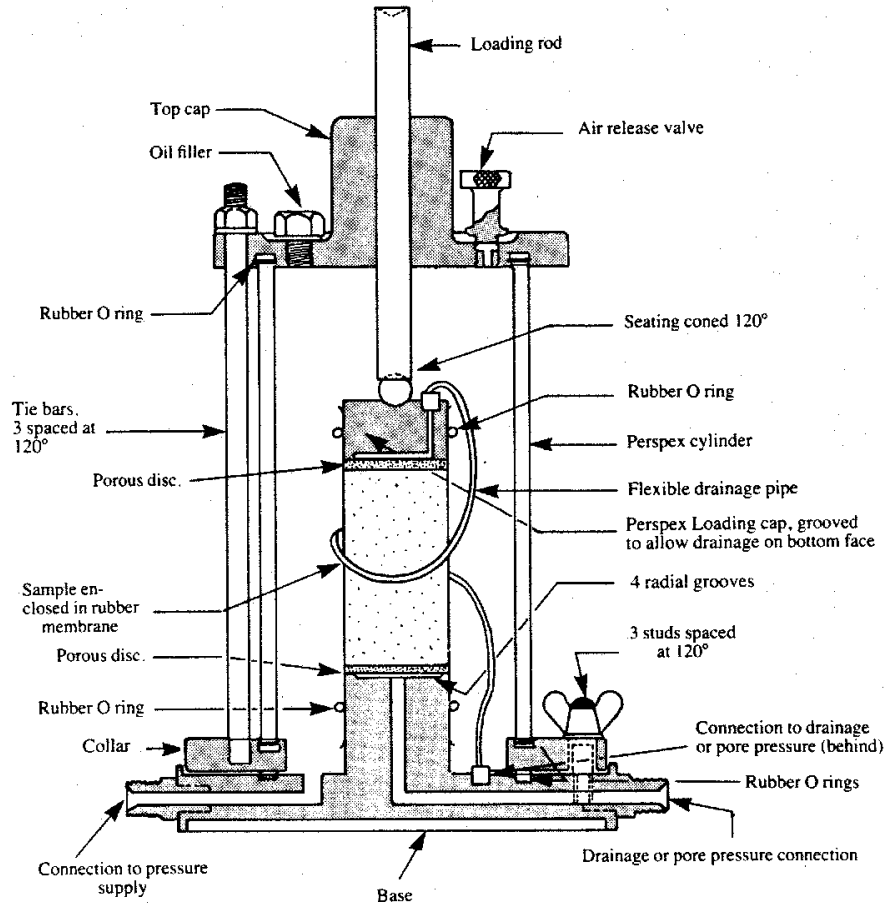


**Figure 2-1 Typical triaxial cell**  
After Craig (Craig 1997)

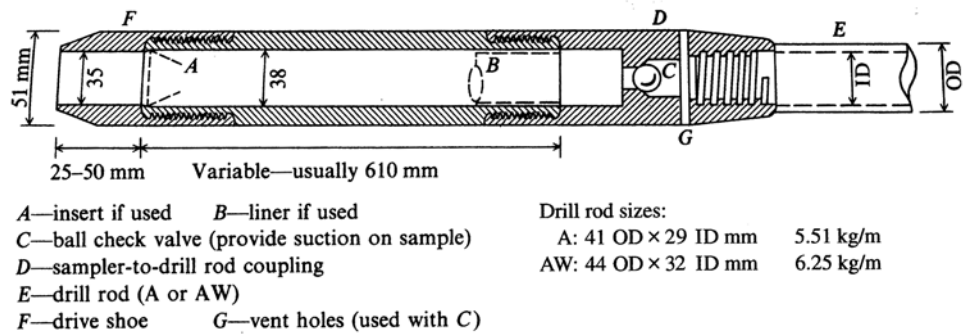


**Figure 2-2 Schematic of split spoon sampler in a standard penetration test**  
After Bowles (1997)

The cone penetration test (CPT) follows a similar procedure to the SPT but does not typically provide a soil sample (Becker 2001). The procedure was developed in Holland in 1965 (Lunne et al. 1986) and comprises a 60° cone at the end of the shaft, as shown in Figure 2-3. The CPT provides a continuous representation of the soil, which yields a distinct

advantage over the standard penetration and flat plate dilatometer tests (Becker 2001). The cone tip resistance,  $q_c$ , and the sleeve friction,  $f_s$ , are correlated to provide an estimate of the shear strength ( $s_u$ ) of the soil (Lunne et al. 1986). Correlations between  $q_c$  and  $f_s$  also exist for the over-consolidation ratio (OCR), angle of friction ( $\phi$ ), elastic modulus ( $E$ ) and the standard penetration  $N$  count (Bowles 1997). The CPT has also been commonly used to estimate the statistical properties of soils because it yields a relatively continuous vertical data sample (Jaksa 1995, Akkaya and Vanmarcke 2003, Kulatilake and Um 2003).

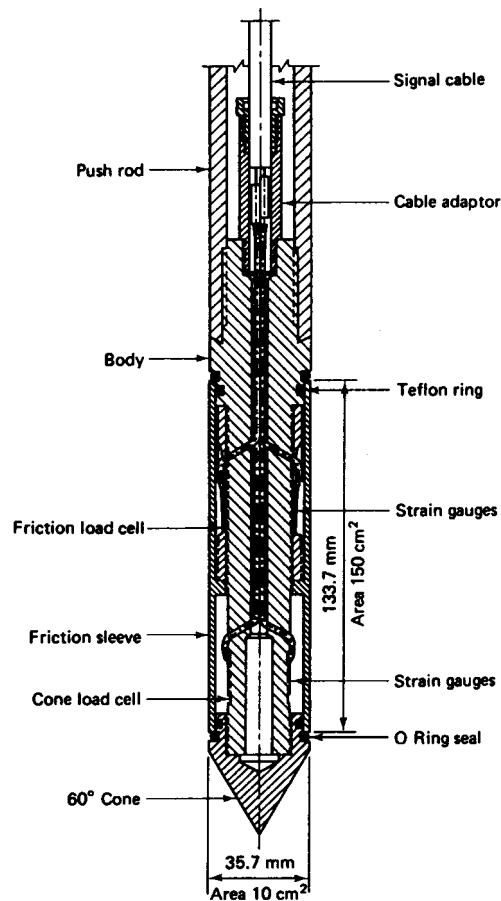


**Figure 2-3 Schematic of the cone penetrometer**  
After Holtz and Kovacs (1981)

The flat plate dilatometer test (DMT) was introduced by Marchetti (1980) and Marchetti and Crapps (1981) and involves pushing a flat plate into the soil and inflating a steel membrane. The arrangement of the flat plate dilatometer is shown in Figure 2-4. The pressure required to inflate the membrane is correlated to soil properties such as the in situ horizontal stress, over-consolidation ratio (OCR), deformation modulus ( $E$ ) and undrained shear strength ( $s_u$ ) (Becker 2001). The DMT is another example of a discrete sampling method, where samples are recorded at discrete depth intervals.

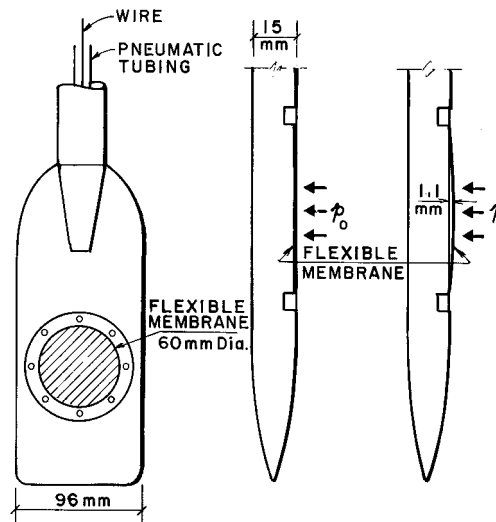


**Figure 2-4 Schematic of the flat plate dilatometer**  
After Marchetti (1980)

The number of samples required in a site investigation is covered by codes in some countries, yet these generally provide direction that only relates to the minimum scope. The Austroads Bridge Design Code (AUSTROADS 1992) recommended that boreholes or test pits should be located every 30 m, and Taiwan's Building Design Code (Moh 2004) recommended that 1 borehole should be drilled every 600 m<sup>2</sup> of site area or 300 m<sup>2</sup> of building area, with a minimum of 2 boreholes being drilled. In the main, however, codes provide little assistance regarding the required scope of an investigation. In fact, countries like Singapore and Malaysia do not have a code or regulation specific to site investigation (Moh 2004). Therefore, it appears that the scope of a site investigation is typically based on budget and time constraints placed on the project (Jaksa et al. 2003).

It is also common that sampling is arranged in patterns to improve the coverage of the site. Ferguson (1992) compared several such sampling patterns and the likelihood they would intercept a known land contamination. Although the regular grid pattern appears to be the most common, it was not found to be the most efficient. Instead, the results indicated that the Herringbone sampling pattern (Figure 2-5) was the most likely to intercept land contamination occupying 5% of the total site area. As an example, with 30 sample locations, the Herringbone pattern showed a 95% probability of intercepting the contamination, whereas the regular grid pattern yielded only a 70% probability of finding the same contamination. A summary of the common sampling patterns described by Ferguson (1992), indicating their popularity and ability to intercept a contamination of unknown extent or location, is shown in Table 2-1. The popular patterns are illustrated in Figure 2-6.

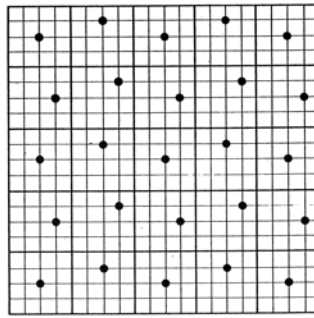


**Figure 2-5 Herringbone sampling pattern**  
After Ferguson (1992)

**Table 2-1 Recommendations for varying site investigation plans**  
After Ferguson (1992)

Source	Random	Regular	Strat. Rand.	Strat. S.U.	W/X Patterns	Comments
Waterhouse (1980)	x	✓	x	x	x	
Bell et al. (1983)	♦	✓	x	x	♦	Regular "perhaps best"
Smith and Ellis (1986)	x	✓	x	x	x	
Department of the Environment / National Water Council (1986)	♦	♦	✓	x	♦	Very confusing account
Interdepartmental Committee for the Redevelopment of Contaminated Land (1987)	♦	✓	x	x	x	Regular preferred for practical reasons
Bridges (1987)	♦	✓	♦	x	♦	
Lord (1987)	♦	✓	♦	x	♦	
British Standards Institution (1988)	x	♦	✓	x	x	Regular "appropriate but not free of bias"
Department of the Environment (1988)	x	✓	x	x	x	

✓ = Recommended      ♦ = Mentioned      x = Not Mentioned

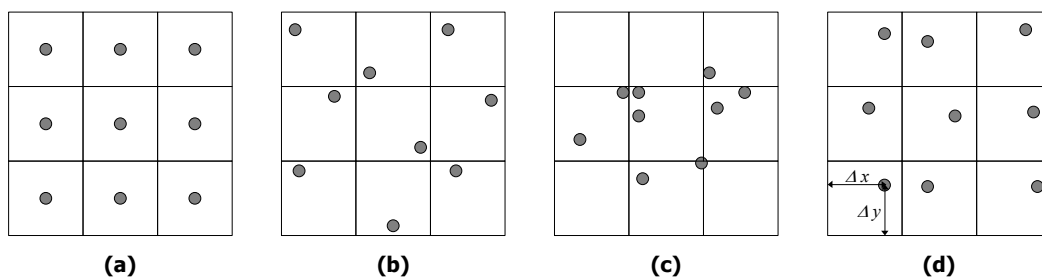


**Figure 2-6 Four different sampling designs: (a) regular (square); (b) stratified random; (c) simple random and (d) stratified systematic unaligned**  
After Ferguson (1992)

The W/X patterns, discussed by Bell et al. (1983), Department of the Environment / National Water Council (1986), Bridges (1987) and Lord (1987), involve locating samples in the outline plan shape of a figure W or X. Lord (1987) suggested that the efficiency of these patterns is likely to be limited.

The regular grid approach, shown in Figure 2-6(a), involves a sample location at the centre of regions that have been defined by subdividing the site investigation area. According to results shown in Table 2-1, this is the most common sampling pattern and is a form of systematic sampling (Baecher and Christian 2003). The stratified random pattern, shown in Figure 2-6(b), is a compromise between the simple random and regular grid patterns, where the site is subdivided into a discrete number of regions and a sample location is randomly selected for each region. This approach is relatively common and is recommended by two sources listed in Table 2-1. The simple random and stratified systematic unaligned patterns, shown in Figures 2-6(c) and (d), respectively, have not been recommended by any of the sources listed in Table 2-1. The stratified systematic unaligned pattern is similar to the Herringbone pattern discussed earlier. Both these patterns require a sufficient number of sample locations to make them distinctly different to the regular grid or stratified random patterns. Furthermore, the regular grid pattern only appears to be slightly less efficient than the Herringbone pattern, as discussed by Ferguson (1992).

### 2.2.2 Shallow Foundations

Shallow foundations are defined as having an embedment depth, which is less than the least characteristic dimension (Chen and McCarron 1991). Foundation types that fall into this category are:

- Pad or spread footings;
- Strip or combined footings; and
- Raft or mat footings.

A shallow foundation is required to meet 2 criteria; stability and serviceability (Bowles 1997, Small 2001). The stability criterion relates to the bearing capacity of the foundation, where it is designed to ensure that failure of the soil does not occur. The serviceability criterion ensures that the foundation and, therefore the structure, do not experience excessive total or differential settlements. The following sections present common procedures of analysing the bearing capacity and settlement of shallow foundations.

### 2.2.2.1 Bearing Capacity of Foundations

In the late 19<sup>th</sup> Century, the concept of bearing pressure in foundation design was introduced to investigate the excessive settlements occurring in buildings (Terzaghi and Peck 1967). However, it wasn't for another 50 years until Terzaghi (1943) developed an analytical bearing capacity equation, based on superposition. Terzaghi's equation is given by:

$$q_{av} = cN_c + \sigma'_n N_q + \frac{\gamma b}{2} N_\gamma \quad (2.1)$$

where  $q_{av}$  is the average pressure over the footing contact area,  $c$  and  $\gamma$  are the cohesion and unit weight of the soil, respectively,  $b$  is the footing width (or least plan dimension),  $\sigma'_n$  is the overburden pressure at the depth of the footing, and  $N_c$ ,  $N_q$ , and  $N_\gamma$  are all parameters that are dependent on the soil's angle of internal friction,  $\phi$ . Terzaghi's equation (2.1) is valid only for strip footings with a centrally applied vertical load (Chen and McCarron 1991).

The bearing capacity factors ( $N_c$ ,  $N_q$ , and  $N_\gamma$ ) have been evaluated by numerous authors (e.g. Terzaghi 1943, Taylor 1948, Meyerhof 1951, Hansen 1961, Sokolovskii 1965, Hansen 1970, Chen 1975) who have used either slip-line, limit equilibrium or limit analysis methods that yield upper- or lower-bound solutions. Moreover, additional correction factors are required for footings of various shapes and with different loading and embedment characteristics. Such factors have been previously calculated by Meyerhof (1963), Hansen (1970) and Chen (1975).

Chen and McCarron (1991) believed that the values of the  $N_c$  and  $N_q$  factors, given by Meyerhof (1951) and Hansen (1961, 1970), are typically accepted as the correct values. Notwithstanding, there is a large range of possible  $N_\gamma$  values. More recently, conventional finite element analyses (Griffiths 1982, Burd and Frydman 1997) and numerical limit analysis methods (Lyamin and Sloan 2002a, Lyamin and Sloan 2002b) have been used to predict the upper- and lower-bounds of bearing capacity. These techniques have reduced the subjectivity and empiricism associated with the bearing capacity factors.

Corrections to the bearing capacity equations are also required for water table location (Small 2001) and the friction angle of the soil obtained using the triaxial test (Meyerhof 1963). Because of the different bearing capacity factors and correction factors, Bowles (1997) suggested a use for the more common solutions, summarised in Table 2-2. How-

ever, he also indicated that more than one solution should be predicted to allow verification.

**Table 2-2 Suggested uses for bearing capacity equations**  
After Bowles (1997)

Method	Recommended for
Terzaghi (1943)	Very cohesive soils where $D/B \leq 1$ or for a quick estimate of $q_{ult}$ to compare with other methods. Do not use for footings with moments and/or horizontal forces or for tilted bases and/or sloping ground.
Hansen (1970), Meyerhof (1963) and Vesic (1973)	Any situation that applies, depending on user preference or familiarity with a particular method.
Hansen (1970) and Vesic (1973)	When base is tilted; when footing is on a slope or when $D/B > 1$ .

The typical bearing capacity equations, given in Equation (2.1), require knowledge of specific soil properties. Alternatively, Bowles (1997) discussed several procedures that yield estimates of the bearing capacity of a soil directly from in situ test results. Both Meyerhof (1956, 1974) and Terzaghi and Peck (1967) were able to determine correlations between the standard penetration  $N$  value and the ultimate bearing capacity of a foundation. The results of the cone penetration test do not appear to have any direct correlation with bearing capacity. Nevertheless, Schmertmann (1978) suggested the cone tip resistance could be correlated to the  $N_q$  and  $N_\gamma$  factors used in Equation (2.1) and Meyerhof (1956) suggested the cone tip resistance could be correlated with the SPT  $N$  value to be used in the methods described above.

The ultimate bearing capacity is typically factored to yield an allowable bearing capacity,  $q_a$ , given by:

$$q_a = \frac{q_{ult}}{FOS} \quad (2.2)$$

where  $q_{ult}$  is the ultimate bearing capacity determined by Equation (2.1) and  $FOS$  is an appropriate factor of safety. Furthermore, the net allowable bearing capacity,  $q_{a_{net}}$ , which accounts for the overburden pressure,  $\sigma'_n$ , is given by:

$$q_{a_{net}} = \frac{q_{ult} - \sigma'_n}{FOS} \quad (2.3)$$

Bowles (1997) suggested that the value of the factor of safety, *FOS*, is typically a function of the type of soil, reliability of the soil properties, use of the structure and overall conservatism of the designer. Phoon et al. (1995) indicated that a *FOS* of 3 is not uncommon. Further discussion regarding the factor of safety have been reserved for later in this chapter.

### 2.2.2.2 Serviceability of Foundations

Bowles (1997) considered settlement estimates of a foundation as a best guess of the footing deformation after a load has been applied. Such estimates are significantly affected by the selection of deformation properties that are representative of the soil variability and level of loading. Holtz (1991) observed that the design of a shallow foundation is typically governed by a limiting settlement criterion and Bowles (1997) noted that most structural distress is caused by excessive settlements and not the shear failures associated with bearing capacity. Settlement occurs in three stages: immediate or distortion; consolidation; and secondary compression settlement (Holtz 1991). A summary of the relative importance of each type of settlement for sands, clays and organic soils is shown in Table 2-3.

**Table 2-3 Relative importance of immediate, consolidation and secondary settlement for different soil types**  
After Holtz (1991)

Soil Type	Immediate Settlement	Consolidation Settlement	Secondary Compression
Sand	Yes	No	No
Clay	Possibly	Yes	Possibly
Organic soil	Possibly (Yes)	Possibly (No)	Yes

Bowles (1997) observed that it is common to treat the material as pseudo-elastic, where the soil properties of concern are either elastic modulus,  $E$ , and Poisson's ratio,  $\nu$ , or shear-strain modulus,  $G$ , and bulk modulus,  $k$ , or the modulus of subgrade reaction,  $k_s$ . Small (2001) suggested that it is generally acceptable to assume elastic behaviour, as the working loads are typically lower than those governing the bearing capacity of the foundation. This is because settlement is typically estimated after the foundation has been designed for bearing capacity (Holtz 1991). However, Small (2001) warned that the adopted elastic modulus must be appropriate for the stress range in the soil.



The general form of most equations used to estimate the settlement of a foundation is given by (Bowles 1997):

$$\delta = \int_0^H \varepsilon dH \quad (2.4)$$

where  $\delta$  is the settlement,  $H$  is the estimated depth of stress change in the layer in question and  $\varepsilon$  is the strain given by:

$$\varepsilon = \frac{\Delta q}{E} \quad (2.5)$$

where  $\Delta q$  is the change in stress at depth,  $H$ . The change in stress,  $\Delta q$ , is a function of  $H$  and the applied footing pressure, while  $E$  is a function of  $H$  and the uncertainty due to soil variability, statistical, measurement and transformation model error, all of which are discussed later in this chapter. Bowles (1997) suggested that the term elastic modulus is not strictly correct as soil is not an elastic medium, even though, the elastic modulus is the most common term used for this parameter and hence has been adopted in this research.

Several methods have been developed to estimate the stress increase,  $\Delta q$ , at any depth below the surface and have been described by several authors (e.g. United States Army Corp of Engineers 1990, Holtz 1991, Bowles 1997). The 2:1 method is a simple application where the stress decreases linearly with depth at a rate of 2:1. The *Newmark* (Newmark 1935) and *Westergaard* (Westergaard 1938) methods are integration techniques of the Boussinesq (ca. 1885) equation, which estimate the stress increase due to a point load on the surface of a semi-infinite, homogeneous, isotropic, weightless, elastic half-space (Bowles 1997). The 2:1 equation is an approximation of:

$$q_z = \Delta q = \frac{3q}{2\pi z^2} \cos^5 \omega \quad (2.6)$$

where  $q$  is the applied stress on the footing,  $z$  is any depth in the soil and  $\omega$  is the angle representing the rate of stress decrease with depth. This angle,  $\omega$ , is equal to 60° for the 2:1 case. The Newmark and Westergaard methods are respectively given by:

$$q_z = \Delta q = q \frac{1}{4\pi} \left[ \frac{2MN_0\sqrt{V}}{V+V_1} \frac{V+1}{V} + \tan^{-1} \left( \frac{2MN_0\sqrt{V}}{V-V_1} \right) \right] \quad (2.7)$$

and

$$q_z = \Delta q = \frac{q}{2\pi} \tan^{-1} \left( \frac{MN_0}{\sqrt{a}(M^2 + N_0^2 + a)^{1/2}} \right) \quad (2.8)$$

where  $q$  is the applied stress on the footing and  $L, B, M, N_0, V, V_1$  and  $a$  are all functions of the footing size, depth of the soil layer and Poisson's ratio. Although the Westergaard equation incorporates Poisson's ratio, Bowles (1997) believed that the Newmark method is better suited to estimating stress distributions.

Additional methods have been used to estimate the immediate settlement under the corner of a footing (Harr 1966, Perloff 1975, Mayne and Poulos 1999). These methods have the general form:

$$\delta = \frac{qbI_p(1-\nu^2)}{E} \quad (2.9)$$

where the settlement,  $\delta$ , is a function of the applied stress,  $q$ , the width of the footing,  $b$ , Poisson's ratio,  $\nu$ , elastic modulus,  $E$ , and an influence factor,  $I_p$ , dependent on the size of the footing and the depth of the soil layer. These techniques have a similar advantage to the Westergaard method described above, where the lateral and axial strains are accounted for through the inclusion of Poisson's ratio,  $\nu$ . Furthermore, they can also be used to estimate both short and long term settlement by selecting appropriate values of  $E$  and  $\nu$ . The influence factor,  $I_p$ , shown in Equation (2.9), varies between authors and is usually a function of the footing size, depth of the soil, footing embedment depth, and the rigidity of the foundation. Timoshenko and Goodier (1951) also proposed a similar relationship described by Bowles (1997) and given by:

$$\delta = qb' \frac{(1-\nu^2)}{E} \left( I_1 + \frac{1-2\nu}{1-\nu} I_2 \right) I_F \quad (2.10)$$

where  $b'$  is the effective width of the footing,  $I_1$  and  $I_2$  are influence factors, as given by:

$$I_1 = \frac{1}{\pi} \left[ M \ln \frac{(1 + \sqrt{M^2 + 1}) \sqrt{M^2 + N_0^2}}{M(1 + \sqrt{M^2 + N_0^2 + 1})} + \ln \frac{(M + \sqrt{M^2 + 1}) \sqrt{1 + N_0^2}}{M + \sqrt{M^2 + N_0^2 + 1}} \right] \quad (2.11)$$

and

$$I_2 = \frac{N_0}{2\pi} \tan^{-1} \left( \frac{M}{N_0 \sqrt{M^2 + N_0^2 + 1}} \right) \quad (2.12)$$

where  $M$  is the ratio of footing length to width and  $N_0$  is the ratio of footing width to soil layer depth. The  $I_F$  correction factor accounts for footing embedment, which assumes a value of 1.0 when all footings are located at the surface of the soil.

Another relationship to estimate the elastic settlement of circular and rectangular foundations has been introduced by Janbu et al. (1956) and later discussed by Christian and Carrier III (1978). Akin to previous methods, the Janbu equation is given by:

$$\delta = \eta_0 \eta_1 \frac{qb}{E} \quad (2.13)$$

where  $\eta_0$  and  $\eta_1$  are correction factors to account for embedment and soil depths, respectively. The  $\eta_0$  correction factor, which accounts for embedment depth, has a value of 1.0 when the footing is located at the soil surface. However, the  $\eta_1$  correction factor is obtained from a series of charts with respect to the width and length of the footing, as well as the depth of the soil layer. Such charts, which were originally developed by Janbu et al. (1956) and later modified by Christian and Carrier III (1978), have been calibrated for a specific Poisson's ratio. Therefore, an analysis in a soil with a different Poisson's ratio requires recalibration.

Similar to the bearing capacity equations discussed above, there are several relationships that predict the settlement of a foundation based on test results. The technique introduced by Schmertmann (1970) is not directly based on the results of a particular geotechnical test. However, it was developed by calibrating measured footing settlements with an elastic modulus determined from a series of cone penetration tests. This method utilises a strain influence factor,  $I_z$ , which varies with depth according to a triangular relationship. The soil is divided into  $n_l$  layers, in which the settlement of each layer is evaluated and then integrated to evaluate the total settlement. The depth of the analysis is determined by the size of the strain influence triangle and, in typical cases, is 2 times the least plan dimension of the footing. The total predicted settlement is estimated using the equation:

$$\delta = C_1 C_2 q \sum_{i=1}^{n_i} \frac{\Delta z_i}{E_i} I_{z_i} \tag{2.14}$$

where  $C_1$  and  $C_2$  are correction factors accounting for the depth of footing embedment and time related effects, respectively,  $q$  is the applied footing pressure, and  $\Delta z_i$ ,  $E_i$  and  $I_{z_i}$  are the depth, elastic modulus and strain influence factor value of the  $i$ th layer, respectively. The  $C_1$  correction factor for depth has a value of 1.0, when the footing is located at the soil surface, while the  $C_2$  value varies little around a value of 1.0, for different time conditions.

The original method proposed by Schmertmann (1970) suggested a strain influence triangle as shown in Figure 2-7(a), while a modified strain distribution, which accounts for the overburden pressure,  $\sigma'_n$ , was developed by Schmertmann et al. (1978) and is given in Figure 2-7(b). The modified strain distribution [Figure 2-7(b)] also accounts for plane strain and axisymmetric conditions, whereby the depth of the strain distribution changes. However, for square and rectangular footings, the distribution shown in Figure 2-7(b) is sufficient.

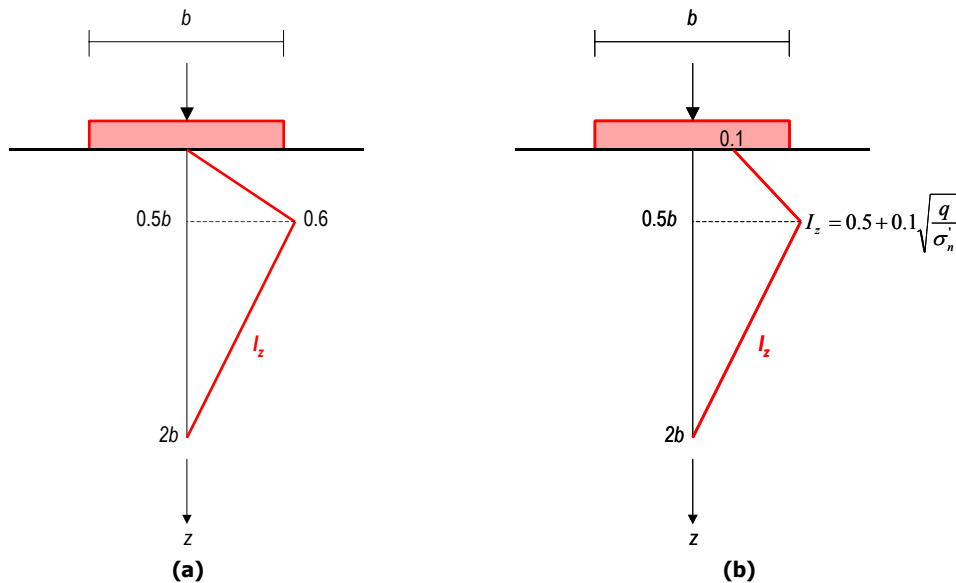


**Figure 2-7 Schmertmann's strain influence triangles: (a) 2B-0.6 triangle from Schmertmann (1970) and (b) modified triangle from Schmertmann et al. (1978)**

Small (2001) and Holtz (1991) both suggested that Schmertmann's method is only suitable for granular soils. However, Bowles (1997) recommended it for all soils and noted that it provides a good alternative settlement relationship. Westergaard (1979) observed that the Schmertmann 2B-0.6 technique predicted settlements 200% larger than the measured settlements of a bridge foundation on fine sand. Bowles (1997) also suggested that the

Schmertmann 2B-0.6 method is conservative in relatively uniform soils or when stiff material overlies a weaker stratum.

### 2.2.2.3 Use of Numerical Methods in Foundation Analysis

Numerical methods in foundation analysis have become increasingly popular with the development of computers (Cook et al. 1989). Such methods typically involve solving numerous simultaneous equations based on soil and structural mechanics. In keeping with traditional methods, numerical techniques predict footing response. The most widely used numerical method is Finite Element Analysis (FEA), which has been recognised as having sound mathematical foundation.

FEA is best described as a numerical procedure to analyse structures or continua (Cook et al. 1989). FEA can be traced back to 1906, when *lattice analogy* was introduced in stress analysis by Wieghardt (1906), Riedel (1927), Hrennikoff (1941) and Ergatoudis et al. (1968).

There are several examples of FEA in geotechnical engineering applications (Baecher and Ingra 1981, Righetti and Harrop Williams 1988, Booker et al. 1989, Smith and Griffiths 2004). FEA is able to suitably predict settlements in linear elastic media, yet in non-linear mediums the analysis becomes more complex. This renders bearing capacity analyses far more complex and, therefore, not as common as serviceability analyses. Three-dimensional FEA in geotechnical applications is also restricted by the large global stiffness matrices (Smith and Griffiths 2004). As such, Smith and Griffiths (2004) have developed a preconditioned iterative conjugate gradient solver to negate the need for a global stiffness matrix. It was first introduced by Griffiths and Smith (1991) and later addressed by Jennings and McKeown (1992).

The use of finite elements to analyse the bearing capacity of a foundation is not common, especially in three dimensions. Problems occur when a region of soil reaches failure and the adjacent regions are required to take additional load (Griffiths and Fenton 2000). This is difficult to model, although, Griffiths and Fenton (2000) simulated this behaviour for a slope stability problem. They assumed an elastic perfectly plastic stress-strain curve to investigate the sensitivity of the factor of safety of a slope, due to soil variability. A reduced integration method was used for both the stiffness and stress redistribution to allow for failed sections of the slope to regain strength from adjacent sections. Figure 2-8 shows the result of the analysis, where darker zones indicate regions of weak soil.

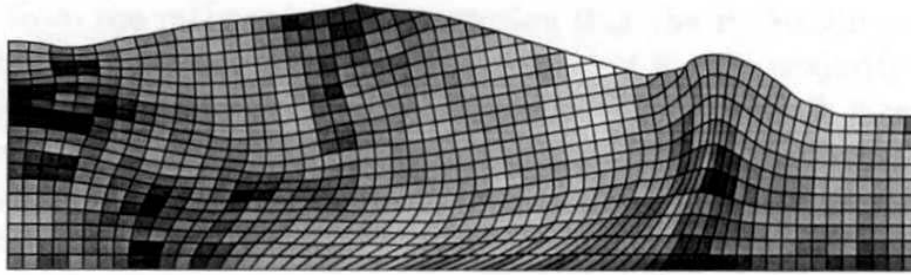


**Figure 2-8 Result of the FEA of a clay slope**  
After Griffiths and Fenton (2000)

Griffiths et al. (2002a) also investigated the bearing capacity of a rough and rigid strip footing using FEA. Similar to the slope stability problem, an elastic perfectly plastic Tresca yield criterion was assumed for the analysis. Griffiths et al. (2002a) noted a finer mesh near the footing is preferred in this type of analysis due to the back computation of the footing load. However, a uniform mesh was used to simplify the generation of the random field and the mapping of the cohesion value. Figure 2-9 presents the resulting deformations associated with bearing capacity of the strip footing.

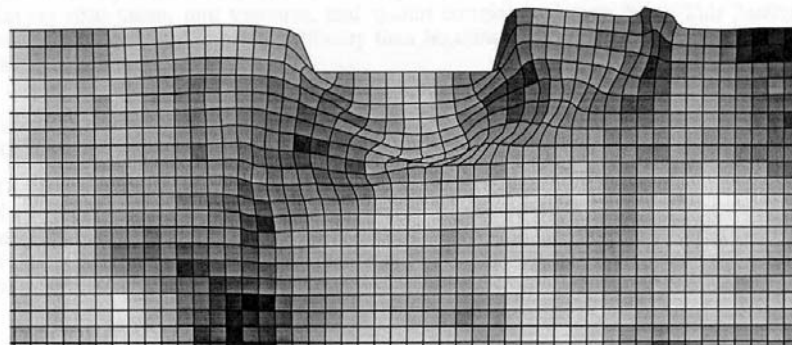


**Figure 2-9 Result of the FEA of the bearing capacity of a rigid strip footing**  
After Griffiths et al. (2002a)

There are several examples of FEA used to predict foundation settlement. Righetti and Harrop-Williams (1988) investigated the settlement of a soil due to a single point load applied on a soil represented by a random field (random fields are discussed later in this chapter). They used properties of the random field to manipulate the finite element equations. This provided a direct method to measure the reliability of a foundation design through FEA. However, Righetti and Harrop-Williams (1988) warned of restrictions due to the discretisation of the original medium. They also investigated stresses in the soil as a

result of the strains. However, only scenarios that produce small strains should be considered if the stresses are to be estimated with some degree of confidence.

Fenton et al. (2003) also used FEA to investigate foundation settlement on a spatially random soil represented by a random field. FEA settlement was compared to settlement from the Janbu equation to observe errors in the method. Using linear elastic theory, the analysis was undertaken in two dimensions. Studies investigating the reliability of footing settlement through FEA have also been undertaken by Fenton et al. (1996) and Fenton and Griffiths (2002) in two-dimensions, and Fenton and Griffiths (2005) in three-dimensions.

#### 2.2.2.4 Design Criteria for Foundations

The procedures described above have suggested means to predict the settlement of a footing or foundation based on the theory of elasticity. However, in a design situation, the footing size is varied to ensure that the bearing capacity of the footing is less than the applied load and that excessive settlements are not allowed or occur. The bearing capacity criterion is relatively straightforward, where the allowable bearing pressure must be greater than the applied load. Means to estimate the allowable bearing capacity have been discussed earlier in this chapter. On the other hand, the settlement criterion varies between different projects and involves both total and differential settlement. Bowles (1997) suggested that differential settlements are the major cause of structural distress and therefore should be controlled by the designer. However, Day (1999) commented that the total settlement of a foundation can have serious effects on the use of the structure being supported. For example, a building that settles 100 mm will have serious impacts on the building services as well as problems for access to the building itself. As such, it is important to consider both total and differential settlements alike.

The Australian Standard for Bridge Design (AS5100, 2004) recommended that the limits adopted for total and differential settlement should be adequate so that the structure being supported is not detrimentally affected. Bowles (1997) provided a summary of research conducted by MacDonald and Skempton (1955) and Wahls (1981) on the tolerable settlements of buildings, with results shown in Table 2-4. A more comprehensive analysis of tolerable settlements for building types and limiting criteria was given by Sowers (1962) and is shown in Table 2-5.

**Table 2-4 Tolerable settlement of buildings in millimetres**

Recommended maximum values in parenthesis  
After Bowles (1997)

Criterion	Isolated foundations	Rafts
Angular distortion (cracking)		1/300
Greatest differential settlement		
Clays		45 (35)
Sands		32 (35)
Maximum settlement		
Clays	75	75 – 125 (65 – 100)
Sands	50	50 – 75 (35 – 65)

**Table 2-5 Summary of Allowable Settlements for Different Buildings and Limiting Criteria**

After Sowers (1962)

Type of movement	Limiting factor	Maximum settlement	
Total settlement	Drainage	15 – 30 cm	
	Access	30 – 60 cm	
	Probability of non-uniform settlement:		
	Masonry-walled structure	2.5 – 5 cm	
	Framed structures	5 – 10 cm	
	Smokestacks, silos, mats	8 – 30 cm	
Tilting	Stability against overturning	Depends on $H_b$ and $W_b$	
	Tilting of smokestacks, towers	$0.004Z$	
	Rolling of trucks, etc.	$0.01Z$	
	Stacking of goods	$0.01Z$	
	Machine operation – cotton loom	$0.003Z$	
	Machine operation – turbogenerator	$0.0002Z$	
	Crane rails	$0.003Z$	
	Drainage of floors	$0.01 - 0.02Z$	
	Differential movement	High continuous brick walls	$0.0005 - 0.001Z$
		One-story brick mill building, wall cracking	$0.001 - 0.002Z$
Plaster cracking (gypsum)		$0.001Z$	
Reinforced-concrete building frame		$0.0025 - 0.004Z$	
Reinforced-concrete building curtain walls		$0.003Z$	
Steel frame, continuous		$0.002Z$	
	Simple steel frame	$0.005Z$	

**Notes:**

$Z$  = distance between adjacent columns that settle different amounts, or between any two points that settle differently. Higher values are for regular settlements and more tolerant structures. Lower values are for irregular settlement and critical structures.  $H_b$  = height and  $W_b$  = width of structure.

Based on the results shown in Tables 2-4 and 2-5, a tolerable settlement appears to be in the order of 25 mm to 75 mm, depending on the type of structure and soil. A tolerable differential settlement of approximately 0.0025 m/m – 0.004 m/m has been suggested by Sowers (1962) from the results shown in Table 2-5 based on a reinforced concrete struc-



ture. Day (1999) also indicated that total and differential settlements within these limits are suitable. Polshin and Tokar (1957) suggested slightly larger maximum tolerable settlements of up to 150 mm for buildings with masonry or reinforced concrete walls.

### 2.2.3 Raft Foundations

A raft or mat foundation is generally required when applied loads are large and pad foundations yield excessive settlements. Rafts distribute the applied loads to reduce the pressure applied to the soil. Although this improves the bearing capacity of the foundation, the total and differential settlements become the governing criteria. A detailed structural design is usually required, dealing with the thickness of the slab and steel reinforcing necessary to resist excessive bending and shear.

Numerical methods like FEA are excellent means for estimating the predicted settlement of a raft. There are, however, several simplified methods that do not require such numerical procedures. In these methods it is important that the actual stiffness of the raft is considered (Small 2001). Small (2001) also warned that analyses representing the raft as a *Winkler* foundation do not represent the true behaviour of the soil and the analysis using an elastic continuum is not site specific. The Winkler foundation idealises the interface between the raft structure and the soil as a series of springs with nominated stiffness.

Kay and Cavagnaro (1982) published a series of charts to predict the settlement of a raft with varying soil types. Similar charts have also been developed by Booker and Small (1983) for circular rafts, and Fraser and Wardle (1976) for rectangular rafts. It should be noted, however, that these charts have typically been developed or calibrated using numerical solutions (Small 2001). The method introduced by Fraser and Wardle (1976) incorporates the rigidity of the raft relative to the underlying soil stiffness. A series of charts are used to determine the required rigidity of the raft to satisfy settlement criteria at the corner, centre and edges of the raft. Additional complexities are introduced into the method when dealing with layered soils or soils of finite depth.

There are also several numerical methods that have been employed to analyse the response of raft foundations. Bowles (1997) discussed a few of these methods, where a detailed discussion was made regarding the Finite Difference Method (FDM), which is similar to finite element analyses, but is not as computationally rigorous. The finite element method has also been used to model raft response. However, finite element analyses suffer from numerically exhaustive computations and run times.

#### 2.2.4 Piled Foundations

Foundation designs discussed thus far have dealt solely with shallow foundations, where the embedment depth is less than the least characteristic dimension of the footing. Deep foundations, on the other hand, transfer loads to underlying bedrock or suitable bearing strata at much greater depths (Poulos 2001). The ultimate load capacity of a pile is a combination of the ultimate shaft capacity, ultimate base capacity and the weight of the pile. The ultimate base capacity is typically determined using bearing capacity theory, while the ultimate shaft resistance is a function of the ultimate shaft friction and the perimeter of the pile. Fellenius (1991) discussed shaft resistance as introduced by Johannessen and Bjerrum (1965) and Burland (1973). Tomlinson (1971) introduced an adhesion factor when dealing with the undrained pile capacity in saturated clays. This is called the  $\alpha$  method (Bowles 1997). The adhesion factor is used in the shaft resistance calculation and was empirically derived by Tomlinson (1971) and others (e.g. Stas and Kulhawy 1984, Kulhawy and Phoon 1993). Other means of estimating the shaft resistance of piles includes the  $\lambda$  (Vijayvergiya and Focht Jnr. 1972) and  $\beta$ -methods (Burland 1973).

The settlement of piles is commonly analysed using the load transfer or  $t$ - $z$  method (Poulos 2001). This method provides a series of curves relating the local load transfer to the displacement of the pile. Although the curves were originally derived empirically, Kraft et al. (1981) and Randolph (1994) have been able to derive them theoretically. Other methods that have been employed to estimate the settlement of a pile include idealising the soil as an elastic continuum (Butterfield and Banerjee 1971, Banerjee and Davies 1977, Poulos and Davis 1980), as well as using numerical analyses (Jardine et al. 1986, Trochanis et al. 1991). Poulos (2001) conducted a critical evaluation of the methods used to investigate the settlement of piles when acting as a group. He suggested that the settlement ratio, equivalent raft and equivalent pier methods are adequate methods that do not require complex calculations. Although both the settlement ratio and the equivalent raft (Tomlinson 1986) methods give satisfactory results (Poulos 1993), Poulos (2001) noted some distinct advantages with the equivalent pier method (Poulos and Davis 1980).

#### 2.2.5 Summary

Bowles (1997) summarised the minimum requirement for a foundation design process into five steps:

1. Locate the site and position of the load;

2. Inspect the site for any anomalies that may affect the design;
3. Plan and implement a field exploration program;
4. Determine necessary soil parameters for the design; and
5. Design an economic foundation based on the soil parameters obtained in steps 3 and 4.

Although the 5 steps above appear straightforward, Bowles (1997) also warned that two foundations will seldom be the same, due to the heterogeneous nature of soil. This influence and those from other sources of uncertainty are discussed in the next section.

---

## **2.3 UNCERTAINTIES IN GEOTECHNICAL ENGINEERING**

---

The design of a foundation, as discussed in the previous section, is prone to significant uncertainties. Many such uncertainties are related to the estimation of suitable soil properties for use in the design relationships discussed above. The following sections identify the many sources of uncertainty inherent in the design process and also describe the methods used to quantify such uncertainties.

### **2.3.1 Sources of Uncertainty for Soil Properties**

Vanmarcke (1977a, 1977b) suggested that three main sources of uncertainty exist in the estimation of suitable soil properties. These are due to inherent soil variability, statistical uncertainty due to limited sampling, and measurement uncertainties due to associated geotechnical testing errors. Filippas et al. (1988) also categorised uncertainties in a geotechnical system into 3 main components:

1. Inherent soil variability;
2. Measurement error; and
3. Transformation model uncertainty.

In addition, Kulhawy (1992) suggested statistical uncertainty, or sampling error, as introduced by Vanmarcke (1977a, 1977b), which results from limited information about the site. This component of uncertainty can be included with measurement error and is minimised through additional sampling (Vanmarcke 1977a, Vanmarcke 1977b, Phoon et al.

1995). Whitman (2000) adopted a simpler explanation, where the uncertainties due to soil variability and random testing errors contribute to data scatter, while the statistical uncertainty and bias in testing error contribute to systematic errors. Kulhawy and Phoon (2002) have also indicated that soil variability and measurement error have an impact on data scatter, as shown in Figure 2-10, which indicates the stages at which each source of uncertainty affects the estimation of a soil property.

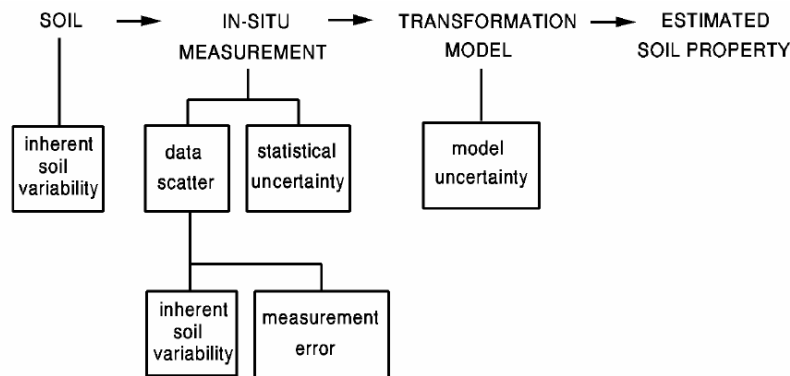


**Figure 2-10 Effects of uncertainties on the estimate of a soil property**  
After Kulhawy (1992)

A slightly different approach to separating the sources of uncertainty has been adopted by Baecher and Christian (2003), who considered the sources to be:

1. Natural variability;
2. Knowledge uncertainty; and
3. Decision model uncertainty.

Essentially the first two sources identified by Baecher and Christian (2003) are equivalent to the sources identified by Kulhawy (1992), where natural and inherent soil variability are the same, and uncertainties due to measurement and transformation model error are equivalent to knowledge uncertainty. Furthermore, Baecher and Christian (2003) categorised knowledge uncertainty into effects dealing with site characterisation, model and parameter uncertainty. Site characterisation uncertainty accounts for both measurement errors and statistical uncertainty, as described by Filippas et al. (1988) and Kulhawy (1992), respectively, while model and parameter uncertainty matches well with transformation model error. The additional source of uncertainty identified by Baecher and Christian (2003), due to decision models, is a function of the decisions an engineer or client makes

regarding conservatism, as well as effects during construction. Such uncertainties are usually due to economic and temporal considerations.

The following sections identify the three sources of uncertainty defined by Filippas et al. (1988), as well as the statistical uncertainty discussed by Kulhawy (1992). Some evidence regarding the magnitude of each source of uncertainty has been quantified. However, in general, the discussion in the following sections deals with the manner in which the uncertainties are best quantified.

### 2.3.2 Inherent Soil Variability

Unlike many civil engineering media, soils are inherently variable, where properties may be significantly different from one location to another. Even when soils are considered reasonably *homogeneous*, soil properties exhibit considerable variability (Vanmarcke 1977a). This variability is due to the complex and varied physical phenomena experienced during their formation (Jaksa 1995). Variability between soil properties is called *spatial variability* and has recently been modelled as a random variable (Spry et al. 1988).

#### 2.3.2.1 Property Randomness

Properties of a soil are suitably represented by a mean trend and a random residual (Spry et al. 1988). As such, the in situ soil property at any depth,  $\xi(z)$ , can be represented by two additive components as given by Brockwell and Davis (1987):

$$\xi(z) = t(z) + w(z) \quad (2.15)$$

where  $t(z)$  is a smoothly varying trend and  $w(z)$  is the fluctuating residual. If sufficient data are available to fit a tractable deterministic function to  $t(z)$ , so that it completely describes  $\xi(z)$ , there is little benefit in analysing the residual,  $w(z)$ . However, in most geotechnical engineering scenarios, there is insufficient data to achieve this (Spry et al. 1988). Therefore, a mathematically tractable function is commonly fitted to the in situ soil property data to best represent the trend. This process is termed detrending, and is necessary for a successful and meaningful statistical analysis (Jaksa 1995). However, Spry et al. (1988) and Fenton (1999) warned that a trend should only be removed if it has physical meaning, akin to the increase of shear strength with depth.

Once the data is detrended, the remaining residual,  $w(z)$ , is modelled as a *stationary* process or field. Vanmarcke (1983) suggested that such modelling is a rational means of quantifying the variability and there is usually economic benefit because it allows the investigation of geotechnical reliability. A random process or field is considered *stationary* if (Brockwell and Davis 1987):

1. The mean is independent of location (no trend exists in the data);
2. The variance is independent of location (homoscedastic);
3. There are no seasonal variations; and
4. There are no irregular fluctuations.

Furthermore, a process or field is also considered to be second-order stationary (also known as *weak stationarity*) if the mean is constant and the correlation between samples is dependent only on the lag between them and not their location (Chatfield 1975, Brockwell and Davis 1987). Vanmarcke (1983) embraced the terminology of *statistical homogeneity* to describe a two- or three-dimensional field that satisfies weak stationarity. However, stationarity is preferred in this thesis to avoid confusion with the use of the term *homogeneous*, which is used in deterministic analyses to describe a soil with uniform properties.

Probabilistic modelling of soils, as defined by Vanmarcke (1977a), involves undertaking a statistical analysis of the residual,  $w(z)$ , shown in Equation (2.15). If the residual is represented by a random variable,  $X$ , then the first two statistical moments of the distribution of the residual are the mean,  $\mu_x$ , given by:

$$\mu_x = E[X] \tag{2.16}$$

and the variance,  $\sigma_x^2$ , given by:

$$\sigma_x^2 = \text{Var}[X] \tag{2.17}$$

In the case of a random field, where each location is defined by its own random variable, it is important to consider the relationship between these two variables. The main descriptor of linear dependence between two random variables,  $X$  and  $Y$ , separated by  $\tau$ , is the covariance,  $\beta_\tau$ , given by:

$$\beta_{\tau} = \text{Cov}[X, Y] = E[XY] - E[X]E[Y] \quad (2.18)$$

In most geotechnical applications the separation,  $\tau$ , is a distance, however it can also be used to describe time as used in a time series analysis (Hamilton 1994). Fenton (1996) made note that the covariance between the same random variable (equivalent to a lag of zero) becomes the variance as given by Equation (2.17). Therefore, the covariance is a second moment statistic. Fenton (1996) also suggested that the magnitude of the covariance may be misleading as it is dependent on the variance of each variable. Therefore, he suggested the use of the correlation,  $\rho_{\tau}$ , between two random variables,  $X$  and  $Y$ , as given by:

$$\rho_{\tau} = \frac{\beta_{\tau}}{\sigma_x \sigma_y} = \frac{\text{Cov}[X, Y]}{\sigma_x \sigma_y} \quad (2.19)$$

The correlation between two properties is bounded by  $-1$  and  $1$ , where  $\rho_{\tau} = \pm 1$  relates to the observations being perfectly correlated (either positively or negatively) and  $\rho_{\tau} = 0$  relates to the observations being completely unrelated or purely random (Vanmarcke 1977a). The correlation of properties within a single sample is termed the *autocorrelation* (Bowerman and O'Connell 1979).

### 2.3.2.2 Statistical Parameters of Soil Properties

In the past, several studies have been conducted to estimate the statistical properties of soils. However, these are generally limited to the first statistical moment or the mean. This is because probabilistic modelling of soils has only been in use for the last 40 years or so (Vanmarcke 1982). Nevertheless, an examination of the literature has yielded information regarding the statistics of soil properties other than the mean.

A comprehensive investigation of soil property variability has been summarised by Phoon et al. (1995) and is shown in Table 2-6. These results represent the outcome of several years of research at Cornell University for the Electric Power Research Institute in the USA regarding the reliability based design of transmission towers (Filippas et al. 1988, Orchard et al. 1988, Spry et al. 1988, Kulhawy et al. 1992). The variability of test results shown in Table 2-6 are presented as a coefficient of variation (COV), which is defined as the standard deviation,  $\sigma$ , divided by the mean,  $\mu$ . The standard deviation is calculated by taking the square root of the variance shown in Equation (2.17). It should be noted that the

COV values, shown in Table 2-6, are also influenced by uncertainties due to measurement error. The magnitude of measurement error will be discussed later.

**Table 2-6 Inherent soil variability based on common test types**  
After Phoon et al. (1995)

Test type	Property	Soil type	Mean	COV (%)
Lab strength	$s_u$ (UC) <sup>a</sup>	Clay	10 – 400 kN/m <sup>2</sup>	20 – 55
	$s_u$ (UU) <sup>a</sup>	Clay	10 – 350 kN/m <sup>2</sup>	10 – 30
	$s_u$ (CIUC) <sup>a</sup>	Clay	150 – 700 kN/m <sup>2</sup>	20 – 40
	$\phi$	Clay and sand	20 – 40°	5 – 15
CPT	$q_c$	Clay	0.5 – 2.5 MN/m <sup>2</sup>	< 20
	$q_c$	Clay	0.5 – 2.0 MN/m <sup>2</sup>	20 – 40
	$q_c$	Sand	0.5 – 30.0 MN/m <sup>2</sup>	20 – 60
VST	$s_u$ (VST) <sup>b</sup>	Clay	5 – 400 kN/m <sup>2</sup>	10 – 40
SPT	$N$	Clay and sand	10 – 70 blows/ft	25 – 50
DMT	$D_A$	Clay	100 – 450 kN/m <sup>2</sup>	10 – 35
	$D_A$	Sand	60 – 1300 kN/m <sup>2</sup>	20 – 50
	$D_B$	Clay	500 – 880 kN/m <sup>2</sup>	10 – 35
	$D_B$	Sand	350 – 2400 kN/m <sup>2</sup>	20 – 50
	$I_D$	Sand	1 – 8	20 – 60
	$K_D$	Sand	2 – 30	20 – 60
	$E_D$	Sand	10 – 50 MN/m <sup>2</sup>	15 – 65
PMT	$p_L$	Clay	400 – 2800 kN/m <sup>2</sup>	10 – 35
	$p_L$	Sand	1600 – 3500 kN/m <sup>2</sup>	20 – 50
	$E_{PMT}$	Sand	5 – 15 MN/m <sup>2</sup>	15 – 65
Lab index	$w_n$	Clay and silt	13 – 100%	8 – 30
	$w_L$	Clay and silt	30 – 90%	6 – 30
	$w_P$	Clay and silt	15 – 25%	6 – 30
	$PI$	Clay and silt	10 – 40%	- <sup>c</sup>
	$LI$	Clay and silt	10%	- <sup>c</sup>
	$\gamma, \gamma_d$	Clay and silt	13 – 20 kN/m <sup>3</sup>	< 10
	$D_r$	Sand	30 – 70%	10 – 40; 50 – 70 <sup>d</sup>

Notes:

<sup>a</sup> UC = unconfined compression test; UU = unconsolidated undrained test; CIUC = consolidated undrained test

<sup>b</sup> VST = vane shear test

<sup>c</sup> COV = (3 – 12%)/mean

<sup>d</sup> The first range of values gives the total variability for the direct method of determination and the second range of values gives the total variability for the indirect determination using SPT values.

Further to the results shown in Table 2-6, Phoon et al. (1995) also compiled a summary of the scale of fluctuation of similar test results, as shown in Table 2-7. The scale of fluctuation is a measure of the correlation between two properties. Treatment of the scale of fluctuation is given later in this chapter. However, in general terms, a larger scale of fluctuation represents a slowly varying field where properties are correlated over long distances. The results shown in Table 2-6 indicate that soils typically show a greater SOF in the hori-



zontal direction than the vertical. This is because soils typically form in layers. In some instances, it appears that the horizontal SOF is a factor 10 times larger than the vertical SOF. This is considered anisotropy and will be discussed in subsequent chapters.

**Table 2-7 Example scale of fluctuation values based of geotechnical properties**  
After Phoon et al. (1995)

Property <sup>a</sup>	Soil type	No. of studies	Scale of fluctuation (m)	
			Range	Mean
Vertical fluctuation				
$s_u$	Clay	5	0.8 – 6.1	2.5
$q_c$	Sand, clay	7	0.1 – 2.2	0.9
$q_c$	Clay	10	0.2 – 0.5	0.3
$s_u$ (VST)	Clay	6	2.0 – 6.2	3.8
$N$	Sand	1	-	2.4
$w_n$	Clay, loam	3	1.6 – 12.7	5.7
$w_L$	Clay, loam	2	1.6 – 8.7	5.2
$\gamma'$	Clay	1	-	1.6
$\gamma$	Clay, loam	2	2.4 – 7.9	5.2
Horizontal fluctuation				
$q_c$	Sand, clay	11	3.0 – 80.0	47.9
$q_c$	Clay	2	23.0 – 66.0	44.5
$s_u$ (VST)	Clay	3	46.0 – 60.0	50.7
$w_n$	Clay	1	-	170.0
Notes:				
<sup>a</sup> $s_u$ and $s_u$ (VST), undrained shear strength from laboratory tests and vane shear tests, respectively; $\gamma'$ , effective unit weight				

The extent of the research summarised by Phoon et al. (1995) in Table 2-6 and 2-7 overshadows most other studies regarding the estimation of statistical soil properties. However, several other authors have also investigated the statistical properties of soils. Jaksa (1995) conducted over 200 cone penetration tests (CPTs) in a 50 m × 50 m area with the aim of characterising the variability of a stiff overconsolidated clay. The results of this research indicated that the COV of the CPT results was close to 60% and the vertical scale of fluctuation was approximately 0.15 m. Jaksa (1995) also estimated the horizontal scale of fluctuation to be approximately 1.5 m.

Akkaya and Vanmarcke (2003) and Kulatilake and Um (2003) also conducted a statistical analysis of extensive soil test data at the Texas A&M University as part of the National Geotechnical Experimentation Sites. They both used the extensive data sets to estimate the mean, COV and scale of fluctuation in both directions in sand and clay sites. The results at the Texas A&M University were primarily based on CPTs. On the other hand, Soulie et al.

(1990) conducted a series of vane shear tests in a soft clay deposit in Quebec, Canada. They too, were able to estimate the mean, COV and scale of fluctuation in both the vertical and horizontal directions of the undrained shear strength. These results are presented in Table 2-8, which summarises the mean, COV and SOF results of the statistical analysis. These results indicate large ranges in COV and SOF values. Furthermore, there does not appear to be any trend with regard to the type of soil. For example, the sand sites do not appear to be consistently more or less variable than the clay sites. This result is similar to the COV values shown in Table 2-6. However, no data indicates that the COV of the soil properties exceeds 100%. Rather, the maximum COV shown is approximately 80% for a sand site described by Phoon et al. (1995) and Phoon and Kulhawy (1999b). Similar to the results shown in Table 2-7, the horizontal SOF is typically larger than the vertical SOF, yet the magnitude of this difference varies for different soil types and sites.

There appears to be no definite trend in the mean values shown in Table 2-6 and 2-8. Instead, the mean appears to be influenced by the type of test and the location of the site. As such, results based on the CPT cannot be directly compared to mean values based on the PMT.

The mean and variability yield good descriptions of the location and shape of the distribution. However, for reliability analyses, it is also important to consider the form of the distribution. Brejda et al. (2000) found it difficult to fit a normal distribution to sampled soil properties, yet they had most success when using a lognormal distribution. On the other hand, Lee et al. (1983) believed that a large majority of soil properties show normal tendency but, as discussed by Fenton (1999), most soil properties are strictly non-negative, which is a condition that is better approximated by a lognormal distribution. As such, Fenton (1999) assumed that the cone tip resistance was lognormally distributed. He also noted the fact that Lumb (1966), Hoeksema and Kitanidis (1985) and Sudicky (1986) all supported the notion that some soil properties are well represented by a lognormal distribution. This was despite the fact that Lumb (1970) believed that soil strength was well represented by a Beta distribution but, if necessary, a normal distribution would be sufficient.

### 2.3.2.3 Modelling Spatial Variability

Not only do properties in the same soil vary from location to location, but they also show a degree of correlation, where properties located closer together are more similar than properties located further apart (Matheron 1963, Journel and Huijbregts 1978, Tabba and Yong 1981, Li and White 1987, Jaksa et al. 1993). This is known as *spatial correlation* and

**Table 2-8 Statistical properties from extensively tested sites**

Site	Soil	Test Type <sup>a</sup>	Mean	COV <sup>b</sup> (%)	SOF <sup>c</sup> (m)		Source
					Vertical	Horizontal	
South Parklands, South Australia	Stiff over-consolidated clay	CPT	2.953 MPa	58	0.15	1.5	Jaksa (1995)
Texas A&M University, USA	Clay site	CPT	1.3 – 5.8 MPa	5 - 36	0.1 - 0.55	-	Kulatilake and Um (2003)
Texas A&M University, USA	Sand site	CPT	8,400 kPa	50	3.25	13.5	Akkaya and Vanmarcke (2003)
New Liskeard, Ontario, Canada	Varved Clay	VST	?	32	5	46	Macasse and Ladd (1973) and Vanmarcke (1977b)
4 Soils	Sand	PMT	5.2 – 15.6 MPa	28 - 68	-	-	
57 Soils	Sand	CPT	0.4 – 29.2 MPa	10 - 81	0.1 – 2.2	3 - 80	
12 Soils	Silty Clay	CPT	0.5 – 2.1 MPa	5 - 40	0.1 – 2.2	3 - 80	Phoon et al. (1995) and Phoon and Kulhawey (1999b)
22 Soils	Sand	SPT	7 – 74 N	19 – 62	2.4	-	
2 Soils	Clay, loam	SPT	7 – 63 N	37 - 57			
Broadback River, Quebec, Canada	Soft Clay	VST	35.8 & 33.6 kPa	23 & 21	3	7	Soulie et al. (1990)

**Notes:**<sup>a</sup> Test Type: CPT – Cone penetration test; VST – Vane shear test; PMT – Pressuremeter test; SPT – Standard penetration test<sup>b</sup> COV – Coefficient of variation (standard deviation divided by mean)<sup>c</sup> SOF – Scale of fluctuation – separation distance within which soil properties are considered reasonably correlated

renders standard statistical analyses like regression, unsuitable to model the spatial variability of soil properties (Matheron 1963). Instead, methods like *geostatistics* (Krigé 1951, Matheron 1965) and *random field theory* (Vanmarcke 1983), which account for spatial correlation, have been used successfully to model the variability of soil properties (Jaksa 1995). Geostatistics and random field models use properties known as the *range* and *scale of fluctuation*, respectively, to describe the magnitude of spatial correlation.

(a) *Random field theory*

Random field theory has a strong relationship with traditional time series statistics that can be traced back to economics and Brownian motion physics in the early 20<sup>th</sup> century (Vanmarcke 1983). Random field models utilise the covariance between properties, as given by:

$$\beta(x, x + \tau) \equiv \beta_\tau = \text{Cov}[X(x), X(x + \tau)] = E[X(x)X(x + \tau)] \quad (2.20)$$

where  $X(x)$  is a sample at position  $x$  and  $X(x + \tau)$  is a sample at a distance  $\tau$  from position  $x$ . Again,  $E[.]$  is the expectation operator. As discussed in the previous section, it is generally preferred that the covariance is expressed by the *correlation*, given by:

$$\rho(x, x + \tau) \equiv \rho_\tau = \frac{\text{Cov}[X(x)X(x + \tau)]}{\sigma_x^2} = \frac{\beta(x, x + \tau)}{\sigma_x^2} \quad (2.21)$$

In a Gaussian or normally distributed field that satisfies the assumption of weak stationarity, the mean and correlation structure uniquely describe the distribution (Vanmarcke 1977a).

The correlation structure defines the degree of correlation between two points in a field. As an additional measure, Vanmarcke (1977a, 1983) introduced the *scale of fluctuation* to describe the correlation structure of the soil. The scale of fluctuation (SOF) is loosely defined as the distance within which two samples in the field are considered reasonably correlated. A large SOF represents properties that vary continuously or show correlations at large separation distances. In fields with large SOFs, the properties appear to vary slowly about the mean. On the other hand, a small SOF is representative of a field where properties vary more erratically or rapidly about the mean. In these fields, properties show little correlation at small separation distances. The SOF has been shown, in the previous sec-

tion, to vary between different test types and for different soils. Vanmarcke (1982) has suggested that the soil SOF is dependent on the initial processes used to form the deposit.

(b) *Geostatistics*

Geostatistics has been extensively used in the mining industry to estimate changes in ore bodies by Krige (1951) and Matheron (1965), but it is also applicable to any spatially or temporally natural phenomena (Journel and Huijbregts 1978, Hohn 1988). Geostatistics is based on a *regionalised variable*, represented by random functions rather than independent random variables. The rate of change of a regionalised variable is measured by the *semivariogram*,  $\gamma_h$  (Matheron 1971), which is given by:

$$\gamma_h = \frac{1}{2} E[(X_{i+h} - X_i)^2] \quad (2.22)$$

where  $E[\cdot]$  is the expected value,  $X_i$  is the value of property  $X$  at location  $i$ ,  $X_{i+h}$  is the value of property  $X$  at location  $i + h$  and  $h$  is the distance between the two points,  $X_i$  and  $X_{i+h}$ .

Jaksa (1995) recognised that it is not possible to know the value of a regionalised variable at all locations, although it is spatially continuous. Therefore, it is necessary to fit a model of the semivariogram to a discrete number of known data pairs. Several common models of semivariogram are available in the literature and include the spherical, exponential, Gaussian and linear. The form of the semivariogram, typically found by a trial-and-error process (Clarke 1979), is used with *kriging* to estimate properties at other locations (Jaksa 1995).

The kriging process provides a method for estimating values at unsampled locations using a nominated semivariogram. Deutsch and Journel (1992) suggested two forms of simulation, which result in a three-dimensional field of properties that are built on a kriging foundation. Such fields conform to a statistical distribution with a target mean and variance, while also conforming to the nominated semivariogram model. The first of these two simulation techniques is Sequential Gaussian Simulation (SGS), which is suitable for homogeneous fields or deposits with a single layer. Sequential Indicator Simulation (SIS) is a more complex formulation but provides ways to simulate 3 dimensional fields that are not necessarily homogeneous. This is more applicable to deposits with multiple layers.

Both SGS and SIS involve conditioning distributions based on previously simulated properties within a nominated neighbourhood area. Both methods begin by defining a random walk. Along this walk, the first property is sampled from the nominated distribution with target mean and variance. The next point along the walk is sampled from a distribution, which is conditioned to conform to the original statistical properties (mean and variance) and the previous sample (or neighbouring samples) through the use of the semivariogram. This procedure continues until all points in the field are simulated.

Baecher and Christian (2003) suggested that the semivariogram is more difficult to use in spatial interpolation and engineering analysis, even though it is less dependent on the assumption of stationarity than the autocovariance. Hence, the autocovariance and random field theory is more commonly used to model the variability in soil properties (Baecher and Christian 2003).

(c) *Fractal and finite scale processes*

Fractals are self-similar processes that show long scale dependence and have infinite SOFs, while finite processes are considered to have short memory and relatively small SOFs (Fenton 1999). Fractals are generally more complex to model than finite processes. However, Jaksa and Fenton (2002) concluded that soils do not explicitly display fractal behaviour.

Vanmarcke (1983) introduced several finite scale models of correlation structure. Fenton (1990) suggested that the exponentially decaying function, or Markov correlation structure, best describes the correlation between properties in a soil. The 1-D exponentially decaying correlation structure is given by:

$$\rho(\tau) = \sigma^2 \exp\left(-\sqrt{\left(\frac{2\tau}{\theta}\right)^2}\right) \quad (2.23)$$

where  $\rho(\tau)$  is the correlation at lag distance  $\tau$ ,  $\sigma^2$  is the variance and  $\theta$  is the scale of fluctuation. The 1-D correlation structure shown in Equation (2.23) becomes the 3-D exponentially decaying correlation structure given by:

$$\rho(\tau_1, \tau_2, \tau_3) = \sigma^2 \exp\left\{-\sqrt{\left(\frac{2\tau_1}{\theta_1}\right)^2 + \left(\frac{2\tau_2}{\theta_2}\right)^2 + \left(\frac{2\tau_3}{\theta_3}\right)^2}\right\} \quad (2.24)$$

where  $\rho(\tau_1, \tau_2, \tau_3)$  is the correlation due to lag distances,  $\tau_1$ ,  $\tau_2$  and  $\tau_3$ ,  $\sigma^2$  is the variance and  $\theta_1$ ,  $\theta_2$  and  $\theta_3$  are the scales of fluctuation in the same direction as the corresponding lag distances. The correlation structure is considered anisotropic if the scale of fluctuation in each direction is different (Vanmarcke 1983). Jaksa et al. (2005) suggested that the correlation of soil properties in the horizontal direction is typically larger than in the vertical direction, due to the layering processes. This is confirmed by the data presented earlier in this chapter.

Vanmarcke (1983) also introduced the variance function, which provides a measure of the variance reduction due to averaging within a finite domain. Such variance reduction is also heavily dependent on the scale of fluctuation, where the variance function corresponding to an exponentially decaying correlation structure, as given by Equation (2.23), is:

$$\gamma(D_v) = 2 \left( \frac{\theta}{2D_v} \right)^2 \left( \frac{2D_v}{\theta} - 1 + e^{-2D_v/\theta} \right) \quad (2.25)$$

where  $\gamma(D_v)$  is the variance function over the averaging domain,  $D_v$ . The variance function is further discussed in Chapter 3.

### 2.3.3 Statistical Uncertainty

The statistical uncertainties associated with a geotechnical model are a result of limited sampling that may not provide an accurate representation of the underlying conditions. Filippas et al. (1988) defined the statistical uncertainty for a set of uncorrelated samples as the variance in the estimate of the mean. In this case, as suggested by DeGroot (1986), the central limit theorem was used, with a formulation given by:

$$\text{Var}(\mu) = \frac{\sigma^2}{n} \quad (2.26)$$

where the  $\text{Var}[\mu]$  is the variance of the sample mean,  $\sigma^2$  is the sample standard deviation and  $n$  is the number of samples. Baecher and Christian (2003) also suggested the use of Equation (2.26) to estimate statistical uncertainty, derived from standard statistical methods (Benjamin and Cornell 1970). However, when considering correlated samples, the sample mean variance becomes:

$$\text{Var}(\mu) = \frac{\sigma^2}{n} + 2 \frac{\sigma^2}{n^2} \sum_{i=1}^n \sum_{j=i+1}^n \rho_{ij} \quad (2.27)$$

where,  $\rho_{ij}$  is the correlation coefficient between the  $i$ th and  $j$ th sample. The value of Equation (2.27) is higher than Equation (2.26) because of redundancy (Filippas et al. 1988). Although Equations (2.26) and (2.27) estimate the statistical uncertainty in the sample mean estimate, neither consider the sampling location. Baecher and Christian (2003) briefly discussed *spatial sampling*, where the variance of the mean estimate is considered a function of the sampling population,  $n$ , and the distance between samples,  $k$ . Discussion was also made regarding the effectiveness of common sampling patterns in terms of estimating the statistical parameters of the sample. For simple random sampling, Baecher and Christian (2003) suggested that the estimation variance has a value given by:

$$\text{Var}(\mu) = \frac{\sigma^2}{n} \frac{n_t - n}{n_t} \quad (2.28)$$

where  $n_t$  is the total population size. In comparison to the values shown in Equation (2.28) the estimation variance for systematic (Cochran 1977) and stratified random sampling (Thompson 2002) is respectively given by:

$$\text{Var}(\mu) = \frac{1}{n} \left( \frac{n_t - n}{n_t} \right) \left( \frac{\sum (x_i - \mu)^2}{n - 1} \right) \quad (2.29)$$

and

$$\text{Var}(\mu) = \sum_i e_i^2 \frac{\sigma_i^2}{n_i} (1 - f_i) \quad (2.30)$$

where  $x_i$  is the sampled value;  $e_i$  is the size of the  $i$ th element divided by the total population size;  $\sigma_i$  is the standard deviation within the  $i$ th element;  $n_i$  is the number of samples taken from the  $i$ th element and  $f_i$  is defined as  $n_i / n_t$ . Like Baecher and Christian (2003), Cressie (1993) also investigated spatial sampling in terms of data analysis. He noted that Olea (1984), Yfantis et al. (1987) and McBratney et al. (1981) found that regular sampling patterns using triangular elements are the most efficient.



### 2.3.4 Measurement Error

Measurement errors arise from the inability of geotechnical tests to accurately estimate the soil properties being tested. Sources of measurement error can be separated into 2 categories: systematic and random (Filippas et al. 1988). Random testing effects are inherent to the test type but cannot be attributed to the spatial variability of soil properties. The effects are generally considered to have zero mean and influence the results of the soil properties equally above and below the mean (Baecher 1979, Snedecor and Cochran 1980). Filippas et al. (1988) suggested the best way to evaluate random testing effects is by undertaking several tests under essentially identical conditions. Systematic errors consistently under or overestimate the property and are generally due to operator and procedural effects and inadequacies with the equipment (Jaksa et al. 1997). Lumb (1974) considered such errors as a bias.

The accurate evaluation of measurement error is inherently difficult due to the presence of other significant sources of errors, such as soil variability and statistical uncertainty (Phoon et al. 1995). Jaksa et al. (1997) suggested a methodology to estimate the measurement error of test results based on the semivariogram and a method originally detailed by Baecher (1982, 1986). This method was based on the proposition that the total uncertainty in a property estimate,  $\sigma_T^2$ , is given by (Orchant et al. 1988):

$$\sigma_T^2 = \sigma_{sv}^2 + \sigma_e^2 + \sigma_{p/o}^2 + \sigma_r^2 \quad (2.31)$$

where  $\sigma_{sv}^2$  is the variance due to spatial variability and  $\sigma_e^2$ ,  $\sigma_{p/o}^2$  and  $\sigma_r^2$  are the uncertainties due to equipment, procedure and operator and random test effects, respectively. The last three terms are sometimes collectively referred to an uncertainty due to measurement error,  $\sigma_m^2$  (Jaksa et al. 1997).

As part of the research conducted at Cornell University for the Electric Power Research Institute (Filippas et al. 1988, Orchant et al. 1988, Spry et al. 1988, Kulhawy et al. 1992), measurement errors were isolated from the uncertainties due to soil variability and statistical uncertainty using random field theory. The resulting errors for several common geotechnical test types were summarised by Phoon and Kulhawy (1999a) and are shown in Table 2-9. These errors are expressed as a coefficient of variation (COV).

The following discussion deals with measurement errors associated with four common test types: the standard penetration test; cone penetration test; flat plate dilatometer test and the

triaxial test. These tests and associated measurement errors are incorporated into the analyses described in subsequent chapters.

**Table 2-9 Measurement errors of common in situ tests expressed as a coefficient of variation**  
After Phoon and Kulhawy (1999a)

Test	Coefficient of variation, COV (%)				
	Equipment	Procedure	Random	Total <sup>a</sup>	Range <sup>b</sup>
Standard penetration test (SPT)	5 – 75 <sup>c</sup>	5 – 75 <sup>c</sup>	12 – 15	14 – 100 <sup>c</sup>	15 – 45
Mechanical cone penetration test (MCPT)	5	10 – 15 <sup>d</sup>	10 – 15 <sup>d</sup>	15 – 22 <sup>d</sup>	15 – 25
Electric cone penetration test (ECPT)	3	5	5 – 10 <sup>d</sup>	7 – 12 <sup>d</sup>	5 – 15
Vane shear test (VST)	5	8	10	14	10 – 20
Dilatometer test (DMT)	5	5	8	11	5 – 15
Pressuremeter test, prebored (PMT)	5	12	10	16	10 – 20 <sup>e</sup>
Self-boring pressuremeter test (SBPMT)	8	15	8	19	15 – 25 <sup>e</sup>

Notes:

<sup>a</sup>  $COV(Total) = [COV(Equipment)^2 + COV(Procedure)^2 + COV(Random)^2]^{0.5}$ .

<sup>b</sup> Because of limited data and judgement involved in estimating COVs, ranges represent probable magnitudes of field test measurement error.

<sup>c</sup> Best to worst case scenarios, respectively, for SPT.

<sup>d</sup> Tip and side resistances, respectively, for CPT.

<sup>e</sup> It is likely that results may differ for  $p_{0r}$ ,  $p_r$  and  $p_{Lr}$ , but the data are insufficient to clarify this issue.

The effectiveness of the standard penetration test (SPT) is highly dependent on its operation (Becker 2001). Orchant et al. (1988) categorised errors associated with the SPT into equipment and procedural/operator effects. Both equipment effects and procedural/operator effects contribute between 5% and 75% of the overall test uncertainty as illustrated in Table 2-9. However, Lee et al. (1983) estimated that the COV of SPT results ranged between 27% and 85%. Furthermore, Lee et al. (1983) concluded that the quality and quantity of information received from an SPT is good when endeavouring to estimate the undrained shear strength of clays and the drained shear strength of sands.

Jaksa (1995) categorised the errors associated with the cone penetration test (CPT) as systematic and random. Orchant et al. (1988) further separated the systematic errors into equipment and operator and procedural effects. Equipment effects result from the manufacture of the cone penetrometer while operator and procedural effects result from techniques such as the angle of inclination or the type of penetration. The results in Table 2-9 indicate that the COV values for the CPT range between 7% and 12%. These COV values include uncertainties due to equipment, operator and procedural and spatial variability effects. The contribution of variation due to equipment effects and operator and procedural effects appear to be 3% and 5%, respectively. Lee et al. (1983) concluded that the quality and quantity of information received by the CPT is very good and good, respectively.

Phoon and Kulhawy (1999a) suggested that COV values for the CPT in sands is larger than in clays.

The dilatometer test (DMT) is relatively new compared to the SPT and CPT and, as such, extensive statistical analyses have yet to be conducted (Orchant et al. 1988). However, the uncertainties in the DMT due to operator and procedural effects are similar to those of the CPT. The contribution of uncertainties due to equipment effects are mainly related to the inflation of the membrane. Results in Table 2-9 indicate that the COV value for the DMT is approximately 11%. Similarly with the CPT, the DMT yields COV values that appear to be higher in sand than in clays (Phoon and Kulhawy 1999a).

Craig (1997) warned that properties obtained using a triaxial test (TT) are only relevant to the drainage conditions simulated. The TT is also limited by the inability to rotate the principal stress axes (Lee et al. 1983). It is also important to note that the cell pressure is assumed to be uniform (Craig 1997), which may result in errors in the soil properties obtained. Equipment effects also influence the accuracy of the test, where leaking seals or faulty transducers severely affect the results. Because the TT is a laboratory test, soil samples must be removed from the site and transported to the laboratory. As such, errors associated with sample disturbance are introduced. Bowles (1997) suggested that errors due to sample disturbance may affect the results up to as much as 50%, if adequate care is not taken. This is despite the fact that the TT is able to obtain very accurate soil properties from the sample.

### **2.3.5 Transformation Model Uncertainty**

The results of common geotechnical in situ tests do not typically provide applicable soil properties that are useful for design relationships (Phoon and Kulhawy 1999b). Rather, the raw test results are processed using a transformation model into a suitable design parameter. Such models are obtained empirically through back substitution or calibration. Accordingly, a degree of uncertainty is added to the estimation of the design parameter. Phoon and Kulhawy (1999b) further stated that uncertainty still exists if the transformation is based on a theoretical relationship because of idealizations and simplifications in the theory. Therefore, it is important to consider the uncertainties due to transformation model error.

Phoon and Kulhawy (1999b) suggested that probabilistic methods could be used to estimate the data scatter associated with a transformation model. For example, the results il-

illustrated in Figure 2-11 show the correlation between a measured property,  $\xi_m$ , and the design property,  $\xi_d$ . An estimation of the transformation model is found by fitting a regression line to the data, while the scatter is modelled by a zero mean random variable. Therefore, the standard deviation of the random variable provides a measure of the uncertainty due to the transformation model error. Such an uncertainty is unique to the relationship between the measured property and the design parameter. Therefore, as an example, the uncertainty due to transformation model error will be different for the correlation between SPT and CPT results with respect to the elastic modulus.

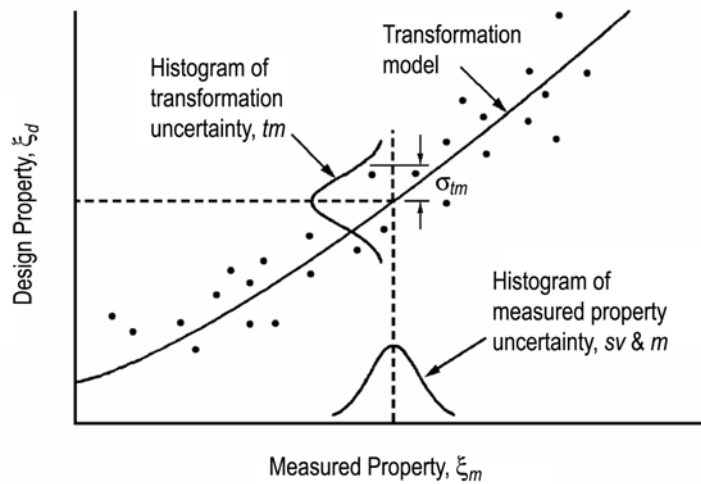


**Figure 2-11 Influence of measurement uncertainty and transformation model uncertainty**  
After Phoon and Kulhawy (1999b)

It should be noted that the correlation between the measured property and the design parameter, shown in Figure 2-11, is also affected by other sources of uncertainty like measurement errors and the inherent soil variability, as discussed earlier in this section. As such, Phoon and Kulhawy (1999b) proposed a relationship for the variance of the design parameter in terms of the different sources of uncertainty, given by:

$$\sigma_{\xi_d}^2 = \left(\frac{\partial T}{\partial sv}\right)^2 \sigma_{sv}^2 + \left(\frac{\partial T}{\partial m}\right)^2 \sigma_m^2 + \left(\frac{\partial T}{\partial tm}\right)^2 \sigma_{tm}^2 \quad (2.32)$$

where  $\sigma_{\xi_d}^2$ , is the variance of the design parameter;  $\sigma_{sv}^2$ ,  $\sigma_m^2$  and  $\sigma_{tm}^2$ , are the variances of the uncertainty due to inherent soil variability, measurement error and transformation model error, respectively;  $sv$ ,  $m$  and  $tm$  are the random variable representations of soil variability, measurement error and transformation model error, respectively; and  $T$  is the transformation function. The uncertainty due to transformation model error may be removed from the relationship shown in Equation (2.32) if the test property yields a direct measure

of the design parameter. For example, the dilatometer test provides a direct measure of the elastic modulus of the soil (Phoon and Kulhawy 1999b).

Kulhawy and Mayne (1990) summarised several of the correlations between soil properties and geotechnical tests, as shown in Table 2-10 - Table 2-10(a) referring to correlations applicable to cohesive soils like clays and Table 2-10(b) referring to correlations applicable to cohesionless soils like sands. The actual transformation models correlating the test type to the soil property have not been shown; rather whether they exist or not.

Phoon and Kulhawy (1999b) used a correlation between the results of a pressuremeter test (PMT) and the standard penetration test (SPT) to estimate the uncertainty due to transformation model error associated with the SPT. They predicted that the uncertainty due to transformation model error for the SPT correlation to PMT results ranged between a COV value of 86% and 93%. This is extremely large and highlights inaccuracies in the correlation investigated. However, another estimation of the uncertainty due to transformation model error between the SPT and the dilatometer test yielded a standard deviation,  $\sigma_m$ , estimate of 0.12. This suggests a considerably more accurate correlation between the SPT and the DMT. Phoon and Kulhawy (1999b) did not examine any correlations between the elastic modulus and the results of a cone penetration test (CPT) or triaxial test. However, they concluded that correlations between test results and the elastic modulus yielded the highest degree of uncertainty.

## **2.4 GEOTECHNICAL DESIGN INCORPORATING UNCERTAINTIES**

---

Geotechnical engineers typically use two methods to account for the uncertainties in a given system. The most common has been to use a global factor of safety, where either the strength is reduced or the loads are increased to ensure the design is sufficiently conservative to meet the specified purpose. Phoon et al. (1995) suggested that the factor of safety is typically applied to the material strength or the capacity of the design, as it is the most uncertain component. This philosophy is common in most geotechnical engineering texts (e.g. Terzaghi and Peck 1968, Fang 1991, Bowles 1997). The factor of safety is generally determined by the experience and judgement of the geotechnical engineer (Phoon et al. 1995). Furthermore, the use of a single factor of safety does not distinguish between model and parameter uncertainties, and hence, does not allow the identification of possible improvements by either increased sampling or alternative testing.

**Table 2-10 Correlations between soil properties and test results for (a) cohesive and (b) non-cohesive soils**  
After Phoon and Kulhawy (1999b)

**(a)**

Property category	Soil property	Laboratory or theory correlation	Field test correlation					
			SPT	CPT	CPTU	PMT	DMT	VST
Basic characterisation	Classification	✓	-	✓	✓	-	✓	-
	Unit weight	✓	-	-	-	-	-	-
	Consistency	-	✓	✓	-	-	-	-
In situ stress	Pre-consolidation stress	✓	✓	✓	✓	✓	✓	✓
	Over-consolidation ratio	✓	✓	-	✓	-	✓	✓
	Coefficient of horizontal soil stress	✓	✓	✓	✓	✓	✓	-
Strength	Effective stress friction angle	✓	-	-	-	-	-	-
	Undrained shear strength	✓	✓	✓	✓	✓	✓	✓
Deformability	Poisson's ratio	✓	-	-	-	-	-	-
	Young's modulus	✓	-	-	-	-	-	-
	Compression indices	✓	-	-	-	-	-	-
	Constrained modulus	✓	✓	✓	-	-	✓	-
	Coefficient of consolidation	✓	-	-	✓	-	✓	-
Permeability	Coefficient of secondary compression	✓	-	-	-	-	-	-
	Hydraulic conductivity	✓	-	-	-	-	-	-

Notes: CPT, cone penetration test; CPTU, piezocone test; DMT, dilatometer test; PMT, pressuremeter test; SPT, standard penetration test; VST, vane shear test.

**(b)**

Property category	Soil property	Laboratory or theory correlation	Field test correlation				
			SPT	CPT	CPTU	PMT	DMT
Basic characterisation	Classification	✓	-	✓	✓	-	✓
	Unit weight	✓	-	-	-	-	-
	Relative density	-	✓	✓	✓	-	✓
In situ stress	Coefficient of horizontal soil stress	✓	-	✓	-	✓	✓
Strength	Effective stress friction angle	✓	✓	✓	-	✓	✓
Deformability	Poisson's ratio	✓	-	-	-	-	-
	Young's modulus	✓	✓	-	-	✓	✓
	Compression index	✓	-	-	-	-	-
	Constrained modulus	✓	-	✓	-	-	-
Permeability	Subgrade modulus	✓	-	-	-	-	-
	Hydraulic conductivity	✓	-	-	-	-	-
Liquefaction resistance	Cyclic stress ratio	-	✓	✓	-	-	✓

Lee et al. (1983) suggested that a factor of safety of 3 is common for permanent structures, but may be reduced to 2 for temporary structures. However, the application of a single factor of safety requires only a global appreciation of the uncertainties in the geotechnical model and is typically non-transparent. In other words, the choice of a factor of safety is unique to the situation and the designer (Phoon et al. 1995), which makes repeatability

almost impossible. Kulhawy and Phoon (2002) discussed the uniqueness of the traditional factor of safety approach, especially with regard to the selection of design parameters. It is also common that engineers will use different calculation methods at different locations or in fact, other engineers may use different calculation methods at the same location (Goble 1999). To illustrate this, Kulhawy (1984) used several design assumptions and equations to compute the design uplift capacity of a drilled shaft in clay. The results are shown in Table 2-11 and illustrate the wide range of actual factors of safety.

**Table 2-11 Design capacity example using several assumptions and equations**  
After Kulhawy (1984)

Design Assumption	Design Equation	$Q_{ud}$ based on FOS = 3 (kN)	$Q_u / Q_{ud}$ ("actual" FOS)
1	$Q_{ud} = (Q_{su} + Q_{tu} + W) / \text{FOS}$	170.7	3.0
2	$Q_{ud} - W = (Q_{su} + Q_{tu}) / \text{FOS}$	214.2	2.4
3	$Q_{ud} = (Q_{su} + W) / \text{FOS}$	108.9	4.7
4	$Q_{ud} - W = Q_{su} / \text{FOS}$	152.4	3.4
5	$Q_{ud} = W / \text{FOS}$	21.8	23.5

Notes:  $Q_{su}$ , side resistance = 261.8 kN;  $Q_{tu}$ , tip resistance = 184.4 kN;  $W$ , weight of shaft = 65.3 kN;  $Q_{u}$ , available capacity =  $Q_{su} + Q_{tu} + W = 511.6$  kN;  $Q_{ud}$ , design uplift capacity;  $\text{FOS}$ , factor of safety

The traditional global factor of safety approach has sufficed in the geotechnical industry for many years (Kulhawy and Phoon 2002). However, recent developments in both structural and geotechnical engineering have seen the implementation of limit state design, which provides a more consistent management of safety levels. Phoon et al. (1995) noted there are three basic requirements in a limit state design:

1. Identifying the potential failure methods;
2. Applying checks for each limit state; and
3. Ensuring that the occurrence of each limit state is adequately improbable.

Limit state design is significantly more complex than the traditional factor of safety approach, yet the outcomes are similar. Instead of a global factor of safety being used to reduce the material strength as in the traditional approach, limit state design involves applying partial factors of safety to all components in the system (e.g. loads and material properties). However, the philosophical difference is that the factors applied to each of

these components are representative of the uncertainty associated with each component. Phoon et al. (1995) noted that both probabilistic and non-probabilistic methods (Hansen 1965, Simpson et al. 1981, Meyerhof 1984, Bolton 1989) have been used to estimate the partial factors of safety. They further commented that the non-probabilistic approach inadequately addresses the shortcomings of the traditional approach. Instead, probabilistic limit state design considers the variation in the design parameters and allows uncertainties to be quantified consistently. However, Whitman (1984) indicated that geotechnical engineers are reluctant to embrace probabilistic analyses because of their lack of proficiency with probability theory. Phoon et al. (1995) further categorised the reasons for avoiding probabilistic analysis into:

1. Difficulty in representing the variability of soil properties;
2. Increased complexity in the design calculations; and
3. Difficulty in interpreting the results as a theoretical probability of failure.

Nevertheless, the increasing legal pressures from regulatory bodies have encouraged geotechnical engineers to understand more about the reliability of their designs through probabilistic analysis (Baecher and Christian 2003). This has been especially true in the power generation industry, nuclear power plants and offshore oil and gas facilities in deep water. Therefore, probabilistic-based designs appear to be the next step towards achieving greater rationality in design (Phoon et al. 1995). Baecher and Christian (2003) also noted that management decisions regarding projects are increasingly based on statistical decision analyses while structural codes already use Load and Resistance Factor Design (LRFD). Such factors have been calibrated based on reliability theory. However, geotechnical LRFD is very different to the structural equivalent because of (Kulhawy and Phoon 2002):

1. The choice of design parameters is typically left at the engineers' discretion;
2. The greatest source of uncertainty due the soil variability is not explicitly considered; and
3. Significant reliability based design calibrations have not been conducted.

Lee et al. (1983) recommended the use of probabilistic methods to account for the variability of soil properties and loadings. Duncan and D'Orazio (1984) also observed through tradition or regulation that it is common for the same factor of safety to be used, even when varying degrees of uncertainty are associated with the different design parameters. They



believed this to be illogical and are convinced it will result in inappropriate factors of safety being adopted. Finally, Phoon et al. (1995) discussed three major advantages of probabilistic analysis where the:

1. Foundation design is more cost-effective;
2. Incompatibility between structural and foundation design is minimised; and
3. Engineer is relieved of assessing the relationship between uncertainties and risk.

Reliability analysis, as adopted in this research, is considered to be the assessment of design risk based on the probabilistic treatment of uncertainties in the parameters specific to that design (Phoon et al. 1995). For example, a reliability analysis of settlement considers the uncertainty in the elastic moduli resulting from the sources indicated earlier in this chapter. Such a reliability analysis assists in the determination of the probability of failure and factors of safety associated with limit state design. Whitman (2000) indicated that such reliability analyses are useful to estimate the factors of safety, as they consistently represent the risks of different types of failure. Furthermore, Wu et al. (1989) suggested reliability analyses provide a systematic method for representing uncertainty in the design parameters and engineering judgement.

Reliability-based design in geotechnical engineering owes its origins to structural engineering and the work of Freudenthal (Freudenthal 1951, Freudenthal and Gumbel 1956, Freudenthal et al. 1966). However, it wasn't until the 1970s that the philosophy was applied to geotechnical engineering.

The basis for reliability-based design is the probabilistic modelling of uncertain quantities using random variables. A random variable is a quantity that cannot be predicted precisely (Phoon et al. 1995). Instead, the variable is drawn from a distribution of properties. Such distributions may define an equal likelihood for all values, although it is more common that some values have a greater likelihood than others. Typical distributions used in reliability analysis of geotechnical systems are the normal and lognormal distributions, as shown in Figures 2-12(a) and (b), respectively.

In a simple reliability approach, the load,  $F$ , and capacity,  $R$ , of a system is represented by random variables. As an example,  $F$  and  $R$  are represented by normal distributions, as shown in Figure 2-13, where  $m_F$  and  $m_R$  are the mean load and capacity, respectively, and  $s_F$  and  $s_R$  are the standard deviation of load and capacity, respectively.

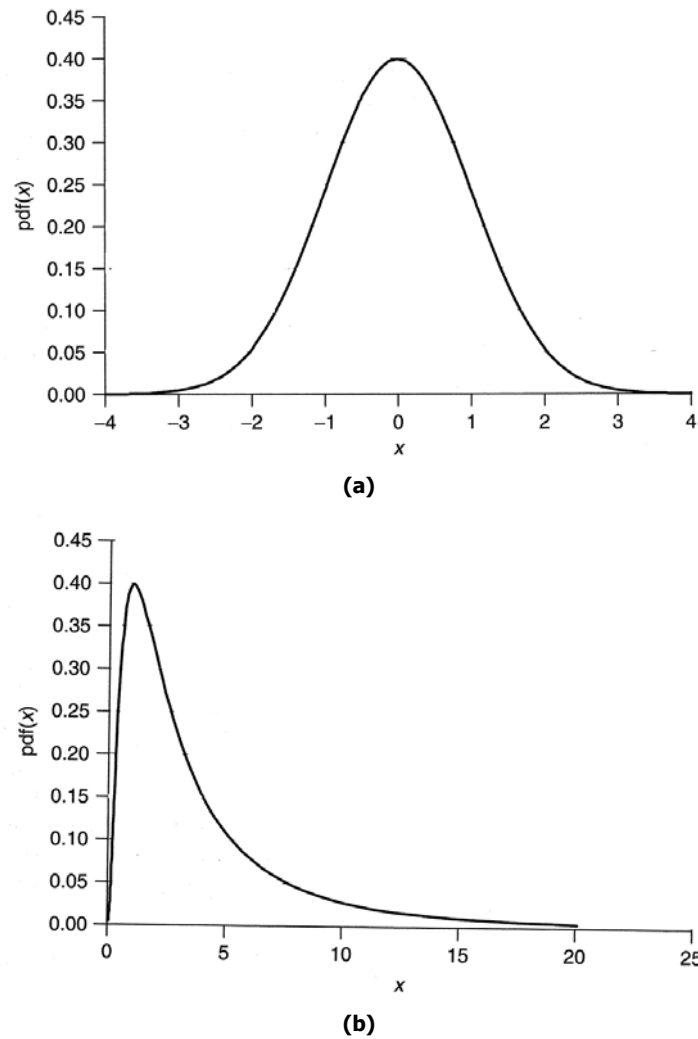


**Figure 2-12 (a) Normal and (b) log normal distributions**  
After Baecher and Christian (2003)

A measurement of reliability can be made through the use of a safety margin or margin of safety,  $MOS$ , which is defined by:

$$MOS = R - F \quad (2.33)$$

The benefit of using the safety margin when  $F$  and  $R$  are both normally distributed is that the safety margin also follows a normal distribution (Baecher and Christian 2003). An example of the probability density function and cumulative probability of the safety margin,  $MOS$ , is shown in Figure 2-14. On the other hand, when  $F$  and  $R$  are lognormally distributed, Baecher and Christian (2003) suggested the use of the factor of safety,  $FOS$ , which is also lognormally distributed and is defined by:

$$FOS = \frac{Q}{F} \quad (2.34)$$

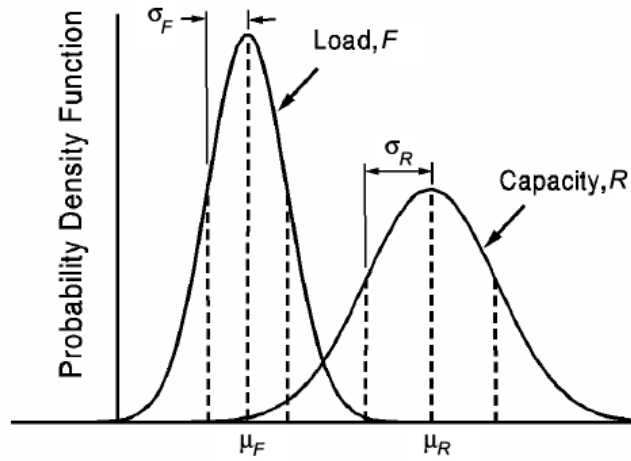
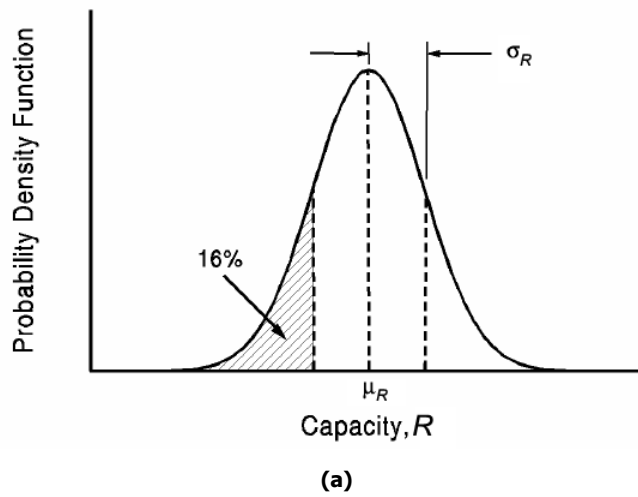
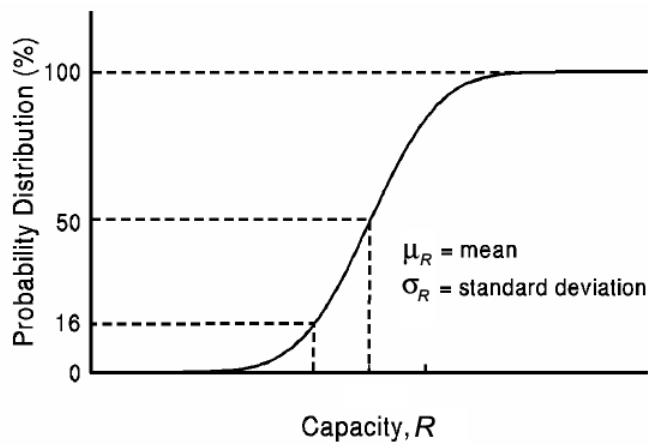


Figure 2-13 Load,  $F$ , and capacity or resistance,  $R$ , distributions (normal)  
After Phoon et al. (1995)



(a)



(b)

Figure 2-14 (a) Probability density and (b) cumulative probability function of safety margin,  $M$ , based on normal  $F$  and  $R$   
After Phoon et al. (1995)

The *reliability index*,  $\beta$ , is determined from the statistical properties of the margin or factor of safety distributions and can, therefore, be directly compared to a probability of failure,  $p_f$ , using probability distributions.

Difficulties in reliability analysis arise with the establishment of an analytical model and the statistical descriptors of the parameters. The parameters in a geotechnical system typically contain many forms of uncertainty and a description is hard to resolve. Phoon et al. (1995) recognised that closed-form solutions of the example shown in Figure 2-13 are rare and typically, the probability of failure must be evaluated numerically. As such, Baecher and Christian (2003) suggested several ways of estimating the reliability of a system based on numerical and simulation methods, including:

- First Order Second Moment (FOSM);
- Second Order Second Moment (SOSM);
- Point Estimation; and
- Monte Carlo simulation.

First order second moment (FOSM) methods use the first order terms in a Taylor series expansion to approximate the mean, variance and standard deviation of the load and resistance functions. Christian et al. (1994) used FOSM to estimate the reliability of the dikes used in the James Bay project. Analyses using FOSM reveal the relative contribution of each source of uncertainty on the total, which Baecher and Christian (2003) suggested is a great advantage. However, FOSM utilises only the first order terms of the Taylor series expansion, whereas the second order second moment methods take into account second order terms. Although this increases complexity in computation, the approximation is typically improved. Point-estimate methods are essentially an extension to the first order reliability method (FORM), as described in detail by Phoon et al. (1995), and, although popular in practice, Baecher and Christian (2003) suggested this technique has many detractors. The method was first introduced by Rosenblueth (1975) and has been used in several applications (Harr 1987, Wolff 1996, Duncan 1999). Harr (1989) suggested that the point estimate method circumvented many of the problems associated with the use of the Taylor series and Monte Carlo methods. However, Baecher and Christian (2003) warned that these methods require large numbers of calculations for multiple variables and may be beyond the scope of practical applications.

Baecher and Christian (2003) also discussed the implementation of stochastic finite elements, which involves mapping soil properties into the finite element mesh. This can be achieved either by using deterministic soil properties, which do not vary across their region (Baecher and Christian 2003), or by using a simulation tool to generate random fields (Vanmarcke 1977a), where soil properties vary within the finite element mesh. The latter case has recently been called the Random Finite Element Method (RFEM) (Fenton 1996) and typically requires Monte Carlo simulations, where each analysis is a representation of the random field (Baecher and Christian 2003). Vanmarcke et al. (1986) conducted an early investigation using this method, which they labelled stochastic finite elements with random fields. However, more recent applications of this technique have been discussed by Fenton et al. (1996, 2003) and Fenton and Griffiths (2002, 2005), who investigated the reliability of settlement on a spatially random soil. The use of finite element methods within a Monte Carlo framework does, however, require a large number of computations (Baecher and Christian 2003). As such, Baecher and Ingra (1981) described a direct evaluation by incorporating the first order estimates of the variance and covariance into the finite element formulation. The benefit of a simulation method is that little knowledge is required regarding the performance function. Instead, the performance function is determined by the results of each realisation in the simulation.

Griffiths et al. (2002b) have compared the use of FOSM and point-estimate methods with the stochastic finite element method. They preferred the stochastic finite element method, as it did not require knowledge of the density function of the input variables and could accommodate the spatial correlation of soil properties. Guan and Melchers (2000) also compared FOSM with Monte Carlo simulation techniques, where they observed that FOSM tends to underestimate the probability of failure with respect to the Monte Carlo solution.

Even after a probability of failure has been determined, Phoon et al. (1995) suggested that comparing this to a target probability is not straightforward. Although the aim of reliability-based design is to ensure that the probability of failure does not exceed a threshold, it is also important that it does not depart significantly from the same threshold. Within this framework, cost-benefit studies are common, yet the consequences affect society as a whole (Whitman 1984, Vick 1992). A cost-benefit philosophy is well illustrated in Figure 2-15, which shows the change in total costs as the probability of failure increases. However, the probability of failure only decreases for an increase in initial cost. This technique also allows the identification of a most efficient design, which yields the least total cost (Baecher et al. 1980, Mortensen 1993).

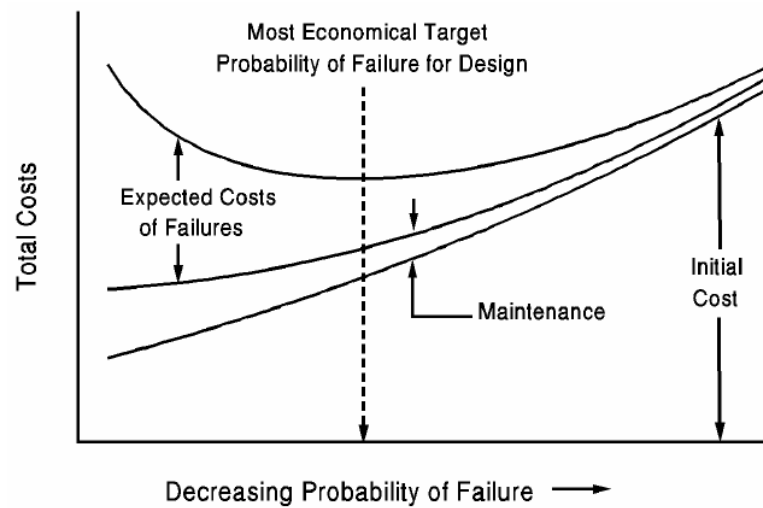


**Figure 2-15 Cost-benefit analysis**  
After Phoon et al. (1995)

Such cost-benefit analysis requires the formulation and inclusion of costs. For the purposes of this research, any analysis including costs associated with failures is referred to as a risk analysis. Vanmarcke (1977b) suggested risk analysis allows the rational consideration of uncertainties in the system that affect the probability of failure.

## 2.5 SUMMARY

The treatment of the literature in this chapter has indicated a general move towards the use of reliability-based foundation design. This is a result of large uncertainties associated with traditional foundation design processes, and potential financial and time costs. The use of reliability-based methods requires an appreciation of uncertainties in the system. In the past, several sources of uncertainty seem to have been investigated more thoroughly than others. A similar situation is also evident in the actual foundation design process, where test methods and design relationships have been well documented and calibrated, yet the design of a site investigation has had little treatment from a reliability point of view.

## Chapter 3 METHODOLOGY DEVELOPMENT

### 3.1 INTRODUCTION

---

This chapter discusses the development of a methodology to quantify the risk of a geotechnical site investigation, based on the impact on the resultant foundation design. An overview of the method is followed by a detailed treatment of the critical aspects and any assumptions or simplifications that are considered necessary.

### 3.2 METHOD OVERVIEW

---

The methodology is used to conduct two types of foundation design. These designs are best described as:

1. *Foundation design based solely on data from a site investigation (SI)*

This design process mimics the real-world design process, where the soil deposit is sampled using a program of common geotechnical tests to determine suitable information to be used in a common footing response prediction technique; and

2. *Foundation design based on complete knowledge of the soil (CK)*

This design process is based on the complete knowledge of the soil where every property is known in detail. The results of this process are considered the optimal or benchmark design and represent the best design for the soil considered.

The second or CK design type is neither feasible nor practical at a real site, as complete knowledge of the soil is never attainable (Clayton 2001). This is because it is not economical to conduct tests at every location, and testing without errors is destructive (e.g. the soil is removed from site and tested in a laboratory). Therefore, the results of this research are based on a simulated soil, where soil properties are generated from a numerical model to conform to the property variability and correlation known to exist in representative soils.

Using a simulated soil allows knowledge of every property at all locations, which in turn makes the second or CK design type possible. The additional benefit of using simulated soils is the ability to generate multiple sites and investigate the effect of many different variables, including soil variability. It is also possible to incorporate the four main sources of uncertainty inherent in a geotechnical model. These sources have been discussed earlier in Chapter 2 and include: (i) inherent soil variability; (ii) statistical uncertainty; (iii) measurement and (iv) model transformation error.

A comparison between the two design types (SI and CK) allows conclusions regarding the performance of the site investigation strategy and soil response prediction technique adopted for the design with respect to the CK design. Furthermore, examination of the resulting design footing area, based on the SI, also allows conclusions regarding the cost effectiveness of that particular investigation strategy. By incorporating these analyses into a Monte Carlo framework, it is then possible to quantify the risk and reliability of the SI design.

The various components of the methodology are developed in the form of a computer code using the FORTRAN 77 compiler language. This conforms to the code used to generate three-dimensional random fields, developed by Professor Gordon Fenton (Dalhousie University, Canada) and a three-dimensional finite element code, developed by Professor Vaughan Griffiths (Colorado School of Mines, United States of America). Extensive programming has also been undertaken by the author to develop additional models needed to conduct the research.

The framework of this methodology was introduced by Jaksa et al. (2003). The methodology has since been modified and deals only with the settlement of foundations, rather than bearing capacity. This is necessary to reduce the number of inherent variables to a manageable quantity as well as yielding reasonable times to achieve computational solutions. Also, Bowles (1997) suggested that foundation settlements, especially differential settlements, are the major cause of structural distress. As such, the framework is illustrated in Figure 3-1, where the highlighted steps are discussed later in this chapter.

The components of the methodology that have not been highlighted in Figure 3-1, deal with the risk analysis of a site investigation with respect to a foundation design. These components incorporate the associated costs with the site investigation and foundation construction, as well as potential failure costs. Details of the implementation of these components are presented in Chapter 8, including the results of the risk analysis.



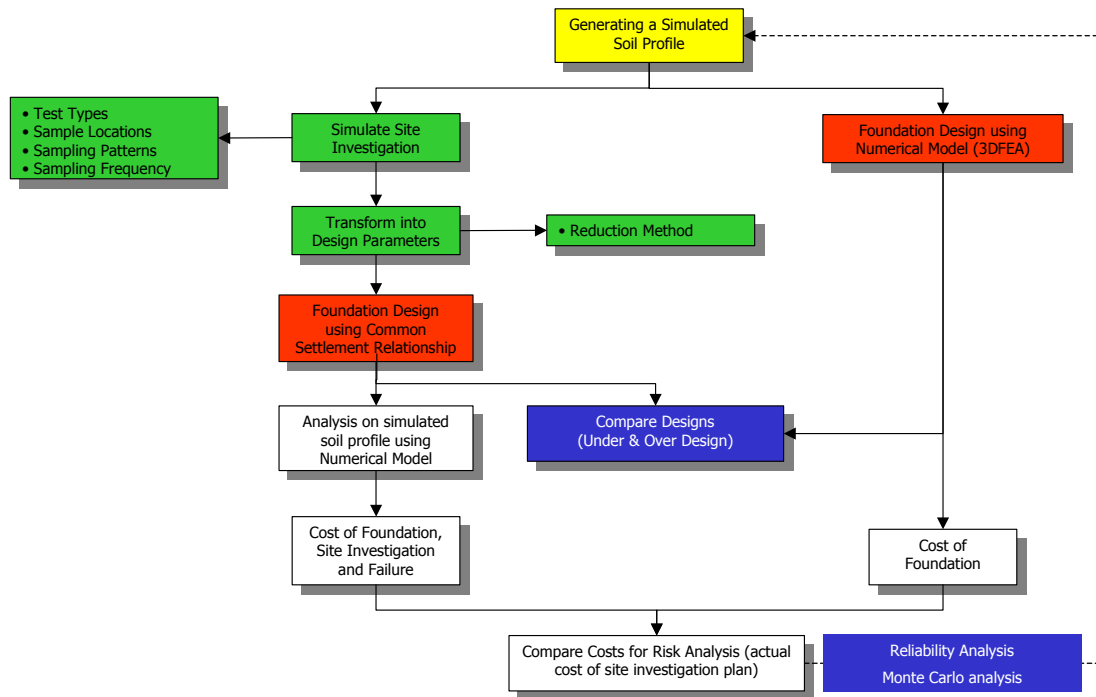


Figure 3-1 Simulation model flowchart

### 3.3 SOIL SIMULATION

To ensure that the results achieved by the methodology are representative of a geotechnical design process, it is essential that the variability and correlation between properties in the simulated soil are similar to real soil deposits. Several researchers have investigated the variability and correlation of soil properties using probabilistic methods such as *random field theory* and *geostatistics* (e.g. Matheron 1965, Vanmarcke 1977a, 1977b, 1983, Souliè et al. 1990, Jaksa et al. 1993, Jaksa 1995). The results and conclusions of these studies are combined with a method to generate three-dimensional random fields to simulate soils. The implementation of this framework is described in the following sections.

#### 3.3.1 Target Distribution and Correlation Structure of Simulated Soil

The target distribution and correlation structure of properties uniquely describes the variability of a soil (Vanmarcke 1983, Fenton and Vanmarcke 1990). The target distribution is typically defined by the mean and variance, or coefficient of variation (COV) of the soil properties, where the COV is adopted in this research. The correlation structure has already been discussed in Chapter 2 (§2.3.2.3), where the use of the scale of fluctuation (SOF) was used to characterise the degree of correlation in a soil.

To illustrate the difference between fields with large and small SOFs, a vertical sample from 6 soil sites with different SOFs is shown in Figure 3-2. Each soil site has the same variability or COV. However, when the elastic moduli are sampled over a finite depth of 30 m, as shown in Figure 3-2, the properties have very different degrees of variability. For example, the sample taken in a soil with a low SOF [Figure 3-2(a)] has a larger variability than in a soil with a high SOF [Figure 3-2(f)]. This is because the properties in a sample with a high SOF show self-similar behaviour, which has a marked influence on the sample variability.

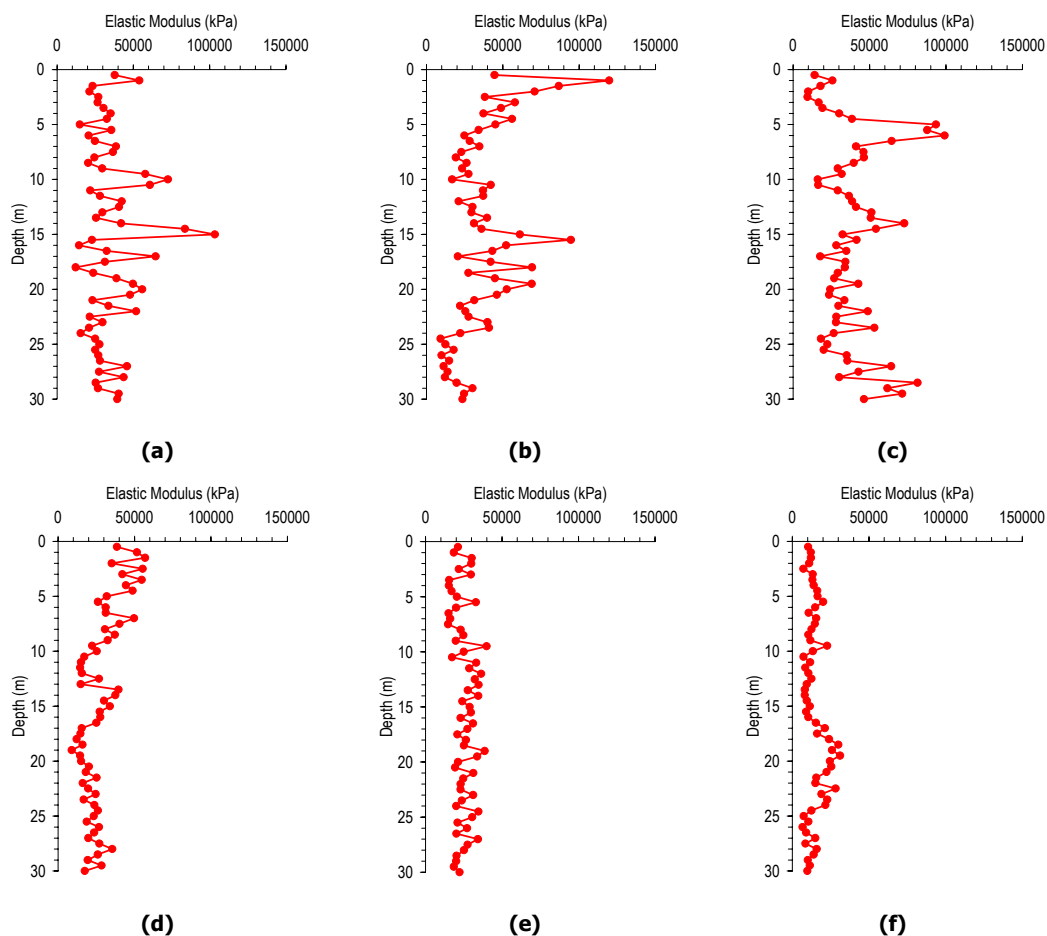


**Figure 3-2 Elastic modulus values for a soil COV of 50% and SOF of (a) 1 m, (b) 2 m, (c) 4 m, (d) 8 m, (e) 16 m and (f) 32 m**

As this research is concerned solely with the settlement or serviceability of a foundation, one need only investigate the properties that affect settlement. Since settlement will be confined to linear-elastic deformation, only the elastic properties of soils are relevant. These are the elastic modulus, or Young’s modulus ( $E$ ), and the Poisson’s ratio ( $\nu$ ). The elastic modulus is a measure of the relationship between stress and strain, while the Poisson’s ratio is a measure of lateral to axial strain. Fenton et al. (1996) concluded that the

variability of Poisson's ratio has little effect on footing settlement. Accordingly, the Poisson's ratio is treated here as a deterministic parameter. Hence, the elastic modulus is the only property used in this research that is treated stochastically as a random variable.

Statistical properties, including the sample distribution and correlation structure, of common soil types have been discussed in Chapter 2. Because there did not appear to be any general trend for the coefficient of variation (COV) and scale of fluctuation (SOF) for different soil types, a range of COV and SOF values is investigated. These ranges are shown in Table 3-1 for the mean ( $\mu$ ), coefficient of variation (COV), and scale of fluctuation (SOF) in both the horizontal,  $\theta_h$ , and vertical directions,  $\theta_v$ . It should be recognised that these ranges are only applicable to the elastic modulus of soil. Poisson's ratio is set to have a uniform value of 0.3. This value of Poisson's ratio appears to be suitable for both sand and clay soils (Lee et al. 1983, Djoenaidi 1985, Bowles 1997).

**Table 3-1 Range of statistical properties used in soil simulation**

Elastic Modulus, $E$	
Mean ( $\mu$ )	10,000 – 40,000 kPa
Coefficient of Variation, COV ( $\sigma / \mu$ )	10, 20, 50, 100%
Scale of Fluctuation, SOF	
Horizontal ( $\theta_h$ )	1, 2, 4, 8, 16, 32 m
Vertical ( $\theta_v$ )	1, 2, 4, 8, 16 m
Poisson's Ratio, $\nu$	
Deterministic Value (uniform)	0.3

In accordance with the discussions in Chapter 2, elastic modulus values are assumed to conform to a lognormal distribution. Essentially this is because the elastic modulus is strictly non-negative, which is a condition well represented by the lognormal distribution (Fenton 1999). Furthermore, Lumb (1966), Hoeksema and Kitaniadis (1985) and Sudicky (1986) stated that most soil properties are well represented by the lognormal distribution. The consequences of assuming a lognormal distribution on the simulated soil properties and the design of the foundation are discussed in subsequent chapters.

For the majority of the results that follow, different mean elastic modulus values are not investigated. This is because the data shown in Chapter 2 indicated that the mean is highly dependent on the site location. Therefore, the mean elastic modulus, for each soil, is based on the magnitude of the footing loads to ensure that a suitable footing design is possible.

It is also important to recognise the assumption of weak stationarity where the mean and correlation of properties in the soil are unaffected by their location. As such, this research has not considered trends in the soil properties. This is due to the limited literature regarding trends associated with the elastic modulus of soil. Furthermore, Spry et al. (1988) and Fenton (1999) suggested that trends in soil data should only be considered when they have physical meaning. Instead, a gradual increase in the mean could be the result of larger scale effects and therefore, should be described by the variability of the property and not a mean trend.

The form of the correlation structure is also used to describe the variability of a soil. This describes how the correlation between values behaves as the separation distance between them increases. Fenton (1996) suggested that a Markov model is common for modelling soil properties. This type of model has been previously discussed in Chapter 2 [§2.2.2.3 – Equations (2.23) and (2.24)].

Simulated soils in this research are all generated with an isotropic correlation structure in the horizontal direction (i.e.  $\theta_x = \theta_y$ ). This allows the use of a single SOF ( $\theta_h$ ) to be adopted. However, this is not necessarily the case for all three directions. Therefore, several simulated soils are also generated with a different SOF in the horizontal and vertical direction. Typically, these soils are identified by the degree of anisotropy ( $\theta_h / \theta_v$ ). Because soils usually show larger correlation in the horizontal rather than in the vertical direction, due to their forming processes in layers (Jaksa et al. 2005), simulated soils with a larger SOF in the vertical direction are not considered. In addition, it is commonplace to adopt a single horizontal SOF.

The Markov exponentially decaying correlation model given in Equations (2.23) and (2.24) is an example of a finite scale model. Such models do not simulate the large-scale dependence that has been shown to exist in some soil deposits (Fenton 1999). Such large-scale dependencies are typically modelled using fractals. However, due to increased complexities dealing with such correlations, and the fact that soils do not explicitly show fractal behaviour (Jaksa and Fenton 2002), the finite scale models given earlier in Chapter 2 [Equations (2.23) and (2.24)] are considered suitable for the purposes of this research.

Throughout this research, abbreviations are used to describe the statistical properties used to generate the elastic modulus field representing the simulated soil. In general, the soil COV is shown with the SOF in parenthesis. For example, a **50(8)** soil refers to a simulated soil with a COV of 50% and SOF of 8 m. In this case, the simulated soil has an isotropic

correlation structure, identified by the single SOF value in the parenthesis. However, when anisotropic conditions are investigated, a notation of **50(8,4)** is used to represent a simulated soil with a COV of 50% and a SOF in the horizontal direction of 8 m and a SOF in the vertical direction of 4 m. Because the results in this research do not consider a fully anisotropic correlation structure, where the SOF is different in all three directions, only two SOF values are used to describe a soil.

### 3.3.2 Generating Random Fields

*Random field theory* and *geostatistics* are two common probabilistic methods that have been successfully used to describe the correlation in soil properties, as already discussed in Chapter 2. Random field theory (Vanmarcke 1983) makes use of a measure called the autocovariance or autocorrelation function, while geostatistics (Matheron 1965) makes use of the semivariogram to describe correlations between properties at different spacings. Baecher and Christian (2003) suggested that the use of the autocovariance function is more common in geotechnical engineering than the use of the semivariogram. This is despite the autocovariance function requiring a greater assumption regarding the stationarity of the sample. These two models have also been used to generate fields that conform to the variability and correlation known to exist in soils. Deutsch and Journel (1992) have discussed the use of sequential Gaussian simulation (SGS) and sequential indicator simulation (SIS) in the geostatistical framework, while Fenton (1996) has compared the efficiency and accuracy of six random field generators.

The random field generators discussed by Fenton (1996), require only the nomination of the distribution with target mean and variance and the target correlation structure. The Moving Average (MA), Discrete Fourier Transformation (DFT) and Covariance Matrix Decomposition methods yield random fields that conform to the target distribution and correlation structure with a high degree of accuracy (Fenton 2002). However, such methods require complex calculations and are therefore, time and computationally exhaustive. Instead, Fenton (2002) suggested the Fast Fourier Transformation (FFT), Turning Bands Method (TBM), and Local Average Subdivision (LAS) as very efficient random field generators, although some loss of accuracy is expected. The LAS method involves discretising the field into a finite number of elements and is the fastest of the approximate methods. This method is able to simulate a two-dimensional field ( $128 \times 128$  elements) 45% faster than the FFT and 370% faster than the TBM using 64 lines (Fenton 1990).

As LAS appears to generate random fields considerably faster than the other approximate random field generator and does not suffer from a symmetric covariance structure, it is adopted for this research. The LAS methodology has been described in detail by Fenton (1990) and is loosely based on the stochastic subdivision algorithm developed by Carpenter (1980) and Fournier et al. (1982). However, Fenton (1990) commented that this algorithm suffered from aliasing problems which were attempted to be rectified by Voss (1984). The method proposed by Fenton (1990) proceeds in a top-down, recursive manner, where a global average of the process is generated at Stage 0, as indicated in Figure 3-3. The values in subsequent stages are estimated by subdividing the parent cell from the previous stage into 2 regions. The local averages of these new cells must conform to the parent cell average, which in turn preserves the global average throughout the process.

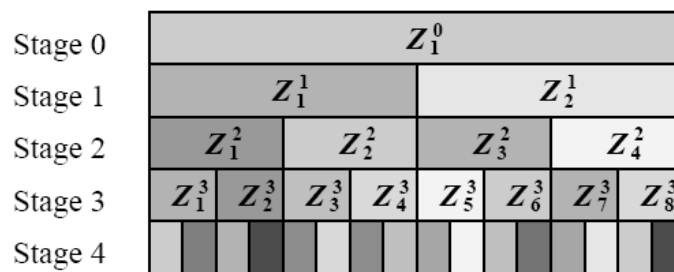


**Figure 3-3 LAS process illustrating a top-down approach**  
After Fenton (1990)

Consider the two new regions below any parent cell as their child cells. The child cell values are approximated by sampling from a distribution that has been conditioned on a range or neighbourhood of parent cell values. For example, the distribution is not only conditioned on the parent cell, but also other cells in the previous stage adjacent to the parent cell. The new child cell values must conform to the following:

1. Their variance must conform to local averaging theory;
2. They must be appropriately correlated with each other;
3. Their averages must conform to the average of their parent cell in the previous stage; and
4. They are appropriately correlated with adjacent cells.

Fenton (1990) examined the accuracy of LAS when estimating a one-dimensional Ornstein-Uhlenbeck process, which has an exponentially-decaying correlation structure.

These results are given in Figure 3-4, comparing the correlation structure of a simulated process generated using LAS and the exact correlation. The results in Figure 3-4 are based on an averaging dimension,  $D$ , and a scale of fluctuation,  $\theta$ . The differences between the exact and LAS correlation structures shown in Figure 3-4 are the result of approximations of cross-cell covariances, whereas covariances within the cells are preserved exactly.

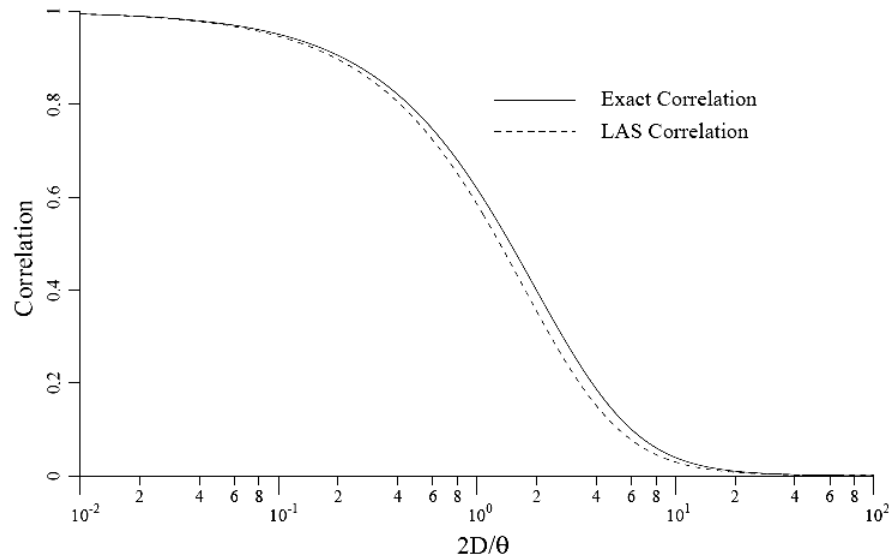


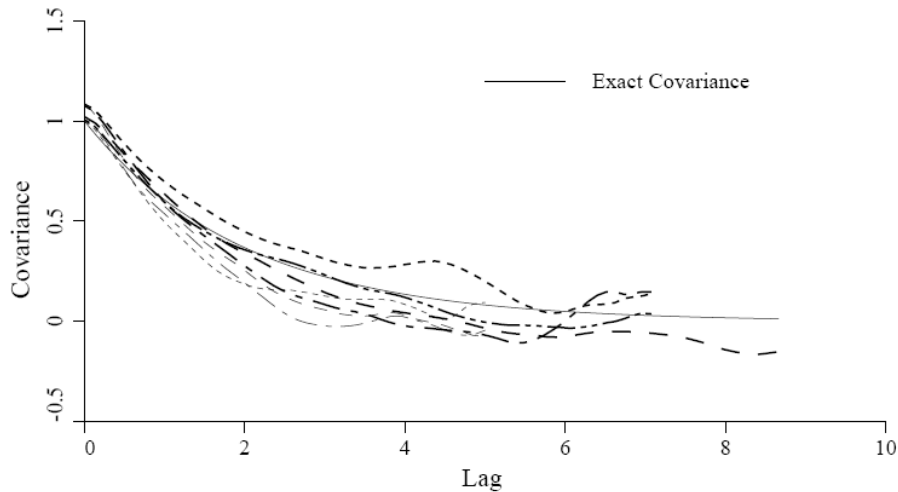
**Figure 3-4 Comparison of estimated and exact covariances across cell boundaries in Local Average Subdivision process**  
After Fenton (1990)

The LAS correlation structure shown in Figure 3-4 was generated using a neighbourhood size of 3, where the distribution used to generate the child cell values was conditioned on the parent cell value and values from the cells either side of the parent cell in the previous stage. Fenton (1990) suggested that a neighbourhood size of 3 is sufficient for the simulation of a process with a monotonically-decreasing correlation structure that is reasonably smooth. However, when the correlation structure is oscillatory a neighbourhood size of 5 is required. Such an increase in neighbourhood size approximately doubles the time required to generate a process (Fenton 1990). Boundary conditions also pose a problem when generating processes using LAS. This is because a neighbourhood size greater than 1 may require the conditioning of a distribution based on parent cell values outside the domain. Fenton (1990) overcame this problem by assuming that the values outside the domain have no bearing on the process being generated.

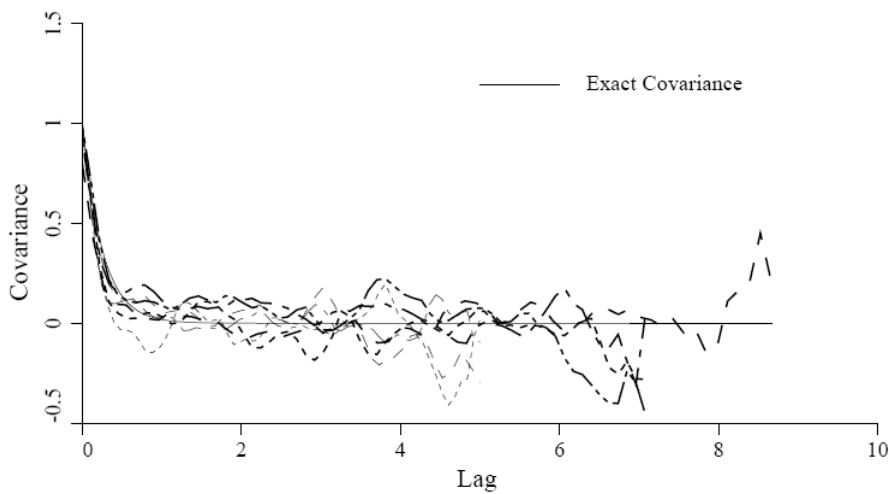
The accuracy of LAS is also improved when the simulated correlation structures are averaged over a suite of realisations. For example, several simulations of the same process are generated and the statistics of the process are averaged over the suite. In other words, the

errors are self-correcting, where the rate of convergence of the estimated statistics to the exact one is  $1/n$ , where  $n$  is the number of realisations (Fenton 1990).

The multi-dimensional extension of LAS has no notable differences in implementation. However, rather than the parent cell being subdivided into 2 child cells, it is subdivided into 4 child cells for a two-dimensional problem and 8 child cells for a three-dimensional field. The multi-dimensional cases still employ the same processes for ensuring that the child cell averages conform to the parent cell average and that values meet within-cell and cross-cell correlations. Results of using LAS to generate three-dimensional fields with an exponentially decaying correlation structure are shown in Figure 3-5(a) and (b) for scales of fluctuation of 4 and  $1/2$ , respectively. These results have been averaged over a suite of realisations and show that LAS appears to simulate the exact correlation structure with an acceptable degree of accuracy.



(a)



(b)

**Figure 3-5 Estimated covariance using LAS for 3-D isotropic field with scale of fluctuation (a)  $\theta = 4$  (Averaged over 50 realisations) and (b)  $\theta = 1/2$  (Averaged over 10 realisations)**  
After Fenton (1990)



The results shown in Figure 3-5 are based on simulated fields with an isotropic correlation structure, where the SOF is the same in all three directions. However, multi-dimensional fields may also possess an anisotropic correlation structure where the SOF is different in all directions. In this case, Fenton (1990) suggested that post-processing of the simulated field is preferred, as their generation tends to target an isotropic correlation structure defined by the lowest specified SOF. Therefore, such fields are generated with an isotropic correlation structure first, and then stretched to conform to the anisotropic correlation structure required.

### 3.3.3 Transformation of the Generated Soil Properties

The local average subdivision (LAS) method discussed in the previous section, generates a three-dimensional random field conforming to a normal distribution and target correlation structure. However, previous discussions have indicated that soil properties typically show lognormal behaviour where properties are strictly non-negative. Therefore, it is necessary to transform the random field simulated by LAS from a normal into a lognormal variable. This is achieved by using the transformation given by:

$$X_{\ln} = \exp(\mu_{\ln x} + \sigma_{\ln x} X) \quad (3.1)$$

where  $X_{\ln}$  is the lognormal variable,  $X$  is the normal variable obtained from LAS generation of the random field and  $\mu_{\ln x}$  and  $\sigma_{\ln x}$  are the mean and standard deviation, respectively, of the lognormal variable given by:

$$\mu_{\ln x} = \ln(\mu_x) - \frac{1}{2} \sigma_{\ln x}^2 \quad (3.2)$$

and

$$\sigma_{\ln x} = \sqrt{\ln\left(1 + \frac{\mu_x^2}{\sigma_x^2}\right)} \quad (3.3)$$

where  $\mu_x$  and  $\sigma_x$  are the mean and standard deviation of the normal variable, respectively. Although the use of a lognormal variable ensures non-negative soil properties, it also introduces a condition whereby the mean is affected by the variance, as shown in Equation (3.2). This influences the results of the soil simulation and is discussed in subsequent chapters. It should be noted, however, that the transformation shown in Equation (3.1)

preserves the median of the field, which is best estimated using a geometric average. The formulation and use of the geometric average is discussed later.

### 3.3.4 Effects of Local Averaging on Random Fields

Properties generated by LAS are averaged values representative of the cell or element size. Although, at first, this may seem inadequate, Fenton (1990) commented that nearly all information about the world is provided as averages. Therefore, it is important to consider the effects of using such averaged values in this research. Vanmarcke (1983) dealt with local averages within a random field and concluded that the averaged value is significantly dependent on the averaging domain and correlation distance or SOF. He determined that the apparent variability of the averaged value decreased, as the domain increased or the SOF became smaller. This is represented by the variance reduction factor (Vanmarcke 1983), which, for a process or field with an exponentially-decaying correlation structure, is given by:

$$\gamma(D_v) = 2 \left( \frac{\theta}{2D_v} \right)^2 \left( \frac{2D_v}{\theta} - 1 + e^{-2D_v/\theta} \right) \quad (3.4)$$

where  $\gamma(D_v)$  is the variance reduction based on an averaging domain of size  $D_v$ . The variance reduction ranges between 0, when the averaging domain is much larger than the SOF, and 1, when the averaging domain is small. Additional discussions concerning local averaging have been made by Vanmarcke (1977a, 1983).

In a field that is based on a target lognormal distribution the effects of local averaging are also observed in the mean. This is due to the presence of the variance of the lognormal variable,  $\sigma_{\ln x}^2$ , in the relationship for the mean,  $\mu_{\ln x}$ , as indicated in Equation (3.2). When the effects of local averaging are included, the mean of the lognormal variable is given by:

$$\mu_{\ln x} = \ln(\mu_x) - \frac{1}{2} \gamma(D_v) \sigma_{\ln x}^2 \quad (3.5)$$

It is also important to consider the effects of local averaging when verifying the accuracy of the simulated soils with respect to the target variability and correlation structure. Such verification measures are discussed in Chapter 4. Effects of local averaging have also influenced the results measuring the performance of site investigations. These effects are discussed in subsequent chapters.

### 3.3.5 Size of the Simulated Soil Site

A site size equal to 50 m × 50 m in plan and 30 m in depth is adopted in this research. This size is chosen because of sampling intervals and computational time considerations that are discussed later in this chapter. Such a site size allows a building with a floor plan size of 20 m × 20 m to be located centrally, while still maintaining sufficient distance to the edge of the site. (The effect of the proximity of the footing location to the edge of the site is discussed later in this chapter.)

As discussed earlier, LAS requires the subdivision of the site into a finite number of elements. The number of elements, and therefore the size of each individual element, is constrained by computational time and relative accuracy. Such restrictions are discussed later in this chapter. The only constraint imposed by LAS is on the total number of elements in each direction. This total must be a power of 2 (Fenton 1990). For example, the number of elements in each direction must be either;  $2^1$ ,  $2^2$ ,  $2^3$ , ...,  $2^n$ . Furthermore, as will be explained later, an element size of 0.5 m × 0.5 m × 0.5 m is adopted. This results in a field size of 100 × 100 × 60 elements. Therefore, to conform to the requirements of LAS, a field with 128 × 128 × 64 elements is generated and the desired field size of 100 × 100 × 60 elements is extracted from it, with the remaining elements being discarded.

## 3.4 SITE INVESTIGATION

As introduced in Chapter 2, a site investigation is essentially a sampling exercise, where samples are taken at specific locations within a site with the aim of accurately and sufficiently characterising the underlying soil conditions. In this research, a site investigation strategy or scope is characterised by:

- The number of samples taken;
- The pattern in which the samples are arranged;
- The method used to reduce the results of multiple samples into a manageable form; and
- The type of geotechnical test used to obtain properties from the samples.

The following sections discuss the adopted definition of a site investigation and the incorporation into the methodology used in this research.

### 3.4.1 Patterns and Quantity of Sampling

Sampling patterns investigated in this research are based on the most common methods, as discussed by Ferguson (1992) and introduced in §2.1. These include the regular grid (RG), stratified random (SR) and simple random (RN) approaches. Such patterns are relatively straightforward to incorporate into the methodology. Although Ferguson (1992) suggested that the herringbone pattern is the most effective, it is essentially a regular grid, and it is rare that site investigations of the scale described in this research would adopt such a pattern.

The first step required in the methodology is to nominate a site investigation size, which is typically centred about the site or the proposed location of the building, as shown in Figure 3-6. The size of the site investigation is defined by the plan area within which sample locations are positioned. Typically, the size of the site investigation is set to be the same size as the building plan. Therefore, based on discussions above, the site size is, for most of the analyses that follow, assumed to be  $50\text{ m} \times 50\text{ m}$ , where  $St_x = St_y = 50\text{ m}$  and the site investigation size is assumed to be  $20\text{ m} \times 20\text{ m}$ , where  $Ip_x = Ip_y = 20\text{ m}$ .

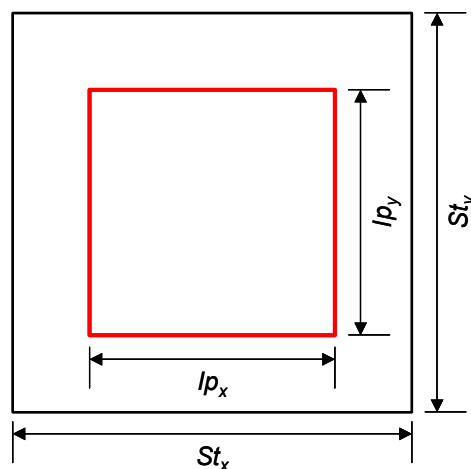


**Figure 3-6** Relative size of site investigation area compared with total site area

Based on the size of the site and the resultant site investigation, a maximum of 25 sample locations is adopted in a single investigation program. As such, the site investigation plan area is divided into segments, relative to the number of sample locations taken. These subdivisions or regions are shown Figures 3-7 and 3-8 for the RG and SR patterns, respectively. Figure 3-7 also indicates the actual sample locations at the centre of each region. This is not possible for the SR pattern, because sample locations are determined randomly within each region. Furthermore, no site investigation plan area divisions are required for

the RN sampling pattern. Rather, the sample locations are selected randomly within the site investigation area using a uniform, or equally likely, distribution.

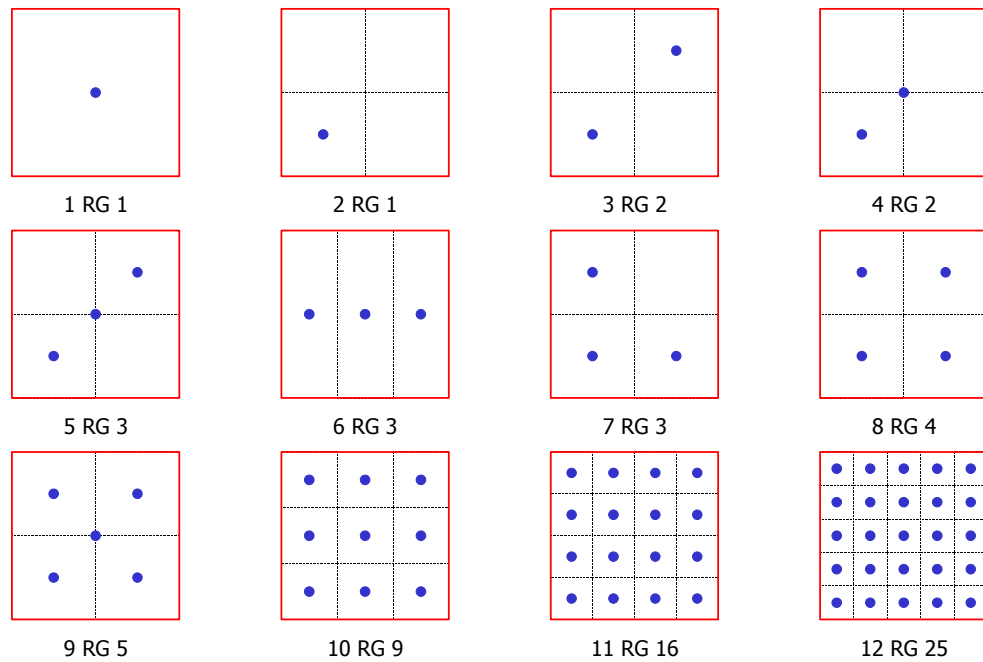


**Figure 3-7 Sampling patterns based on a regular grid (RG) pattern**

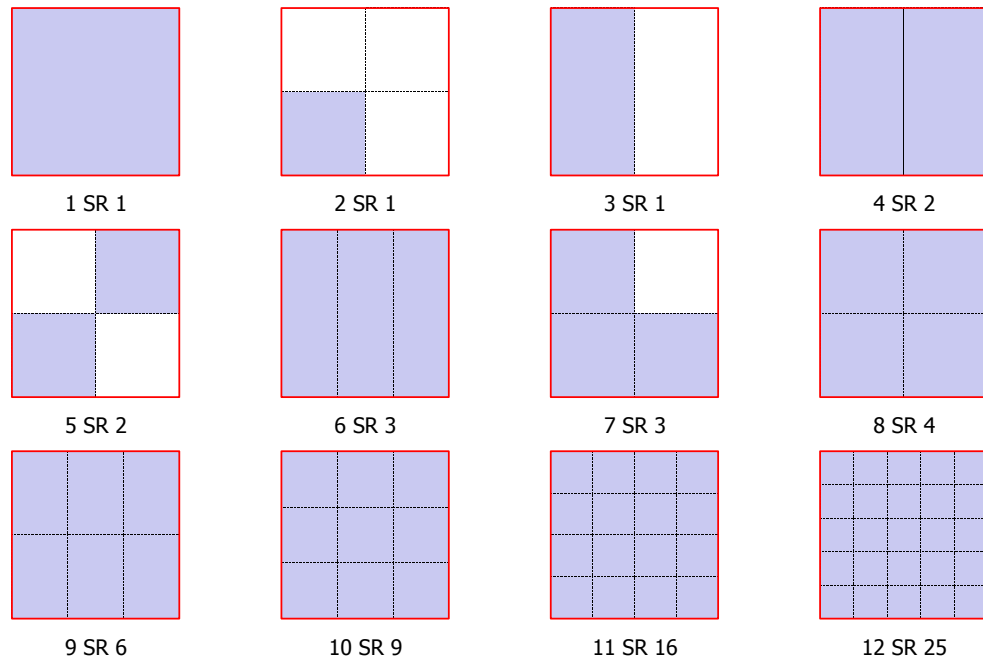


**Figure 3-8 Sampling patterns based on a stratified random (SR) pattern**

All patterns include 12 different site investigation programs, ranging from a single sample location up to 25 locations. The nomenclature indicated in Figure 3-7 and 3-8 is adopted to describe the sequential number of the investigation plan (1 – 12), the pattern (RG, SR or

RN) and the number of sample locations in the site investigation (1 – 25). This nomenclature is used throughout this thesis.

The majority of the results presented in this research deal with the number of sample locations that constitute a particular site investigation strategy. However, many standards or codes treat the scope of site investigation in terms of sampling density, which is defined as the number of samples within a given area. Such sampling densities are discussed in later chapters. To compare these recommendations with the sampling frequency discussed above, Table 3-2 presents the corresponding number of samples required within a given area based on a specified sampling density. Table 3-2 shows the equivalent number of samples per 300 m<sup>2</sup>, for each of the site investigation strategies, based on varying site investigation area size.

**Table 3-2 Sampling density based on 1 sample/300 m<sup>2</sup> compared with adopted sampling density for research methodology**

Plan Area	Samples / 300 m <sup>2</sup> based on total number of samples							
	1	2	3	4	5	9	16	25
20 m x 20 m	0.75	1.50	2.25	3.00	3.75	6.75	12.00	18.75
20 m x 30 m	0.50	1.00	1.50	2.00	2.50	4.50	8.00	12.50
30 m x 30 m	0.33	0.67	1.00	1.33	1.67	3.00	5.33	8.33
30 m x 40 m	0.25	0.50	0.75	1.00	1.25	2.25	4.00	6.25
40 m x 40 m	0.19	0.38	0.56	0.75	0.94	1.69	3.00	4.69
40 m x 50 m	0.15	0.30	0.45	0.60	0.75	1.35	2.40	3.75
50 m x 50 m	0.12	0.24	0.36	0.48	0.60	1.08	1.92	3.00

As discussed in Chapter 1, several codes recommend or require a minimum of 1 sample per 300 m<sup>2</sup> as being sufficient for a building of relative significance. This density relates to 0.8 samples in the site investigation area of 20 m × 20 m, or 0.1 samples, if the density considers the full site area of 50 m × 50 m. Another means of interpreting the results shown in Table 3-2 is that, for example, the sampling program consisting of 25 sample locations within a 20 m × 20 m plan area corresponds to a sampling density that is nearly 20 (18.8) times more intensive than the recommended 1 sample per 300m<sup>2</sup>. Alternatively, if these results are based on the entire site area (50 m × 50 m), then the sampling program consisting of 25 sample locations is equivalent to a sampling density of 3 times more intensive than that recommended. In addition, for the entire site area, 9 sample locations are approximately equivalent to the recommended 1 sample per 300 m<sup>2</sup>.

### 3.4.2 Soil Parameter Reduction Techniques

Most of the settlement prediction techniques introduced in Chapter 2 and discussed later in this chapter do not accommodate the horizontal variability of elastic modulus values. Instead, they require knowledge of a single vertical sample of elastic moduli. In fact, some techniques do not accommodate for elastic modulus values that vary in the vertical direction either. Therefore, it is necessary to specify a technique to combine the results from multiple sample locations into a suitable set of elastic moduli. Such a process can also be seen as the selection of a characteristic value from a set of sample or test results. The process is shown schematically in Figure 3-9, where the results of 4 different vertical samples are combined to attain a single vertical sample. Note that the addition signs shown in Figure 3-9 are for indicative purposes only, as several of the techniques adopted do not involve addition.

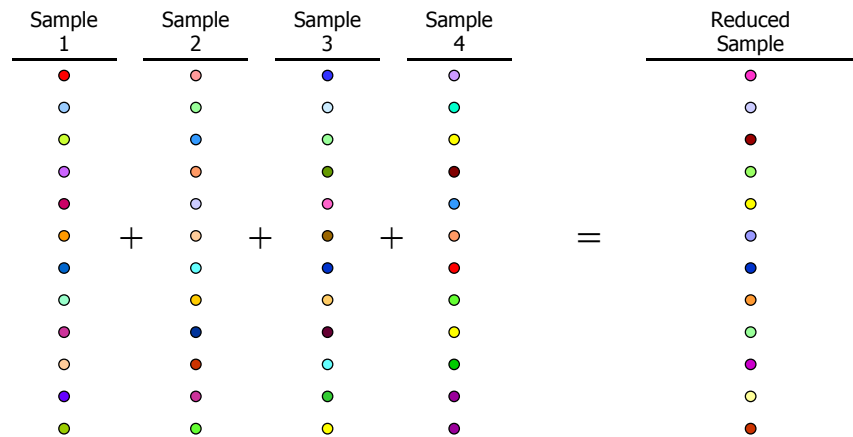


**Figure 3-9 Process of combining results from multiple samples into a reduced sample**  
 (Note: addition signs are for indication purposes only and do not necessarily infer a summation)

The process of combining the results of multiple samples into a single vertical sample is, in this research, referred to as a *reduction technique*. The reason for adopting this terminology in lieu of “averaging” or “combination” is that the various techniques examined involve a combination of averaging, weighting and selecting a threshold value.

Three of the reduction techniques adopted in this research are based on an average of the results from the different sample locations. These are the standard arithmetic average, SA, given by:

$$SA = \frac{1}{n} \sum_{i=1}^n x_i \tag{3.6}$$

the geometric average, GA, given by:

$$GA = \left( \prod_{i=1}^n x_i \right)^{1/n} \quad (3.7)$$

and the harmonic average, HA, given by:

$$\frac{1}{HA} = \frac{1}{n} \sum_{i=1}^n \frac{1}{x_i} \quad (3.8)$$

where  $n$  is the number of samples and  $x_i$  is the value of each property in the sample. The standard arithmetic average estimates the mean of the sample population and weights all individual properties equally, while the geometric and harmonic average are low-value dominated, where a single zero value in the sample yields a zero and infinite result, respectively. Fenton and Griffiths (2002) suggested that the geometric average of elastic moduli provides a better representation in a spatially random medium. This is because the standard arithmetic average is suited to strongly vertical layered media and the harmonic average is suited to strongly horizontal layered media. Therefore, in a spatially random soil, which is somewhere between a strongly vertical and horizontal layered medium, the geometric average appears to be better suited. However, these conclusions were based on averaging all elastic moduli located beneath a footing, whereas the reduction technique is concerned with combining results from a series of sample locations, not necessarily beneath a footing.

Two reduction techniques considered in this research are determined based on the separation distance between the sample location and the footing. These methods are the inverse distance weighted technique, ID, given by:

$$ID = \sum_{i=1}^n \frac{S_i}{S_{tot}} x_i \quad (3.9)$$

and the inverse distance squared technique, I2, given by:

$$I2 = \sum_{i=1}^n \frac{S_i^2}{S_{tot}^2} x_i \quad (3.10)$$



where  $s_i$  is the distance between the  $i$ th sample location and the proposed footing and  $s_{tot}$  is the total distance between all sample locations and the proposed footing. Both the inverse distance and inverse distance squared techniques result in a greater importance or weight being assigned to the results of sample locations that are closer to the proposed footing. This is, in fact, the manner in which actual soil properties have been shown to behave, as discussed in the previous chapter. The limiting case is when the sample location coincides with the proposed footing. In this case, the results from this sample location are given a weight of 1.0 and the results from the remaining sample locations are ignored. This has important consequences on the variability of the design, as discussed in subsequent chapters.

The final two reduction techniques involve selecting a single value from the set of results. The first, the minimum threshold technique (MN) involves adopting the minimum value from each of the sample locations. This is an extremely conservative solution, where the weakest soil property is chosen from the sampled data. On the other hand, the 1<sup>st</sup> quartile technique (1Q) involves determining the value that is equivalent to 25% of the range of values in the sample set. For example, if the minimum and maximum value from the sample data is 10,000 and 20,000 respectively, then the 1<sup>st</sup> quartile value is 12,500. Although this also appears to be conservative, it is not nearly as conservative as the minimum threshold technique.

It should be noted that different reduction techniques are only used to combine the results from multiple sampling locations. If a single elastic modulus value is required, the reduction technique is used to obtain a single vertical sample of values, and then these values are averaged using a standard arithmetic average.

### **3.4.3 Types of Soil Tests**

The discussion in Chapter 2 indicated that the performance between different types of soil tests is generally a function of uncertainties due to measurement and transformation model error. Four test types have been exclusively investigated throughout this research, as these are the most common tests used to characterise a soil for serviceability design. These include:

- Standard penetration test (SPT);
- Cone penetration test (CPT);

- Triaxial test (TT); and
- Flat plate dilatometer (DMT).

The first difference between these test types is the vertical sampling frequency. For example, the CPT is a relatively continuous in situ test, where soil properties are sampled at less than or equal to 20 mm depth intervals. However the SPT and DMT are examples of discrete vertical sample in situ tests, where soil properties are usually sampled at much larger depth intervals, i.e. 1.5 m. Furthermore, the TT is a laboratory test, where soil specimens are first sampled on site, and then transported to a laboratory where the TT is subsequently performed. Therefore, due to the costs associated with the TT, it is common that only a few samples per borehole (or sample location) are removed from the site for laboratory testing. The adopted vertical sampling rate of each test type is summarised in Table 3-3, based on an element size of 0.5 m × 0.5 m × 0.5 m and a soil layer depth of 30 m. For example, for the SPT, a sample is obtained every third element, representing a sampling depth frequency of 1.5 m. An analysis of the vertical sampling rates assume for the TT is also undertaken. The results of this analysis are discussed in Chapter 7 (§7.4.2). However, for most of the results that follow, the TT is based on 2 tests per sampling locations.

**Table 3-3 Vertical sampling frequencies for each test type**  
(element size = 0.5 m × 0.5 m × 0.5 m)

Test Type	Vertical Sampling Frequency	
	Depth Interval (m)	Element
Standard Penetration Test (SPT)	1.5	3
Cone Penetration Test (CPT)	0.5	1
Triaxial Test (TT)	15 (2 / sample location)	30
Flat Plate Dilatometer Test (DMT)	1.5	3

It should also be noted that the vertical sampling rate of 0.5 m assumed for the CPT is much larger than would be expected in the field. Therefore, differences between the CPT and other tests are not expected to be as noticeable. However, due to the restrictions imposed on element size regarding computational time, as discussed later in this chapter), an element size of 0.5 m is necessary.

The different types of soil tests are also distinguished by the degree of uncertainty attributed to their measurement and transformation model errors. Firstly, it is important to consider the methodology adopted to attribute such uncertainties to each test type. Consider

that  $E_f$  represents the elastic modulus values retrieved directly from the simulated soil. As such, the resulting elastic modulus value incorporating uncertainties due to measurement and transformation model error,  $E_r$ , is given by:

$$E_r = (tm)(m_b m_r)E_f \quad (3.11)$$

where  $tm$ ,  $m_b$  and  $m_r$  are the unit mean, lognormal variables representing the uncertainty due to transformation model error, bias and random measurement effects, respectively. These random variables are defined by a COV value based on published results discussed in Chapter 2. Such values for each test are given in Table 3-4. An analysis examining the influence of the values of  $m_b$  and  $m_r$  is also conducted. Results of this analysis are discussed in Chapter 7 (§7.4.2). However, the values shown in Table 3-4 are assumed to be representative of the errors in the test types for the majority of analyses undertaken.

**Table 3-4 Uncertainties due to measurement and transformation model error for each test type**

Test Type	Uncertainties Measured as COV		
	Transformation Model, $tm$	Measurement	
		Bias, $m_b$	Random, $m_r$
Standard Penetration Test	25	20	40
Cone Penetration Test	15	15	20
Triaxial Test	0	20	20
Flat Plate Dilatometer Test	10	15	15

It is also important to consider at what stage the uncertainties due to measurement and transformation model errors are included into the analysis. In other words, when the values of  $tm$ ,  $m_b$  and  $m_r$  are incorporated.

Uncertainties due to measurement errors are incorporated in a two-step process. To illustrate this process the soil data shown in Figure 3-10 provides an example of an original data set taken directly from a simulated soil. The broken line in Figure 3-10(a) indicates the sample mean of the original data set, which is evaluated over the entire depth of the sample. The bias mean is then determined by multiplying the sample mean of the original data set by the random variable,  $m_b$ , as shown by the green line in Figure 3-10(b). The test bias is assumed to be the difference between the sample mean of the original data set and the bias mean. This test bias value is then added to each value in the original data set to yield the green series shown in Figure 3-10(c), which is considered the biased sample.

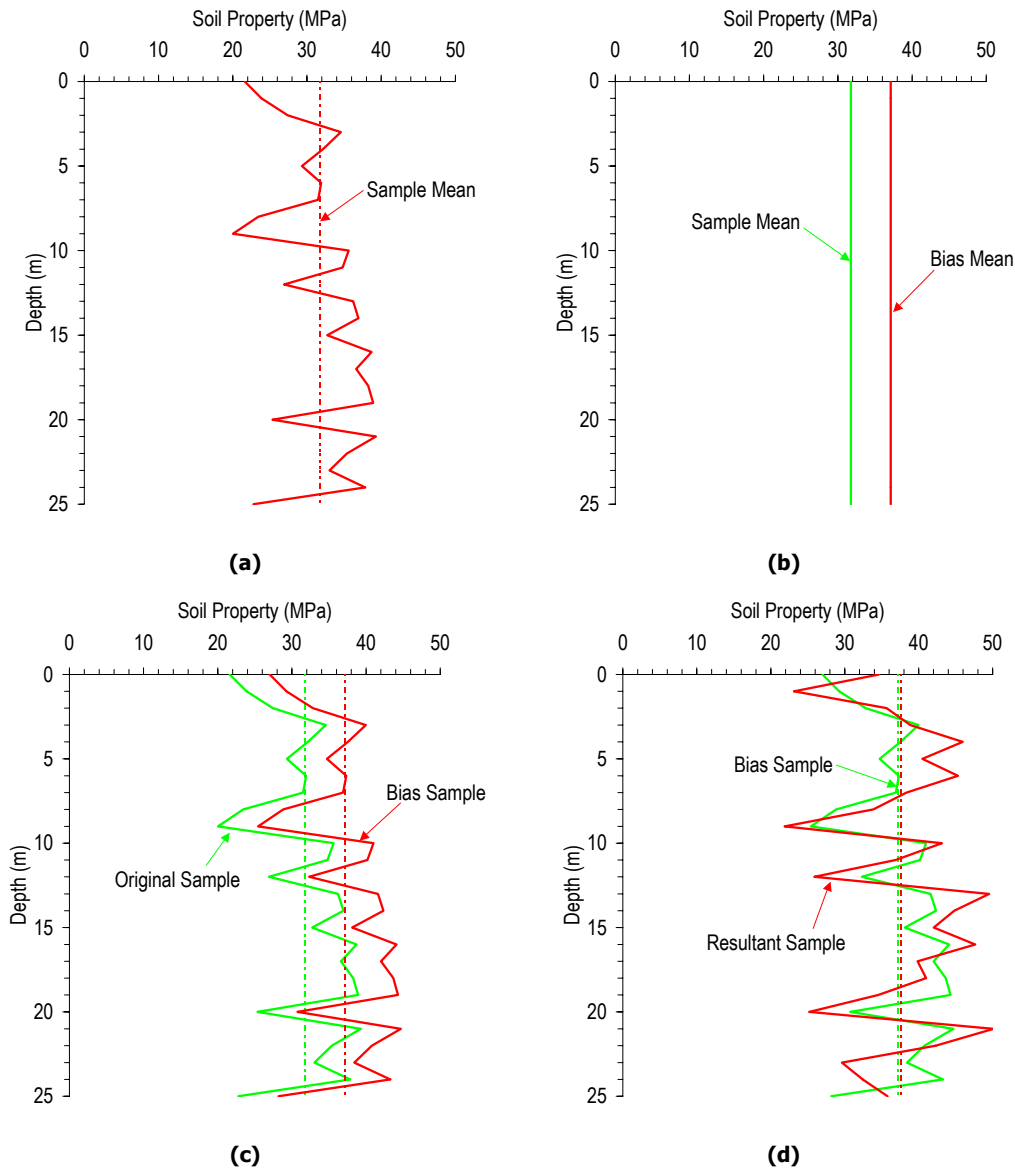


**Figure 3-10 Process of attributing test uncertainties**

The second step involves adding the uncertainties due to the random component of measurement error. This is achieved by multiplying each value in the biased sample by the random variable,  $m_r$ , to give the resultant sample set, shown in red in Figure 3-10(d). A comparison between the original data set and the resulting sample is shown in Figure 3-11 where the resulting sample is shown in red and the original in green.

The uncertainties due to transformation model error are included in the analysis after the uncertainties due to measurement error have been incorporated. Similarly, with the bias component of the measurement error, the uncertainties due to transformation model error are based on the mean of all the samples and the random variable,  $tm$ . It should be noted,

however, that the uncertainty due to transformation model error is constant for all samples in the site investigation program. For example, if the site investigation program consists of 9 sample locations and the uncertainty due to transformation model error yielded an increase of 500 kPa, then the results at each sample location are increased by 500 kPa. However, the next site investigation program may have a different uncertainty.

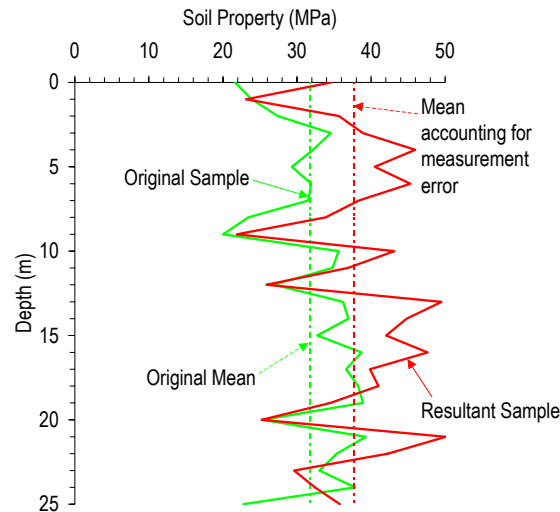


**Figure 3-11 Comparison of test values with bias and random effects and actual soil properties**

As this research is solely concerned with the serviceability design of a foundation, only the performance of the types of soil tests in relation to the elastic modulus of the soil are investigated. Therefore, conclusions regarding the effectiveness and suitability of the types of soil tests from this research are applicable only to situations dealing with the serviceability design of a foundation.

### 3.5 FOUNDATION DESIGN METHODOLOGY

The method adopted to design a foundation in this research is no different to the processes described by many well-known foundation engineering books (e.g. Fang 1991, Bowles 1997). Essentially, the method involves determining a footing size that meets the specified design criteria. The method exclusively deals with the design of pad foundations, where the size of the footing is relatively small and internal bending moments are typically not significant. However, consideration is also taken when a pad foundation does not meet the design criteria and, as such, an alternative foundation type is required. These conditions are discussed later in this section. Furthermore, the design is based solely on a serviceability criterion, dealing with the settlement and differential settlement of the foundation. No

consideration is given to bearing capacity design because the numerical procedure to estimate the bearing capacity of a foundation involves non-linear soil models, which dramatically increases computational time. In addition, Bowles (1997) indicated that differential settlements are the major cause of structural distress.

The discussions in this section deal with the manner in which the footing geometry is varied to accommodate different footing sizes and the criteria used to determine the need for an alternative foundation type. The techniques adopted to estimate the settlement of the footing and the limits imposed on the design are discussed later.

### 3.5.1 Pad Foundation Geometry

Pad footings are designed to be either square or rectangular in plan. Since the adopted settlement prediction techniques (introduced in Chapter 2) estimate only the settlement of the footing and do not directly yield design dimensions, an iterative process is required, where the settlement for a given footing size is evaluated and compared to the design criteria, discussed in the following section. To target the most efficient design, the first footing size is the smallest possible footing, and then the size is increased until a suitable size, which conforms to the design criteria, is obtained. The process of increasing the footing size is shown in Figure 3-12, where the darker shaded area is the original footing size and the lighter shaded area shows progressively increasing footing sizes. The footing is increased in such a manner as to ensure that the load is applied centrally.

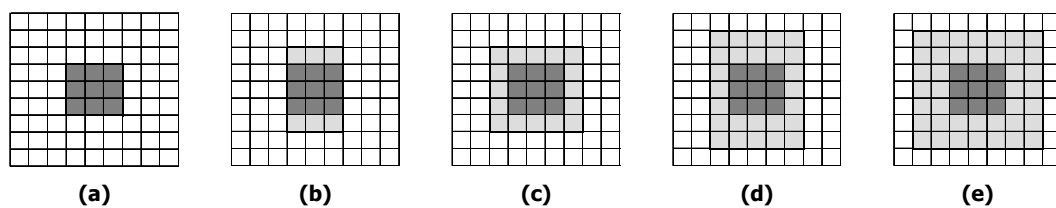


Figure 3-12 Process of increasing footing size

A drawback to the process shown in Figure 3-12 is the discretisation of the footing area. This becomes a significant issue when the analysis includes a three-dimensional finite element analysis (3DFEA). The use of 3DFEA requires the footing size to be constrained to the element size, which in this case is 0.5 m. This means that the footing is increased by 1 m for subsequent iterations. As such, it becomes difficult to target a footing size that meets the design criteria exactly. Instead, the smallest footing that conforms to the design criteria is selected. Although the footing size is constrained to the element size only when 3DFEA is used, the same process is adopted for all settlement relationships. However,

some of the results presented in subsequent chapters are based on the implementation of the methodology without 3DFEA and the optimal design has been found by other means. In this case, the footing size is increased by 0.1 m for subsequent iterations. This is discussed later, when these analyses are presented.

### 3.5.2 Requirement for an Alternative Foundation Type

In some of the analyses that follow, a pad foundation system that meets the serviceability criteria is not achievable. Typically, the threshold of concluding that a pad foundation is not suitable is based on the size of the individual pad footings. Therefore, a similar threshold is incorporated into this methodology, which controls when an alternative foundation type, such as a raft or piles, is required. This is based on the size of the individual pad footings and their proximity to adjacent footings. The threshold is reached when the design of a pad footing yields a dimension that is larger than half the distance to the closest footing, as shown in Figure 3-13. Computational and time constraints have limited this research solely to the design of pad foundations. The design of raft and pile foundations is beyond the scope of this study.

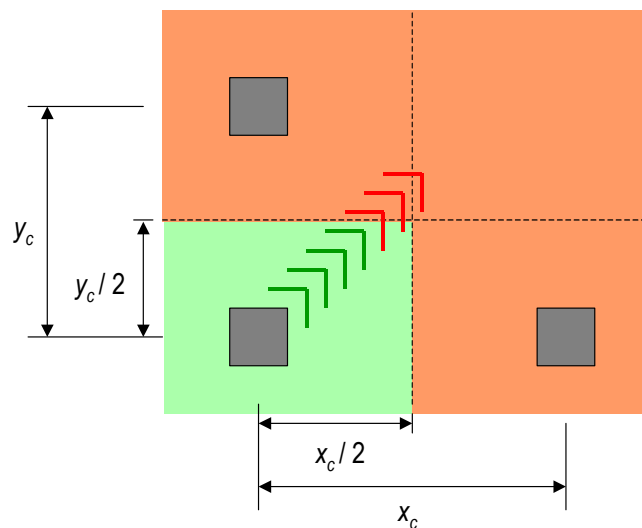


**Figure 3-13 Threshold yielding an alternative foundation type**  
(green – pad footing is suitable, red – requires an alternative foundation type)

## 3.6 PAD FOUNDATION DESIGN

The methods used to predict footing settlement, introduced in Chapter 2, require information regarding the loading conditions, elastic properties of the underlying soil and the size of the footing. However, as mentioned above, none of the methods directly yield a footing

size. As such, they are referred to in this research as settlement prediction techniques or methods, and are used in conjunction with limits regarding the individual total footing settlement and differential settlement between footings. The discussion in this section deals with the adoption of suitable limits that constitute the design criteria, as well as the implementation of the settlement prediction techniques introduced in Chapter 2. Several calibrations and corrections are required to ensure that the prediction techniques are consistent and therefore, comparable.

### 3.6.1 Pad Foundation Design Criteria

The design criteria adopted nominates limits regarding the total settlement of a single footing and the differential settlement between two adjacent footings. Based on the discussions in Chapter 2, a total settlement limit of 25 mm and a differential settlement limit of 0.0025 m/m is assumed for this research. The total settlement of each footing in the system is estimated using the settlement prediction techniques discussed in the following section. The differential settlement between two footings is calculated using the estimated settlement of each footing and the centre-to-centre spacing. For example, the condition shown in Figure 3-14 illustrates a two-footing foundation system, where footings suffer settlements  $\delta_1$  and  $\delta_2$ . Therefore, the differential settlement,  $\lambda_{1-2}$ , between these two footings, is given by:

$$\lambda_{1-2} = \frac{|\delta_1 - \delta_2|}{Z} \quad (3.12)$$

where  $Z$  is the centre-to-centre spacing.

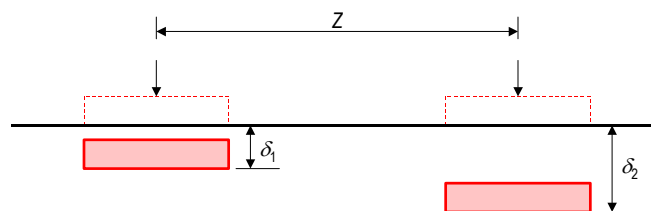


Figure 3-14 Calculation of differential settlement between two adjacent footings

In the case of a foundation system that consists of more than 2 footings, the differential settlement between each pair of footings is calculated and compared to the differential settlement limit of 0.0025 m/m.



### 3.6.2 Settlement Prediction Techniques

Aside from the 3DFEA numerical method described later, eight prediction techniques for estimating the settlement of a footing are considered in this research. These techniques are compared in Table 3-5, in terms of whether or not they:

- Predict the settlement of a rigid or flexible loaded area;
- Accommodate soil variability in the vertical direction; and
- Incorporate an analysis depth that is limited by some function of the footing geometry.

**Table 3-5 Comparison of settlement prediction techniques adopted in the methodology, not including the numerical method**

Settlement Prediction Method	Abbreviation	Rigid Loaded Area	Flexible Loaded Area	Property Variation in the Vertical Direction	Depth Limit
Schmertmann 2B-0.6	Sch2B	✓	-	✓	✓
Timoshenko and Goodier	T&G	-	✓	-	-
Newmark	New	-	✓	✓	-
Westergaard	Wst	-	✓	✓	-
2:1	2:1	-	✓	✓	-
Janbu	Jan	✓	-	-	-
Perloff	Per	✓	-	-	-
Schmertmann Modified	SchM	✓	-	✓	✓

In order to maintain consistency with the numerical analysis method discussed later, all footings are treated as rigid. Therefore, the settlement prediction methods that yield estimates of a flexible footing are converted to a rigid footing settlement. This conversion process is discussed in the next section. It is also evident from Table 3-5 that there are also inconsistencies between methods dealing with the depth of analysis. Two methods (Schmertmann 2B-0.6, and Schmertmann Modified) limit the analysis to a depth determined by the geometry of the footing. The other methods either use influence factors, which are typically a function of the soil layer depth, or integrate strain contributions at depth intervals extending to the base of the layer. The numerical method also accommodates small strains at deep locations, which generally causes an over estimation of settlement (Seycek 1991). Further discussion regarding the depth of analysis is given in Chapter 4, where settlement estimates from the numerical method are compared to measured settlements of constructed footing.

Additional analyses are also required for the Janbu technique to calibrate the  $\eta_1$  correction factor, with respect to a Poisson's ratio of 0.3. Fenton et al. (2003) has previously calibrated this coefficient for a constant Poisson's ratio of 0.25 using a logarithmic function of soil depth to footing width ratio, as given by:

$$\eta_1 = \eta_a + \eta_b \ln\left(\frac{D}{b}\right) \quad (3.13)$$

where  $\eta_a$  and  $\eta_b$  are constants of the fitted relationship, and  $D$  and  $b$  are the depth of the soil layer and width of the footing, respectively. A similar relationship is also used for the calibration of the coefficient with Poisson's ratio of 0.3 undertaken in this research. Figure 3-15 shows the results of the calibration using 3DFEA settlement estimates, where the Janbu  $\eta_1$  coefficient is plotted against the soil layer depth to footing width ratio on a logarithmic scale.

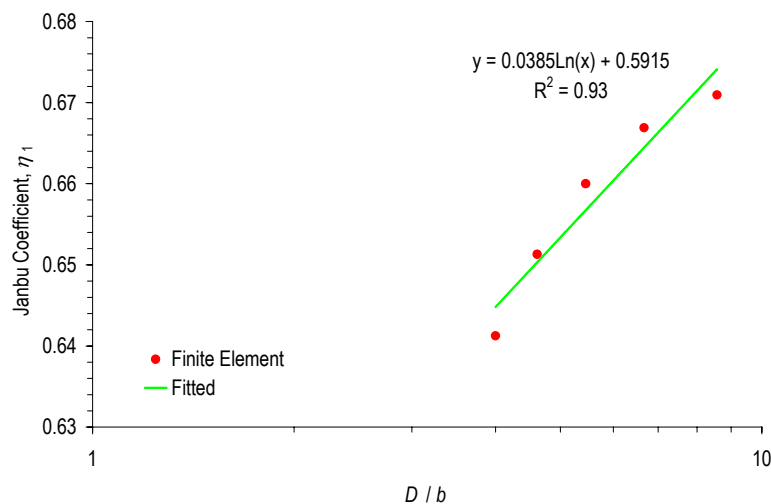


**Figure 3-15 Janbu settlement equation coefficient  $\mu_a$  for varying soil depth to footing width ratio**

The fitted relationship between the Janbu  $\eta_1$  coefficient and the soil depth to footing ratio shown in Figure 3-15, yields values of  $\eta_a$  and  $\eta_b$  equal to 0.5915 and 0.0385, respectively. These values compare to the calibration undertaken by Fenton et al. (2003), where  $\eta_a$  and  $\eta_b$  were estimated to be 0.4294 and 0.5071, respectively. A reasonable match between Equation (3.13) and the 3DFEA results is shown in Figure 3-15, with an  $R^2$  goodness-of-fit of 0.93. Similar to the Timoshenko and Goodier and Perloff prediction techniques, the Janbu method requires a single elastic modulus value. However, Fenton et al. (2003) suggested that a geometric average of the soil properties located directly beneath the footing

provides a better approximation in a spatially random soil than an arithmetic average. Accordingly, the elastic modulus value required by the Janbu technique is estimated using a geometric average.

The implementation of the Perloff relationship given in Equation (2.9) utilises influence values published by Harr (1966) based on a rigid footing. However, since this technique was originally proposed by Perloff (1975), it has been assigned this name for the results that follow.

### 3.6.3 Determination of Rigid Footing Displacements

As detailed above, few of the prediction techniques estimate the settlement of a flexible footing, which is in contrast to the numerical method, as discussed later. As such, it is necessary to use the settlement predictions of the flexible footing to estimate the settlement of a corresponding rigid footing. This conversion process is achieved to correspond with the distribution of settlement and contact pressures under flexible and rigid footings, as shown in Figure 3-16.

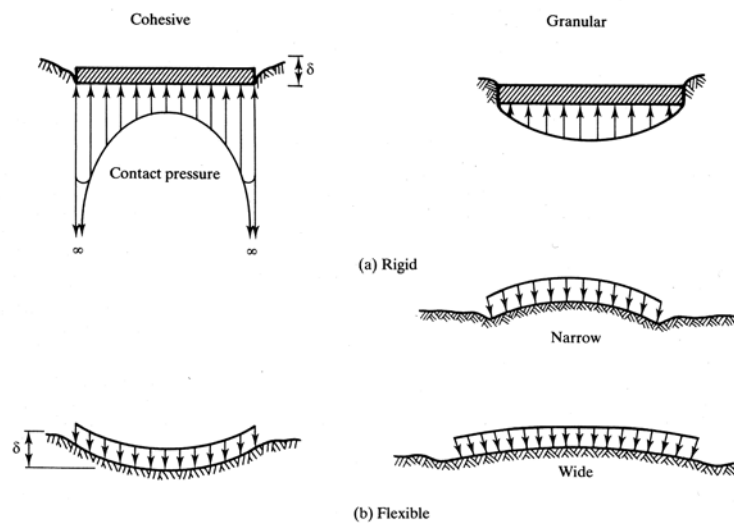


**Figure 3-16 Distribution of settlements for (a) rigid and (b) flexible loaded areas**  
After Holtz (1991)

To convert the settlement estimates of a flexible footing to a corresponding rigid footing settlement, the following steps are adopted:

1. Estimate the settlement at the middle,  $\delta_m$ , of the flexible footing by dividing the footing into 4 equal segments and estimating the settlement at the corner of each

segment. The settlement at the middle of the flexible footing is therefore, the sum of the settlements at the corner of each of the 4 segments (Bowles 1997).

2. Estimate the settlement at the corner of the flexible footing,  $\delta_c$ .
3. Assume a parabola represents the settlement distribution of a flexible loaded area, as shown in Figure 3-17. Since three points are required to define a parabola, the centre and two corner settlements are used.

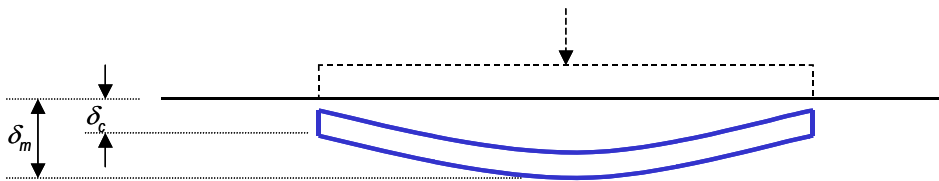


Figure 3-17 Settlement of a flexible footing

4. Let the settlement of a corresponding rigid footing be  $\delta_r$ , as shown in Figure 3-18.

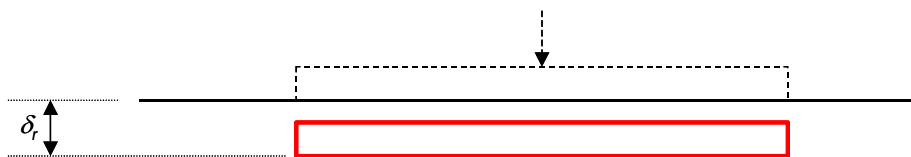


Figure 3-18 Settlement of a rigid footing

5. The rigid settlement,  $\delta_r$ , is estimated as the weighted average of the flexible loaded area, as shown in Figure 3-19.

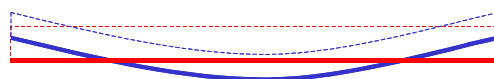


Figure 3-19 Overlay of settlement distribution of a flexible and rigid footing

6. The weighted average of the flexible displacement is estimated using the parabolic centroid, as shown in Figure 3-20, where  $x_d$  is the distance to the parabolic centroid and  $h$  is the difference between the corner and middle settlements, as given by:

$$h = \delta_m - \delta_c \quad (3.14)$$

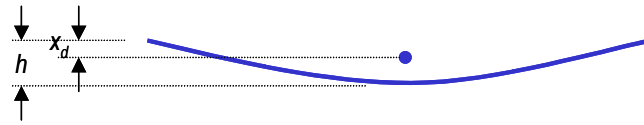


Figure 3-20 Centroid of the settlement distribution of a flexible footing

7. The distance to the parabolic centroid,  $x_d$ , is, therefore, expressed in terms of the flexible footing settlements as:

$$\begin{aligned} x_d &= \frac{2}{5} h \\ &= 0.4h \\ &= 0.4(\delta_m - \delta_c) \end{aligned} \quad (3.15)$$

8. Finally, the rigid footing settlement is estimated in terms of the flexible footing settlement using:

$$\begin{aligned} \delta_r &= \delta_c + x_d \\ &= \delta_c + 0.4(\delta_m - \delta_c) \\ &= 0.4\delta_m + 0.6\delta_c \end{aligned} \quad (3.16)$$

### 3.6.4 Procedure used to Account for Multiple Footing Interactions

The settlement prediction methods discussed above estimate the settlement of a footing based on an applied load. However, the numerical method discussed later, also considers the settlement of a footing due to the presence of an adjacent footing. Therefore, to maintain consistency between the two techniques, the settlement of one footing due to an adjacent footing, is estimated and added to the settlement prediction of the footing due to the applied load. For example, refer to the condition shown in Figure 3-21. The adopted method estimates the settlement of Footing 1, due to the load applied to Footing 2. This settlement is added to the predicted settlement of Footing 1, due to its own load,  $P_1$ , to yield the total settlement of Footing 1.

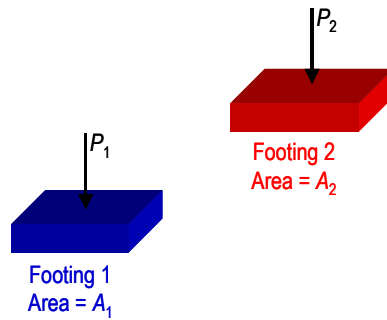


Figure 3-21 Two adjacent footings with areas  $A_1$  and  $A_2$ , and applied loads,  $P_1$  and  $P_2$

The method adopted to predict the settlement of Footing 1 due to an adjacent footing (Footing 2) is based on superposition and best described by the following steps:

1. Calculate the distance between the centre of Footing 1 and the inside and outside edge of Footing 2, as given in Figure 3-22 by  $r_i$  and  $r_o$ , respectively.



Figure 3-22 Determination of (a) internal and (b) external radius of annulus

2. Estimate the settlement of the shaded annulus,  $\delta_{ann}$ , as shown in Figure 3-23, which has an internal radius of  $r_i$ , external radius of  $r_o$  and an applied pressure equal to  $P_2 / A_2$  (the applied pressure on Footing 2). Use influence factors published by Harr (1966) based on a rigid footing.

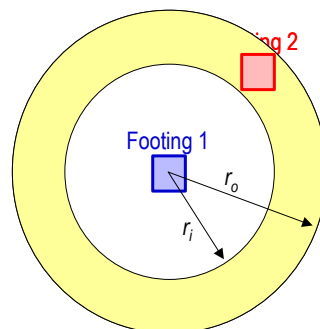


Figure 3-23 Schematic of shaded annulus

3. Estimate the proportion of area occupied by Footing 2 in relation to the annulus, by determine the angle  $\psi$ , with two lines from the centre of Footing 1 to the midpoint of each closest side of Footing 2, as shown in Figure 3-24.

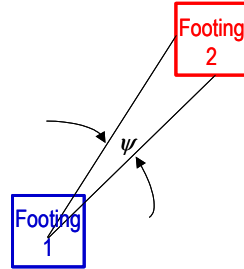


Figure 3-24 Determination of angle,  $\alpha$

4. Calculate the settlement of Footing 1 due to Footing 2,  $\delta_{1|2}$ , as given by:

$$\delta_{1|2} = \frac{\psi^\circ}{360} \delta_{ann} = \frac{\psi^c}{2\pi} \delta_{ann} \quad (3.17)$$

It is not expected that the settlement of one footing due to an adjacent footing will have a significant impact on the results, because the minimum spacing in the analyses with multiple footings is 8 m. However, to maintain consistency with the numerical method, the effects of adjacent footings are incorporated into the analyses that follow.

### 3.6.5 Numerical Modelling of Footing Settlement

The use of a numerical model, such as three-dimensional finite element analysis (3DFEA), allows analyses to accommodate the spatial variability of the soil in all directions. This does, however, come at a cost of increased computational time and discretisation limitations. A 3DFEA model, developed by Smith and Griffiths (2004), is used to estimate the settlement of a rigid footing, assuming linear-elastic behaviour and no footing rotation.

Since 3DFEA estimates only the settlement of a footing of known size, an iterative process is adopted to yield a footing design. This process is similar to the process adopted for the other settlement prediction techniques, where the size of the footing is varied until the design meets the settlement criteria. However, an iterative process further increases the computational time, by requiring multiple 3DFEA to yield a single footing design. Therefore, the Schmertmann settlement prediction technique using the 2B-0.6 strain influence distribution is used to provide an initial footing design. From this starting point, 3DFEA is

employed to achieve the final footing design. This measure significantly reduces the number of 3DFEA iterations required to yield a single footing design.

Furthermore, an investigation of the accuracy and performance of the 3DFEA model is also undertaken to ensure that the resultant footing designs are not significantly affected by discretisation errors and that the method implementation is efficient. In this case, four separate investigations are conducted, concerning the:

- Convergence tolerance;
- Number of elements under the footing;
- Number and size of elements in the mesh; and
- Distance between the edge of the footing and the mesh boundary.

The following sections discuss the results of the investigations conducted regarding the accuracy and efficiency of 3DFEA. Furthermore, decisions regarding the number and size of elements in the mesh and under the footing, the convergence tolerance, and the minimum distance between the edge of the footing and the mesh boundary, are also documented.

#### 3.6.5.1 Convergence tolerance

The 3DFEA method uses a preconditioned iterative conjugate gradient solver to overcome the need to assemble a global stiffness matrix (Smith and Griffiths 2004). Although this reduces memory and storage requirements, it uses an iterative solver that is more time consuming and requires the specification of a suitable convergence tolerance. A higher tolerance reduces the number of iterations required and, therefore, reduces the computational time. However, a higher tolerance also increases the possibility of errors in the settlement estimate. Therefore, an investigation is conducted to measure the effect of increasing the convergence tolerance on the accuracy of the settlement estimate and the computational time.

For this investigation, 9 different convergence tolerances are examined, ranging from 0.0001 to 1. These tolerances are relative measures of error. The analysis involves estimating the settlement of a single pad footing, founded on a soil with a uniform elastic modulus of 10,000 kPa and a Poisson's ratio of 0.3. The footing size is nominated to be



1.5 m × 1.5 m and it is centrally located on a 50 m × 50 m site, with a 30 m deep soil layer. A point load of 1,500 kN is applied to the centre of the footing. Results of this analysis are shown in Figure 3-25, for the settlement estimate, relative settlement error and computational time. The relative settlement error is determined by comparing the settlement at each convergence tolerance, with the settlement estimate from the analysis with a convergence tolerance of 0.0001. In this case, the settlement estimate at the lowest convergence tolerance is 65 mm. Therefore, the relative settlement,  $SE$ , is calculated using:

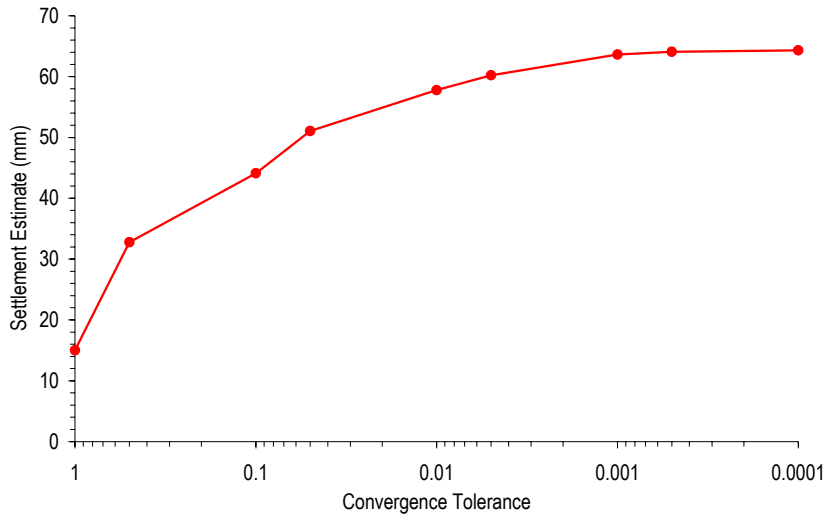
$$SE = \frac{|s - 65|}{65} \quad (3.18)$$

where  $s$  is the settlement for another convergence tolerance.

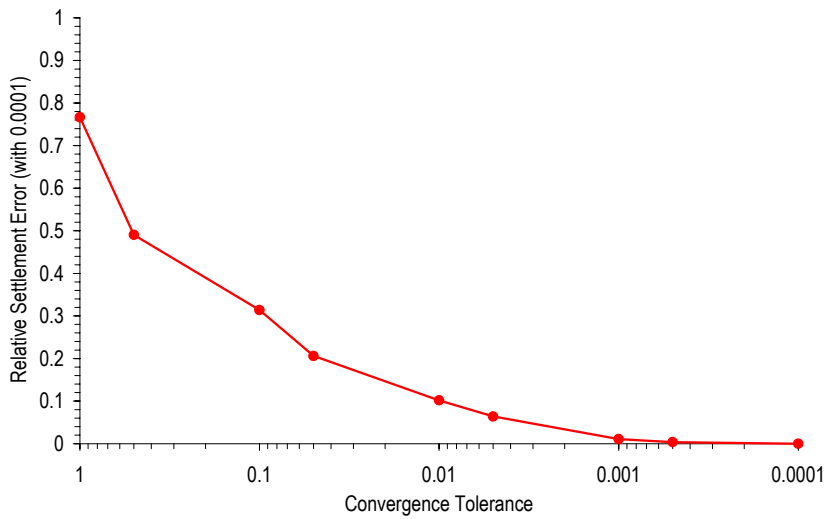
Results clearly indicate that the settlement estimate increases as the convergence tolerance is decreased. However, the results shown in Figure 3-25(a) also indicate that the settlement estimate asymptotes to a constant value of approximately 65 mm. As evident in Figure 3-25(c), the increase in accuracy comes at a high cost of computational time, where the analysis based on a convergence tolerance of 0.0001, requires approximately 900 seconds (15 minutes). This is compared to the computational time with a convergence tolerance of 0.005 of approximately 120 seconds (2 minutes), which leads to a relative error of only 5%. In this case, a 5% error relates to approximately 1 mm of settlement, which is considered acceptable for this research and most design situations. Ideally, the lowest convergence tolerance leading to the most accurate settlement estimate would be adopted. However, considering the computational time suggested in Figure 3-25(c), and that tens of thousands of Monte Carlo realisations are required in this research, a convergence tolerance of 0.005 is an appropriate compromise.

It should also be noted that all analysis conducted in this section required less than 500 iterations of the conjugate gradient solver to reach the nominated convergence tolerance. Therefore, it is reasonable to conclude that a maximum of 500 iterations will be sufficient to achieve a tolerance of 0.005.

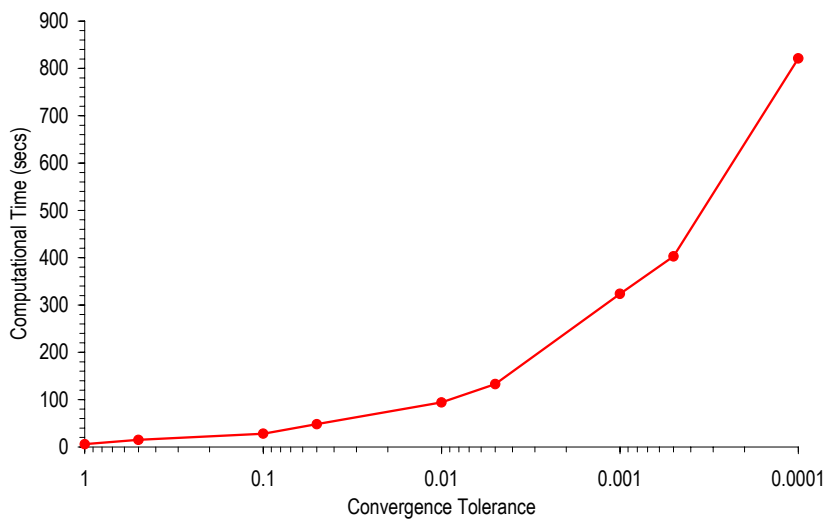
**A 3DFEA convergence tolerance of 0.005 with a maximum number of iterations of 500 is adopted.**



(a)



(b)



(c)

**Figure 3-25 Effect of convergence tolerance on the (a) settlement estimate, (b) relative settlement error and (c) computational time using 3DFEA**

### 3.6.5.2 Effect of number of elements beneath the footing

The number of elements located under the footing also affects the accuracy of 3DFEA settlement estimates. This is because stresses are simulated at nodal points. Therefore, stresses are more accurately simulated by an increased number of nodal points. However, additional nodal points infer more elements required under the footing and therefore, a larger minimum footing size. For example, if a single element resulted in suitable simulation of stresses under the footing, a minimum footing size of 0.5 m × 0.5 m is possible (assuming an element size of 0.5 m × 0.5 m). However, if one element was not sufficient to accurately simulate the stresses under the footing, the minimum footing size would be larger. Therefore, analyses are conducted to measure the impact of increasing the number of elements under the footing on the settlement estimate. This leads to the determination of a minimum footing size.

As with the analysis regarding the convergence tolerance above, this investigation involves a single pad footing of size 1.5 m × 1.5 m. The footing is loaded with a 1,500 kN centrally applied point load, with the elastic modulus is set to 10,000 kPa (uniform). The Poisson's ratio is also the same as the above analysis, with a value of 0.3. Based on the results in the previous section, a convergence tolerance of 0.005 is adopted with a maximum of 500 solver iterations.

To increase the number of elements under the footing, without changing the footing size or increasing the total number of elements in the mesh, the element size is decreased. This also reduces the site size. The element sizes used in this analysis are shown in Table 3-6 along with the corresponding site sizes. Results are shown in Figure 3-26 as settlement estimates and a relative settlement error. In this case, the relative settlement error is based on comparisons with the results considering 36 elements beneath the footing. This is because the analysis with 36 elements yields the largest settlement of approximately 62 mm.

**Table 3-6 Element and site sizes used to increase the number of elements beneath the footing**

No. of elements beneath footing	No. of elements in mesh	Element size	Site size
1	100 × 100 × 60	1.5 m × 1.5 m × 0.5 m	150 m × 150 m × 30 m
4	100 × 100 × 60	0.75 m × 0.75 m × 0.5 m	75 m × 75 m × 30 m
9	100 × 100 × 60	0.5 m × 0.5 m × 0.5 m	50 m × 50 m × 30 m
16	100 × 100 × 60	0.3 m × 0.3 m × 0.5 m	30 m × 30 m × 30 m
25	100 × 100 × 60	0.25 m × 0.25 m × 0.5 m	25 m × 25 m × 30 m
100	100 × 100 × 60	0.15 m × 0.15 m × 0.5 m	15 m × 15 m × 30 m
225	100 × 100 × 60	0.1 m × 0.1 m × 0.5 m	10 m × 10 m × 30 m

A relative error of approximately 0.2 (20%) was found when the settlement estimate is based on a single element beneath the footing, as shown in Figure 3-26. This error reduces dramatically as the number of elements increases. However, because it is also important to ensure the site size is sufficiently larger than the footing size (to accommodate multiple footing systems and to minimise boundary effects), a compromise between accuracy and number of elements beneath the footing is required. In this case, the relative error of considering 9 elements beneath the footing is less than 5% (3.2%), which is considered acceptable for this research and most design scenarios. Therefore, a minimum of 9 elements is required beneath the footing, to ensure that stresses are simulated with sufficient accuracy and the settlement error is acceptably low.

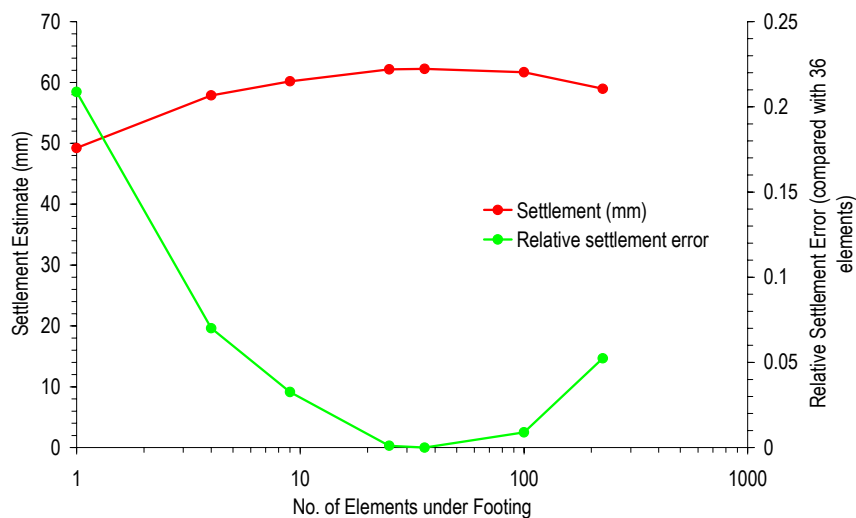


**Figure 3-26 Effect of increasing the number of elements beneath a footing on the accuracy of 3DFEA settlement estimates**

**A minimum of 9 elements (3 elements × 3 elements) are required beneath each footing to ensure the accurate simulation of stresses when using 3DFEA.**

It is also interesting to note that the relative error increases when more than 36 elements are considered beneath the footing. However, this is likely to be a result of boundary effects, where the edge of the footing is close to the finite element mesh boundary. Such effects are discussed later.

### 3.6.5.3 Effect of the size and total number of elements

The total number or size of elements in the finite element mesh also affects the accuracy of the settlement estimate. For instance, it is reasonable to assume that more elements with a

smaller size will yield a result with improved accuracy. However, analyses using increasing number of elements will require increasing computational time. Therefore, another investigation is conducted to investigate the effect of element size and number. This is achieved by analysing the settlement of a single pad footing of size  $1.5 \text{ m} \times 1.5 \text{ m}$ , founded on a soil with a uniform elastic modulus of 10,000 kPa and Poisson's ratio of 0.3.

As with the preceding investigations, the footing is loaded with a 1,500 kN centrally applied point-load and is assumed to be located at the centre of the site. Twelve different element sizes are considered, while the size of the site is maintained constant at  $50 \text{ m} \times 50 \text{ m}$  and a depth of 30 m. The different element sizes are summarised in Table 3-7, where they are grouped based on the number of elements in the horizontal plane. Note that the last element size in each group has the same total number of elements as the first element size in the next group. However, the results shown in Figure 3-27 suggest that analyses with more elements in the vertical direction require additional computational time even though they have the same total number of elements. This is because stresses and strains are greater in the vertical direction and therefore, require additional time to converge to a solution.

**Table 3-7 Element size and number used to investigate the influence of**

Element size	No. of elements in mesh	No. of elements in horizontal plane	Total no. of elements
$1 \text{ m} \times 1 \text{ m} \times 1 \text{ m}$	$50 \times 50 \times 30$	2,500	75,000
$1 \text{ m} \times 1 \text{ m} \times 0.5 \text{ m}$	$50 \times 50 \times 60$	2,500	150,000
$1 \text{ m} \times 1 \text{ m} \times 0.3 \text{ m}$	$50 \times 50 \times 90$	2,500	225,000
$1 \text{ m} \times 1 \text{ m} \times 0.25 \text{ m}$	$50 \times 50 \times 120$	2,500	300,000
$0.5 \text{ m} \times 0.5 \text{ m} \times 1 \text{ m}$	$100 \times 100 \times 30$	10,000	300,000
$0.5 \text{ m} \times 0.5 \text{ m} \times 0.5 \text{ m}$	$100 \times 100 \times 60$	10,000	600,000
$0.5 \text{ m} \times 0.5 \text{ m} \times 0.3 \text{ m}$	$100 \times 100 \times 90$	10,000	900,000
$0.5 \text{ m} \times 0.5 \text{ m} \times 0.25 \text{ m}$	$100 \times 100 \times 120$	10,000	1,200,000
$0.25 \text{ m} \times 0.25 \text{ m} \times 1 \text{ m}$	$200 \times 200 \times 30$	40,000	1,200,000
$0.25 \text{ m} \times 0.25 \text{ m} \times 0.5 \text{ m}$	$200 \times 200 \times 60$	40,000	2,400,000
$0.25 \text{ m} \times 0.25 \text{ m} \times 0.3 \text{ m}$	$200 \times 200 \times 90$	40,000	3,600,000
$0.25 \text{ m} \times 0.25 \text{ m} \times 0.25 \text{ m}$	$200 \times 200 \times 120$	40,000	4,800,000

The results shown in Figure 3-27 suggest that all analyses with 10,000 elements in the horizontal plane result in a relative settlement error of less than 4%, whereas analyses with 2,500 elements in the horizontal direction yield relative errors closer to 10%. Furthermore, the computational time associated with an element size that yields 40,000 elements in the horizontal planes is too great considering the number of Monte Carlo realisations that are

required for this research. Therefore, an element size that results in 10,000 elements in the horizontal plane is considered appropriate.

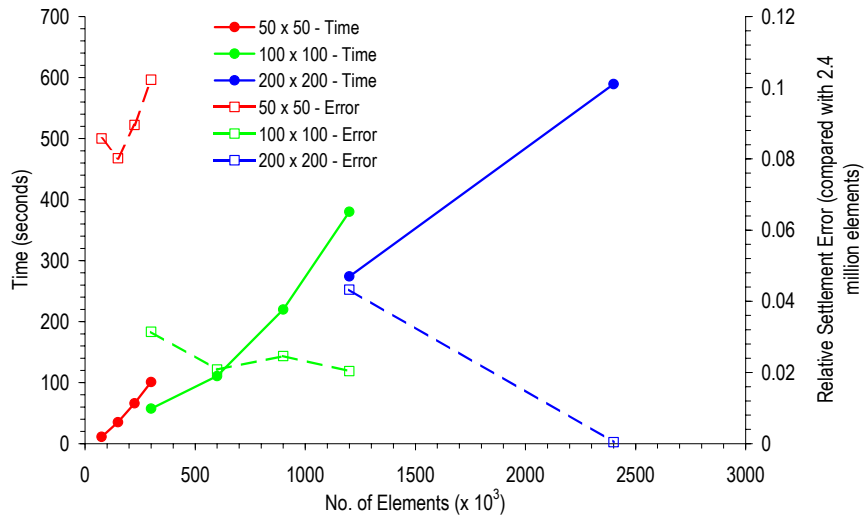


**Figure 3-27 Effect of the number of elements in the mesh (element size) on the accuracy and computational time of 3DFEA settlement estimates**

The adopted element size in the vertical direction does not only affect the accuracy of 3DFEA, it also impacts on the resolution of elastic modulus properties that will be mapped to the finite element mesh. Therefore, instead of adopting the element size that requires the least computational time, an element size of 0.5 m  $\times$  0.5 m  $\times$  0.5 m is adopted. This allows the elastic modulus properties generated using LAS (see §3.3) to be mapped directly to the elements in the mesh without additional averaging.

**An element size of 0.5 m  $\times$  0.5 m  $\times$  0.5 m is adopted leading to a finite element mesh of 100  $\times$  100  $\times$  60 elements representing a 50 m  $\times$  50 m site with a depth of 30 m.**

#### 3.6.5.4 Effect of distance of footing edge to finite element mesh boundary

Another important modelling consideration, which affects the accuracy of 3DFEA, is boundary conditions. These affect the analysis when stresses exist at the boundary of the mesh and have to be modelled as a continuum. This requires simplifications and assumptions in the model. In this case, nodes along the boundary are only free to move in the vertical direction (e.g. lateral movement is assumed zero). This infers that horizontal stresses at the boundary are zero. However, if the footing is close to the boundary of the

mesh, horizontal stresses will be large. Therefore, it is necessary to ensure that there is sufficient spacing between the edge of the footing and the mesh boundary, to avoid large horizontal stresses.

To determine the minimum distance between the edge of the footing and the mesh boundary, settlement analyses are conducted where the footing location is moved closer to the mesh boundary. In this case, the footing is assumed to have a plan size of 1.5 m × 1.5 m, while the site size remains the same at 50 m × 50 m in plan and 30 m deep. The footing is loaded with a 1,500 kN centrally applied load and the soil is assumed to have a uniform elastic modulus of 10,000 kPa and a Poisson's ratio of 0.3. Results of this analysis are shown in Figure 3-28, where the distance between the centre of the footing and the finite element mesh boundary is expressed in terms of the footing width. This allows direct comparisons with the conclusion made by Desai and Abel (1972), who indicated that the centre of a footing should be at least 5 times the footing width from the finite element boundary.

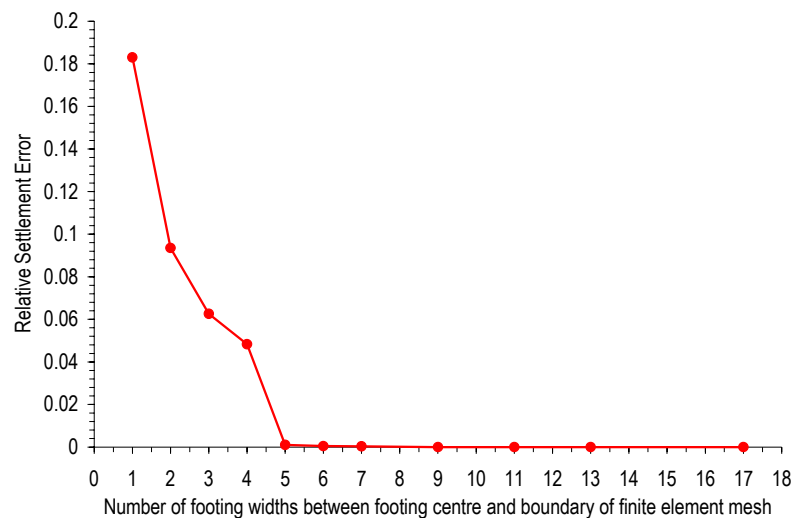


**Figure 3-28 Influence of boundary effects on the accuracy of 3DFEA settlement estimates**

Results shown in Figure 3-28 clearly indicate that, when the centre of the footing is more than 5 times the footing width from the edge of the finite element mesh boundary, the relative settlement error is negligible (less than 0.1%). When the footing is one width closer to the boundary, the relative settlement error increases to approximately 5%. Therefore, it is important to ensure that footings are positioned on the site so that their centre is never closer than 5 times the footing width from the edge of the mesh boundary.

Footings are positioned so that the centre is more than 5 times the footing width from the finite element mesh boundary.

#### 3.6.5.5 Summary

The results presented in this section have dealt with the implementation of the 3DFEA model and influences such as mesh size and convergence tolerance. Further discussions regarding the accuracy of 3DFEA to estimate footing settlements are presented in Chapter 4.

### 3.7 MONTE CARLO ANALYSIS

---

The Monte Carlo analysis adopted in this research involves generating simulated soils based on a random selection, while still conforming to the same spatial statistics (mean, COV and SOF). Each simulated soil is then used to yield foundation designs based on site investigation data (SI) and complete knowledge of the soil (CK). This section deals with the nomenclature adopted to describe results from the Monte Carlo analysis, as well as the required number of realisations and methods of optimisation to reduce computational time.

#### 3.7.1 Nomenclature and Metrics

The results of the analyses are generally output in the form of footing areas,  $A$ , designed on the basis of either the results of a site investigation and one of the settlement prediction techniques, or the complete knowledge of the soil and 3DFEA. However, some results shown later take the form of settlement estimates,  $S$ , where the footing area is specified and settlements are predicted based on the results of a site investigation and a particular settlement prediction technique or complete knowledge and 3DFEA.

Each realisation of the Monte Carlo analysis yields footing areas or settlement estimates. Footing areas are compared to determine whether the design based on the site investigation data is less than or greater than the design based on the complete knowledge and 3DFEA. A footing is considered to be under-designed when the design based on the site investigation yields a smaller footing than that based on complete knowledge, and over-designed when the site investigation design is larger. Alternatively, an optimal condition occurs when the site investigation design yields a footing size equal to that obtained using 3DFEA and complete knowledge.



The footing areas and number of occurrences of over-, under-, or an optimal design are recorded for each realisation in the Monte Carlo analysis. The results are then compiled over the suite of Monte Carlo realisations to generate the sample mean or average footing area and probabilities of under-, over- and optimal design. The general nomenclature for the footing areas resulting from the analysis in each Monte Carlo realisation is shown in Figure 3-29, where:

- $A$  is the area of the design footing ( $\text{m}^2$ ) and  $S$  is the settlement (mm) of a given footing size;
- $k$  is the designator of the settlement method used (\* = optimal or 3DFEA)
- $r$  is the realisation number of the Monte Carlo analysis
- $i$  is the footing number in the foundation system; and
- $j$  is the designator of the site investigation program, as discussed in §3.4.

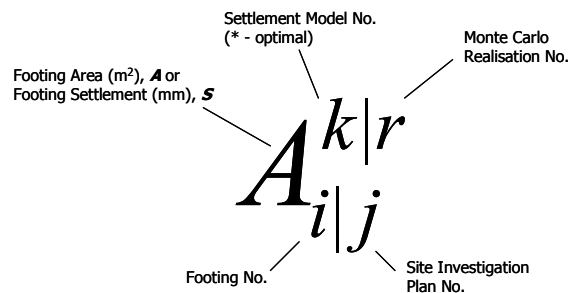


**Figure 3-29 Notation of footing area or footing settlement**

Using the footing areas,  $A$ , or settlement estimates,  $S$ , from each Monte Carlo realisation, and knowledge of the average footing area or settlement estimate, it is also possible to determine the variance and standard deviation of each. This provides a measure of the spread of values and aids in the definition of the distribution of the footing area or settlement estimates.

The design error,  $DE$ , for footing design and settlement error,  $SE$ , for settlement estimation, are additional measures of the differences between the design or analysis based on the site investigation data and complete knowledge of the soil. These measures are included to illustrate the magnitude of over- and under- design or settlement estimate. The design and settlement errors are defined as the difference between the site investigation and complete knowledge design or settlement estimate divided by the complete knowledge design or

estimate. This measure is calculated for each Monte Carlo realisation and averaged over the suite of realisations to yield an expected or average design and settlement error. The range of results used throughout this research are summarised in Table 3-8, using nomenclature shown in Figure 3-29.

**Table 3-8 Statistical properties obtained from Monte Carlo simulation to measure effectiveness of site investigation scope**

Statistical Values	
Sample Mean	$\hat{\mu}_{A_j^k} = \frac{1}{n_r n_f} \sum_{r=1}^{n_r} \sum_{i=1}^{n_f} A_{i j}^{k r}$
Sample Variance	$\hat{\sigma}_{A_j^k}^2 = \frac{1}{(n_r - 1)} \sum_{r=1}^{n_r} \left( \left( \frac{1}{n_f} \sum_{i=1}^{n_f} A_{i j}^{k r} \right) - \mu_{A_j^k} \right)^2$
Probabilities ( <i>j</i> th site investigation plan, <i>k</i> th settlement method)	
Under design Probability	$p_{ud_j}^k = \frac{1}{n_r n_f} \sum_{r=1}^{n_r} \sum_{i=1}^{n_f} \left\{ 1 \Leftrightarrow A_{i j}^{k r} < A_{i j}^{* r} \right\}$
Over design Probability	$p_{od_j}^k = \frac{1}{n_r n_f} \sum_{r=1}^{n_r} \sum_{i=1}^{n_f} \left\{ 1 \Leftrightarrow A_{i j}^{k r} > A_{i j}^{* r} \right\}$
Optimal Probability	$p_{op_j}^k = \frac{1}{n_r n_f} \sum_{r=1}^{n_r} \sum_{i=1}^{n_f} \left\{ 1 \Leftrightarrow A_{i j}^{k r} = A_{i j}^{* r} \right\}$
Errors – typically expressed as an average or expected error E[.] ( <i>j</i> th site investigation plan, <i>k</i> th settlement method)	
Design Error	$DE_j^k = \frac{A_{i j}^{k r} - A_{i j}^{* r}}{A_{i j}^{* r}}$
Settlement Error	$SE_j^k = \frac{S_{i j}^{k r} - S_{i j}^{* r}}{S_{i j}^{* r}}$

### 3.7.2 Number of Realisations

With a Monte Carlo analysis, it is important to determine a suitable convergence point or number of realisations where the results become stable. Accordingly, an investigation is undertaken to determine the number of realisations that yields a relatively constant average footing area. This is considered to be the convergence and is influenced by the spatial statistics of the elastic modulus in the soil, as well as the process used to determine the footing size.

The average footing area determined after each realisation, for a design based on complete knowledge of the soil and 3DFEA settlement estimates, is shown in Figure 3-31. These results are based on a foundation system consisting of 9-pad footings, as shown in Figure 3-30, centred on a 50 m × 50 m site with a 30 m deep soil layer. The mean elastic modulus is set to 20,000 kPa, while the elastic modulus coefficient of variation (COV) and scale of fluctuation (SOF) is set to 50% and 8 m, respectively. Figure 3-31 shows the mean footing area, as well as the relative error associated with the mean footing area after 10,000 realisations.

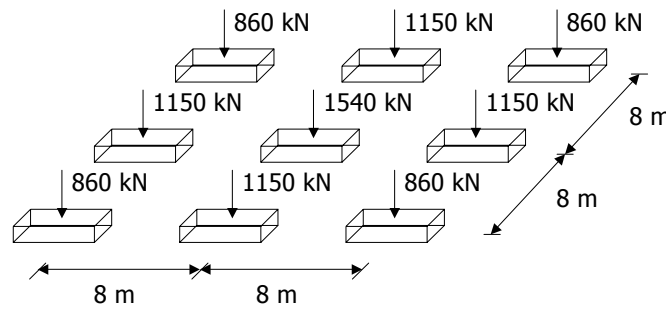


**Figure 3-30 Pad foundation system used in analysis to determine suitable number of Monte Carlo realisations**

It can be seen that a relatively constant average footing area is achieved after approximately 4,000 Monte Carlo realisations (Figure 3-31). At this number of realisations, the average footing area has a relative error of approximately 0.5%, which is significantly more accurate than the errors associated with the implementation of 3DFEA discussed earlier in this chapter. Therefore, it is considered appropriate to investigate the use of fewer realisations yielding a slightly greater error. In fact, after 1000 realisations, the relative error in the average total footing area is less than 1%. This is considered acceptable for this research and therefore, is adopted as the required number of realisations to yield convergence.

**A Monte Carlo analysis consisting of 1,000 realisations produces stable conditions and is therefore adopted for subsequent analyses.**

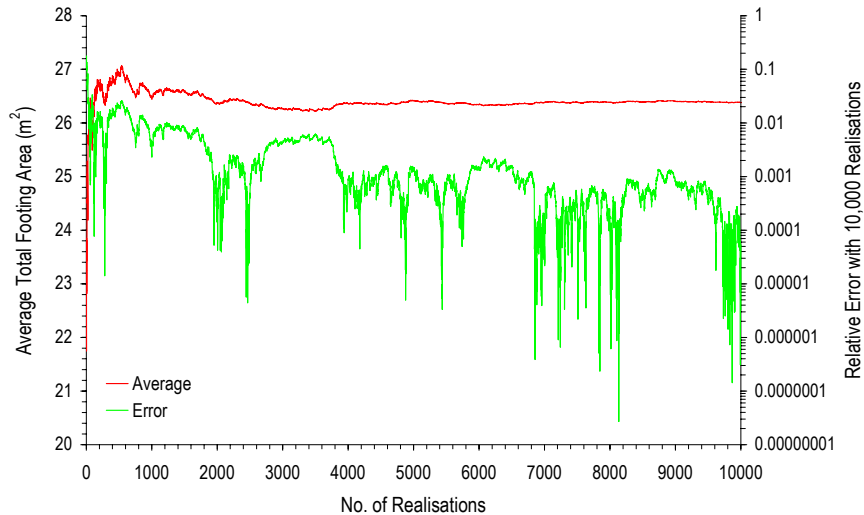


**Figure 3-31 Convergence rate of 9-pad system designed using 3DFEA and based on a soil COV of 50% and SOF of 8 m**

### 3.7.3 Optimisation of Computational Time

With the inclusion of large 3DFEA within a Monte Carlo framework, consisting of 1,000 realisations, the computational times are significant. As such, it is desirable to investigate means of increasing the productivity of the methodology by improving the code and utilising available computing resources. These are discussed in the following sections.

#### 3.7.3.1 Software Optimisation

The first step in optimising the run times is to identify the code segments associated with the most computationally intensive tasks. Table 3-9 provides the results of such an assessment based on a single pad footing on a soil with uniform properties. It is clearly shown in Table 3-9 that the numerical design, using 3DFEA, is overwhelmingly the most computationally intensive task. As a result, two improvements are possible. The first, is to target only the numerical design process by improving the performance of the code or changing the process altogether. The other option is to undertake a full optimisation of the entire process by code improvement, compiler optimisation and/or the use of additional resources. It is considered of greater benefit to investigate the possibilities associated with the entire method, rather than just the numerical design. This allows the performance of all parts of the method to be optimised, while retaining the numerical design in its current form.

**Table 3-9 Code profiling results**

Task	Time (secs)	% of Time
Program Preliminaries	0.001	0.0001%
Random Field Generation	0.039	0.0048%
Traditional Design (with 1 Site Investigation Plan)	0.004	0.0005%
Numerical Design (including Finite Element Analysis)	810.887	99.8846%
Post-processing Results	0.365	0.0450%
Entire Program	811.824	
Notes: Field size 100 × 100 × 60 (Uniform Field) – 1 Design Load		

Several FORTRAN compilers are also investigated to determine the most efficient compiler. The majority of the code is written in FORTRAN 77. However, numerous FORTRAN 90 commands are incorporated due to their convenience. The text editor included in Compaq Visual FORTRAN for Windows (Compaq Computer Corporation 2000) was used to write and assemble the various sections of code, due to its simplicity, flexibility and Windows compatibility. However, an alternative compiler is required to enable the program to be compiled and executed on Unix-based platforms. For this purpose the Intel FORTRAN Compiler (Intel Corporation 2004) is used due to its comprehensive libraries, especially dealing with parallel processing, which is discussed later in this chapter.

Benchmark speeds for the three compilers considered in this research are shown in Table 3-10, as sourced from Polyhedron Software (2004). Although the benchmarks shown in Table 3-10 indicate the availability of the Intel and Lahey compilers for a Windows environment, neither is used to compile the code under Windows.

**Table 3-10 Benchmark results for various FORTRAN 77 and FORTRAN 90 compilers**  
After Polyhedron Software (2004)

Compiler	FORTRAN 77		FORTRAN 90	
	Win32	Unix	Win32	Unix
Compaq Visual FORTRAN for Windows	7.83	-	13.32	-
Intel FORTRAN Compiler	6.52	6.86	13.47	12.19
Lahey FORTRAN Compiler	8.47	7.72	16.63	13.53

It is apparent from the results of the benchmark tests that there is no great advantage in running a FORTRAN 77 or 90 program on a Unix platform compared with Windows. However, there are slight differences between the three compilers investigated. The results

show that the Intel FORTRAN Compiler yields the fastest run-time on either a Unix or Windows platform using FORTRAN 77 or 90. It must be noted, however, that the benchmark results, shown in Table 3-10, are based on generic FORTRAN code and are not specific to this research.

### 3.7.3.2 Hardware Optimisation

Different chipsets and computer configurations also lead to varying computational times for the same computer code. An analysis of computer types and configurations is also undertaken, where the systems examined include:

- Toshiba Pentium P4 Laptop with 512 MB RAM and 40 GB HDD running Windows XP Home Edition and Compaq Visual FORTRAN 6.0;
- AMD Athlon 1800+ Desktop with 512 MB RAM and 60 GB HDD running Linux and Intel FORTRAN Compiler 7.1;
- AMD Athlon 2100+ Dual Server with 1.0 GB RAM and 60 GB HDD running Linux and Intel FORTRAN Compiler (2 of: *Terzaghi* and *Vanmarcke*); and
- IBM eServer 1350 Linux cluster consisting of 129 nodes, with each node having dual 2.4 GHz Xeon Processors (Pentium P4), 2.0 GB RAM and running RedHat Linux (*Hydra*).

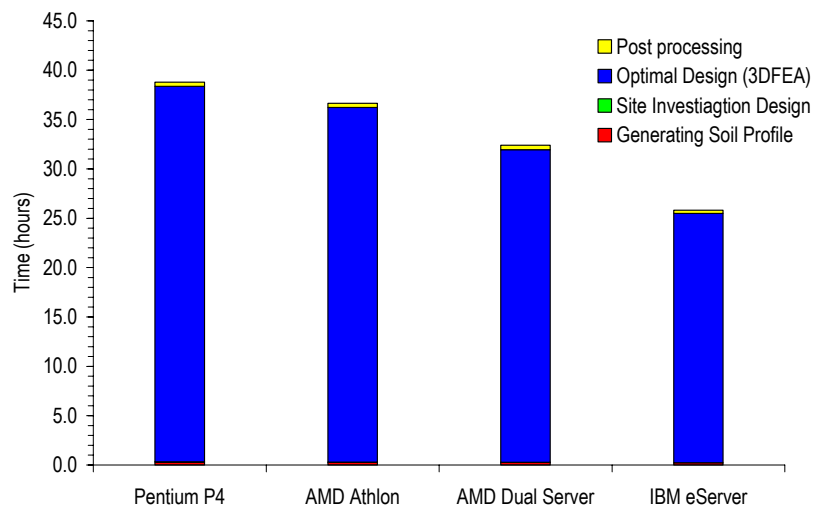
The computational time for each computer configuration running 1,000 Monte Carlo realisations of a foundation problem consisting of 9-pad footings (Figure 3-30), on a three-dimensional soil with a COV of 50% and SOF of 8 m, consisting of 600,000 ( $100 \times 100 \times 60$ ) elements is shown in Table 3-11. The computational times for each system are also shown graphically in Figure 3-32.

The computational time results shown in Table 3-11 and Figure 3-32 suggest that the IBM eServer is noticeably faster than the other computer configurations. This is most likely caused by the large amount of random access memory (RAM) available on this computing system. The performance of the Pentium P4 is heavily affected by the availability of only 512 MB of RAM. However, since all computers have been available during this research, they have all been utilised. It is important, however, to identify the most efficient computer configuration to enable the more time consuming, computationally exhaustive analyses to be directed to that computing system.

**Table 3-11 Cross platform computational times for 1000 Monte Carlo realisations for a soil COV of 50% and SOF of 8 m**

Computer	No. of Realisations	Time (hours)	Multiple Processor**
Pentium P4*	1,000	38.8	×
AMD Athlon	1,000	36.6	×
AMD Dual Server: Terzaghi and Vanmarcke	1,000	32.4	✓
IBM eServer: Hydra	1,000	25.8	✓

Notes:  
 \* - the analysis on the Pentium P4 was undertaken on a Windows XP platform using Compaq Visual FORTRAN 6.0  
 \*\* - results in this table have not been based on multi-processing.

**Figure 3-32 Cross platform computational times**

### 3.7.3.3 Parallel Processing

Parallel processing involves using numerous processors, connected through shared memory or a network, to undertake computations within the program at the same time. Parallel programming controls and directs the communications between processors to ensure all are conducting the correct computations. Message passing interface (MPI) controls communication to allow a single program to be concurrently run using multiple processors (Snir et al. 1996). MPI programming can be used with both FORTRAN and C programming languages and contains various intrinsic subroutines to communicate between processors.

MPI programming controls the processors using a single code. Common terminologies in MPI programmes include the master processor, which controls most of the preliminary computations, and the slave processors, which undertake the mass computations. The master sends the required information to the slaves for computation and then receives the calculated information. The MPI programming environment controls these transmissions

between the master and slaves. Figure 3-33 shows a typical process for an MPI program, where the master processor reads inputs and undertakes preliminary calculations, then sends information to the slaves, which undertake the bulk of the calculations. Once the slaves have completed their calculations, they send the information back to the master, which compiles results and then sends the next series of calculations back to the slaves.

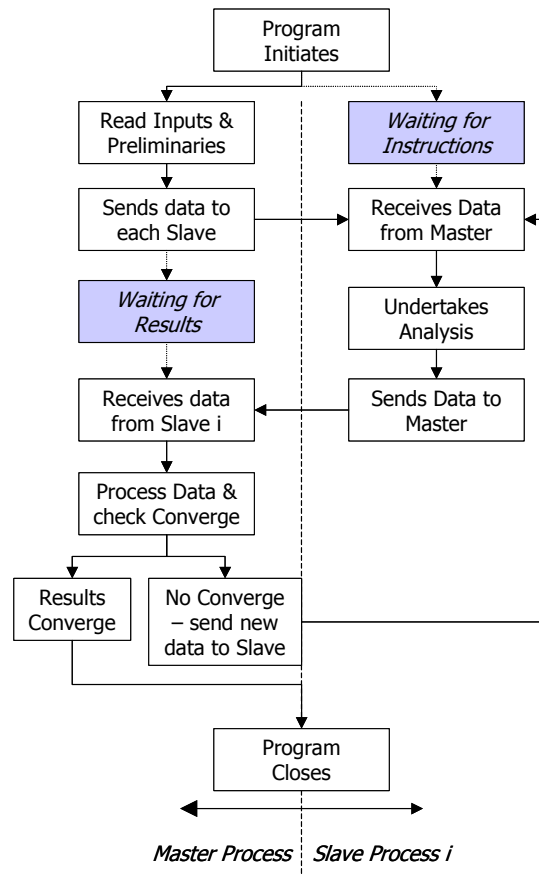


**Figure 3-33 Typical steps in an MPI program**

MPI programming is ideal for Monte Carlo analyses as it enables concurrent realisations to be undertaken by each processor. This greatly improves speed, where the reduction in computation time is approximated by a linear function of the number of processors used. In other applications of MPI programming, there is typically a threshold speed increase that can be achieved, due to communication time delays between processors.

The MPI code for this research is adopted directly from the original single-processor code, where information necessary for a Monte Carlo realisation is sent to each one of the slaves. The slave processor then runs the same code as would be run on the single processor computer and returns the results to the master, which compiles the results. This procedure is repeated until 1,000 realisations are completed. The realisations are proportioned to the



number of slaves available to the code and, when one processor finishes a single realisation, it receives another task immediately from the master, rather than waiting for all processors to finish. This greatly improves the efficiency of the code.

The benefit of using multiple processors is evaluated by conducting an analysis based on the same site and foundation conditions as the investigation of the computer configurations above. Results of this analysis are shown in Table 3-12 for all multi-processor systems and in Figure 3-34 for the Hydra system only. Computational times using a single processor are based on the single processor code. These are included as the benchmark result with which to compare the increase in speed when using an increasing number of processors. Furthermore, time comparisons and speed increases shown in Table 3-12, are for comparisons on the same platform (i.e. the speed increase for Hydra with 4 processors is based on a comparison with the computational time using Hydra with a single processor). The speed increase is a ratio, calculated by dividing the benchmark time of a single processor by the computational time based on an increasing number of processors.

**Table 3-12 Comparison of program run times for varying number of processors using Message Passing Interface (MPI)**

Computer	No. of Processors	No. of Realisations	Time (mins)	Time (hours)	Speed Increase (multiple of 1 process)
AMD	1*	1000	131898	36.6	-
Terzaghi	1*	1000	116639	32.4	-
Vanmarcke	2	1000	113190	31.4	1.0
Hydra	1*	1000	92910	25.8	-
Hydra	2	1000	83304	23.1	1.1
Hydra	4	1000	28171	7.8	3.3
Hydra	8	1000	1224	3.4	7.6
Hydra	16	1000	7869	2.2	11.8
Notes:					
* - single process runs undertaken without MPI code					

Results shown in both Table 3-12 and Figure 3-34 indicate that considerable time is saved when 4 or more processors are used with MPI implementation. This is not shown, however, with 2 processors. This is because the master processor sits idle while the slave processor does the majority of the analysis, resulting in a similar computation time to a single processor. This suggests that a multiple processor implementation should be faster than the single processor implementation by a factor equal to one less than the number of processors being used. However, the results indicate that, when 8 processors are used, the multiple processor implementation is 7.6 times faster than a single process implementation.

This is due to more efficient use of the processors, where the master can compile the results while the slaves are able to start on the next realisation. In this case, most of the processors are working at all times, rather than when 2 processors are used and the master sits idle for long periods.

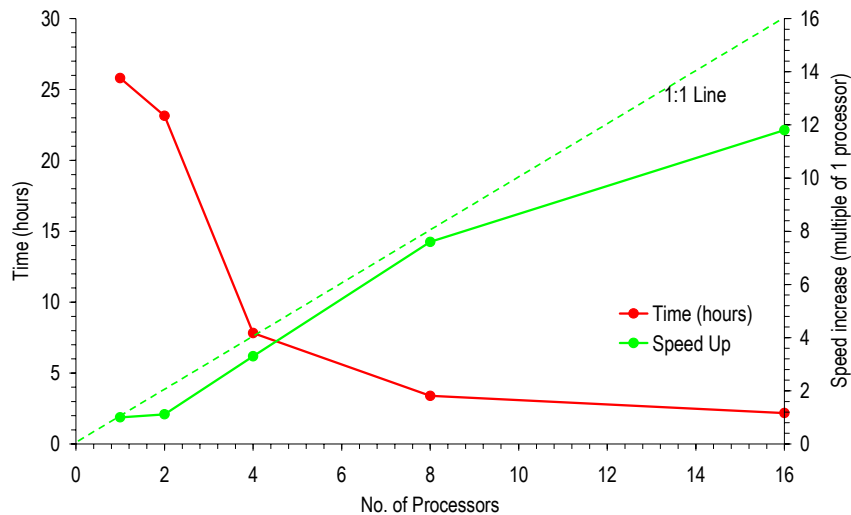


**Figure 3-34 Effect of additional processors on the computational time and relative speed increase**

The results shown in Figure 3-34 also indicate that implementing the MPI code with 8 processors yields the optimal speed increase, relative to the number of processors used. This is evident in Figure 3-34, where the speed increase using 8 processors appears to be the nearest the 1:1 speed increase line. When the MPI code is implemented with more than 8 processors, the speed increase trends away from the 1:1 line, indicating little benefit with 16 processors. This is due to the increased communication between master and slaves and the possibility that the master delays the slaves while compiling results. As such, it a MPI implementation with 8 processors is adopted when possible.

**When the MPI code is implemented, 8 processors on the Hydra supercomputer are used.**

It should be noted that the results shown in Figure 3-34 illustrate that the speed increase never exceeds the 1:1 line. Therefore, it is faster to run 8 separate single processor codes than a single MPI implementation with 8 processors. However, the single implementation of the MPI code using 8 processors will be completed approximately 7.6 times faster than each of the separate single processor runs and, as such, a complete set of results is achieved earlier. It is also possible to run multiple MPI implementations using 8 processors on the

Hydra supercomputer, as the system consists of 256 processors. As a result, the MPI implementation is used for most of the analyses presented in this research.

### **3.8 SUMMARY**

---

This chapter has dealt with the quantification of errors and risks associated with design of a foundation based on information from a site investigation. The methodology aimed to incorporate all forms of uncertainty that are inherent in a geotechnical design, including soil variability, statistical uncertainty, uncertainties due to measurement and transformation model error, and the use of simplified foundation response prediction methods. Although the adopted methodology is primarily used for the design of a pad foundation, it is also used to determine when an alternative foundation design is required.

The adopted methodology was also shown to require an extensive computational effort, which required optimisation to reduce computational time to manageable proportions. Such optimisation tools included the use of several available computers, including a supercomputer, where parallel processing is employed.



## **Chapter 4 VERIFICATION OF METHODOLOGY**

### **4.1 INTRODUCTION**

---

The ability of any site investigation program to derive representative soil properties depends on two major factors. These are the type and extent of the tests performed and the variability of the soil properties. Therefore, it is essential, for the accuracy of the results presented in this research, that the simulated soils yield properties that are representative of in situ values. It is also important to ensure that the implemented settlement prediction techniques are accurate. As a result, this chapter presents the results of verification undertaken to ensure that the soil simulation and the settlement prediction techniques are accurate.

### **4.2 VERIFYING THE PROPERTIES IN THE SIMULATED SOIL**

---

The local average subdivision (LAS) method, discussed in Chapter 3, is adopted in this research for generating a three-dimensional random field to conform to a target normal distribution with a mean and variance, and a target correlation structure defined by the scale of fluctuation (SOF). Furthermore, the normal variables generated by LAS are transformed to lognormal variables to adequately represent soil properties. Therefore, it is necessary to verify that the properties of the simulated soil meet the specific lognormal distribution and correlation structure. It is also necessary to investigate any effects associated with transforming the properties.

#### **4.2.1 Verifying the Target Distribution**

To ensure that both the random field generator and transformation method are appropriately implemented, an analysis to investigate the statistical properties of the simulated soil

is conducted. This involves analysing both the sample distribution of properties within the simulated soil, and the sample mean and variance of that distribution.

The results shown in Figure 4-1 illustrate the sample distribution of the elastic modulus properties of nine different simulated soils, defined by their COV and SOFs. The sample distributions clearly illustrate the non-negative property of the lognormal distribution. However, it should be noted that there is no upper limit, and extremely high properties are possible. The influences of a lack of an upper limit are discussed later.

On visual inspection, the sample distributions shown in Figure 4-1 appear to demonstrate good lognormal behaviour. However, when Chi-square goodness-of-fit tests (D'Agostino and Stephens 1986) are performed on the generated data, it is clear that only fields with a low COV and SOF conform to a lognormal distribution with a high degree of confidence. The results of the Chi-square goodness-of-fit tests, for each of the nine fields, are shown in Table 4-1, where a higher *p*-value represents a higher probability of the data belonging to a lognormal distribution.

**Table 4-1 Goodness-of-fit statistics for simulated soil with a lognormal distribution**

Soil		Sample Statistics		Fit Statistics	
COV	SOF	Mean	Standard Deviation	$\chi^2$	$\chi^2$ p-value
10	1	9,977	723	59.43	0.8740
10	8	9,988	960	60.49	0.8520
10	32	10,022	881	102.89	0.0121
50	1	9,485	3353	70.48	0.5618
50	8	9,921	4,760	147.93	0.0000
50	32	10,016	4,340	271.23	0.0000
100	1	8,490	5,656	79.10	0.2926
100	8	9,840	9,426	117.52	0.0007
100	32	10,147	8,460	123.02	0.0002

It is clear from the results in Table 4-1 that, as the SOF increases, the probability that the data belongs to a lognormal distribution decreases. This is because properties in a field with a higher SOF are correlated. This infers that properties are more self-similar, which therefore skews the distribution. It should also be noted that the assumed bin size has a considerable impact on the Chi-square test. In this case, a constant bin size was adopted to simplify the analysis. This has an influence on the results shown in Table 4-1.

It is also important to verify that the sample mean and variance of the generated fields represent the target mean and variance. It should be noted, that the target mean and variance

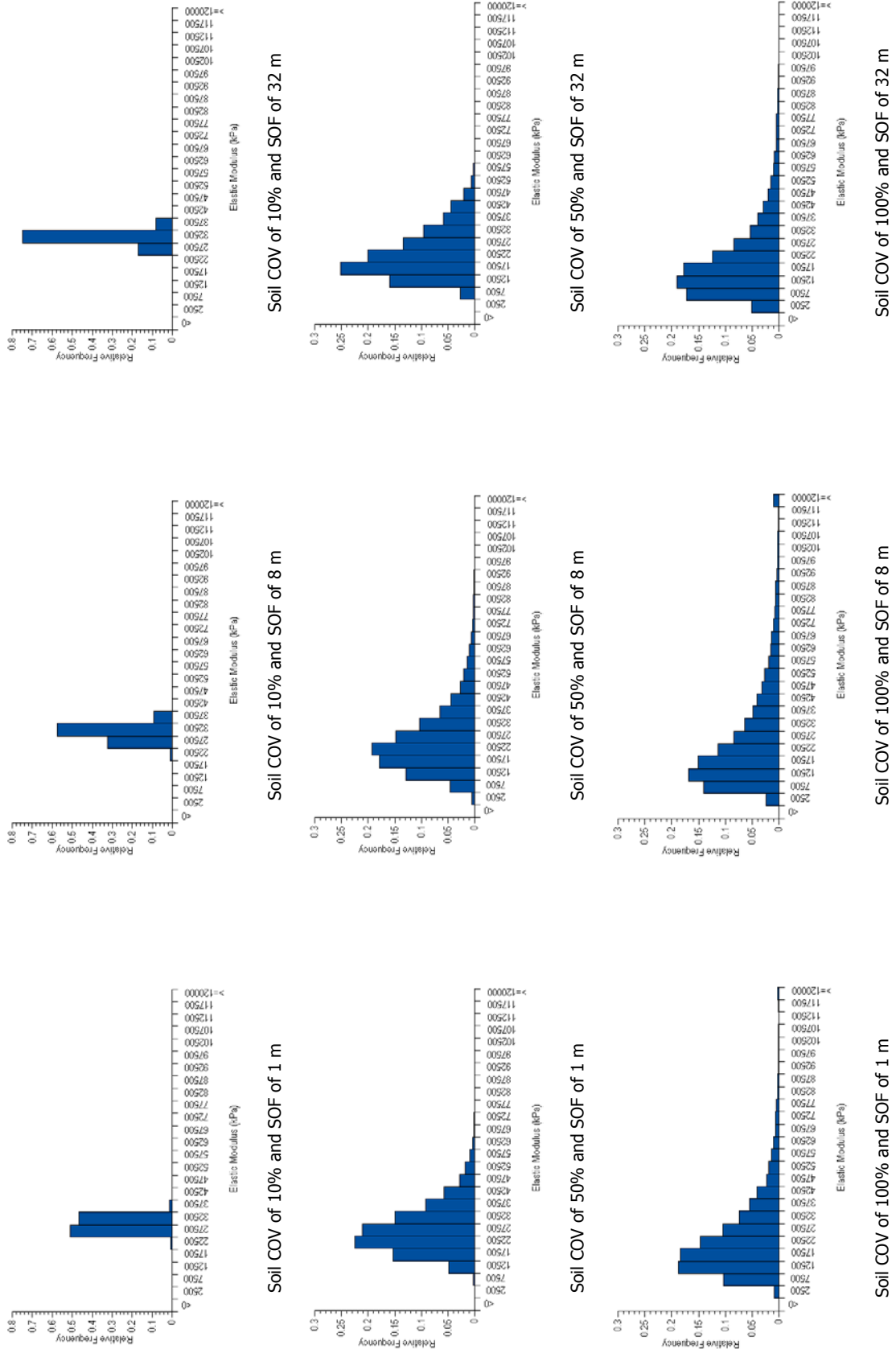


**Figure 4-1** Frequency distributions of elastic modulus values from the simulated soil using LAS (based on soil properties at the surface)

are point estimates, while the resultant sample mean and variance are local averages that are affected by the element size and the SOF (Vanmarcke 1983). Effects of local averaging have been briefly discussed in Chapter 2, but are also shown in greater detail by the results in Table 4-2, where the sample mean and standard deviation for 9 different soils are compared to the target mean and standard deviation.

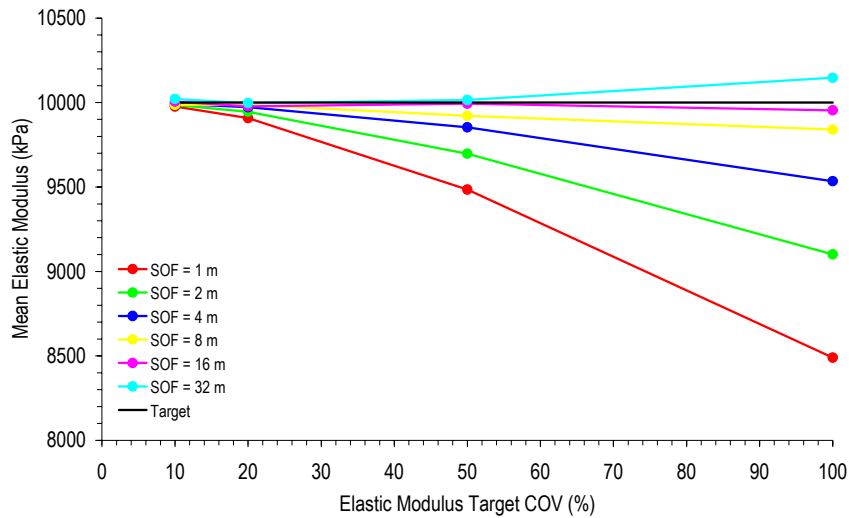
**Table 4-2 Comparison between target and sample mean and standard deviation of simulated soils**

Soil		Mean (kPa)		Error (%)	Standard Deviation (kPa)		Error (%)
COV	SOF	Target	Sample		Target	Sample	
10	1	10,000	9,977	0.2	1,000	723	27.7
10	8	10,000	9,988	0.1	1,000	960	4.0
10	32	10,000	10,022	0.2	1,000	881	11.9
50	1	10,000	9,485	5.2	5,000	3,353	32.9
50	8	10,000	9,921	0.8	5,000	4,760	4.8
50	32	10,000	10,016	0.2	5,000	4,340	13.2
100	1	10,000	8,490	15.1	10,000	5,656	43.4
100	8	10,000	9,840	1.6	10,000	9,426	5.7
100	32	10,000	10,147	1.5	10,000	8,460	15.4

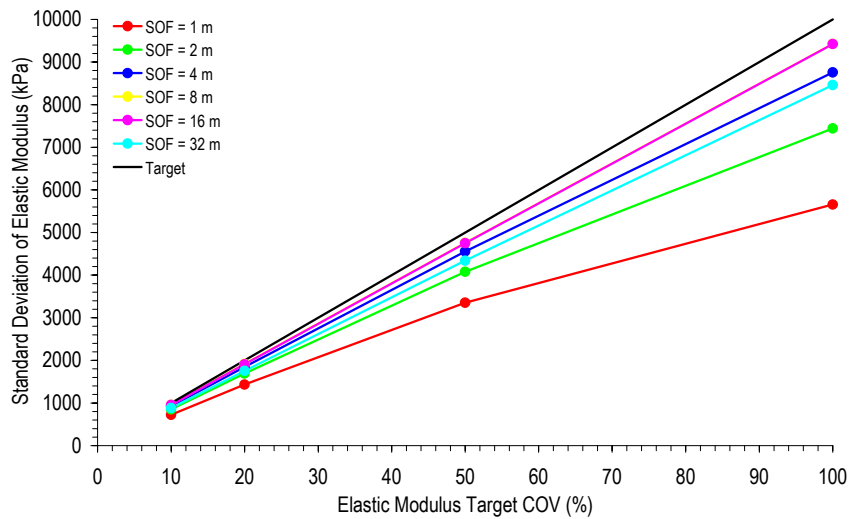
The sample mean is calculated by averaging the properties in each elastic modulus field, as well as for the 1,000 Monte Carlo realisations. Similarly, the sample standard deviation is calculated by averaging the standard deviation for each elastic modulus field over the suite of realisations. The results shown in Table 4-2 are presented graphically in Figures 4-2 and 4-3 to illustrate trends between the sample and target mean and standard deviation. Results shown in Figures 4-2(a) and (b) highlight the effect of increasing the target COV on the sample mean and standard deviation, respectively. On the other hand, results shown in Figures 4-3(a) and (b) illustrate the influence of an increasing target SOF on the sample mean and standard deviation, respectively.

The results shown in Figures 4-2 and 4-3 suggest that the sample mean and standard deviation are dependent on the target COV and SOF. For example, the sample mean diverges from the target mean as the target COV increases, as shown in Figure 4-2(a). This is especially true when the target SOF is 1 m, yet results in Figure 4-2(b) further indicate that the sample standard deviation diverges from the target as the COV increases. Again, this is exacerbated when the target SOF is small.





(a)



(b)

**Figure 4-2 Effect of target soil COV on the sample (a) mean and (b) standard deviation**

The target SOF is also shown to have an influence on the sample mean and standard deviation, by the results presented in Figures 4-3(a) and (b). Such results suggest that the sample mean approaches the target mean as the target SOF increases. In fact, the sample mean appears to equal the target mean, when the soil SOF has a specific value. However, this SOF value also appears to be a function of the target COV, where fields generated with larger COV require a larger SOF for equality.

Although the results shown in Figure 4-3(a) suggest that the sample mean approaches the target mean for an ever-increasing target SOF, the results shown in Figure 4-3(b) indicate a peak sample standard deviation for a specific target SOF value, which appears to occur when the target SOF is between 8 m and 16 m and seems to be unaffected by the target

COV. At no time, for the conditions investigated, does the sample standard deviation exceed the target standard deviation, as shown in Figure 4-2(b).

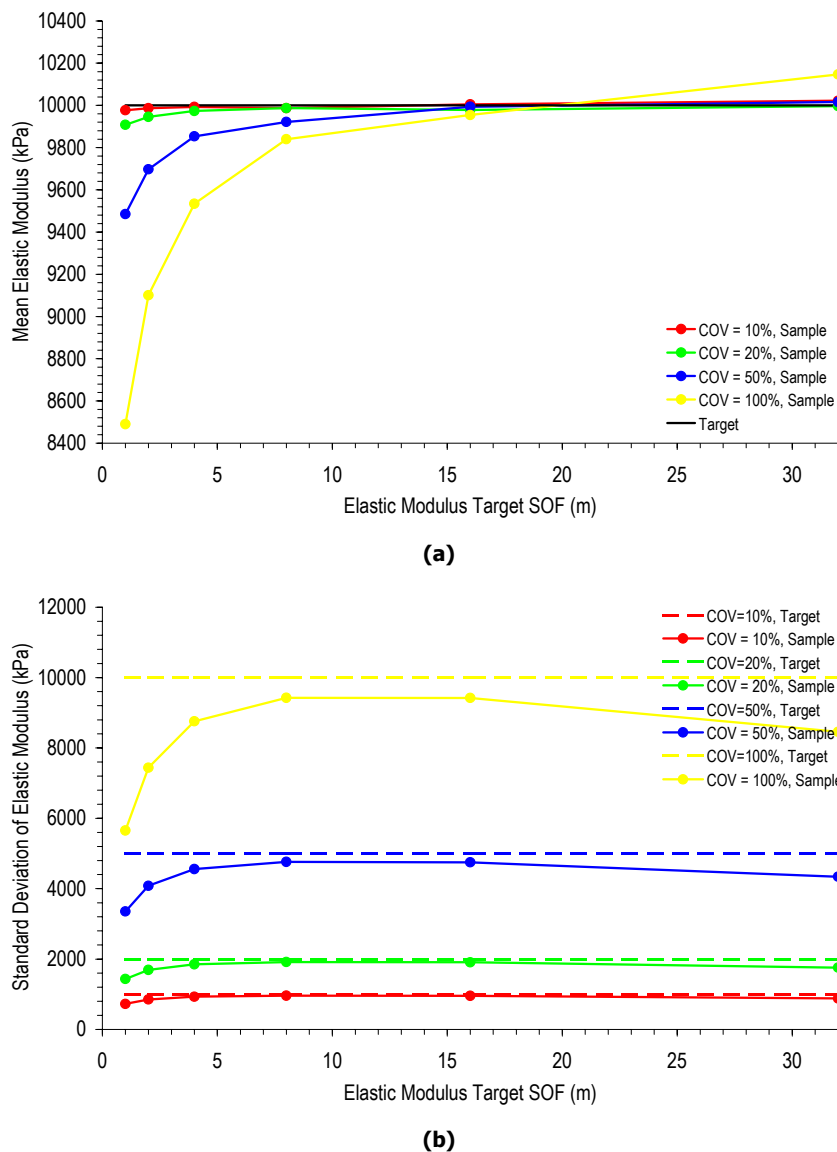


**Figure 4-3 Effect of target soil SOF on the sample (a) mean and (b) standard deviation**

The results in Figure 4-3 that indicate a maximum sample standard deviation, for a specific target SOF, warrant further investigation. As such, two different analyses are undertaken to examine the impact of a varying target SOF, element and field size. The first analysis investigates the effect of increasing the element size, while the field size is kept constant at 50 m × 50 m × 30 m. These results are provided in Figure 4-4(a) for soils with five different SOFs and a COV of 50%. The element size of 0.5 m is also identified in Figure 4-4(a) since this size is assumed for all the analyses that follow, as discussed in Chapter 3 (§3.6.5.3).

The second type of analysis investigates the effect of increasing the field size, where the element size is held constant at  $0.5 \text{ m} \times 0.5 \text{ m} \times 0.5 \text{ m}$ . In this case, only four different soil SOFs are investigated, but the soil COV is again kept constant at 50%. These results are given in Figure 4-4(b), which illustrates the field size in terms of field width. The width of 50 m is identified in Figure 4-4(b), since a field size of  $50 \text{ m} \times 50 \text{ m} \times 30 \text{ m}$  is assumed for the remainder of analyses, as discussed in Chapter 3 (§3.3.5).

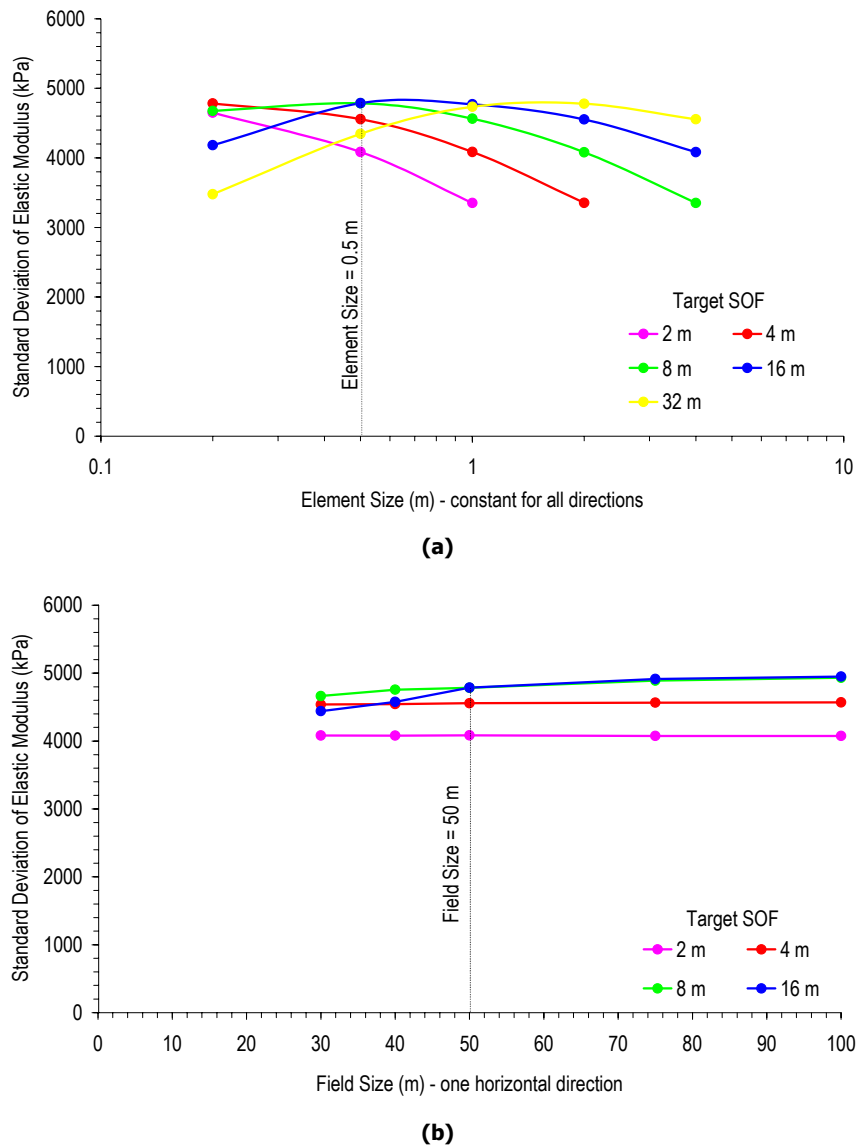


**Figure 4-4 Sample standard deviation of the elastic modulus field for an increasing (a) element size and (b) target SOF**

Figure 4-4 clearly indicates that the element size has a greater impact on the sample standard deviation than the field size. In fact, the site size appears to have little influence on the standard deviation, as shown in Figure 4-4(b). Figure 4-4(a) also indicates that, for the

element size assumed in the analyses that follow, the maximum standard deviation occurs when the target SOF is 8 m. This is therefore, considered the worst case SOF and causes the highest variability in the simulated soil. A worst case SOF has previously been identified in a similar type of analyses by Fenton and Griffiths (2002).

Further evidence to support that the worst case SOF is a function of the element size is shown in Figure 4-5, which shows the effect of increasing the ratio of SOF to element size on the sample standard deviation of the field. These results indicate that the maximum standard deviation occurs when the ratio between target SOF and element size is 16. Therefore, as estimated above, the target SOF that causes the maximum standard deviation is 8 m, for a 0.5 m element size.

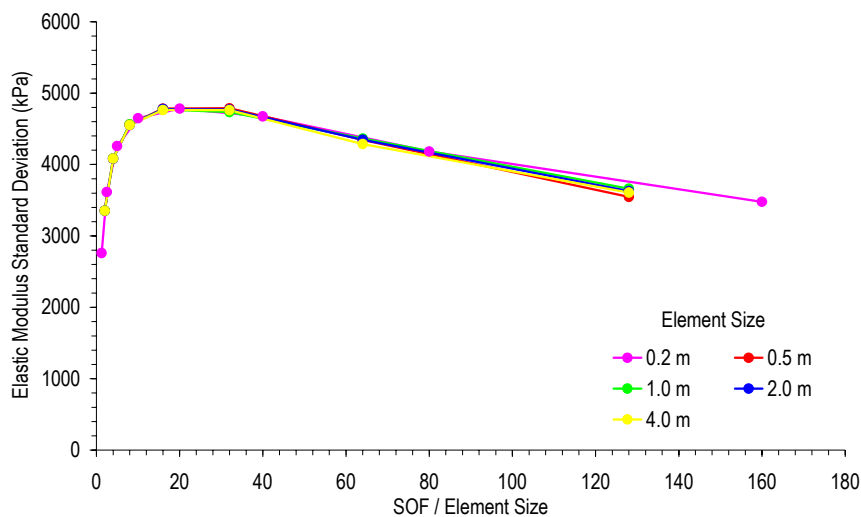


**Figure 4-5 Sample standard deviation of elastic modulus field based on different element sizes**

**A maximum sample standard deviation occurs when the ratio of SOF to element width is 16. In this case, where the element size is assumed to be 0.5 m, the SOF is 8 m. This is considered the worst case SOF.**

By using the worst case SOF in the results that follow, all resulting conclusion can be considered conservative. As such, it is not necessary to accurately characterise the soil SOF. Instead, the results regarding the required sampling effort to characterise a site, based on a worst case SOF, are over-conservative and therefore, should also be sufficient for soils with different SOFs.

The occurrence of a worst case SOF that causes a maximum standard deviation is also intuitive. For example, when the SOF is small, the elastic modulus properties vary rapidly about the mean over short distances. However, because the variations are so rapid, the variability averages out over a reasonable averaging domain, leading to a small standard deviation. At the other end of the spectrum, when the SOF is high, the properties in the soil are highly correlated or self-similar. Therefore, over a finite domain, the variability or standard deviation is also small. Consequently, with the standard deviation being close to zero when the target SOF is either small or large, the inference is for a high standard deviation, or variability, when the SOF value lies between the extreme cases. This phenomenon is clearly shown in the results shown in Figures 4-3(b), 4-4(a) and 4-5.

The variability in the sample mean for varying target SOF and COV, as shown in Figure 4-2, is also explained using local averaging, with the inclusion of a variance reduction term, as discussed by Vanmarcke (1983). However, it is first necessary to recall the method used to transform a normal variable into a lognormal one, as discussed in Chapter 3. This process involves calculating the mean,  $\mu_{\ln x}$ , and variance,  $\sigma_{\ln x}^2$ , of the lognormal variable using:

$$\mu_{\ln x} = \ln(\mu_x) - \frac{1}{2} \sigma_{\ln x}^2 \quad (4.1)$$

and

$$\sigma_{\ln x}^2 = \ln\left(1 + \frac{\mu_x^2}{\sigma_x^2}\right) \quad (4.2)$$

respectively, where  $\mu_x$  and  $\sigma_x^2$  are the mean and variance of the normal or standard variable, respectively. The variance reduction relationship,  $\gamma(D_v)$  for an exponentially-decaying correlation structure, in a domain of size of  $D_v$ , is incorporated in Equation (4.2) to give the relationship for the sample mean as:

$$\hat{\mu}_x = \mu_x \exp\left\{\frac{1}{2}(\gamma(D_v) - 1) \ln\left(1 + \frac{\sigma_x^2}{\mu_x^2}\right)\right\} \quad (4.3)$$

Therefore, Equation (4.3) infers that:

$$\text{as } \frac{\sigma_x^2}{\mu_x^2} = COV_x^2 \rightarrow \infty, \hat{\mu}_x \rightarrow 0 \quad (4.4)$$

$$\text{as } \frac{\sigma_x^2}{\mu_x^2} = COV_x^2 \rightarrow 0, \hat{\mu}_x \rightarrow \mu_x \quad (4.5)$$

$$\text{as } \theta \rightarrow \infty, \gamma(D) \rightarrow 1 \therefore \hat{\mu}_x \rightarrow \mu_x \quad (4.6)$$

$$\text{as } \theta \rightarrow 0, \gamma(D) \rightarrow 0 \therefore \hat{\mu}_x \rightarrow \exp\{\mu_{\ln x}\} \quad (4.7)$$

where  $\exp\{\mu_{\ln x}\}$  is the median of the normal variable. The conditions in Equations (4.4) to (4.7) are consistent to the trends shown previously shown in Figure 4-2(a) where, as the target COV increases, the sample mean approaches zero [Equation (4.4)]. On the other hand, when the target COV decreases, the sample mean approaches the target [Equation (4.5)]. These results are very different when considering the target SOF, where the sample mean approaches the median as the target SOF is reduced [Equation (4.7)], while, as the SOF increases, the sample mean approaches the target mean [Equation (4.6)].

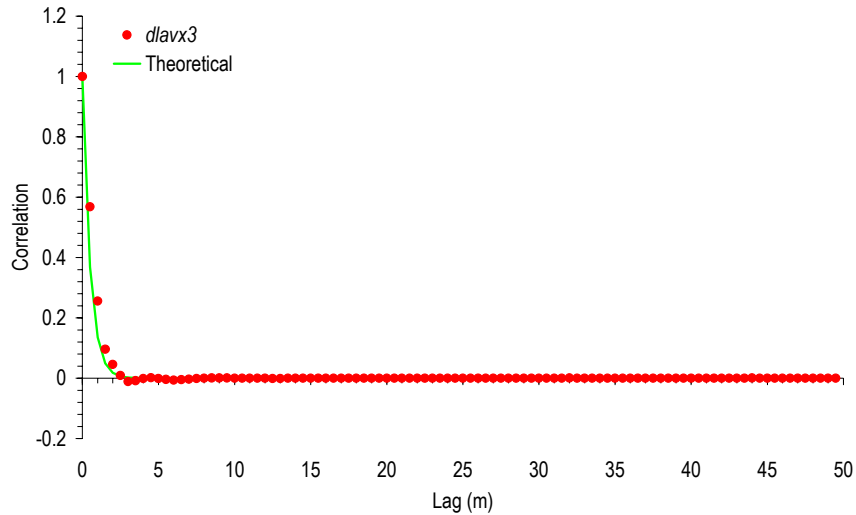
#### 4.2.2 Verifying the Correlation Structure

The local average subdivision methodology adopted to generate three-dimensional random fields, discussed in Chapter 3, uses two functions to simulate the target correlation structure. The *dlavx3* and *dlspx3* function represent a three-dimensional averaging variance function and a three-dimensional partially separable variance function, respectively. These functions are part of the *mrsetl3d* code developed by Fenton and Griffiths (2005). Both aim to simulate an exponentially-decaying correlation structure or Markov model.

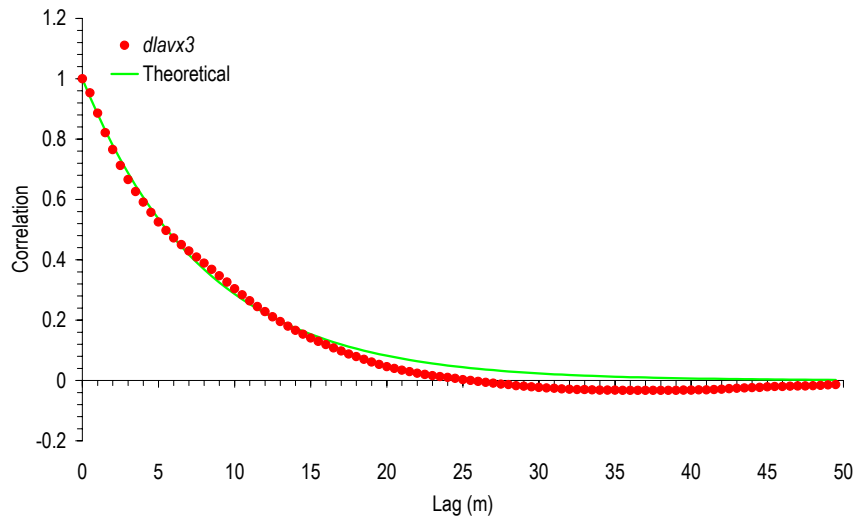
In order to validate the correlation functions generated by *dlavx3* and *dlspx3*, their output is compared with the target correlation structure in Figures 4-6 and 4-7, respectively. The theoretical relationship of a three-dimensional exponentially-decaying correlation structure is given by:

$$\rho(\boldsymbol{\tau}) = \exp\left(\frac{-2|\boldsymbol{\tau}|}{\theta}\right) \quad (4.8)$$

where  $\rho(\boldsymbol{\tau})$  is the correlation between two points in the field separated by the distance vector  $\boldsymbol{\tau} = \{\tau_x, \tau_y, \tau_z\}$  and  $\theta$  is the target SOF. In this analysis, only fields with an isotropic correlation structure have been investigated, hence the use of a single SOF value in Equation (4.8).



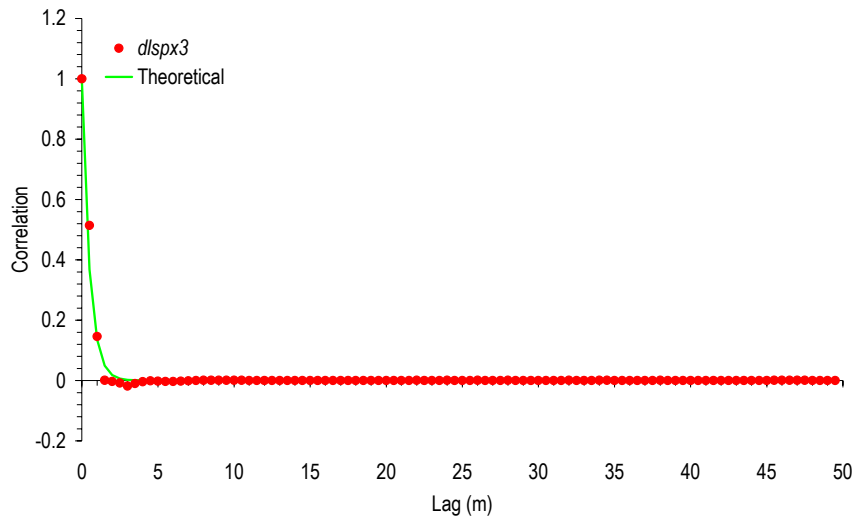
(a)



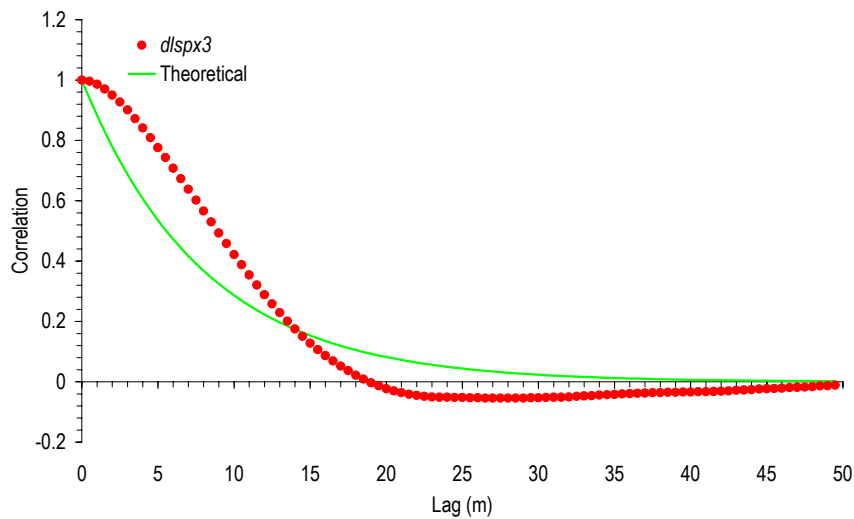
(b)

**Figure 4-6 Correlation structure of simulated field using *dlavx3* and a (a) COV of 50% and a SOF of 1 m and (b) COV of 50% and a SOF of 16 m**

The results shown in Figures 4-6 and 4-7 suggest that the *dlavx3* function appears to simulate fields that yield a better representation of the target correlation structure than the *dlspvx3* function. This is especially true for fields with larger SOFs, as shown in Figures 4-6(b) and 4-7(b). However, both functions appear to simulate fields that comply sufficiently well when the SOF is 1 m, as shown in Figures 4-6(a) and 4-7(a).



(a)



(b)

**Figure 4-7** Correlation structure of simulated field using *dlsp3* and a (a) COV of 50% and a SOF of 1 m and (b) COV of 50% and a SOF of 16 m

The difference between soil simulations using each variance function is shown more clearly by profile outputs as given in Figures 4-8 and 4-9, which illustrate the elastic modulus values on the  $x$ - $y$  plane located at the surface ( $z = 0$ ). The outputs in Figure 4-8 are based on a simulated soil with a target COV of 50% and SOF of 1 m, while the outputs in Figure 4-9 are based on a soil with a target COV of 50% and SOF of 16 m.

The results shown in Figure 4-9, for a SOF of 16 m, show a clear difference between the use of *dlavx3* and *dlsp3*. The field generated using *dlavx3* [Figure 4-9(a)] appears to have greater resolution than the field generated using *dlsp3* [Figure 4-9(b)]. This difference is also exhibited when comparing the sample correlation structure with the target correlation structure, shown in Figures 4-6(b) and 4-7(b), for the *dlavx3* and *dlsp3* functions, respec-



tively. Based on these results, the  $dlavx3$  function is adopted to simulate the correlation between properties in the simulated soil.

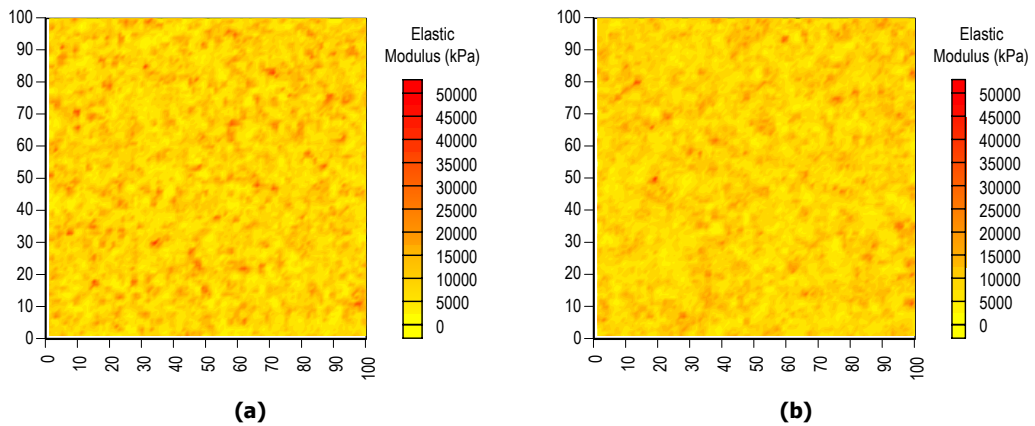


**Figure 4-8** Surface properties for a soil COV of 50% and a SOF of 1 m using (a)  $dlavx3$  and (b)  $dlspvx3$  variance functions

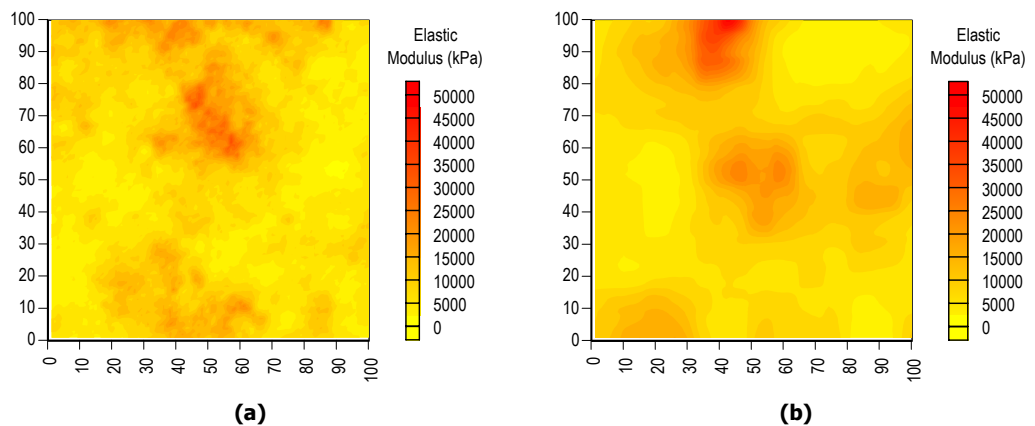
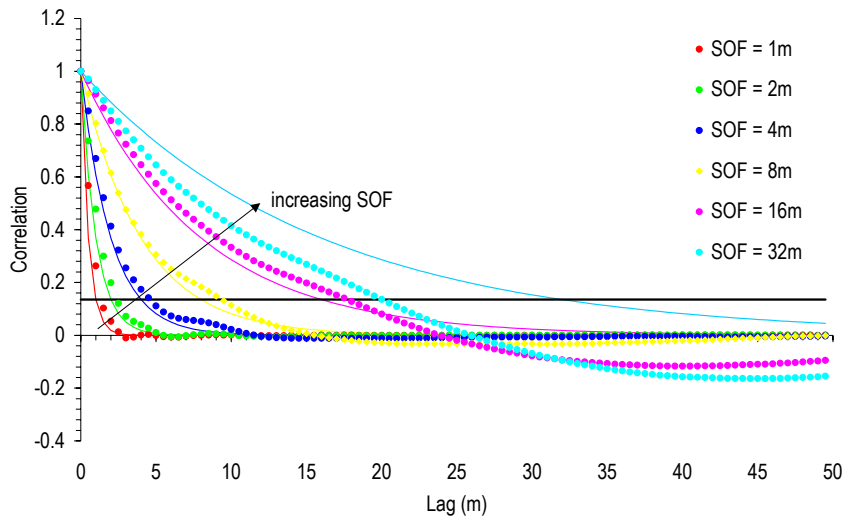


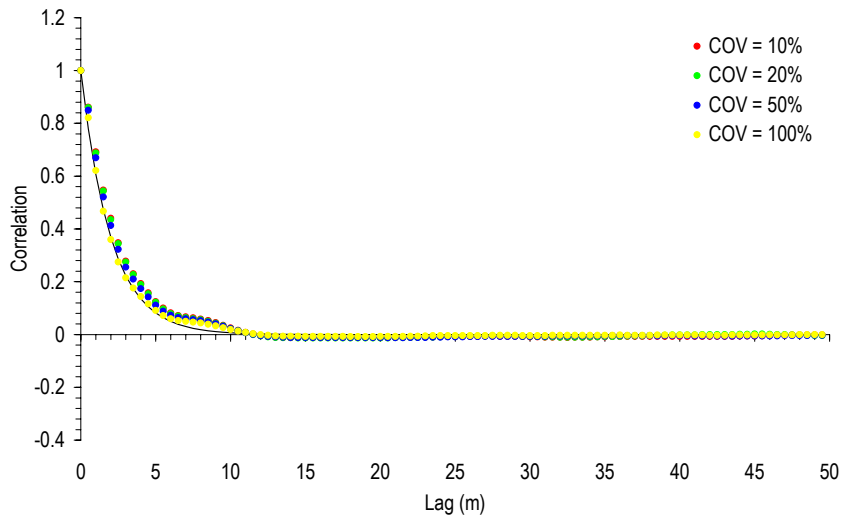
**Figure 4-9** Surface properties for a soil COV of 50% and a SOF of 16 m using (a)  $dlavx3$  and (b)  $dlspvx3$  variance functions

The three-dimensional averaging variance function ( $dlavx3$ ) is used to simulate the correlations between points, when generating fields using the local average subdivision technique.

The ability of  $dlavx3$  to accurately simulate the correlation structure of a field is further tested for a range of target SOF and COV values. The results shown in Figures 4-10(a) and 4-10(b) illustrate this ability, as the target SOF and COV is increased, respectively. The target correlation structure for each SOF value is also shown in Figure 4-10, based on the relationship given previously in Equation (4.8).



(a)



(b)

**Figure 4-10 Correlation structures generated by *dlavx3* function for (a) increasing target SOF and (b) increasing target COV**

Results shown in Figure 4-10(b), suggest that the target COV does not affect the accuracy of the *dlavx3* function in simulating the target correlation structure. However, the target SOF does appear to have an impact, as shown in Figure 4-10(a). The black line, shown in Figure 4-10(a), indicates the theoretical correlation when the lag equals the target SOF. It is, therefore clear, from Figure 4-10(a), that *dlavx3* less accurately models fields with larger SOFs.

### 4.2.3 Investigation of Transformation Effects

As explained above, to yield a soil whose properties conform to a lognormal distribution, it is necessary to transform the normal distribution properties, as generated by using local

average subdivision (LAS). Therefore, it is important to investigate any effects associated with this transformation. This is achieved by plotting the sample element mean and standard deviation of the simulated soil averaged over 1,000 Monte Carlo realisations, as shown in Figure 4-11. This figure illustrates the sample mean and standard deviation for the surface plane ( $z = 0$ ) for soils with three different SOFs.

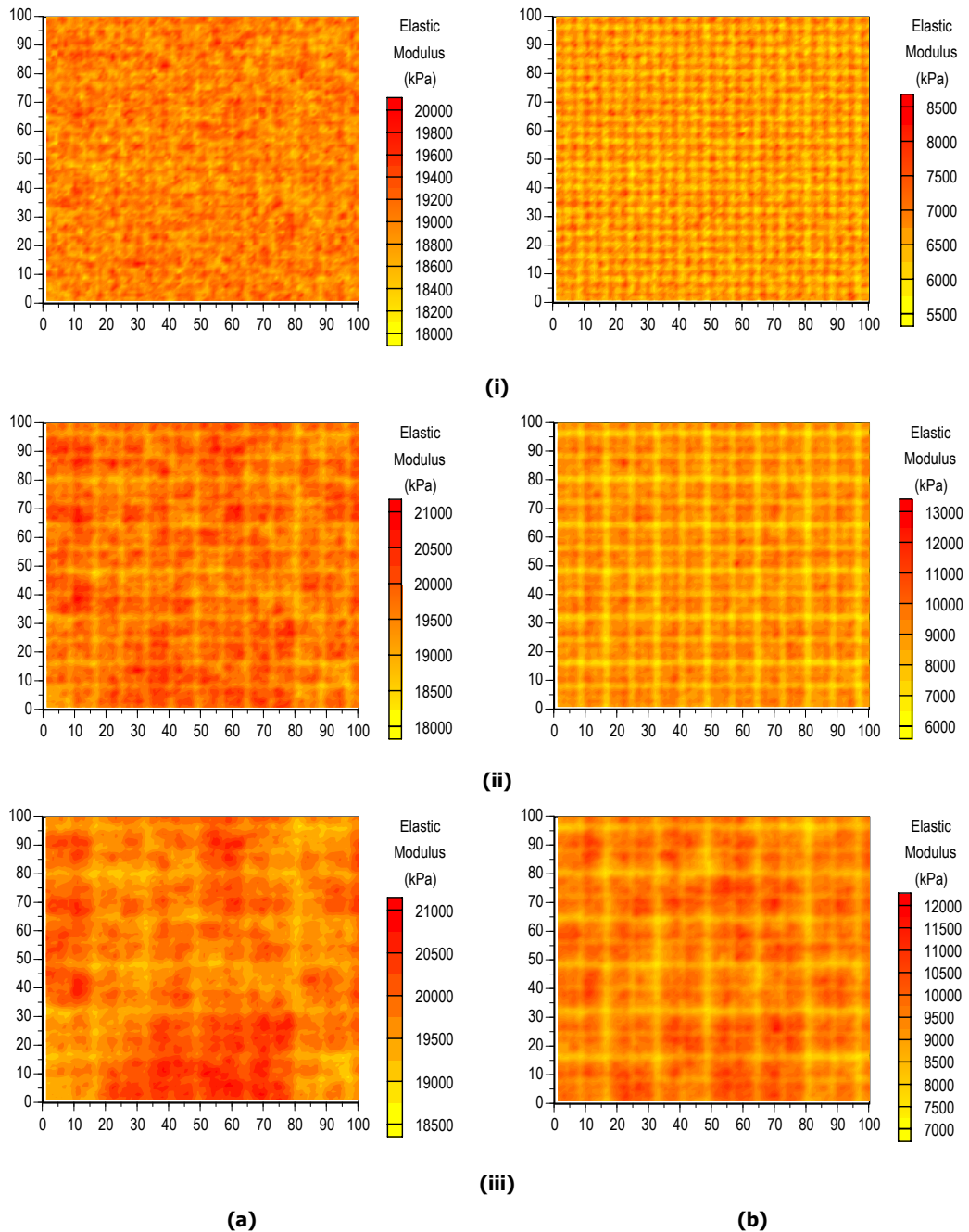


**Figure 4-11** Sample element (a) mean and (b) standard deviation of elastic modulus values at the surface ( $z = 1$ ) from a simulated soil with a COV of 50% and a SOF of (i) 1 m, (ii) 4 m and (iii) 16 m

The sample element mean is the average of the property located at the same relative position in the soil taken over the 1,000 realisations. Similarly, the sample element standard deviation is a measure of the variability of a soil property in the same relative position in the soil taken over 1,000 realisations.

The results shown in Figure 4-11 clearly demonstrate the presence of *gridding* or *aliasing* in the sample element mean and standard deviation for all three soils investigated. At first glance, the size of the gridding appears to increase as the SOF increases. However, on closer inspection, smaller gridding in the soil with the high SOF is still evident. Fenton (1994) observed a similar phenomenon when investigating the sample standard deviation of random fields with a normal distribution with zero mean and unit variance. However, the gridding was not evident in the sample element mean. This is because no transformation to a lognormal variable had been undertaken. The transformation to the lognormal variable incorporates the effect of the variance of the lognormal variable in the mean of the lognormal variable, as discussed earlier in this section and in Chapter 3 (§3.3.3). As a consequence, this induces the gridding effect into the sample element mean.

Fenton (1994) concluded that the gridding was a result of the cross-cell covariance in the LAS. To overcome these effects in the sample element mean, a field translation process is implemented. This involves generating a field that is significantly larger than the required field. The desired field is then sub-sampled from within the larger field with an origin ( $x = 0, y = 0, z = 0$ ). The location of each sub-sample changes for each subsequent Monte Carlo realisation. The locations of the origin are controlled along a diagonal to ensure a uniform selection of origin locations.

The result of using the field translation process is shown in Figure 4-12, for the sample element mean and standard deviation of the same fields as shown in Figure 4-11. Very little gridding is evident in Figure 4-12 after field translation is employed.

**A field translation procedure is implemented to eliminate gridding in the sample mean due to the lognormal transformation process.**

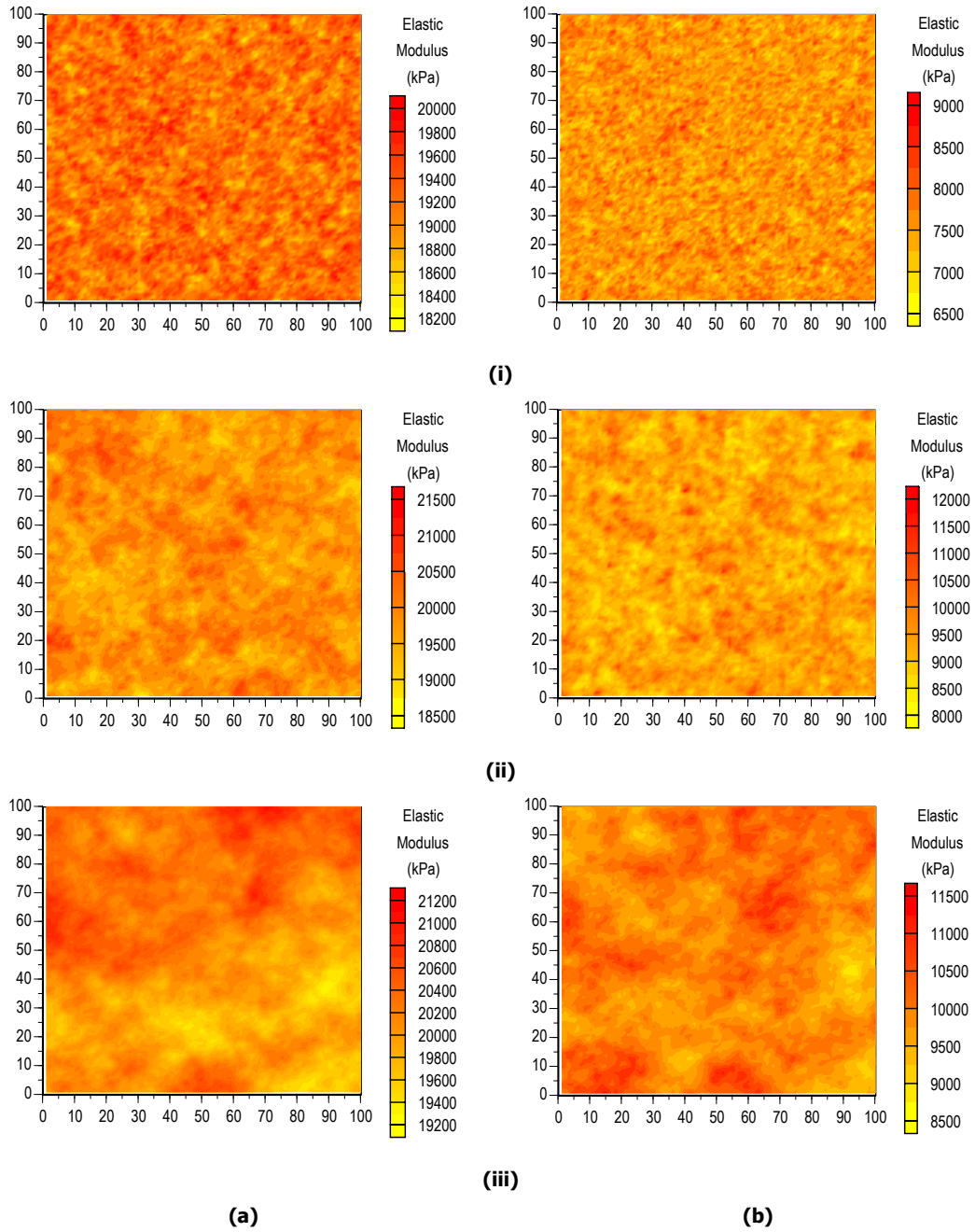


Figure 4-12 Sample element (a) mean and (b) standard deviation of elastic modulus values using field translation and a soil with a COV of 50% and a SOF of (i) 1 m, (ii) 4 m and (iii) 16 m

### 4.3 VERIFICATION OF THE IMPLEMENTATION OF SETTLEMENT PREDICTIONS TECHNIQUES

This section presents comparisons between settlement estimates using the methodology described in Chapter 3 and calculated settlements. Also included in this section are comparisons between settlement estimates using 3DFEA and measured settlements of constructed footings. These comparisons are undertaken with an aim to correlate the 3DFEA

model, described in Chapter 3 (§3.6.5), with measured footing settlements, so that a footing design using this method represents an optimal result.

### 4.3.1 Comparing Simulation and Calculated Settlement Predictions

Comparisons between the implemented settlement prediction techniques and settlements calculated by hand are conducted for a single pad footing on a soil with a uniform elastic modulus of 10,000 kPa. A constant deterministic elastic modulus is used so that errors associated with inherent soil variability and sampling are removed. The footing is positioned at the centre of a 50 m × 50 m site, with a depth of 30 m. Settlement estimates are based on a footing with an applied load of 1,500 kN and a plan size ranging from 1.5 m × 1.5 m to 3.5 m × 3.5 m. The results of the analysis are shown in Table 4-3 for each settlement prediction technique, excluding 3DFEA. These results demonstrate that the implementation of the methodology is accurate and yields the same settlement estimates as those calculated by hand. Results also indicate the differences in each settlement method.

**Table 4-3 Verification of settlement estimates for single pad footing**

Footing Size	Settlement (mm)							
	1.5 m × 1.5 m		1.5 m × 2.5 m		2.5 m × 2.5 m		2.5 m × 3.5 m	
Settlement Method	Sim. <sup>a</sup>	Calc. <sup>b</sup>	Sim. <sup>a</sup>	Calc. <sup>b</sup>	Sim. <sup>a</sup>	Calc. <sup>b</sup>	Sim. <sup>a</sup>	Calc. <sup>b</sup>
Schmertmann 2B-0.6	60.00	60.00	36.00	36.00	36.00	36.00	25.71	26.00
Schmertmann Modified	69.00	69.00	51.83	52.00	40.41	40.00	33.47	33.00
Timoshenko and Goodier	61.99	62.00	37.8	38.00	31.27	31.00	27.49	27.00
Newmark	61.98	62.00	47.78	48.00	38.13	38.00	31.91	32.00
Westergaard	80.42	80.00	62.85	63.00	49.82	50.00	41.92	42.00
2:1	70.68	71.00	47.04	47.00	41.23	41.00	32.04	32.00
Janbu	79.54	80.00	66.01	66.00	47.69	48.00	42.88	43.00
Perloff	86.00	86.00	47.09	47.00	40.86	41.00	28.15	28.00

Notes:

<sup>a</sup> simulation estimates are based on the implementation of the adopted methodology

<sup>b</sup> calculated estimates are based on hand calculations of the settlement relationships

The implementation of the methodology is also verified by evaluating settlements of a 9-pad footing system, as shown in Figure 4-13. As the elastic modulus is deterministic and uniform throughout the site, footings with the same applied load and the same relative position in the foundation system should suffer the same settlement.

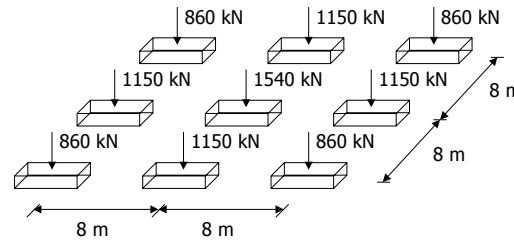


**Figure 4-13 System of 9-pad footings**

Table 4-4 shows the results of the settlement analysis of the 9-pad system founded on a soil with uniform elastic modulus of 30,000 kPa. The settlements of the corner footings and the central-edge footings are recorded for comparison purposes. The results indicate that the footings in a multiple pad system undergo the same settlements for footings that have the same applied load and the relative position in the system on a soil with a uniform elastic modulus. These results also confirm that the method adopted to account for the effects of adjacent footings is also reliable. There are slight differences between the predicted settlements of the corner and central edge footings, for each settlement prediction techniques, as shown in Table 4-4. These are a function of the approximate method used to estimate the settlement increase due to adjacent footings, as discussed in Chapter 3 (§3.6.4).

**Table 4-4 Settlement estimates for corner and central edge footings of the 9-pad system**

Settlement Method	Settlement (mm)							
	Corner Footings				Central-Edge Footings			
3DFEA	42.93	42.93	42.93	42.93	58.49	58.49	58.49	58.49
Schmertmann 2B-0.6	43.37	43.37	43.37	43.37	56.4	55.66	55.66	56.4
Timoshenko and Goodier	44.5	44.5	44.5	44.5	57.92	57.18	57.18	57.92
Newmark	44.5	44.5	44.5	44.5	57.92	57.18	57.18	57.92
Westergaard	55.07	55.07	55.07	55.07	72.06	71.32	71.32	72.06
2:1	49.49	49.49	49.49	49.49	64.59	63.85	63.85	64.59
Janbu	54.57	54.57	54.57	54.57	71.38	70.64	70.64	71.38
Perloff	53.63	53.63	53.63	53.63	73.15	72.41	72.41	73.15
Schmertmann Modified	48.53	48.53	48.53	48.53	63.3	62.56	62.56	63.3

To further verify the suitability of the method adopted to account for the effects of adjacent footings, an investigation is conducted comparing the predicted settlement of the footings in the 9-pad system with those predicted from 9 single footings. In this case, two separate analyses are conducted. The first examines the settlement of each of the nine footings as part of the foundation system. For the common settlement prediction techniques, this

analysis type requires the use of the method described in Chapter 3 to account for the settlement of adjacent footings. The second analysis type involves estimating the settlement of each of the 9 footings separately. This analysis does not include the effects of adjacent footings. The results of these analyses are shown in Figure 4-14 for 3DFEA, the Schmertmann 2B-0.6 and Timoshenko and Goodier prediction techniques. These results are based on a soil with a uniform elastic modulus of 10,000 kPa and each footing is assumed to have a size of 1.5 m × 1.5 m.

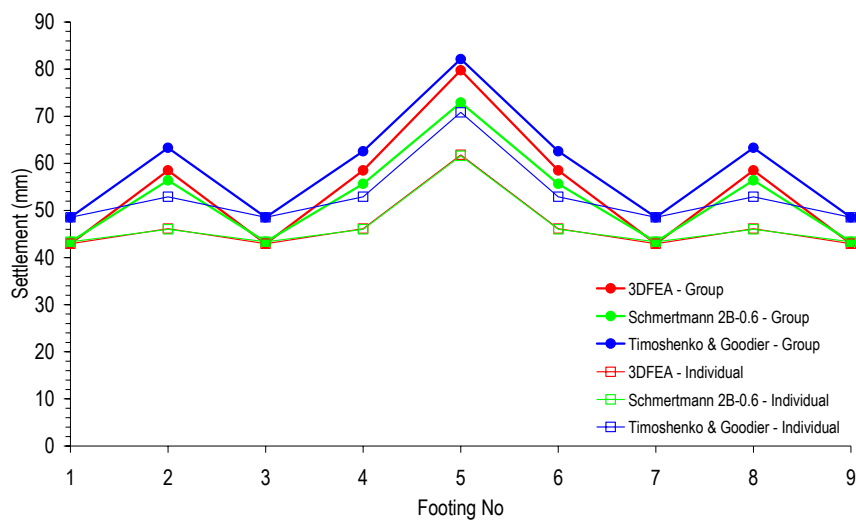


**Figure 4-14 Comparison between group and individual settlement for each footing in the 9-pad foundation system**

The results in Figure 4-14 suggest that, the methodology discussed in Chapter 3 (§3.6.4) to account for effects due to adjacent footings using the settlement prediction techniques, yields effects similar to those modelled by 3DFEA. It should be noted however, that the settlement increase shown for footing 5 is noticeably larger for 3DFEA than for the Schmertmann 2B-0.6 and Timoshenko and Goodier techniques. This difference is most likely the result of proportioning the settlement of the rigid circular footing, as described in Chapter 3 (§3.6.4). However, this is not expected to noticeably affect the results presented in the following chapters.

#### 4.3.2 Calibration of 3DFEA to Measured Settlements

The accuracy of the 3DFEA model is influenced by the adopted convergence tolerance and the size and number of elements in the finite element mesh. A discussion regarding the impact of these variables on the accuracy of the model has already been given in Chapter 3 (§3.6.5). However, this discussion did not deal with the accuracy of 3DFEA, as compared



to measured settlements. This comparison is considered necessary as the analysis or design, based on 3DFEA settlement estimates, is subsequently used as the optimal or benchmark analysis or design throughout this research and hence, should be as accurate as possible.

To determine the accuracy of 3DFEA settlement estimates with respect to measured settlements, an investigation is undertaken comparing settlement estimates using 3DFEA and the measured settlements of constructed footings, as documented by several authors (Kantey 1965, D'Appolonia 1968, Schmertmann 1970, Webb and Milvill 1971, Davisson and Salley 1972, Fischer 1972, Tschebotarioff 1973, Swiger 1974). The measured settlements used for this analysis are shown in Table 4-5, as an adaptation from Bowles (1997). It should be noted that the elastic modulus values were calculated using correlations with the CPT and SPT. These calculations were completed by the sources and no information was provided regarding the correlation models used. Furthermore, no information was provided regarding the property variability and hence, deterministic parameters are adopted. A few sources also failed to detail information regarding the depth of the soil layer. In these cases, the depth is assumed to be 30 m.

**Table 4-5 Measured settlements obtained from various literature sources including analysis parameters**

Source	$b$ m	$l$ m	$H$ m	$D$ m	$E^1$ kPa	$\nu$	$P$ kN	$\delta$ mm
Kantey (1965)	6.10	6.10	<sup>-2</sup>	21	12,449	0.30	7,117	82.55
D'Appolonia et al. (1968)	3.81	6.10	1.91	15	57,456	0.33	3,781	8.38
Schmertmann (1970)	2.59	22.80	2.02	13	14,843	0.40	10,577	36.83
Schmertmann (1970)	2.99	12.55	2.99	15	29,686	0.30	5,993	17.02
Schmertmann (1970)	18.90	18.90	<sup>-2</sup>	94	16,758	0.45	26,674	67.06
Schmertmann (1970)	26.52	58.34	2.65	27	11,012	0.30	306,654	297.18
Schmertmann (1970)	0.61	0.61	0.34	3	5,267	0.30	41	8.89
Webb and Milvill (1971)	53.95	53.95	<sup>-2</sup>	46	52,668	0.30	627,113	32.26
Davisson and Salley (1972)	37.80	37.80	<sup>-2</sup>	27	18,673	0.30	214,763	142.24
Fischer et al. (1972)	152.40	152.40	30.48	518	2,786,631	0.45	7,784,388	12.70
Tschebotarioff (1973)	27.43	30.18	2.74	22	12,928	0.30	285,362	99.06
Swiger (1974)	9.75	9.75	<sup>-2</sup>	39	186,733	0.30	12,526	6.10

Notes:  
<sup>1</sup> – elastic modulus values has been transformed from CPT and SPT results  
<sup>2</sup> – no depth was recorded

The results of this analysis are shown in Figure 4-15, where the 3DFEA settlement estimates are plotted against the measured settlements, including the equality line. The correlation between the measured and 3DFEA settlements appears low from the results shown in Figure 4-15. This is because of the uncertainties regarding the estimation of an elastic modulus and the unknown degree of variability in the analysis parameters. It should also be recognised that the 3DFEA settlement estimates are based on an estimate of a rigid loaded area, whereas footings do not deflect as a perfectly rigid area. Seycek (1991) also suggested that finite element analyses tend to over-estimate the settlement of a footing due to contributions of small strains at large depths in the soil layer. He suggested that it might be more suitable to restrict the zone of deformation within a soil, rather than analysing the total depth.

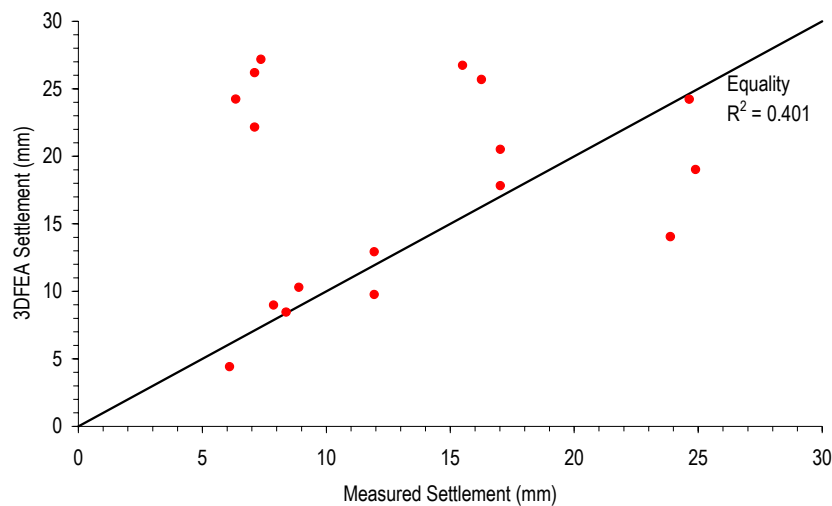
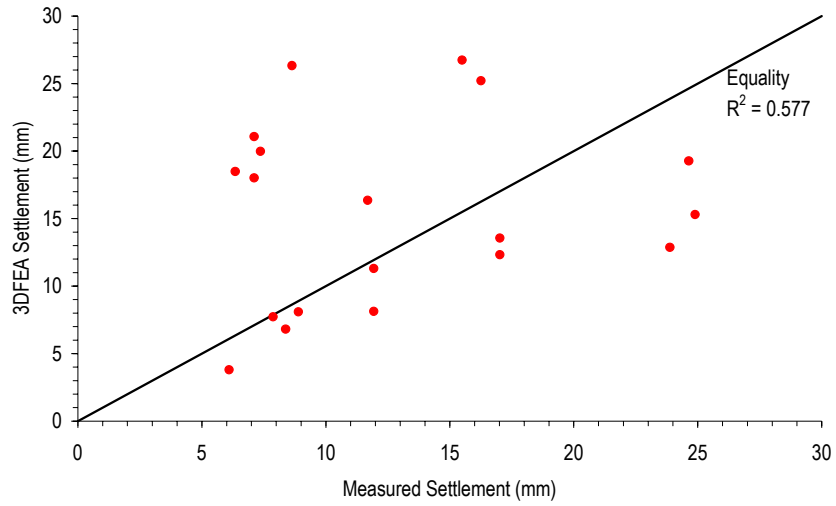
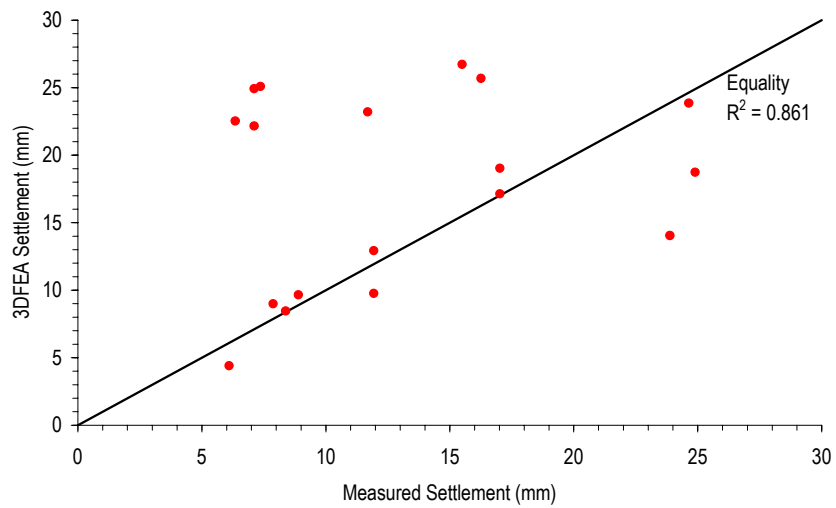


**Figure 4-15 Comparison between measured settlement and 3DFEA settlement using a full depth analysis**

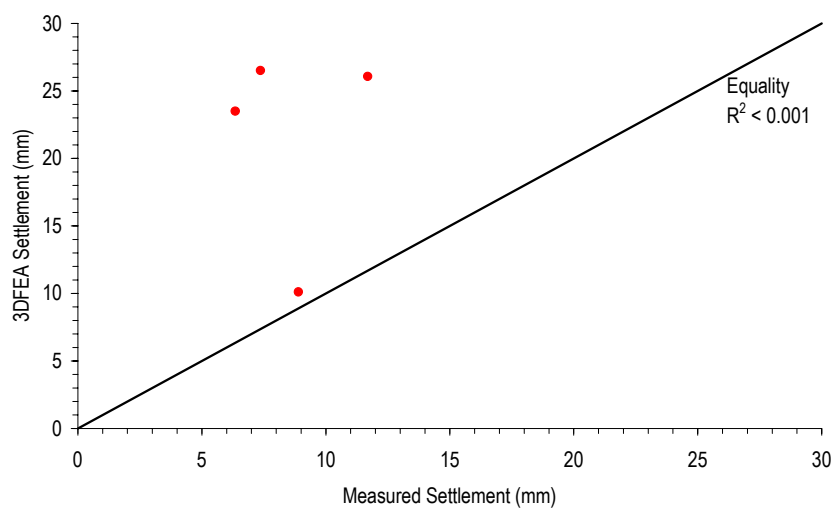
Holtz (1991) and Bowles (1997) suggested that 95% of stresses resulting from a loaded area exist within a depth of approximately 5 times the least plan dimension of the footing. As such, a comparison between 3DFEA settlement estimates and measured settlements is also conducted using a 3DFEA with a depth restriction equal to 2, 5 and 8 times the least plan dimension of the footing. These results are shown in Figure 4-16, based on the measured settlements and the parameters given in Table 4-5. These results yield slight improvements, where the correlation between estimated and measured settlements appears stronger for the depth restriction of 5 times the least plan dimension. In the cases where the 3DFEA settlement estimates are poorly correlated with the measured settlement, the 3DFEA estimates are typically larger. This corresponds to a conservatism, which, in some



(a)



(b)



(c)

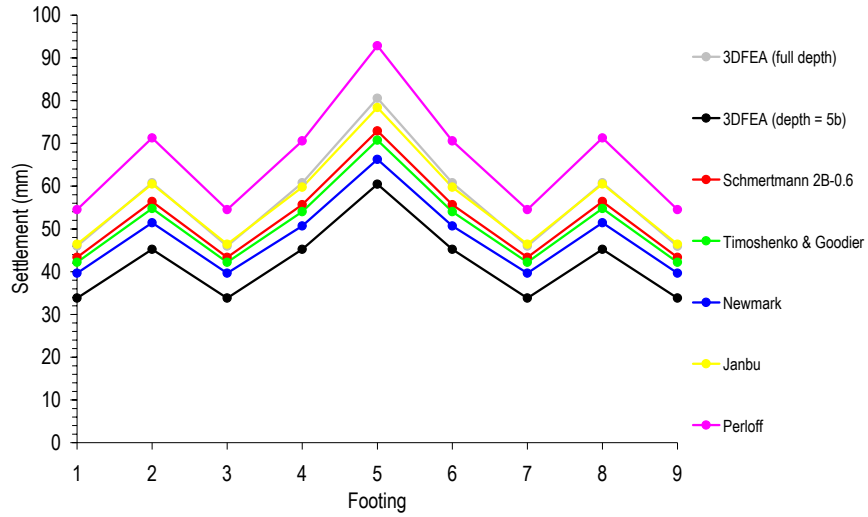
**Figure 4-16 Comparison between measured settlement and 3DFEA settlement using an analysis depth of (a)  $2b$ , (b)  $5b$  and (c)  $8b$ , where  $b$  is the least plan dimension of the footing**

cases, is by a factor of 4 or 5 times. Although this is not ideal, it does guard against potential failures and is therefore, more desirable than an under-conservatism, where the 3DFEA estimates settlements are much less than measured.

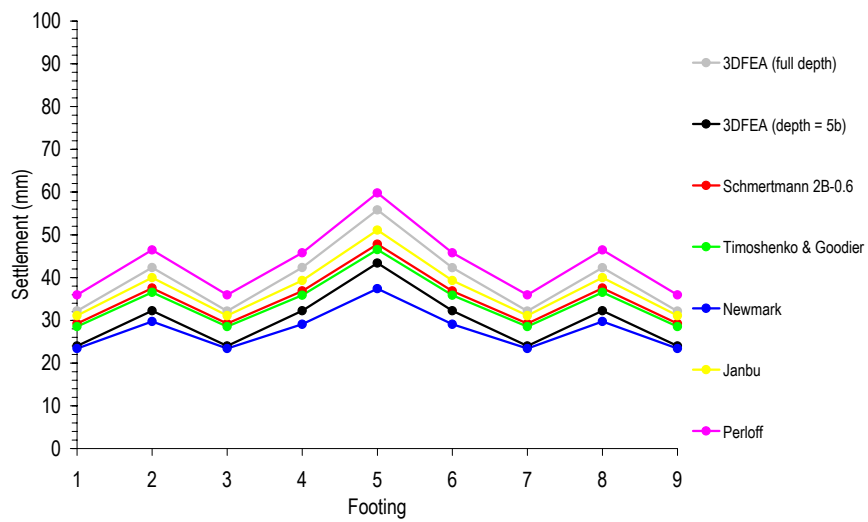
The results shown in Figure 4-17 compare the effect of adopting a depth restriction for 3DFEA on the settlement estimate for a system of 9 footings. In these results, 3DFEA is only restricted to a depth equal to 5 times the least plan dimension of the footing, where each footing in the system has the same width. Results are also compared to settlement estimates using four of the settlement prediction techniques discussed in Chapter 3. Analyses are shown for footing widths of 1.5 m, 2.5 m and 3.5 m, in Figure 4-17(a), (b) and (c), respectively. In all cases, footings are considered square and loaded with a 1,500 kN point load.

It is apparent from Figure 4-17 that the inclusion of a depth restriction for the 3DFEA yields, as expected, a smaller settlement estimate. However, the difference between estimates based on a full depth and the depth restriction analysis appears to reduce as the footing width increases. This is because the depth restriction approaches the full depth of the soil. The results shown in Figure 4-17 also suggest that a depth restriction of 5 times the footing width yields settlement estimates that are similar to Schmertmann's 2B-0.6 technique. Furthermore, this technique is based on correlations with measured settlements, as discussed in Chapter 2 (§2.2.2). On the other hand, settlement estimates using a full depth 3DFEA yields similar settlements to Janbu's relationship. This is because the coefficients of the Janbu relationship have been previously calibrated using the 3DFEA model, as discussed in Chapter 3 (§3.6.2).

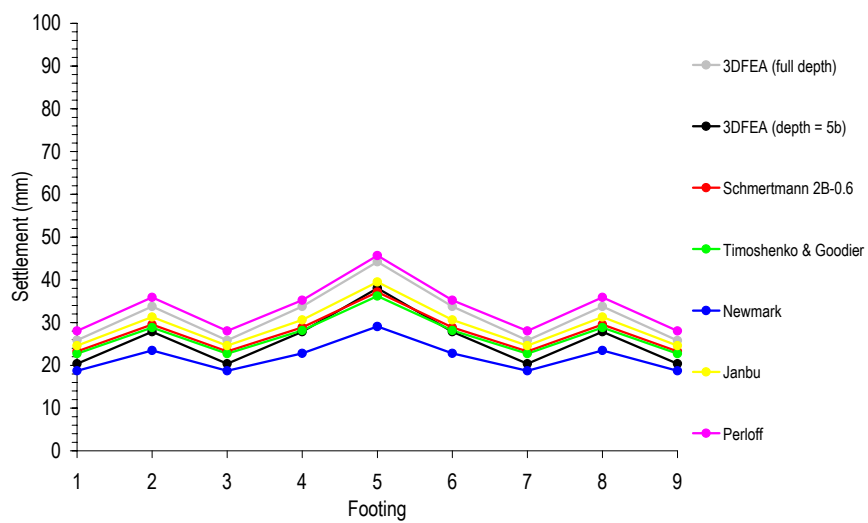
The results shown in Figure 4-17 indicate that 3DFEA estimates, based on a depth restriction of  $5b$ , yield a notably smaller settlement than the other settlement relationships investigated when the footing size is small. The cause of this difference is due to the manner in which the effects of adjacent footings are accommodated in the methodology. However, the results shown in Figure 4-17(c) show that, when the footing width is 3.5 m, 3DFEA, based on a full depth analysis, yields settlements close to the Perloff approximation, which is the most conservative of all the settlement techniques investigated. On the other hand, 3DFEA estimates, based on a depth restriction of  $5b$ , are similar to most of the settlement relationships investigated, including the Schmertmann 2B-0.6 technique. Therefore, the results shown in Figure 4-17 confirm that 3DFEA, based on a depth restriction of 5 times the footing width, yields a settlement that is closer to the measured settlement than a full depth analysis.



(a)



(b)



(c)

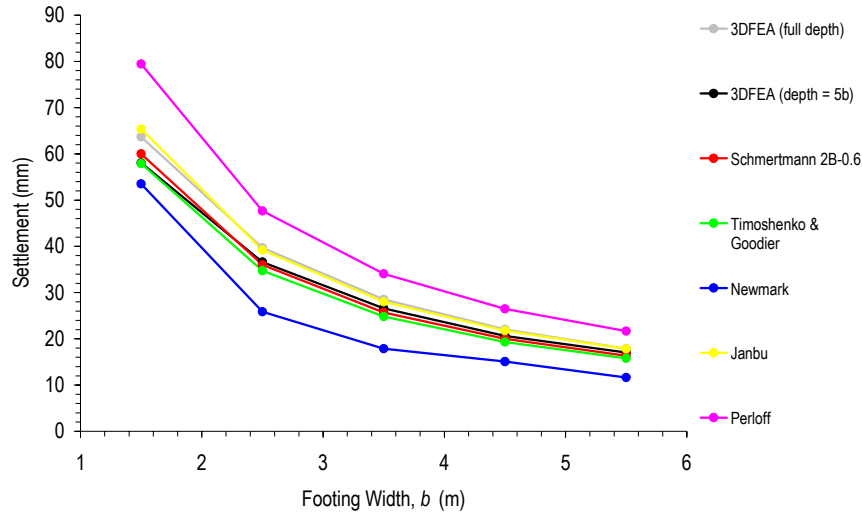
**Figure 4-17 Comparison between 3DFEA settlement with varying depth analyses and other settlement prediction techniques for 9 the pad footing foundation system with widths equal to (a) 1.5 m, (b) 2.5 m and (c) 3.5 m**

Results shown in Figures 4-18(a) and (b) compare 3DFEA settlement analyses based on a depth restriction of 5 times the footing width, with estimates using settlement prediction techniques for a single pad footing with varying width and a constant point load or constant pressure, respectively. Settlement estimates presented in Figure 4-18(a) are based on a single point load of 1,500 kN, whereas the results shown in Figure 4-18(b) are based on an applied pressure of 800 kPa. In both cases, the elastic modulus field is uniform (10,000 kPa) and all footings are considered square. These results indicate that 3DFEA, based on a depth restriction of  $5b$ , yields settlement estimates that are close to the Schmertmann 2B-0.6 technique. This is consistent with the results shown in Figure 4-17, for the multiple footing scenario. Furthermore, the results shown in Figure 4-18 indicate that a change in footing width or applied pressure does not cause the 3DFEA settlement estimate to diverge to any great extent from the Schmertmann 2B-0.6 estimate. On the other hand, the 3DFEA estimate, based on a full depth analysis, yields a larger settlement, which is in close agreement with the Janbu technique. This close agreement is due to the calibration of the Janbu coefficients, as discussed in Chapter 3 (§3.6.2).

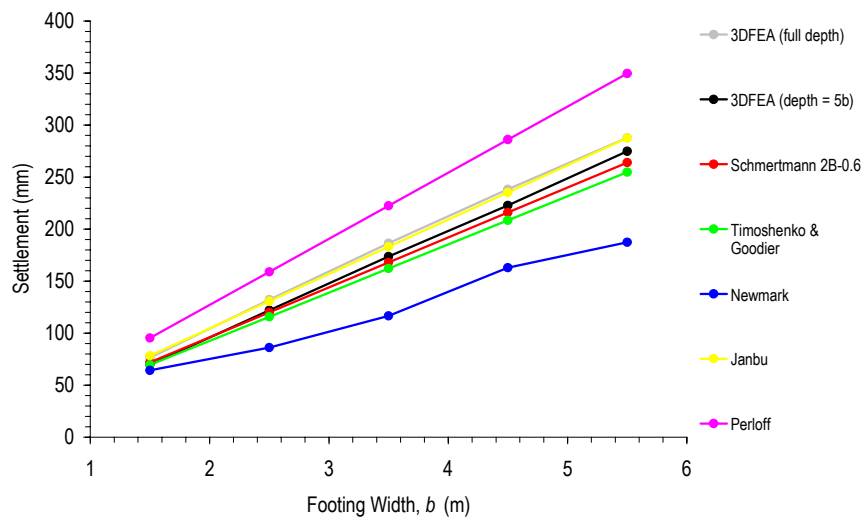
The results shown in Figure 4-18 also suggest that the 3DFEA settlement estimate, based on a depth restriction of  $5b$ , yields results that are split between the other prediction techniques. For example, in all conditions investigated, the Newmark and Timoshenko and Goodier techniques yield settlement estimates that are less than 3DFEA, based on a  $5b$  depth restriction. However, both the Janbu and Perloff techniques result in larger settlement estimates for all conditions investigated. Furthermore, settlement estimates based on the Perloff technique, are of a similar degree larger as the estimates based on the Newmark technique are smaller. This infers that 3DFEA, with a  $5b$  depth restriction, allows good comparisons between the other settlement prediction techniques, as well as showing better correlation with measured settlements.

Since the correlation between measured settlements is higher for 3DFEA, with a  $5b$  depth restriction, and because 95% of the stresses induced by a loaded area at the surface exist within a depth equal to 5 times the least plan dimension of the footing, all analyses that follow are based on a depth restriction equal to 5 times the least plan dimension of the footing. This includes the settlement techniques that integrate the strains at depth intervals as discussed in Chapter 2 (§2.2.2.2). This ensures consistency between all settlement estimates.

**The analysis of settlement using 3DFEA and settlement techniques that integrate strains over depth is restricted to an analysis depth equal to 5 times the least plan dimension of the footing.**



(a)



(b)

**Figure 4-18 Comparison between settlement estimates of 3DFEA with full and  $5b$  depth with common settlement prediction techniques of a single pad footing of varying width under (a) constant load and (b) constant pressure**

#### 4.4 VERIFICATION OF MEAN AND VARIABILITY OF SETTLEMENT ESTIMATES

This section evaluates the results of the Monte Carlo analysis, where comparisons are drawn between the output and a theoretical evaluation of footing settlement. Settlement estimates are based on elastic modulus data taken from different sampling locations within a  $50\text{ m} \times 50\text{ m}$  site, with an assumed depth of  $30\text{ m}$ . All footings are assumed to be  $1.5\text{ m} \times 1.5\text{ m}$  in plan dimension and loaded with a  $1,500\text{ kN}$  centrally-applied point load.

Both settlement estimates using the method described in Chapter 3 and the theoretical evaluation are based on the Schmertmann 2B-0.6 technique. Four different simulated

soils, defined by their target COVs and SOFs are investigated. The Monte Carlo analysis consists of 1,000 realisations for each soil. Settlement averages and standard deviations are determined for each soil and compared to a theoretical evaluation.

The theoretical evaluation is formulated by rearranging the Schmertmann equation to yield an expression for the settlement of the footing,  $\delta$ , in terms of the elastic modulus values,  $E_i$ . This is given by:

$$\begin{aligned}\delta &= C_1 C_2 \frac{P}{A} \sum_{i=1}^n \frac{I_{z_i}}{E_i} \Delta z \\ \delta &= C_1 C_2 \frac{P}{A} \sum_{i=1}^n \frac{I_{z_i}}{E_i} \Delta z \\ \delta &= C^* \sum_{i=1}^n \frac{I_{z_i}}{E_i} \\ \delta &= \sum_{i=1}^n \frac{C^{**}}{E_i}\end{aligned}\tag{4.9}$$

where  $C^*$  and  $C^{**}$  are both functions of the Schmertmann settlement influence factors and information regarding the load and footing size. Since the elastic modulus,  $E_i$ , is stochastic and represented by a random field, the settlement can also be expressed in terms of a stochastic variable,  $S$ . Furthermore, the expected or average settlement,  $E[S]$  or  $\mu_s$ , is directly related to the statistical description of the elastic modulus and is given by:

$$E[S] = \hat{\mu}_s = \sum_{i=1}^n C_i^{**} E\left[\frac{1}{E_i}\right] = \left(\frac{1 + COV_E^2}{\mu_E}\right) \sum_{i=1}^n C_i^{**}\tag{4.10}$$

where  $COV_E$  and  $\mu_E$  is the coefficient of variation and the average of the elastic modulus field, respectively. This relationship yields an estimation of the average settlement of a footing based on results from a sample of elastic moduli located anywhere around the site. However, because the relationship given in Equation (4.10) is independent of the location of  $E_i$ , the average settlement is constant for all sampling locations. This is because the elastic modulus field is assumed to be stationary, where the mean elastic modulus is independent of position in the field. Although stationarity infers that the average settlement is independent of location, the settlement is still stochastic and is, therefore, variable. Furthermore, a settlement estimate based on two different sampling locations within the same in-



dividual realisation may be different. As such, it is possible to define the covariance between two settlement estimates  $S_1$  and  $S_2$  as:

$$\text{Cov}[S_1, S_2] = \left( \frac{1 + COV_E^2}{\mu_E} \right)^2 \left[ \sum_{i=1}^n \sum_{j=1}^n C_i^{1**} C_j^{2**} (1 + COV_E^2)^{\rho_{ij}} - \sum_{i=1}^n C_{i, A_1}^{**} \sum_{j=1}^n C_{j, A_2}^{**} \right] \quad (4.11)$$

where  $\rho_{ij}$  is the correlation between two elastic moduli in the soil. (Note the difference between  $COV_E$  and  $\text{Cov}[\cdot, \cdot]$ , where the former refers to the coefficient of variation of  $E$  and the latter is the covariance operator.) The coefficients,  $C^{1**}$  and  $C^{2**}$  are the coefficients defined in Equation (4.9), based on sampling location 1 and 2, respectively. Considering the same settlement prediction technique and footing size is used,  $C^{1**}$  and  $C^{2**}$  are also the same.

The correlation between two elastic moduli is dependent on the vertical spacing of the soil properties in the field and the sample separation distance, as shown in Figure 4-19. When the sample separation distance becomes zero ( $x = 0$  in Figure 4-19), the covariance between  $S_1$  and  $S_2$  becomes the variance of  $S$ ,  $\text{Var}[S]$ , and the correlation is dependent only on the vertical spacing of soil properties. Similarly with the average or expected settlement estimate, the variance of settlement estimate is also independent of location and yields a constant value for all sampling locations.

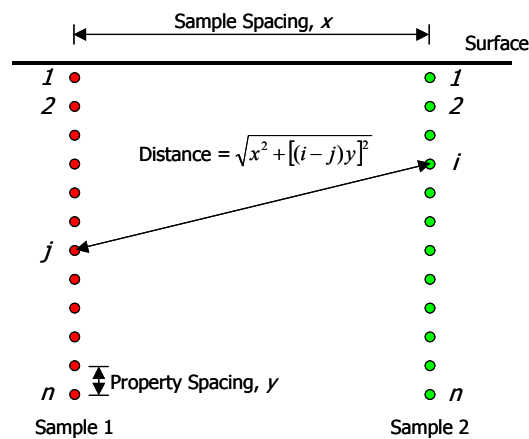
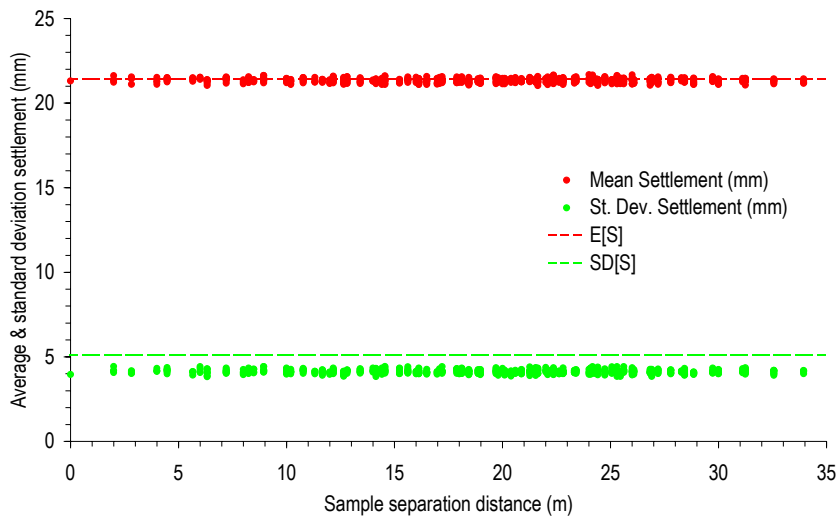


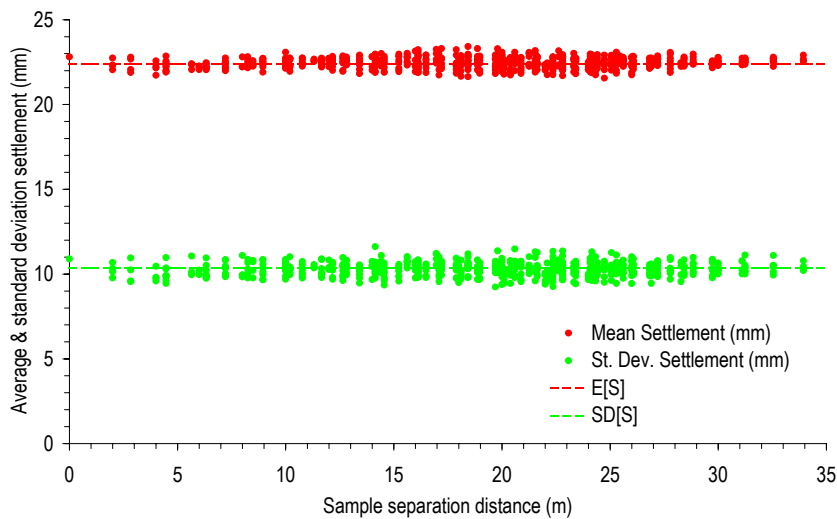
**Figure 4-19** Distance used to determine correlation,  $\rho_{ij}$ , between two sample locations and between soil properties spaced in the vertical direction

Results shown in Figures 4-20 and 4-21 compare the average and standard deviation of settlements obtained using the adopted methodology and the theoretical evaluation using Equations (4.10) and (4.11). The variance of the settlement estimate given in Equation (4.11) is converted to a standard deviation to enable direct comparisons with the results of

the methodology. The results in Figures 4-20(a) and (b) show the average and standard deviation of settlement estimates based on an increasing sample separation for a soil COV of 50% and a SOF of 1 m and 16 m, respectively. On the other hand, results shown in Figures 4-21(a) and (b) are based on soils with SOF of 4 m and a COV of 50% and 100%, respectively.



(a)



(b)

**Figure 4-20 Effect of increasing the sample separation distance on the average and standard deviation of settlement estimates using the adopted methodology and theoretical evaluation for a soil COV of 50% and SOF of (a) 1 m and (b) 16 m**

The effect of stationarity is clearly highlighted in the results shown in Figures 4-20 and 4-21 where the settlement average and standard deviation are unaffected by the spacing between the footing and the sample location. For each of the site conditions shown in these figures, the results of the methodology appear to be adequately correlated with the theo-

retical evaluation. This is also true for the settlement variance in all conditions, except when the soil COV and SOF are 50% and 1 m, respectively, as shown in Figure 4-20(a). In this situation, the results of the methodology yield a notably smaller settlement variance than the theoretical evaluation. This may be the result of increased local averaging, which has not been accounted for in the theoretical evaluation. Nevertheless, the majority of results show good correlation.

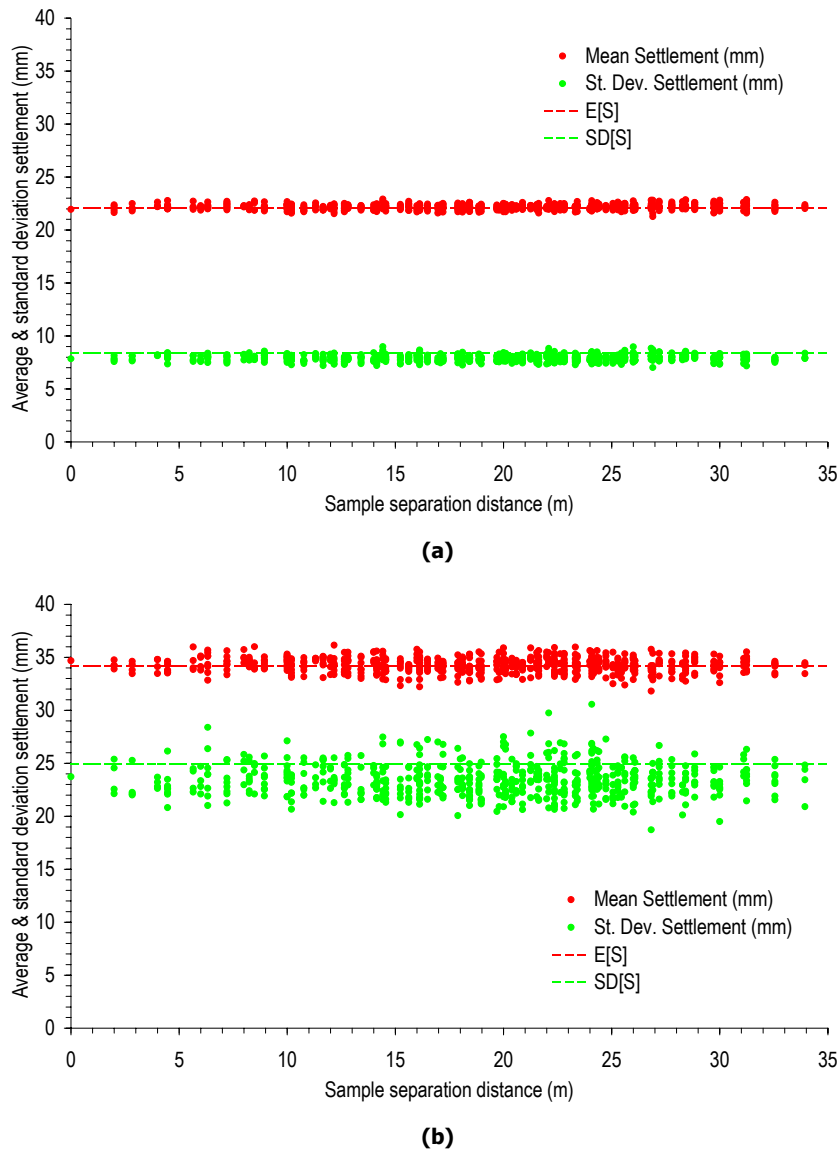


**Figure 4-21 Effect of increasing the sample separation distance on the average and standard deviation of settlement estimates using the adopted methodology and theoretical evaluation for a soil SOF of 4 m and COV of (a) 50% and (b) 100%**

Although the settlement average and variance have been shown to be independent of sample location, it is expected that the average settlement error, defined in Chapter 3 (§3.7.1), will be influenced by the sample location. This is because the settlement error is calculated

for each individual realisation and then averaged over the suite of realisations. Therefore, the variability of the settlement estimate infers that predictions based on different sample locations within the same realisation will be different and as such, the settlement error will be non-zero. The theoretical average settlement error is formulated using the expression for the expected settlement error,  $E[SE]$ , given by:

$$E[SE] = E\left[\frac{S_1 - S_2}{S_2}\right] = E\left[\frac{S_1}{S_2} - 1\right] = E\left[\frac{S_1}{S_2}\right] - 1 \quad (4.12)$$

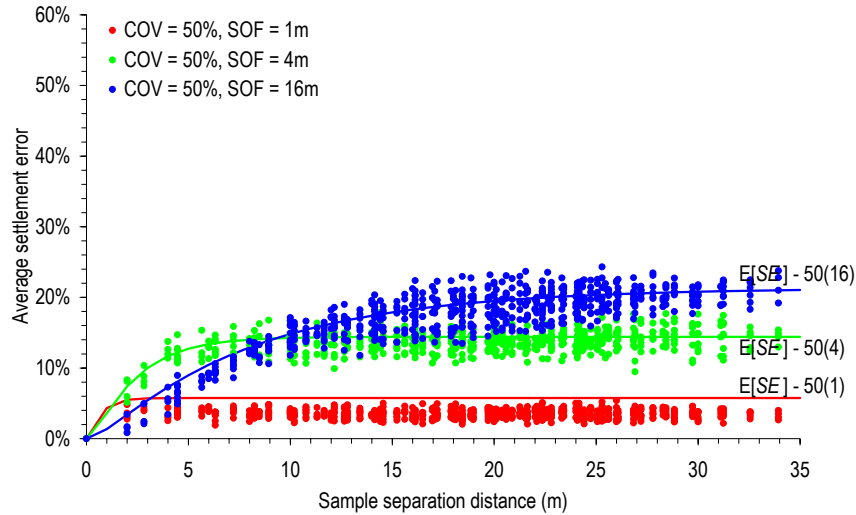
where  $S_1$  is the settlement estimate based on a sample location 1 and  $S_2$  is the settlement estimate based on a sample location 2. In this case, the settlement estimate based on sample location 2 is considered the benchmark or optimal result. A first order approximation of Equation (4.12) yields a zero value because the average settlement estimate is independent of sample location. However, a second order Taylor series expansion given by:

$$E[g(S_1, S_2)] = g(\mu) + \frac{1}{2} \sum_{i=1}^2 \sum_{j=1}^2 \text{Cov}[S_i, S_j] \left( \frac{\partial^2 g}{\partial S_i \partial S_j} \Big|_{\mu} \right) \quad (4.13)$$

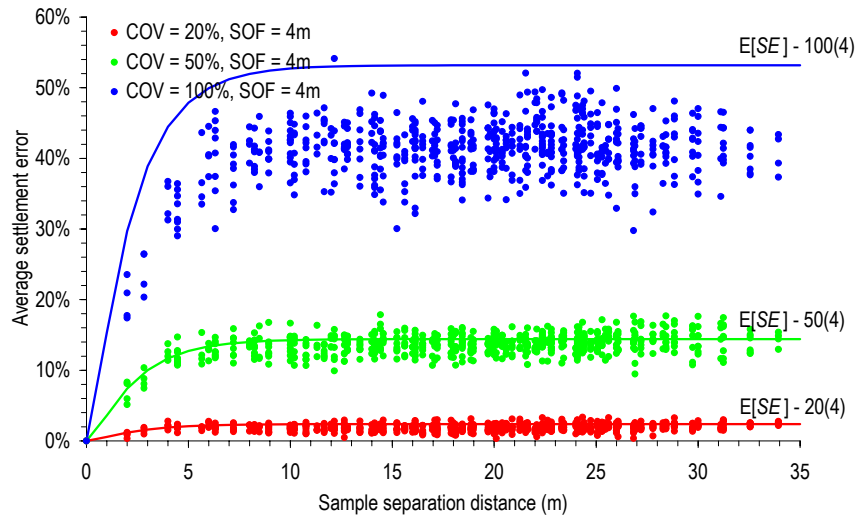
leads to a non-zero solution. By substituting the expressions for the settlement mean and variance, given by Equations (4.10) and (4.11), respectively, and the covariance between two settlement estimates, given by Equation (4.11), the second order Taylor series expansion becomes:

$$E[SE] = \frac{1}{E[S]} (\text{Var}[S] - \text{Cov}[S_1, S_2]) \quad (4.14)$$

where  $E[S]$  and  $\text{Var}[S]$  are the mean and variance of the settlement estimate and  $\text{Cov}[S_1, S_2]$  is the covariance between the settlement estimates. Comparisons between the theoretical evaluation of the average settlement error, using the second order Taylor series approximation, and the results of the adopted methodology, are shown in Figure 4-22. Results indicate the effect of increasing the distance between sampling locations on the average settlement error. The results in Figure 4-22(a) are based on a soil with the same COV of 50% and varying SOF, while the results shown in Figure 4-22(b) are based on a soil with the same SOF of 4 m and a varying COV. The average settlement error from the Monte Carlo simulation is determined by predicting the settlement using elastic modulus values from two distinct sampling locations. The settlement error is compiled for each Monte Carlo realisation and then averaged over the suite of 1,000 realisations.



(a)



(b)

**Figure 4-22 Effect of increasing the sample separation distance on the average settlement error using the adopted methodology and theoretical solution on a soil with an increasing elastic modulus (a) SOF (COV of 50%) and (b) COV (SOF of 4 m)**

The relationship between the sample separation distance and the average settlement error for the adopted methodology shows good correlation with the theoretical evaluation, as shown in Figure 4-22. However, the methodology appears unable to replicate the theoretical solution for a soil COV of 100% and SOF of 4 m or a COV of 50% and SOF of 1 m. In these situations, the results of the methodology yield a smaller average settlement error than the theory, regardless of the sample separation distance. Such differences are most likely due to the second order Taylor series approximation. However, reasonable correlation exists between the results from the methodology and from theory.

## 4.5 SUMMARY

---

Discussion in this chapter has dealt with verification analyses undertaken to ensure that the methodology described in Chapter 3, accurately simulates the variability of soil properties, predicts settlements in accordance with the settlement relationships and estimates the average and variance of settlement estimates within a reliability analysis. The sample statistics of the simulated soil compare favourably with the target statistics adopted to generate the field. Such agreement has verified that the methodology adopted is suitable to simulate the variability of soil properties.

An examination of the implementation of the settlement relationships has demonstrated that the method adopted to account for the effects of adjacent footings yields suitable settlements when compared to 3DFEA settlement estimates. A further investigation regarding the accuracy of 3DFEA settlement estimates, when compared to measured settlements, has identified that the 3DFEA should be adopted with a depth restriction equal to 5 times the least plan dimension or the width of the footing.

A theoretical evaluation of the settlement average and variance based on the results of two distinct sample locations, has also verified that the implementation and convergence rate of the reliability analysis and the adopted methodology is sufficiently accurate. It has also been shown that the methodology is able to replicate the theoretical trend between average settlement errors, for an increasing sample separation.

## **Chapter 5 EFFECT OF DIFFERENT SETTLEMENT PREDICTION TECHNIQUES ON THE DESIGN AND ANALYSIS OF A PAD FOUNDATION**

### **5.1 INTRODUCTION**

---

The settlement prediction techniques that have been introduced in Chapter 2 (§2.2.2) each possess a certain degree of uncertainty or error. Such errors are typically due to the simplifications or assumptions in the method. For example, some of the techniques idealise a three-dimensional problem into two-dimensions, while some are based on correlations with measured settlements of constructed footings. Using the methodology described in Chapter 3, and assuming that a 3DFEA settlement estimate is a benchmark that accommodates the total variability of the soil, it is possible to estimate the degree of conservatism associated with each settlement prediction technique, and how such conservatism is affected by changing site conditions.

Throughout this chapter, three different foundation systems are investigated consisting of a single pad footing and a group of 4 and 9 pad footings, as shown in Figure 5-1. Each pad footing is constrained to conform to the restrictions discussed in Chapter 3 (§3.6), where they have been considered rigid and unable to rotate. Each system is centred on a 50 m × 50 m site, which has an assumed depth of compressible soil of 30 m. The single pad footing resists a single point load of 1,500 kN, while the system of 4 and 9 pad footings resist column loads representative of a 3-storey 20 m × 20 m structure with a 5 kPa live load and 3 kPa dead load. Each footing in the 4-pad system resists the same 2,400 kN load, while the footings in the 9-pad system resist loads representative of their column loads determined using tributary floor areas. Corresponding footing loads for the 9-pad system are shown in Figure 5-1(c).

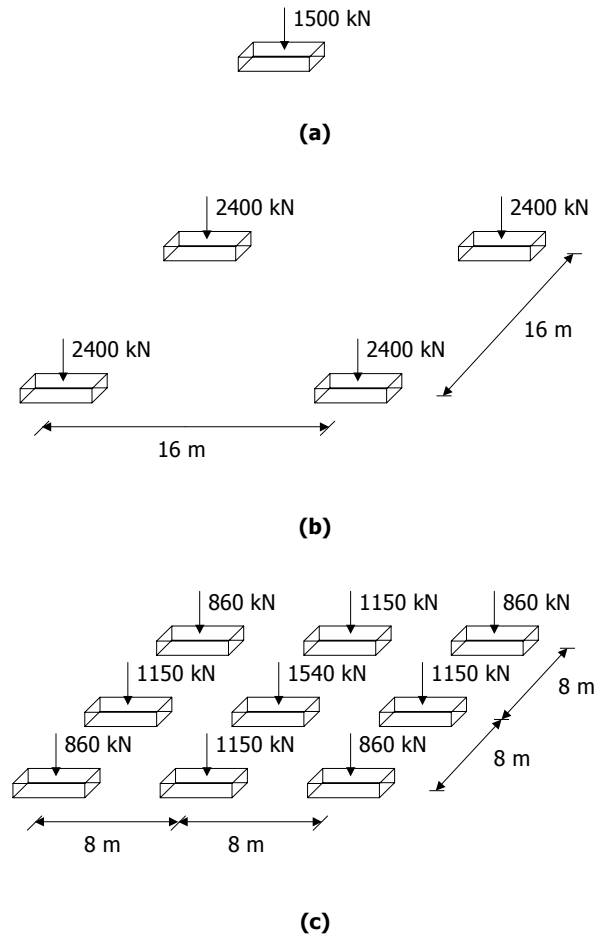


**Figure 5-1** Layout of (a) single, (b) 4-pad and (c) 9-pad system foundation system

Results presented in this chapter are divided into two categories. The first section deals with settlement estimates of the footing system, where the footing size is known *a priori*. Such results indicate the relative conservatism of each settlement prediction technique with respect to the estimated settlement. The second section elaborates on this analysis by undertaking a design process using the settlement prediction technique, where footing sizes are varied to meet a specific design criterion. The results in this section demonstrate the relative conservatism of the settlement prediction technique in relation to the design of a foundation.

The effects of sampling and testing are not included in this chapter. Instead, the results are based on the complete and exact knowledge of the soil. It should be noted at this stage, that the settlement prediction techniques investigated do not accommodate all elastic moduli in the soil deposit. Rather, they either require a single elastic modulus value, or a set of data that varies in the vertical direction. This set of data is considered a single vertical sample. Therefore, complete knowledge of the soil (CK) is regarded as the elastic



moduli in a single vertical sample located at the centre of the proposed footing. In the case of a multiple pad system, each footing is analysed or designed separately, based on a single vertical sample of moduli located directly beneath the centre of that footing. Although this does not strictly constitute CK, it is considered reasonable for the purposes of the comparisons that follow.

---

## **5.2 SETTLEMENT ANALYSES**

---

Results presented in this section are limited to investigating the predicted settlement of a foundation system with footings of known size using one of the settlement prediction techniques discussed in earlier chapters. A probabilistic analysis is undertaken, where the average, variability and distribution of settlement estimates are evaluated. The effect of soil variability and footing size is investigated, as well as comparisons between the settlement prediction techniques and 3DFEA, which is based on the total variability of the soil. An influence region is also introduced later in this section, where elastic moduli within a region are averaged with the aim of determining a suitable characteristic value that accommodates the variability of the soil. However, in the main, the analyses in this section are based on elastic moduli from a single vertical sample located at the centre of the footing.

### **5.2.1 Settlement Analysis on a Soil with Uniform Properties**

It has been stressed in earlier chapters that soils are inherently variable and geotechnical properties are likely to be different at different locations. In contrast, it is almost universal in practice for a site to be characterised into a uniform layer that greatly simplifies the analysis. Despite this, differences still exist between settlement prediction techniques due to model uncertainty (this should not be confused with transformation model uncertainty, as discussed in §2.3.5). As a result, an analysis is undertaken to measure the conservatism of several prediction techniques using a soil with a uniform elastic modulus. In other words, the elastic modulus is the same at all locations in the soil. Consequently, these results are deterministic and a Monte Carlo analysis is not necessary. This form of analysis is beneficial, as it is not affected by uncertainties due to sampling errors (statistical uncertainty), measurement errors, transformation model errors or soil variability. Rather, these results are only a function of the error associated with different settlement prediction techniques, i.e. model error.

Figure 5-2(a) illustrates the settlement estimates from all settlement prediction techniques examined (including 3DFEA) for a single pad footing founded on a soil with a uniform

elastic modulus of 10,000 kPa. Figure 5-2(b) shows the relative conservatism associated with the techniques, as compared to 3DFEA. These results are measured using the settlement error defined in Chapter 3 (§3.7.1). Results shown in Figure 5-2(b) suggest that five of the eight settlement relationships show conservatism with respect to 3DFEA. Such conservatism infers that the technique yields a larger predicted settlement than 3DFEA. The results of the Schmertmann 2B-0.6 method are consistent with conclusions made by Bowles (1997), where it is expected to yield larger settlements on a soil with uniform properties. This is primarily due to the transformation model used to convert cone penetration test results into elastic moduli.

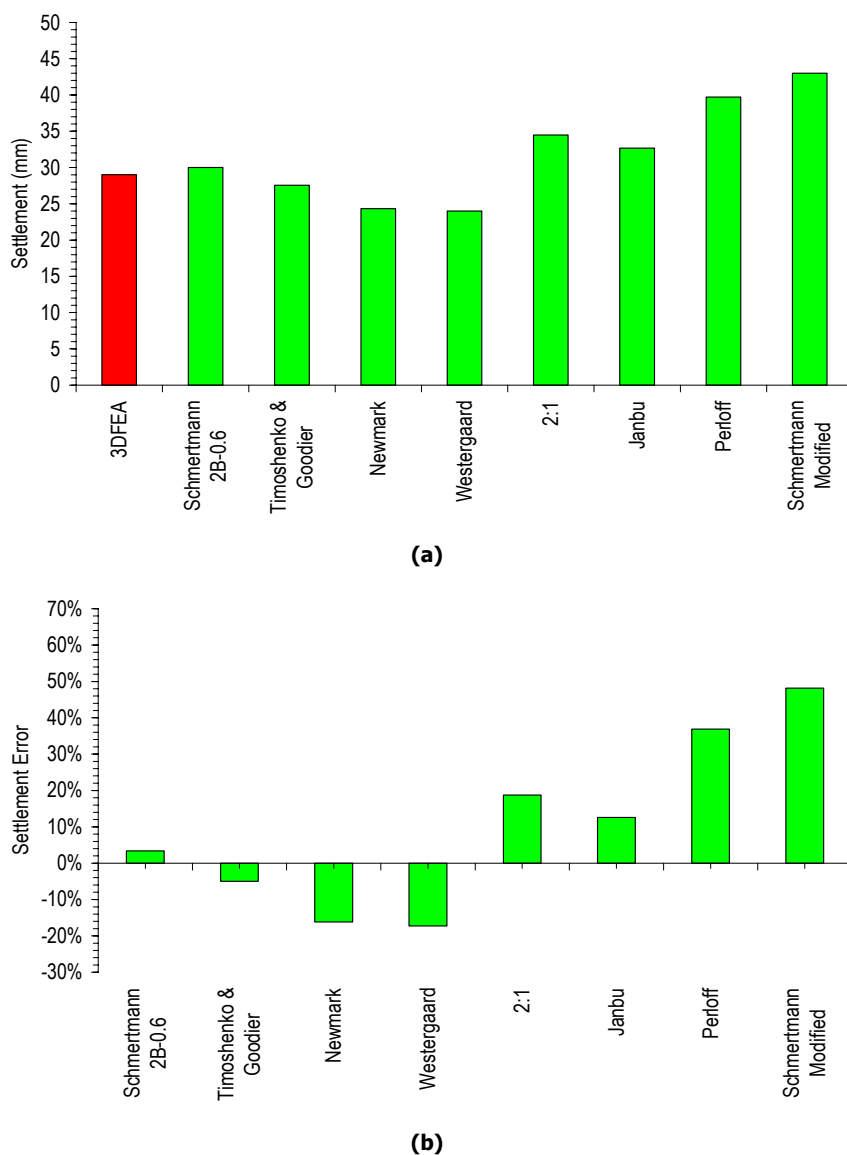


**Figure 5-2 Results of the settlement prediction techniques for a single pad footing for a soil with a uniform elastic modulus showing (a) absolute settlement and (b) relative to 3DFEA**

The relative conservatism of the settlement prediction techniques is also shown using a theoretical evaluation in Table 5-1. These formulations are based on the same loading conditions, elastic moduli and footing sizes used to yield the results shown in Figure 5-2. The results shown in Table 5-1 suggest that, for the methods examined, the Schmertmann 2B-0.6 technique yields the least conservative settlement estimate, with the smallest coefficient of 0.6. The other techniques appear to be slightly more conservative, with coefficients ranging from 0.69 (Timoshenko and Goodier) to 0.86 (Schmertmann Modified). Comparisons, such as those shown in Table 5-1, are valid only when the soil has a constant elastic modulus. However, in such conditions, the Schmertmann 2B-0.6 technique will always yield a settlement estimate less than the other four methods shown in Table 5-1, due to it having the smallest coefficient of 0.6. The relative conservatism of the five techniques shown in Table 5-1 is also evident in Figure 5-2, where the Schmertmann 2B-0.6 technique yields the smallest settlement estimate and the Schmertmann Modified technique yields the largest, of the methods examined in Table 5-1.

The results for the analysis of the 4 and 9 pad systems are shown in Figures 5-3 and 5-4, respectively. Since each footing in the 4-pad system is designed to resist the same load, the settlement on a soil with a uniform elastic modulus will be the same for each footing. Therefore, the results in Figure 5-3 display the settlement estimates for only one footing in the system. This is also the case for the 9-pad system, where Figure 5-4 shows the settlement estimates of three representative footings.

Results for all foundation systems indicate that the Schmertmann Modified technique yields the most conservative settlement estimate. This relationship appears only slightly more conservative than the Perloff approximation, using influence values for a rigid loaded area adopted from Harr (1966), which represents the theoretical evaluation based on elastic theory. Therefore, the modifications made by Schmertmann et al. (1978) to the original method proposed by Schmertmann (1970), yields settlement estimates that are closer to the theoretical solution but further from the 3DFEA model adopted in the methodology.

Settlement estimates based on 3DFEA appear to be amongst the least conservative predictions. A similar result has also been observed by Seycek (1991), because finite element analyses are unable to approximate the infinite stresses at the edges of a rigidly loaded area, as prescribed by theory. Therefore, stresses simulated by finite element analysis tend to be less than theoretical, resulting in smaller settlements. This is shown in Figures 5-2, 5-3 and 5-4 where 3DFEA settlements appear to be significantly less than the theoretical solution, i.e. Perloff approximation.

**Table 5-1 Comparison of settlement prediction technique coefficients based on a 1.5 m × 1.5 m footing for a soil with a uniform elastic modulus**

Schmertmann 2B-0.6	Schmertmann Modified
$\delta = C_1 C_2 q \sum_{i=1}^{n_i} \frac{I_{z_i}}{E_i} \Delta z_i$	$\delta = C_1 C_2 q \sum_{i=1}^{n_i} \frac{I_{z_i}}{E_i} \Delta z_i$
$C_1 = C_2 = 1$	$C_1 = C_2 = 1$
no time or embedment effects	no time or embedment effects
$\sum_{i=1}^{n_i} \frac{I_{z_i}}{E_i} \Delta z_i = \frac{0.6b}{E}$	$\sum_{i=1}^{n_i} \frac{I_{z_i}}{E_i} \Delta z_i = \frac{(0.05 + I_{z_p})b}{E} = \frac{0.88b}{E}$
integration of strain distribution with constant E	integration of strain distribution with constant E
$\delta = 0.6 \frac{P}{El}$	$\delta = 0.88 \frac{P}{El}$
Timoshenko and Goodier	Perloff
$\delta = qb \frac{(1-\nu^2)}{E} \left[ I_1 + \frac{(1-2\nu)}{1-\nu} I_2 \right] I_f$	$\delta = \frac{qbI_p(1-\nu^2)}{E}$
$I_f = 1$	$\delta = 0.91I \frac{P}{El}$
no embedment effects	with a Poisson's ratio of 0.3
$I_1 = 0.437 \quad I_2 = 0.00306$	$I = 0.873$
corner and centre influence factors from width to length and depth to width ratios	based on the soil layer depth to footing width ratio (bearing in mind the depth restrictions)
$\delta = 4(0.4) \frac{P}{Ebl} 0.91 \frac{b}{2} (0.439)$ $+ 0.6 \frac{P}{Ebl} 0.91b(0.439)$	$\delta = 0.79 \frac{P}{El}$
transformation to rigid settlement	
$\delta = 0.56 \frac{P}{El}$	
Janbu	
$\delta = \eta_0 \eta_1 \frac{qb}{E}$	
$\mu_0 = 1$	
no embedment effects	
$\eta_1 = 0.5915 + 0.0385 \ln \left( \frac{D}{b} \right)$	
calibration from 3DFEA with $\nu = 0.3$	
$\delta = 0.71 \frac{P}{El}$	

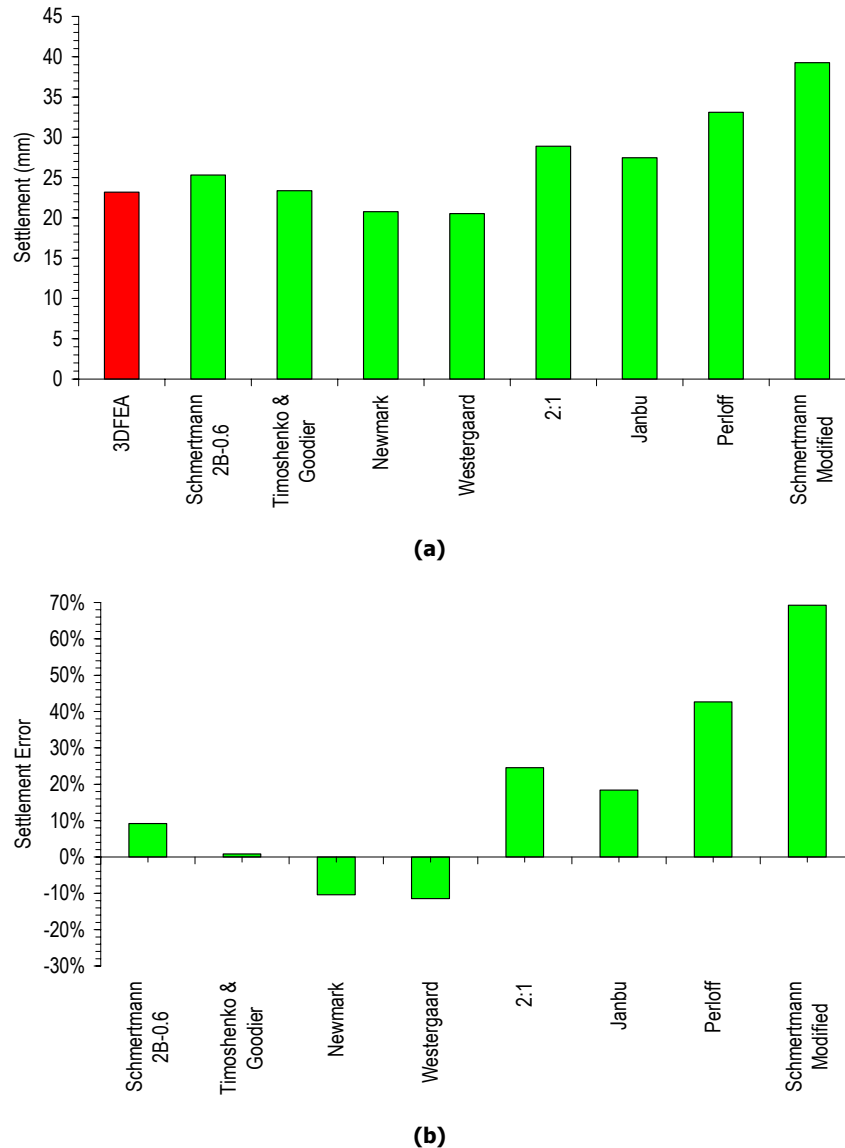
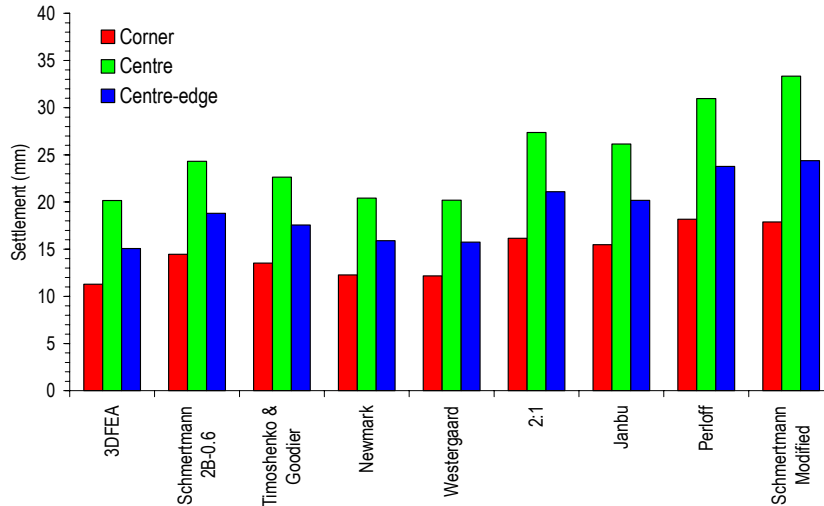
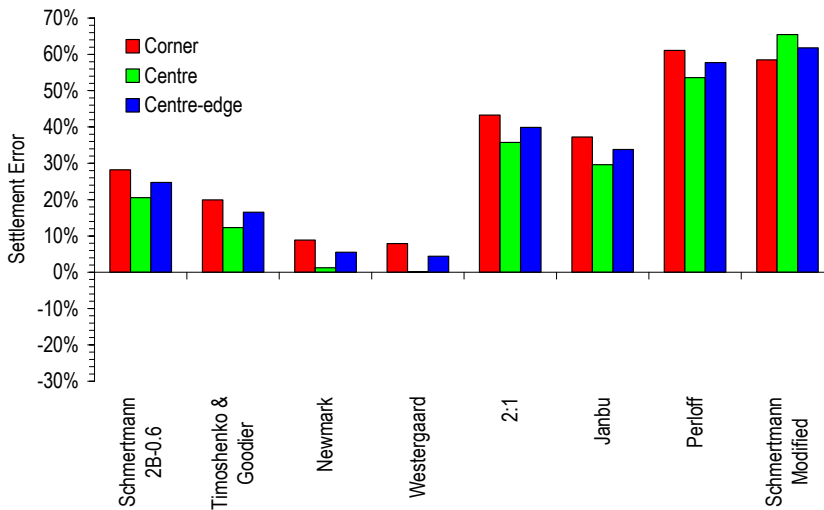


**Figure 5-3 Results of the settlement prediction techniques for each footing in the 4-pad system for a soil with a uniform elastic modulus showing (a) absolute settlement and (b) settlements relative to 3DFEA**

The difference between settlement estimates based on 3DFEA and the theoretical solution raises a concern regarding the applicability of finite element analysis to yield settlement estimates consistent with those measured (§4.3.2). However, predictions based on 3DFEA accommodate both the horizontal and vertical variability of soil, which is not possible in the other techniques. Hence, 3DFEA is used throughout the subsequent analysis to provide predictions of ‘actual’ settlements, bearing in mind that these are based on elastic theory, which, by its very nature, is a simplification of reality. However, as mentioned previously (§2.2.2.3), finite element analysis is used in the geotechnical community as a state-of-the-art methodology for predicting stresses and settlement. As a result, comparisons between settlement estimates given in this chapter are relative to those predicted by 3DFEA.



(a)



(b)

**Figure 5-4 Results for the corner, centre and remaining footings in the 9-pad system, for a soil with a uniform elastic modulus showing (a) absolute settlement and a (b) settlement error with 3DFEA**

The relative settlement error of the single pad footing scenario, shown in Figure 5-2, is also shown in Figure 5-5 for footings of varying plan size. In total, three different footing sizes are investigated with plan dimensions of 1.5 m × 1.5 m, 2.5 m × 2.5 m, and 3.5 m × 3.5 m. In all cases, the applied point load is maintained constant, leading to a decreasing applied pressure as the footing size increases. The results shown in Figure 5-5 indicate little difference in settlement error for most of the settlement methods, as the footing size increases. The differences of note are shown for the Newmark, Perloff and Schmertmann modified techniques. The differences indicated by the Newmark and Perloff relationships are likely due to their initial degree of conservatism for a of 1.5 m × 1.5 m footing. However, the differences observed for the Schmertmann Modified technique warrants further attention.

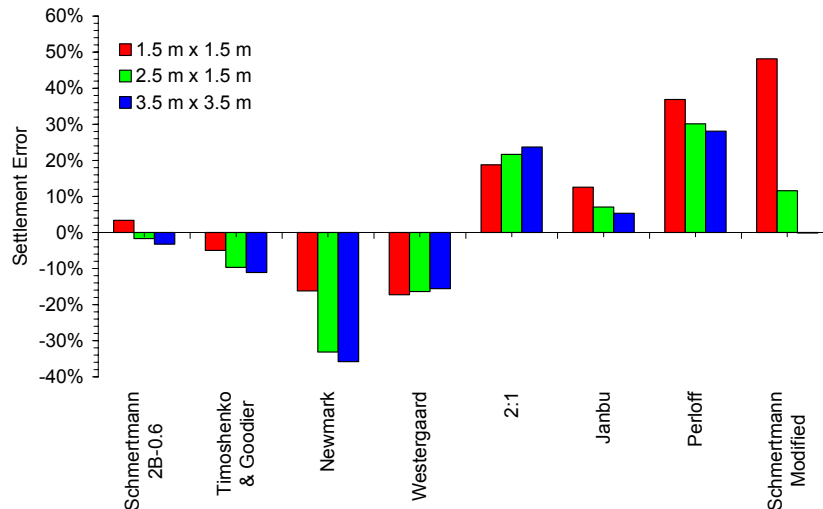


**Figure 5-5 Settlement error relative to 3DFEA settlement for a single pad footing of varying size for a soil with a uniform elastic modulus**

The Schmertmann technique, based on the modified strain distribution, appears to yield settlement estimates that are close to 3DFEA estimates when the footing has a plan size of  $3.5 \text{ m} \times 3.5 \text{ m}$ . This is in stark contrast to the results when the footing has a plan size of  $1.5 \text{ m} \times 1.5 \text{ m}$ . Although errors are expected when analysing a small footing with 3DFEA (§3.6.5.2), it is more likely that the Schmertmann Modified technique yields settlements with a varying degree of conservatism for different footing sizes. This is because the Schmertmann strain distribution was calibrated to the measured settlement of a series of footings constructed on sand. Therefore, the calibration should yield suitable settlement estimates when the size and footing conditions are similar to those used to calibrate the method. However, in other situations, the settlement estimates may be inadequate.

### 5.2.2 Settlement Analysis on a Spatially Random Soil

As discussed in previous chapters, soils are inherently variable, where their properties may vary considerably from one location to another (Vanmarcke 1977a). Such variability also affects the estimated settlement based on the prediction techniques discussed above. As a result, the analysis presented in this section investigates the footing settlement based on soils with spatially random elastic moduli. Similar studies have been conducted by others (e.g. Fenton et al. 1996, Fenton and Vanmarcke 2003, Fenton et al. 2003, Fenton and Griffiths 2005, Fenton et al. 2005), who investigated the finite element analysis of settlement estimates on a spatially random soil. The reason for using a finite element analysis is that it more appropriately accommodates variability of the soil. This is achieved by mapping the elastic moduli from the simulated soil to the properties of the finite element mesh. As

mentioned in Chapter 2 (§2.4), Fenton et al. (1996) referred to this as a random finite element method (RFEM). Although others have investigated the predicted settlement of a foundation using finite element analyses on a spatially random soil, it is important to compare such predictions with the estimates obtained using the other settlement techniques discussed in earlier chapters.

The estimated settlements based on the settlement prediction techniques (not including 3DFEA) do not accommodate the total variability of the soil but, instead, are based on elastic moduli located under the centre of each footing. Results are presented in a probabilistic framework based on 1,000 Monte Carlo realisations, where the random field representation of the elastic modulus field is generated from a random seed and conforms to the same target distribution (including mean and variance) and correlation structure.

Since the analysis is probabilistic, and estimates from the same settlement relationship will vary between Monte Carlo realisations depending on the elastic moduli located under the footing, it is important to observe the resulting sample distribution of settlement estimates. Figure 5-6 shows such sample distributions of estimates for each settlement prediction technique investigated, including 3DFEA. These results are based on a single pad footing loaded with a 1,500 kN point load and founded on a soil with a mean elastic modulus of 20,000 kPa, a COV of 50% and a SOF of 8 m. Additional sample distributions for other soil types are included in Appendix A. It is apparent from these sample distributions that the settlement estimates show good lognormal behaviour, which is consistent with the conclusion made by Fenton and Griffiths (2002). It is convenient to assume lognormal behaviour for settlement estimates, as it allows analytical description of exceedance levels and comparisons between methods. Such comparisons are discussed later in this section.

To confirm lognormal behaviour of the settlement estimates, a Chi-square goodness-of-fit test (D'Agostino and Stephens 1986) is undertaken. The lognormal distribution used to fit the settlement estimates is determined using the frequency function for a lognormal distribution, given by:

$$f(x) = \frac{1}{x\sigma_{\ln x}\sqrt{2\pi}} e^{-\frac{1}{2}\left(\frac{\ln x - \mu_{\ln x}}{\sigma_{\ln x}}\right)^2} \quad (5.1)$$



where  $f(x)$  is the frequency of property  $x$ , in this case the estimated settlement, and  $\mu_{\ln x}$  and  $\sigma_{\ln x}$  are the mean and standard deviation of the lognormal distribution, respectively, given by:

$$\mu_{\ln x} = \ln(\mu_x) - \frac{1}{2} \sigma_{\ln x}^2 \quad (5.2)$$

and

$$\sigma_{\ln x} = \ln\left(1 + \frac{\sigma_x^2}{\mu_x^2}\right) \quad (5.3)$$

where  $\mu_x$  and  $\sigma_x^2$  are the mean and variance of the normal variable, respectively. The mean and variance of the normal variable given in Equations (5.2) and (5.3) are estimated by the sample mean, or average, and sample variance of the settlement over 1,000 Monte Carlo realisations. Using the sample distributions shown in Figure 5-6, and the corresponding lognormal distributions determined using Equation (5.1), the Chi-square statistic is calculated. These results, for each settlement relationship and for seven different soils, are given in Table 5-2. A comparison between the sample and idealised lognormal distributions is also given in Figure 5-7 for the 3DFEA estimates of a single pad footing, founded on a soil with a COV of 50% and SOF of 4 m.

The shaded values in Table 5-2 highlight the conditions where the Chi-square  $p$ -value is greater than 0.5. This infers that these results conform to a lognormal distribution, within a 50% confidence limit. It is, therefore, clear that the settlement methods show closer agreement with a lognormal distribution when the soil COV is high (e.g. 100%). In fact, for a soil COV of 10%, every settlement technique investigated yielded a  $p$ -value less than 0.5, which represents low confidence of the data conforming to a lognormal distribution. However, the Chi-square test is heavily influenced by the assumed bin size, which in this case, is maintained constant for all soils and settlement methods. Therefore, when the settlement has a low variability, as is expected when the soil COV is 10%, all results may reside in the same bin, which therefore affects the outcome of the Chi-square test. This is also the case when the soil SOF is high, where the apparent variability of the elastic moduli is reduced, as discussed previously in Chapter 4 (§4.2.1). Therefore, it is not an unexpected result that the settlement estimates do not show good agreement with a lognormal distribution when the soil COV is low, or the SOF is high.

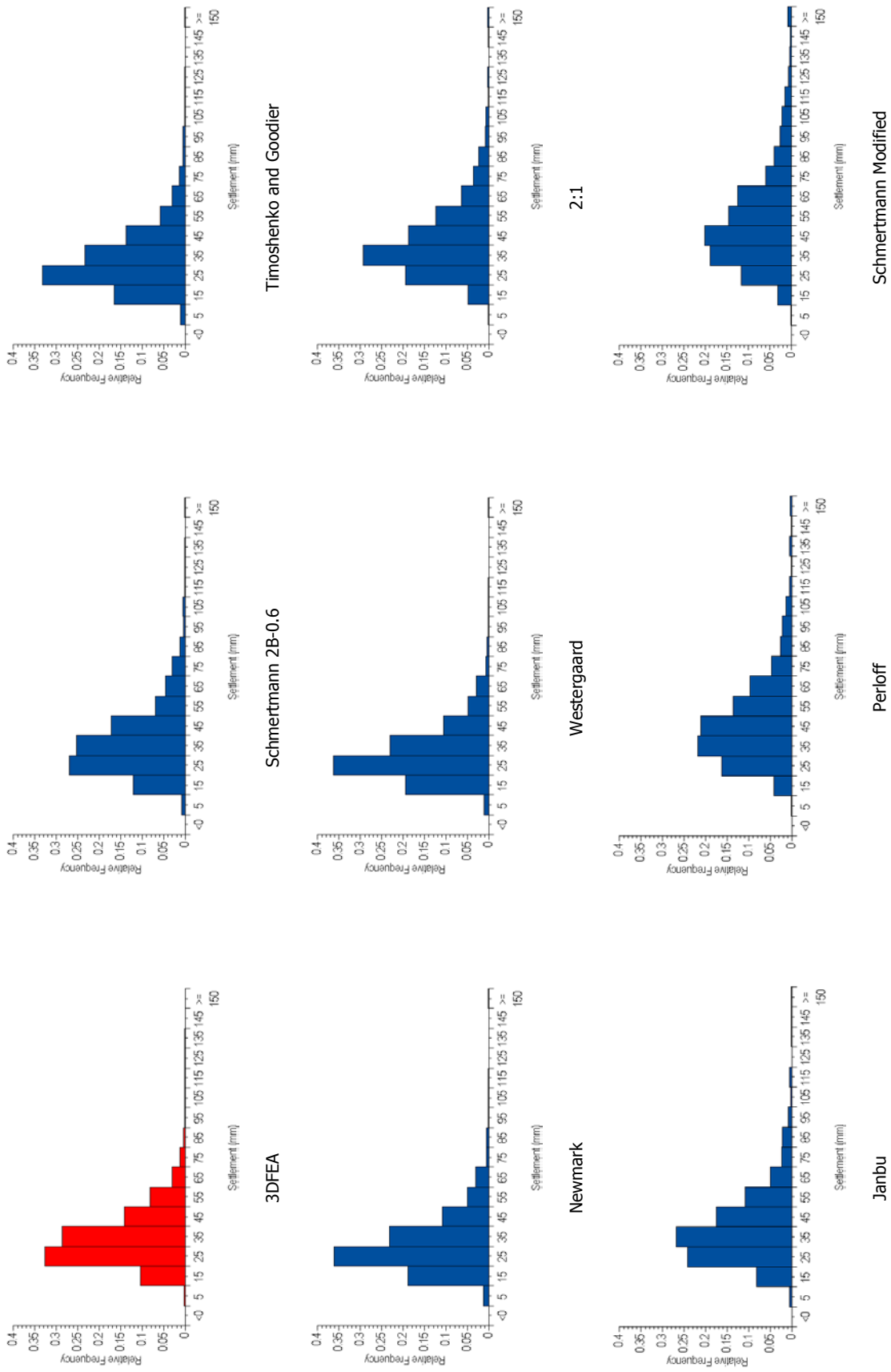
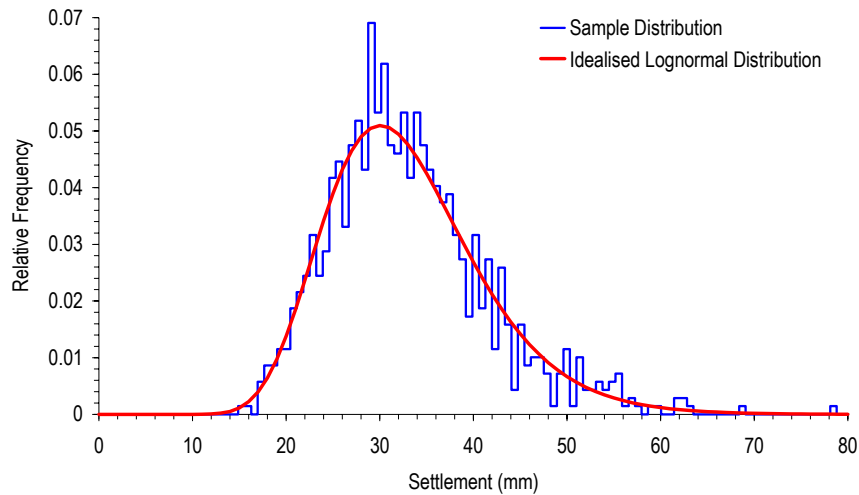


Figure 5-6 Frequency distribution of estimated settlement of a single pad footing, for a soil COV of 50% and SOF of 8 m

**Table 5-2 Results of the Chi-square goodness-of-fit test for settlement estimates with a log-normal distribution ( $p$  value shown in parenthesis)**

Settlement Relationship	COV	10%	20%	50%	50%	50%	50%	100%
	SOF	8 m	8 m	1 m	4 m	8 m	16 m	8 m
3DFEA		42.43 (0.039)	42.14 (0.042)		17.15 (0.946)	38.03 (0.098)		18.77 (0.905)
Schmertmann 2B-0.6		48.76 (0.009)	27.82 (0.474)	32.92 (0.239)	31.76 (0.284)	14.01 (0.987)	31.30 (0.304)	21.55 (0.802)
Timoshenko and Goodier		57.92 (0.001)	23.87 (0.688)	26.54 (0.543)	32.40 (0.259)	35.18 (0.165)		15.46 (0.973)
Newmark		30.83 (0.325)	21.15	28.17 (0.456)	41.85 (0.045)	28.40 (0.444)	43.36 (0.032)	26.02 (0.572)
Westergaard		46.84 (0.014)	38.43 (0.091)	26.54 (0.543)	29.96 (0.365)	22.77 (0.744)	33.15 (0.230)	20.80 (0.834)
2:1		42.14 (0.042)	42.72 (0.037)	22.08 (0.778)	24.34	32.86 (0.241)	29.79 (0.373)	31.88 (0.280)
Janbu		27.59 (0.487)	38.43 (0.091)	18.54 (0.912)	39.13 (0.079)	27.70 (0.480)	35.82 (0.147)	27.30 (0.502)
Perloff			24.34 (0.664)	25.21 (0.617)	27.12 (0.512)	35.94 (0.144)	29.38 (0.393)	15.75 (0.969)
Schmertmann Modified		39.65 (0.071)	21.50 (0.804)	43.01 (0.035)	33.39 (0.222)	14.48 (0.983)	36.29 (0.136)	23.18 (0.724)



**Figure 5-7 3DFEA settlement distribution with idealised lognormal distribution, for a soil COV of 50% and SOF of 4 m**

Using the idealised lognormal distributions for each technique, comparisons between the settlement methods and 3DFEA are shown in Figures 5-8 and 5-9, for soils with an increasing COV and SOF, respectively. It is evident from these results that the settlement methods yield estimates that have greater variability than those given by 3DFEA. The average estimated settlement is also shown to be different between 3DFEA and the other

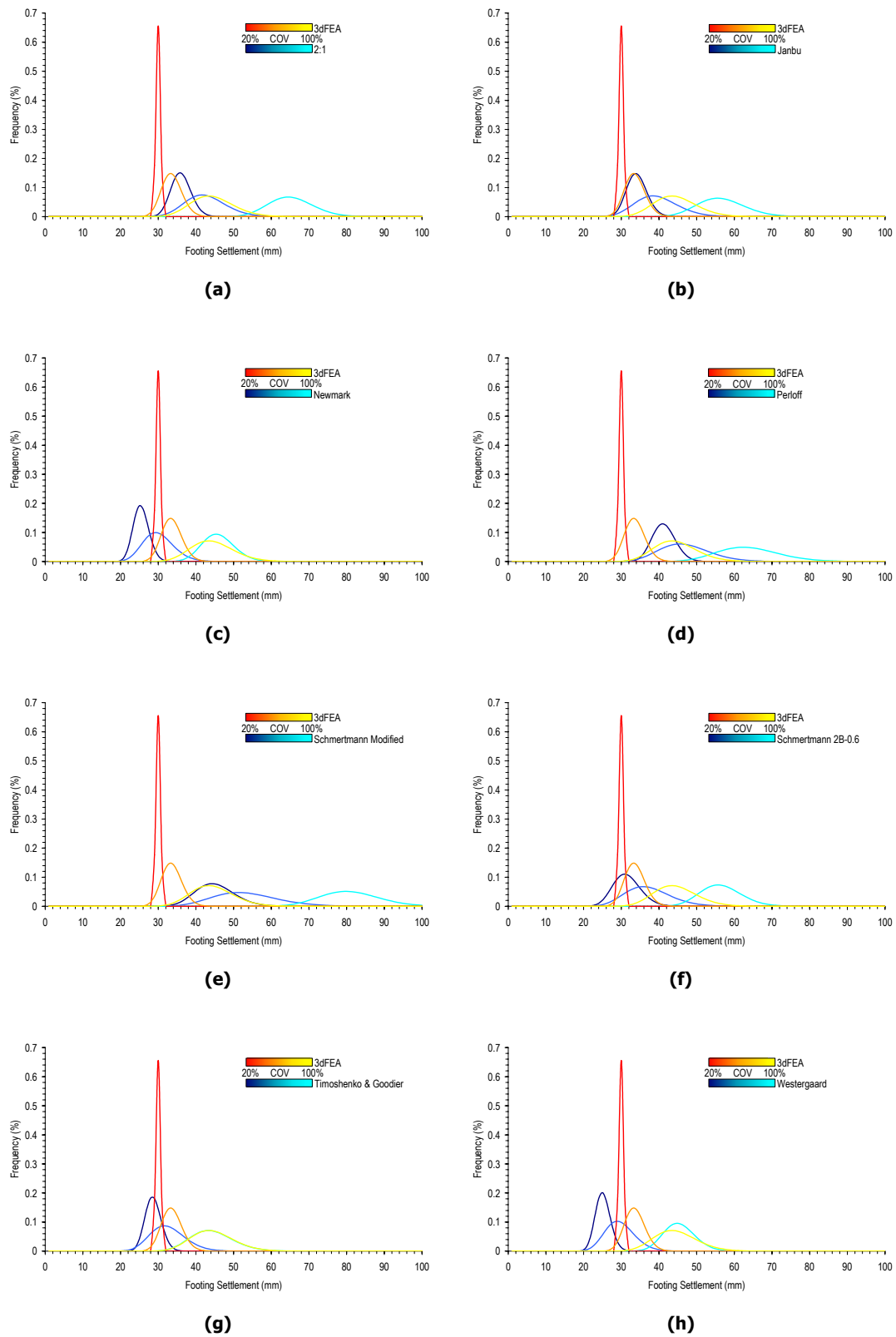


**Figure 5-8 Comparison of idealised settlement distributions, for a soil SOF of 4 m, with respect to the (a) 2:1, (b) Janbu, (c) Newmark, (d) Perloff, (e) Schmertmann Modified, (f) Schmertmann 2B-0.6, (g) Timoshenko and Goodier and (h) Westergaard settlement prediction techniques**

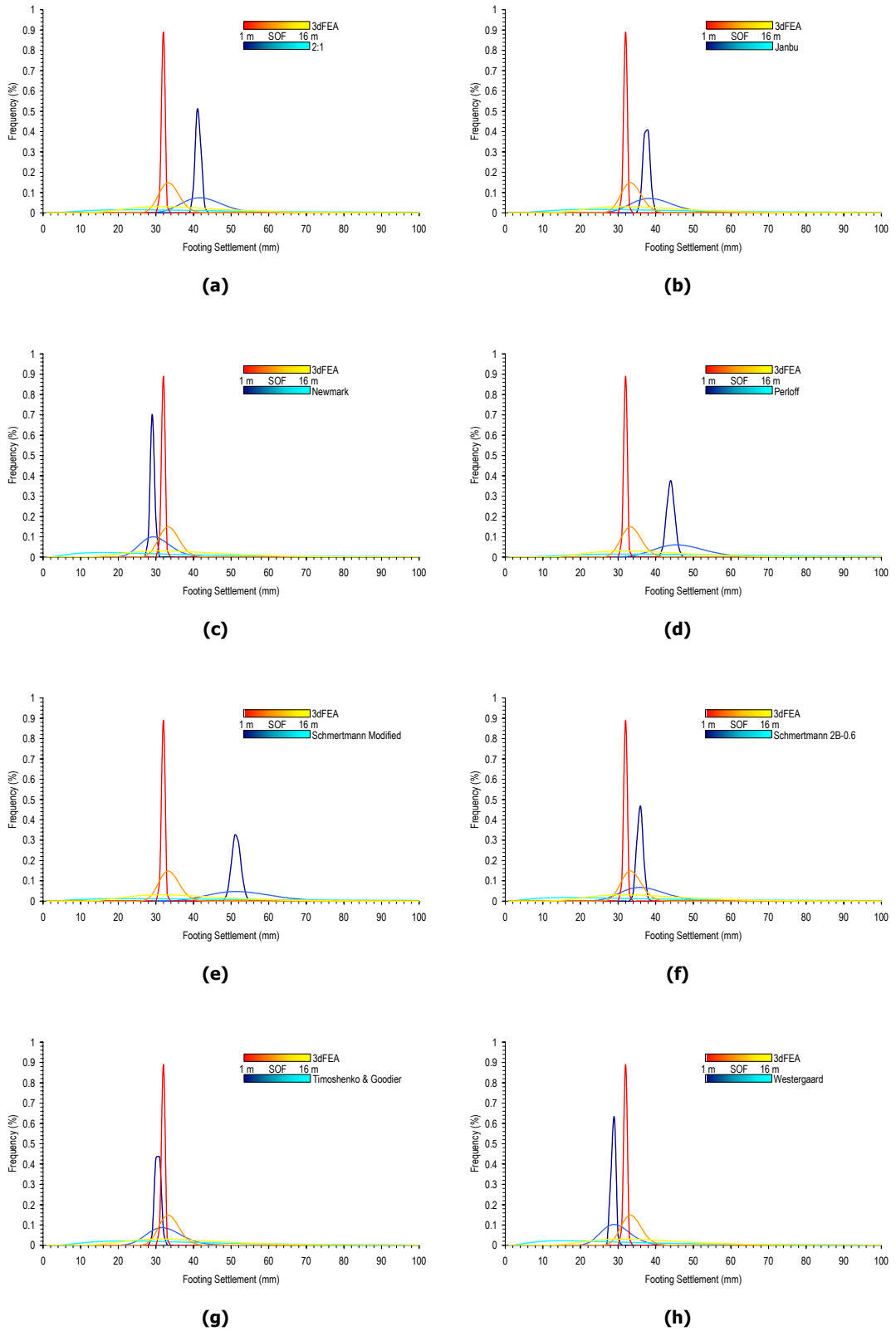


**Figure 5-9 Comparison of idealised settlement distributions, for a soil COV of 50%, with respect to the (a) 2:1, (b) Janbu, (c) Newmark, (d) Perloff, (e) Schmertmann Modified, (f) Schmertmann 2B-0.6, (g) Timoshenko and Goodier and (h) Westergaard settlement prediction techniques**

methods. The Timoshenko and Goodier (T&G) technique appears to provide a reasonable estimate of the average settlement when the soil SOF is 4 m. In fact, the Timoshenko and Goodier technique closely approximates 3DFEA when the soil COV is 100% and SOF is 4 m. As expected, the distribution of settlement estimate using the Schmertmann Modified (SchM) technique is far greater than 3DFEA.

The effect of increasing the soil SOF on the idealised lognormal distributions (Figure 5-9) suggests that the average appears unaffected. This is in contrast to the results shown in Figure 5-8, where the average settlement increases as the soil COV increases. A rise in the soil SOF does, however, affect the variability of the settlement estimate for all methods. In this case, the variability of settlement grows as the soil SOF increases. It also appears that such an escalation in variability is independent of the method used, where all techniques, including 3DFEA, appear to show a similar increase.

The effect of increasing the soil COV and SOF on the average settlement estimate is perhaps better illustrated by the results shown in Figures 5-10 and 5-11, respectively. Results shown in Figures 5-10(a) and 5-11(a) are based on settlement estimates using 3DFEA, while Figures 5-10(b) and 5-11(b) are based on the Schmertmann 2B-0.6 (Sch2B) technique. Similar results for the other techniques are included in Appendix A. Effects of footing size are also included in Figures 5-10 and 5-11, where the plan size is increased from 1.5 m × 1.5 m to 3.5 m × 3.5 m. It is important to bear in mind that all footings discussed in this section are assumed to be square in plan.

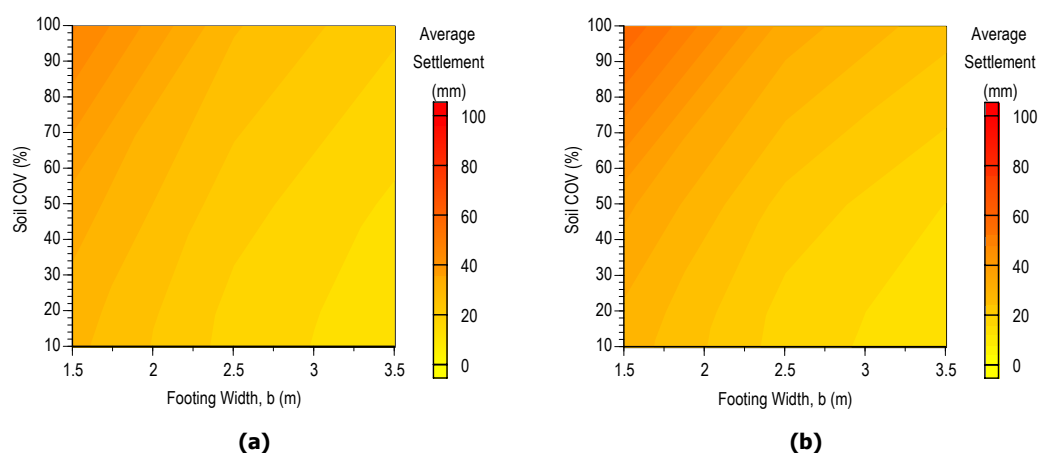


**Figure 5-10 Effect of increasing the soil COV (SOF of 8 m) on the average settlement of a single pad footing using (a) 3DFEA and (b) the Schmertmann 2B-0.6 technique**

Trends shown in Figure 5-10 suggest that an increasing soil COV causes an increase in the average settlement estimate. This appears true for both the average settlement using

3DFEA and the Schmertmann 2B-0.6 technique (Figure 5-10) but can also be concluded for all prediction techniques from the idealised lognormal distributions shown in Figure 5-8 and the additional results in Appendix A. Although an increase in average settlement suggests that the elastic moduli located below the footing are reduced, it is important to consider the effects of increased variability and the shape of the lognormal distribution. For example, the effects of increasing the soil COV on the variability of the settlement estimate (measured as the settlement COV) is shown in Figures 5-12(a) and (b), for 3DFEA and the Schmertmann 2B-0.6 method, respectively. These results suggest that an increasing soil COV yields an increasing settlement estimate COV. Furthermore, because the settlement estimates are lognormally distributed, where negative settlements are not possible, an increase in variability infers an increase in average, since the distribution is flattened and the average moves to the right. Therefore, a rising variability, results in an increase in the average. This is also illustrated by relationship for the lognormal mean given by:

$$\mu_{\ln x} = \ln(\mu_x) - \frac{1}{2} \sigma_{\ln x}^2 \quad (5.4)$$

Rearranging this yields:

$$\mu_x = \exp\left\{ \mu_{\ln x} + \frac{1}{2} \sigma_{\ln x}^2 \right\} \quad (5.5)$$

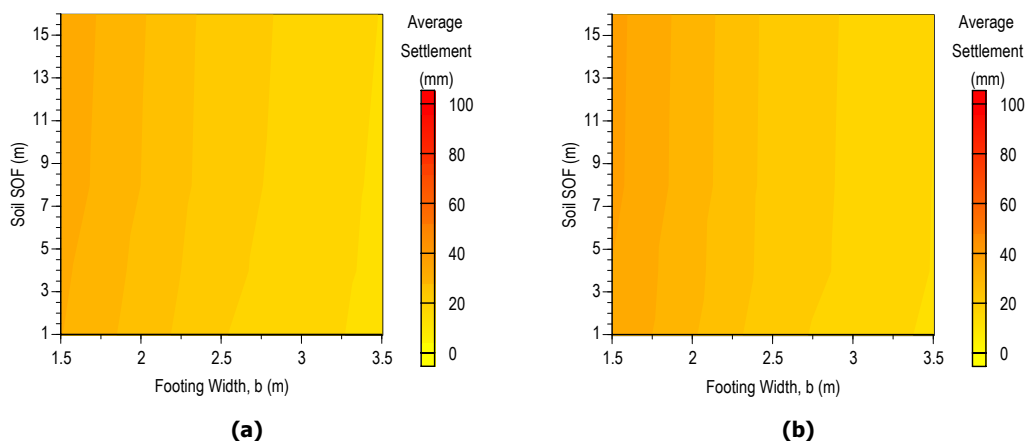


**Figure 5-11 Effect of increasing the soil SOF (COV of 50%) on the average settlement of a single pad footing using (a) 3DFEA and (b) the Schmertmann 2B-0.6 technique**

Hence, as the variance of the lognormal variable increases, so too does the average of the standard variable. Consequently, the increase in settlement average for a rising soil COV,

is driven by the growing settlement variability, and does not necessarily infer that the elastic moduli located beneath the footing are smaller.

**An increase in soil COV causes an increase in the average settlement.**

The average settlement estimate also appears to be influenced by the width of the footing, as one might expect. Such effects are due to the prediction of settlement being dependent on the area and, in most cases, the width of the footing. However, the results shown in Figure 5-10(a), for 3DFEA, indicate that a 1.0 m increase in footing width is equivalent to a 90% reduction in soil COV. However, when using the Schmertmann 2B-0.6 technique, a 1.0 m increase in footing width is equivalent to a 60% reduction in soil COV. This suggests that the soil COV has a greater effect on the average settlement than the footing width when the Schmertmann 2B-0.6 method is used, as compared to 3DFEA. In contrast to the effects of an increasing soil COV, the SOF is shown to have little impact on the average settlement estimate for both 3DFEA and the Schmertmann 2B-0.6 method, as shown in Figures 5-11(a) and (b), respectively.

The results shown in Figure 5-12 suggest that the soil COV has a greater effect on the COV of the settlement estimate than the footing width. In fact, the latter is shown to have little effect on the COV of the settlement estimate, especially for the Schmertmann 2B-0.6 technique [Figure 5-12(b)]. However, it is important to realise that the results shown in Figure 5-12 are a coefficient of variation, which is a normalised measure of variance. Therefore, given the shading in Figure 5-10 for the average settlement, and in Figure 5-12 for the COV of settlement estimate, the standard deviation is also influenced by the width of the footing. Furthermore, the soil SOF is shown to have an influence on the settlement COV, as shown in Figure 5-13. These results suggest that a rising soil SOF yields an increasing settlement COV for both 3DFEA and the Schmertmann 2B-0.6 method. It also appears that the settlement COV is larger when using the Schmertmann 2B-0.6 technique compared to 3DFEA, for all soil SOFs and footing width combinations investigated. However, it appears that the footing width has a greater effect on the settlement COV when using 3DFEA.

**The footing width has a greater impact on the settlement COV using the Schmertmann 2B-0.6 method, as compared to 3DFEA.**



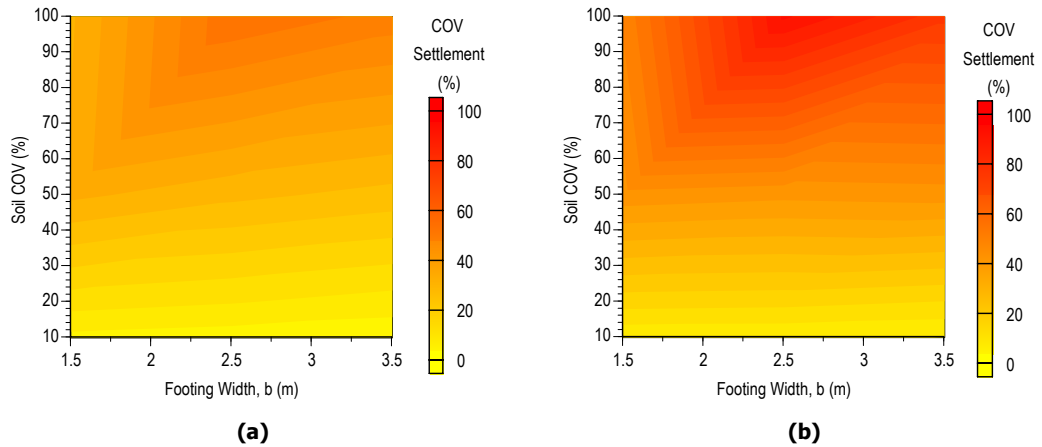


**Figure 5-12 Effect of increasing the soil COV (SOF of 8 m) on the COV of settlement of a single pad footing using (a) 3DFEA and (b) Schmertmann's 2B-0.6 relationship**

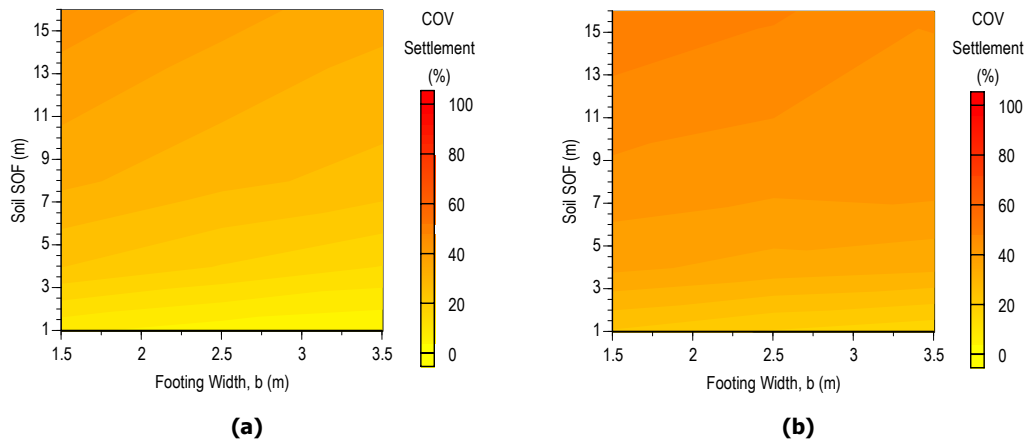


**Figure 5-13 Effect of increasing the soil SOF (COV of 50%) on the COV of settlement of a single pad footing using (a) 3DFEA and (b) Schmertmann's 2B-0.6 relationship**

The settlement COV is affected by the soil SOF due to local averaging. When the soil SOF is low, there is sufficient averaging to yield a reasonably constant elastic modulus, which results in a reasonably constant settlement estimate. However, as the soil SOF increases, the local averaging is reduced and the difference between the simulated and target elastic moduli increases. This was shown in Chapter 4 (§4.2.1). Although this effect is averaged over 1,000 Monte Carlo realisations, in order to obtain a relatively constant average settlement, as shown in Figure 5-11, the variance between realisations is great, and therefore, the settlement COV is large.

**The soil COV and footing width affect the mean settlement estimate, while the soil SOF affects the settlement COV.**

Using idealised lognormal distributions similar to those shown in Figure 5-8 and 5-9, where the shape of the distribution is defined by the average and standard deviation of the settlement estimate, it is possible to determine a bi-variate probability distribution that compares the sample distributions of settlements from 3DFEA with those given by the other methods. Furthermore, levels of exceedance can also be estimated by examining the probability that the estimates based on the prediction techniques, yield a smaller settlement than those from 3DFEA. This probability is given by:

$$P[Y > X] = P\left[\frac{Y}{X} > 1\right] = P[Z > 1] = P[\ln Z > 0] \quad (5.6)$$

where  $X$  is a random variable representation of the settlement technique estimate,  $Y$  is the random variable representation of the 3DFEA settlement and  $Z$  is the bi-variate probability distribution of  $X$  and  $Y$ . Since  $X$  and  $Y$  are lognormal, from discussions earlier in this section, the bi-variate distribution will also be lognormally distributed with mean,  $\mu_{\ln Z}$ , and standard deviation,  $\sigma_{\ln Z}$ . From Equation (5.6) and using the normal distribution function  $\Phi(x)$ , the probability that the settlement based on the prediction techniques is larger than that from 3DFEA, is given by:

$$P[\ln Z > 0] = 1 - \Phi\left(-\frac{\mu_{\ln Z}}{\sigma_{\ln Z}}\right) = 1 - \Phi\left(-\frac{(\mu_{\ln Y} - \mu_{\ln X})}{\sqrt{(\sigma_Y^2 + \sigma_X^2)}}\right) \quad (5.7)$$

where  $\mu_{\ln X}$  and  $\mu_{\ln Y}$  are the means of the lognormal variables  $X$  and  $Y$  and  $\sigma_{\ln X}$  and  $\sigma_{\ln Y}$  are the standard deviations of the lognormal variables  $X$  and  $Y$ , respectively.

Using Equation (5.7), Table 5-3 gives the probability that the 3DFEA settlement estimate exceeds that given by the other techniques, for nine different soils defined by their COV and SOF. It is important to note the probability that the prediction technique estimated settlement is less than that from 3DFEA is the situation where possible foundation failure may occur. This is referred to as the probability of under-estimation, and is a manifestation of the prediction technique under-estimating the true settlement, given by 3DFEA.

Results in Table 5-3 suggest that the probability of under-estimation is dependent on both the soil COV and SOF, which is in agreement with earlier results that showed that the average and standard deviation are greatly influenced by the spatial statistics of the soil. However, the changes in soil COV and SOF appear to affect the probability of under-

estimation differently for different methods. For example, an increase in soil COV appears to reduce the probability of under-estimation for the Newmark (New), Schmertmann 2B-0.6 (Sch2B), Timoshenko and Goodier (T&G) and Westergaard (Wst) techniques. For the other methods, it appears that, when the soil COV is 50%, the probability of under-estimation is greatest.

**Table 5-3 Probability that prediction technique settlement is less than 3DFEA settlement**

Prediction Technique	Soil COV:	Probability (%)								
		20%			50%			100%		
		Soil SOF:	1 m	4 m	16 m	4 m	16 m	1 m	4 m	16 m
2:1		0	1	45	0	6	53	0	1	40
Janbu		0	6	47	0	18	54	0	8	44
Newmark		100	98	72	100	78	68	0	40	58
Perloff		0	0	24	0	3	42	0	2	35
Schmertmann Modified		0	0	40	0	1	48	0	0	30
Schmertmann 2B-0.6		1	38	61	0	32	62	0	6	47
Timoshenko and Goodier		100	74	62	95	60	60	88	51	53
Westergaard		100	99	73	100	81	69	0	43	58

The main reason for the inconsistent trends, shown in Table 5-3, is due to the different effects of increasing soil COVs and SOFs on the settlements estimates using 3DFEA and the other methods. Such differences were shown in Figures 5-8 and 5-9 by the translation of the idealised lognormal distributions along the  $x$ -axis. These distributions were affected by the soil COV and SOF at different rates, and therefore, the probabilities of under-estimation are influenced differently by the soil COV and SOF.

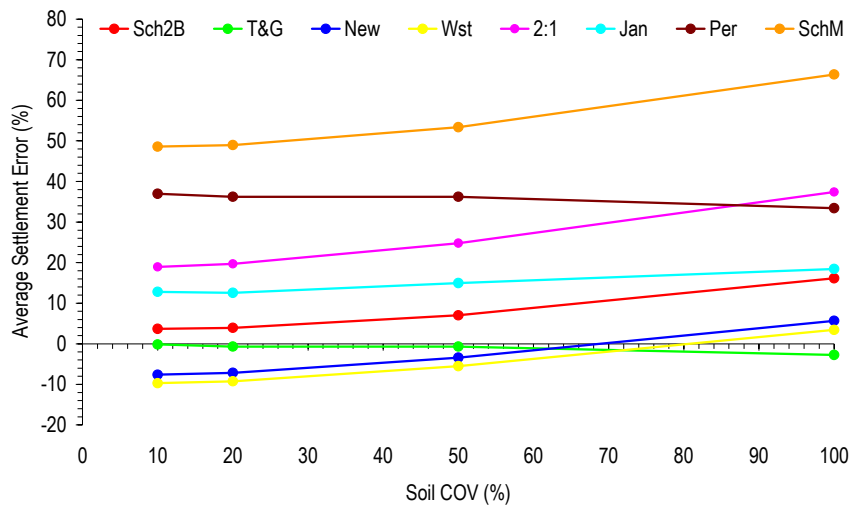
Although the probability of underestimation provides a measure of the likelihood that a settlement prediction technique will yield a settlement estimate less than 3DFEA, it does not indicate the overall conservatism of the technique. Such conservatism must also include the degree of underestimation and overestimation. This is the primary reason for introducing the settlement error,  $SE$ , as defined previously in Chapter 3 (§3.7.1), and repeated here as:

$$SE = \frac{S_i - S_{opt}}{S_{opt}} \quad (5.8)$$

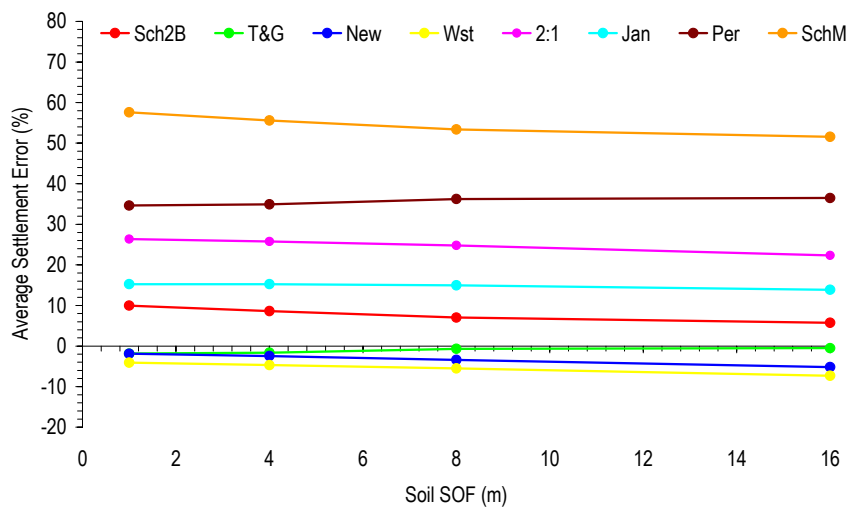
where  $S_i$  is the prediction technique estimated settlement and  $S_{opt}$  is the 3DFEA settlement estimate.

The *SE* is the normalised difference between the settlement estimate using a prediction technique and 3DFEA. It is calculated for each realisation in the Monte Carlo analysis and then expressed as an expected, or average, settlement error,  $E[SE]$ . Although the average settlement error is not a true probabilistic measure, it does account for the variability in the settlement estimates, and provides a measure of the degree of underestimation or overestimation with respect to 3DFEA.

The average settlement error of a single pad footing, based on results from the prediction techniques discussed previously, is shown in Figure 5-14. Figure 5-14(a) is based on a footing founded on a soil with a SOF of 8 m and increasing COV, while Figure 5-14(b) is based on a soil COV of 50% and increasing SOF.



(a)



(b)

Figure 5-14 Average settlement error for an increasing soil (a) COV (SOF of 8 m) and (b) SOF (COV of 50%)

As shown in Figure 5-14(a), the average settlement error increases as the soil COV increases for all methods, except those of Perloff (Per), Timoshenko and Goodier (T&G) and, to a lesser extent, Janbu (Jan). It is important to note that these techniques are the only ones investigated that do not accommodate elastic modulus variability in the vertical direction. Instead, an average elastic modulus is considered. Such averaging reduces the apparent variability of the elastic moduli leading to a diminished effect with respect to settlement error. The other techniques appear to yield a similar increase in average settlement error for increasing soil COV. The relative difference between the average settlement errors shown for each settlement prediction technique appears to be in similar proportion to the results of the analysis based on a uniform elastic modulus field, as shown previously in Figure 5-3.

Figure 5-14(b) shows that an increasing soil SOF has less influence on average settlement error than the soil COV. Instead, the average settlement error appears almost constant for all SOFs investigated. However, there does appear to be a slight reduction in average settlement error as the soil SOF increases. On the other hand, the settlement methods that do not accommodate soil variability in the vertical direction appear to have a slightly increasing average settlement error as the soil SOF rises. These trends are in direct contrast to those in Figure 5-14(a). Nevertheless, the soil COV appears to have a greater impact on the average settlement error than the SOF.

**The average settlement error increases as the soil COV increases. Furthermore, the soil COV has a greater influence on the average settlement error than the soil SOF.**

The average settlement error, shown in Figure 5-14, also indicates the relative conservatism of each method with respect to 3DFEA. For instance, a large positive settlement error corresponds to a highly conservative method, while a large negative error refers to a method with small conservatism. Such conservatisms have been shown throughout this section, where the Newmark, Westergaard and Timoshenko and Goodier methods have all been shown to be the least conservative. At the other end of the spectrum, the Schmertmann Modified and Perloff techniques have been shown to be highly conservative.

Each of the methods investigated in this section have also shown to be affected similarly by the spatial statistics of the soil. However, settlement estimates based on 3DFEA and complete knowledge of the soil (CK) appear to be influenced differently by the soil COV than the other techniques. This is because the other methods do not technically consider

the complete knowledge of the soil. Therefore, it is considered relevant to explore an alternative means of incorporating the complete knowledge of the soil into the settlement methods. This is discussed in the following section.

### 5.2.3 Analysis Using an Influence Region of Properties

Results presented thus far have indicated that settlement estimates, based on 3DFEA and complete knowledge of the soil (CK), are affected differently by the soil COV and SOF than the estimates using the other methods. This is due to the number of elastic moduli used in the analysis, where the 3DFEA considers all moduli at the site and the other methods account for only the soil properties in a single vertical sample, located under the footing. Although in the previous section, a single vertical sample was considered suitable for comparison between methods, it does not constitute complete knowledge of the soil. In reality, the soil surrounding the footing also influences settlement (Holtz 1991, Bowles 1997). Therefore, a better representation of complete knowledge is to consider the elastic moduli in a region surrounding the footing. However, it is not clear what the size of this region should be. Figure 5-15 illustrates the well-established dispersion of stresses throughout a soil, due to a square and continuous, or strip, footing. In this figure, the  $q/q_0$  isobars indicate the percentile of pressure distribution throughout the soil, where  $q$  is the stress at any point in the profile and  $q_0$  is the applied footing pressure. It is evident from these contours that a square loaded area affects soil up to a distance of approximately 1.5 times the footing width from the edge of the footing. Bowles (1997) and Holtz (1991) suggested that stresses less than 5% of the applied stress are insignificant and do not contribute to footing settlement.

The isobars shown in Figure 5-15 suggest it is appropriate to use an *influence region* within which soil properties should be averaged to determine a characteristic elastic moduli to use in the settlement methods examined above. If the size of the influence region is based on the extent of the isobars shown in Figure 5-15, properties should be averaged within a region that has a plan area 225% larger than the footing size. However, the isobars in Figure 5-15 indicate that higher stresses occur closer to the centre of the footing. Therefore, a region that is 225% larger than the footing size may not be suitable, as the outlying soil properties have reduced impact in relation to settlement. As such, an analysis investigating the most appropriate influence region size is undertaken. This involves averaging the elastic moduli within an influence region of progressively increased size. The resultant characteristic value is then used in each of the settlement methods to estimate the footing settlement. This estimate is compared with a 3DFEA settlement, which utilises

complete knowledge of the soil (CK), accommodating total variability of the elastic modulus.

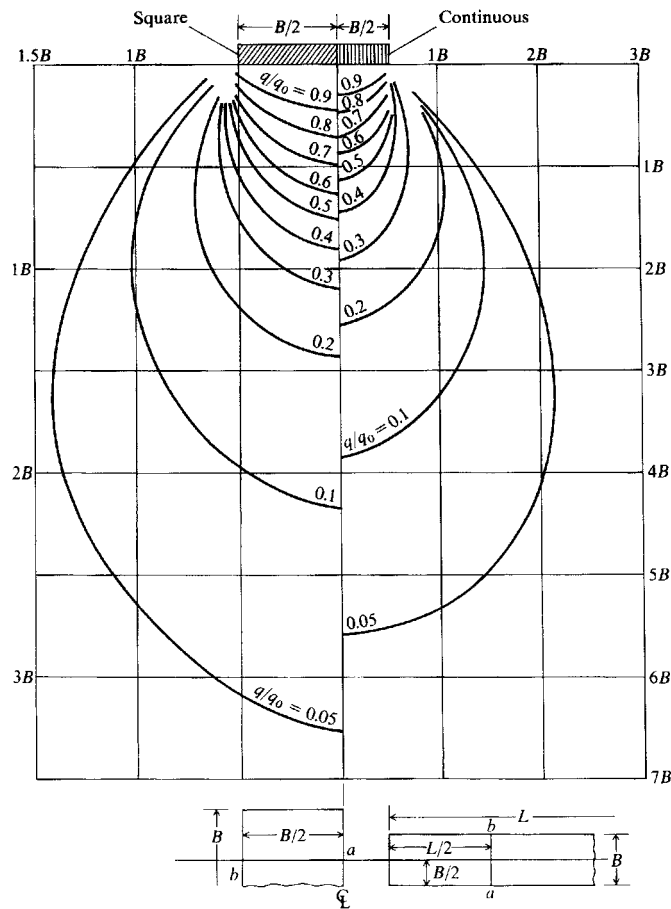


**Figure 5-15 Pressure isobars shown for a square and strip footing**  
After Bowles (1997)

Knowledge of an optimal influence region also has implications when planning site investigations or deciding how the results from a site investigation should be considered in the design or analysis of a footing. During the planning phase of a site investigation, a borehole should be located within the optimal influence region to ensure that the representative properties are sampled. The effect of sample location on the design of a foundation will be treated in later chapters. It is also plausible to conclude whether the results of a sample location should be considered in the settlement analysis based on knowledge of the optimal influence region. Consider the situation presented in Figure 5-16, where 10 sample locations are randomly located on a site in order to characterise the underlying soil with the aim to design a 4-pad foundation system. The broken lines surrounding each of the 4 footings represent the plan area of the optimal influence region. Therefore, for the example shown in Figure 5-16, the results from borehole T1 and T2 should be used in the design of

Footing 1; boreholes T3 and T4 should be used for Footing 2; boreholes T6 and T7 should be used for Footing 3, and boreholes T8 and T9 should be used for Footing 4. The results from boreholes T5 and T10 should not be considered for any of the footings in the system.

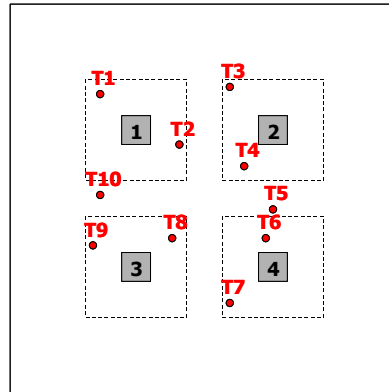


**Figure 5-16 Example of a site investigation programme consisting of 10 random borehole locations for a foundation system with 4 pad footings and their corresponding optimal influence region areas**

To identify the size of the optimal influence region, an analysis is conducted, where the plan area of the region is centred about the footing and progressively increased in size, as shown in Figure 5-17. The footing is assumed to have a plan size of 1.5 m × 1.5 m for the majority of analyses. However, footings of a different size are also investigated. The mean elastic modulus of the simulated soil is set to 20,000 kPa and different combinations of COV and SOF are used to simulate the soil. The mean elastic modulus is not expected to affect the results – only the total settlement. The elastic moduli within the influence region are averaged using one of three different averaging techniques: standard arithmetic average (SA), geometric average (GA), and harmonic average (HA), as defined in Chapter 3 (§3.4.2).

Figures 5-18 and 5-19 show the effect of increasing the size of the influence region on the average settlement error of the pad footing, in relation to increasing soil COV and SOF, respectively. These results compare settlement estimates based on elastic moduli contained within the influence region and the Schmertmann 2B-0.6 technique (Sch2B), with those based on 3DFEA and CK. The average settlement error is plotted against a ratio of the influence region plan area to footing plan area ( $A_i/A_f$ ). The results shown in both figures also demonstrate the effect of averaging the properties within the influence region using different averaging techniques, where results in Figures 5-18(a) and 5-19(a) are based on a standard arithmetic average (SA); results in Figures 5-18(b) and 5-19(b) are based on a geometric average (GA); and results in Figures 5-18(c) and 5-19(c) are based on a harmonic average (HA).



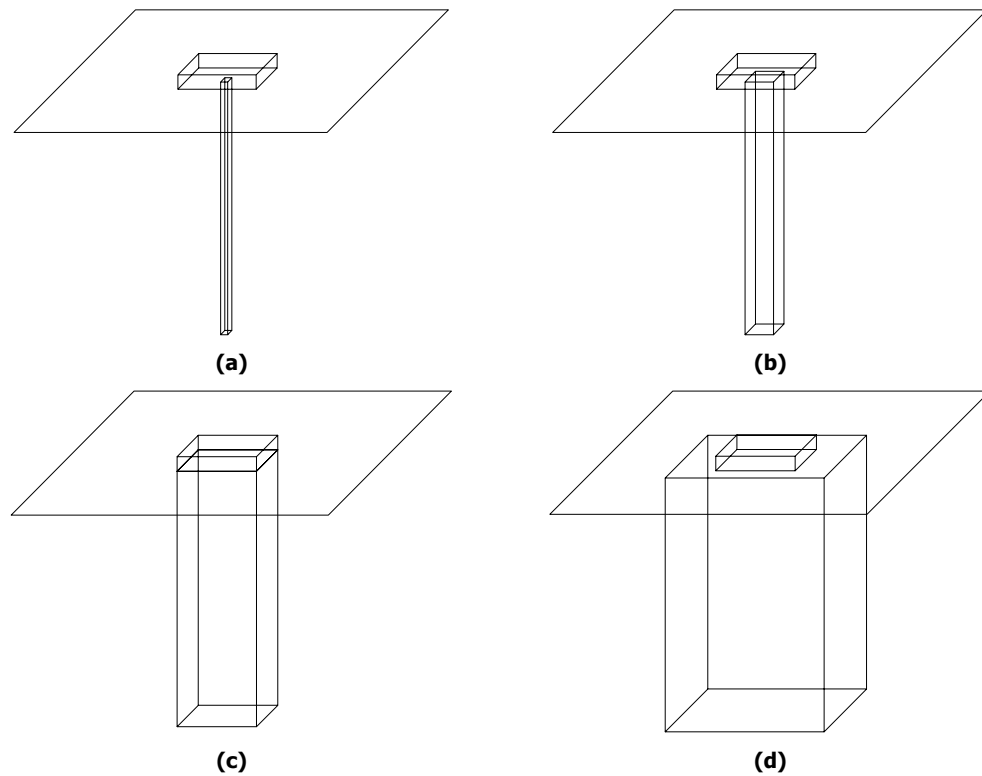
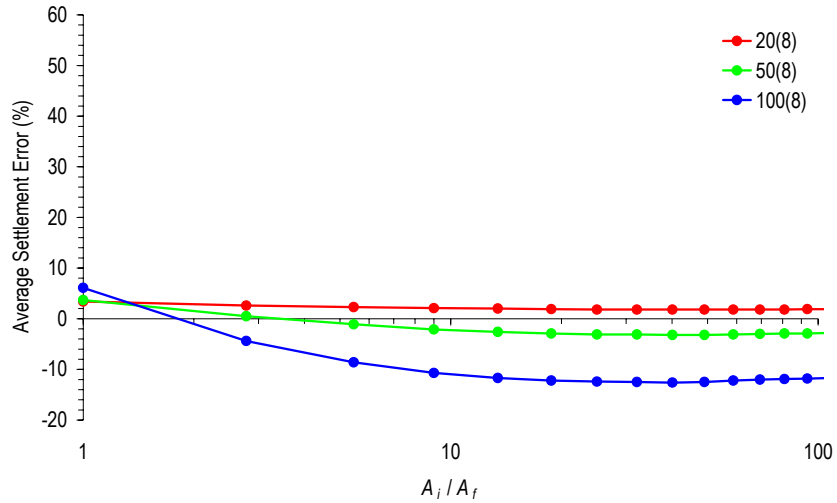


**Figure 5-17 Increasing influence areas from a (a) vertical line to a (d) comparatively large region**

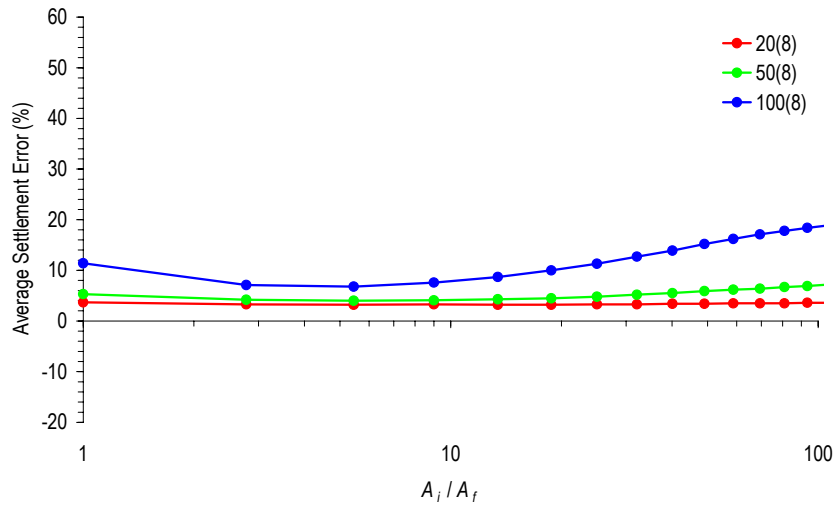
Several relevant conclusions regarding the use of an influence region are evident from the results shown in Figures 5-18 and 5-19. Such conclusions are:

- The average settlement error is reduced as the influence region size increases, when the SA method is used;
- The average settlement error increases as the influence region size grows, when the HA is used. As a result, this technique is not suited to averaging properties within an influence region;
- An optimal influence region,  $A_{opt}$ , occurs, where the average settlement error is a minimum;
- The  $A_{opt}$  is not affected by the soil COV; and
- The soil SOF has a significant impact on the  $A_{opt}$ . Furthermore, a worst case SOF is also evident, where the  $A_{opt}$  is a maximum.

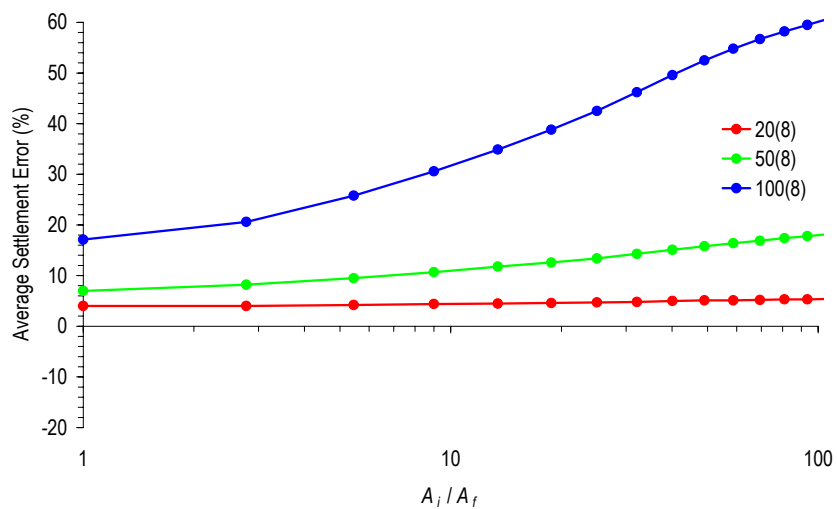
Since the SA is the only averaging technique that yields close to a zero average settlement error, for a given influence region, it follows that this method provides a better



(a)

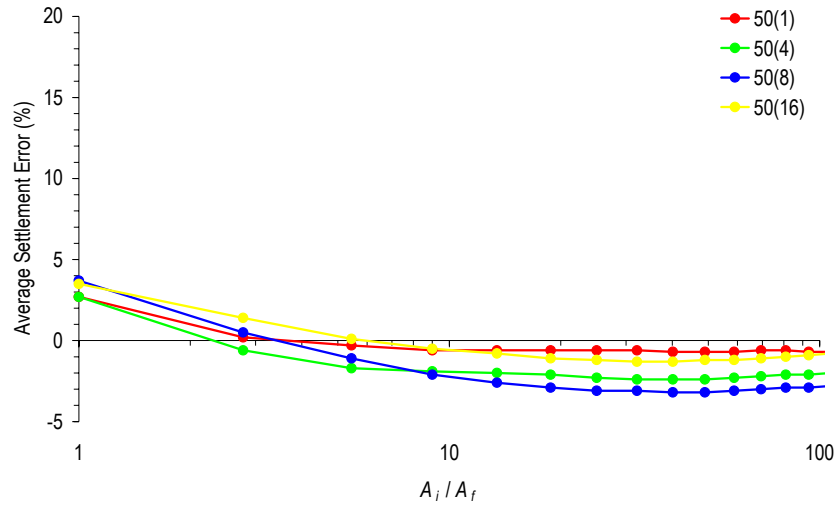


(b)

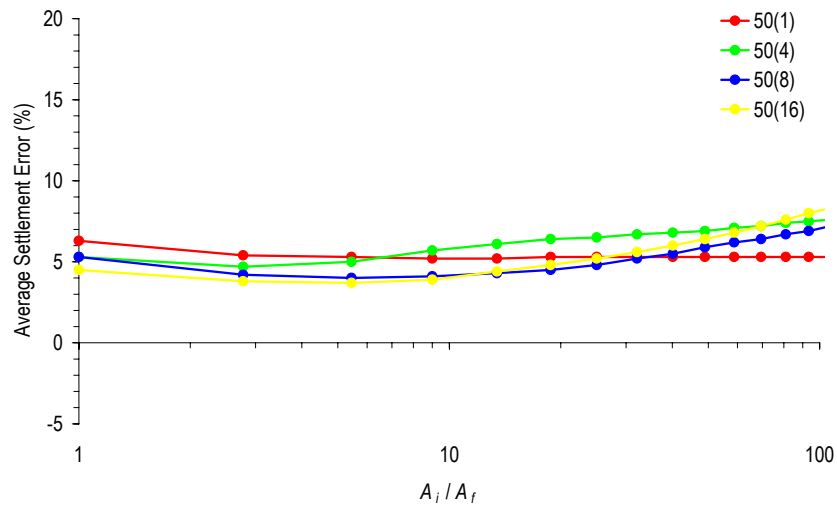


(c)

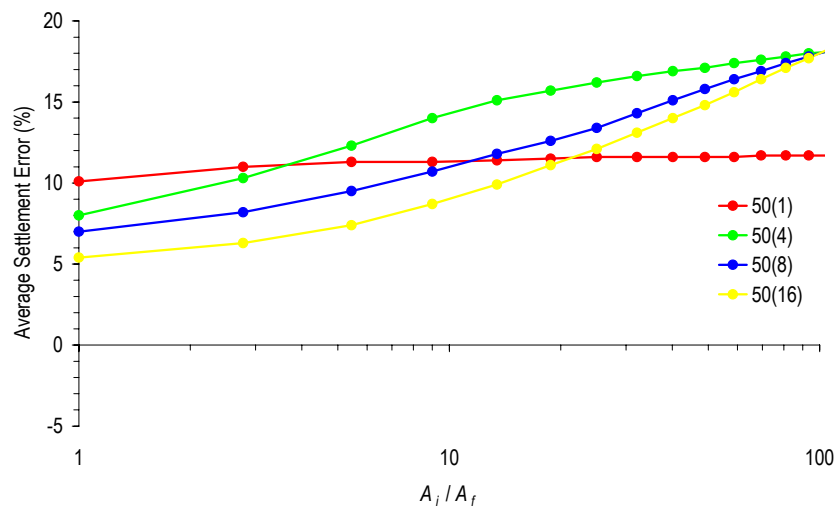
**Figure 5-18 Effect of increasing the size of the influence region within which properties are averaged using (a) SA, (b) GA and (c) HA on the average settlement error of a single pad footing, for an increasing soil COV and SOF of 8 m**



(a)



(b)



(c)

**Figure 5-19 Effect of increasing the size of the influence region within which properties are averaged using (a) SA, (b) GA and (c) HA on the average settlement error of a single pad footing, for an increasing soil SOF and COV of 50%**

representation of the underlying soil conditions. However, it is important to remember that Schmertmann 2B-0.6 method (Sch2B) was shown earlier (Figure 5-2) to yield conservative settlement estimates. In fact, such results indicated that settlement estimates, based on the Schmertmann 2B-0.6 method, were approximately 4% larger than 3DFEA estimates on a soil with a uniform elastic modulus. Such conservatism is again shown in Figure 5-18(a), using the SA, for a soil COV of 10%. However, as the soil COV increases, the average settlement error reduces and becomes negative, which implies a reduction in conservatism. On the other hand, the results in Figure 5-18(b), based on the GA, suggest a minimum average settlement error that varies between 4% and 8% for a soil COV of 10% and 100%, respectively. This infers that the GA preserves the conservatism associated with the Schmertmann 2B-0.6 technique. On the other hand, the average settlement error grows considerably, for an increasing influence region size using the HA [Figures 5-18(c) and 5-19(c)]. Therefore, the optimal influence region,  $A_{opt}$ , when using the HA, is equivalent to a single vertical sample of elastic moduli located at the centre of the footing. This is the condition that was investigated earlier in this chapter (§5.2.2). Hence, the HA is not suited to this form of analysis and, as a result, is not considered further.

The size of the optimal influence region,  $A_{opt}$ , appears to be affected by only the soil SOF, and not the soil COV. As a result, the  $A_{opt}$  is constant for all soil COVs investigated. This is shown in Figures 5-18(a) and (b) for the SA and GA, respectively. In the case of the SA, the  $A_{opt}$  occurs when the influence region is approximately 20 times the footing area, while for the GA, the  $A_{opt}$  occurs when the influence region is approximately 6 times the footing size. However, it should be noted that soils with low COV (i.e. less than 50%) do not show large variations in average settlement error. Furthermore, the analysis based on the SA also indicates that influence regions larger than the  $A_{opt}$  yield the same average settlement error.

In contrast, the soil SOF has a definite impact on the  $A_{opt}$ , as shown in Figures 5-19(a) and (b), for the SA and GA, respectively. For example, when using the SA, the  $A_{opt}$  increases in size from 9 to 21 times the footing area, as the soil SOF rises from 1 m to greater than 4 m. However, an influence region size of 21 times the footing area will still yield the minimum average settlement error for a soil SOF of 1 m. A similar result is also apparent when using the GA. In this case, the  $A_{opt}$  increases from 3 times the footing area, when the soil SOF is less than 4 m, to 5 or 6 times the footing area when the soil SOF is greater than 4 m. Therefore, both Figures 5-19(a) and (b) suggest that, as the soil SOF increases, the  $A_{opt}$  increases. However, it also appears that such an increase is not universal, where a maximum  $A_{opt}$  is achieved when the soil SOF is greater than 4 m and less than 8 m. Such a

SOF is in agreement with the expected worst case SOF, as described in Chapter 4 (§4.2.1). Furthermore, a comparison between the average settlement errors, when a very large influence region size is considered, also confirms the presence of a worst case SOF. This is best illustrated by the SA results, shown in Figure 5-19(a), where the average settlement error, based on an influence region size equal to 100 times the footing area, appears to reduce as the soil SOF increases from 1 m to 8 m. However, as the soil SOF increases beyond 8 m, the average settlement error increases. This infers that a soil SOF of 8 m yields a limiting case, which in this instance, is the maximum negative average settlement error.

**For the SA, an optimal influence region of approximately 21 times the footing area should be used. In contrast, for the GA, an optimal influence region of 6 times the footing area is suited. However, for lower soil SOFs, the region size, using the GA, should also be reduced.**

It is important to consider that the GA is greatly influenced by low elastic moduli. In fact, if a zero elastic moduli occurred within the influence region, the GA would equal zero, yielding an infinite settlement. On the other hand, the SA weights all values equally and is not biased by low or high values. Fenton and Griffiths (2002) suggested that a GA may be more suited to characterising a soil because it is spatially random, whereas a SA applies to vertically layered media and a HA applies to a horizontally layered soil. Fenton and Griffiths (2002) also observed that foundations appear to find the weakest failure path. Therefore, the capacity or settlement of a foundation is heavily dependent on the low strength or stiffness regions of soil. The GA, rather than the SA, more appropriately accommodates these low strength or stiffness regions.

The GA also appears to reach a minimum average settlement error faster than the SA. This suggests that the GA makes better use of limited information. However, the results shown in Figures 5-18(b) and 5-19(b) also suggest that the average settlement error will increase if a GA is applied to a region larger than the  $A_{opt}$ . This is not evident for the SA technique, where additional information does not appear to greatly affect the result. Therefore, it is of great importance that the  $A_{opt}$  is identified when using a GA.

To this point, the examination of settlement estimates using an influence region has been confined to the average settlement error of a pad footing with a plan size of 1.5 m × 1.5 m. However, an analysis is also conducted to investigate the use of an influence region for a pad footing of varying size. These results are given in Figure 5-20 and suggest that the size of footing has little impact on the  $A_{opt}$ . Instead, it appears that an increase in the footing size reduces the conservatism of the Schmertmann 2B-0.6 method by causing a reduc-

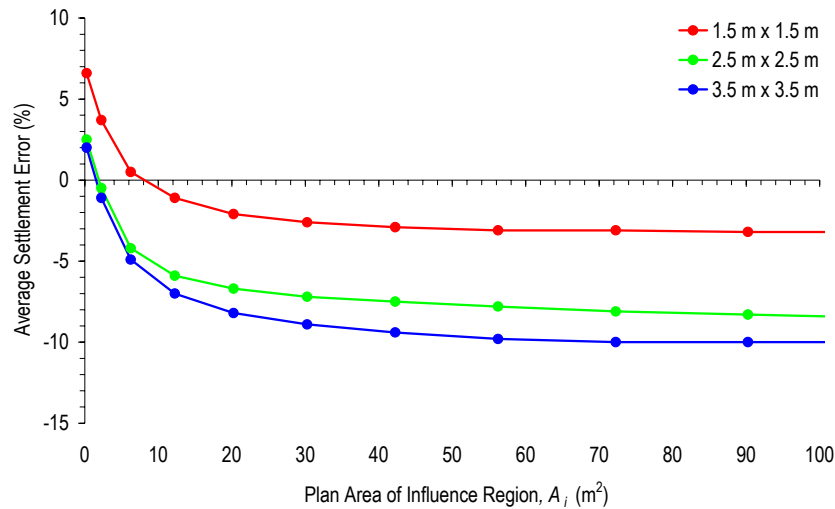
tion in the average settlement error. A reduction in conservatism has also been observed earlier in this chapter (Figure 5-5), where analyses were conducted on a soil with uniform properties. However, the relationship between average settlement error and influence region size appears to be unaffected. This suggests that, for footings up to a plan size of 3.5 m × 3.5 m - a common size for pad footings - the  $A_{opt}$  is constant. Figure 5-20 also confirms the conclusions made above, regarding the effectiveness of the SA and GA methods, where the GA appears to preserve the conservatism in the method and makes better use of limited information, achieving a minimum average settlement error at a smaller influence region. However, the reduction in conservatism associated with larger footings causes the average settlement error from the GA to become negative for certain influence regions. Therefore, careful consideration is required when selecting the  $A_{opt}$  for both the SA and GA, as negative average settlement errors infer a possible failure condition.

**The footing size has little impact on the required dimensions of the optimal influence region.**

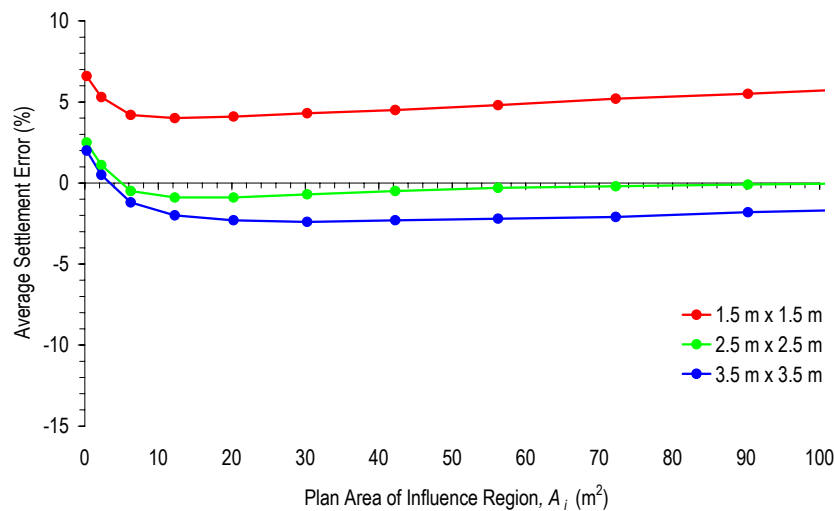
Analyses are also undertaken to investigate the effect of increasing influence region on the average settlement error using the different settlement prediction techniques described earlier. The results of this analysis are shown in Figures 5-21 and 5-22, based on a soil COV of 50% and SOF of 8 m, and a soil COV of 100% and SOF of 16 m, respectively. Figures 5-21(a) and 5-22(a) are based on the SA, while Figures 5-21(b) and 5-22(b) use the GA. Such results indicate that:

- Different settlement prediction techniques have little effect on the relationship between average settlement error and the size of the influence region; and
- The Perloff (Per) and Timoshenko and Goodier (T&G) methods show no benefit in averaging elastic moduli within an influence region. Instead, a single vertical sample of elastic moduli yields the smallest average settlement error.

Although the different settlement methods show little impact on the relationship between influence region size and average settlement error, they do illustrate their relative conservatisms, as discussed previously in this chapter. As such, it is possible to identify which settlement methods will yield an average settlement error that is close to zero. In this case, it appears that the Schmertmann 2B-0.6 technique provides the best solution, when using the SA. On the other hand, the Timoshenko and Goodier method is better when using the GA. However, this will be affected by the footing size, as discussed above in Figure 5-20.



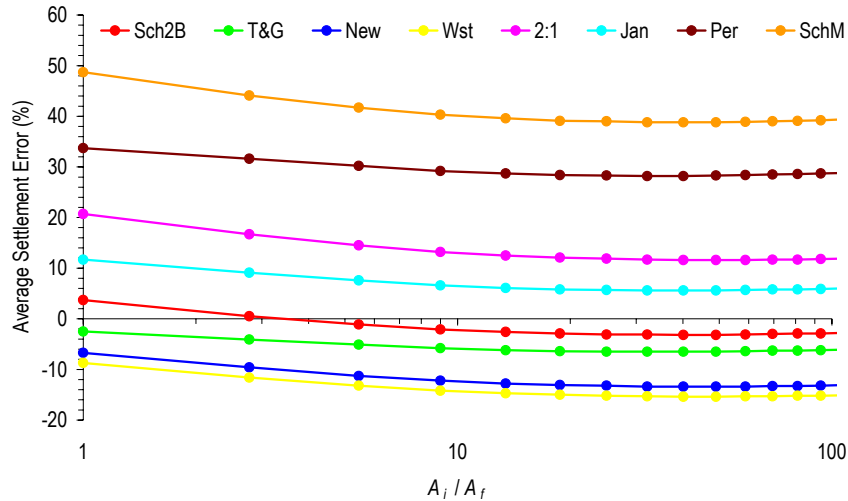
(a)



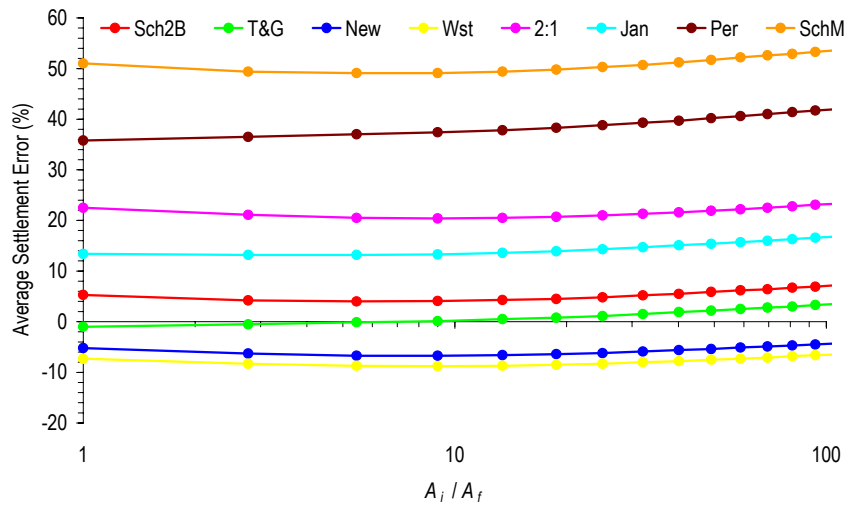
(b)

**Figure 5-20 Effect of increasing the influence region within which soil properties are averaged with the (a) SA and (b) GA on the average settlement error of a single pad footing of varying widths, for a soil COV of 50% and SOF of 8 m**

It is not unexpected that the Perloff and Timoshenko and Goodier methods show no benefit in using an influence region of elastic moduli. This is because these methods have already been shown previously (Figure 5-14) to behave differently than the other techniques. In those particular results, the Perloff and Timoshenko and Goodier relationships were shown to have a reducing average settlement error for increasing soil COV and SOF, while the other methods all indicated an increasing error. Those differences were believed to be a result of the Perloff and Timoshenko and Goodier techniques using a single elastic modulus, rather than a vertical sample. Therefore, it is also expected that the differences shown in Figures 5-21 and 5-22 are a result of the same cause.



(a)



(b)

**Figure 5-21 Effect of increasing the influence region within which soil properties are averaged using the (a) SA and (b) GA on the average settlement error of a single pad footing using different prediction relationships, for a soil COV of 50% and SOF of 8 m**

Although the analysis regarding the influence region of soil properties yields an optimal region, it is important to note that it is not expected that all elastic moduli within this region would be known with any degree of confidence. Instead, this analysis has identified the region within which elastic moduli have the greatest impact on footing settlement. The example shown earlier in Figure 5-16, is for illustration purposes only and should not be adopted as the ultimate solution. Results in subsequent chapters will demonstrate that using the results from every sample location will increase the confidence and therefore, the accuracy of the analysis. However, based on the analysis presented in this section, it is recommended that an influence region with a size of approximately 6 times the footing width, should be considered and properties should be averaged using the GA. This yields a



slightly conservative result for a footing of size 1.5 m × 1.5m. However, if the footing size increases, or the soil SOF reduces below 4 m, this region size should be reviewed.

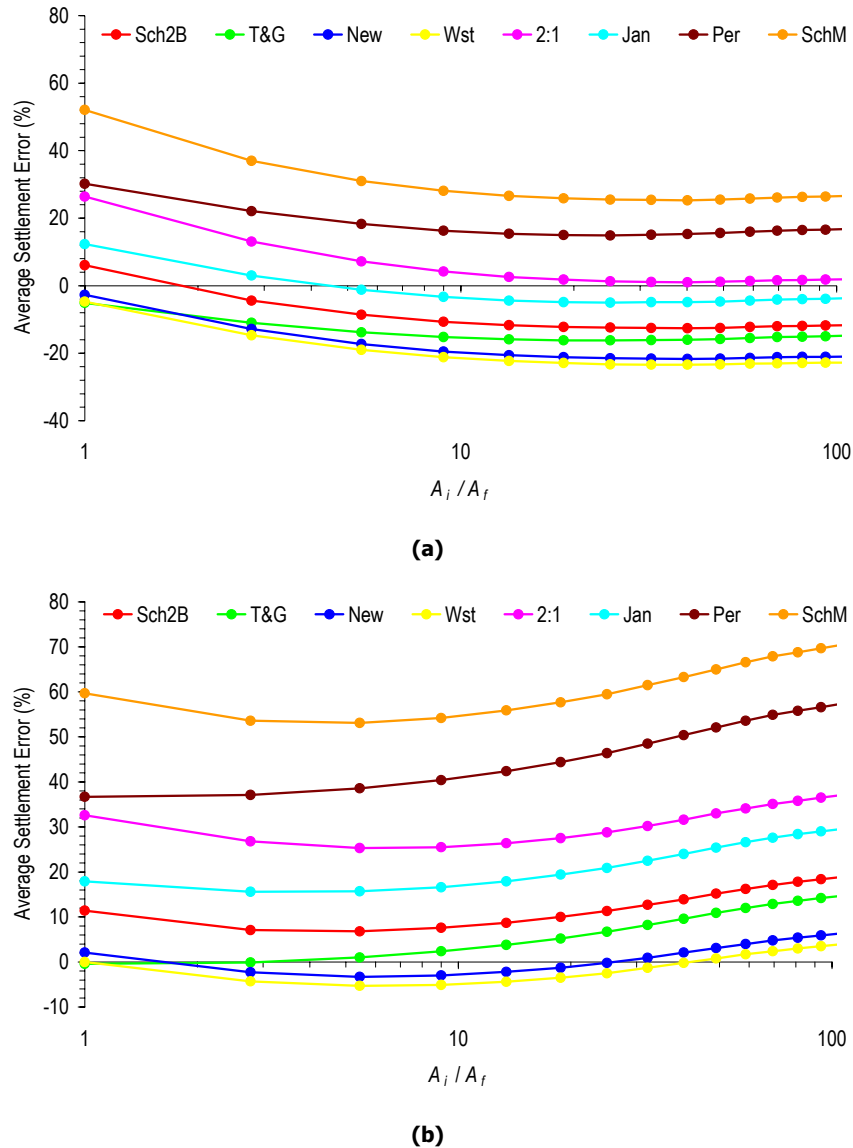


**Figure 5-22 Effect of increasing the influence region within which soil properties are averaged using the (a) SA and (b) GA on the average settlement error of a single pad footing using different prediction relationships, for a soil COV of 100% and SOF of 8 mm**

### 5.2.4 Summary

Results in this section have identified the differences between settlement methods on the prediction of footing response. In most cases, the relative conservatism of the techniques have been identified where the Schmertmann Modified was shown to yield the largest settlements and the Newmark or Westergaard method provided the smallest. It has also been shown that settlement estimates are affected by the spatial statistics of the soil. However,

an increasing soil COV and SOF was shown to have little impact on the relative conservatism of the methods.

Most of the results presented were based on a *pseudo* complete knowledge of the soil, which was assumed to be a single vertical sample of elastic moduli, located beneath the centre of the footing. However, comparisons between the pseudo complete knowledge and the full complete knowledge, which accounted for all elastic moduli, indicated that variations in soil COV and SOF had different impacts. Therefore, another measure of complete knowledge was introduced, which involved averaging the soil properties within an influence region. Furthermore, an optimal influence region was identified for different averaging techniques. This optimal region was shown to be unaffected by the soil COV and has applications when planning site investigations. In this case, the optimal influence region was found to be approximately 6 times the footing area when the GA is used to average properties. However, this size varied with the soil SOF and the footing width.

The next section of this chapter extends the analysis undertaken here to include settlement estimates from different methods in a design process. This identifies the relative conservatism of each prediction technique to provide a footing design that meets a specified criterion.

### **5.3 PAD FOUNDATION DESIGN USING DIFFERENT SETTLEMENT PREDICTION TECHNIQUES**

---

The results thus far have dealt exclusively with the predicted settlement of a footing of a specific size. In a design scenario however, the size of the footing is not known and different footing sizes are examined until the specified design criteria are met. As such, an analysis is undertaken to examine the use of different settlement methods on the design of a pad foundation. The design process adopted here is an iterative one, which involves beginning with an initial footing size and comparing the predicted settlement to the limits nominated in the design criteria. If the predicted total settlement, or differential settlement between two footings is greater than the specified limit, the footing size is increased until the predicted settlement meets the design criteria, as discussed in Chapter 3 (§3.5.1). The analysis also examines the impact of varying the soil COV and SOF on the design of the foundation. However, for this form of analysis, the settlement methods use complete knowledge of the soil (CK), where CK consists of a single vertical sample of elastic moduli located beneath the centre of the footing. For 3DFEA, CK involves using all elastic moduli.

The increments that are used to increase the size of the footing have already been discussed in Chapter 3 (§3.5.1) and are dependent on whether or not 3DFEA is used in the analysis. The effect of using different size increments is illustrated in Figure 5-23, where sample distributions of designed footing areas are given. Results in Figure 5-23(i) are based on a size increment of 1 m, while the results in Figure 5-23(ii) are based on an increment of 0.1 m. The sizing increment of 1 m is required when 3DFEA settlement estimates are included. On the other hand, a 0.1 m sizing increment is adopted when 3DFEA is not considered. This is possible, since the footing size is not tied to the element size. It should be noted, however, that the element size remains 0.5 m × 0.5 m × 0.5 m for all analyses.

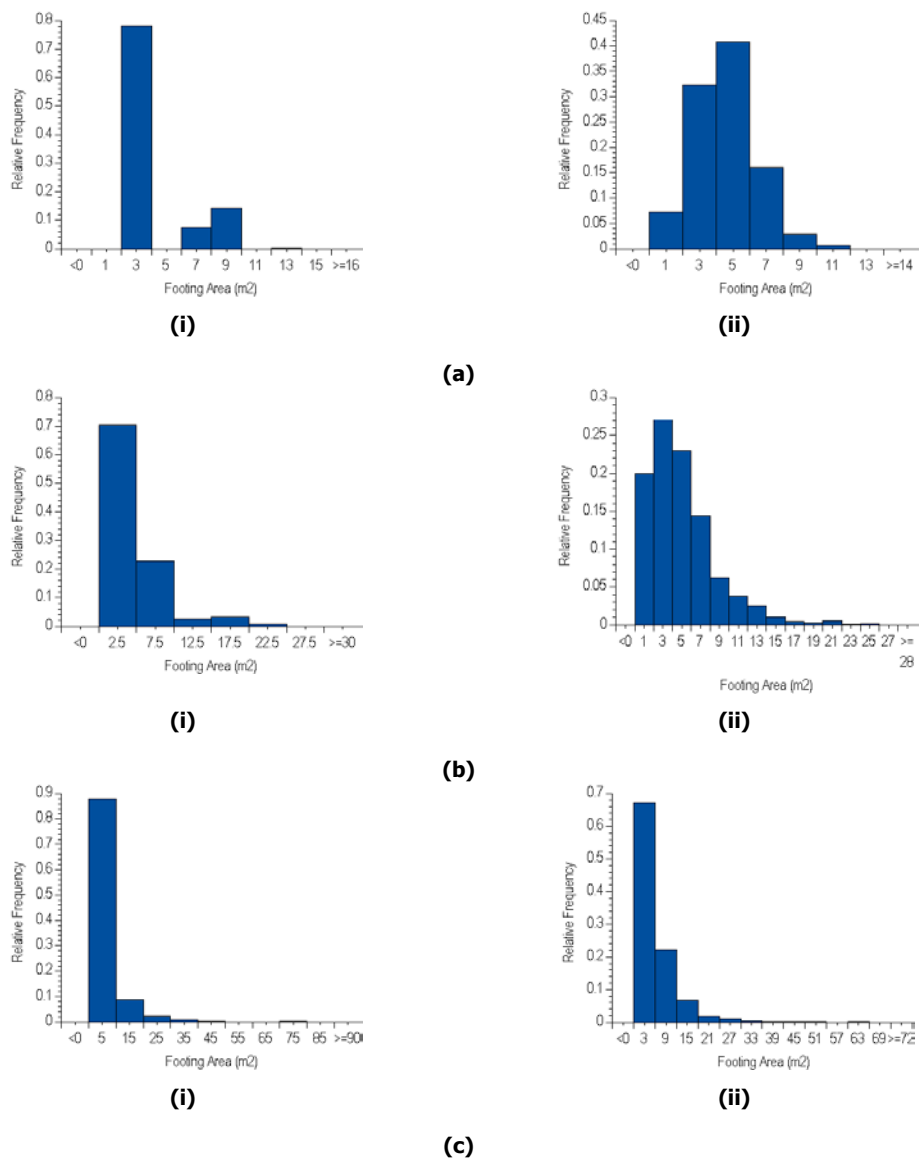


**Figure 5-23** Difference between design area distributions using the Schmertmann 2B-0.6 prediction technique with a (i) 0.5 m and (ii) 0.05 m discretisation for a single pad footing, for a soil COV of 50% and SOF of (a) 1 m, (b) 4 m and (c) 16 m

The results for the 0.1 m sizing increment, shown in Figure 5-23(ii), yield a sample distribution that has a lognormal shape. However, the sample distributions based on a 1 m sizing increment, shown in Figure 5-23(i), almost appear discrete and have less resolution than the 0.1 m sizing increment. As such, it is difficult to adequately describe the sample distribution based on a 1 m increment using a common statistical distribution. Furthermore, the minimum footing size constraint also makes it difficult to describe the distribution of design area. This constraint sets the minimum footing size to 9 square elements ( $3 \times 3$ ), which, in the case of 1 m size increment, is  $2.25 \text{ m}^2$ . The requirement for a minimum footing size has been previously discussed in Chapter 3 (§3.6.5.2).

**The resulting footing design areas from the analysis cannot be adequately described by a lognormal distribution due to the minimum footing size constraint and the discretisation of elements.**

Given that it is difficult to describe foundation design areas using a common statistical distribution, a theoretical analysis of probabilities and exceedance levels similar to that conducted in the previous section, is not possible. Instead, the results presented in this section rely on the output of the Monte Carlo simulation. However, the use of a Monte Carlo simulation has been shown to be sufficiently accurate in Chapter 4 (§4.4). Therefore, this is considered a suitable alternative to a theoretical evaluation.

The majority of results presented in this section, are based on a foundation system consisting of 9-pad footings, as shown previously in Figure 5-1(c). This allows the investigation of the relative conservatism of each settlement prediction technique for individual footings in the system. Analyses are based on a soil with spatially random elastic moduli with a mean of 30,000 kPa. The deterministic situation, when the elastic modulus is uniform throughout the soil, has already been investigated earlier in this chapter as a settlement analysis (§5.2.1), and therefore, a repeat of the analysis for a design scenario is unnecessary. The design criteria adopted includes a maximum absolute settlement limit of 25 mm and a maximum differential settlement limit of 0.0025 m/m. Since 3DFEA is used in this section, a sizing increment of 1 m is adopted where the footing sizes are increased by 1 m in one direction (0.5 m each side of the centre) if the predicted settlement is larger than the limits.

The effect of increasing the soil COV and SOF on the average and COV of total footing area for both 3DFEA and the Schmertmann 2B-0.6 (Sch2B) technique, is shown in Figures 5-24 and 5-25, respectively. The minimum total footing area for the 9-pad system is

20.25 m<sup>2</sup>, based on each footing having a minimum area of 2.25 m<sup>2</sup>, or plan dimensions of 1.5 m × 1.5 m. Such a minimum design is shown to adequately meet the design criteria for both 3DFEA and the Schmertmann 2B-0.6 method when the soil COV is less than 50%, (Figure 5-24). However, when the soil COV is greater than 50%, a total footing area greater than 20.25 m<sup>2</sup> is required. It is apparent, from the results shown in Figure 5-24, that a foundation designed using 3DFEA requires a larger footing area to meet the design criteria than a foundation designed using the Schmertmann 2B-0.6 technique, for soils with a COV greater than 50%.

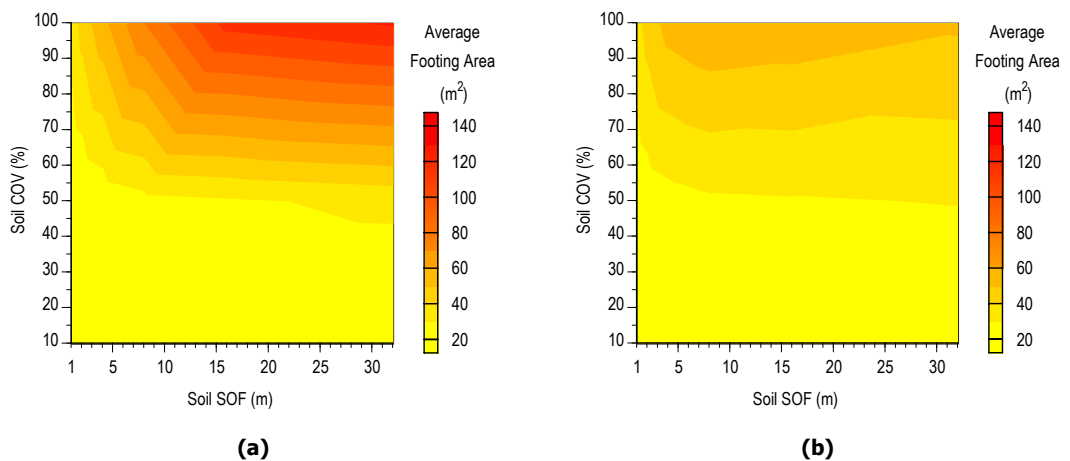


**Figure 5-24** Effect of increasing soil COV and SOF on the average total footing area of a system of 9-pad footings, designed using (a) 3DFEA and (b) the Schmertmann 2B-0.6 prediction technique

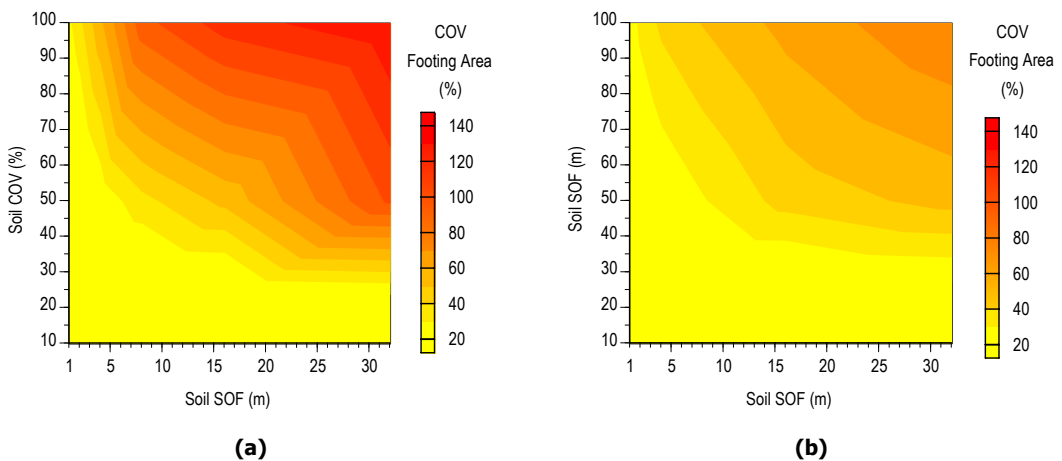


**Figure 5-25** Effect of increasing soil COV and SOF on the COV total footing area of a system of 9-pad footings, designed using (a) 3DFEA and (b) the Schmertmann 2B-0.6 prediction technique

**A foundation design using 3DFEA yields a larger footing than the Schmertmann 2B-0.6 technique, when the soil COV is greater than 50%.**

The soil COV has a notable effect on the average total footing area, as shown in Figure 5-24, by the strong horizontally layered appearance of the shading. However, when the soil SOF is low (less than approximately 8 m), the COV does not appear to impact the results to the same degree. This is due to increased averaging at low SOFs, where the apparent variability in the elastic modulus is less than the actual. Similar results are shown in Figure 5-25 for the COV of total footing area,  $COV_A$ , where the  $COV_A$  is influenced to a greater extent by the soil SOF, when it is low. However, when the soil SOF is high, the soil COV has the greatest influence on the  $COV_A$ .

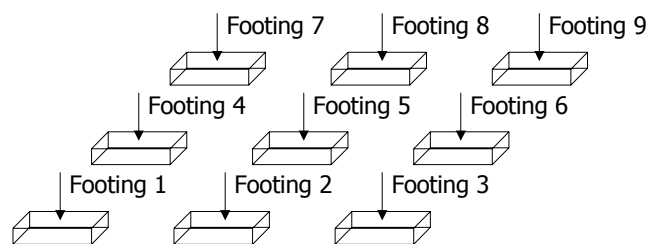
A comparison between the results shown in Figure 5-24(a) and (b) suggests that the soil COV has a greater impact on the average total footing area designed using 3DFEA as compared to using the Schmertmann 2B-0.6 method. Although this was shown earlier in this chapter (§5.2.2) for the settlement analysis, the differences are more exaggerated in Figure 5-24. The cause of the greater difference between a settlement analysis and a design scenario is the size of the footing and the number of elastic moduli considered in the analysis. For example, an increase in soil COV was shown earlier in this chapter (§5.2.2), to increase the average settlement of a footing with a set size. However, in a design scenario, an increase in average settlement may result in an increase in footing area to ensure that the settlement limits prescribed in the design criteria are met. Although this does not have a significant impact on the number of elastic moduli considered in most of the prediction relationships, which are based on a single vertical sample of values, it does have a marked impact on the number of values considered in 3DFEA. This is because, as the footing size increases, elastic moduli located further from the footing are included and additional values, which are lower in the soil, are considered due to the depth of the analysis being a function of the footing width (§4.3.2). Such an increase has an influence on the apparent variability of the elastic moduli, which in turn affects the variability and average total footing area. Consequently, the total footing area variability is increased, where the maximum  $COV_A$ , based on 3DFEA, is 140% but only 80% using the Schmertmann 2B-0.6 method (Figure 5-25). Although the shading in both Figures 5-25(a) and (b) appear similar, the effect of increasing the soil COV and SOF is much greater when using 3DFEA than the Schmertmann 2B-0.6 method. It should be noted however, that footing designs based on most of the prediction techniques, will not always consider a single vertical sample of elastic moduli located directly beneath the footing, since it is not always practical to sample the soil at these locations. The effects of sampling at locations that do not coincide with the footing are considered in subsequent chapters.

Results in Figures 5-24(a) and (b) show that the soil SOF has a greater effect on the average total footing area when it is less than approximately 8 m. When the soil SOF is greater than 8 m, it appears to have little effect and the average total footing area is solely dependent on the soil COV. This suggests a worst case SOF, as discussed previously in Chapter 4 (§4.2.1).

The results of the analysis dealing with the  $COV_A$ , shown in Figures 5-25(a) and (b), suggest there are three distinct regions where the soil COV and SOF have a different affect on the  $COV_A$ . For example, when the soil COV is low, the soil COV appears to have little influence on the  $COV_A$ . On the other hand, the soil SOF has a large impact where a small increase infers a large rise in  $COV_A$ . In addition, when the soil SOF is large, the soil COV has a large effect on the  $COV_A$  and a change in soil SOF has little effect. In this case, a small rise in soil COV has a considerable impact where the  $COV_A$  also increases. This behaviour is evident for both the results based on 3DFEA and the Schmertmann 2B-0.6 technique, as shown in Figures 5-25(a) and (b), respectively. However, the influence of varying the soil COV and SOF appears greater for designs based on 3DFEA. Therefore, it is concluded that designs based on 3DFEA are more susceptible to changes in soil COV and SOF.

**Footing designs based on 3DFEA are more dependent on the soil COV and SOF than the other settlement prediction methods.**

Results shown in Figures 5-24 and 5-25 are based on the total footing area of the foundation system, where the footing areas from each of the 9 pads are added together. However, an analysis is also undertaken to examine the average and COV of footing area for each individual footing in the foundation system. The numbering convention for footings is given in Figure 5-26, while the results of the analysis are shown in Figure 5-27. Such results are based on a soil COV of 50% and SOF of 8 m.



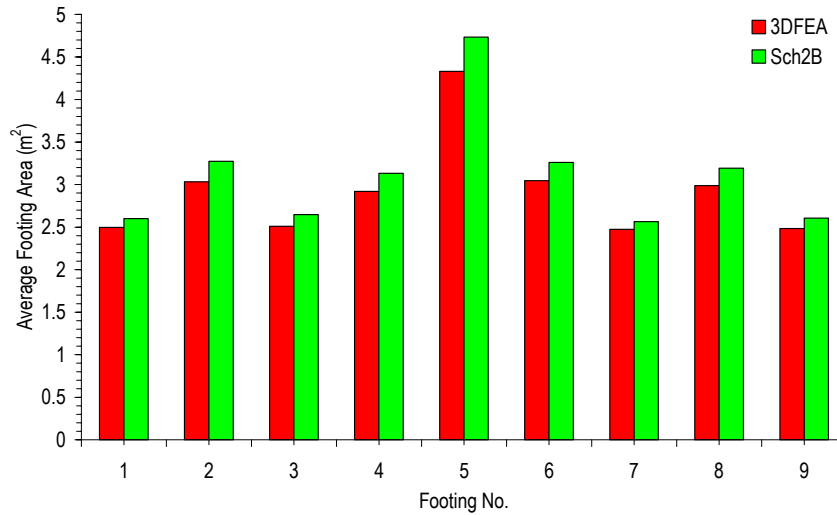
**Figure 5-26 Footing number convention for the 9-pad system shown in 5-1(c)**

Figure 5-27(a) implies that 3DFEA yields smaller footing designs for all footings in the system, when compared to the Schmertmann 2B-0.6 method. This is consistent with results shown for the average total footing area (Figure 5-24) where, for a soil COV of 50% and SOF of 8 m, the design based on 3DFEA is shown to have a smaller average total footing area than the design based on the Schmertmann 2B-0.6 method. Furthermore, the relative design areas for each of the footings appear to be consistent with the applied loads, where: Footings 1, 3, 7 and 9 are designed with an applied load of 860 kN; Footings 2, 4, 6 and 8 are designed with an applied load of 1,150 kN; and Footing 5 is designed with an applied load of 1,540 kN, as discussed previously in this chapter (§5.1). Additionally, the difference between the average design areas based on 3DFEA and the Schmertmann 2B-0.6 technique appears similar for each footing. This infers that the relative conservatism between the settlement prediction techniques is independent of load magnitude and footing location, bearing in mind that this conclusion is based solely on a soil COV of 50% and SOF of 8 m.

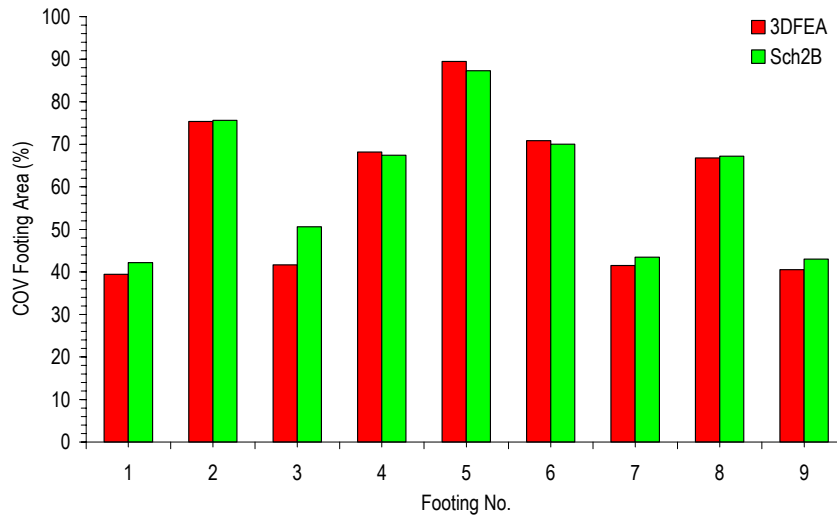
The results shown in Figure 5-27(b) suggest that designs based on 3DFEA have a larger relative COV than the Schmertmann 2B-0.6 method, when the footing is designed to resist a larger load. This is because larger footings are required to support larger applied loads. Furthermore, a larger footing infers that additional elastic moduli are considered in the analysis through the use of the depth restriction (§4.3.2) and the width of the footing. Although additional elastic moduli are considered for both designs, the Schmertmann 2B-0.6 method considers only moduli in a single vertical sample, as discussed previously, while 3DFEA considers moduli from the entire soil.

The results and discussion presented thus far have been confined to soils with an isotropic correlation structure. In other words, the soil SOF is the same in all three orthogonal directions. However, as discussed in Chapter 2 (§2.3.2.2), anisotropic behaviour is common and soils generally exhibit higher correlation horizontally than vertically, due to their formation process (Jaksa et al. 2005). As such, an analysis involving soils with an anisotropic correlation structure is undertaken. For this analysis, the degree of anisotropy, defined as the ratio of the horizontal SOF to the vertical ( $\theta_h / \theta_v$ ), is increased. Results of this analysis are given in Figures 5-28(a) and (b) for the average and COV of total footing area for the 9-pad system, respectively. Figure 5-28 is based on foundation designs using only 3DFEA and the Schmertmann 2B-0.6 method. However, similar trends are also evident for the other settlement prediction techniques. These results are included in Appendix B.





(a)



(b)

**Figure 5-27 Footing area (a) average and (b) COV for individual footings in the 9-pad system designed using 3DFEA and the Schmertmann's 2B-0.6 technique, for a COV of 50% and SOF of 8 m**

The results shown in Figure 5-28 indicate that an increasing degree of anisotropy reduces both the average and COV of total footing area,  $COV_A$ . However, this is more likely a function of a reduction in the vertical SOF than the result of increasing degree of anisotropy. This is because the vertical SOF has a greater impact on the design, where the settlement prediction techniques use the elastic moduli in the vertical direction. Both the average and  $COV_A$  appear to tend towards a constant as the degree of anisotropy increases. Again, this is likely a result of the vertical SOF tending towards a small value, which represents erratic variations and a reduced variance due to increased averaging. This conclusion is confirmed by comparisons of the average footing area for soils with the same vertical SOF, as shown in Figure 5-29. In this case, the average total footing area remains almost constant for all degrees of anisotropy investigated. Hence, the vertical SOF con-

trols the settlement estimate, and therefore, the size of the footing design. At this stage, while the design is based on the complete knowledge of the soil, the horizontal SOF appears to have little influence. However, when designs are based on the results from a site investigation, where sampling locations are distributed around the site, the horizontal SOF has a definite influence. Such effects are discussed in later chapters.

**The vertical SOF has the greatest impact on the design of a foundation, when such a design is based on the complete knowledge of the soil.**

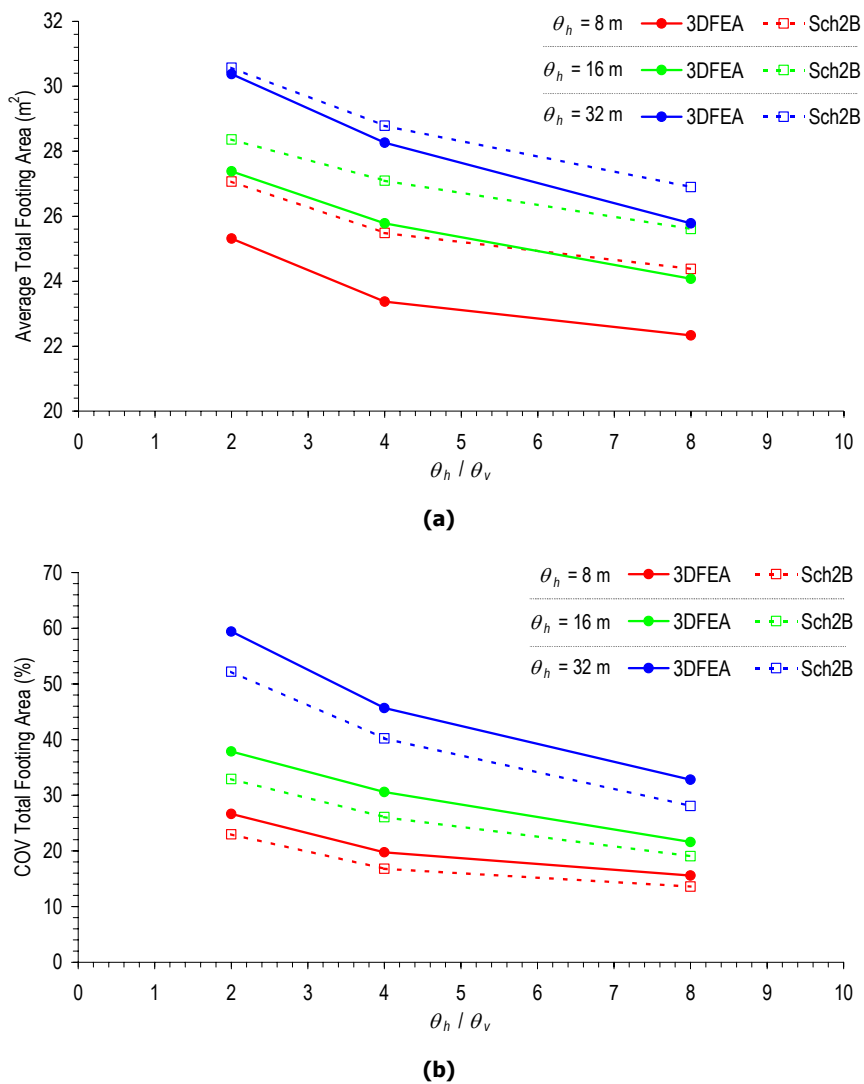


**Figure 5-28 Effect of increasing the horizontal to vertical SOF ratio (COV of 50%) on the (a) average and (b) COV total footing area, of the 9-pad system, designed using 3DFEA and Schmertmann 2B-0.6 technique**

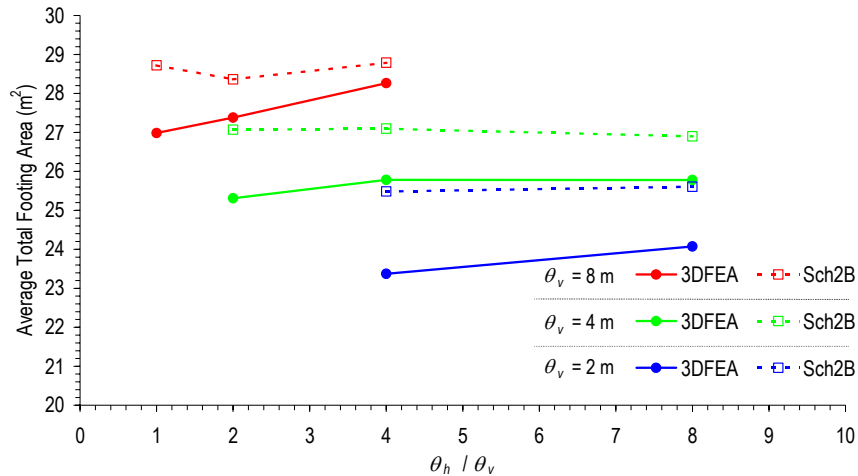


**Figure 5-29 Effect of increasing the horizontal to vertical SOF ratio (COV of 50%) on the average total footing area, of the 9-pad system, designed using 3DFEA and Schmertmann 2B-0.6 technique**

Additional to the results already presented regarding the effect of soil variability on the average and COV of total footing area, a reliability analysis is also conducted. In this case, two probabilistic measures are considered: under- and over-design. These measures have already been introduced in Chapter 3 (§3.7.1) and involve comparing the foundation design based on 3DFEA with the design based on the other settlement methods. An over-design is assumed to occur if the design, based on settlement estimates using the Schmertmann 2B-0.6 method, yields a footing area that is larger than the design based on 3DFEA. Conversely, an under-design occurs when the design, based on the Schmertmann 2B-0.6 technique, yields a smaller footing area than the 3DFEA design. Probabilities are generated by summing the number of under- and over-design conditions from the 1,000 Monte Carlo realisations. In the case of a foundation system consisting of multiple footings, like the results presented in this section, under- and over-design conditions are recorded for each footing in the system. Therefore, the probabilities of under- and over-design are determined based on 9 footings and 1,000 Monte Carlo realisations.

The results of the probabilistic analysis are shown in Figure 5-30, for increasing soil COVs and SOFs. Figure 5-30(a) indicates the probability of under-design, while Figure 5-30(b) presents the probability of over-design. As discussed in Chapter 4 (§4.3.2), the results are based on the assumption that a 3DFEA design yields a benchmark or optimal design.

Figure 5-30(a) suggests that an increasing soil COV yields a higher probability of under-design. This result is expected, as an increasing soil COV causes the average footing area and COV, based on 3DFEA, to increase at a faster rate than those based on the Schmert-

mann 2B-0.6 method, as was shown in Figures 5-24 and 5-25. This results in designs using 3DFEA yielding a larger footing area than the Schmertmann 2B-0.6 technique when the soil COV is high, which results in an increased probability of under-design.

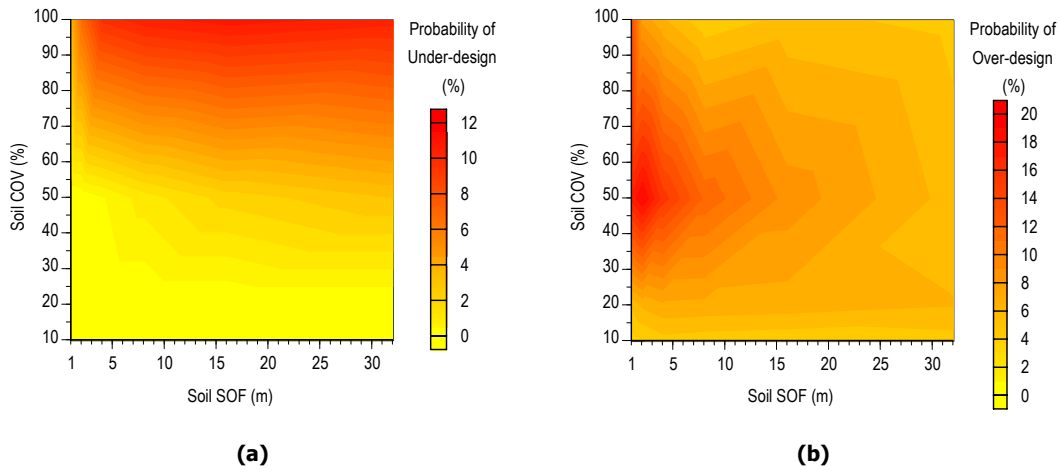


**Figure 5-30 Effect of increasing soil COV and SOF on the probability of (a) under- and (b) over-design of a 9-pad system designed using the Schmertmann 2B-0.6 technique (SCH)**

**An increasing soil COV yields a higher probability of under-design.**

The soil SOF does not appear to affect the probability of under-design to the same extent as the soil COV. This is because the SOF does not have the same impact on the average or COV of footing area. However, the probability of under-design does appear to increase slightly as the soil SOF increases, when the SOF is less than the worst case SOF of approximately 8 m. Beyond this worst case, the probability of under-design appears to be constant for increasing soil SOF.

The relationship between the probability of over-design and soil COV and SOF [Figure 5-30(b)] is notably different to the relationship involving the probability of under-design [Figure 5-30(a)]. Rather than the occurrence of a general trend, Figure 5-30(b) suggests a worst case combination of soil SOF and COV that cause the largest probability of over-design. For this analysis, the worst case occurs when the soil COV is 50% and the SOF is less than 8 m. As the soil COV increases or decreases, or the SOF becomes larger than 8 m, the probability of over-design diminishes. This trend is caused by the comparative rates at which the soil COV and SOF affect the average and COV of total footing areas, which have been shown previously in Figures 5-24 and 5-25.

**A worst case SOF of approximately 8 m is evident where the probability of under-design becomes relatively constant and the probability of over-design is a maximum.**

The probabilities of under- and over-design are also examined for each of the settlement prediction techniques discussed throughout this chapter. These results are given in Figures 5-31 and 5-32, where Figures 5-31(a) and 5-32(a) are for an increasing soil COV and Figures 5-31(b) and 5-32(b) are for an increasing soil SOF.

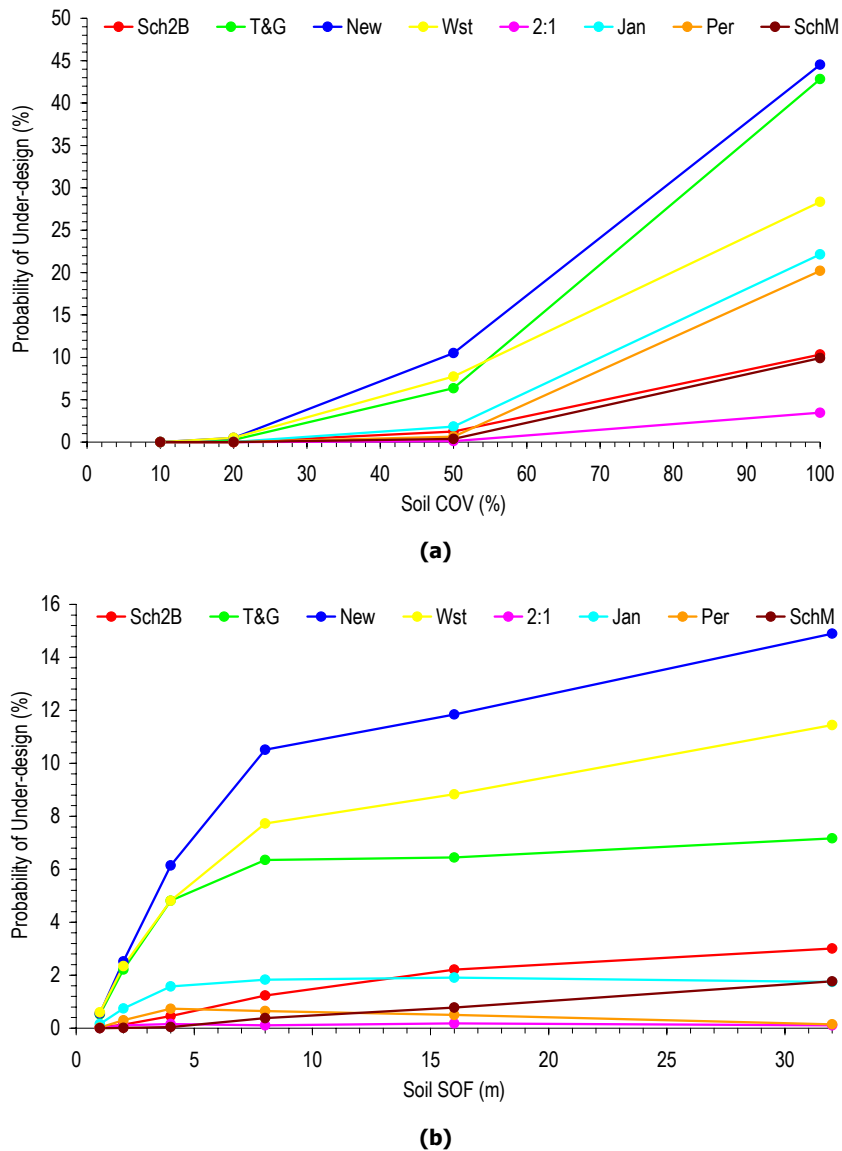
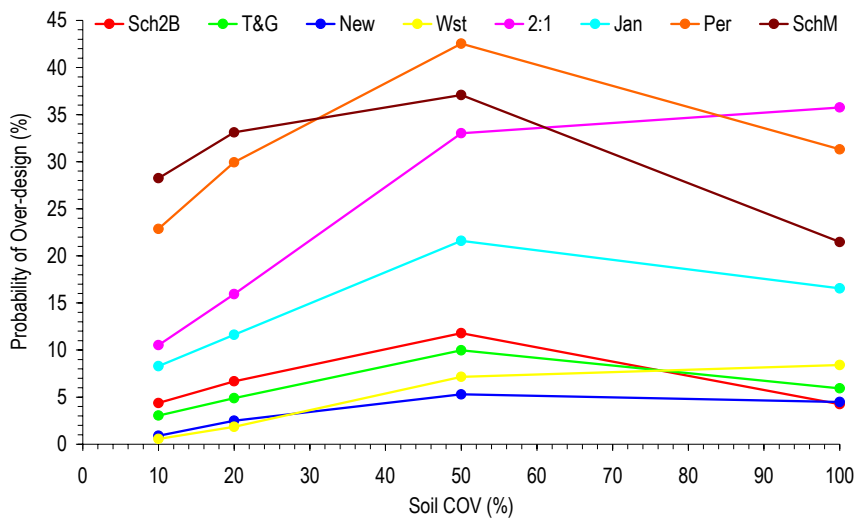


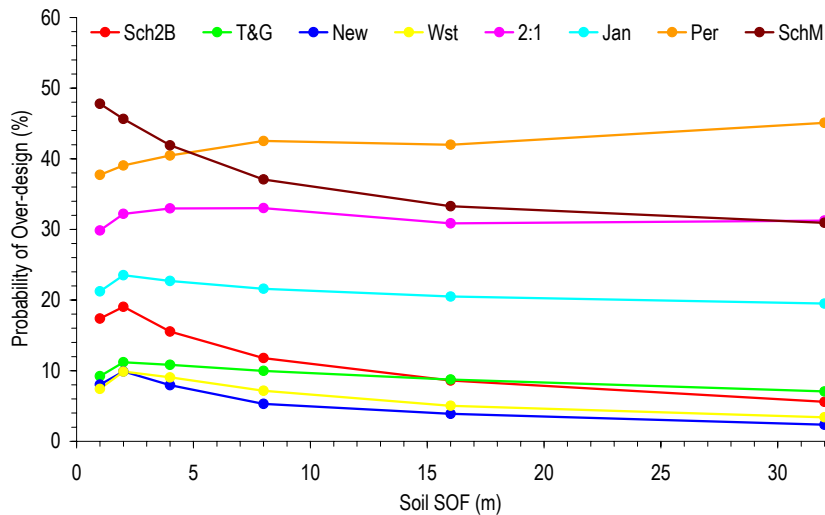
**Figure 5-31 Effect of increasing soil (a) COV (SOF of 8 m) and (b) SOF (COV of 50%) on the probability of under-design of a 9-pad system, designed using each settlement prediction technique**

For all prediction techniques investigated, an increasing soil COV or SOF appears to increase the probability of under-design [Figures 5-31(a) and (b)]. However, Figure 5-31(b)

suggests that a maximum probability of under-design is reached for most techniques, when the soil SOF is approximately 8 m. This again corresponds to the worst case SOF. For the settlement methods that do not yield a same maximum probability of under-design, it appears that an increasing soil SOF affects the probability of under-design at a greater rate when it is less than 8 m. The trends shown in Figure 5-31(a) between the probability of under-design and an increasing soil COV, infer that the probability of under-design continues to increase as the soil COV rises. Since the probability of under-design cannot exceed 100%, it is expected that these results will asymptote at 100%.



(a)



(b)

**Figure 5-32 Effect of increasing soil (a) COV (SOF of 8 m) and (b) SOF (COV of 50%) on the probability of over-design of a 9-pad system, designed using each settlement prediction technique**

Figures 5-31(a) and (b) indicate that when the soil COV and SOF is low, the settlement methods yield a probability of under-design that is close to zero. This either suggests that

the soil variability has a considerable influence on the accuracy of the prediction technique or, the techniques are over-conservative, leading to large footing designs on soils that are relatively uniform or have a low soil SOF. The former conclusion appears to be more reasonable, considering the results shown in Figure 5-32, where most of the settlement methods also yield a relatively low probability of over-design (less than 30%) for soils with low COV and SOF. Consequently, it is expected that a high proportion of designs based on the prediction techniques, yield the same footing area as those based on 3DFEA when the soil has a low COV and SOF. However, it should be noted that the minimum footing area constraint has an impact on this conclusion, where it is not been possible to yield a footing with a plan size less than 1.5 m × 1.5 m. Furthermore, the results shown earlier in this chapter indicated that a reducing soil COV and SOF infer a decreasing average total footing area. Therefore, the results shown in Figures 5-31 and 5-32, on soils with low COV and SOF, may be influenced by the minimum footing constraint.

Observations were made earlier in this chapter identifying the differences between settlement prediction techniques that either accommodate vertical variability of elastic moduli or require a single elastic modulus value. The results shown in Figure 5-31(a) also highlight such differences, where the techniques that use a single elastic modulus appear to be more affected by an increasing COV than the other method when the COV is greater than 50%. Furthermore, the techniques that only use a single elastic modulus also appear to achieve a maximum probability of under-design at a lower soil SOF [Figure 5-31(b)]. This suggests that these techniques are more influenced by a high soil COV and low SOF.

**The probability of under-design, for designs based on settlement prediction methods that use a single elastic modulus, are more influenced by soils with high COVs and low SOFs.**

The relative conservatism of each settlement prediction technique is shown clearly in Figures 5-31 and 5-32, where the techniques that show a relatively high probability of under-design have a relatively low probability of over-design. These techniques (New, Wst and T&G) are examples of under-conservative prediction methods. The other techniques that show a high probability of over-design and a low probability of under-design (2:1, SchM and Per) are examples of very conservative settlement prediction methods. The Schmertmann 2B-0.6 and Janbu methods appear to yield probabilities of under- and over-design that are neither noticeably high nor low. This suggests that these techniques are good estimators of settlement when compared to 3DFEA. The relative conservatism of the settlement prediction techniques in a design situation is similar to the conservatism of the same

methods in the settlement analysis situations, shown previously in Figure 5-5 for the deterministic case, and Figure 5-14 for the analysis with a spatially random soil.

The probability of under- and over-design indicates the frequency that the common settlement prediction technique yields a footing design which is less than or greater, respectively, than the 3DFEA design on the same soil. However, such measures do not demonstrate the degree by which an under- or over-design occurs. Furthermore, it is the degree of under- and over-design that controls the severity of foundation failures or additional costs of a foundation design. As such, a measure called the *design error* is adopted, which provides a normalised measure of the degree of under- or over-design. The design error,  $DE$ , has been previously defined in Chapter 3 (§3.7.1) and is repeated here as:

$$DE = \frac{A_i - A_{opt}}{A_{opt}} \quad (5.9)$$

where  $A_i$  is the design footing area based on a settlement prediction technique and  $A_{opt}$  is the designed footing area based on 3DFEA. Both designs make use of the complete knowledge of the soil (CK), bearing in mind that CK for the prediction techniques (not 3DFEA) consists of a single vertical sample of elastic moduli located beneath the centre of each footing in the foundation system.

Similar to the settlement error used earlier in this chapter, the design error is calculated for each realisation in the Monte Carlo analysis and then expressed as an average or expected design error,  $E[DE]$ . The average design error for the 9-pad system [Figure 5-1(c)] is shown in Figure 5-33. These results are based solely on a footing design using the Schmertmann 2B-0.6 method. Additional results, comparing the average design error for each settlement method, are given in Figures 5-34(a) and (b), for soils with an increasing COV and SOF, respectively.

The results in Figure 5-33 are similar to the results of the probability of over-design, shown in Figure 5-30(b). This suggests that an over-design condition has a greater influence on the design error than an under-design condition. This is a result of the minimum footing area constraint, where the size of an over-design has no limit (for instance, the Schmertmann 2B-0.6 design could very large), whereas the smallest allowable total footing area of  $20.25 \text{ m}^2$  limits the size of an under-design. Further discussions regarding the bias of the design error towards an over-design condition are given in Chapter 7.



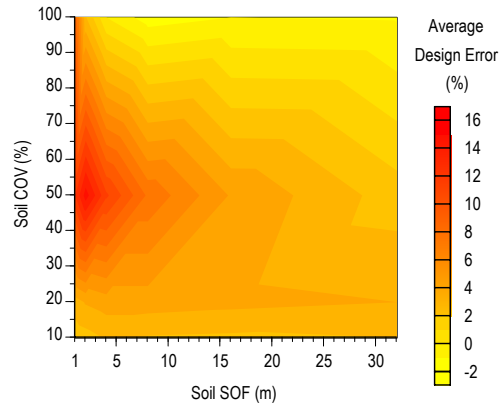
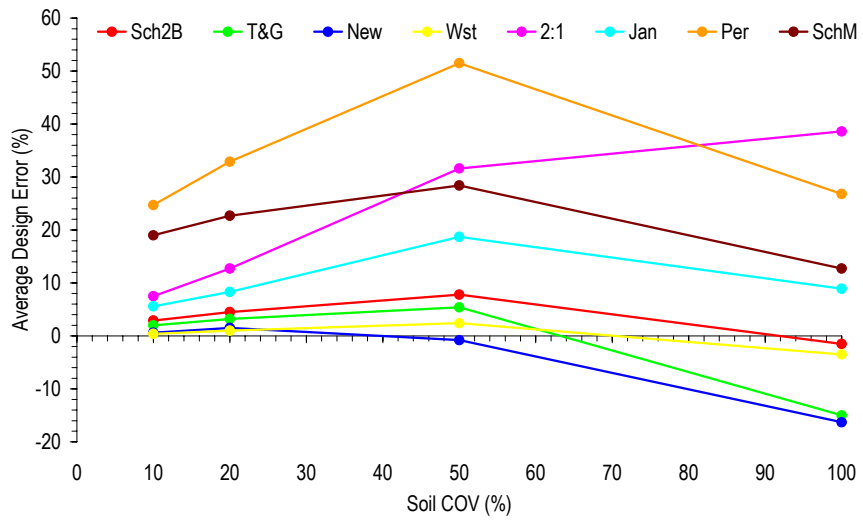
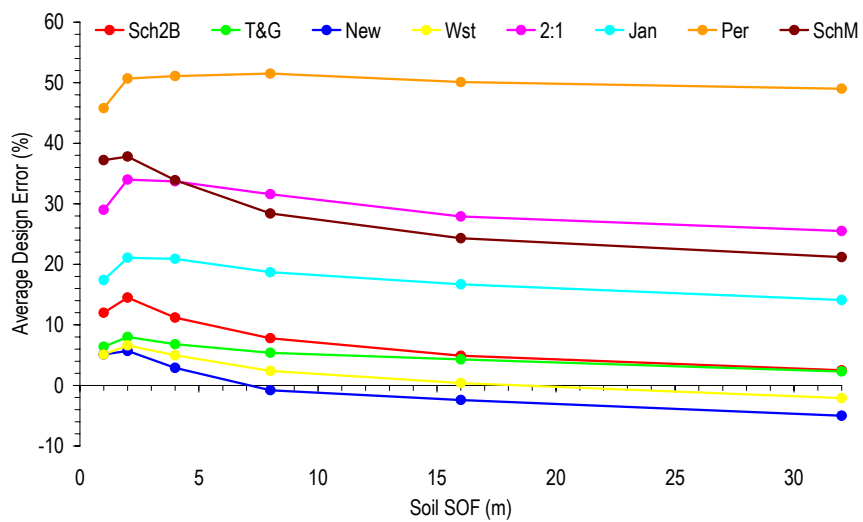


**Figure 5-33 Effect of increasing soil COV and SOF on the average design error of a 9-pad system designed using the Schmertmann 2B-0.6 prediction technique**



**(a)**



**(b)**

**Figure 5-34 Effect of increasing soil (a) COV (SOF of 8 m) and (b) SOF (COV of 50%) on the average design error of a 9-pad system, designed using each settlement prediction technique**

As with the probability of over-design [Figure 5-30(b)], the average design error appears to yield a maximum when the soil COV is 50% and the SOF is less than the worst case of approximately 8 m [Figure 5-33]. This is also shown in Figures 5-34(a) and (b), where most of the settlement methods yield a design with a maximum average design error when the soil SOF is less than 8 m and the COV is 50%. The only technique not to show this behaviour is the 2:1, where the average design error increases as the soil COV rises. This is consistent with the results shown in Figure 5-32(b), for the probability of over-design, and is due to the high variability of design areas and large conservatism of 2:1.

**The maximum average design error occurs when the soil COV is 50% and the SOF is less than the worst case of 8 m.**

As shown in Figure 5-34(a), only two prediction techniques appear to yield a negative average design error when the soil has a COV of 50%. The Westergaard method results in a negative average design error only when the soil SOF is greater than 16 m, while the Newmark technique yields negative average design errors when the soil SOF is greater than 7 m. The Schmertmann 2B-0.6 and Timoshenko and Goodier methods appear to be the best performing techniques, yielding designs with the smallest positive average design error for a soil COV of 50% and all SOFs investigated [Figure 5-34(a)]. However, when the soil COV is increased to 100%, both techniques yield negative average design errors [Figure 5-34(b)]. Whether a large positive design error is preferred over a small negative design error depends on the cost of potential failures and construction. These factors are examined in Chapter 8, together with the effects of site investigations.

The relative conservatisms of the settlement methods investigated have a notable impact on the design of the foundation. However, each of the techniques appears to be influenced by the variability of the soil in a similar manner. As such, it is difficult to provide a clear recommendation regarding which settlement prediction technique performs the best. Furthermore, the analysis presented in this section is based solely on the complete information of the soil, whereas it is unlikely that a single vertical sample of elastic moduli would be known under each and every footing. Therefore, final conclusions and recommendations regarding the most appropriate settlement methods for a foundation design are reserved for the analyses in future chapters, which account for uncertainties due to sampling and testing.

---

## 5.4 SUMMARY

---

The research presented in this chapter dealt with the use of several different settlement prediction techniques, in both analysis and design frameworks. The results have shown that each settlement prediction technique possesses varying degrees of conservatism that affect the analysis and design of a footing. Furthermore, these effects have been shown to vary for different soil COVs and SOFs. Settlement predictions conducted in this chapter have been based on soil properties located beneath the centre of the footing, or within an influence region located below the footing. In the case of the optimal settlement prediction or footing design based on 3DFEA, all elastic moduli were considered. Uncertainties due to sampling errors and measurement and transformation model errors were not included in this chapter. However, the effect of such errors is discussed in subsequent chapters.

The Schmertmann 2B-0.6 and Janbu settlement prediction techniques have been shown to yield settlement estimates close to 3DFEA for the majority of site conditions investigated. However, the Schmertmann Modified technique has also been shown to give excellent results when the footing size is comparatively large (i.e. greater than  $3.5 \text{ m} \times 3.5 \text{ m}$ ). The Perloff prediction technique, which is based on influence values adopted from Harr (1966) and provides the ‘theoretical’ solution, has been shown to yield much larger settlements than the 3DFEA technique adopted.

An influence region within which elastic moduli are averaged has also been introduced to account for soil variability. It was found that a geometric average (GA) of elastic moduli, within the influence region, preserved the conservatism in the prediction technique and yielded a small average settlement error when the region was relatively small. On the other hand, a standard arithmetic average of elastic moduli was shown to negate the conservatism in the prediction technique and yield a negative average settlement error for several conditions investigated.

The performance of the settlement prediction techniques has been shown to be notably different in a design situation. It was found that a soil with a COV of 50% and SOF of 8 m resulted in designs with the highest probability of over-design and average design error. However, it is important to recognise that the results presented in this chapter were based on the complete knowledge of the soil (CK), where for most of the settlement prediction techniques (excluding 3DFEA), CK is defined as the elastic moduli in a single vertical sample located directly beneath each and every footing. This is a condition that is unlikely to occur. Therefore, the analysis presented in the next chapter deals with a foundation de-

sign incorporating uncertainties due to limited sampling (statistical) and the measurement and transformation model errors inherent to different geotechnical tests. The choice of design parameters based on a site investigation is also examined in the following chapter.

## **Chapter 6 EFFECT OF SITE INVESTIGATIONS ON DESIGN PARAMETERS AND THE DESIGN OF A PAD FOUNDATION**

### **6.1 INTRODUCTION**

---

As introduced in Chapter 1, the aim of a site investigation is to characterise adequately the subsoil conditions. Therefore, a characterisation typically yields a series or set of values that, when implemented into a design or analysis relationship, allows one to predict the response of the soil. However, the selection of these values, referred to as characteristic values or design parameters, is dependent on the number of samples, sample location and the technique adopted to combine the results of multiple samples. Furthermore, as expected, design parameters have a direct effect on the resulting foundation design. Therefore, analyses in this chapter investigate the effect of site investigations of varying scope, on design parameters and the resulting foundation design.

This chapter is separated into three sections. The first section investigates the impact of sampling and site investigation scope on design parameters. In this analysis, the average and variability of design parameters obtained using a simulated site investigation, are compared to the known mean and variability of the simulated soil. The results of this form of analysis indicate the performance of a site investigation to characterise the spatial variability.

The second section of the chapter investigates the impact of a site investigation on the design of a foundation. In this section, the effect of increased sampling, different sampling patterns, test types and techniques to select a characteristic value, referred to here as the reduction technique, are measured by the average or expected footing design. This analysis allows conclusions regarding the relative conservatism of a site investigation.

The third and final section examines the effect of using site investigation data on the variability of a foundation design. This is achieved by comparing the size of the foundation designed from each of the 1,000 Monte Carlo realisations, with the average footing area, evaluated in the second section of the chapter. These results demonstrate how the scope of the site investigation affects the difference between foundation designs for soils with the same spatial statistics. A reliability analysis of the foundation design, which describes the performance of a site investigation in terms of probabilities, is reserved for later treatment in Chapter 7.

## 6.2 EFFECT OF SITE INVESTIGATION SCOPE ON DESIGN PARAMETERS

---

The inherent variability of soil infers that site investigation programs of varying scope lead to the resolution of different design parameters. By simulating a three-dimensional soil using local average subdivision (LAS), where all properties are known in detail, it is possible to investigate the ability of a site investigation program to estimate the statistics of the generated field. No foundation analysis or design is undertaken in this section. Instead, the results of a data analysis, using the elastic moduli sampled in a site investigation, are compared to the statistics of the simulated soil. This measures the ability of the site investigation program to characterise the variability. Each source of uncertainty, described in Chapter 2 (§2.3), is included in the analysis. Such uncertainties include soil variability, sampling error, and measurement and transformation model errors.

### 6.2.1 Soil Variability

To investigate the influence of soil variability on design parameters, an analysis is undertaken with a site investigation plan consisting of a single sampling location that is randomly located within a 20 m × 20 m area. A sampling location includes all elastic moduli in a vertical sample, leading to 60 values spaced a 0.5 m. Results show comparisons between the average and standard deviation of the sampled data with the average and standard deviation of the elastic modulus field representing the soil. Analyses are conducted considering 24 different soils defined by their target COVs and SOFs. Target soil COVs range from 10% to 100% and SOFs range from 1 to 32 m. The results shown in Figure 6-1 illustrate the influence of COV and SOF on the ability of the sampled data to represent the statistics of the soil.

In this section, an *average* is used to represent the sample mean. This is to avoid confusion with the target mean of the soil, which has been discussed previously in Chapter 3 (§3.3).

The soil average is the sample mean of the entire elastic modulus field, for all 1,000 Monte Carlo realisations. Therefore, in this case, where the simulated field consists of  $100 \times 100 \times 60$  elements, the soil average considers 600,000 elastic moduli in each field multiplied by 1,000 Monte Carlo realisations. On the other hand, the average sample data is the sample mean of the elastic moduli in the single sample locations. In other words, the average sample data considers 60 properties for each of the 1,000 Monte Carlo realisations.

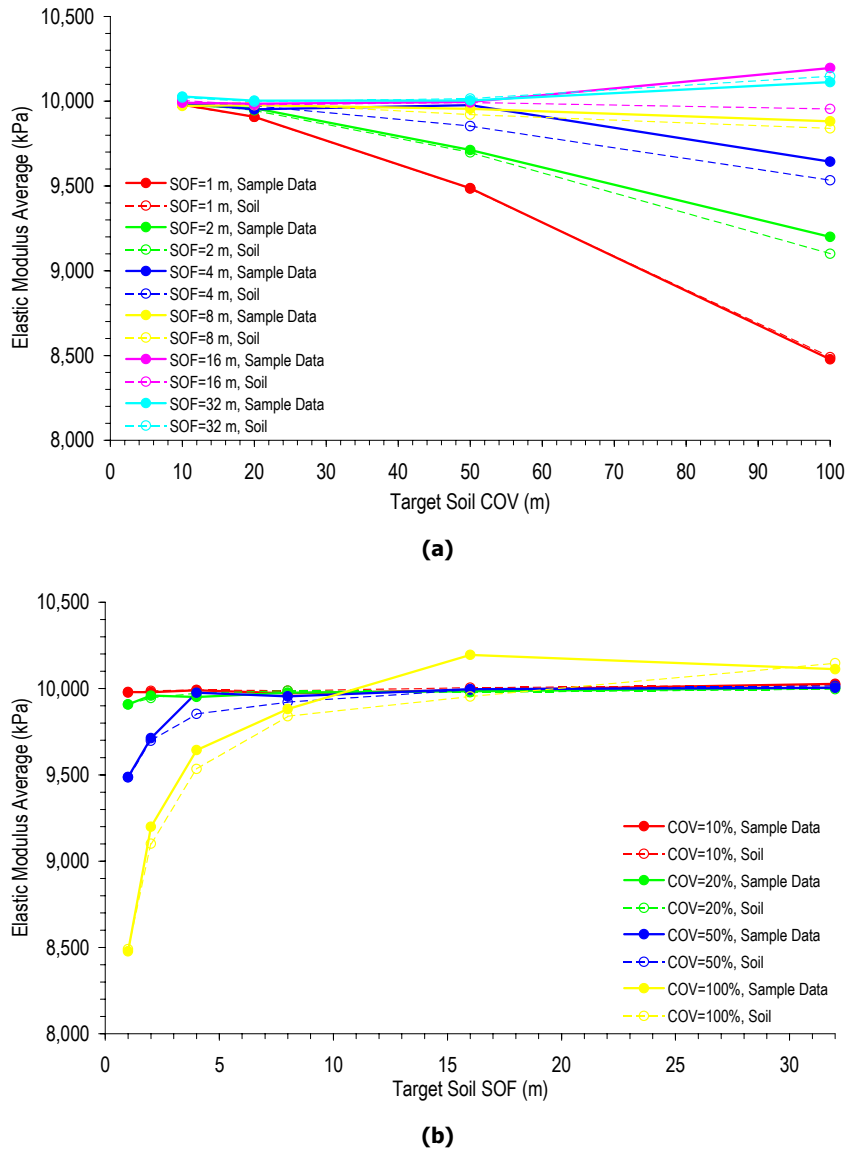


**Figure 6-1 Effect of increasing the soil (a) COV and (b) SOF on the sampled data and soil average**

A comparison between the sample data and soil average, shown in Figure 6-1(a), suggests that:

- The sample data average is typically greater than the soil average. This is especially true when the target soil SOF is between 2 m and 16 m;
- For low and high target SOFs (1 m and 32 m), the sample data average is similar to the soil average; and
- Both the sample data and soil average reduce when the soil COV approaches 100%, and the SOF is 1 m.

A reduction in the sampled data and soil average is not as noticeable when the soil SOF is high. In fact, when the target SOF is greater than 8 m, the sampled data and soil averages are shown to increase as the COV becomes larger. This phenomenon is a function of local averaging, which has been discussed in earlier chapters (§3.3.4). In the case when the target SOF is low, there is increased local averaging and the variability of properties within a domain is reduced. This reduction in variance results in a decrease in the average, due to the presence of a lognormal distribution. However, when the SOF is large, local averaging is reduced and the variability of the properties within the domain tends toward the target or point variance. These effects are clearly shown in Figure 6-1(b), where the sampled data and soil averages escalate as the SOF rises from 1 to 32 m. Both the sampled data and soil averages approach the target or point mean of 10,000 kPa as the SOF increases.

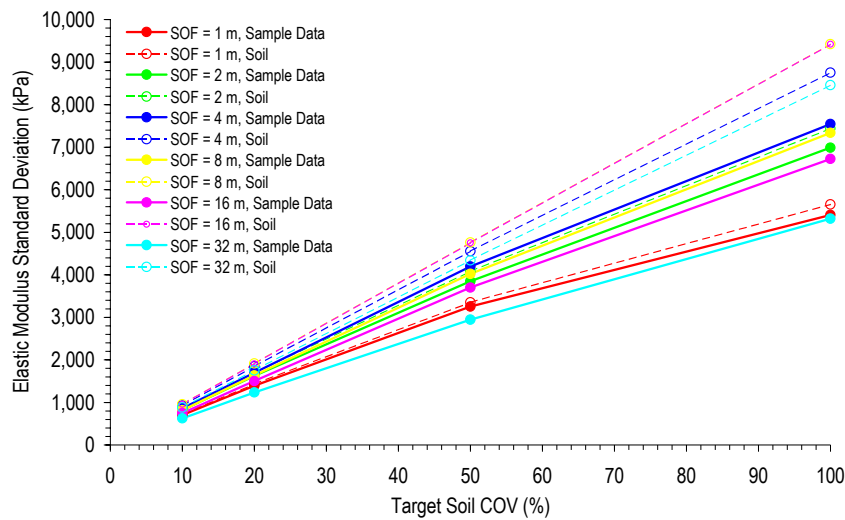
It is important to remember that the results shown in Figures 6-1(a) and (b) are based on two very different sample sizes or domains, as discussed above. This has a considerable impact on local averaging, and therefore, the variance reduction. Such a difference is illustrated by the comparison between the sampled data and soil standard deviation, as shown in Figure 6-2(a), for increasing COVs and Figure 6-2(b), for increasing SOFs. These results suggest that, for all site conditions investigated, the sampled data standard deviation is less than the soil standard deviation.

The results presented in Figure 6-2 also highlight noticeable differences between the sample data and soil standard deviation, especially when the target soil SOF is large. Again, this is a result of local averaging and variance reduction, where the domain used to estimate the sample data standard deviation is much smaller than the soil. With a smaller domain, but the same SOF, the local averaging and variance reduction is increased resulting in a smaller variance, as shown in Figure 6-2. It is also clear, from the results shown in Figure 6-2(b), that a maximum standard deviation occurs for both the sample data and the soil. This phenomenon has been discussed previously in Chapter 4 (§4.2.1), and is a func-

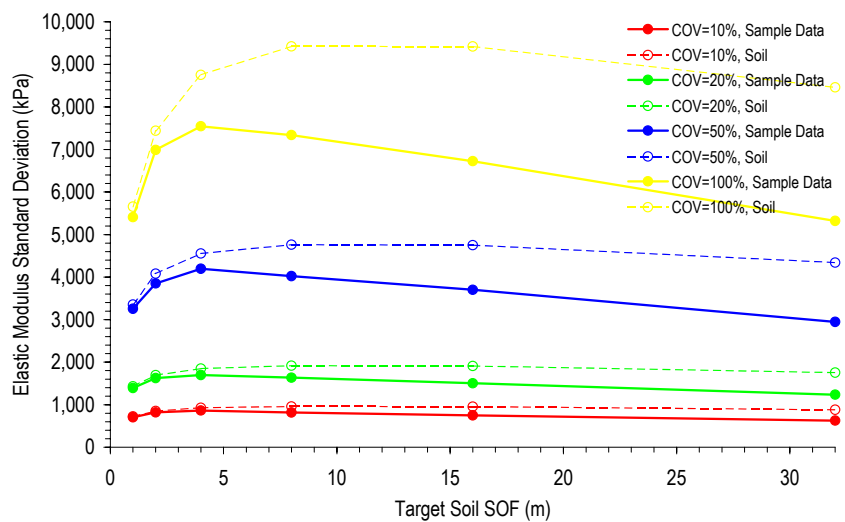


tion of the domain size and the target soil SOF. The results shown in Figure 6-2(b) confirm such conclusions, where:

- The maximum standard deviation occurs at a different target SOF for the sample data and the soil; and
- The maximum standard deviation is achieved at a smaller target SOF for the sample data than for the soil. This is because the domain size used to evaluate the sample data standard deviation is much smaller than that for the soil.



(a)



(b)

Figure 6-2 Effect of increasing the target soil (a) COV and (b) SOF on the sample data and soil standard deviation

The sample data variability is typically less than the soil variability because the sampling domain is much smaller.

## 6.2.2 Sampling Patterns and Reduction Techniques

Design parameters obtained from a site investigation are also affected by the scope of the investigation. This is because the number of samples has an impact on the variability of the data. Consequently, this has an influence on the average, due to the underlying log-normal distribution. Furthermore, the manner in which design parameters are selected from a series of data also requires attention. This process is referred to as the reduction technique and has been discussed previously in Chapter 3 (§3.4.2).

To illustrate the effect of increasing the number of samples on the design parameter, an analysis using the regular grid arrangement of samples, with up to 25 locations, is investigated. The RG arrangement was shown previously in Chapter 3 (Figure 3-7), but is also repeated here, in Figure 6-3. The results of the analysis are presented as distributions of sampled data for each of the sampling arrangements shown in Figure 6-3. These distributions are displayed in Figure 6-4.

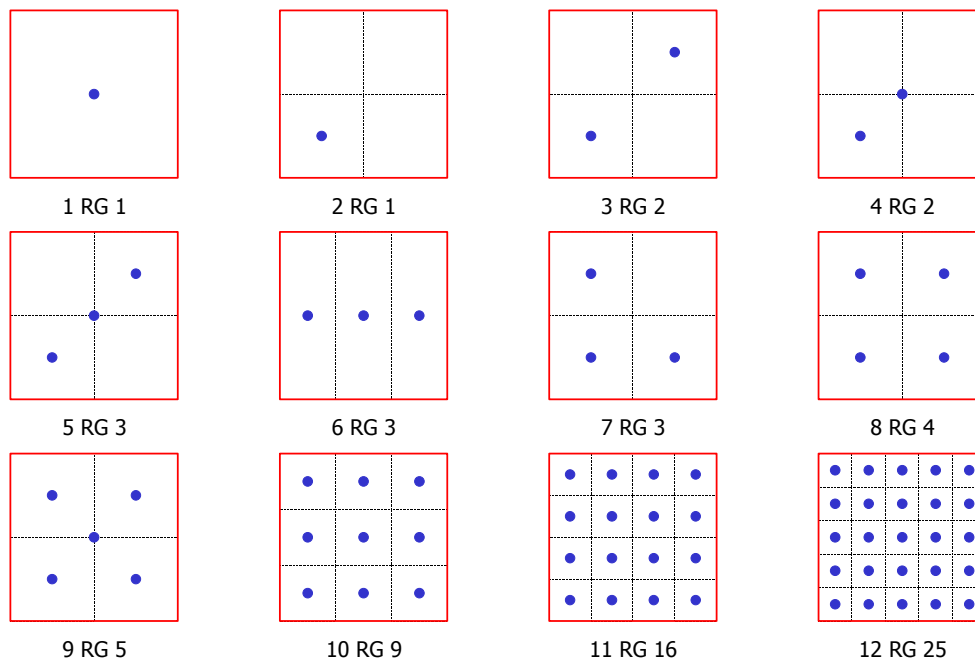


**Figure 6-3 Sampling locations based on the regular grid pattern**  
Repeated from 3-7

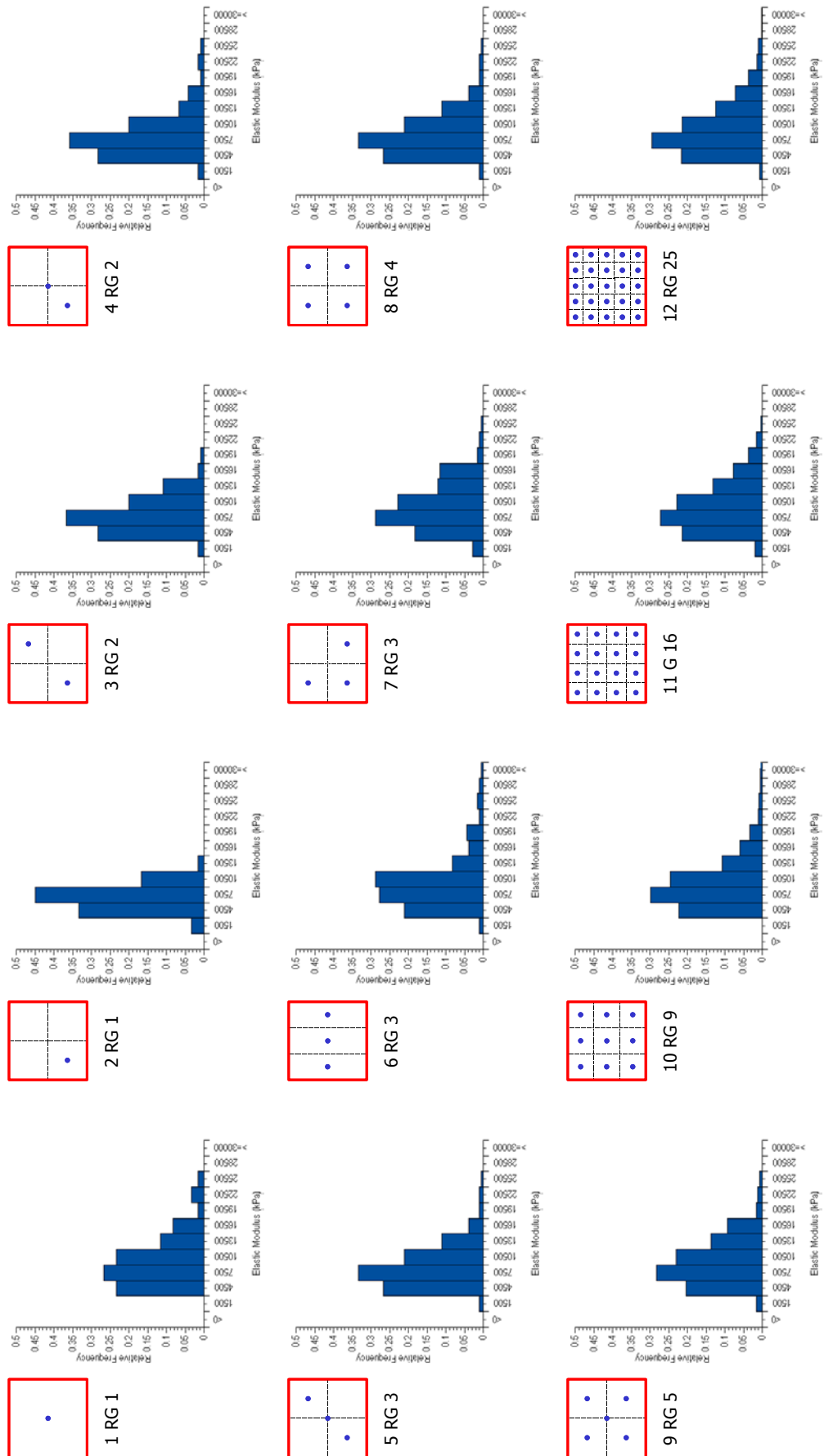


**Figure 6-4** Histogram of elastic modulus values resulting from a site investigation program consisting of sample locations arranged in a regular grid pattern for a soil COV of 50% and SOF of 8 m

As discussed in Chapter 3 (§3.4.1), sample locations are arranged within a plan area of 20 m × 20 m, which is centred on a 50 m × 50 m site with an assumed depth of 30 m. Each sample location consists of a single vertical sample of elastic moduli. In this case, where the type of test is not considered, all 60 elastic moduli are obtained at each sample location, representing a vertical sampling interval of 0.5 m. The results in Figure 6-4 are based solely on a soil with a COV of 50% and SOF of 8 m. Results from a single realisation are only considered to clearly illustrate the effect of increased sampling. When using all 1,000 Monte Carlo realisations, the results undergo significant averaging and the design parameters become similar for different sampling patterns. Therefore, in this situation, it is better to illustrate the results from a single realisation.

The results presented in Figure 6-4 do not allow many conclusions regarding the effect of increased sampling on the design parameter. However, it is apparent that a higher sampling effort results in an elastic modulus distribution that closely resembles a lognormal distribution. This is an expected result as the underlying elastic modulus field is based on a lognormal distribution. However, the distributions based on an investigation consisting few sampling locations do not exhibit the same lognormal appearance. Furthermore, it also appears that the variance of the elastic moduli increases as the sampling effort escalates. For example, the variance from 25 sample locations is greater than the results from a single sample location at the corner of the site investigation plan. This is a result of an additional number of samples increasing the apparent variance of the elastic moduli. It should also be emphasised that an increase in variance also affects the average elastic modulus because of the underlying lognormal distribution. Therefore, an increasing number of sample locations causes an increase in the average design parameter. This is further discussed later in this section.

Although the results shown in Figure 6-4 suggest that an increased sampling effort yields a higher variability in the sampled elastic moduli, the results are not yet reduced into a single vertical sample. This is achieved using one of the reduction techniques discussed in Chapter 3 (§3.4.2) and has a significant effect on the average, standard deviation and distribution of elastic moduli. Therefore, an analysis is undertaken to compare the effect of using different reduction techniques on the resultant design parameter. In this case, comparisons are made between two vertical samples of elastic moduli. One vertical sample is obtained by using the sample data from the site investigation, which is reduced using one of the techniques described in Chapter 3 (§3.4.2). The other sample, which is considered the ‘actual’ data, consists of the elastic moduli in a vertical profile located at the centre of the site (i.e. a plan position of 25 m × 25 m). For the inverse distance (ID) and inverse

distance squared (I2) reduction techniques, this central location is considered to be the position of the footing.

Comparisons between the two vertical samples are given in Figure 6-5, for a soil with a target COV of 50% and SOF of 8 m. Like the results presented above, these are based on a single Monte Carlo realisation in order to minimise the effects of averaging. Comparisons in Figure 6-5 indicate that:

- The variability of the reduced sample diminishes for an increasing sampling effort, as one would expect;
- The ID and I2 replicate the ‘actual’ data perfectly when a sample location is positioned at the centre of the site. This is because the sample location at the centre of the site is assigned a weighting of 1 and the elastic moduli from the other sample locations are ignored;
- The minimum reduction technique (MN) yields smaller values than the other techniques, as one would expect. Furthermore, the MN yields a reduced sample that continues to decrease as the number of sample locations increases;
- The 1Q reduction technique yields elastic moduli that are slightly larger than the MN, but are typically less than the standard arithmetic average (SA), geometric average (GA) and harmonic average (HA) methods; and
- The GA yields elastic moduli that are typically larger than the HA, but less than the SA.

The results presented in Figure 6-5 also represent the conservatism of each reduction technique. In a settlement analysis context, higher elastic moduli represent a smaller settlement and therefore, less conservatism. Hence, Figure 6-5 indicates that:

- The MN is the most conservative reduction technique, which also shows an escalating conservatism for increasing sampling effort;
- The 1Q is only slightly less conservative than the MN, but, generally more conservative than the other methods;
- The GA is typically more conservative than the SA, but less than the HA.

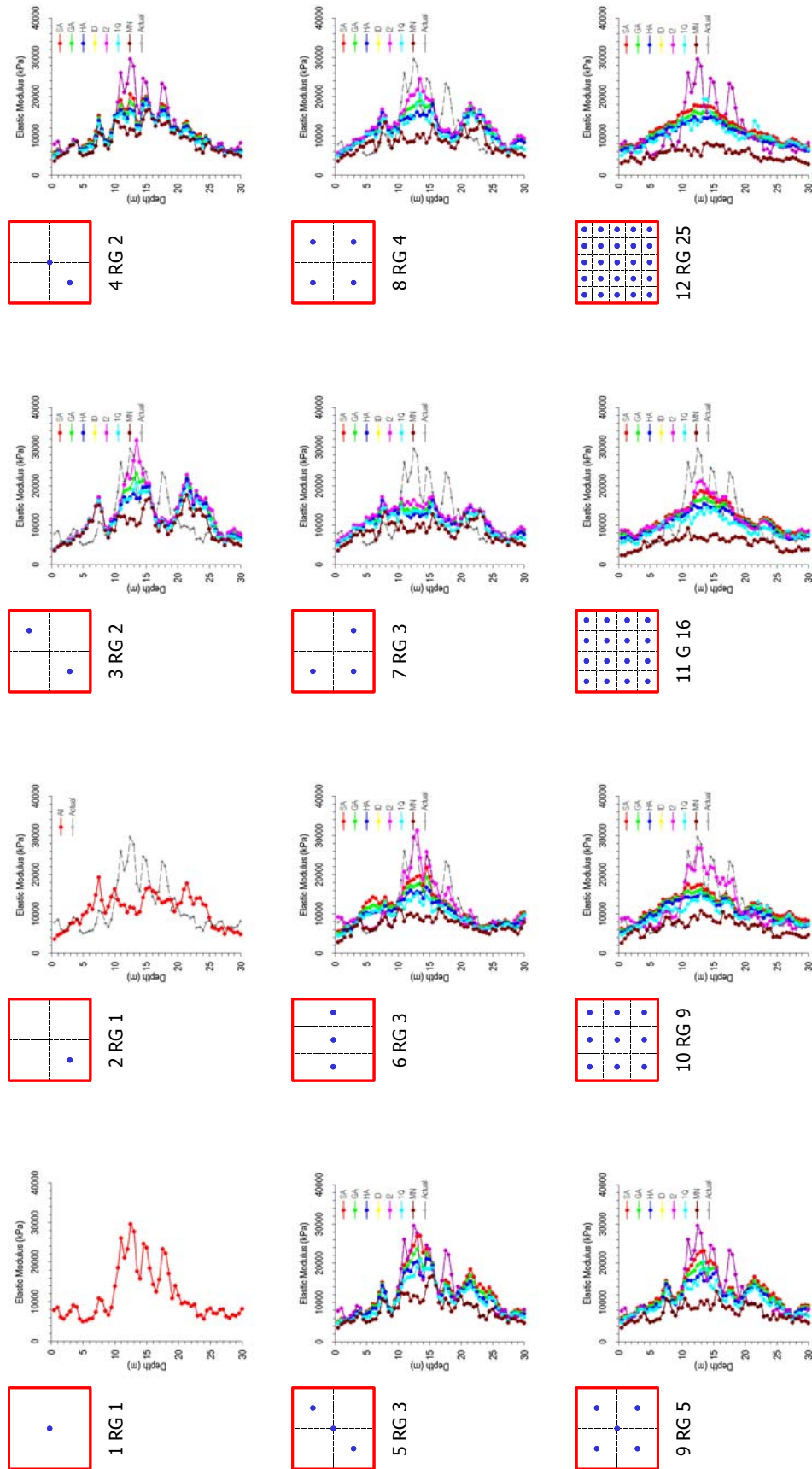


**Figure 6-5** Effect of using different reduction techniques on the estimate of soil properties based on a site investigation program consisting of sample locations arranged in a regular grid pattern for a soil COV of 50% and SOF of 8 m

**The conservatism in the design parameter increases as the sampling effort rises, when using the MN reduction technique.**

The relative conservatisms for the SA, GA and HA, confirm the conclusions made by Fenton and Griffiths (2002), who suggested that a GA yields a result that is between a HA and SA. This is because both the HA and GA are low-strength dominated, where a zero elastic modulus value yields an undefined or zero result, respectively. The effect of these reduction techniques on a foundation design is discussed, in greater detail, later in this chapter and in subsequent chapters.

It should be noted that the results in Figure 6-5 do not include all sampling patterns and reduction techniques. This is because some coincide directly with the results of another reduction technique. For example, the ID and I2 result in the same vertical sample of elastic moduli for a single pad footing located at the centre of the site. Therefore, these results coincide perfectly and as a result, the ID results are not shown in Figure 6-5. This is also the case for the SA when all samples locations are equidistant from the footing or centre of the site. In this case, the SA yields the same values as the ID and I2.

To examine the effect of using different reduction techniques to achieve a single vertical sample for the different sampling arrangements, sample distributions for the resulting elastic moduli are given in Figures 6-6 and 6-7, based on the use of 5 and 25 sample locations, respectively. The ID and I2 reduction techniques are not shown in these figures because they yield the same vertical sample of elastic moduli as the data sampled directly from the soil, due to one sampling location always coinciding with the footing.

Figures 6-6 and 6-7 are essentially frequency plots of the elastic moduli, shown in Figure 6-5, for the corresponding sampling pattern and reduction technique. However, the results shown in Figures 6-6 and 6-7 also illustrate the effect of the reduction technique on the average and variability of the single vertical sample and the shape of the distribution. It is apparent from these results that by reducing the results from multiple sampling locations, the distribution of elastic moduli tends to diminish the lognormal shape. In fact, several of the results shown in Figures 6-6 and 6-7 indicate a triangular distribution. Yet, even a triangular shape distribution is not common for all reduction techniques. It is also apparent that the MN yields a single vertical sample with a smaller average than the other techniques, which is consistent with the results shown in Figure 6-5 above.

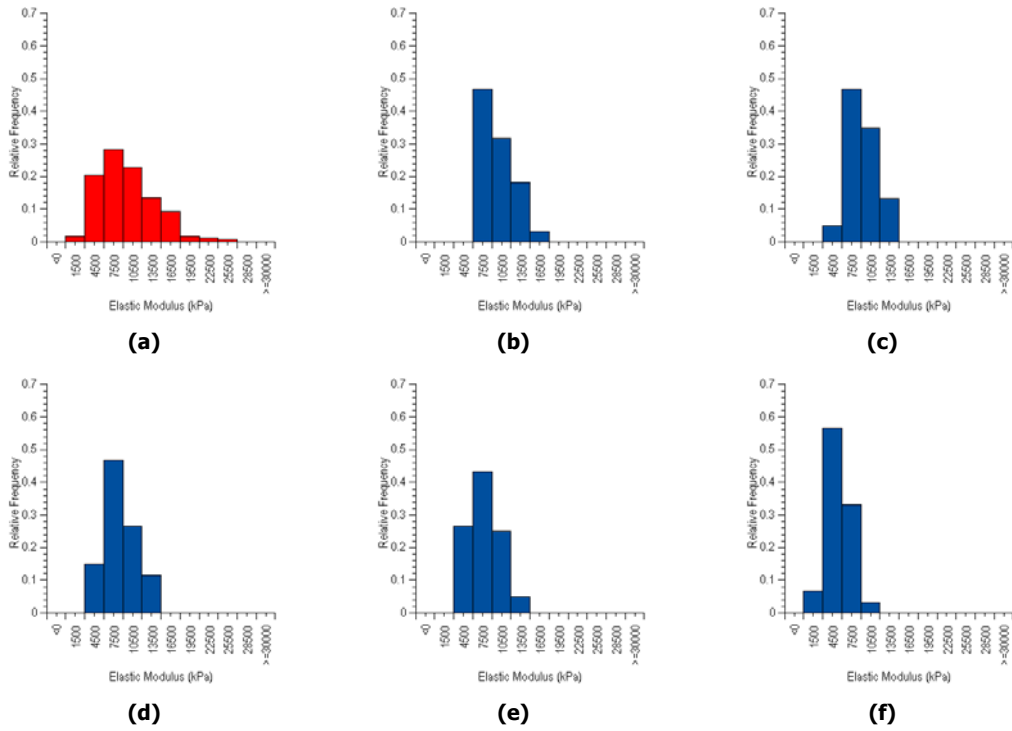


**Figure 6-6 Sample distributions of the (a) non-reduced sampled data and the reduced sample using the (b) SA, (c) GA, (d) HA, (e) MN and (f) 1Q from 5 sample locations, for a soil COV of 50% and SOF of 8 m**

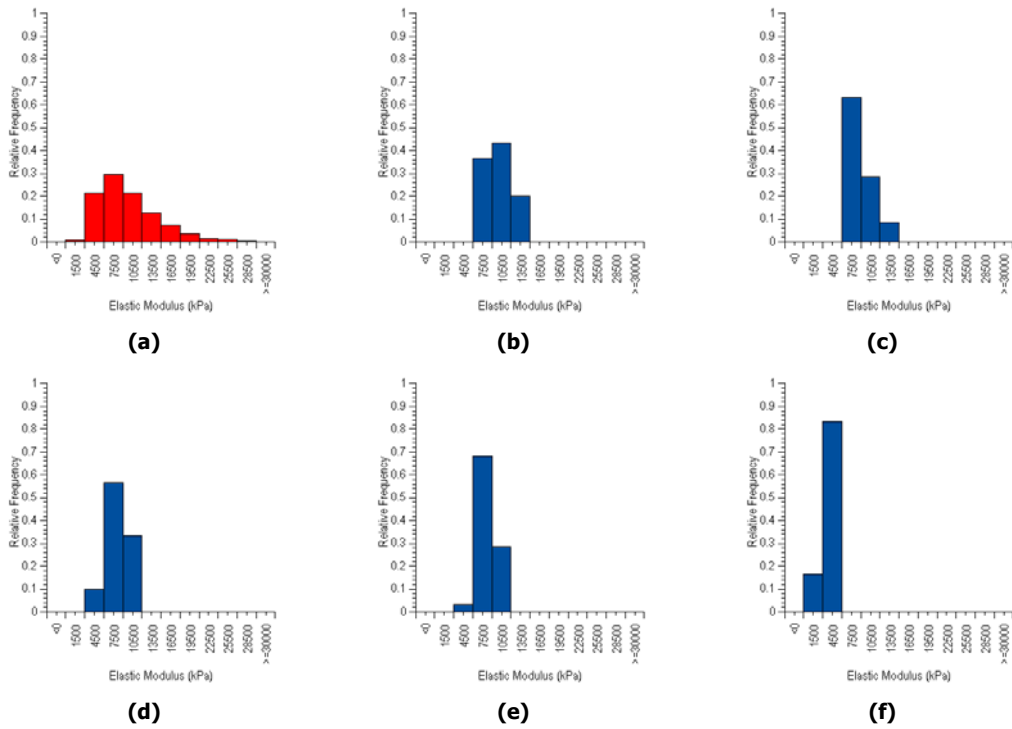


**Figure 6-7 Sample distributions of the (a) non-reduced sampled data and the reduced sample using the (b) SA, (c) GA, (d) HA, (e) MN and (f) 1Q from 25 sample locations, for a soil COV of 50% and SOF of 8 m**



To measure the ability of a reduction technique and sampling program to adequately characterise the soil site, two measures are introduced. These are the reduced sample average and standard deviation, where the reduced sample is defined as the vertical profile of elastic moduli. Both the reduced sample average and standard deviation are evaluated for each Monte Carlo realisation and then averaged over the suite of 1,000 realisations. The results of this analysis are given in Figure 6-8 for the average, and in Figure 6-9 for the standard deviation. Both sets of results are based on a soil with a target COV of 50% and SOF of 8 m, and a site investigation consisting of up to 25 sample locations arranged in a regular grid (RG). Similar to the results shown earlier, the ID and I2 are based on a single footing located at the centre of the site.

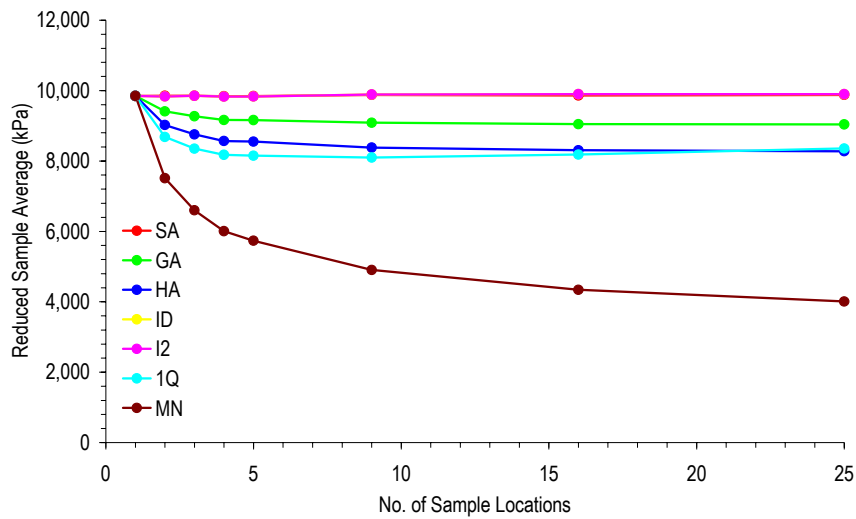


**Figure 6-8** Effect of increased sampling using different reduction techniques on the reduced sample average for a soil COV of 50% and SOF of 8 m

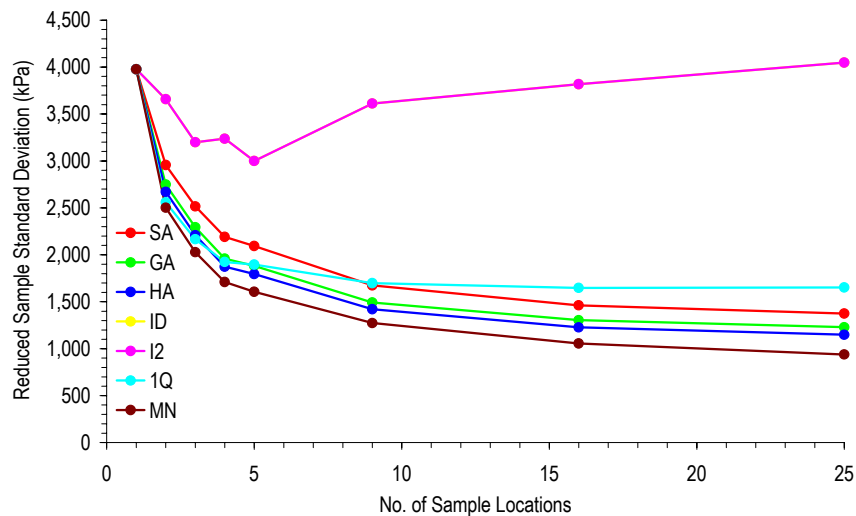


**Figure 6-9** Effect of increased sampling using different reduction techniques on the reduced sample standard deviation for a soil COV of 50% and SOF of 8 m

The results shown in Figure 6-8 confirm the general conclusions made regarding the results shown in Figure 6-5, where:

- The MN yields the most conservative solution; and
- The GA technique yields a reduced sample average that is larger than the HA, but less than the SA.

Furthermore, the results in Figure 6-8 suggest that by considering the results of an increasing number of sample locations, the reduced sample average decreases. This is the case for all reduction techniques, except the SA, ID and I2, which all appear to be relatively independent of sampling effort. A decreasing reduced sample average implies a diminishing design parameter and hence, increasing conservatism. The impact of this is discussed later in this chapter and in subsequent chapters.

**The reduced sample average, for all reduction techniques, except SA, ID and I2, decreases as the sampling effort increases.**

The results shown in Figure 6-9 suggest that the variability of the reduced sample decreases as the sampling effort increases, except when the ID and I2 methods are used. Furthermore, Figure 6-9 indicates that:

- The reduced sample standard deviation is greater for the ID and I2 than for any other technique. Additionally, the reduced sample standard deviation, based on the ID and I2, reaches a minimum when 5 sample locations are considered;
- The MN yields a reduced sample with the least standard deviation; and
- The decrease in reduced sample standard deviation for increased sampling is similar for all reduction techniques, except the ID and I2.

The minimum standard deviation, shown in Figure 6-9 for the ID and I2 methods, is caused by the weighting of data based on the sample and footing location, as discussed in Chapter 3 (§3.4.2). Such weighting implies that, when a sample coincides with the footing location, the results of the other sample locations are ignored. In this case, the reduced sample consists of the results from a single sample location. The effects of this are shown in Figure 6-9, where the reduced sample standard deviation is the same for 1 and 25 sample locations using the ID and I2. Therefore, it is somewhat misleading to plot the reduced

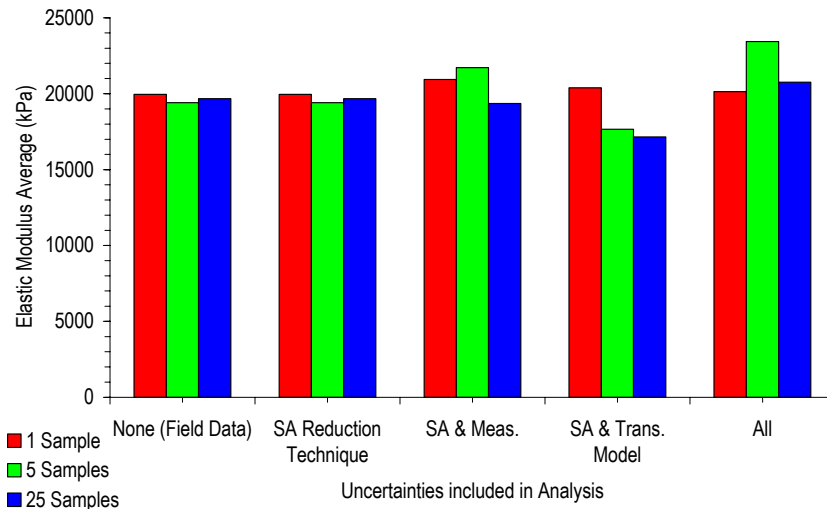
sample average and standard deviation for the ID and I2, against an increased sampling effort when, in fact, the results considering 25 sample locations are based only on the results of a single sample location. The impact of using the ID and I2 on the design of a pad foundation is discussed later in this chapter.

It appears that the sampling effort has a greater influence on the reduced sample standard deviation than the reduction technique. This is because, for most of the reduction methods, the decrease in standard deviation is similar. Furthermore, this implies that, as one would anticipate, an increasing sampling effort results in a more robust design parameter. It is therefore, expected that a foundation design based on the results of a large number of sample locations will be more robust than a design that is based on few sample locations. This is investigated later in this chapter and in subsequent chapters.

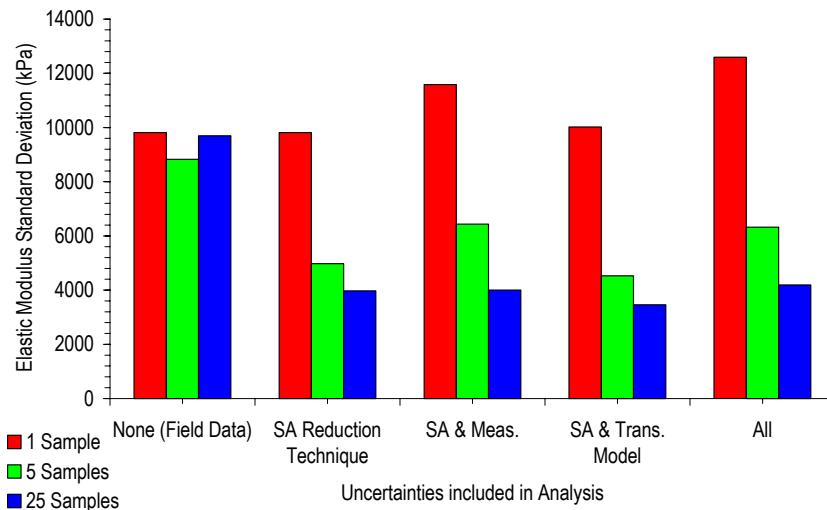
### **6.2.3 Types of Soil Tests**

Measurement and transformation model errors have been discussed previously in Chapter 2 (§2.3.4 and §2.3.5) and are measures of the inherent uncertainties in a geotechnical test. The methodology adopted to include these errors into the analysis involves adding uncertainty to the elastic moduli obtained at sample locations, as described in Chapter 3 (§3.4.3). This increased uncertainty affects both the average and variance of the design parameter. As a result, an analysis is conducted to investigate the impact of including measurement and transformation model errors on the design parameter. The results of this analysis are given in Figures 6-10(a) and (b), for the average and standard deviation of the design parameter, respectively. These results are based on a site investigation program consisting of 1, 5 and 25 sample locations, that are arranged in a regular grid, as shown previously in Figure 6-3. In this case, the SA is used to determine the reduced sample and the analysis is conducted for a soil with a target COV of 50% and SOF of 8 m.

At this stage, the measurement and transformation model errors used in the analysis are representative of the cone penetration test (CPT). Therefore, the bias and random components of measurement error are represented by a unit-mean lognormal variable with a COV of 15% and 20%, respectively. Additionally, the transformation model error is represented by a unit-mean lognormal variable, with a COV of 15%. The use of these variables to represent the measurement and transformation model errors has been discussed previously in Chapter 3 (§3.4.3).



(a)



(b)

**Figure 6-10 Effect of including uncertainties on the design parameter (a) average and (b) standard deviation based on 1, 5 and 25 CPT samples, arranged in a RG for a soil COV of 50% and SOF of 8 m**

The results shown in Figure 6-10 suggest that:

- Uncertainties due to measurement error have a greater impact on the average design parameter than uncertainties due to transformation model error;
- The average design parameter reduces, for an increased sampling effort, when transformation model errors are included;
- Errors associated with the SA have a greater influence on the design parameter standard deviation than both the measurement and transformation model errors; and

- Unlike the average, the standard deviation reduces as the sampling effort increases, when all errors are included.

#### **6.2.4 Summary**

The analysis dealing with the effect of site investigations on the design parameter has typically shown that the design parameter standard deviation reduces as the sampling effort increases. This implies that a more robust design parameter results when based on additional data. However, the conservatism of the design parameter and furthermore, the effect of increased sampling on the conservatism, has been shown to be dependent on the reduction technique used. Such effects are investigated further in the following section, where the design parameters are used in the design of a pad foundation.

### **6.3 EFFECT OF SITE INVESTIGATION SCOPE ON THE EXPECTED PAD FOUNDATION DESIGN**

---

In Chapter 5, the performance of common settlement prediction techniques was evaluated based on a settlement analysis and foundation design. However, these results were based on complete knowledge of the soil (CK), where the elastic moduli located directly beneath the footing were considered. Therefore, such results were not affected by sources of uncertainty including sampling, measurement and transformation model errors. On the other hand, the results in the previous section demonstrated that such uncertainties have a notable impact on design parameters. As a result, this section considers the effect of using information from a site investigation (SI), which incorporates the geotechnical system uncertainties described in Chapter 2 (§2.3), on the design of a pad foundation for settlement. The section is further divided into sub-sections, dealing with individual sources of uncertainty and their influence over the design of the foundation.

#### **6.3.1 Soil Variability**

The results presented in Chapter 5 and the previous section of this chapter, demonstrated that the inherent variability of the soil has a noticeable impact on design parameters and the estimation of settlements using the prediction techniques investigated. In brief, the results in Chapter 5 indicated that the soil COV has a marked influence on the average footing area of a resultant design, while the soil SOF has a greater impact on the COV of footing area. However, these results were based on elastic moduli obtained from the proposed footing location and as such, were not influenced by uncertainties due to sampling,

measurement and transformation model errors. Hence, an analysis is undertaken to investigate the effect of sampling on the design of a pad foundation, for soils with increasing COV and SOF. This is achieved by evaluating the foundation design area of the 9-pad system [Figure 5-1(c)], based on the information from a site investigation (SI). Results are presented as an average total footing area, which is the sum of the pad footings in the 9-pad system averaged over 1,000 Monte Carlo realisations.

Results in this chapter and subsequent chapters are typically presented in a standardised manner, with a legend as shown in Figure 6-11. It is also important to note that both the regular grid (RG) and stratified random sampling (SR) patterns, which are used in this chapter and subsequent chapters, include different arrangements for investigations with the same number of sample locations. These are given in Figures 6-12(a) and (b) for the RG and SR patterns, respectively. In these cases, the results are averaged to yield a single solution for a given number of sample locations. This clearly illustrates the effect of additional sampling on the foundation design. However, later in this chapter and in subsequent chapters, the arrangements with the same number of sample locations are investigated individually to examine the effect of sampling location.

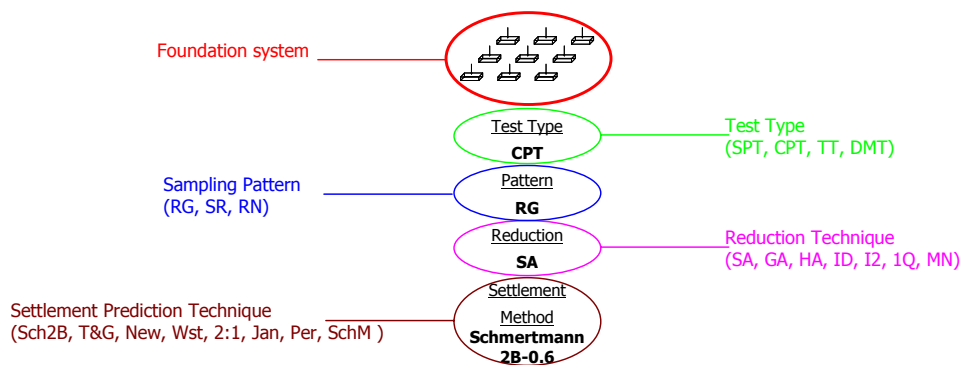


**Figure 6-11 Standard legend of results for Chapter 6, Chapter 7, Chapter 8 and Chapter 9**

The results illustrating the effect of increased sampling on the average total footing area for soils with varying COV and SOF, are shown in Figures 6-13(a) and (b), respectively. In general, these results indicate that:

- The average total footing area reduces as the sampling effort increases;
- There is greater benefit in additional sampling for soils with a higher COV;
- Larger average footing areas result when the soil COV or SOF is higher; and
- The effect of increased sampling is negligible when the soil COV is low.

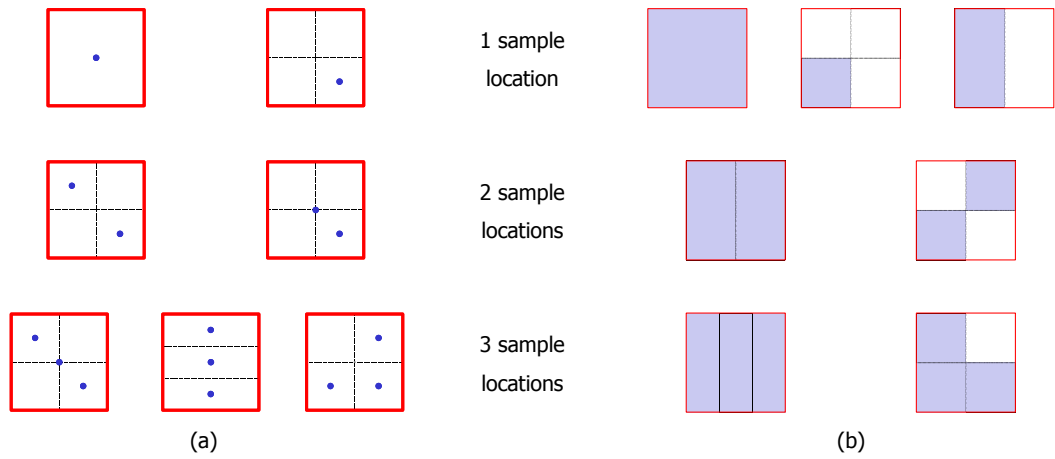


**Figure 6-12 Sampling arrangements with the same number of sampling locations for the (a) RG and (b) SR**

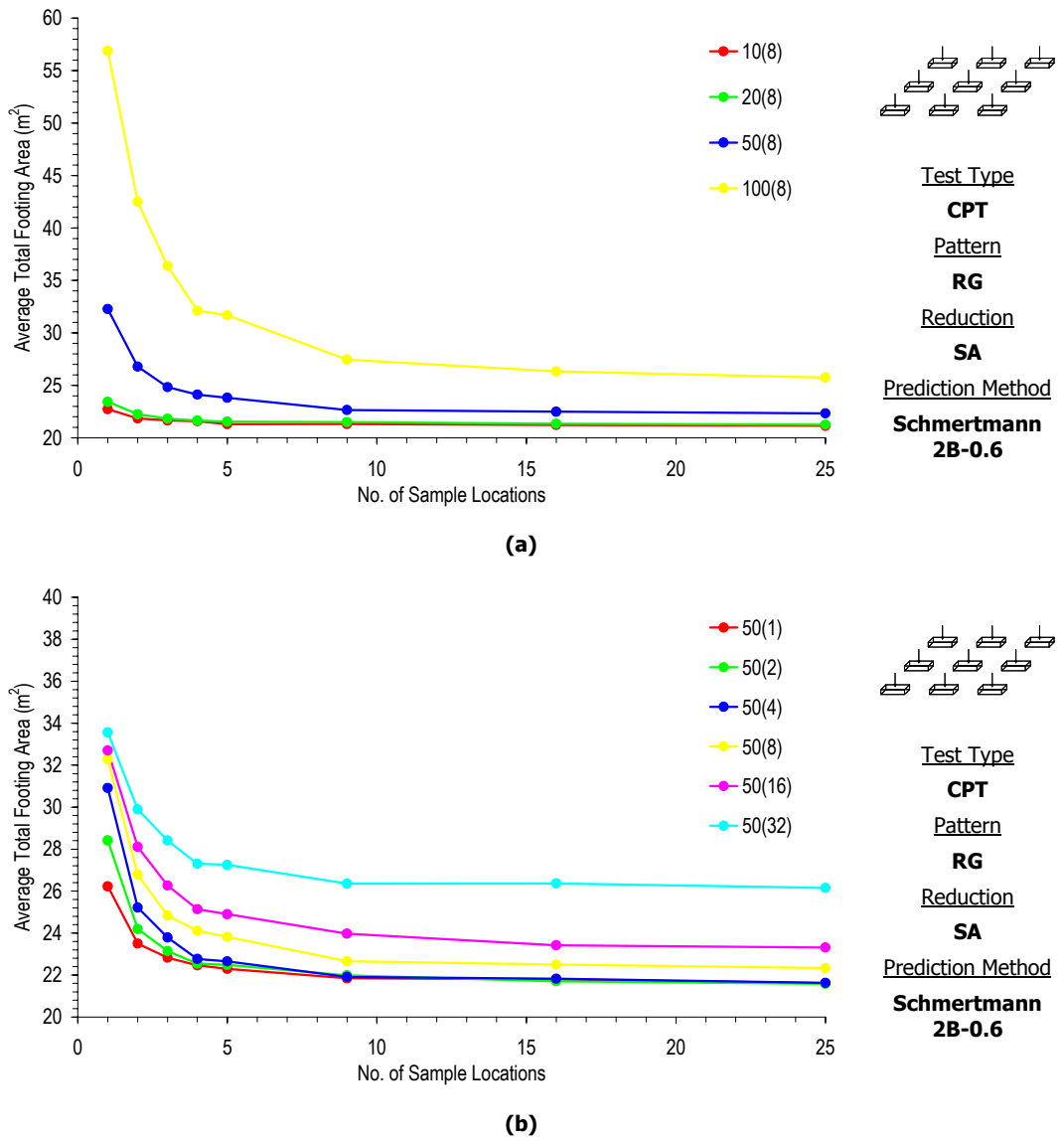


**Figure 6-13 Effect of sampling on the mean total footing area, for an increasing soil (a) COV (SOF of 8 m) and (b) SOF (COV of 50%)**

The reduction in average total footing area for increasing sampling effort is consistent with the results shown in the previous section, where the average design parameter was shown to be larger when additional sampling locations were considered. This infers a reduction in conservatism where a site investigation consisting of few sample locations yields a conservative result. Furthermore, the results in Figure 6-13 suggest that the average total footing area asymptotes to a minimum,  $A_{min}$ . However, the number of sampling locations required to achieve  $A_{min}$ , increases as the soil COV rises [Figure 6-13(a)]. In contrast, the soil SOF is observed to have little impact on the number of samples required to reach  $A_{min}$ , as shown in Figure 6-13(b).

Consistent with the results presented in Chapter 5 (§5.3), the average total footing area increases as the soil COV rises. However, the results in Figure 6-13(b) also suggest that the average total footing area increases as the soil SOF rises. Although a similar increase was shown in Chapter 5 [Figure 5-24(a)] when the soil SOF was lower than 8 m, the same results indicated little impact when the soil SOF was higher than 8 m. Furthermore, the results shown in Figure 6-13(b) indicate that at low sampling rates (e.g. 1 sampling location), the difference in average total footing area for soil SOFs larger than 8 m, is less than for high sampling rates (e.g. 25 sampling locations). This trend is reversed for soil SOFs less than 8 m, where the difference between average total footing areas at low sampling rates is greater than the difference for higher sampling efforts. This implies a special condition when the soil SOF is approximately 8 m. This phenomenon has been discussed previously as the worst case SOF.

Since  $A_{min}$  is generally achieved well before significant sampling is undertaken, it can be concluded that  $A_{min}$  is the best possible design, given the input information and prediction techniques. In this case, it appears that the best design for a soil COV of 50% and SOF of 8 m, is a footing system with a total area of approximately 23 m<sup>2</sup>. This is based on a site investigation program consisting of 9 or more sampling locations arranged in a regular grid pattern, and reduced using the standard arithmetic average. Whether this design is conservative or not depends on the optimal design achieved using complete knowledge of the soil and 3DFEA. Comparisons between the two design types are discussed in subsequent chapters.

Results in Figure 6-13 are based solely on soils with an isotropic correlation structure. However, it is common, as discussed previously in Chapter 2 (§2.3.2), that soils show greater correlation horizontally. Therefore, an analysis is also undertaken to investigate the impact of increased sampling on the expected foundation design for soils with an anisot-



ropic correlation structure. The results of this analysis are given in Figures 6-14(a), (b) and (c) for soils with a horizontal SOF of 8, 16 and 32 m, respectively. In each case, the soil COV is kept constant at 50% and degrees of anisotropy equal to 2, 4 and 8, are examined (where a degree of 8 relates to the horizontal SOF being eight times larger than the vertical).

In general, the results presented in Figure 6-14 indicate that:

- The vertical SOF influences the size of the footing required to meet the design criteria; and
- The horizontal SOF influences the benefits of increased sampling.

These results are consistent with the result shown in Chapter 5 (§5.3), where the horizontal SOF was shown to have little impact on the design of a foundation using complete knowledge of the soil. However, the horizontal SOF appears to affect the influence of sampling on the foundation design. In the case presented, a higher sampling effort is required to yield the minimum average total footing area,  $A_{min}$ , when the horizontal SOF is larger. This is consistent with the results shown in Figure 6-13.

### 6.3.2 Sampling Patterns and Reduction Techniques

In Chapter 3, a site investigation scope was characterised by the number of sampling locations, the pattern in which the locations were arranged, the reduction method employed and the type of test used. In this section, the effect of different sampling patterns and reduction methods on the expected, or average, total footing area is examined. However, it is also worthwhile to explore the effect of the plan size of the site investigation, which was defined in Chapter 3 (§3.4.1) by  $Ip_x$  and  $Ip_y$  (Figure 3-6). In most of the analyses that follow, the site investigation plan size is assumed to be 400 m<sup>2</sup> where  $Ip_x = Ip_y = 20$  m. However, in this section, an analysis is conducted to examine the impact of increasing the plan size from 400 m<sup>2</sup> (20 m × 20 m) to 2,500 m<sup>2</sup> (50 m × 50 m). In this form of analysis, a smaller sizing increment of 0.1 m is used, where the footing size is increased by 0.05 m, either side of centre, if the footing settlement exceeds the limits nominated in the design criteria. This is in contrast with most of the results presented to date, which have been based on a sizing increment of 1 m, where the footing size is increased by 0.5 m either side of centre. A smaller increment is used in this analysis to yield a better resolution of average design area, which makes the comparisons between the effects of site investigation size and sampling

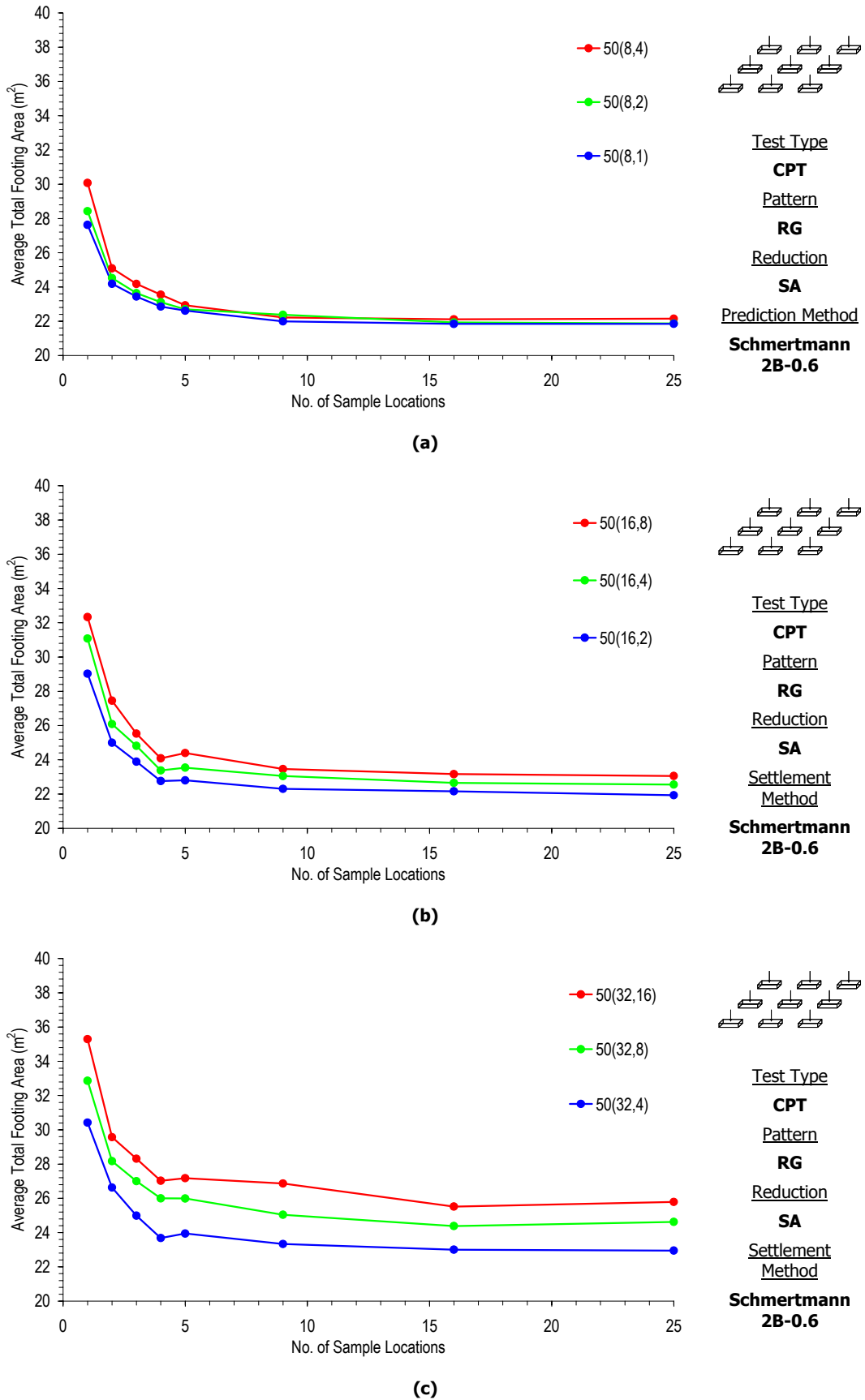


Figure 6-14 Effect of increasing the degree of anisotropy for a horizontal soil SOF,  $\theta_{hr}$ , of (a) 8 m, (b) 16 m and (c) 32 m on the average total footing area based on a site investigation

patterns clearer. Results are given in Figures 6-15 and 6-16, based on a soil COV of 50% and SOF of 8 m. Figure 6-15 indicates the impact of increasing the number of sampling locations on the average total footing area, while Figure 6-16 expresses the sampling effort in terms of a sampling rate, which is defined as the number of samples per 300 m<sup>2</sup>.

The results shown in both Figures 6-15 and 6-16 suggest that:

- The size of the site investigation has little impact on the average total footing area;
- A minimum average total footing area,  $A_{min}$ , is achieved when more than 5 sampling locations are considered for all site investigation plan sizes; and
- A sampling rate, expressed in terms of the number of samples per 300 m<sup>2</sup>, should not be used to determine the optimal sampling effort that yields  $A_{min}$ .

Although the results shown in Figures 6-15 and 6-16 indicate that the site investigation size has little impact, this is only relevant to an increase from 400 m<sup>2</sup> to 2,500 m<sup>2</sup>. However, the results do suggest that a sampling rate, defined as the number of samples per area, should be avoided. Instead, the total number of sampling locations has a greater impact on the foundation design.

**The number of sampling locations has a greater impact on the foundation design than a sampling rate.**

The results shown in both Figures 6-15 and 6-16 also indicate that there is little difference between the three different sampling patterns investigated. Each pattern yields a similar result with an  $A_{min}$  of approximately 11 m<sup>2</sup>, when 25 sample locations are considered. A better comparison of the use of different sampling patterns is given in Figure 6-17. These results are based on a site investigation area of 20 m × 20 m and, similar to Figures 6-15 and 6-16, a soil COV of 50% and SOF of 8 m. However, in this case and for the remaining analysis in this chapter, a sizing increment of 1 m is adopted. This is to ensure consistency between results shown in subsequent chapters that require the use of 3DFEA. It is also evident from the results in Figures 6-15 and 6-16 that the effect of increased sampling for a sizing increment of 0.1 m, is similar to that for the sizing increment of 1 m, shown above (§6.3.1). However, it is important to recall that, for a 1 m sizing increment and the 9-pad system, the minimum total footing size is 20.25 m<sup>2</sup>.

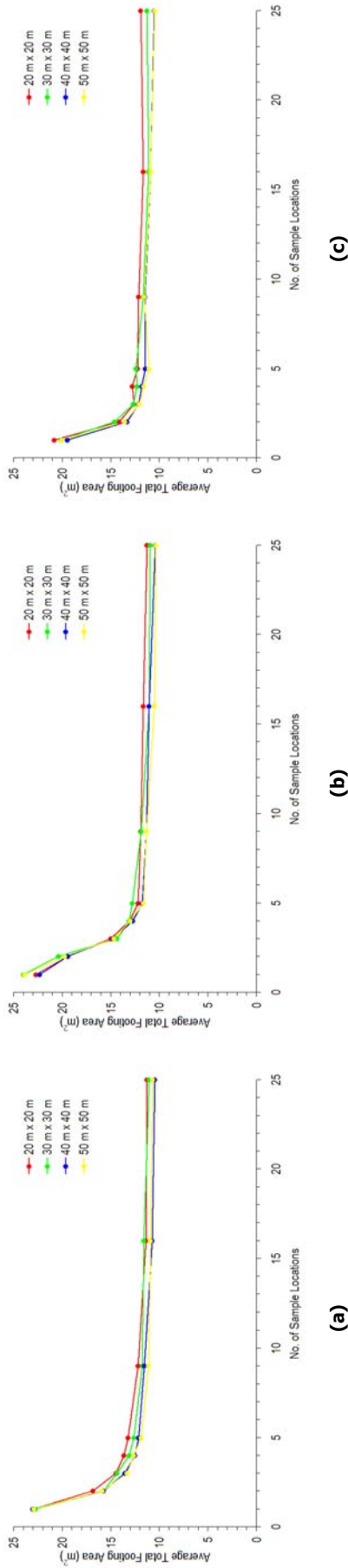


**Figure 6-15** Effect of increased sampling on a site investigation of varying size, where samples are arranged in (a) RG, (b) SR and (c) RN pattern and reduced using the SA for a soil COV of 50% and SOF of 8 m

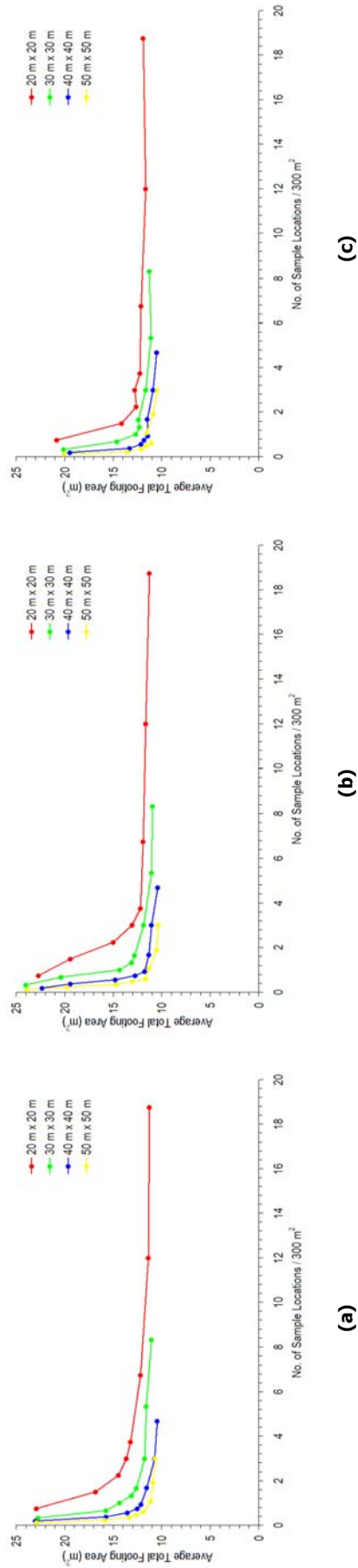


**Figure 6-16** Effect of sampling rate per 300 m<sup>2</sup> on a site investigation of varying size, where samples are arranged in (a) RG, (b) SR and (c) RN pattern and reduced using the SA for a soil COV of 50% and SOF of 8 m

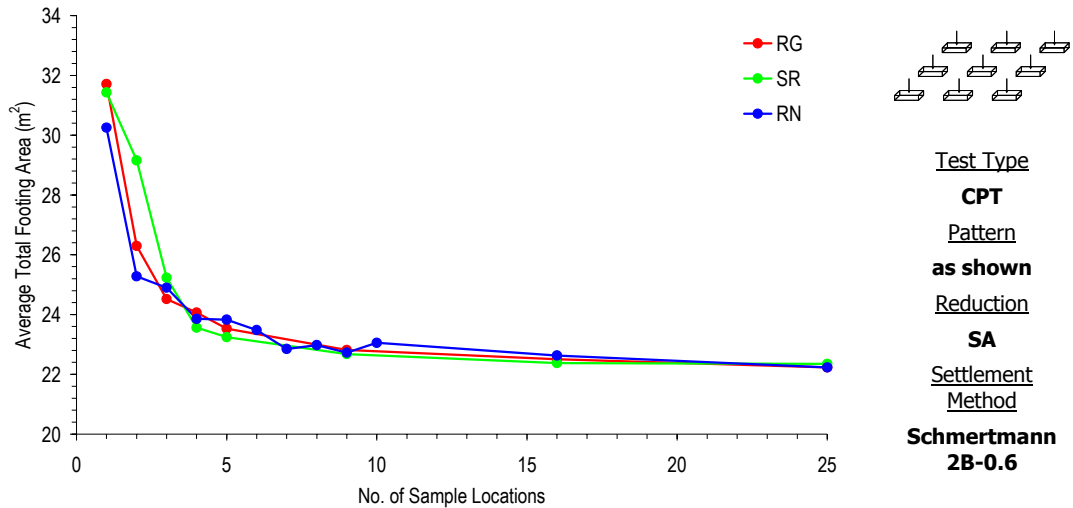


**Figure 6-17 Effect of increased sampling with different sampling patterns on the average total footing area, for a soil COV of 50% and SOF of 8 m**

For each of the sampling patterns shown in Figure 6-17, the average total footing area appears to reduce at the same rate, as the sampling effort increases. Consequently, the sampling pattern appears to have little influence on the relationship between average total footing area and sampling effort. Instead, the number of sample locations is more important for the design of a foundation.

The similarities between the RG and SR sampling patterns are a result of the site investigation area of 20 m × 20 m, or 40 × 40 elements. Since the investigation plan area is relatively small, a large number of sample locations causes little distinction between each sampling location for the RG and SR methods. For example, when 25 sample locations are considered, each sample location in the SR pattern is randomly selected within a 4 m × 4 m (8 × 8 element) region. Therefore, for a soil SOF of 8 m, the elastic moduli within this region are highly correlated and therefore, similar. Although this is not the case for the simple random pattern, the relationship between the average total footing area and increased sampling is also very similar to the RG and SR patterns. Again this is due to the overall plan size of the investigation. However, the results shown in Figures 6-15 and 6-16, suggest that there is also little difference in average total footing area, between a site investigation size of 20 m × 20 m and a size of 50 m × 50 m. Therefore, it appears again that the number of sample locations has the greatest impact on the average total footing area.

Since the results shown in Figures 6-15, 6-16 and 6-17 indicate that the arrangement of samples within a site investigation has little impact on the design of foundation, it is con-

sidered sufficient, for the remainder of this section, to investigate only the use of the regular grid (RG) pattern. The RG has also been described by Ferguson (1992) as the most common and, together with the herringbone layout, the optimal sampling pattern.

**The number of sample locations in a site investigation with a plan size of 20 m × 20 m has a greater importance on the foundation design than the arrangement of such sampling locations.**

Analyses are also conducted to investigate the influence of different reduction techniques on the effect of increased sampling. For this form of analysis, a RG sampling pattern is used together with measurement and transformation errors representative of a CPT. Results are given in Figures 6-18(a) and (b), which illustrate the effect of increased sampling on the average total footing area, with and without the MN reduction technique, respectively. Like results shown previously, this analysis is based on a soil COV of 50% and SOF of 8 m. Results for other soil types are given in Appendix B.

The results in Figure 6-18(a) indicate that, for the MN reduction technique, the average total design area:

- Is considerably larger than the other reduction techniques; and
- Increases as the sampling effort increases.

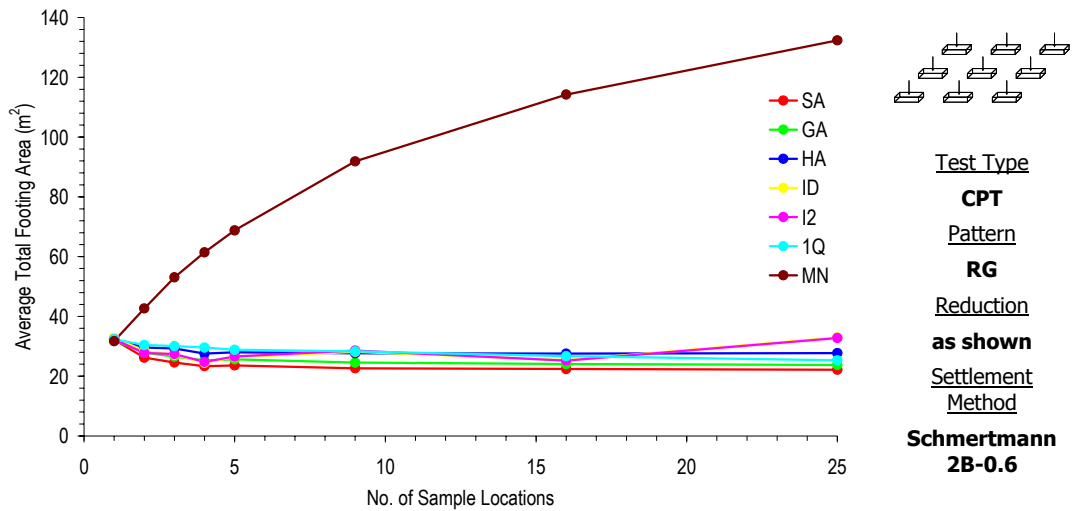
As such, increased sampling using the MN increases conservatism. Whether this infers an increasing error depends on the optimal foundation design, which is discussed in the next chapter. However, because the relationship between increased sampling and the average total footing area, based on the MN, is opposite to the other techniques, it is not considered further in this section.

**The MN yields highly conservative foundation designs that increase as the sampling effort grows.**

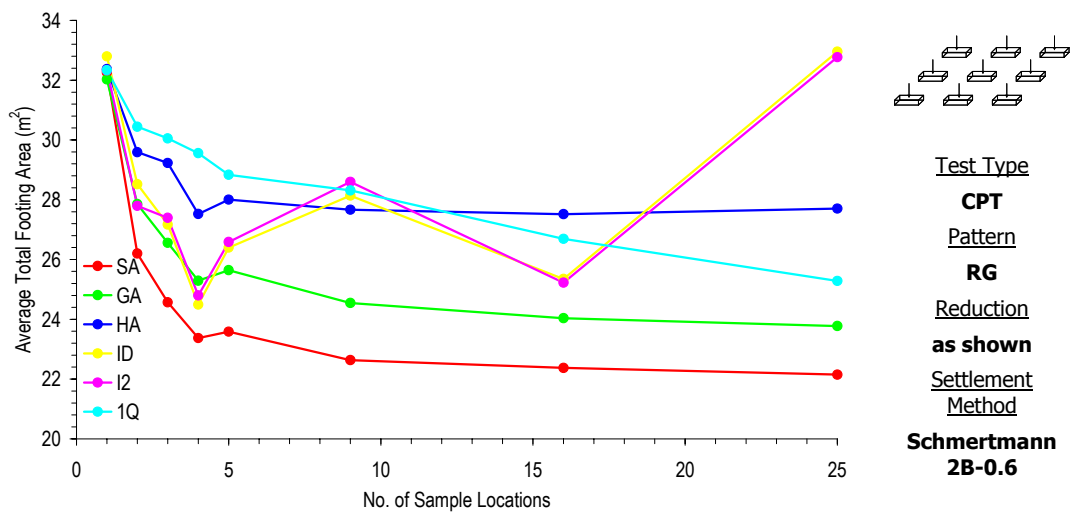
Conclusions, from the results shown in Figure 6-18(b), include:

- The SA technique yields the least conservative solution;
- The GA yields an average total footing area that is greater than the SA, but less than the HA;

- A minimum average total footing area,  $A_{min}$ , is achieved for the SA, GA and HA techniques after 15 sampling locations are considered;
- The 1Q technique requires more than 15 sampling locations to achieve  $A_{min}$ ; and
- The relationship between increased sampling and average total footing area using the ID and I2 techniques is erratic and does not follow a general trend.



(a)



(b)

**Figure 6-18 Effect of sampling with different reduction techniques on the average total footing area, for a soil COV of 50% and SOF of 8 m, (a) including MN and (b) excluding MN**

The relative conservatisms between the reduction techniques based on averaging (SA, GA and HA) are consistent with the results shown earlier in this chapter (§6.2.2), regarding the selection of design parameters. Such results indicated that the SA yielded a larger design

parameter than both the GA and HA. A larger design parameter infers a smaller foundation design and therefore, reduced conservatism. The GA and HA techniques yield larger designs because they are low-value dependent, where a low elastic moduli has a greater bearing on the characteristic value than higher values, as discussed earlier (§6.2.2).

Although  $A_{min}$  appears to be achieved, when using the SA, GA and HA, after 15 sampling locations are considered, the size of  $A_{min}$  is different for each technique. For example,  $A_{min}$ , using the SA is approximately 22 m<sup>2</sup>, while  $A_{min}$ , based on the GA and HA, is approximately 23.8 m<sup>2</sup> and 27.8 m<sup>2</sup>, respectively. These differences are consistent with the relative conservatisms inherent in the reduction technique, as discussed earlier in this chapter (§6.2.2). However, the 1Q technique does not appear to reach  $A_{min}$  after 25 sample locations are considered. At this point, the average total footing area is approximately 25.4 m<sup>2</sup>, which is slightly larger than the GA, yet less than the HA. Therefore, it is expected that the average total footing area using the 1Q will continue to decrease when more than 25 sample locations are considered. Furthermore, it appears that a greater sampling effort is required to yield  $A_{min}$  when the 1Q technique is used in comparison with the SA, GA and HA methods.

The erratic relationship between increased sampling and average total footing area shown for the ID and I2 reduction techniques exists, despite the fact that the same methods were shown earlier in this chapter to yield design parameters that closely approximated the actual elastic moduli (§6.2.2). However, those particular results (Figure 6-5) were based on sampling locations that were randomly selected within the site investigation area and a single pad footing located at the centre of the site. In the case shown in Figure 6-18(b), the sampling locations are arranged in a regular grid and the results are used to design 9 separate pad footings as part of a foundation system. As such, for increased sampling, the average total footing area, based on the ID and I2, decreases until 5 sample locations are considered, after which the average total footing area increases. Furthermore, it appears that the designs based on the results of 1 and 25 sample locations, yield similar average total footing areas. Although this seems counter-intuitive, the ID and I2 involve weighting the results from each sample location, based on the distance from the footings in the system. Therefore, in some circumstances the results from some sample locations may be ignored. This occurs for the case when the sampling effort consists of 25 locations, because one sample location always coincides with each footing location. Therefore, the design based on the ID and I2, using results from 25 sample locations, is only representative of the results of 9 different sampling locations. This has an impact on the variability of the sam-



pled data, where the domain size has been previously shown to have a considerable influence on the apparent variability (§4.2.1).

To demonstrate the effect of using the ID and I2 methods with a RG sampling pattern, an analysis is undertaken comparing the different reduction techniques shown in Figure 6-18(b) with a stratified random (SR) pattern and a simple random (RN) arrangement of sampling locations. These results are given in Figures 6-19(a) and (b), for the SR and RN patterns, respectively. Such results indicate that the ID and I2 techniques yield similar relationships as the other methods. This is in stark contrast to the results shown in Figure 6-18(b), where the ID and I2 methods were shown to have no general trend with increased sampling.

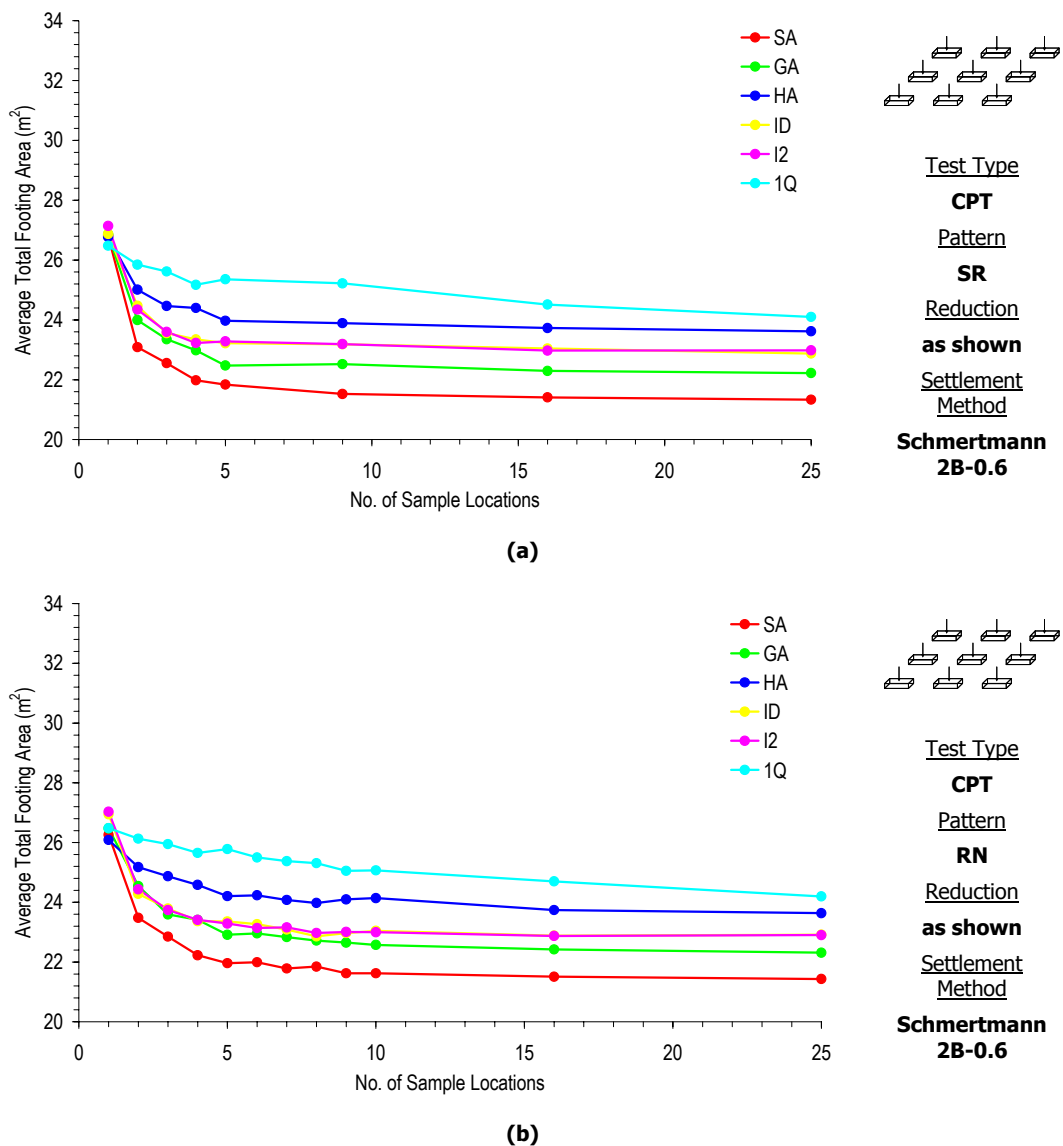


**Figure 6-19** Effect of sampling with different reduction techniques on the average total footing area based on a (a) SR and (b) RN sampling pattern for a soil COV of 50% and SOF of 8 m

The difference between the results shown in Figure 6-18(b) based on the RG, and those in Figures 6-19(a) and (b) based on the SR and RN, respectively, is because a sampling location in the RG pattern consistently coincides with the footing. This has an impact on the apparent variability of the elastic moduli and therefore, an effect on the average, due to the presence of a lognormal distribution. Alternatively, because the sampling locations are chosen randomly in the SR and RN patterns, it is rare that a sampling location will coincide with the footing. Hence, the elastic moduli from all locations are considered in the design and the benefits of increased sampling are evident. Based on the results in Figures 6-19(a) and (b), it appears that the conservatism of the ID and I2 methods yields a footing design that is slightly larger or more conservative than the HA technique.

The results shown thus far have been based on the total footing area, which is the sum of all 9 footing sizes in the system. However, the effect of increased sampling on the average footing area for each individual pad in the foundation system is also examined. These results are given in Figure 6-20, for a soil COV of 50% and SOF of 8 m, and a site investigation based on a RG, CPT and either the SA, GA, HA, ID, I2 or 1Q.

The results shown in Figure 6-20 suggest that, for each reduction technique, the effect of increased sampling is similar for each footing in the 9-pad system. Therefore, the effect of increased sampling and the impact of using a different reduction technique do not favour one footing in the system. The only notable difference appears to be when the results of the site investigation are reduced using either the ID or I2. This effect appears to be exaggerated for the central footing, which is designed to resist the largest load. It should also be noted that, for the central footing, the designs based on ID and I2 using results from 1, 5 and 25 sample locations are the same. This is because these sampling plans have a location that coincides with that of the central footing.

### 6.3.3 Types of Soil Tests

It has already been discussed in Chapter 2 (§2.3.4 and §2.3.5), that different test types possess varying degrees of uncertainty, which in turn affect the design process of a foundation. Therefore, an analysis is conducted to compare the resulting foundation designs, based on the use of the SPT, CPT, triaxial test (TT) and DMT. The test types are distinguished by the measurement and transformation model errors assumed, as discussed in Chapter 3 (§3.4.3). The analysis that follows is based solely on a site investigation consisting of

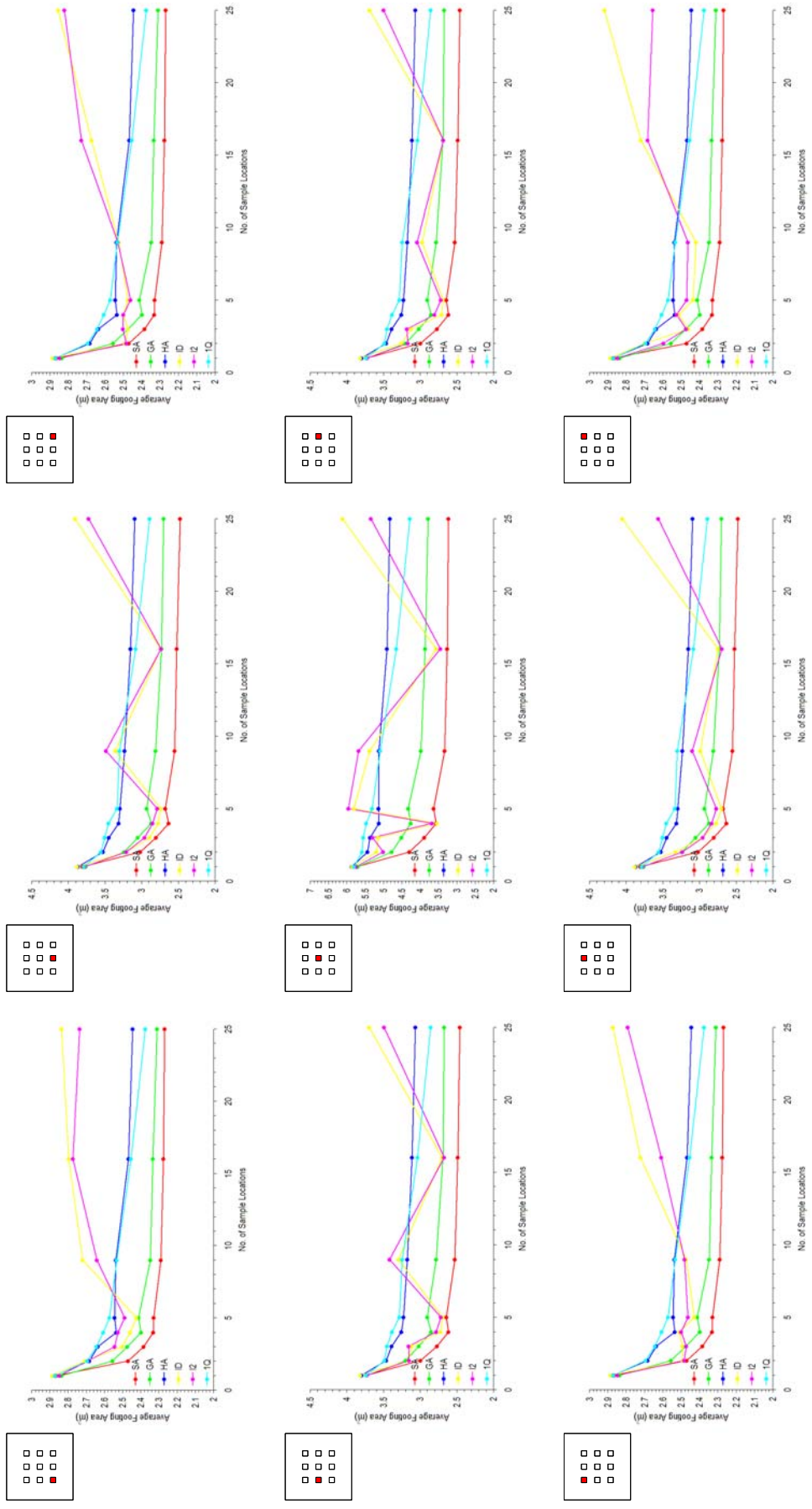


**Figure 6-20** Effect of sampling on the average footing area of each footing in the 9-pad system for a soil COV of 50% and SOF of 8 m

sampling locations arranged in a RG and reduced using the SA. Results are given in Figures 6-21 and 6-22 for an increasing soil COV and SOF, respectively. It is also important to reiterate the relative vertical sampling rates for each test type. More specifically, the SPT, DMT and TT are examples of discrete sampling techniques, whereas the CPT is a continuous sampling technique. As a result, elastic moduli are sampled at 1.5 m depth intervals (3 elements), for the SPT and DMT while, for the CPT, values from each element (0.5 m) are sampled. The results using the TT are based on 2 elastic moduli per sample location, where one is sampled just below the surface at a depth of 0.5 m, and the second is sampled at a depth of 15 m, which is half the depth of the soil layer. Only two samples are used for the TT at each location as samples are required to be tested offsite in a laboratory. However, an analysis investigating the effect of the assumed vertical sampling rate of the TT is discussed later in Chapter 7 (§7.4.2).

Before discussing the results in Figures 6-21 and 6-22, it is important to recall the degree of uncertainty due to measurement and transformation model error assumed for each test type. These were given in Chapter 3 (Table 3-4) but are also summarised in Table 6-1.

**Table 6-1 Adopted uncertainties due to measurement and transformation model error for each test type investigated**

Test Type	Abbreviation	Measurement Error (COV - %)		Transformation Model Error (COV - %)
		Bias / Systematic	Random	
Standard penetration test	SPT	20	40	25
Cone penetration test	CPT	15	20	15
Triaxial test	TT	20	20	0
Dilatometer test	DMT	15	15	10

It is clear from the adopted uncertainties summarised in Table 6-1 that the SPT is assumed to yield the most uncertain results, as suggested by the literature reviewed in Chapter 2 (§2.3.4). Such an increased uncertainty causes greater conservatism of the foundation design, as shown in Figures 6-21 and 6-22. In this case, the designs based on the SPT were shown to yield footings that had notably larger average total areas. However, the effect of increased sampling does not appear to vary between the different test types, indicating that the sampling effort still has the greatest impact on the design of a foundation. In fact, it appears that the differences between test types are the same, irrespective of the sampling effort. Instead, only the conservatism of the foundation design is affected by the assumed testing uncertainties, including measurement and transformation model error.

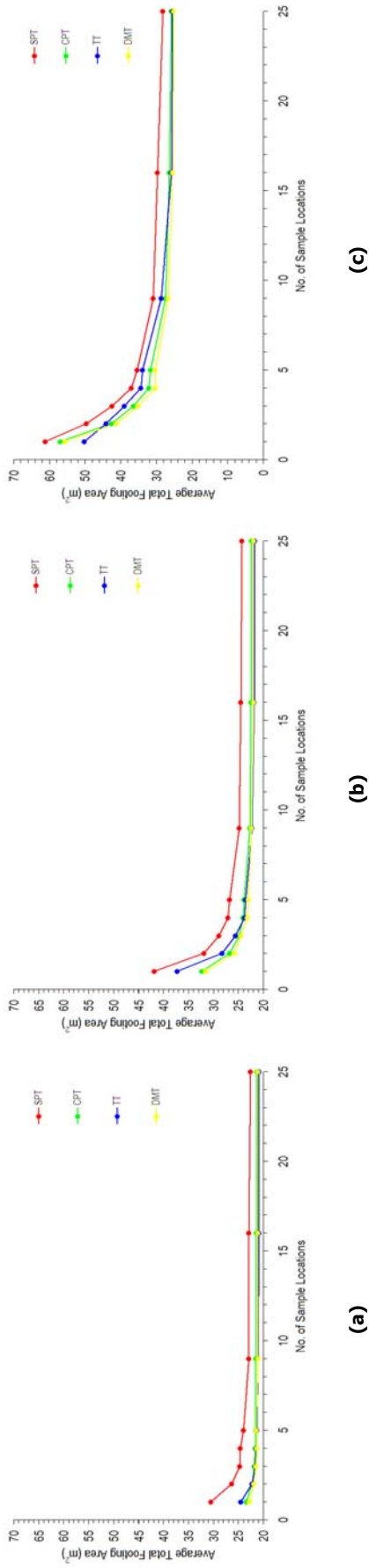


**Figure 6-21** Effect of sampling using different test types on the average total footing area of the 9-pad system for a soil SOF of 8 m and COV of (a) 20%, (b) 50% and (c) 100%

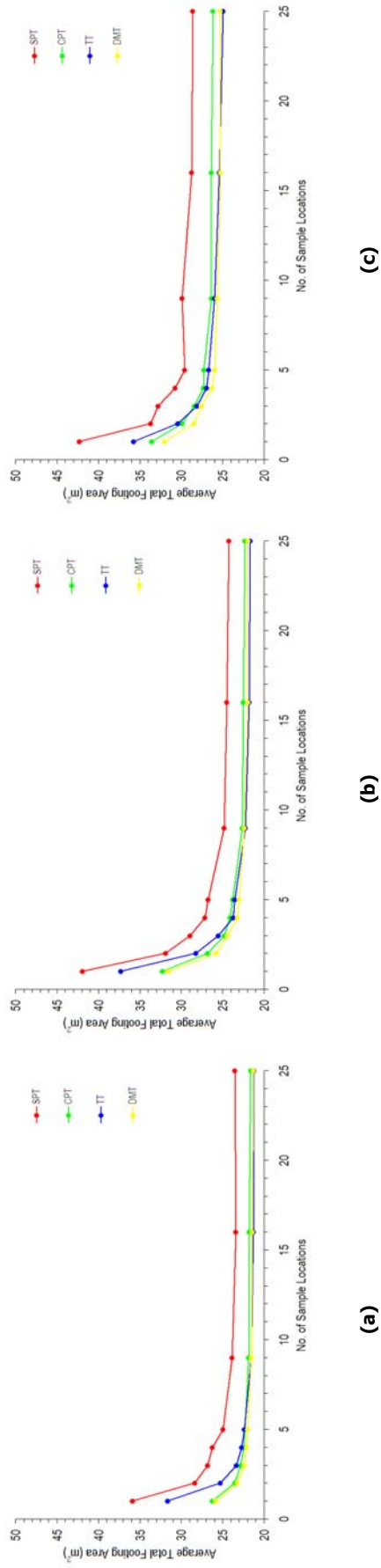


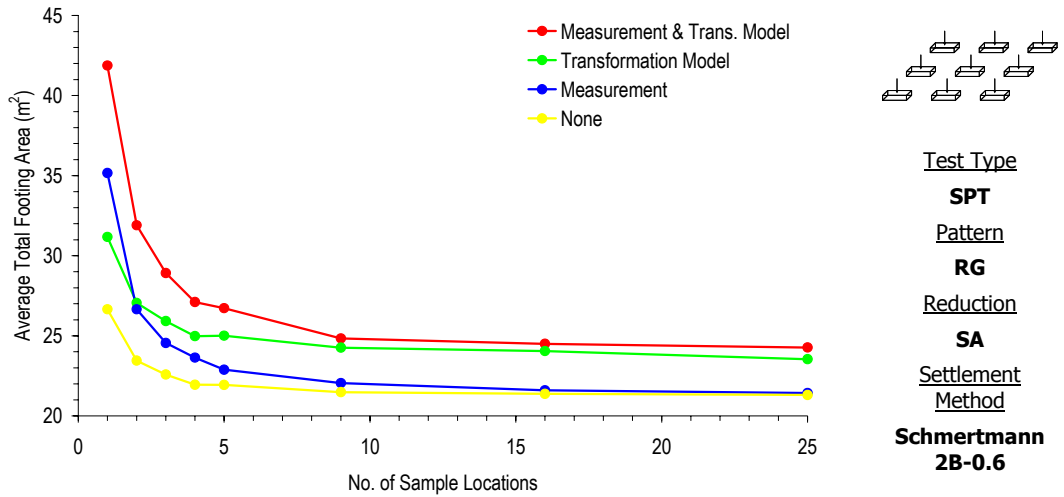
**Figure 6-22** Effect of sampling using different test types on the average total footing area of the 9-pad system for a soil COV of 50% and SOF of (a) 1 m, (b) 8 m and (c) 32 m

As discussed in Chapter 3 (§3.4.3), uncertainties exist regarding the methodology used to incorporate uncertainties due to measurement and transformation model error for each test type. This is due to the limited available research regarding measurement and transformation model errors and the large ranges of values in the literature. As such, the impact of measurement and transformation model errors on the average total footing area is also examined. These results are given in Figure 6-23 for a soil COV of 50% and SOF of 8 m. Analyses are conducted based solely on the SPT [Figure 6-23(a)] and the CPT [Figure 6-23(b)]. However, additional results for all test types and other soils are given in Appendix B.

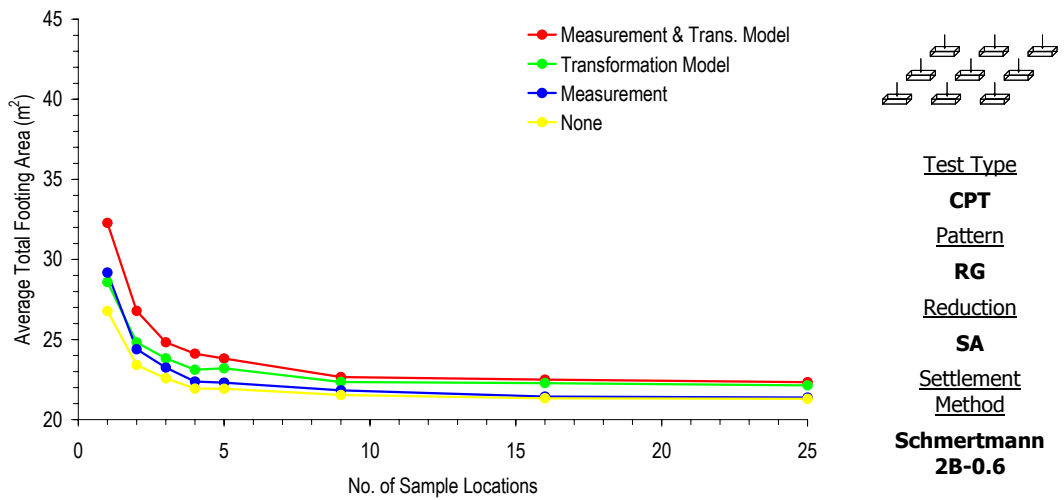
In Figure 6-23, the average total footing area is shown to increase with the incorporation of both measurement and transformation model errors. However, it is interesting to observe the relative increases in average total footing area for different sampling efforts. For example, when the results from 25 sample locations are considered, the uncertainty due to measurement error appears to have little effect on the results, where the average total footing area is the same as the case when no measurement uncertainty is included. However, when the design is based on a single sample location, the uncertainty due to measurement error appears to have a notable effect on the result where the average total footing area is larger. This suggests that the effects of including measurement errors are reduced as the sampling effort increases.

**The effects of measurement error are reduced as the sampling effort is increased.**

The inclusion of transformation model errors appears to affect the results by the same degree, irrespective of sampling effort. This is because this form of uncertainty is similar to a bias where all results are affected by the error and increased averaging has no effect. However, it is also important to consider the relative importance of both sources of uncertainty, when the results from an increasing number of sample locations are considered. In this case, measurement errors have the most significant impact when only a limited number of sample locations are considered. However, when the site investigation consists of three or more locations, the transformation model errors have the greatest influence. These conclusions appear to be valid for both the results of the SPT [Figure 6-23(a)] and the CPT [Figure 6-23(b)]. However, the effects of measurement and transformation model error appear to be less for the CPT. This is because the uncertainties assumed for the SPT are larger than the CPT.



(a)



(b)

Figure 6-23 Effect of sampling, including measurement and transformation model errors for the (a) SPT and (b) CPT on the average total footing area, for a soil COV of 50% and SOF of 4 m

The uncertainties due to measurement error have a greater influence than the transformation model errors, when the site investigation consists a limited number of samples. The uncertainties due to transformation model error become of greater significance, when the site investigation consists of 3 or more samples.

The increasing average total footing area, shown for the inclusion of measurement and transformation model errors, is also explained by investigating the manner in which the errors are included in the methodology, as described in Chapter 3 (§3.4.3). For example, if  $E_f$  represents an elastic modulus generated at any location in the field, then the resulting elastic modulus,  $E_r$ , including measurement and transformation model errors, is given by:

$$E_r = (tm)(m_b m_r)E_f \quad (6.1)$$

where  $tm$  represents the transformation model error and  $m_b$  and  $m_r$ , represent the bias and random parts of the measurement uncertainty, respectively. The difference between the bias and random parts of the measurement uncertainty has been described previously in Chapter 3 (§3.4.3).

The lognormal transformation of Equation (6.1) leads to the expression given by:

$$\ln E_r = \ln tm + \ln m_b + \ln m_r + \ln E_f \quad (6.2)$$

where the mean,  $\mu_{\ln E_r}$  and variance,  $\sigma_{\ln E_r}^2$  of the resultant elastic modulus, are given by:

$$\mu_{\ln E_r} = \mu_{\ln tm} + \mu_{\ln m_b} + \mu_{\ln m_r} + \mu_{\ln E_f} \quad (6.3)$$

and

$$\sigma_{\ln E_r}^2 = \sigma_{\ln tm}^2 + \sigma_{\ln m_b}^2 + \sigma_{\ln m_r}^2 + \sigma_{\ln E_f}^2 \quad (6.4)$$

respectively, and are the summation of the mean and variances of the natural logarithm of the individual parts shown in Equation (6.2). The relationships given by Equations (6.3) and (6.4) have also been used by others (e.g. Jaksa et al. 1997) to describe the combination of several sources of uncertainty. Furthermore, based on the assumption that the footing area,  $A$ , is inversely proportional to the resultant elastic modulus,  $E_r$ , it is possible to develop an expression for the average,  $\mu_A$ , of the footing area, in terms of the resultant elastic modulus, as given by:

$$\begin{aligned} A &\propto \frac{\kappa}{E_r} \\ \ln A &= \ln \kappa - \ln E_r \\ \mu_A &= \ln \kappa - \mu_{E_r} \end{aligned} \quad (6.5)$$

where  $\kappa$  is a deterministic constant dependent on the settlement prediction technique used and the limits nominated in the design criteria.



Using the expressions for the average of the footing area, shown in Equation (6.5), and the relationships for the mean and variance of the resultant elastic modulus, shown in Equations (6.3) and (6.4), the average footing area can be expressed as:

$$\mu_A = \frac{\kappa(1 + \sigma_{im}^2)(1 + \sigma_{m_b}^2)(1 + \sigma_{m_r}^2)(1 + \text{COV}_{E_f}^2)}{\mu_{E_f}} \quad (6.6)$$

where  $\text{COV}_{E_f}$  is the coefficient of variation of the elastic modulus field, which is defined as the standard deviation,  $\sigma_f$ , divided by the mean,  $\mu_f$ . The results given in Equation (6.6) infer that, as:

$$\sigma_{im}^2, \sigma_{m_b}^2, \sigma_{m_r}^2, \text{COV}_{E_f}^2 \uparrow \Rightarrow \mu_A \uparrow \quad (6.7)$$

This also confirms the results shown in Figure 6-23, where the average total footing area increases as the measurement and transformation model errors rise or become non-negative. The expression in Equation (6.7) also infers that an increase in the soil COV results in a larger average total footing size. This has previously been observed in the results shown in Chapter 5 (§5.2.2 and §5.3) and earlier in this chapter (§6.3.1).

The relationship in Equation (6.6), for the mean footing area, yields:

$$\sigma_{im}^2 = \sigma_{m_b}^2 = \sigma_{m_r}^2 = \text{COV}_{E_f}^2 = 0 \Rightarrow \mu_A = \frac{\kappa}{\mu_{E_f}} \quad (6.8)$$

This states that, when the sources of uncertainty due to measurement and transformation model errors and inherent soil variability are zero, the average footing area is equal to the coefficient representing the design criteria and settlement relationship,  $\kappa$ , divided by the mean of the elastic modulus field. In other words, this becomes the case when the soil has a uniform elastic modulus field, which has been addressed in Chapter 5 (§5.2.1).

It is important to note that the relationship between the average footing area and the variances from the several sources of uncertainty, given by Equation (6.6), does not account for the statistical uncertainty resulting from a limited number of samples. Therefore, the trends indicated in Equations (6.7) and (6.8) are suitable only for general conditions, and are inappropriate for absolute conclusions. The results shown in Figure 6-23 illustrate such an occurrence, where the conclusions drawn in Equation (6.6) do not accurately predict the

observed behaviour. This is because the theoretical evaluation does not consider the effects of increased sampling and the measurement errors are not averaged out when 25 sample locations are considered.

#### **6.3.4 Settlement Prediction Techniques**

An analysis is also undertaken to compare the average total footing area of a 9-pad system, based on information from a site investigation and the use of the different settlement relationships discussed in Chapter 3 (§3.6.2). Such an analysis indicates whether different settlement prediction techniques have a greater impact on the effect of increased sampling. The results of this analysis are given in Figures 6-24 and 6-25, for an increasing soil COV and SOF, respectively. Both figures are based on a site investigation consisting of samples arranged in a RG, reduced using the SA and uncertainties representative of the CPT.

Both Figures 6-24 and 6-25 indicate that the use of different prediction techniques has little influence on the effect of increased sampling. Instead, like the results shown for different test types, the different settlement methods yield designs with varying degrees of conservatism. Therefore, it appears again, that sampling has the greatest effect on the foundation design where an increased sampling effort reduces the average total footing area.

Figures 6-24 and 6-25 also indicate the average total footing area of the design based on 3DFEA and complete knowledge of the soil (CK). Obviously, this design does not vary for different sampling efforts because it is based on CK. However, it is interesting to note the effect of increased sampling and the use of different settlement prediction techniques on the average total footing area, with respect to the design based on 3DFEA. For example, with a soil COV of 50% and SOF of 8 m [Figure 6-24(b)], increased sampling using the Janbu method yields an average total footing area that tends towards the design based on 3DFEA. This infers that increased sampling improves the design, if 3DFEA is considered the optimal. However, for a soil COV of 100% and SOF of 8 m [Figure 6-24(c)], increased sampling using the same technique increases the difference between 3DFEA. This infers that increased sampling actually worsens the result. In fact, this is true for all prediction techniques investigated when the soil has a COV of 100% and SOF of 8 m. This is because 3DFEA yields a relatively large average total footing area when the soil COV is large. Further comparisons between the foundation designs, based on the results of a site investigation data and the optimal design utilising CK, are discussed in Chapter 7.

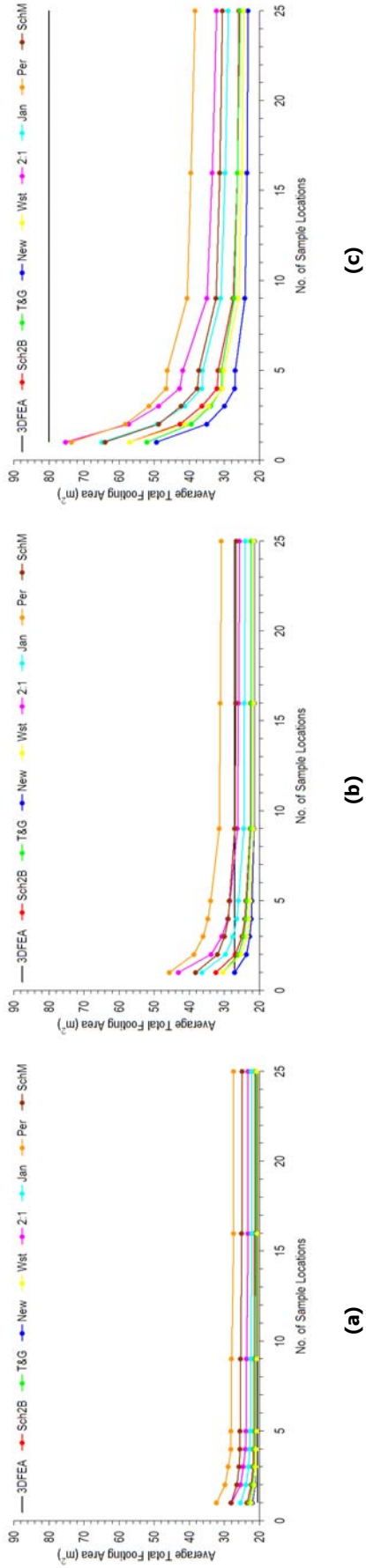


**Figure 6-24** Effect of sampling and the use of different settlement relationships on the average total footing area of the 9-pad system for a soil SOF of 8 m and COV of (a) 20%, (b) 50% and (c) 100%

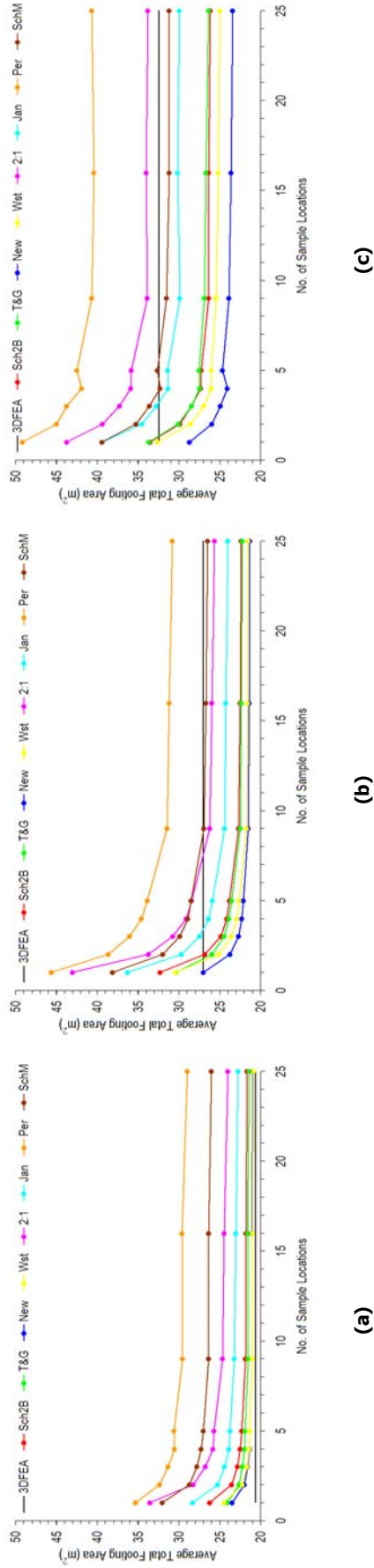


**Figure 6-25** Effect of sampling and the use of different settlement relationships on the average total footing area of the 9-pad system for a soil COV of 50% and SOF of (a) 1 m, (b) 8 m and (c) 32 m

### 6.3.5 Summary

Based on the results shown in this section, the following general conclusions regarding the impact of increased sampling on the expected, or average, total footing area are made:

- The soil COV has a greater impact on the foundation design than the soil SOF. Furthermore, soils with high COV require increased sampling to achieve the minimum total footing area,  $A_{min}$ . The soil SOF has little impact on the required sampling effort to achieve  $A_{min}$ ;
- The MN reduction technique yields a very conservative foundation design that increases in conservatism as the sampling effort is increased. Therefore, this method should be avoided, especially when the sampling effort is high;
- Increased sampling has no general affect on the foundation design when the data are reduced using the ID or I2 methods;
- Test types with larger measurement and transformation model errors, like the SPT, lead to more conservative solutions; and
- Increased sampling has the greatest impact on the average total design area, where a greater sampling effort leads to a reduced footing design in most cases.

## 6.4 EFFECT OF SITE INVESTIGATION SCOPE ON THE VARIABILITY OF A PAD FOUNDATION DESIGN

---

The results shown in the previous section of this chapter illustrated the effect of increased sampling on the average total footing area of a foundation design. However, it is also useful to investigate the effect of sampling on the variability of the foundation design. This is achieved by observing the effect of increased sampling on the sample distribution of footing areas and the sample standard deviation, or coefficient of variation (COV), of the total footing area. Like the results shown earlier in this chapter, it is expected that the effect of increased sampling on the variability of the foundation design will be influenced by the statistical properties of the elastic moduli, the scope of the site investigation, and uncertainties due to measurement and transformation model errors. As such, the influences of each source of uncertainty are investigated below.

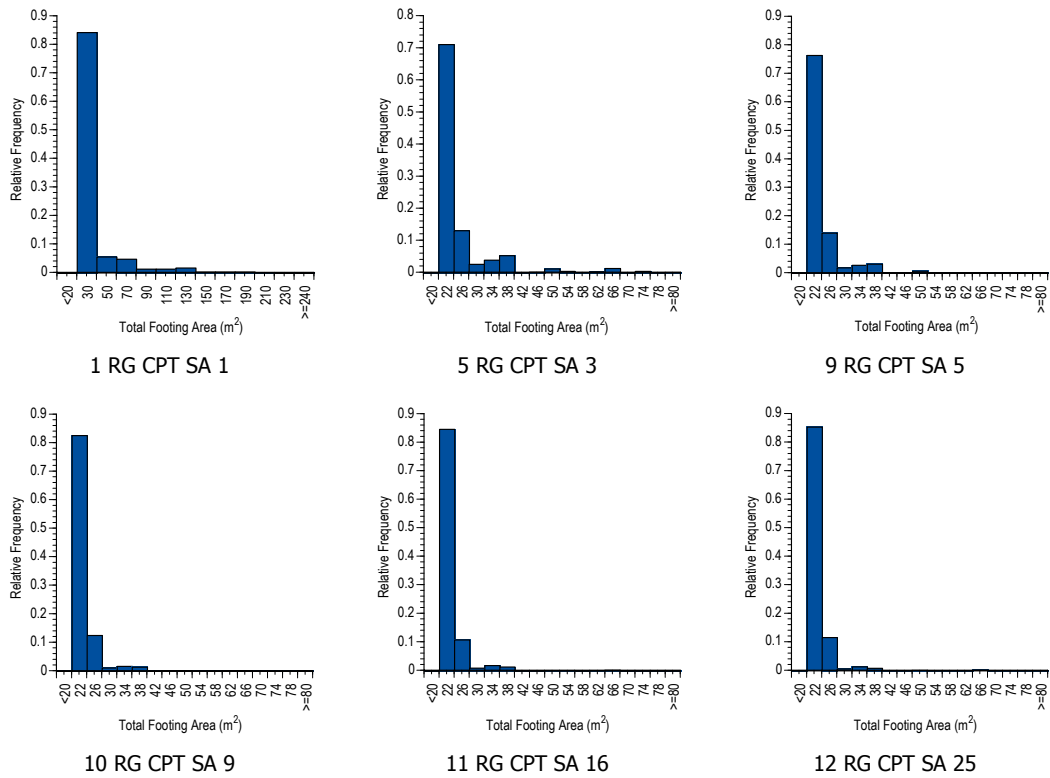
### 6.4.1 Soil Variability

Soil variability has been shown, earlier in this chapter, to have a notable influence on the effect of increased sampling on design parameters and the resulting foundation design. Therefore, it is reasonable to suggest that the soil COV and SOF will also have an impact on the variability of the foundation design. As such, the sample distributions of total footing area are examined by recording design areas from each of 1,000 Monte Carlo realisations. This analysis illustrates the variation of footing area and therefore, a measure of the robustness of the design. Sample distributions of total footing area are given in Figures 6-26(a) and (b) for a soil COV of 50% and 100%, respectively. An increase in soil COV is only examined, as it was shown earlier in this chapter (§6.3.1) that the COV has the greatest impact on the design. At this stage of the analysis, the Schmertmann 2B-0.6 settlement method (Sch2B) is used exclusively and the site investigation is based on a RG, SA and CPT. The nomenclature used in Figure 6-26 indicates the sampling arrangement, as discussed previously in Chapter 3 (§3.4.1) and revisited earlier in this chapter (Figure 6-12).

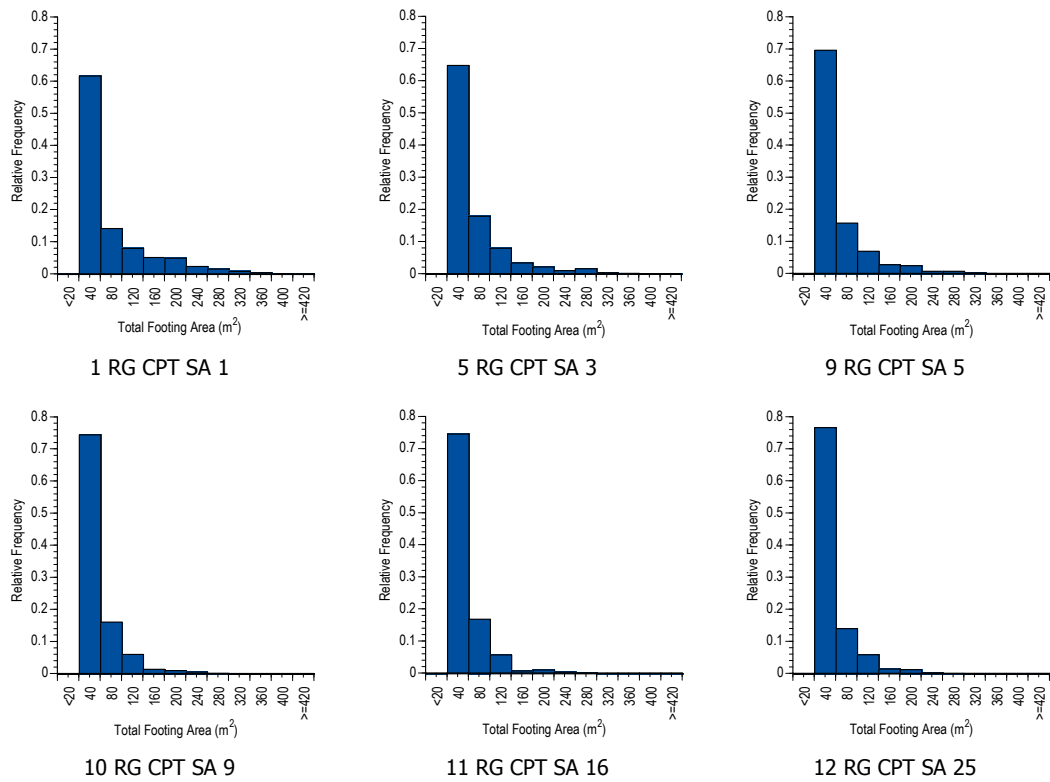
It is apparent that the variability of the total footing area is reduced as the sampling effort increases. This is shown in Figure 6-26 by the reducing width of the sample distribution. Such narrowing also infers a reduction in the sample mean or average total footing area, due to the minimum footing constraint, as discussed in Chapter 3 (§3.6.5.2), and the presence of a lognormal distribution. A reducing average total footing area was also observed in the previous section of this chapter and, furthermore, has significant consequences regarding the probability of under-design, over-design and design error, which is discussed later in Chapter 7. Although the sample distributions, shown in Figures 6-26(a) and (b) for soil COVs of 50% and 100%, respectively, appear different, the effect of increased sampling appears to be similar.

It is difficult to represent the sample distributions of total footing area using common statistical distributions because of the minimum footing constraint. Although it appears that several of the sample distributions, shown in Figure 6-26, mimic an exponential shape, it is important to consider that the method does not allow a total footing area of less than 20.25 m<sup>2</sup>, as discussed previously in Chapter 3 (§3.6.5.2). Therefore, any fitted distribution is required to be skewed to provide the shape shown by the results in Figure 6-26.

**It is difficult to describe the sample distribution of total footing area using typical statistical distributions due to the minimum footing constraint.**



(a)



(b)

Figure 6-26 Sample distributions of total footing area for the Schmertmann 2B-0.6 settlement relationship for a soil SOF of 8 m and COV of (a) 50% and (b) 100%

Although the results in Figure 6-26 provide a reasonable measure of the effect of sampling and soil COV on the variability of footing design, Figure 6-27 yields a clearer indication, where the results illustrate the effect of increased sampling on the COV of total footing area. These results are based on an increasing soil COV [Figure 6-27(a)] and SOF [Figure 6-27(b)].

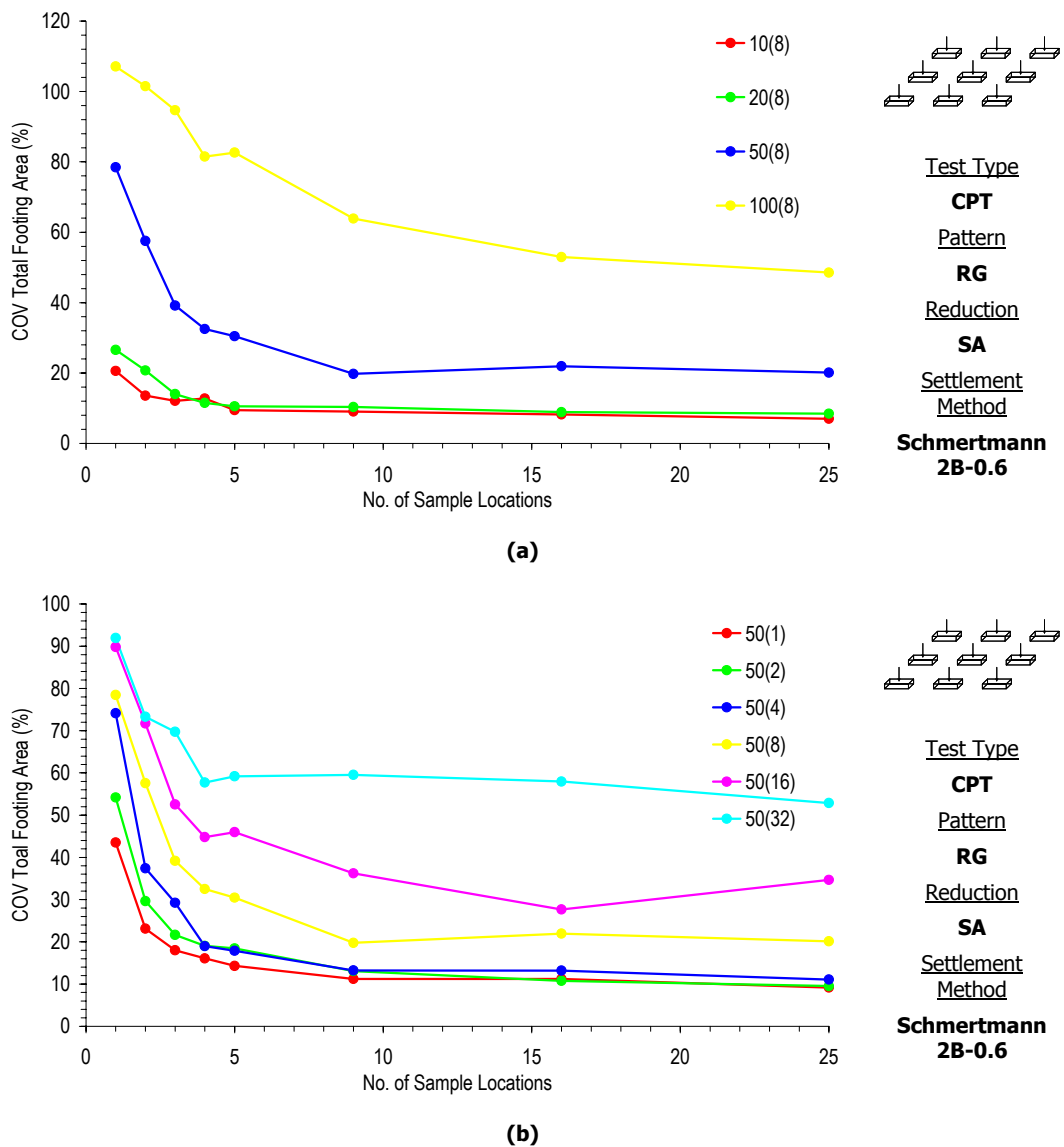


Figure 6-27 Effect of sampling on the COV of total footing area, for an increasing soil (a) COV (SOF of 8 m) and (b) SOF (COV of 50%)

It appears from Figure 6-27 that:

- The effect of increased sampling on the COV of total footing area,  $COV_A$ , is affected more by the soil COV than the soil SOF; and

- The number of sampling locations required to achieve a minimum  $COV_A$  is affected by the soil COV, but not the soil SOF.

The second conclusion suggests that additional sampling is required to yield the most robust design, with the least variation. This complements the results shown earlier in this chapter, which indicated that additional sampling is required to achieve the minimum total footing area. In the case presented, 9 or more sampling locations are required to yield the least variable design when the soil COV is 50%. However, additional sampling effort is required when the soil COV increases to 100%.

**The number of sample locations required to obtain the least variable design is affected by the soil COV, where additional sampling is required when the COV is higher. The soil SOF does not appear to have a significant effect.**

Although most comparisons between an SI and CK design are reserved for later chapters, the difference between the average total footing area, based on CK, and the range of footing areas from an SI design, are also examined. In this case, the CK design is achieved using 3DFEA and all elastic moduli, while the SI design is based on the same conditions investigated in Figure 6-27. The results of this analysis are given in Figure 6-28, where the range of SI designs are based on  $\pm 1$  standard deviation from the average. This range is employed because specific ranges of significance are not possible, due to the difficulty of describing the sample distribution using a common statistical distribution. It should also be reiterated that the total footing area is constrained by a minimum of 20.25 m<sup>2</sup>. Therefore, this applies to all cases in Figure 6-28. An upper limit is also applied to the total footing area, whereby the methodology records the need for an alternative foundation when a pad foundation is not achievable, as discussed in Chapter 3 (§3.5.2). However, this maximum is equivalent to a total footing area of 506.25 m<sup>2</sup>, and the results shown in Figure 6-28 do not reach this maximum.

The results shown in Figure 6-28 clearly indicate that increased sampling not only reduces the average total footing area, but also the range of footing areas that meet the design criteria. Furthermore, because the footing size is constrained to be greater than 20.25 m<sup>2</sup>, the ranges become smaller as the average total footing area tends towards 20.25 m<sup>2</sup>. Therefore, when the SI design is based on 25 sampling locations, the range of footing areas is less than the average total footing area of the CK design. This has considerable implica-



tions when investigating the probability of under-design, where the design using 3DFEA and CK is considered the optimal design. This is discussed further in Chapter 7.

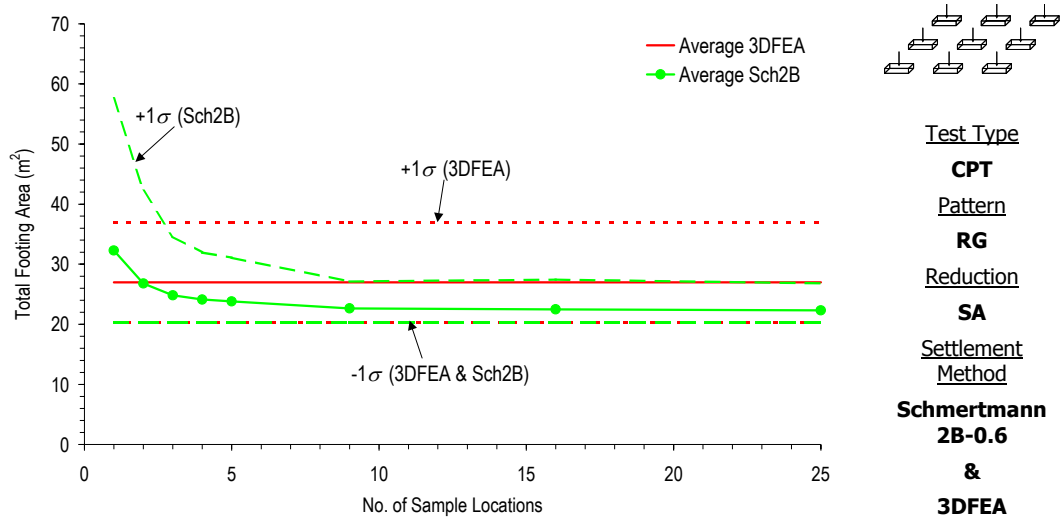


**Figure 6-28** Effect of sampling on the spread of total footing area using  $\pm 1$  standard deviation from the average using Schmertmann 2B-0.6 and 3DFEA for a soil COV of 50% and SOF of 8 m

### 6.4.2 Sampling Patterns and Reduction Techniques

In keeping with the analyses undertaken earlier in this chapter, regarding the average total design area, the impact of additional sampling in different patterns on the design variability has also been examined. These results are given in Figure 6-29 for a soil COV of 50% and SOF of 8 m and show much the same trend as those presented earlier (Figure 6-17). In this case, the COV of total footing area is shown to reduce as the sampling effort increases. However, like the results shown earlier (Figure 6-17), there appears little difference between the sampling patterns. This again indicates that the sampling pattern has little impact on the effects of increased sampling.

Analyses are also undertaken to examine the impact of using different reduction techniques on the variability of total footing area. In this case, the site investigation is based solely on the RG arrangement of sampling locations. Furthermore, as with previous analyses, only a soil COV of 50% and SOF of 8 m is examined. Results of analyses for other soil types are included in Appendix B. As such, the effect of increased sampling on the standard deviation and COV of total footing area is given in Figures 6-30 and 6-31, respectively. The effect on the standard deviation is included to indicate that the reduction in the average total footing area, shown in the previous section, is not the sole influence on the COV. In this case, Figure 6-30 clearly indicates that the standard deviation, for all but the MN re-

duction technique, reduces as the sampling effort rises. Furthermore, the reduction in standard deviation is so great that it also causes a diminishing COV, as shown in Figure 6-31. This is despite the fact that the average total footing area is also shown to reduce for an increased sampling effort (Figure 6-18).

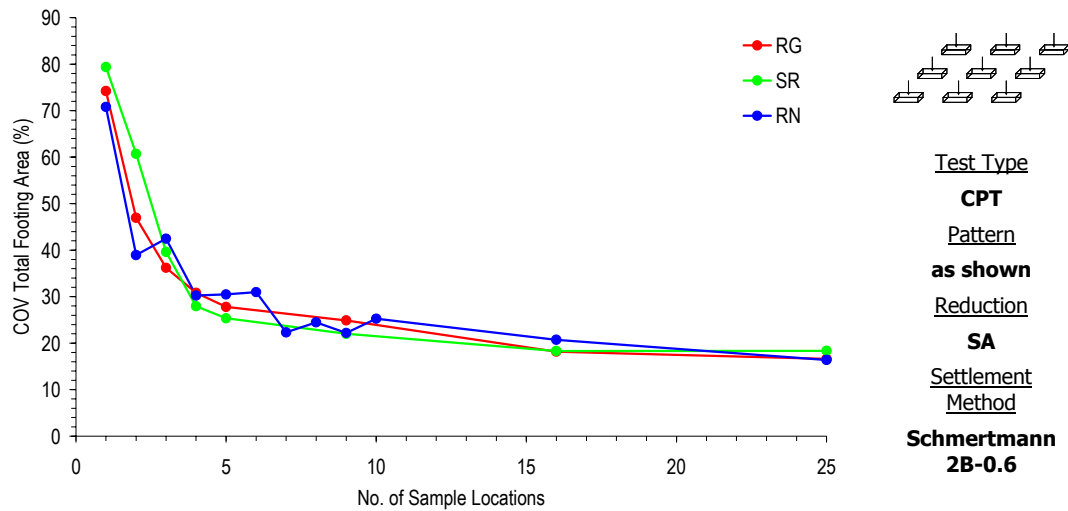


**Figure 6-29 Effect of increased sampling with different sampling patterns on the COV of total footing area, for a soil COV of 50% and SOF of 8 m**

In contrast to the sampling pattern, the reduction technique is shown to have a marked influence on the relationship between increased sampling and the design variability (measured as the standard deviation and  $COV_A$ ). The results in Figures 6-30 and 6-31 indicate that:

- The SA yields the most robust foundation designs;
- The MN yields a highly variable design compared with the other methods. Furthermore, the variability of the design based on the MN increases as the sampling effort grows; and
- The effect of increased sampling is similar for all reduction techniques investigated, except for the MN.

As with the results shown earlier in this chapter (§6.3.2), the ID and I2 techniques yield an erratic relationship between increased sampling and the variability of the design. However, the results in Figures 6-30 and 6-31 suggest that the relationship between increased sampling and design variability, for the ID and I2, also shows a general trend, where the COV of total footing area is reduced as the sampling effort increases. Furthermore, the

reduction in design variability for increased sampling, appears to be larger than the reduction in average total footing area, as shown earlier in this chapter (§6.3.2). This intimates that increased sampling has a greater impact on the variability of the design, than the average or expected foundation design.

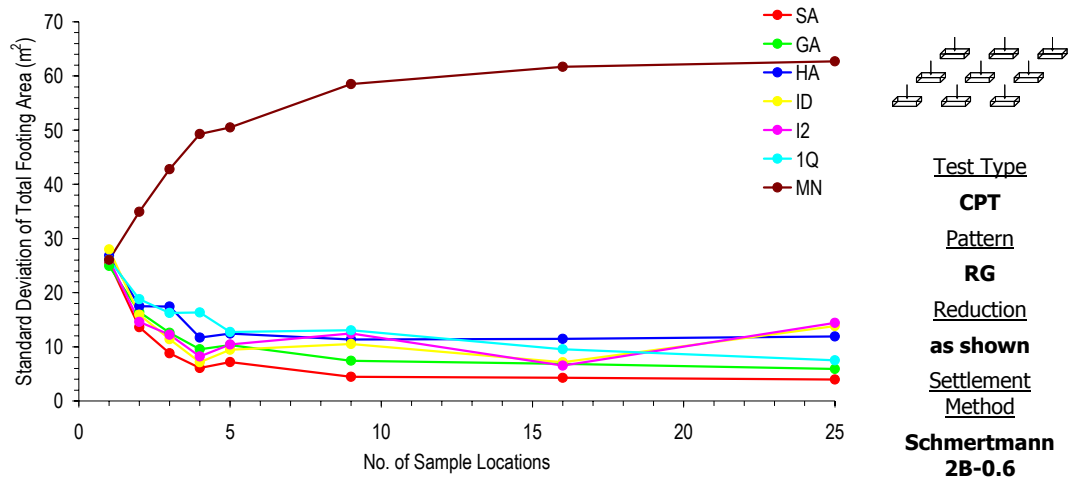


Figure 6-30 Effect of sampling with different reduction techniques on the standard deviation of total footing area, for a soil COV of 50% and SOF of 8 m

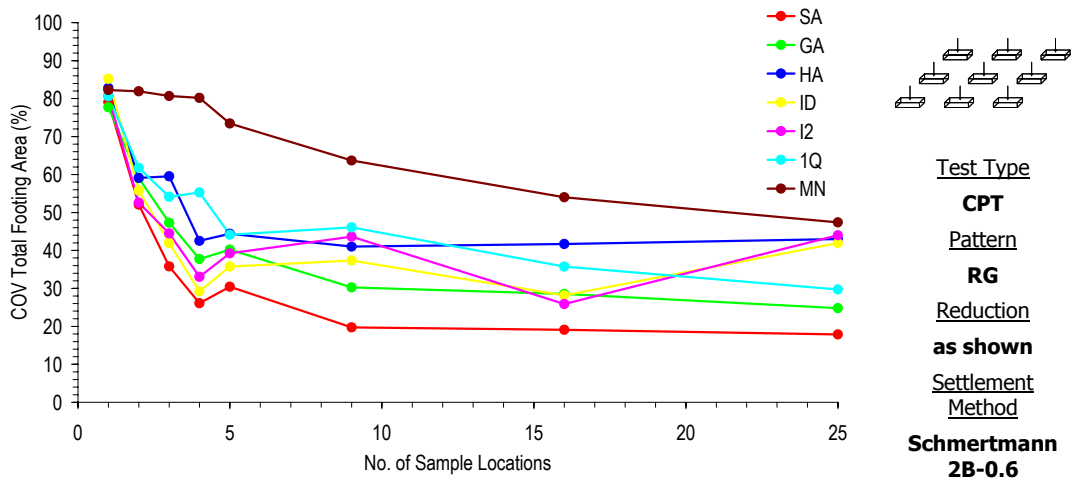


Figure 6-31 Effect of sampling with different reduction techniques on the COV of total footing area, for a soil COV of 50% and SOF of 8 m

### 6.4.3 Types of Soil Tests

Since different test types directly affect the variability of the design parameters (§6.2.3), it is also expected that they will have an impact on the variability of the footing design. As

such, the effect of increased sampling on the COV of total footing area based on different test types, is also examined. In this case, the analysis considers a site investigation that consists of sampling locations arranged in a RG and reduced using the SA. Results are given in Figures 6-32 and 6-33 for soils with an increasing COV and SOF, respectively.

Figures 6-32 and 6-33 suggest that the test type has an impact on the relative benefits of increased sampling. For instance, the design variability reduces at a faster rate, and by a greater percentage, for the TT than for any other test. However, this is largely a function of the vertical sampling rate, as the results using the TT appear to show the greatest benefit when the soil SOF is low (Figure 6-33). Given that the results using the TT are based on sampling 2 elastic moduli separated by 15 m at each sampling location, this test does not suffer from redundant information like the other types. However, when the soil SOF reaches 32 m [Figure 6-33(c)] the 2 samples taken for each sample location are more correlated.

The SPT is shown to have the least effect on the COV of total footing area for increased sampling. This test type is also shown to yield the footing design with the highest variability. This is a direct result of the large uncertainties assumed for the SPT, as shown in Table 6-1. The impact of a highly variable design on the reliability of the foundation design is discussed in subsequent chapters. However, the SPT has already been shown to yield highly conservative footing designs in Figures 6-21 and 6-22. Therefore, it is expected that the design error due to sampling with the SPT, will be large when compared to the CPT, TT and DMT.

As with the discussion earlier in this chapter (§6.3.3), it is also possible to describe theoretically the impact of measurement and transformation model errors on the design variability. Using the formulation shown in Equation (6.1), together with the expressions given in Equations (6.2) to (6.4), and given that the footing area,  $A$ , is proportional to a constant,  $\kappa$ , and inversely proportional to the resultant elastic modulus,  $E_r$ , as given by:

$$\begin{aligned}
 A &\propto \frac{\kappa}{E_r} \\
 \ln A &= \ln \kappa - \ln E_r \\
 \sigma_A^2 &= \sigma_{E_r}^2
 \end{aligned}
 \tag{6.9}$$

where  $\sigma_A^2$  and  $\sigma_{E_r}^2$  are the variances of the footing area and resultant elastic modulus value, respectively, then the relationship for the variance of the footing area,  $\sigma_A^2$ , is given by:

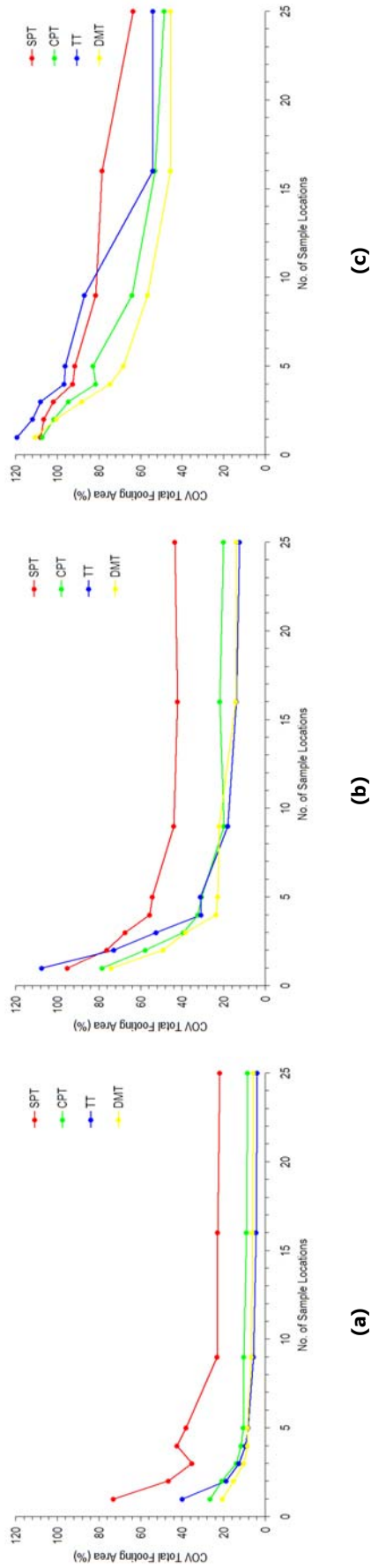


**Figure 6-32** Effect of sampling with different test types on the COV of total footing area of the 9-pad system, for a soil SOF of 8 m and COV of (a) 20%, (b) 50% and (c) 100%

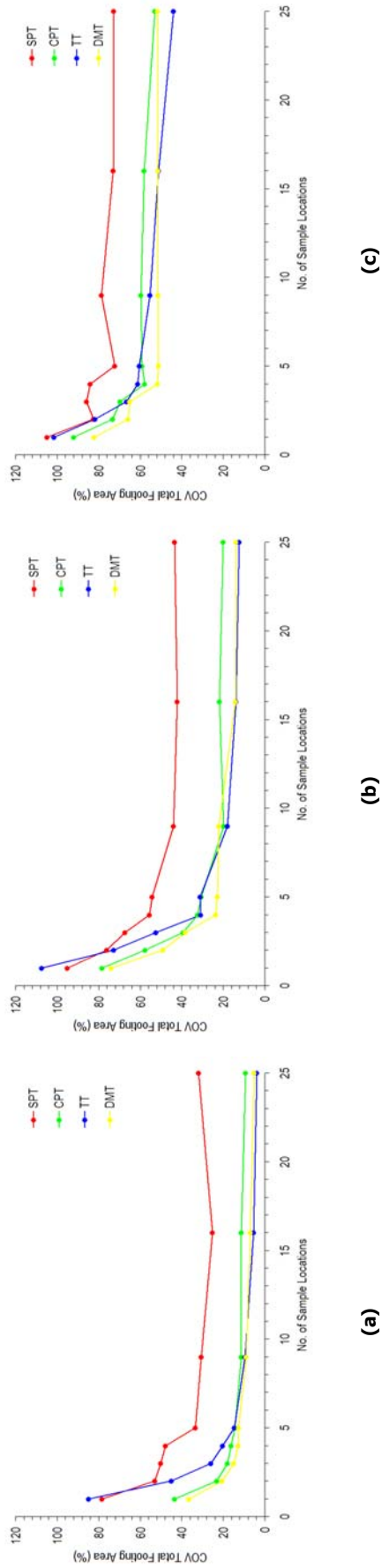


**Figure 6-33** Effect of sampling with different test types on the COV of total footing area of the 9-pad system, for a soil COV of 50% and SOF of (a) 1 m, (b) 8 m and (c) 32 m

$$\sigma_A^2 = \sigma_{E_r}^2 = \mu_{E_f}^2 \left\{ (1 + \sigma_{tm}^2)(1 + \sigma_{mb}^2)(1 + \sigma_{mr}^2)(1 + COV_{E_f}^2) - 1 \right\} \quad (6.10)$$

where  $\mu_{E_f}$  is the mean of the elastic modulus field value,  $COV_{E_f}$  is the coefficient of variation of the elastic modulus field and  $\sigma_{tm}^2$ ,  $\sigma_{mb}^2$  and  $\sigma_{mr}^2$  are the assumed variances of the transformation model and bias and random components of the measurement error, respectively, as defined by the COV values given in Table 6-1. Conditions in Equation (6.10) infer that, as:

$$\sigma_{tm}^2, \sigma_{mb}^2, \sigma_{mr}^2, COV_{E_f}^2 \uparrow \Rightarrow \sigma_A^2 \uparrow \quad (6.11)$$

and

$$\sigma_{tm}^2, \sigma_{mb}^2, \sigma_{mr}^2, COV_{E_f}^2 \rightarrow 0 \Rightarrow \sigma_A^2 \rightarrow 0 \quad (6.12)$$

Hence, as each source of error increases the variability of design area will also rise. However, as each source of error decreases the variability approaches zero. This effect has been shown earlier in this chapter in relation to the influence of soil variability, where the  $COV_A$  approached zero as the soil COV decreased. However, the conditions given in Equations (6.11) and (6.12) are also shown in Figure 6-32 and 6-33, where an increase in measurement and transformation model error, as represented by the different test types, yields a larger  $COV_A$ .

#### 6.4.4 Settlement Prediction Techniques

The influence of the different settlement methods on the design variability is also examined. Like the analysis for the different test types, this analysis considers only site investigations where the sampling locations are arranged in a RG and reduced using the SA technique. Furthermore, measurement and transformation model errors representative of the CPT are only considered. Results are expressed in terms of the COV of total footing area,  $COV_A$ , and are given in Figures 6-34 and 6-35 for an increasing soil COV and SOF, respectively.

Additional to the  $COV_A$ , based on the information from a site investigation, the results presented in Figures 6-34 and 6-35 also indicate the design variability based on 3DFEA and

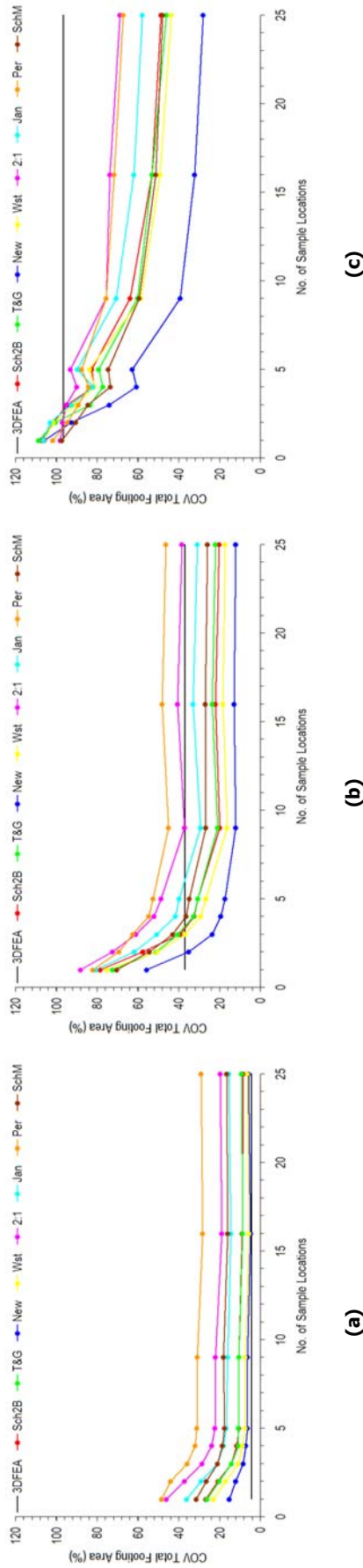


**Figure 6-34** Effect of sampling and settlement technique on the COV total footing area of the 9-pad system, for a soil SOF of 8 m and COV of (a) 20%, (b) 50% and (c) 100%

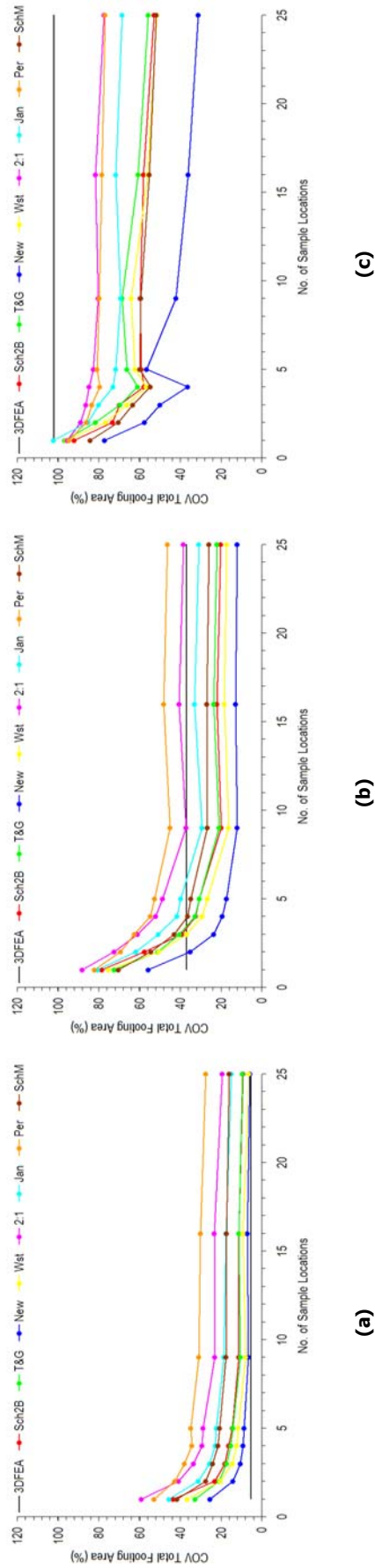


**Figure 6-35** Effect of sampling and settlement technique on the COV total footing area of the 9-pad system, for a soil COV of 50% and SOF of (a) 1 m, (b) 8 m and (c) 32 m

complete knowledge of the soil (CK). This allows comparisons between the variability of the design based on a site investigation (SI). In general, the results suggest that:

- The effect of increased sampling on the design variability is similar for each settlement method;
- The difference in design variability between settlement methods is exaggerated when the soil COV or SOF is large; and
- The design variability, based on 3DFEA and CK, is affected by an increasing soil COV and SOF more than the design based on a site investigation.

The similar trends shown for each settlement method is consistent with the results shown earlier in this chapter (§6.3.4), regarding the average total footing area. Furthermore, the increase in difference between settlement methods for soils with higher COV and SOF is a function of the apparent variability of the elastic moduli. A similar trend was observed in Chapter 5 (§5.3) where a larger footing was required when the soil COV and SOF was high. However, it is also important to consider that Figures 6-34 and 6-35 indicate the COV of total footing area, which is a normalised measure of the variability and is dependent on the average. Therefore, it is important to consider these results in conjunction with the effect of increased sampling on the average total footing area, as shown in the previous section (Figures 6-24 and 6-25).

**Increased sampling has a greater impact on the design variability than the use of different settlement prediction techniques.**

The sensitivity of the CK design to an increasing soil COV or SOF has been shown previously in Chapter 5 (§5.3). In those results, a similar trend to that shown in Figures 6-34 and 6-35 was apparent, where the variability of the design based on 3DFEA increased at a greater rate than the design based on the other settlement methods. In that case, however, both design types were based on complete knowledge of the soil. Nevertheless, the comparisons between the design types in Figures 6-34 and 6-35 has an impact on the probability of under- and over-design and the average design error, as discussed in the next chapter.

Since the effect of increased sampling is similar for each settlement prediction technique, it again appears that increased sampling has a greater impact on the design variability. This is consistent with the other results shown earlier in this section regarding the soil variabil-



ity, sampling pattern, reduction method and test type. Therefore, the greatest impact on design variability is the sampling effort where, in most cases, a high effort yields a less variable or more robust design.

## **6.5 SUMMARY**

---

The results in this chapter have identified the effect of site investigations on the design parameters and the design of a pad foundation. It was shown that both the design parameter and foundation design are significantly affected by the scope of the site investigation. It was also observed that the foundation design was affected by the settlement prediction technique used. However, this had little influence on the impact of increased sampling.

An investigation with an increased sampling effort was shown to yield a foundation design that is smaller than a design based on a limited site investigation. It was also illustrated that increased sampling has a similar effect on the variability of the design. The rate at which the footing area and variability reduced for an increased sampling effort, was shown to be a function of the reduction technique and variability of the underlying soil. However, this rate appears to be unaffected by the sampling pattern and the settlement method used.

The uncertainties due to measurement error were shown to have a notable influence on the foundation design, when the site investigation consists of few sampling locations. However, this quickly reduced as the number of locations increases and the measurement error is averaged out. At this point, the uncertainties due to transformation model error dominate. In all cases, the addition of uncertainties due to measurement and transformation model error increased the average and variability of the footing area.

Throughout this chapter, some comparisons between an optimal design and a design based on the result of a site investigation were possible. However, the majority of such comparisons are reserved for subsequent chapters. Instead, the results presented in this chapter illustrated the effect of including different forms of uncertainty and using site investigations of differing scopes on the conservatism of a foundation design.

The following chapter extends the analysis presented in this chapter by comparing the design based on a site investigation, with one based on complete knowledge, in a reliability framework. Such an analysis indicates whether the site investigation design yields a conservative solution, where the foundation is larger than required, or whether the design is prone to a failure, where the size is less.



## **Chapter 7    RELIABILITY ASSESSMENT OF A SITE INVESTIGATION IN TERMS OF FOUNDATION DESIGN**

### **7.1            INTRODUCTION**

---

The reliability analysis of a design generally involves investigating the effect of uncertain variables on the performance of the design in a probabilistic framework. Traditionally, this has meant that uncertainties in the strength and loads have been incorporated into the analysis to estimate the probability of failure. However, in this case, where a foundation design is sought, the uncertainties in strength have been incorporated into the analysis to estimate the probability that the resulting design is less than (under-design) or greater than (over-design) an optimal design. The uncertainties associated with the loads are not considered, as they are peripheral to the overall investigation. As such, the analyses presented in this chapter illustrate the effect of increased sampling on the probability of under- and over-design, as well as an additional measure called the design error. Probabilities and the design error are determined by comparing the foundation design based on the results from a site investigation, with the optimal design based on 3DFEA and complete knowledge of the soil, for each realisation of the Monte Carlo analysis. Although the design error is not technically a probabilistic measure, it is discussed in this chapter as it quantifies the degree of under- and over-design. Furthermore, it is used to demonstrate the reliability of a site investigation to provide a suitable site characterisation.

This chapter is divided into three sections. The first two sections examine the effect of sampling on the probabilities of under- and over-design and the design error. In these sections, the influences of soil variability and different site investigation scopes are explored. The third section of the chapter concerns the influence of individual sources of uncertainty on the design error. This section identifies the sensitivity of sampling location and the effect of measurement errors.

## **7.2 EFFECT OF SITE INVESTIGATION SCOPE ON THE PROBABILITY OF UNDER- AND OVER-DESIGN**

---

Reliability analyses in geotechnical applications typically present results in the form of a probability of failure or non-conformance, where the design does not meet the specified criteria. Such analyses make use of knowledge regarding the distribution of two random variables describing the capacity and load or, in the case presented in this research, the design area based on site investigation data (SI), and the design area based on complete knowledge (CK). With information regarding the distribution of the two variables, it is possible to use one of the reliability methods discussed in Chapter 2 (§2.4) to estimate representative probabilities, including a probability of failure. However, the distribution of footing area has been shown to be sufficiently complex where it is unable to be described adequately using a common statistical distribution. This makes the use of numerically based reliability analysis techniques inherently difficult. Therefore, it is necessary to use the results of the Monte Carlo analysis to derive probabilities of exceedance.

Rather than an analysis situation, where the performance of a nominated design or footing area is analysed to determine failure probabilities, the situation in this research is to compare a design based on a SI, with an optimal one based on CK. Therefore, instead of using the terminology of a probability of failure, it is more appropriate to refer to probabilities of under- and over-design. For example, as mentioned previously in Chapter 5 (§5.3), an under-design occurs when the footing design based on a SI is smaller than the optimal design. On the other hand, an over-design occurs when the SI design is larger than the optimal.

The results in this section illustrate the effect of increased sampling on the probability of under- and over-design of a pad foundation, where the SI design uses one of the settlement prediction techniques discussed in previous chapters, and the optimal design is based on 3DFEA and CK. The influence of inherent soil variability, different sampling programs, reduction techniques, test types and prediction techniques is also investigated.

### **7.2.1 Soil Variability**

The variability and correlation of the soil elastic moduli has been shown, in Chapter 6, to affect both the design parameter and the statistics of a footing design. Therefore, it is expected that the spatial variability will also have an impact on the reliability of a site investigation. As such, an examination of the effect of increased sampling on the probability of

under- and over-design for a 9-pad foundation system is undertaken for soils with varying COV and SOF. In this case, the site investigation is assumed to consist solely of sampling locations arranged in a regular grid (RG), reduced using the standard arithmetic average (SA), and including uncertainties that are representative of the CPT. Furthermore, the design based on the site investigation data (SI) uses the Schmertmann 2B-0.6 method, while the complete knowledge design (CK) is based on 3DFEA settlement estimates. All analyses presented in this chapter concerning the 9-pad system, assume a mean elastic modulus of 30,000 kPa. Results are given in Figures 7-1 and 7-2 for soils with an increasing COV and SOF, respectively. Each figure is separated into two parts, where Figures 7-1(a) and 7-2(a) show the probability of under-design and Figures 7-1(b) and 7-2(b) illustrate the probability of over-design.

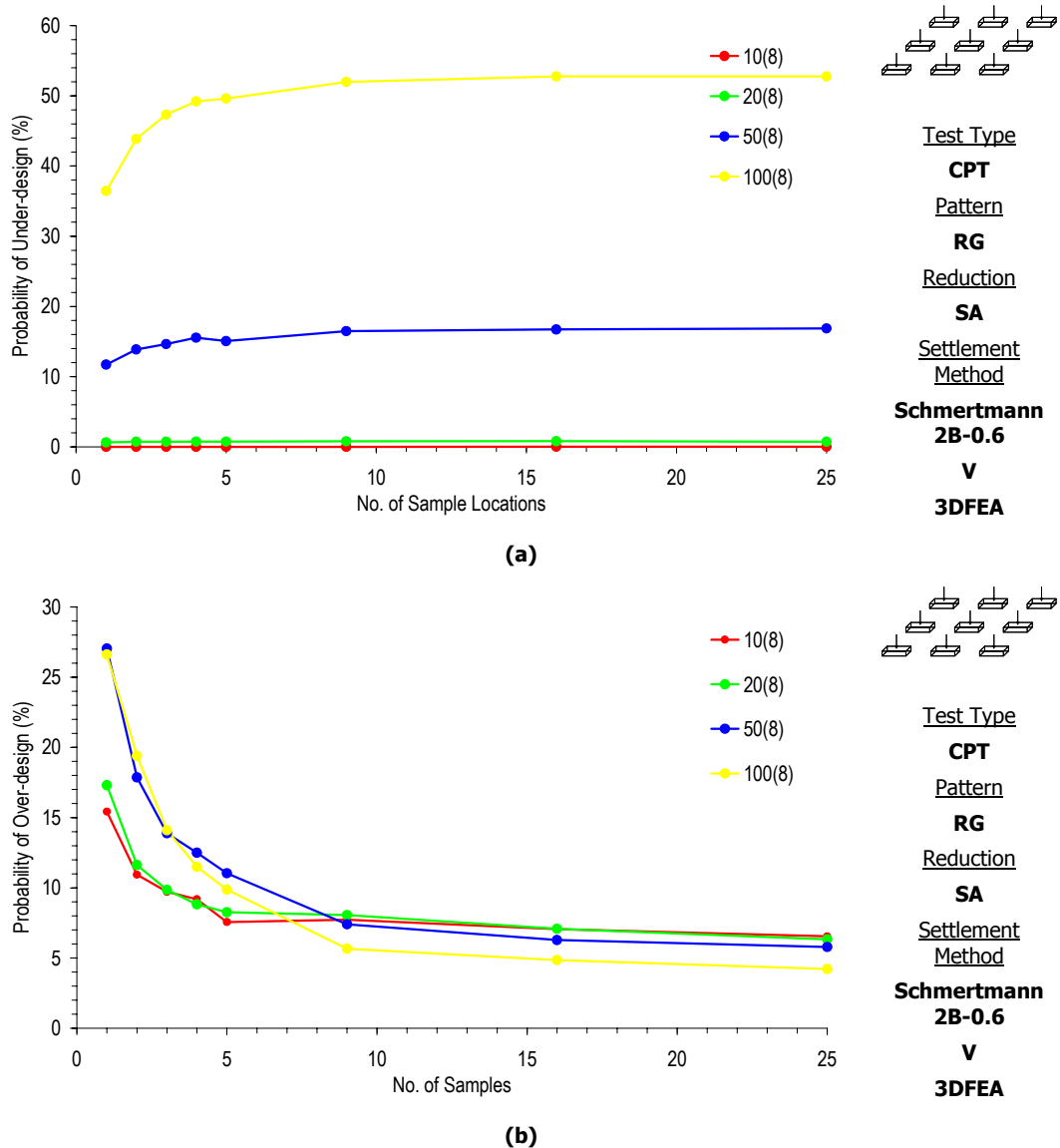


Figure 7-1 Effect of sampling on the probability of (a) under- and (b) over-design, for an increasing soil COV (SOF of 8 m)

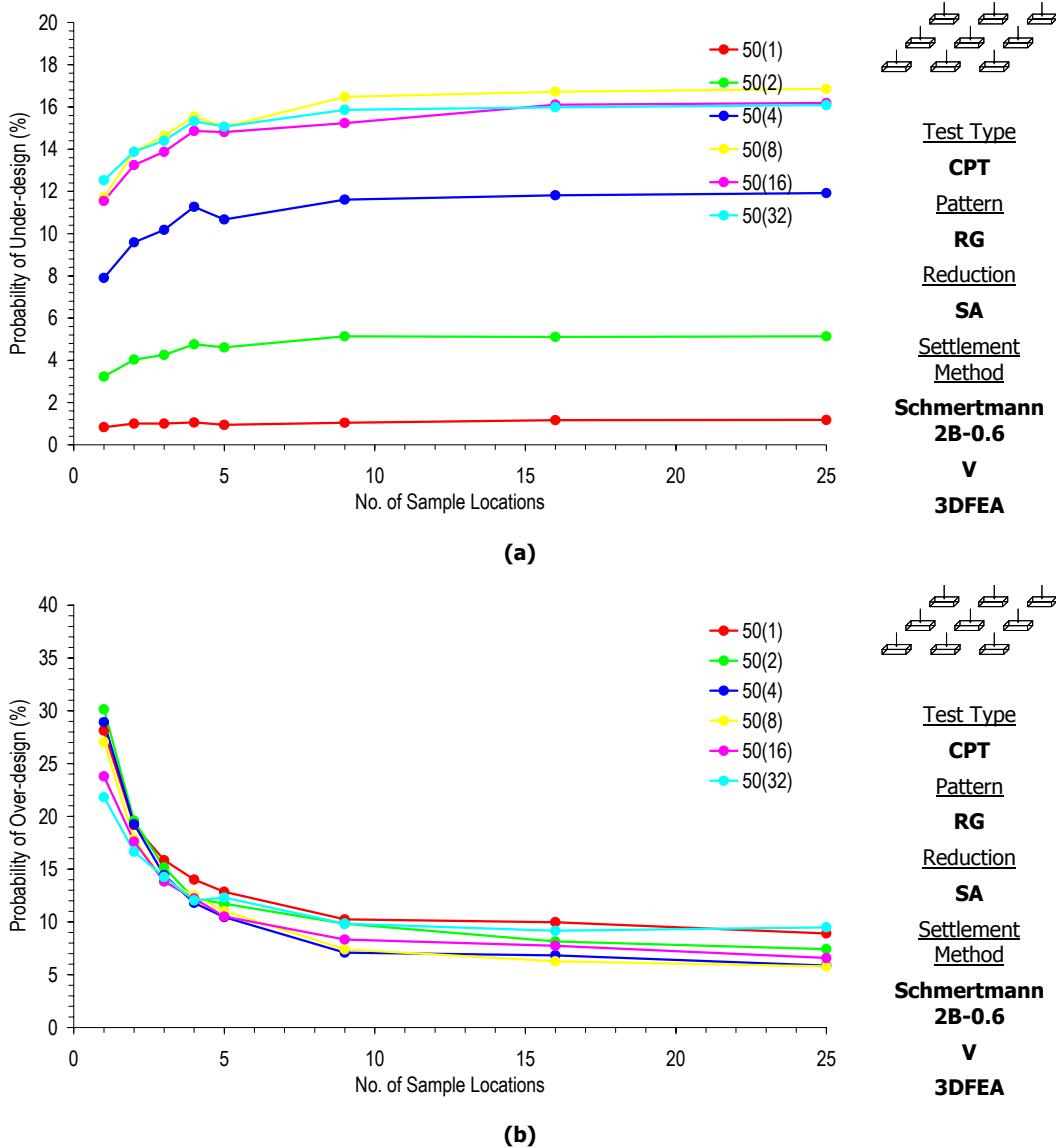


Figure 7-2 Effect of sampling on the probability of (a) under- and (b) over-design, for an increasing soil SOF (COV of 50%)

From the results shown in Figures 7-1(a) and (b), the following general trends are observed:

- As the sampling effort increases, the probability of under-design rises and the probability of over-design diminishes;
- The impact of increased sampling is greater on the probability of over-design than the probability of under-design;
- For an intensive sampling effort (e.g. 25 sampling locations) the probability of over-design is less for foundations on soils with a higher COV. On the other

hand, when the sampling effort is low (e.g. 1 sample location), the probability of over-design is greater when the soil has a high COV;

- The probability of under-design is hardly affected by increased sampling for a soil with a COV of 20% or less;
- The soil COV has a greater impact on the probability of under-design than the probability of over-design; and
- The probabilities of under- and over-design are relatively constant when more than 10 sample locations are considered.

The increase in probability of under-design may seem at first, counter-intuitive. However, it is important to recall that increased sampling leads to a reduction in the average total footing area, as shown in Chapter 6 (§6.3.1). Therefore, as the average footing area reduces, the probability of under-design increases, because the likelihood that a design will be less than the optimal rises. However, such an increase in probability of under-design is mirrored by a reduction in over-design, as shown in Figure 7-1(b).

Although the soil COV is shown to have a notable influence on the probabilities, the results in Figure 7-1(b) for the over-design condition, indicate that the benefits of increased sampling are similar for a soil COV of 50% and 100%. This contradicts the results shown in Figure 7-1(a), where the probability of under-design increases as the soil COV escalates. Such differences between the probability of under- and over-design have been shown previously in Chapter 5 (Figure 5-30) for varying soil COVs, where the effects of sampling were not considered. In those results, the probability of under-design grew continually as the soil COV increased. However, the probability of over-design was shown to reach a maximum when the soil COV was 50%. As discussed in Chapter 5 (§5.3), this discrepancy is a result of the comparative rates at which the soil COV and SOF affect the average and variability of the design. To some extent, these influences have been discussed in Chapter 6 (§6.3 and §6.4).

The soil SOF is shown to have less impact on the probability of under- and over-design than the soil COV, as shown in Figure 7-2. However, the results do indicate that:

- In most cases, the probability of under-design is the highest, and the probability of over-design is the lowest, when the soil has a SOF of 8 m. This corresponds with a worst case SOF, as discussed in previous chapters;

- Increased sampling has little impact on the probability of under-design when the soil SOF is lower than 2 m; and
- The soil SOF has a greater influence on the probability of under-design than the probability of over-design.

The worst case SOF, as discussed in previous chapters and illustrated in Figure 7-2, is a function of the apparent variability of the elastic moduli and local averaging effects. Such a worst case SOF allows the estimation of a limiting condition without accurate estimation of the soil SOF. This has been discussed previously in Chapter 4 (§4.2.1) and observed in results shown in Chapter 5 and 6.

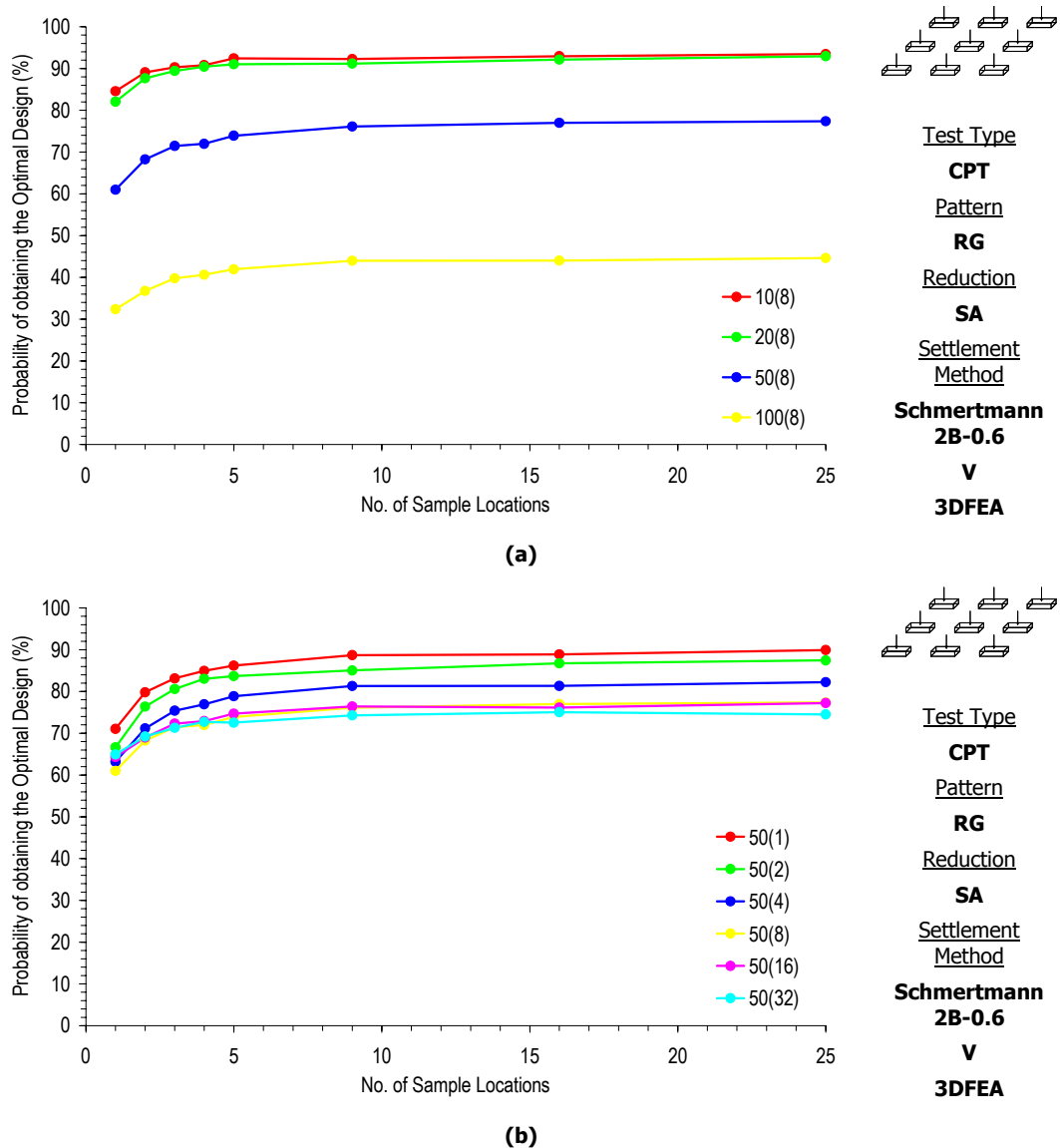
Since the results shown in Figures 7-1 and 7-2 indicate opposing trends for the probability of under- and over-design, an analysis examining the probability of obtaining an optimal design is undertaken. This is the condition where the SI design yields the same area for each footing as the design using 3DFEA and CK. These results are given in Figure 7-3(a) and (b) for increasing COV and SOF, respectively. It should be noted that for an optimal design to occur, the SI footing design must be exactly the same as the optimal design. Therefore, an optimal design does not occur if, by chance, the total footing areas are the same, but the individual footing areas are different. In this case, the number of footings that are less than, or greater than, their corresponding optimal design, contribute to the probability of under- and over-design, respectively.

Figure 7-3 indicates that the probability of obtaining an optimal design rises as the sampling effort increases. As opposed to the results regarding the probability of under- and over-design, shown in Figures 7-1 and 7-2, there appears to be little benefit for increased sampling in soils with a higher COV. Instead, the probability of obtaining an optimal design appears to increase at the same rate for each of the soil conditions investigated. However, the results shown in Figure 7-3(b) do suggest the presence of a worst case SOF, where the probability of obtaining an optimal design is the least. As before, this worst case SOF appears to occur when the soil SOF is approximately 8 m.

Although previous analyses have indicated that the site investigation design does not favour one footing in the foundation system, the probability of under- and over-design, as well as the probability of obtaining an optimal design, is also examined for each individual pad footing. These results are given in Figure 7-4 for four different soils and the same site investigation conditions used in the analyses presented above. As such, the probability of



under- and over-design, as well as the probability of obtaining an optimal design, are almost identical for footings that share the same loads and same relative position in the foundation system. However, there are differences between footings that do not share the same applied load or relative position. For example, the central edge footings show a greater probability of over-design, and smaller probability of under-design than the corner footings. Furthermore, the central footing shows a larger probability of over-design, and a smaller probability of under-design. This suggests that the probabilities are heavily dependent on the applied load where the centre footing is required to carry the greatest load, and the central edge footings are designed to support a larger load than the corner footings.



**Figure 7-3** Effect of sampling on the probability of obtaining the optimal design, for an increasing soil (a) COV (SOF of 8 m) and (b) SOF (COV of 50%)

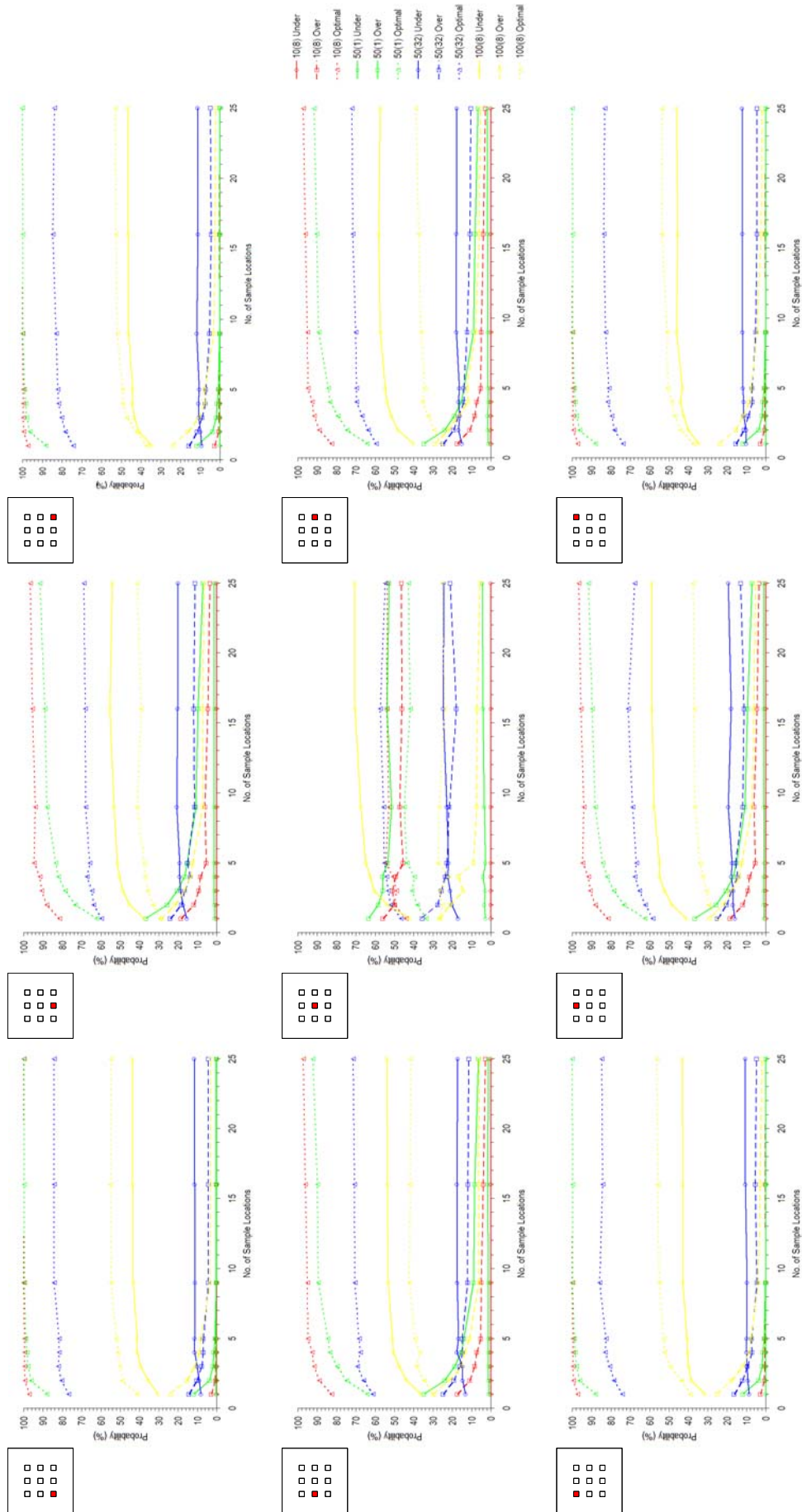


**Figure 7-4** Effect of sampling on the probability of under- and over-design, and probability of obtaining an optimal design, for each footing in the 9-pad system, based on a SI (RG, SA, CPT)

Figure 7-4 also indicates that the effect of increased sampling has a greater effect on the probability of under- and over-design, as well as the probability of obtaining an optimal design, for the central edge footings as compared to the other footings in the foundation system. Hence, it is not possible to conclude that the effect of increased sampling is dependent on the size of the applied load. Rather, it is a function of the relative position of the footing in the foundation system and the arrangement of sampling locations. This explains why there is little effect of sampling shown for the central footing. In this case, a sample location is typically located near the central footing for most of the RG sampling plans (Figure 3-7).

In addition to the probabilities of under- and over-design, and the probability of obtaining an optimal design, a probability that a pad foundation will not satisfy the design criteria, is also examined. This condition is considered the probability of requiring an alternative design where such an alternative design may be a strip, raft or piled foundation. The criteria for requiring an alternative foundation design has been previously discussed in Chapter 3 (§3.5.2) and is based on the total size of the foundation design. The results illustrating the effect of increased sampling on the probability of requiring an alternative design are given in Figures 7-5(a) and (b), for soils with an increasing COV and SOF, respectively. As before, the SI designs are based on the Schmertmann 2B-0.6 method, with sampling locations arranged in a RG, reduced using the SA and including uncertainties representative of a CPT.

The relatively low probability of requiring an alternative design, in Figure 7-5, suggests that the assumed mean elastic modulus of 30,000 kPa allows a viable pad foundation design for most situations. However, the results also show that, as the sampling effort increases, the probability of requiring an alternative foundation decreases. This is consistent with the results shown in Figures 7-1(b) and 7-2(b), for the probability of over-design. The similarities between the probability of over-design and requiring an alternative design are due to the manner in which an alternative foundation type is required. As discussed in Chapter 3 (§3.5.2), an alternative foundation type is needed when the pad foundation design is large, which is when the foundation is largely over-designed.

Figure 7-5(a) indicates that an alternative foundation design is generally required only when the soil COV is 100%. This is because larger footings are required when the COV is high, as discussed previously in Chapter 5 (§5.3) and Chapter 6 (§6.3). Furthermore, the results in Figure 7-5(b) indicate that as the soil SOF increases, the probability of requiring an alternative foundation type also rises. However, the effect of increased sampling does

not appear to be influenced greatly by the soil SOF, as was the case for the probability of over-design [Figure 7-2(b)].

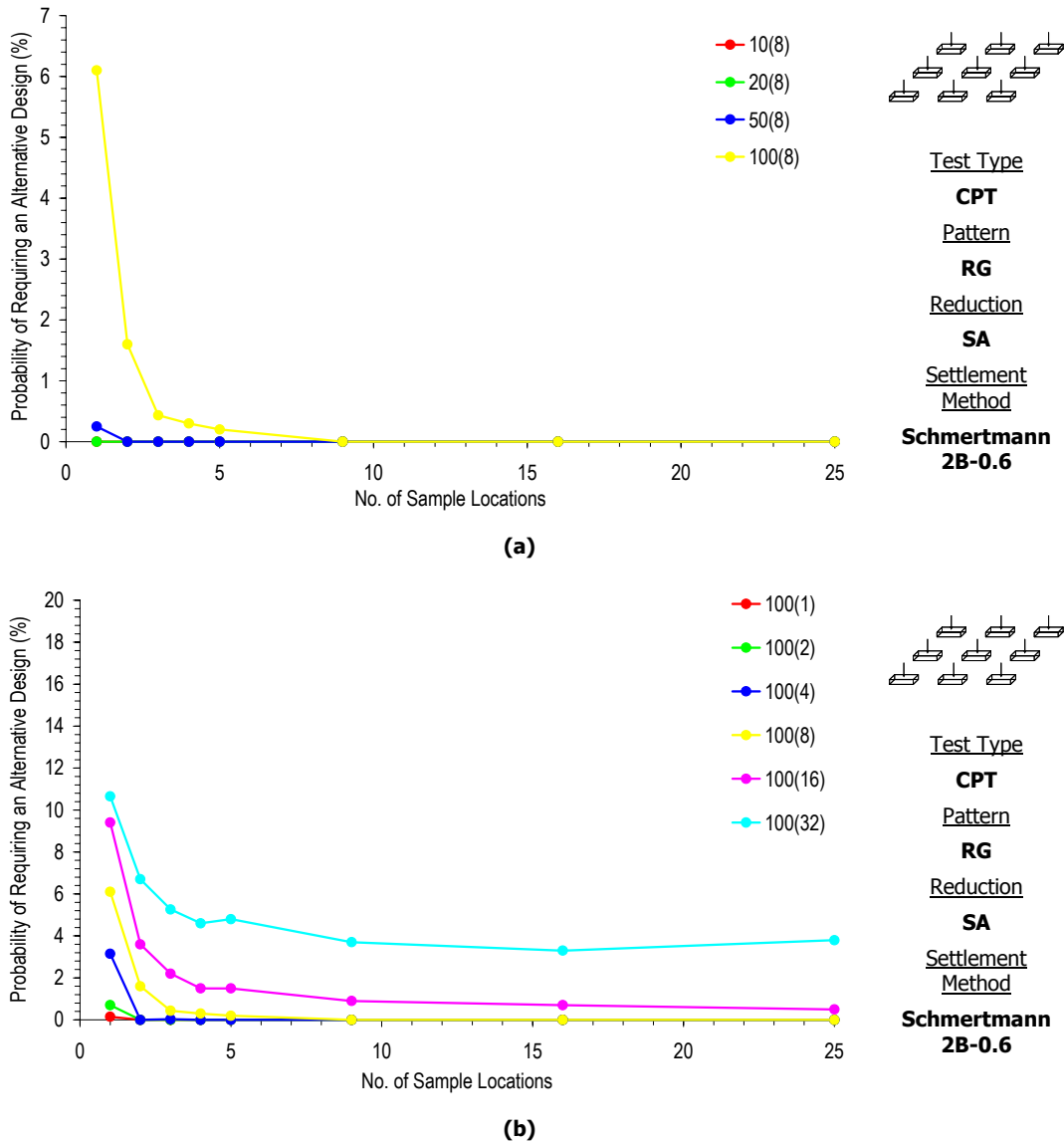


Figure 7-5 Effect of sampling on the probability of a requiring an alternative design for the 9-pad system for an increasing soil COV and SOF of 8 m

### 7.2.2 Sampling Patterns and Reduction Techniques

In addition to the analysis examining the effect of increased sampling on the probability of under- and over-design for soils with varying COV and SOF, an analysis is also conducted to measure the impact of using different sampling patterns and reduction techniques. Similar to the analysis in the previous section, the SI design is based on the Schmertmann 2B-0.6 method and uncertainties representative of the CPT. However, rather than investigating the effects of increased sampling for several different soils, only a soil COV of 50% and

SOF of 8 m is examined. Such a SOF of 8 m corresponds to the worst case SOF, discussed previously, and a COV of 50% was shown to yield results that were similarly affected by increased sampling as a soil COV of 100% [Figure 7-1(b)]. Nevertheless, the effects of increased sampling with different sampling patterns and reduction techniques on the probability of under- and over-design, as well as the probability of obtaining an optimal design for other soil types, are given in Appendix B.

Results based on different patterns are presented in Figure 7-6. These results indicate that the use of different patterns has little impact on the probabilities, or the effect of increased sampling. The only minor differences occur when the sampling effort is low (e.g. less than 5 sampling locations). In these cases, the SR is slightly more conservative than the other patterns, leading to a higher probability of over-design. However, this difference is never more than 5%, which, considering the errors associated with the Monte Carlo analysis (§3.7.2) and the convergence of 3DFEA (§3.6.5), is almost negligible. Furthermore, when more than 5 sampling locations are considered, the probabilities are almost identical for the three different patterns. This result is consistent with those presented in Chapter 6 (§6.3.2), where the average total footing area was shown to be very similar for all sampling conditions and patterns.

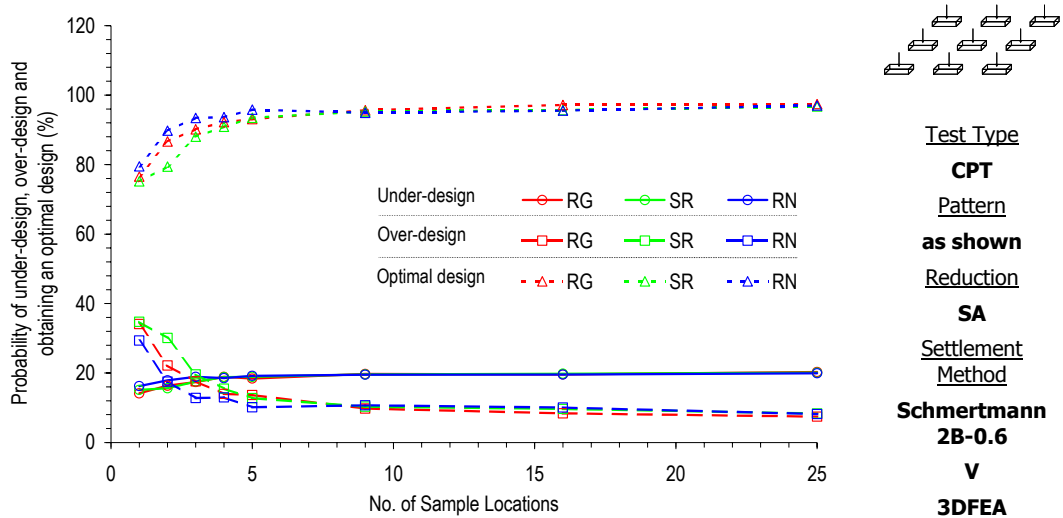


**Figure 7-6 Effect of sampling with different sampling patterns on the probability of under- and over-design and the probability of obtaining an optimal, for a soil COV of 50% and SOF of 8 m**

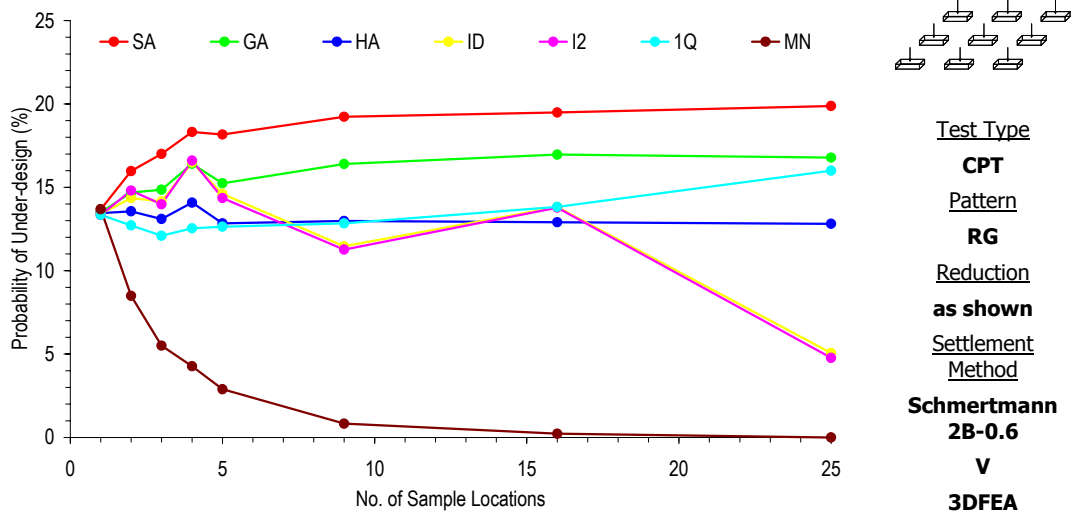
The results of the analysis dealing with different reduction techniques are given in Figure 7-7. Such results indicate that the reduction technique has a notable impact on the probabilities. As such, the following general conclusions are made:

- The MN technique yields a design with a very high probability of over-design and low probability of under-design;
- The probability of under-design increases and the probability of over-design diminishes as the sampling effort rises for all methods except the MN;
- Excluding the MN, the SA technique is affected by increased sampling more than any other method;
- The ID and I2 methods yield an erratic relationship between the probabilities and increased sampling; and
- The probability of obtaining an optimal design increases as the sampling effort grows, for all methods except the MN.

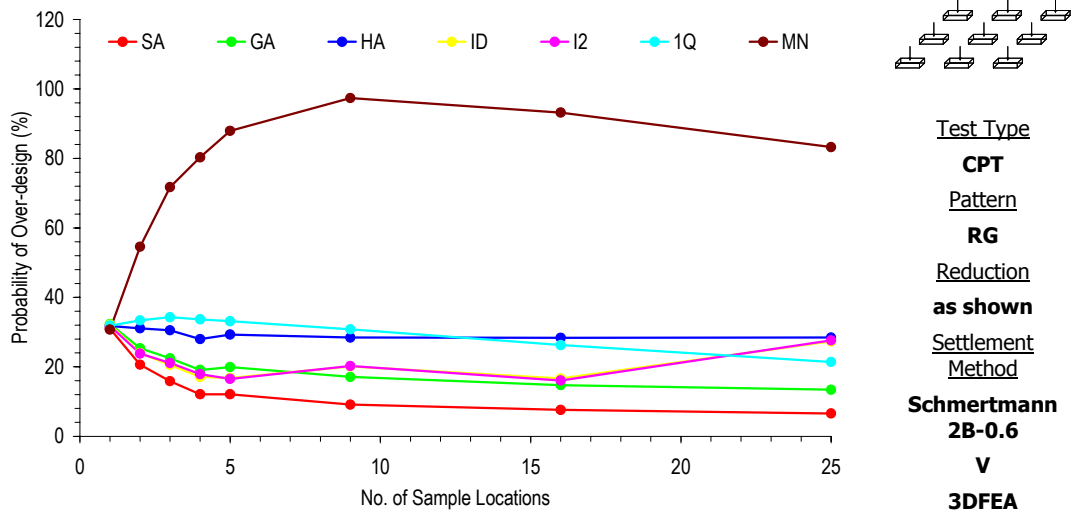
The high probability of over-design shown by the MN is consistent with the results presented in Chapter 6 (§6.3.2), where the MN yielded highly conservative designs that became more conservative as the sampling effort grew. However, the high probability of over-design is mirrored by a low probability of under-design that decreases as the sampling effort increases. This is in stark contrast to the other techniques that all show opposing trends.

**The MN reduction technique yields designs with a high probability of over-design that increases as the sampling effort grows.**

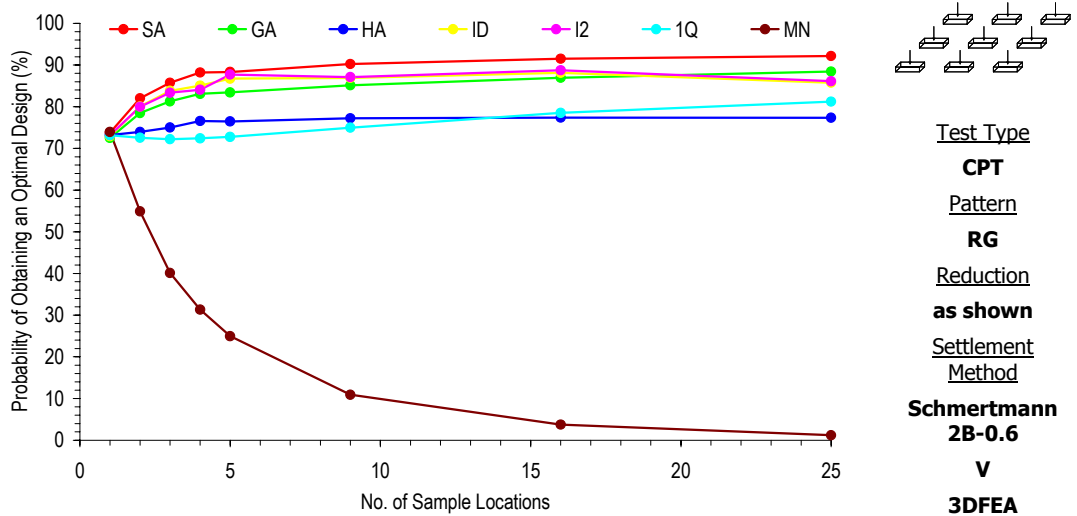
The SA technique is shown to yield the foundation design with the least probability of over-design. As such, it is also the method that is affected the most by increased sampling, excluding the MN. However, because the SA yields a low probability of over-design, it also results in the highest probability of under-design. This is consistent with the results shown in Chapter 6 (§6.3.2), where the SA produced the least conservative design with the smallest average total footing area. The other reduction techniques (not including MN) appear to yield designs with varying degrees of increased conservatism, where the probability of under-design is smaller and the probability of over-design is larger than the results using the SA. Again, these results appear to be consistent with those presented in Chapter 6 (§6.3.2), where the methods that resulted in more conservative designs show a lower probability of under-design [Figure 7-7(a)] and a higher probability of over-design [Figure 7-7(b)].



(a)

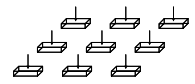


(b)



(c)

**Figure 7-7 Effect of increased sampling with different reduction techniques on the probability of (a) under- and (b) over-design and (c) the probability of obtaining an optimal, for a soil COV of 50% and SOF of 8 m**



Test Type

CPT

Pattern

RG

Reduction

as shown

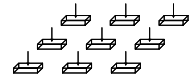
Settlement

Method

Schmertmann  
2B-0.6

V

3DFEA



Test Type

CPT

Pattern

RG

Reduction

as shown

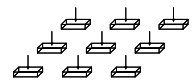
Settlement

Method

Schmertmann  
2B-0.6

V

3DFEA



Test Type

CPT

Pattern

RG

Reduction

as shown

Settlement

Method

Schmertmann  
2B-0.6

V

3DFEA

**The SA yields a low probability of over-design, but a high probability of under-design.**

The GA technique is only marginally less affected by increased sampling when compared to the SA. The reduction techniques based on weighting the distance between the sample and footing locations (ID and I2) appear to be erratically affected by increased sampling. This was also observed in Chapter 6 (§6.3.2), where no particular trend was apparent for the effect of increased sampling on the average total footing area. As discussed in Chapter 6 (§6.3.2), the erratic behaviour is caused by the occurrence of a sampling location coinciding with a footing. In that particular case, the design of the footing considers only the elastic moduli from the single sampling location and the remaining data is ignored. This has an impact on the apparent variability of the elastic moduli and therefore, the foundation design. As such, it is recommended that, when using the ID or I2, the elastic moduli from all sampling locations should be considered, even if one sampling location coincides with the footing.

**When using the ID and I2, information from all sampling locations should be considered.**

The 1Q and HA reduction techniques are the least affected by increased sampling. Both techniques yield designs that have probabilities of under- and over-design, as well as probabilities of obtaining an optimal design, which are very similar for all sampling conditions. However, the formulation of the 1Q and HA are quite different, where the HA is an averaging technique and the 1Q is a selection process. Although the results in Figure 7-7 suggest that the probabilities for these two techniques are similar, they do appear to be affected differently by increased sampling. For example, increased sampling with the 1Q has a near-linear affect on the probability of under-design and obtaining an optimal design. Such a linear relationship suggests that the probabilities may continually increase or decrease. By definition however, the results must reach a constant probability (it is not possible to increase past 100% probability or reduce past 0%). Nevertheless, the results shown in Figure 7-7 suggest that such a constant is not reached before the results from 25 sample locations are considered. Unlike the 1Q, the techniques based on averaging (SA, GA, and HA) seem to show an exponential behaviour, where probabilities of under- and over-design, as well as probabilities of obtaining an optimal design, vary considerably for small changes in sampling effort when only few sample locations are considered. After approximately 9 sample locations, these methods reach a relatively constant probability.



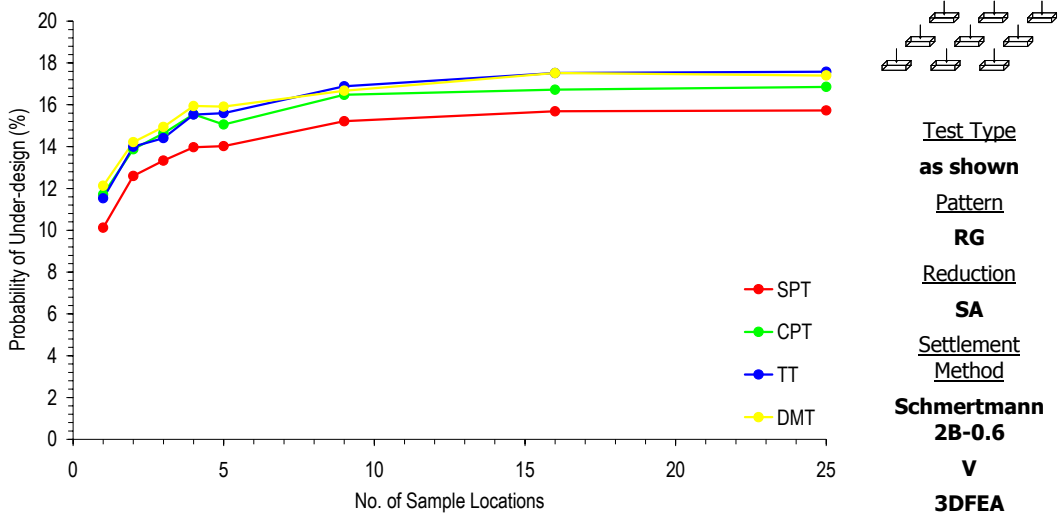
The SA method yields the highest probability of obtaining an optimal design, which at first glance, suggests that it is the best performing technique. However, the difference between settlement methods must also be considered, where the Schmertmann 2B-0.6 method (Sch2B) was shown, in Chapter 5 (§5.2.1), to yield slightly conservative settlement estimates. Therefore, the high probability of achieving an optimal design shown for the SA, infers that the conservatism in the Schmertmann 2B-0.6 method is negated by the site investigation. A similar effect was also observed in Chapter 5 (§5.2.3), where the averaging of elastic moduli within an increasing influence region was shown to negate the conservatism of the Schmertmann 2B-0.6 method.

### 7.2.3 Types of Soil Tests

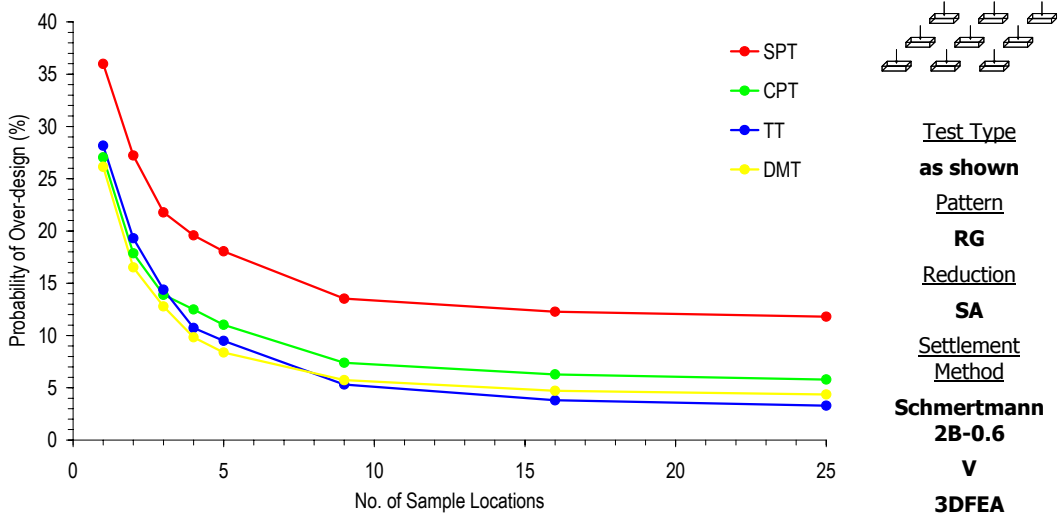
The four different test types investigated in this research (SPT, CPT, DMT and TT) were shown in Chapter 6 (§6.3.3) to yield designs with different degrees of conservatism. As such, each test type is expected to have an impact on the probability of under- and over-design, as well as the probability of obtaining an optimal design. Therefore, an analysis is conducted to investigate the impact of different test types on the probability of under- and over-design, as well as the probability of obtaining an optimal design. Again, this is achieved by comparing designs based on information from a site investigation (SI) with an optimal design using 3DFEA and CK. The SI design, in this case, is based on a site investigation where sample locations are arranged in a RG and reduced using the SA. As with previous analyses, the SI designs are based on the Schmertmann 2B-0.6 settlement method. The different test types are distinguished by the assumed measurement and transformation model errors, as discussed in Chapter 3 (§3.4.3). The results comparing the tests are presented in Figure 7-8. These results are based on a soil COV of 50% and SOF of 8 m. Additional results are also given in Appendix C.

The results in Figure 7-8 lead to the following general conclusions:

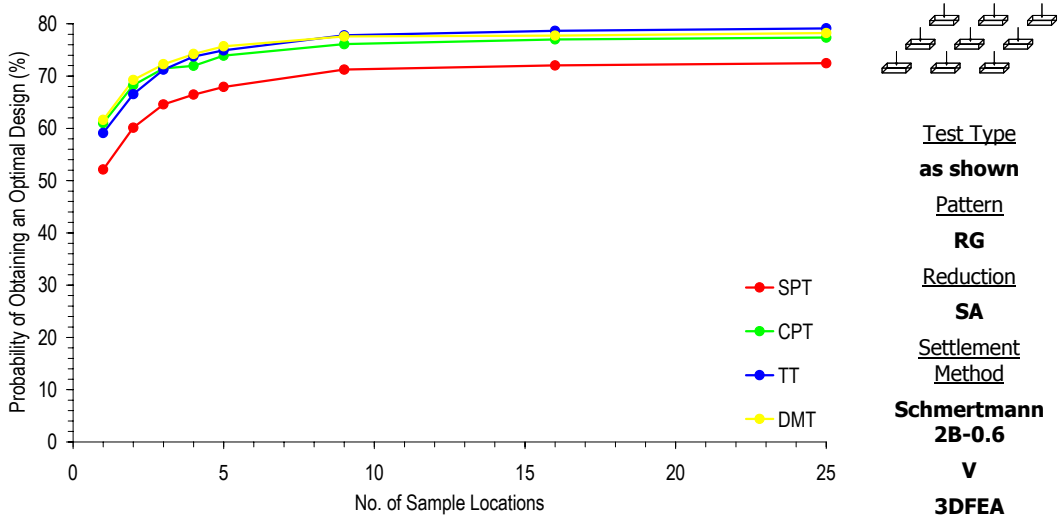
- The SPT yields the lowest probability of under-design and highest probability of over-design for all sampling conditions;
- The TT is more affected by increased sampling than the CPT or DMT. This leads to the TT showing the least probability of over-design when 25 sample locations are considered; and



(a)



(b)



(c)

Figure 7-8 Effect of sampling with different test types on the probability of (a) under- and (b) over-design and (c) the probability of obtaining an optimal design, for a soil COV of 50% and SOF of 8 m

- The CPT and DMT yield very similar probabilities of under- and over-design, as well as probabilities of obtaining an optimal design. The relationship between increased sampling and such probabilities is very similar for the CPT and DMT.

The low probability of under-design and high probability of over-design shown by the SPT infers that this test type is the most conservative. This is consistent with results shown in Chapter 6 (§6.3.3) and is a function of the assumed measurement and transformation model errors (§3.4.3). Furthermore, the SPT appears to be least affected by increased sampling, which is due to its high transformation model error that does not average out with increased sampling.

It is difficult to distinguish many differences between the CPT and DMT. This is because the assumed measurement and transformation model errors for both tests are very similar. The main difference between these two test types is the vertical sampling rate. However, due to the constraints on the element size (§3.6.5.3), the relative vertical sampling frequency for the CPT is not truly representative of the test implementation. Instead, in real applications, the CPT is expected to yield many more properties than the DMT.

Figure 7-8 also allows conclusions regarding the effect of measurement and transformation model errors. These effects have also been discussed previously in Chapter 6 (§6.3.3 and §6.4.3), where the effect of measurement error was observed to progressively reduce, as the sampling effort increased. A similar phenomenon is observed in Figure 7-8, where the TT yields a design with a higher probability of over-design than both the CPT and DMT, when 1 sampling location is considered. However, as the sampling effort increases, the probability of over-design, based on the TT, reduces and becomes less than the CPT and DMT. This is because the measurement errors associated are averaged out with increased sampling, leaving only the transformation model error that, for the TT, is assumed to be zero. As a result, it appears to be of greater benefit to use a test type that has a low transformation model error when a large number of sample locations are used. On the other hand, when only few samples are considered, it appears beneficial to use a test type that has a low measurement error. This does not however, infer that test types with a high measurement error and a low transformation model error will necessarily yield designs with less probability of over-design than a test type with a moderate measurement and transformation model error. Although, it does allow a better selection of test type, given knowledge regarding the sampling effort. Additional discussion regarding the use of different types of tests is reserved for later in this chapter and Chapter 8.

**It is recommended to use a test type with a low transformation model error when a large number of locations are possible. However, if only few sampling locations are possible, it is recommended to use a test type with a low measurement error.**

#### **7.2.4 Settlement Prediction Techniques**

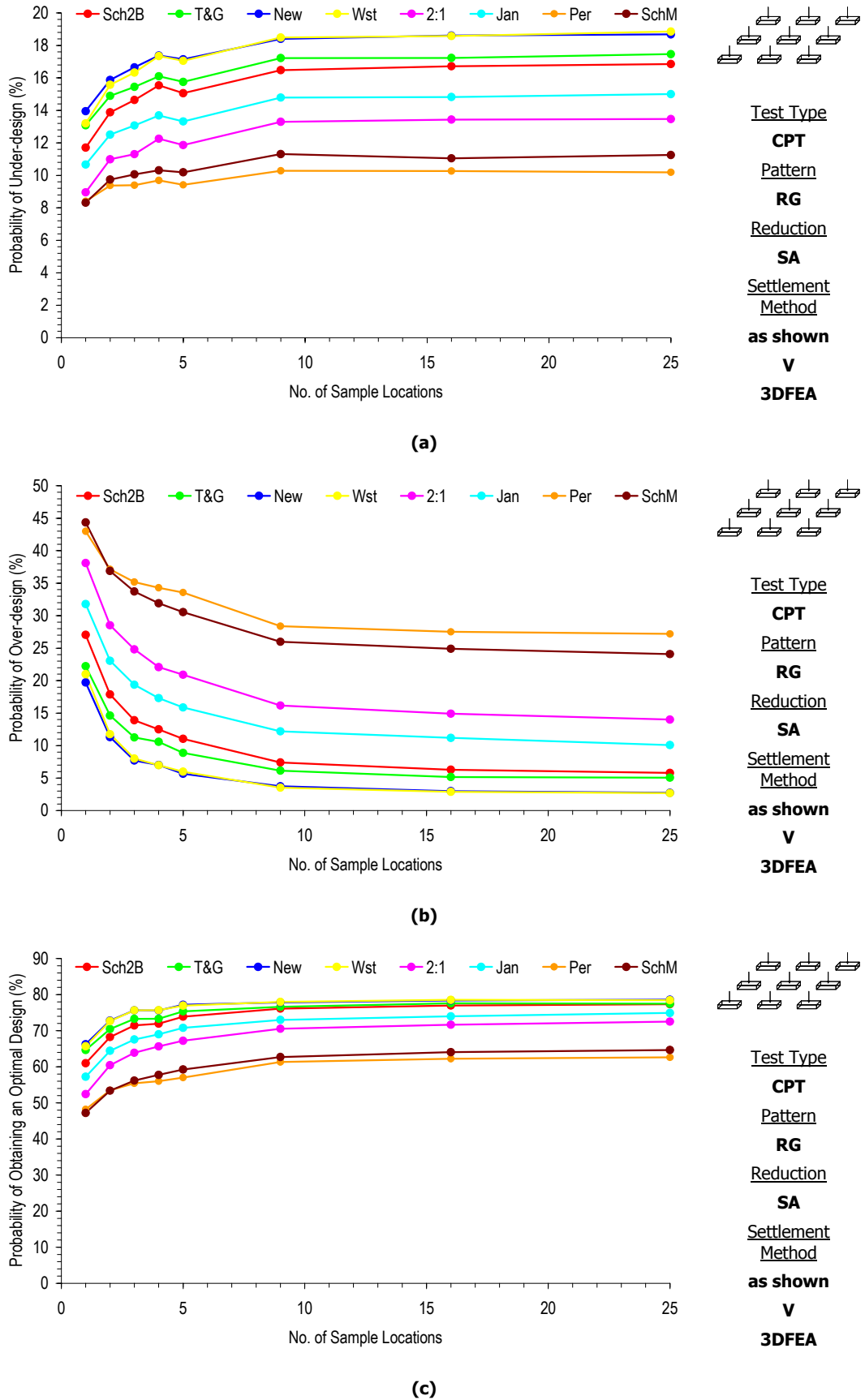
The final examination of the effect of increased sampling on the probability of under- and over-design, as well as the probability of obtaining an optimal design, involves the different settlement prediction techniques, as discussed in Chapter 3 (§3.6.2). In this case, the data for the SI design is based on sampling locations arranged in a RG, reduced using the SA and with uncertainties representative of the CPT. As with all previous analyses presented in this chapter, the SI design is compared to an optimal design that is based on the complete knowledge of the soil (CK) and 3DFEA. Results are given in Figure 7-9 for a soil COV of 50% and SOF of 8 m. Additional results for other soil COVs and SOFs are included in Appendix C.

Figure 7-9 indicates that the effect of increased sampling on the probabilities of under- and over-design, as well as the probability of obtaining an optimal design, is hardly influenced by the use of different settlement prediction techniques. This is consistent with the results shown in Chapter 6 (§6.3.4), where increased sampling was shown to have a similar effect for all settlement methods investigated. However, Figure 7-9 does allow some conclusions regarding the conservatism of the settlement methods and their impact on the probabilities. These conclusions include:

- The Perloff method yields the most conservative design, resulting in a high probability of over-design and a low probability of under-design;
- The Newmark model yields the least conservative design, resulting in a low probability of over-design and high probability of under-design; and
- Settlement methods that yield a high probability of under-design also result in a high probability of obtaining an optimal design.

#### **7.2.5 Summary**

It is important to note that all results in this section are based on comparisons with designs using 3DFEA and complete knowledge of the soil (CK). Therefore, as discussed in



**Figure 7-9** Effect of sampling and the use of different settlement prediction techniques on the probability of (a) under- and (b) over-design and (c) the probability of obtaining an optimal, for a soil COV of 50% and SOF of 8 m

Chapter 4 (§4.3.2), all conclusions made in this section regarding the performance of site investigation programs are relative to a foundation design using 3DFEA and CK. In addition, it is important to recognise the difficulty in determining an optimal site investigation program based solely on the probabilities discussed in this section. Such difficulties were briefly discussed in Chapter 2 (§2.4), in relation to defining an acceptable probability of failure. However, the following general recommendations have been identified from the discussions in this section:

- The probability of under-design increases as the sampling effort grows. This is mirrored by a reducing probability of over-design;
- The trend between the probability of obtaining an optimal design and increased sampling is similar to that of the probability of under-design;
- A soil SOF of 8 m causes a limiting case where the effect of increased sampling on the probabilities is the greatest;
- The SA reduction technique provides the highest probability of obtaining an optimal design and is affected the greatest by increased sampling (excluding the MN); and
- The difference between the SPT and the other test types is exaggerated for the probability of over-design. This indicates that the SPT is highly conservative and increased sampling is not as beneficial as it is for the other tests.

Since it is difficult to base decisions regarding the site investigation solely on the probabilities of under- and over-design, another measure of error is adopted. This measure is the design error and is discussed in detail in the following section. The design error provides a measure of the degree of under- or over-design, and allows additional conclusions regarding the impact of additional sampling.

### **7.3 EFFECT OF SITE INVESTIGATION SCOPE ON THE DESIGN ERROR**

---

The relative benefits of increased sampling on the probability of under- and over-design, shown in the previous section, identified opposing trends. For example, the probability of under-design was typically shown to rise as the sampling effort increased, whereas the probability of over-design decreased. A similar phenomenon was also observed in Chapter 5 (§5.3), when two different settlement techniques using complete knowledge of the soil

(CK) were compared. As such, it was difficult to determine an optimal solution. Therefore, another measure of error is introduced, which directly compares the results of one design type with another. The *design error*, which was previously introduced and defined in Chapter 3 (§3.7.1), and briefly used in Chapter 5 (§5.3), provides a measure of the degree of under- and over-design, by normalising the error between the SI and optimal designs.

The analysis presented in this section examines the effect of sampling on the design error of a foundation system. In general, the results are restricted to the analysis of the 9-pad system, shown previously in Chapter 5 [Figure 5-1(c)]. However, an analysis of a single pad system is also discussed. Results also illustrate the sensitivity of the design error with respect to the sources of uncertainty already identified and discussed earlier in this chapter. Such uncertainties include inherent soil variability, different sampling patterns and reduction techniques, measurement and transformation model errors and different settlement relationships.

Results in this section are presented in terms of an average design error, where the design error is calculated for each Monte Carlo realisation and then averaged for the suite of 1,000 realisations. Furthermore, in the case of a foundation system with multiple footings, the design error is calculated for each footing and then averaged to yield an average design error for the foundation system. Full details regarding the formulation of the design error have been given previously in Chapter 3 (§3.7.1).

### 7.3.1 Soil Variability

Since the spatial variability of the soil has been shown in previous results to have a substantial influence on the effect of sampling, it is also expected that the soil COV and SOF will have an impact on the average design error. As such, the analysis in this section examines the impact of increasing the soil COV and SOF on the average design error for different sampling efforts. Such an analysis is undertaken for the 9-pad foundation system used throughout this research [Figure 5-1(c)], where the site investigation design is based on sampling locations arranged in a regular grid (RG), the use of the standard arithmetic average (SA) reduction method, and uncertainties representative of a CPT. The results of the analysis are given in Figures 7-10 and 7-11, for an increasing soil COV and SOF, respectively. In both figures the red shading indicates a high positive average design error, the blue shading represents a large negative average design error and the yellow shading indicates a close to zero design error.

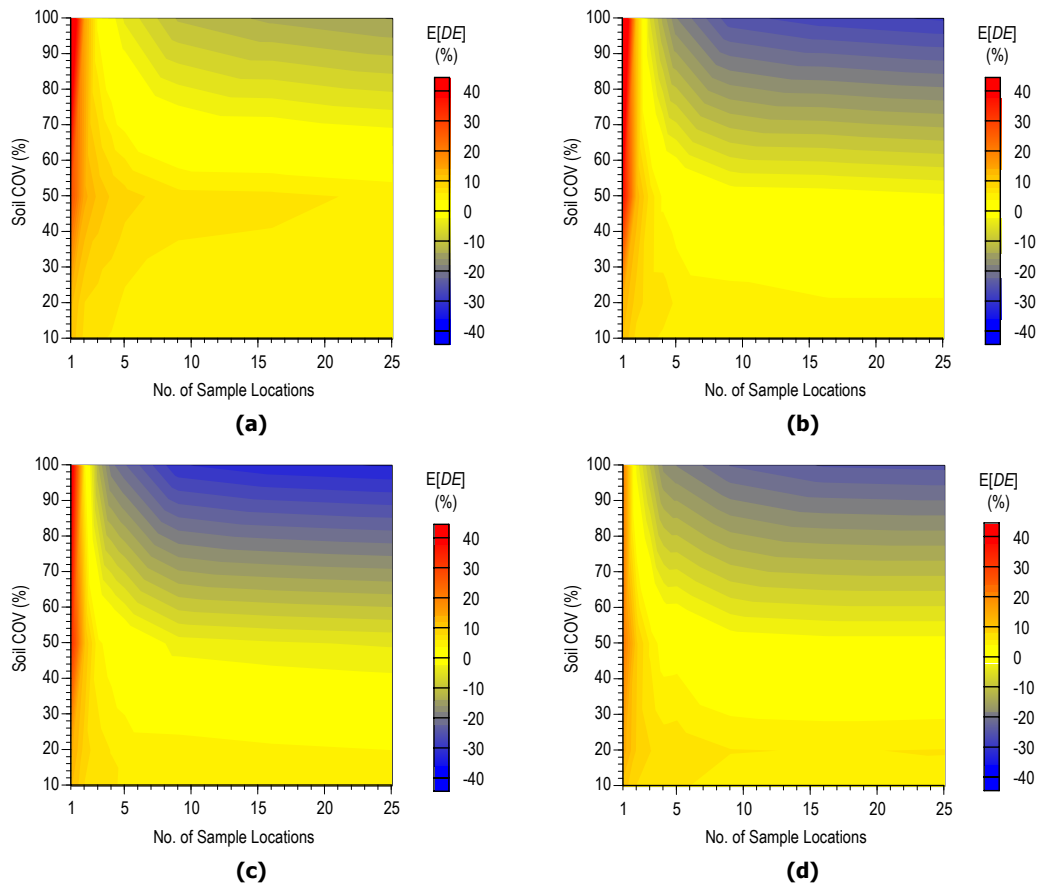


**Figure 7-10 Effect of increased sampling on the average design error, for an increasing soil COV and SOF of (a) 1 m, (b) 4 m, (c) 8 m and (d) 32 m**

Both Figures 7-10 and 7-11 indicate similar trends between sampling and average design error for soils with increasing COVs and SOFs, respectively. In all cases, the average design error reduces as the sampling effort increases. A clearer representation of the results shown in Figures 7-10 and 7-11 is presented in Figures 7-12(a) and (b), for soils with an increasing COV and SOF, respectively. Similar results for other soil COVs and SOFs are given in Appendix D. These results, as well as the surface plots in Figures 7-10 and 7-11, allow more specific conclusions regarding the influence of spatial variability on the effect of increased sampling, including:

- Increased sampling has a greater effect on the average design error for soils with a high COV (e.g. 100%);
- A worst case SOF exists, where the effects of increasing sampling on the average design error are the greatest. In this case, the worst case SOF appears to be approximately 8 m;



- When the soil COV is high (e.g. greater than 50%), the average design error becomes negative for large sampling efforts (e.g. greater than 5 sampling locations);
- The effects of increased sampling are negligible for a soil COV of 10%; and
- The soil SOF has less effect on the impact of increased sampling than the soil COV.

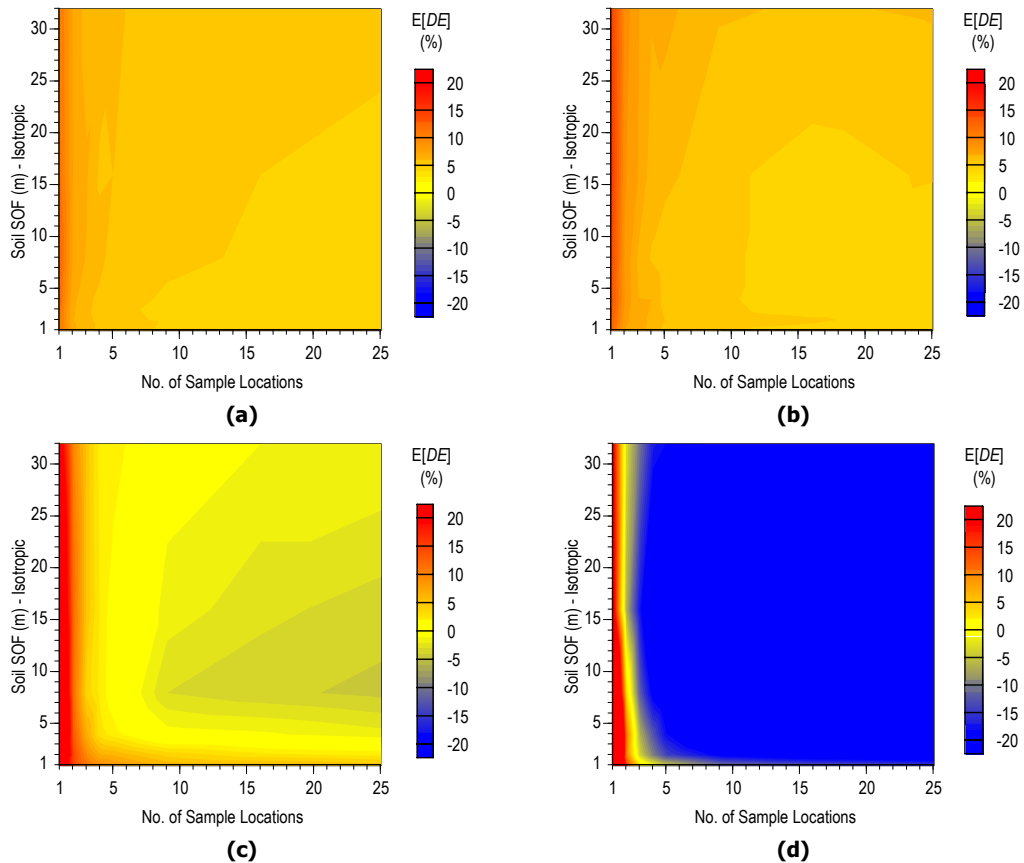


**Figure 7-11 Effect of increased sampling on the average design error, for an increasing soil SOF and COV of (a) 10%, (b) 20%, (c) 50% and (d) 100%**

Most of the conclusions made from the results in Figures 7-10 to 7-12 are consistent with the observations made earlier regarding the average total foundation design (§6.3.1) and the probabilities of under- and over-design (§7.2.1). However, it is clear that the average design error is dominated by the over-design condition where similar trends are shown between the design error and the probability of over-design [Figure 7-1(b)]. In fact, the reduction in average design error for increased sampling yields highly negative design errors when both the sampling effort and soil COV are large. Again, this is consistent with the results shown earlier (§7.2.1), where the probability of under-design was much larger than the probability of over-design, when both the soil COV and sampling efforts were high.

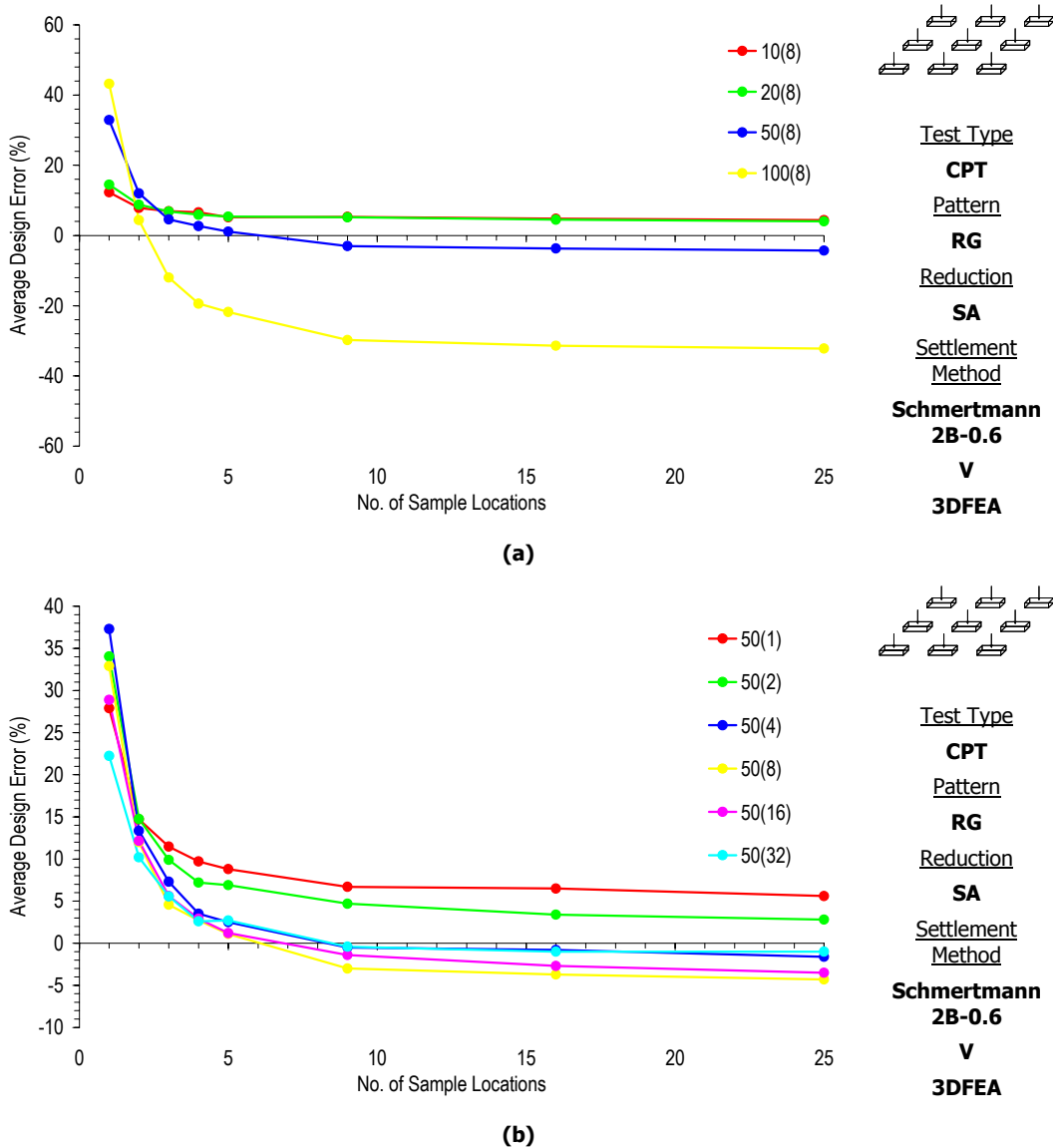


**Figure 7-12 Effect of increased sampling on the average design error, for an increasing soil (a) COV (SOF of 8 m) and (b) SOF (COV of 50%)**

The negative average design error implies that the design based on a SI is, on average, less than the optimal design. This is reflected in Figure 7-13, which illustrates the effect of increased sampling on the average total footing area using a SI (Sch2B) and CK (3DFEA). These results indicate that the SI design yields a larger average total footing area than the optimal, when the soil has a SOF that is less than 2 m. This is true for all sampling conditions, even though the average total footing area is shown to decrease for an increasing sampling effort. However, when the soil SOF is greater than 2 m, and more than 3 sample locations are considered, the average total footing area based on a SI is shown to be less than the optimal. This infers that the SI design is, on average, less than the optimal design. However, the sampling effort that causes the average total footing area to be less than optimal (Figure 7-13) does not coincide with the sampling effort that yields a negative aver-

age design error [Figure 7-12(b)]. Instead, a negative average design error is only achieved when additional sampling locations are considered. This is due to the formulation of the design error itself.

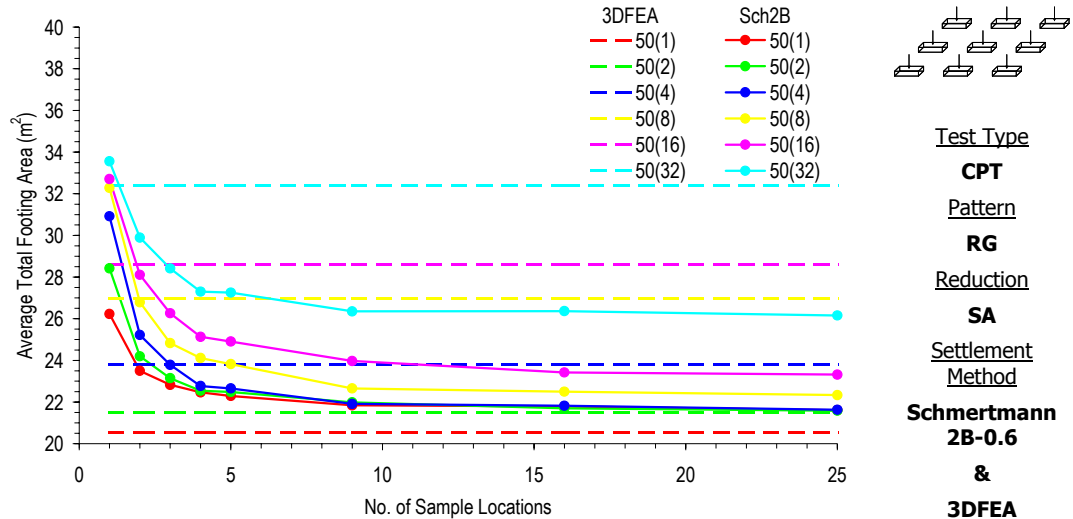


**Figure 7-13 Effect of increased sampling on the average total footing area, for an increasing soil SOF and COV of 50%**

Recall that the design error,  $DE$ , is given by:

$$DE = \frac{A_i - A_{opt}}{A_{opt}} \quad (7.1)$$

where  $A_i$  is the footing area based on a SI and  $A_{opt}$  is the footing area based on the optimal design. For the design error to be negative, the SI design must be less than the optimal design (e.g.  $A_i < A_{opt}$ ). However, when this occurs,  $A_{opt}$  is generally large, because there is a minimum limit on the size of  $A_i$  (§3.6.5.2). Therefore, although  $DE$  is negative, it is also relatively small. On the other hand, when  $DE$  is positive the SI design is larger than the optimal design, (e.g.  $A_i > A_{opt}$ ). Considering that the maximum footing size is relatively large (§3.5.2), there is almost no limit on the maximum  $DE$ . Therefore, the magnitude of the design error is exaggerated when the SI design is larger than the optimal. In other words, the over-design condition has a greater effect on the design error than an under-design. This causes the average design error to be strongly positive as shown in Figure 7-12, even though the average total footing area of the site investigation design is less than the average total footing area of the optimal design (Figure 7-13).

Similar to previous analyses, the effect of increased sampling on the average design error for each individual footing is also investigated. These results are given in Figure 7-14 for five different soils. Such results clearly indicate that the average design error and the effect of increased sampling, is influenced by the magnitude of the applied load. For example, the largest influence of increased sampling and the maximum and minimum average design error, is shown for the footing that is designed to resist the largest load (central footing). However, Figure 7-14 also suggests that, when the soil COV is 100%, the average design error of the footing with the highest applied load (central footing) is less than the other footings. Yet, when the soil COV is 20% or 50%, the error is less. Therefore, it appears that the conservatism of the central footing is increased as the soil COV approaches 100%. This is because a higher COV yields a larger design (§6.3.1) and, due to the formulation in Equation (7.1), a larger average design error.

It is also apparent from Figure 7-14 that the minimum average design error (whether positive or negative) occurs for each footing at the same sampling effort of approximately 3 sampling locations for soils with a COV of 20%, and 5 and 9 sampling locations for soils with a COV of 50% and 100%, respectively. This infers that a SI using the RG and SA does not favour one footing over another. Therefore, the optimal sampling effort that results in least average design error is consistent for every footing in the system. However, it should be noted that the least average design error might be negative, as is the case when the soil COV is 100%.

**The optimal sampling effort, which yields the least average design error, does not favour a footing in the foundation system.**

### 7.3.2 Sampling Patterns and Reduction Techniques

An analysis examining the influence of different sampling patterns and reduction techniques on the average design error is conducted with the aim of recommending an optimal site investigation strategy. Based on the results in the previous section, which indicated that a soil COV of 50% and SOF of 8 m provided a limiting condition, the analyses in this section investigate the impact of sampling for this soil only. The results for other soil COVs and SOFs are included in Appendix D. Results dealing with the sampling pattern are given in Figure 7-15. These are based on the standard arithmetic average (SA) reduction technique and indicate that the simple random arrangement of sampling locations

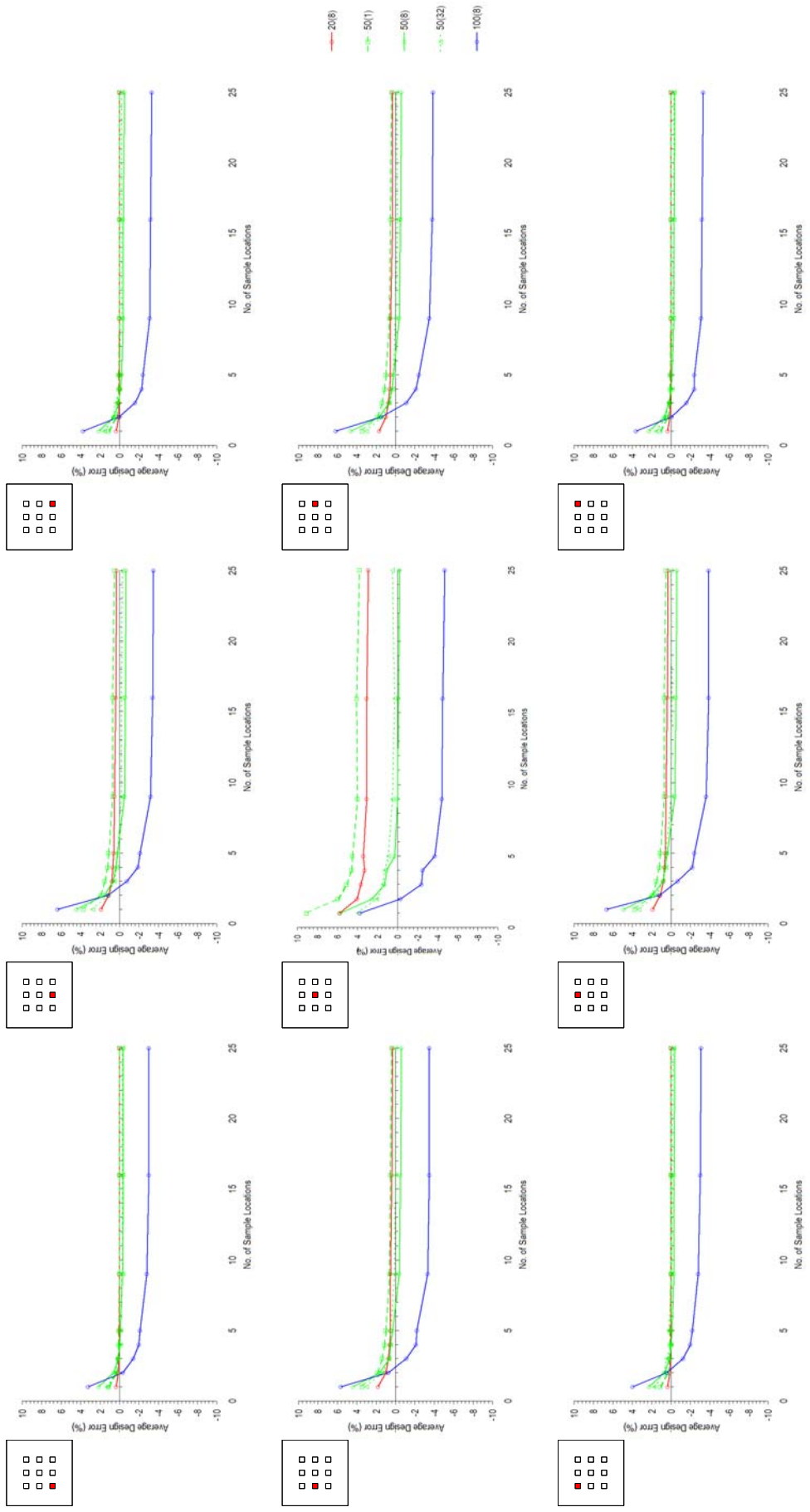


**Figure 7-14** Effect of sampling on the average design error of each footing in the 9-pad system, based on a design using Sch2B and a SI (CPT, RG, SA) and an optimal design using 3DFEA and CK, for a soil COV of 50% and SOF of 8 m

(RN) yields a design with the least average design error when the sampling effort is low. However, when more than 5 sampling locations are considered, all three patterns appear to yield similar average design errors. These results are consistent with the effect of increased sampling on the probability of over-design given earlier in this chapter [Figure 7-6]. Therefore, the sampling pattern appears again, to have little impact on the design.

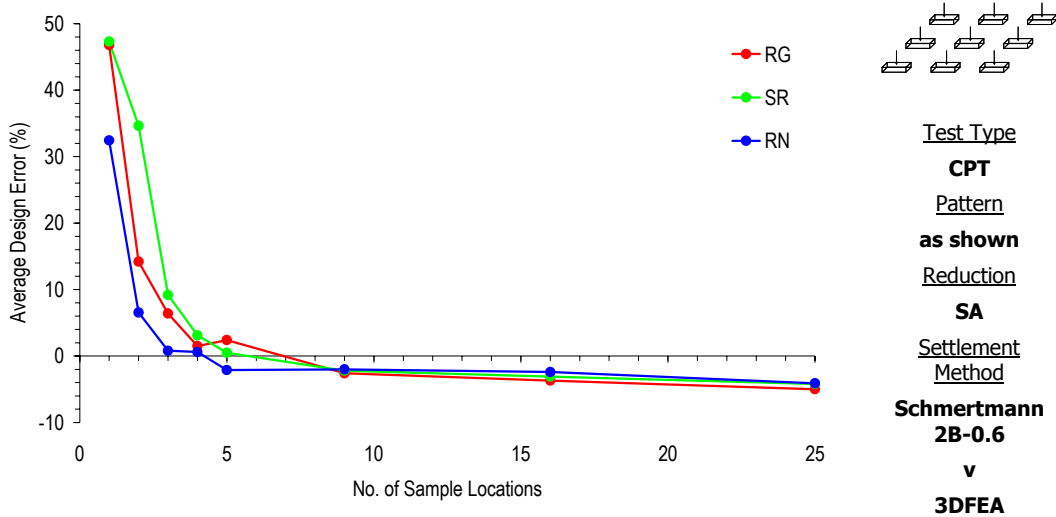


**Figure 7-15 Effect of sampling using different patterns on the average design error, for a soil COV of 50% and SOF of 8 m**

On the other hand, the use of different reduction techniques has been shown previously in Chapter 6 and earlier in this chapter, to have a marked influence on the effect of increased sampling on the design of a foundation. Therefore, it is important to closely examine the influence of each technique on the average design error. This analysis does not consider the MN reduction technique due to its very high level of conservatism, which also increases as the sampling effort rises. As such, it was recommended earlier in this chapter and in Chapter 6 (§6.3.2) that the MN method should not be considered when characterising soils for a foundation design. By excluding the MN from this analysis, comparisons between the other methods are also much clearer. Therefore, results examining the impact of additional sampling with different reduction techniques on the average design error are given in Figure 7-16. Such results are based on a RG sampling pattern and a soil COV of 50% and SOF of 8 m.

In general, the results in Figure 7-16 show similar trends with the probability of over-design, as given earlier in this chapter [Figure 7-7(b)]. However, because the average design error can be negative, the results in Figure 7-16 allow the following additional conclusions:

- The SA method yields the least average design error. However, the error becomes negative when more than 5 sampling locations are considered;
- The GA yields the design with the least positive average design error, when the sampling effort is the greatest (e.g. 25 sampling locations); and
- Comparisons between the relative average design errors for each technique are very similar to those for the probability of over-design [Figure 7-7(b)].

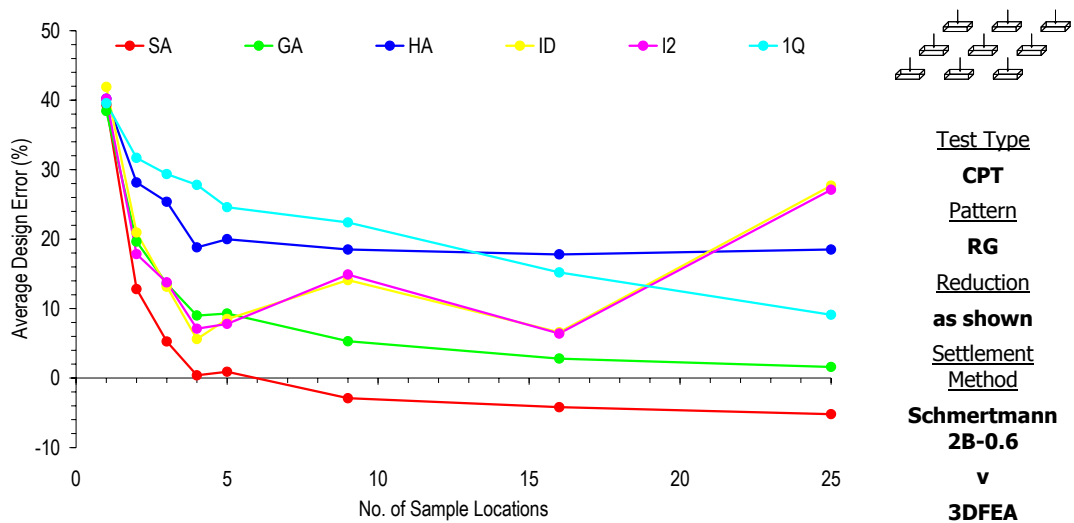


**Figure 7-16 Effect of sampling and different reduction techniques on the average design error, for a soil COV of 50% and SOF of 8 m**

Based on the results given in Figure 7-16, the GA method is recommended as the preferred technique, which leads to the smallest positive average design error, when the sampling effort is the greatest. However, because the average design error is considerably reduced as the sampling effort increases, the SA method is suited for site investigations with limited sampling (e.g. less than 5 sampling locations).

**The GA reduction technique is recommended to yield the smallest positive average design error, for all sampling conditions. However, when the sampling effort is low, the SA yields reasonable results.**

In Figure 7-16, the ID and I2 techniques show erratic results that do not indicate a general trend for increased sampling. This is consistent with the results shown in Chapter 6 (§6.3.2), regarding the average total footing area and is caused by a sample location coinciding with the footing. When this occurs, the footing design only considers one sampling location, which has an impact on the variability of the design (§6.4.2). Recommendations

regarding the use of the ID and I2 methods have been made previously in Chapter 6 and earlier in this chapter.

### 7.3.3 Types of Soil Tests

Keeping with the results of the analysis presented until now, an analysis dealing with the use of different types of soil tests is also undertaken. This form of analysis is based on a site investigation design where sampling locations are arranged in a RG and reduced using either the SA, GA or 1Q methods. Results are given in Figure 7-17 and are, again, based on a soil with a COV of 50% and SOF of 8 m. As similar with the other analyses in this section, results for additional soil COVs and SOFs are included in Appendix D.

In general, Figure 7-17 confirms the conclusions made earlier in this chapter and in Chapter 6 (§6.3.3), where the test type has slight influences on the effect of increased sampling. Closer examination of the results yield the following conclusions:

- The TT yields the second largest average design error when the sampling effort is low, yet it provides the lowest error when the sampling effort is high;
- The difference between the SPT and the other test types is exaggerated when the GA reduction technique is used. This is due to the GA being dominated by low elastic moduli (§5.2.3);
- The DMT consistently provides the lowest average design error, for most sampling conditions; and
- the difference between the CPT, TT and DMT is negligible, at high sampling efforts .

The greater reduction in average design error for the TT is consistent with results in Chapter 6 (§6.2.3), where the measurement errors were shown to average out as the sampling effort increased. However, since the TT yields a larger average design error than both the CPT and DMT at low sampling efforts, it is not recommended for use. Furthermore, the large average design errors shown for the SPT also suggest that other tests should be explored first. However, when the sampling effort is high and the SA method is used, the SPT yields a small positive average design error whereas the other test types yield negative errors. In this case, the conservatism of the SPT is beneficial.



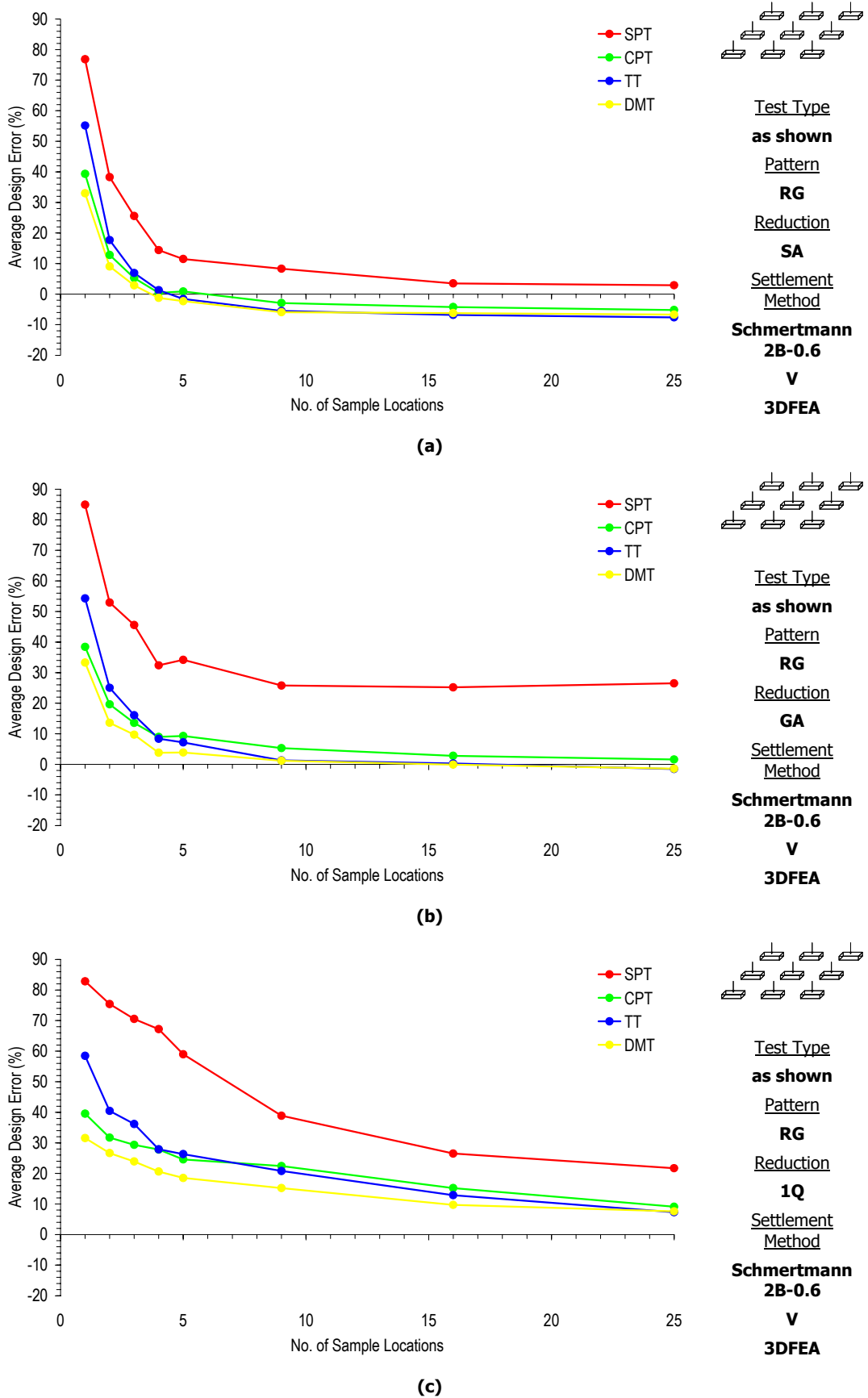


Figure 7-17 Effect of sampling and different test types using the (a) SA, (b) GA and (c) 1Q reduction techniques on average design error, for a soil COV of 50 % and SOF of 8 m

**When the sampling effort is high and a SA reduction technique is used, the conservatism of the SPT is beneficial, with respect to the average design error.**

The best performed test types, based on the average design error, are the CPT and DMT. This is due to the relatively low measurement and transformation model errors assumed for each test (§3.4.3). Although the results in Figure 7-17 suggest that the DMT performs slightly better than the CPT, the assumed vertical sampling rate for the CPT is not representative of its real implementation. This is due to the constraints placed on the element size for computational time purposes (§3.6.5.3). In reality, the vertical sampling rate of the CPT is much larger than the DMT. However, in this case, the CPT only samples three times more elastic moduli, than the DMT. This causes similar results between the CPT and DMT and, hence, no clear recommendation between the two test types is possible.

#### **7.3.4 Settlement Prediction Techniques**

To complete the examination on the effect of increasing sampling on the average design error, an analysis of each settlement prediction technique is undertaken. In this case, each method discussed in Chapter 3 (§3.6.2) is used to design a 9-pad foundation system [Figure 5-1(c)], based on data from a site investigation consisting of sampling locations arranged in a RG, reduced using the SA, and with uncertainties representative of the CPT. Since the results in Chapter 6 (§6.3.4), dealing with the average total footing area, indicated that the comparison between the SI and optimal designs, varied for increasing soil COVs and SOFs, this analysis is also conducted for different soils. Such results are given in Figures 7-18 and 7-19. Additional results are also given in Appendix D for a site investigation using the GA reduction method.

The results in Figures 7-18 and 7-19 yield greater conclusive evidence that the settlement techniques have little influence on increased sampling. This is because the relationship between increased sampling and average design error is preserved for each settlement method and all soils investigated. The only notable differences are those due to the relative conservatisms inherent in each method.

An interesting observation from Figures 7-18 and 7-19 is whether the SI designs, which are based on different settlement methods, yield a positive or negative average design error. It appears in Figure 7-19(a) that, for a soil COV of 20%, designs that are based on every

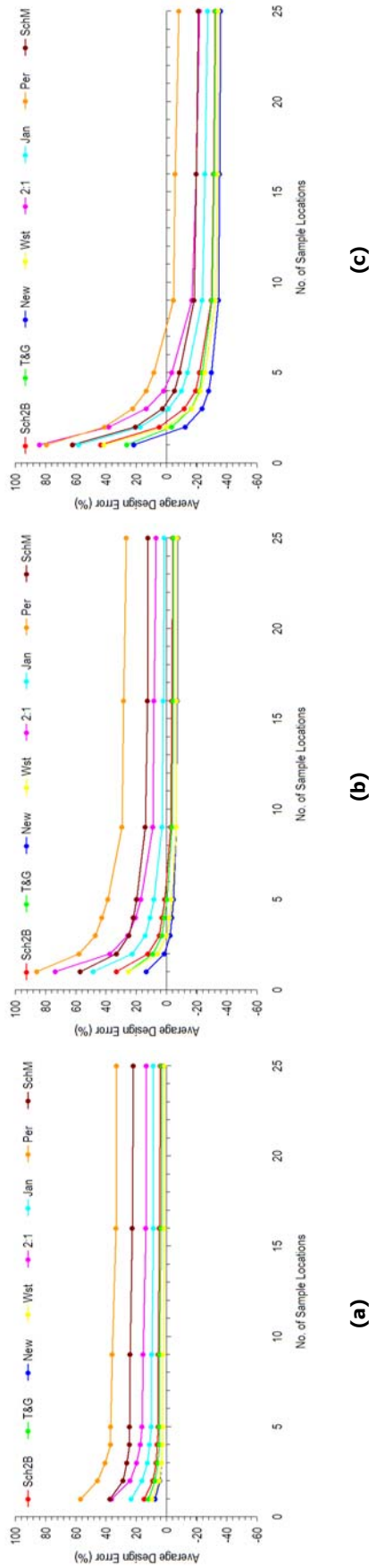


**Figure 7-18** Effect of sampling and different settlement prediction techniques for the design based on a SI (CPT, RG, SA) on the average design error of the 9-pad system, for a soil SOF of 8 m and COV of (a) 20%, (b) 50% and (c) 100%

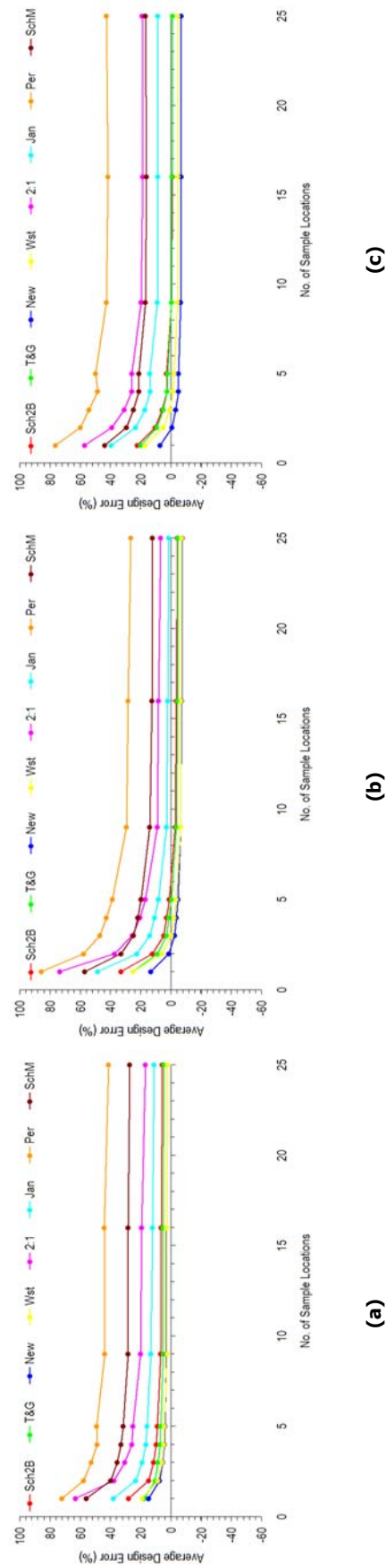


**Figure 7-19** Effect of sampling and different settlement prediction techniques for the design based on a SI (CPT, RG, SA) on the average design error of the 9-pad system, for a soil COV of 50% and SOF of (a) 1 m, (b) 8 m and (c) 32 m

prediction technique yield positive errors for all sampling conditions investigated. However, when the soil COV is increased to 100% and the results of more than 9 sample locations are considered [Figure 7-19(c)], every prediction technique yields a design with a negative average design error. In fact, for several of the prediction techniques, a sampling effort of more than 2 sample locations yields a design with a negative average design error. Therefore, even the Perloff and Schmertmann Modified methods, which were shown in Chapter 5 (§5.2.1) to yield highly conservative settlement estimates for a 1.5 m × 1.5 m footing on a uniform soil, result in a negative average design error. This infers that the uncertainties incorporated in the analysis due to soil variability, measurement and transformation model errors, and the statistical uncertainty due to the site investigation plan, reduces the conservatism in relation to 3DFEA.

### 7.3.5 Analysis of a Single Pad Footing

The analyses presented in this chapter, thus far, have exclusively dealt with a foundation system consisting of 9 pad footings. However, additional analyses are also conducted to measure the effect of increased sampling on the design of a foundation consisting a single pad footing. Essentially, these results are very similar to those shown previously in this chapter. Of particular note, however, is the effect of increased sampling on the average design error of the single pad footing, based on different reduction techniques. These results are given in Figures 7-20(a) and (b), for soils with an increasing COV and SOF, respectively. Additional results are also given in Appendix D for individual soil types. The results in Figures 7-20 are based on a site investigation with sample locations arranged in a RG and with uncertainties representative of a CPT. The Schmertmann 2B-0.6 technique is used to estimate the settlements for the SI design.

The biggest difference between the results shown in Figure 7-20, and the results shown earlier in this chapter (§7.3.2), is the effect of increased sampling on the average design error using the ID. Figure 7-20 suggests that the relationship between average design error and increased sampling for the ID, is smooth and far less erratic than shown earlier in this chapter for the 9-pad system (Figure 7-16). This is because the formulation of the ID works well with only a single pad footing, when the results from the sample locations are weighted in accordance with their distance from the footing. Similar results for a single pad footing, and sample locations arranged using a RN, are also given in Appendix D. This infers that the ID and I2 techniques yield reasonable results when the foundation system consists of a single pad footing, or the sampling locations are not arranged in a systematic manner.

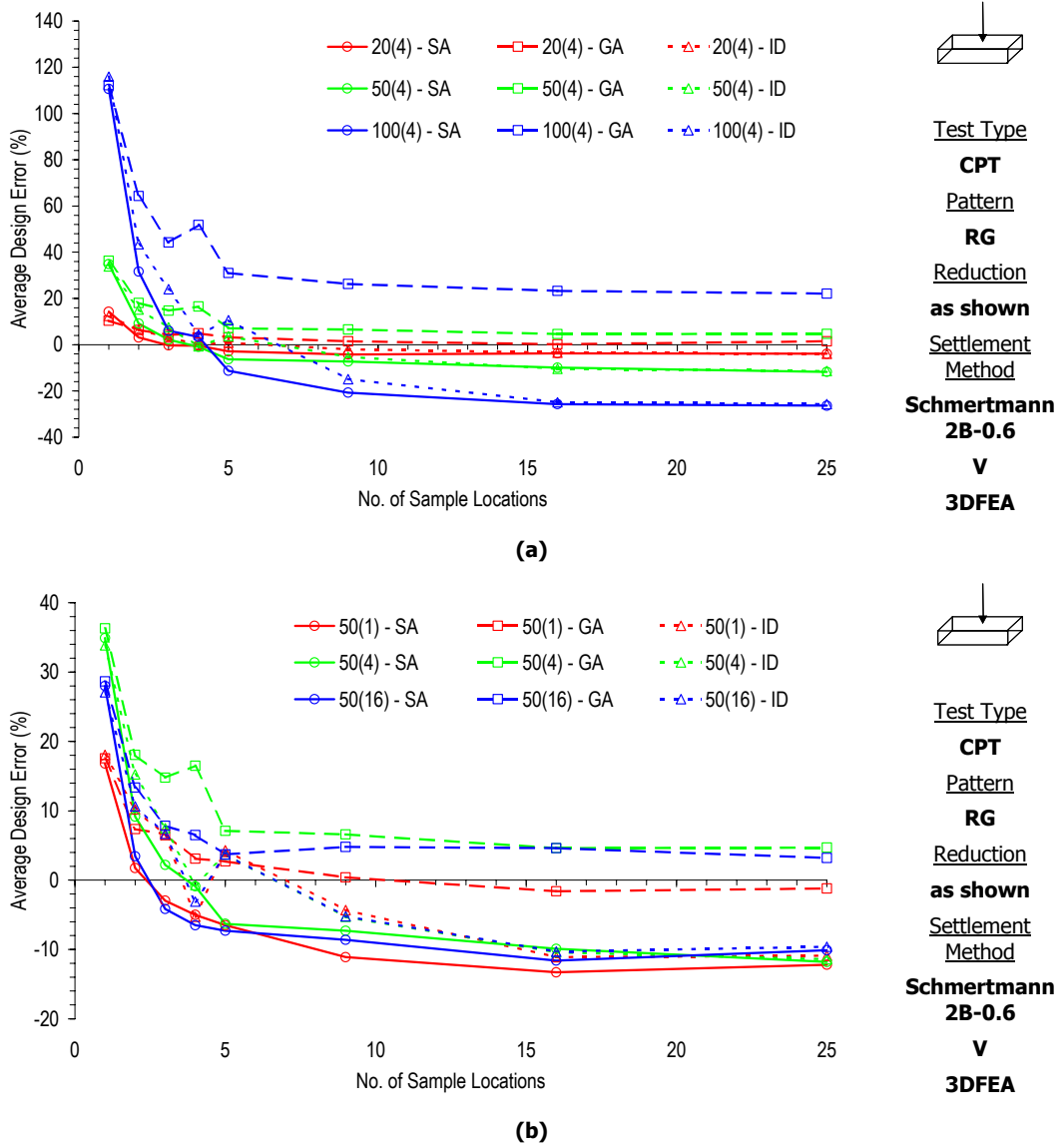


**Figure 7-20** Effect of sampling on the average design error of a single pad footing, for an increasing soil (a) COV (SOF of 4 m) and (b) SOF (COV of 50%)

The ID and I2 reduction methods yield better results when used to design a single pad foundation, rather than a multiple pad system.

### 7.3.6 Summary

The results presented in this section enable several specific conclusions regarding the use of a site investigation. These are:

- The design error reduces as the sampling effort increases. This infers a reduction in conservatism;

- A negative average design error is achieved for many site conditions when the sampling effort is high. This is an under-design condition and may lead to a foundation failure;
- The average design error is controlled by an over-design condition;
- The ID and I2 reduction techniques perform better when the foundation system consists of only a single pad footing or when the sampling locations are not systematically arranged so that one location coincides with a footing;
- Increased sampling has the greatest impact on the average design error; and
- The optimal site investigation strategy, based on the average design error, consists of a regular grid (RG) arrangement of sampling locations, the geometric average (GA) reduction technique, and either the CPT or DMT. This yields the lowest positive average design error for all sampling conditions.

It should be remembered, however, that conclusions made in this section are based on the average design error, which is formulated using the 3DFEA design. Furthermore, the design error is also controlled by an over-design condition where a reduction in over-design yields a reduction in design error. However, it is expected that the under-design of a foundation may be more critical for the total risk of a design. This is discussed further in Chapter 8.

## **7.4 RELIABILITY ASSESSMENT DUE TO INDIVIDUAL SOURCES OF UNCERTAINTY**

---

The analyses presented thus far have been based on a foundation design incorporating all sources of uncertainty. However, results have also indicated that the sources of uncertainty have a different impact on the foundation design. As such, additional analyses are undertaken to examine the affect of statistical uncertainty and the uncertainties due to measurement error. This form of analysis allows the individual modelling of errors associated with each uncertainty.

### **7.4.1 Statistical Uncertainty**

The statistical uncertainty inherent in a site investigation is a function of the number and spatial location of samples used to estimate the characteristic value. The influence of sampling rate, or the number of samples, has been examined earlier in this chapter and in

Chapter 6. However, it is also relevant to investigate the sensitivity of sampling location on the design of a foundation. To achieve this, an analysis using 625 individual sample locations is undertaken. This involves designing a foundation based on the results of single vertical sample of elastic moduli taken at each sample location, as shown in Figure 7-21, with respect to the 9-pad system that has been shown previously in Chapter 5 [Figure 5-1(c)]. This design is compared to an optimal one that is based on the elastic moduli located beneath the centre of each footing. Results are presented as an expected or average design error,  $E[DE]$ .

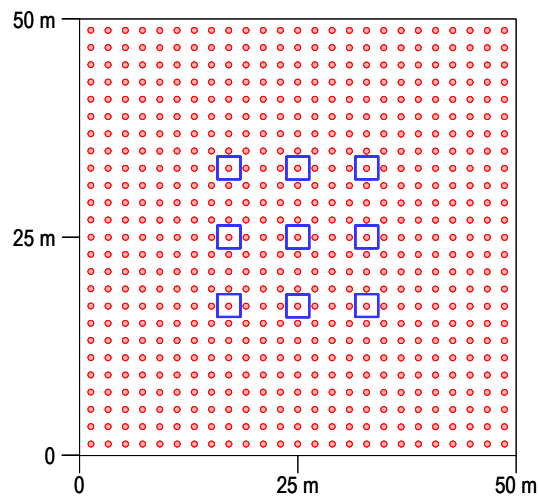


**Figure 7-21 Sampling locations in the site area with respect to the system of 9-pad footings**

The average design error of the single pad footing case designed using data from each of the 625 sample locations individually, is given in Figures 7-22 and 7-23, for soils with an increasing COV and SOF, respectively. All foundation designs in this section are based on settlement estimates using the Schmertmann 2B-0.6 technique. Furthermore, the analysis does not account for measurement or transformation model errors. Elastic moduli are sampled at every 0.5 m depth interval for both the sample and optimal designs.

Figure 7-22 shows that an increase in soil COV has little effect on the sensitivity of sample location. Instead, it appears that a rise in COV increases the average design error, irrespective of the sample location. However, an increase in soil SOF, as shown in Figure 7-23, does affect the sensitivity of the sample location. Such results also suggest the presence of a worst case SOF, as discussed earlier. This is illustrated by the varying magnitude of the average design error for the four different soils examined. For example, when the soil SOF is 1 m [Figure 7-23(a)], the results show a low average design error for all locations around the site. However, as the soil SOF rises to 4 m [Figure 7-23(b)] and 16 m [Figure 7-23(c)],

the average design error increases, especially around the perimeter of the site. However, Figures 7-23(b) and (c) illustrate a region of small average design error that increases in size as the SOF rises. Furthermore, when the analysis is conducted for a soil SOF of 100 m [Figure 7-23(d)] this region of small design error has grown to encompass almost the entire site. In fact, Figure 7-23(d) is similar to Figure 7-23(a) for a soil with a SOF of 1 m. Therefore, it is expected that the region of small average design error will continue to increase in size until the entire site has a zero error. This infers that, in this case, it is of no importance where the sample location is positioned. This is consistent with the theory, that states when the SOF approaches infinity, all the soil properties are the same and sampling will yield the same values irrespective of location.

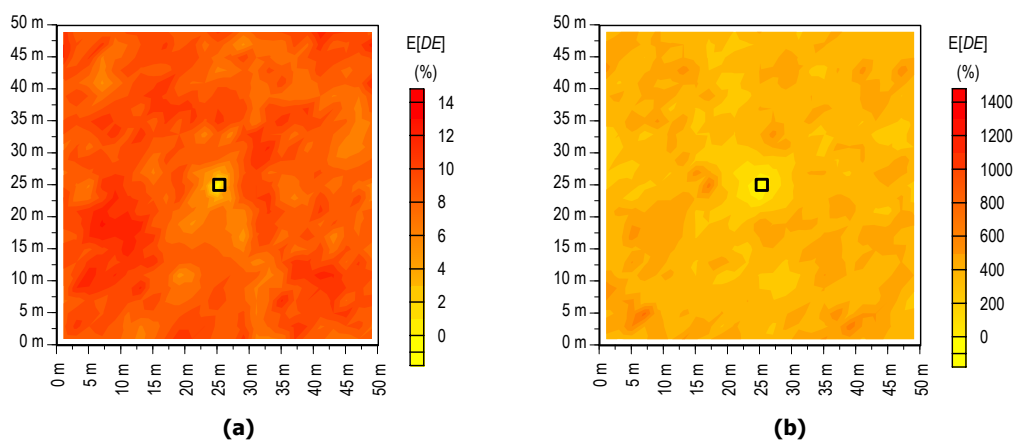


**Figure 7-22 Average design error of a single pad footing at sample locations, for a soil SOF of 4 m and COV of (a) 20% and (b) 100%**  
(Note the change in scale of E[DE])

With two limiting cases suggesting that every location on the site has a zero average design error when the soil SOF is either very small or very large, it is apparent that there is a condition in between that yields a maximum average design error. This condition also appears to be a function of the soil SOF that, throughout this research, has been considered the worst case SOF.

The results shown in Figure 7-23, and to a lesser degree in Figure 7-22, indicate a relationship between the average design error and the separation distance of the sample and footing location. This relationship is further examined in Figure 7-24 for soils with a constant COV of 50% and different SOFs. In this situation, the concept of a worst case SOF implies that the maximum error will occur when the soil SOF is equal to the worst cast. This does not necessarily infer that all sampling locations will have a maximum average design error when the SOF is the worst case. However, it does suggest that a sample location positioned at the site boundary will yield a maximum error.



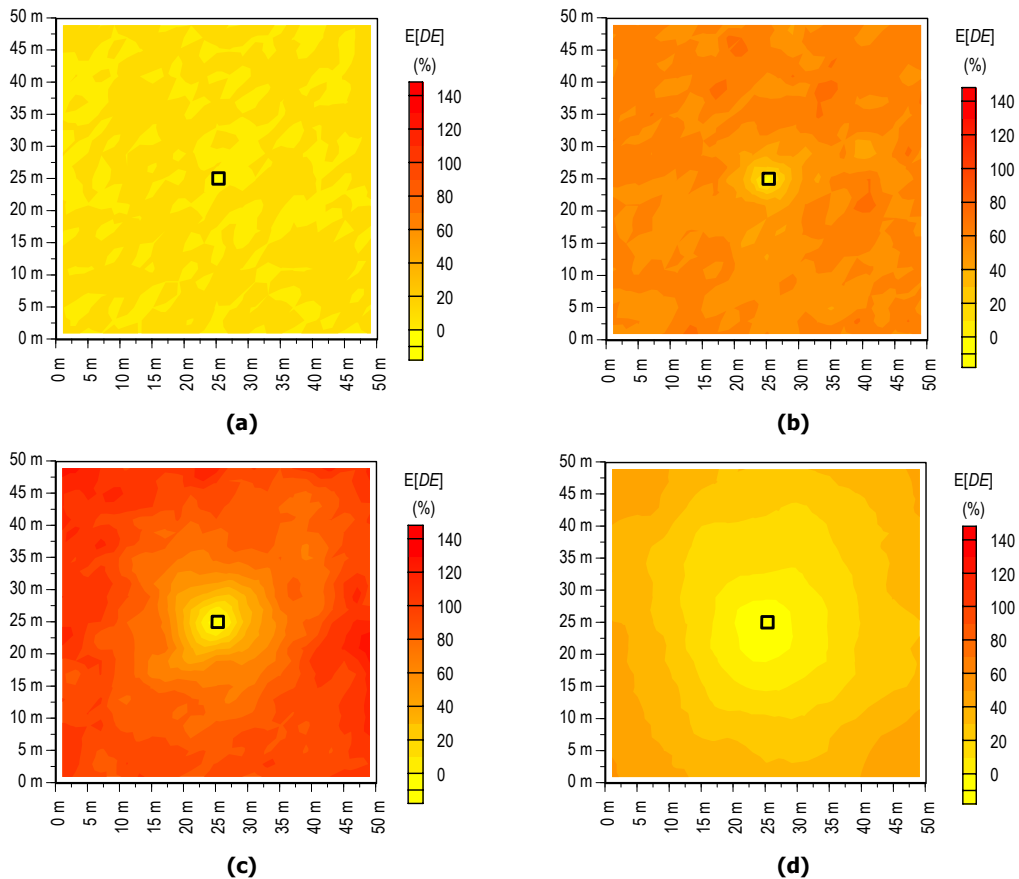


**Figure 7-23 Average design error of a single pad footing at sample locations, for a soil COV of 50 % and SOF of (a) 1 m, (b) 4 m, (c) 16 m and (d) 100 m**

Figure 7-24 illustrates that the average design error increases to a maximum value as the distance separating the sample and footing location increases. However, the maximum error, and the rate at which it increases, appears to be a function of the soil SOF. For example, when the soil has a SOF of 1 m, the maximum average design error of approximately 20% occurs when the separation distance is greater than 2 m. However, when the soil SOF is 4 m, the maximum error of approximately 70% occurs when the separation distance is greater than 10 m.

It is often not possible to sample at the proposed footing location. Therefore, the results in Figure 7-24 can be used to estimate the errors associated with locating a sample at a position other than the footing location. Furthermore, these results can also be utilised to justify locating a sample closer to the footing. For example, if a sample location is moved 5 m closer to a footing from a distance of 10 m, the average design error reduces from 80% to 40% for a soil with a COV of 50% and SOF of 16 m.

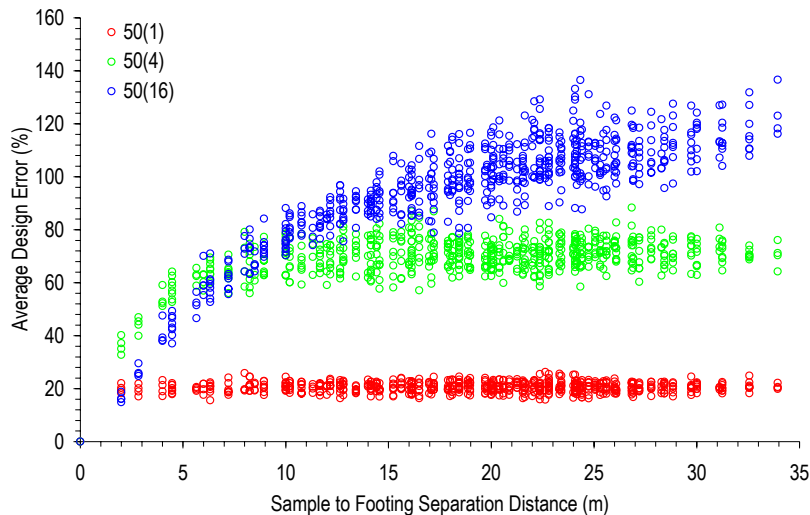


**Figure 7-24 Effect of increasing the sample-to-footing separation distance on the average design error of a single pad footing, for an increasing soil SOF and COV of 50%**

The results shown in Figure 7-24 closely resemble those presented in Chapter 4 (§4.4) for the average settlement error based on a sample location at a distance from the centre of the site. However, the results shown in Figure 7-24 represent the average design error, which is a function of the footing design. As such, the magnitude of the average design error is different to the magnitude of settlement error. As in Chapter 4 (§4.4), a similar analysis was attempted to develop a theoretical evaluation of the average design error. However, because the relationship between settlement and footing design is non-linear, such an analysis requires high-order approximations of non-linear equations. This yielded an unsatisfactory solution.

Analyses are also undertaken to estimate the effects of using the results from a single sample location on the design of a foundation system consisting 4- and 9-pad footings. These results are given in Figures 7-25 and 7-26, respectively. Figures 7-25(a) and 7-26(a) are based on a soil with a COV of 50% and SOF of 1 m, while Figures 7-25(b) and 7-26(b) are based on a soil with a COV of 50% and SOF of 16 m.

Figures 7-25(a) and 7-26(a) illustrate a similar behaviour to the results shown in Figure 7-23 for the single pad footing and a soil with the same COV and SOF. However, the results presented in Figures 7-25(b) and 7-26(b) indicate slightly different behaviour, where the least average design error appears to occur when the sample location coincides with the footing locations. This is especially true for the 4-pad system, shown in Figure 7-25(b), where the average design error is noticeably lower when the sample location coincides with one of the footings, rather than at the centre of the system. Therefore, it appears of

greater benefit, as one might expect, to sample in a location coincident with the proposed footing. This also appears true for the 9-pad system, as shown in Figure 7-26(b). However, because the 9-pad system consists of a footing located at the centre of the site, the average design error is also low at this location. Furthermore, it appears that the average design error at the centre of the site is lower than at the locations of the other footings. This is likely to be a result of two factors. First, the central footing is a point of symmetry for the entire system. Therefore, a sample located at this point should yield a reasonable design with a relatively low average design error. Second, the central footing is designed to resist the largest load (1,540 kN compared with 1,150 kN and 860 kN). Therefore, the design of this footing is of greater importance than the other footings because it typically yields a larger area. As such, it appears of greater benefit to sample at this location, for the case presented.

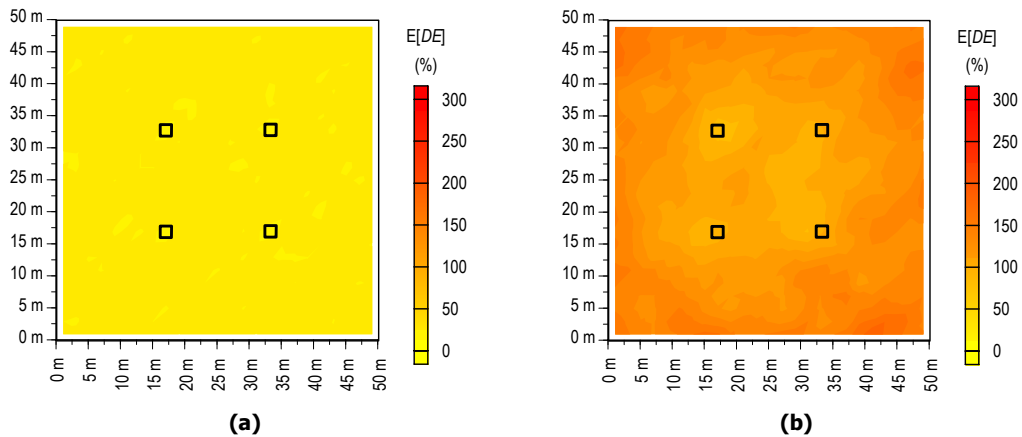


**Figure 7-25 Average design error of a 4-pad system at sample locations for a soil COV of 50% and SOF of (a) 1 m and (c) 16 m**

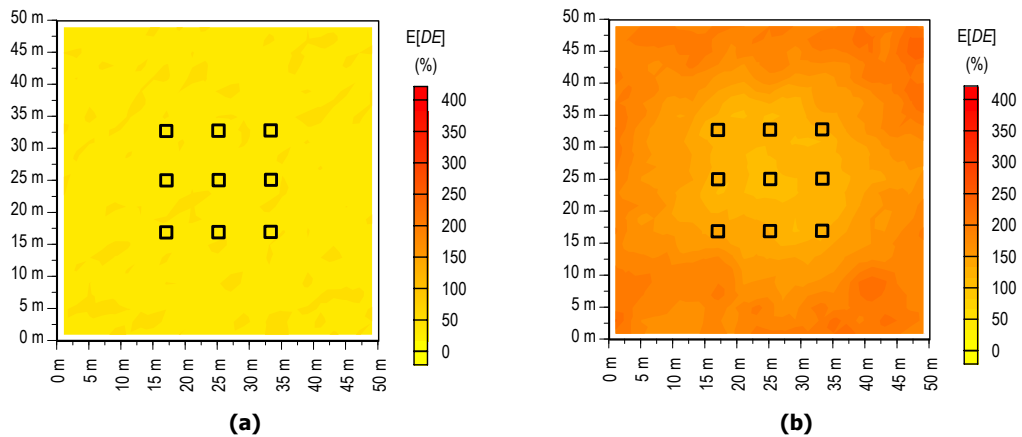


**Figure 7-26 Average design error of a 9-pad system at sample locations, for a soil COV of 50% and SOF of (a) 1 m and (c) 16 m**

Although these results have indicated that the best sampling location is as close to the footing or the centre of the foundation system, they also allow conclusions regarding the relative benefits of sampling location. For instance, these results identify the errors or uncertainties associated with using soil data from a sample location that is not under the centre of the footing. This aids with the planning and design of a site investigation.

### 7.4.2 Measurement Error

In this section, the impact of assuming different measurement errors for the four test types used throughout this research, is examined. This is achieved by comparing two foundation designs based on a single vertical sample of elastic moduli under the centre of the footing. The first design uses elastic moduli that incorporate measurement errors, in accordance with the discussion in Chapter 3 (§3.4.3). The second design is based on elastic moduli sampled directly from the simulated soil, without measurement error.

The degrees of uncertainty due to measurement error investigated in this analysis are shown in Table 7-1. Such values represent the COV of the unit mean lognormal variable used to represent the test bias and random test effects as described in Chapter 3 (§3.4.3). These values are based on the ranges of uncertainties found in the literature regarding measurement errors, as discussed in Chapter 2 (§2.3.4). The uncertainties assumed for the analyses shown in Chapter 6 and earlier in this chapter are highlighted in Table 7-1.

**Table 7-1 Range of uncertainties used in sensitivity analysis of test measurement error**

Test Type	Test Bias ( <i>m</i> )	Random Effects ( <i>m</i> , as COV %)
Cone Penetration Test (CPT)	10, <span style="background-color: yellow;">15</span> , 30, 40, 50, 60, 70, 80	10, 20, 30, <span style="background-color: yellow;">40</span> , 50, 60, 70, 80
Standard Penetration Test (SPT)	5, 10, <span style="background-color: yellow;">15</span> , 20, 25, 30	5, 10, 15, <span style="background-color: yellow;">20</span> , 25, 30
Triaxial Test (TT)*	5, 10, 15, <span style="background-color: yellow;">20</span>	5, 10, 15, <span style="background-color: yellow;">20</span>
Flat-Plate Dilatometer (DMT)	5, 10, <span style="background-color: yellow;">15</span> , 20, 25, 30	5, 10, <span style="background-color: yellow;">15</span> , 20, 25, 30
Notes:		

It should also be noted that the vertical sampling intervals related to each test type are also included in this analysis. For example, the SPT and DMT are assumed, again, to sample every 3rd element in the vertical direction. This represents a vertical sampling interval of 1.5 m. On the other hand, the CPT is assumed, again, to sample every element in the vertical direction, representing a vertical sampling interval of 0.5 m. Although the CPT is generally able to sample continuously, where vertical sample spacing may be less than 20 mm, the constraints imposed on this research, in reference to computational time and available

resources (§3.6.5 and §3.7.3), has necessitated the adoption of a 0.5 m element size. Therefore, a vertical sampling interval of 0.5 m is the smallest interval possible given the element constraints. The vertical sampling frequency assumed for the TT is also treated as a variable in this analysis. In this case, four different sampling intervals are investigated, where the TT samples 1, 2, 4 or 8 elastic moduli from the single vertical sample of properties. These sampling rates represent a sampling interval of 30 m, 15 m, 7.5 m and 4 m, respectively.

The results presented in this section are exclusively expressed in terms of a design error as defined in Chapter 3 (§3.7.1), and used in previous sections of this chapter. The same formulation of the average design error is adopted where the error between the two footing designs is computed for each realisation and then averaged over the 1,000 Monte Carlo realisations. Designs are based solely on a single pad footing located at the centre of a 50 m × 50 m site with an assumed depth of 30 m. The footing is designed to resist an applied load of 1,500 kN, with a maximum settlement of 25 mm. As this analysis considers a single pad footing only, there is no need to examine differential settlements. Analyses are undertaken for a soil with a uniform elastic modulus of 10,000 kPa and soils with a spatially random elastic modulus, defined by a COV and SOF.

The sensitivity of bias test errors and random test effects on the average design error of the foundation are illustrated in Figures 7-27(a) and (b) for the SPT and CPT, respectively. These results are based on a soil with a uniform elastic modulus. Results presented in Figures 7-28 and 7-29 illustrate the effect of increasing the bias and random components of the SPT measurement error, for a soil with an increasing COV and SOF, respectively. Likewise, the results in Figures 7-30 and 7-31 indicate the impact of an increasing bias and random component of the CPT measurement error, for a soil with an increasing COV and SOF, respectively.

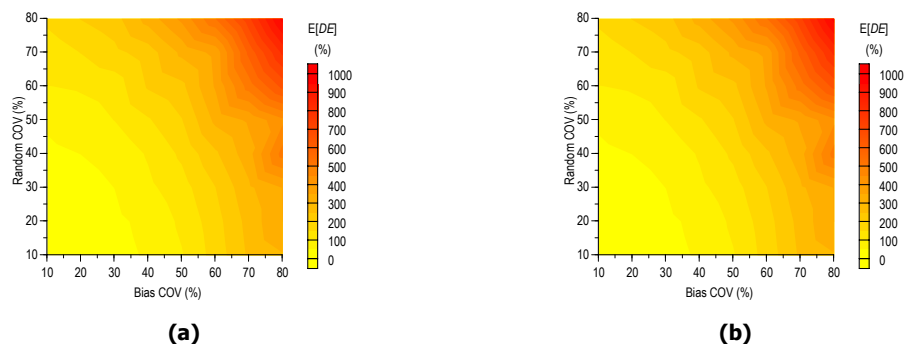


**Figure 7-27 Effect of increasing the bias and random components of measurement error for the (a) SPT and (b) CPT, on the average design error, for a soil with a uniform elastic modulus**

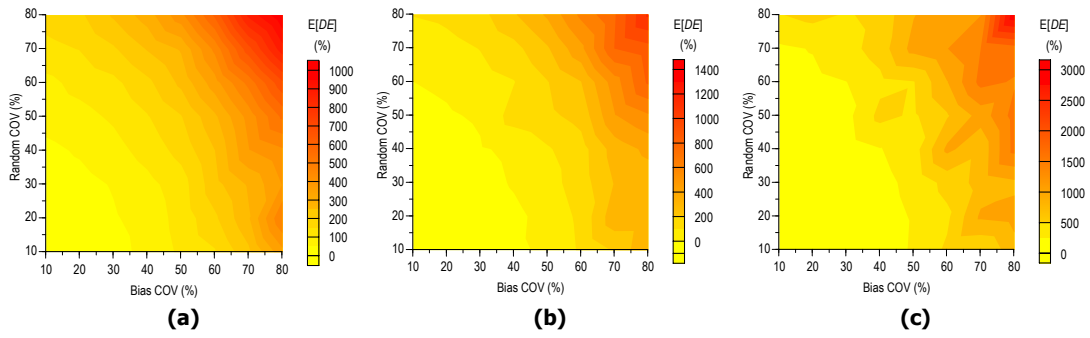


**Figure 7-28 Effect of increasing the bias and random components of measurement error for the SPT, on the average design error, for a soil with a SOF of 4 m and COV of (a) 20%, (b) 50% and (c) 100%**

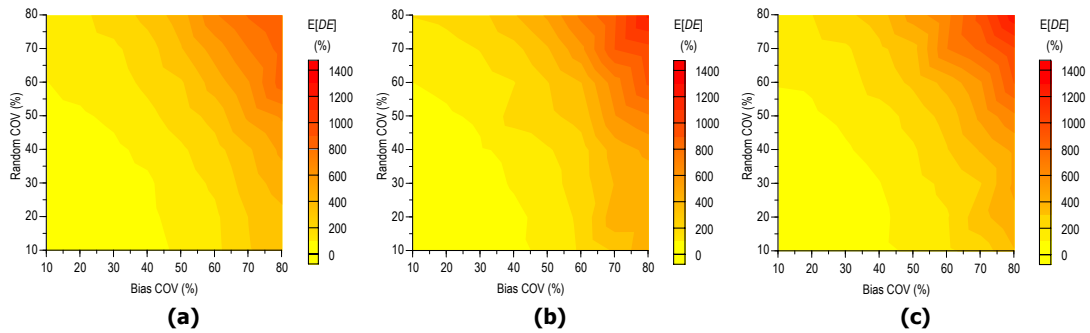


**Figure 7-29 Effect of increasing the bias and random components of measurement error for the SPT, on the average design error, for a soil with a COV of 50% and SOF of (a) 1 m, (b) 4 m and (c) 16 m**

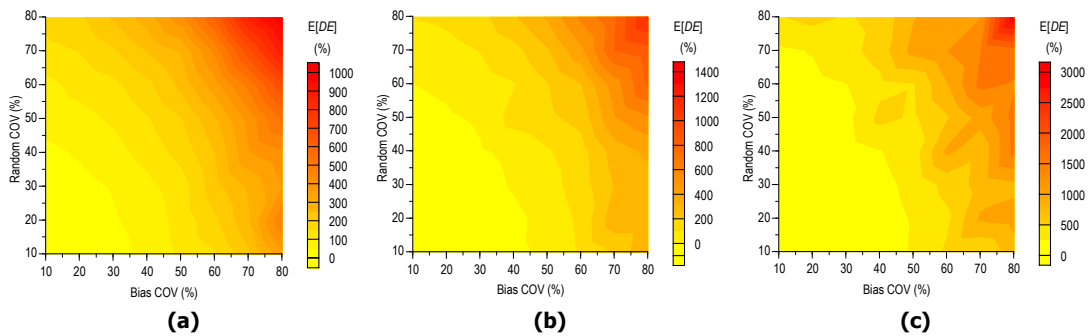


**Figure 7-30 Effect of increasing the bias and random components of measurement error for the CPT, on the average design error, for a soil with a SOF of 4 m and COV of (a) 20%, (b) 50% and (c) 100%**

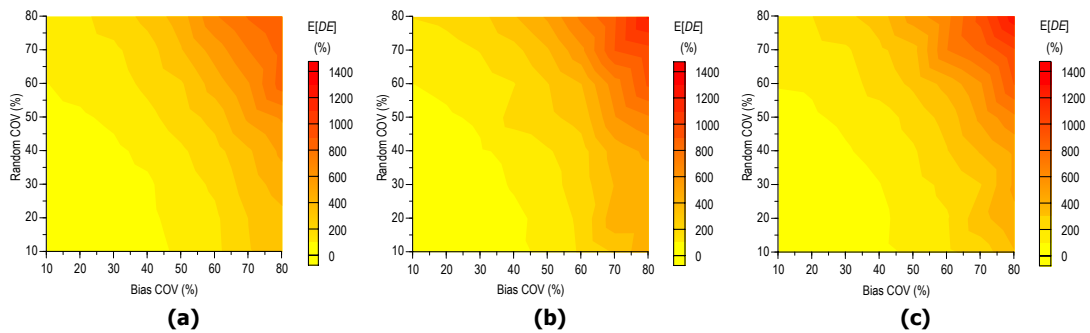


**Figure 7-31 Effect of increasing the bias and random components of measurement error for the CPT, on the average design error, for a soil with a COV of 50% and SOF of (a) 1 m, (b) 4 m and (c) 16 m**

The results given in Figures 7-27 to 7-31 indicate that the effect of the bias and random components of measurement error have a consistent effect on the average design error. For example, as the bias increases, the average design error also increases. However, it also appears that an increase in the bias has a greater effect on the error than the random component. Therefore, the average design error is more sensitive to the bias component of measurement error. This is because the bias alters the average elastic moduli used in the design, while the random component has a greater impact on the variability.

Furthermore, it appears from Figures 7-28(c) and 7-30(c) that, for a soil COV of 100%, the relationship between the average design error and an increasing bias and random component is not as well defined. However, it is important to recognise that a soil COV of 100% yields highly variable designs that cause erratic errors. Furthermore, because the elastic moduli are sampled from a single location, there is little scope for averaging. However, the underlying nature of the results shown in Figures 7-28(c) and 7-30(c) suggests that the relationship between average design error and the bias and random components of measurement error, is still similar to the results for a soil with a uniform elastic modulus (Figure 7-27).

It is noted that the range of average design error, shown in Figure 7-28 for the SPT, changes as the soil COV becomes larger. As such, the average design error increases noticeably as the soil COV rises. This increase is more notable than for the CPT (Figure 7-30). However, Figure 7-28 also indicates that there is little increase in the average design error when the bias and random components are less than 30%. This coincides with the maximum bias and random components of measurement error considered for the CPT. Therefore, it appears that the average design error increases exponentially as the bias and random components rise. As such, the SPT, which is assumed to have a large bias and random component, yields designs with considerably larger errors. This has been shown previously in this chapter (§7.3.3), when the effect of increased sampling on the average design error was investigated. However, this effect may be related more to the formulation of the design error, rather than the increasing bias and random errors. Recall from the theoretical evaluation of measurement errors, given in Chapter 6 (§6.3.3 and §6.4.3), that an increase in error yielded larger design areas, which were also more variable. Furthermore, it was observed earlier in this chapter (§7.3.1) that the design error is dominated by an over-design condition that infers larger footings. Therefore, larger footings are expected to yield higher design errors. This is shown in Figures 7-27 to 7-31.

Although the soil COV is shown to affect the relationship between the average design error and the bias and random components of measurement error (Figures 7-28 and 7-30), the results in Figures 7-29 and 7-31 suggest that the soil SOF has little impact. In this case, the results appear similar in shape and magnitude. It also appears that the vertical sampling frequency has little impact on the relationship between the average design error and the bias and random components of measurement error. As such, it is expected that a similar analysis for the DMT will yield similar results. This is because the assumed measurement errors for the CPT and DMT are similar, and there appears little difference between the results for a vertical sampling frequency of 1.5 m (SPT and DMT) and 0.5 m (CPT). However, as mentioned in previous chapters, a vertical sampling frequency of 0.5 m is not representative of the CPT.

Although there appears little difference between a vertical sampling frequency of 1.5 m and 0.5 m, the results shown in Figure 7-32 for the TT suggest otherwise. Such results illustrate the effect of increasing the bias and random components for 4 different vertical sampling rates. It appears that the average design error is noticeably reduced as the sampling rate increases. In fact, the average design error, based on 4 samples per location, is approximately 50% less than a vertical sampling rate when 1 sample is considered.

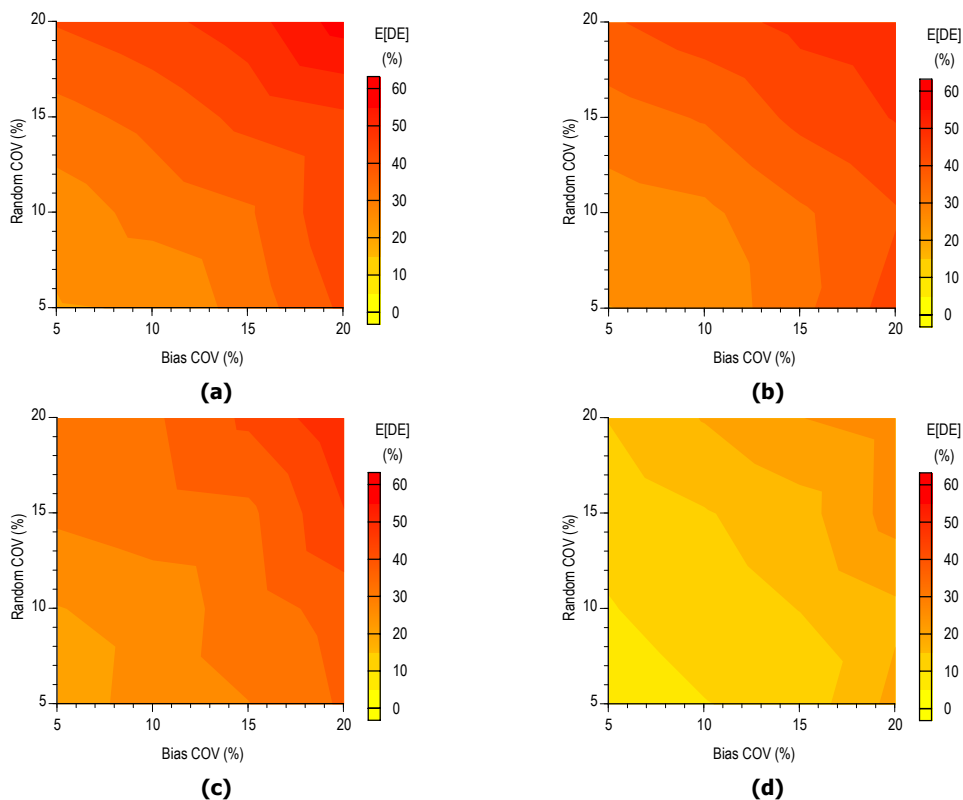


**Figure 7-32 Effect of increasing the bias and random components of measurement error, based on a TT with a vertical sampling rate of (a) 1, (b) 2, (c) 4 and (d) 8 samples per borehole, for a soil COV of 50% and SOF of 4 m**



Even though the results in Figure 7-32 suggest that the vertical sampling rate appears to affect the average design error, it does not appear to affect the influence of increasing the bias and random components of measurement error. Instead, the trends in Figure 7-32 are very similar to those in Figures 7-28 to 7-31, for the SPT and CPT, respectively. However, there are differences in magnitudes of design error, which is an expected results considering the different measurement errors examined for each type of test. As a result, it appears that there is no special relationship between the average design error and the bias and random components of measurement error. The only notable difference between the two components of error is that the bias appears to have a slightly greater effect on the average design error. However, in the main, an increase in the bias and random components infers a larger average design error.

---

## 7.5 SUMMARY

---

The results in this chapter have shown that increased sampling has a definite impact on the reliability of a footing design. These results indicated that a greater sampling effort leads to a higher probability of under-design and therefore, a lower probability of over-design. Furthermore, the probability of obtaining an optimal design was shown to increase as the sampling effort rose. The average design error was dominated by over-design, where a decrease in average design error was apparent for increasing sampling effort. However, in some cases such a decrease resulted in a negative average design error, suggesting that the design, based on the results of the site investigation, was considerably smaller than the optimal design.

The sampling pattern appeared to have little effect on either the probability of under- or over-design or the average design error. However, the technique adopted to reduce the results from multiple sample locations into a single set of design values, was shown to have a marked impact, where the GA technique provided designs with a consistently low positive average design error. Both results showing probabilities of under- and over-design and the average design error indicated that a soil SOF of approximately 8 m yields a limiting case. This has been observed in previous chapters and as such, has been labelled the worst case SOF.

A strong relationship between the distance separating a single sample location and an individual pad footing on the average design error was also identified in this chapter. These analyses indicated the presence of a worst case SOF that results in a maximum average design error. It was also demonstrated that the bias and random components of measure-

ment error have similar effects on the average design error of a single footing. Furthermore, it appeared that the vertical sampling frequency of the TT had a notable impact on the results, where the average design error was shown to decrease as the vertical sampling frequency increased.

Although the results presented in this chapter have allowed some conclusions regarding the optimal site investigation and settlement prediction technique, they are still based on comparisons with a 3DFEA design. Furthermore, it is difficult to determine a suitable probability limit to target and the design error is controlled by an over-design condition. As such, the analysis in the next chapter uses a risk analysis to identify the optimal site investigation and the relative benefits of increased sampling. The results in the following chapter complement those presented in this chapter to target the optimal site investigation with the aim of reducing the risk of foundation failures to achieve an economical solution.

## **Chapter 8 RISK ASSESSMENT OF SITE INVESTIGATIONS IN TERMS OF FOUNDATION DESIGN**

### **8.1 INTRODUCTION**

---

In previous chapters, the effects of increased sampling on the design of a pad foundation has been measured using the expected or average size of the footing and the probabilities that the design is larger or smaller than required. In general, the results have indicated that increased sampling reduces the size of the footing, leading to a lower probability of over-design and a higher probability of under-design. However, a foundation design that has a small footing area does not necessarily infer the most efficient design with the least financial risk. This is because the smaller total footing area has also been shown to have a larger probability of under-design, which is similar to a foundation failure. As a result, this chapter investigates the effect of increased sampling and the use of different site investigations on the financial risk of the foundation design. This is achieved using a risk analysis, where the costs associated with the design and potential failures are incorporated into the methodology discussed in Chapter 3. This allows direct comparisons between the results expressed in terms of a total cost, which includes costs associated with the site investigation, construction of the foundation and the building, and any costs associated with rehabilitation due to foundation failures.

The first part of this chapter details the method adopted to include costs associated with each phase of the design. Results later in the chapter inject the formulation of these costs into the methodology described in Chapter 3, to investigate the effect of an increased site investigation expenditure on the total cost, or financial risk, of a foundation design. As with the analyses conducted in Chapter 7, the results presented in this chapter are based on the inclusion of all sources of uncertainty identified in Chapter 2 (§2.3). The results enable the direct comparison of different sampling patterns, reduction techniques, test types, and

the use of different settlement prediction techniques. This allows the identification of an optimal site investigation that provides a design with the lowest total cost. Analyses also illustrate the benefits of increased site investigation expenditure in terms of cost savings.

## 8.2 CALCULATION OF TOTAL FOUNDATION COST

The *total cost* of a foundation is defined in this research as the sum of the costs associated with the site investigation, construction of the foundation and building, and any costs associated with failures due to inadequate foundation design. It is therefore, necessary to assign costs representative of each of these components to allow a risk analysis to be performed. The following sections describe the formulation of such costs, which have been incorporated into the methodology described in Chapter 3. It should be noted that all costs used in this chapter are in Australian dollars. However, comparisons between costs are valid for all financial denominations.

### 8.2.1 Site Investigation and Construction Costs

The assumed costs for each test type investigated in this research are shown in Table 8-1. These costs are adopted from common industry rates in South Australia, as described by Jaksa (2004). The costs are also based on production rates and drilling costs adopted from Jaksa (2004). The triaxial test (TT) is assumed to be the standard isotropic consolidated, undrained test.

**Table 8-1 Costs associated with different site investigation tests**  
Adapted from Jaksa (2004)

Test Type	Costs				sample location
	Cost	Drilling Rate	Test Cost	Test Rate	
Standard penetration test (SPT)	\$150 / hr	1.9 m / hr	\$25 / test	15 test / sample	\$2,900
Cone penetration test (CPT)	\$150 / hr	1.9 m / hr	\$150 / hr	5 m / hr	\$3,300
Triaxial Test (TT)	\$150 / hr	1.9 m / hr	\$725 / test	2 test / sample	\$2,650
Dilatometer test (DMT)	\$150 / hr	1.9 m / hr	\$150 / hr	3.75 m / hr	\$3,600
Notes:					
Drilling costs for SPT, CPT and DMT are based on a depth of 30 m per sample location.					

The building construction costs as shown in Table 8-2, are adopted from Rawlinsons (2004) and based on a fully serviced office building in the form of a rate per square metre of plan area. It should also be recognised that the costs shown in Table 8-2 include the

foundation construction that, in the analyses that follow, is considered a variable that is dependent on the site conditions, site investigation and design technique. Therefore, the substructure costs are deducted from the total building cost in Table 8-2. This provides the superstructure costs as a function of building height in terms of the number of storeys. A polynomial trend line is fitted to the results with an  $R^2$  value of 0.99. The equation of the fitted polynomial trend line is given by:

$$y = 26.797x^2 + 2191.7 \tag{8.1}$$

where  $y$  is the building cost per square metre of plan area and  $x$  is the number of storeys. This relationship is adopted to estimate the cost of the building construction.

**Table 8-2 Building construction and substructure costs by number of storeys**

Building Height (storeys)	Cost Range (\$ / m <sup>2</sup> incl. substructure)	proportion (%)	Substructure cost (\$ / m <sup>2</sup> building plan area)
1	1075 – 1175	6	68
2	1230 – 1330	3.1	40
3	1395 – 1520	2.2	32.5
4-7	1565 – 1715	1.8	30.25
8-20	2230 – 2280	1.3	30
21-35	2990 – 3190	0.9	29
36-50	3285 – 3535	0.8	26.5

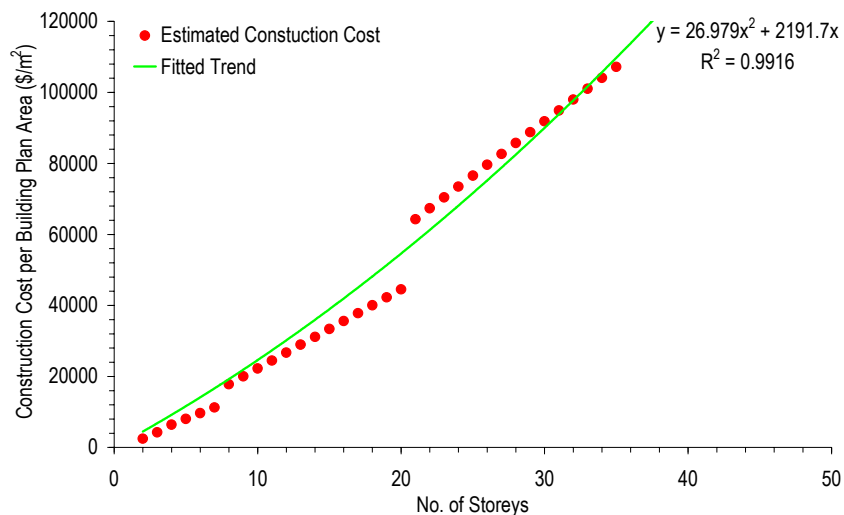


**Figure 8-1 Relationship between construction cost (excluding substructure) and number of storeys**

The construction cost of the foundation is based on a cubic metre rate including excavation, preparation of the base, supply and placement of steel reinforcing, supply and placement of concrete and finishing of the concrete. Again, the costs are adopted from Rawlinsons (2004) and yield a total cubic metre rate of \$510. However, the footing design methodology described in Chapter 3, yields only a square metre footing plan area. Therefore, it is necessary to estimate the thickness of the footing design. This is achieved using a procedure described by Warner et al. (1998), which involves designing the thickness of the footing in terms of beam shear and then checking to ensure that the designed thickness meets the punching shear criterion. The methodology described by Warner et al. (1998) utilises a shear reduction factor,  $\phi_{red}$ , which, for the purposes of this research, is assumed to be 0.7. The beam shear capacity,  $V_{uc}$ , of the footing is given by:

$$V_{uc} = \beta_1 b d (\rho_{min} f'_c)^{1/3} \quad (8.2)$$

where  $\beta_1$  is a shape factor assumed to be 1.1,  $b$  is the least plan dimension of the footing,  $d$  is the depth of the footing,  $\rho_{min}$  is the minimum percentage of steel reinforcing in the footing, which is assumed to be 1.5% and  $f'_c$  is the yield strength of the concrete, which is assumed to be 28 MPa. The applied shear load on a critical section of the footing is given by:

$$V^* = qb \left( \frac{b - c_w}{2} - d \right) \quad (8.3)$$

where  $c_w$  is the width of the column assuming it is square in plan shape. Therefore, for the design to meet the beam shear criterion, the inequality given by:

$$\phi_{red} V_{uc} \geq V^* \quad (8.4)$$

must be met. Furthermore, by substituting Equations (8.2) and (8.3) into Equation (8.4), equating and solving for the depth,  $d$ , the result becomes:

$$d = \frac{V_1^* V_2^*}{\phi_{red} \beta_1 b (\rho_{min} f'_c)^{1/3} + V_1^*} \quad (8.5)$$

where  $V_1^*$  and  $V_2^*$  are components of Equation (8.3) and are given by:

$$V_1^* = qb \quad (8.6)$$

and

$$V_2^* = \frac{b - c_w}{2} \quad (8.7)$$

respectively. It should be noted that the depth,  $d$ , given in Equation (8.5) is a depth to the top of the reinforcement. Therefore, assuming an additional 65 mm is required to account for the size of the reinforcing and the cover, the depth,  $d$ , is increased by 65 mm, to give the total depth of the footing,  $d_t$ . Furthermore, the total depth of the footing is rounded up to the nearest 100 mm. Therefore, the new depth to the top of the reinforcing,  $d_r$ , is given by:

$$d_r = d_t - 65 \quad (8.8)$$

Using the new depth to the top of the reinforcing,  $d_r$ , the punching shear capacity,  $V_{u0}$ , is estimated by:

$$V_{u0} = 4(c_w + d_r)d_r f_{cv} \quad (8.9)$$

where  $f_{cv}$  is the shear capacity of the concrete and is given by:

$$f_{cv} = 0.34\sqrt{f'_c} \quad (8.10)$$

The punching shear capacity given in Equation (8.9) is compared to the applied punching shear of the footing, given by:

$$V_3^* = q(bl - (c_w - d_r)^2) \quad (8.11)$$

where  $l$  is the length of the footing or the dimension perpendicular to the least plan dimension. For the design to meet the punching shear criterion, the expression:

$$\phi_{red} V_{u0} \geq V_3^* \quad (8.12)$$

must hold. Therefore, if Equation (8.12) is not satisfied by the depth to the top of the reinforcing,  $d_r$ , then the depth is increased by 100 mm and the punching shear criterion is

checked again. The beam shear criterion is satisfied if the depth to the reinforcing cover is equal to or greater than the depth required.

### 8.2.2 Failure Costs

The methodology discussed in Chapter 3 describes a process where the size of the footing is designed to meet the required criteria. However, the design process is always based on a possibly inaccurate characterisation of the soil through a limited or inadequate site investigation. Consequently, this design may result in a foundation failure, where the actual footing settles excessively. To determine whether a footing settles in excess of the settlement criteria, the designed footing is analysed using the complete knowledge of the soil (CK). The results of such an analysis indicate the ‘true’ settlement of the footing. Furthermore, these settlements are then used to determine whether the foundation fails or not. For example, if the ‘true’ settlement of the design exceeds the settlement limit, the footing is considered to fail. However, if the ‘true’ settlement is less than the limit, the footing is considered safe and no failure exists. Instead, this footing is either over-designed, in which case additional costs will be evident in the cost of the foundation construction, or the footing is equivalent to the optimal size, in which case no cost penalties are attributed. However, if the CK analysis of the SI design yields settlements greater than 25 mm, a failure occurs and the consequences of such a failure are added to the total cost.

It is important to consider that a failure in this case does not necessarily infer a catastrophic failure. Instead, a failure implies that the design has failed to meet the specified design criteria. In other words, there are various degrees of failure. These are described by failure severity categories, as given in Table 8-3. Similar categories have been used by Day (1999) and Boone (2004) to describe the works required to rectify foundation problems. The categories shown in Table 8-3 are adopted to be consistent with the description of refurbishment works, as discussed by Rawlinsons (2004) and shown in the third column of Table 8-3. This enables simple mapping of refurbishment costs to the failure severity categories.

To demonstrate the costs associated with each category of failure severity, Figure 8-2 illustrates the relationship between the size of the building and the expected failure cost associated with each category. The expected costs are expressed as a ratio of rehabilitation to the original construction cost, where a value of 0.5 is associated with a failure or rehabilitation cost equal to 50% of the original building cost. The relationship between cost and building size indicates that the minor rehabilitation and demolish and rebuild categories yield a rela-



tively constant cost ratio, which is essentially independent of building size. However, the ratio associated with a major foundation failure decreases as the building size increases. This is due to the requirement of foundation underpinning, as described in Table 8-3, where costs associated with underpinning are assumed to be independent of building size.

**Table 8-3 Description of failure severities and rehabilitation works**

Severity of Failure / Rehabilitation Category	Failure Description and Rehabilitation Works	Rehabilitation Works in terms of cost description in Rawlinsons (2004)	Cost Makeup
Minor	Some cracking evident from excessive settlement – requires patching and repainting	Minor refurbishment works	\$410 / m <sup>2</sup> building plan area / storey
Major	Major cracking and structural failures – requires significant patching, structural retrofitting and foundation underpinning	Major refurbishment works + Foundation underpinning	\$2035 / m <sup>2</sup> building plan area / storey for major refurbishment + \$1730 / m <sup>2</sup> footing area for underpinning
Demolish and Rebuild	Building can no longer be used for intended purpose – requires complete demolition and rebuild	Demolish costs + Rebuild costs	\$90 / m <sup>2</sup> building plan area / storey for demolition

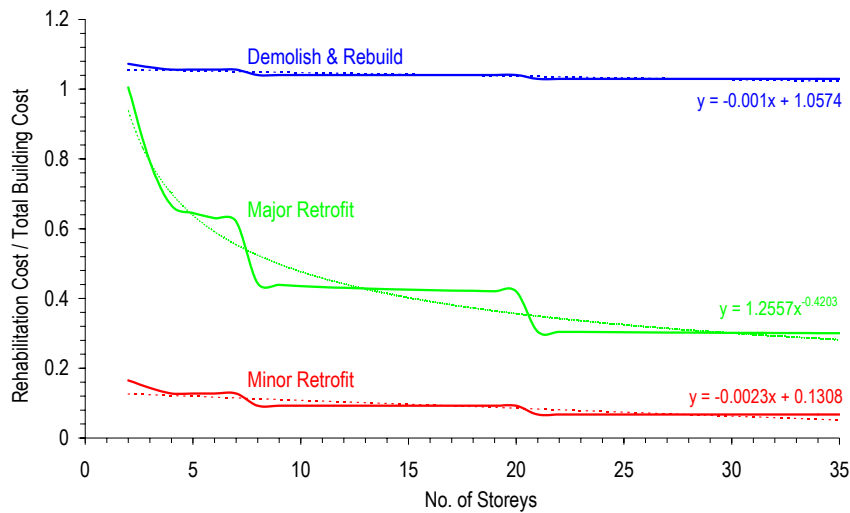


**Figure 8-2 Relationship of minor and major retrofit and demolish and rebuild for buildings of varying storeys**

The settlements associated with the various rehabilitation works are determined using the severity of cracking damage, as discussed by Bjerrum (1963) and Day (1999), and given in Figure 8-3 and Table 8-4, respectively. These results have provided the settlements limits given in Table 8-5. Such limits control the costs associated with the failure of the founda-

tion, and therefore, have an impact on the total cost. Later in this chapter, a brief analysis is undertaken to investigate the sensitivity of these limits. Table 8-5 also includes differential settlement limits that are adopted based on the severity of cracking damage resulting from the angular distortions shown in Figure 8-3 and the differential settlements shown in Table 8-4.

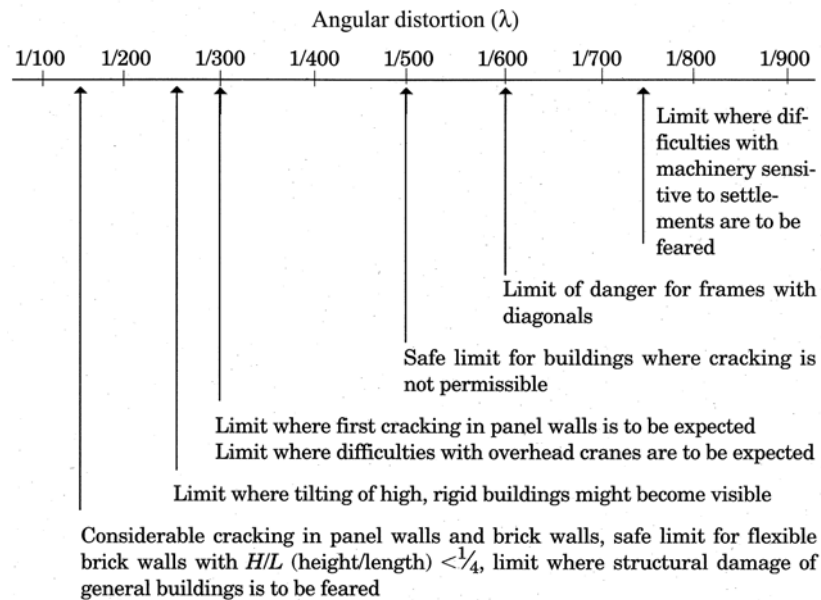


**Figure 8-3 Criteria of damage based on angular distortion**  
After Bjerrum (1963)

By incorporating the relationship between rehabilitation cost ratio and building size (Figure 8-2) and the settlement limits to cause each category of failure or rehabilitation works (Table 8-5), it is possible to illustrate the rehabilitation cost ratio associated with the ‘true’ total and differential settlements of the foundation design for buildings of varying number of storeys, as shown in Figure 8-4(a) and (b), respectively. These results are used to assign costs associated with foundation failure, which are added to the total cost of the design.

Costs associated with failure are based on the maximum total or differential settlements in the foundation system. Therefore, if two of the footings in the system settle excessively, the failure costs associated with the foundation design are based on the footing that undergoes the maximum settlement. As with total settlement, the maximum differential settlement determines the failure cost associated with the design. In the cases where both the total and differential settlement exceeds the limits, the maximum failure cost is adopted. This infers that only one footing, or one pair of footings in the foundation system, controls the associated failure cost, as would be the case in reality.

**Table 8-4 Severity of cracking damage**  
After Day (1999)

Damage category	Description of typical damage	Approx. crack width	Settlement	Differential settlement
Negligible	Hairline cracks	< 0.1 mm	< 30 mm	< 1/300
Very slight	Very slight damage including fine cracks that can easily be treated during normal decoration, perhaps an isolated slight fracture in building, and cracks in external brickwork visible on close inspection.	1 mm	30 to 40 mm	1/300 to 1/240
Slight	Slight damage includes cracks that can be easily filled and redecoration would possible be required; several slight fractures may appear showing on the inside of the building; cracks that are visible externally and some repointing may be required; and doors and windows may stick.	3 mm	40 to 50 mm	1/240 to 1/175
Moderate	Moderate damage includes cracks that require some opening up and can be patched by a mason; recurrent cracks that can be masked by suitable linings; repointing of external brickwork and possibly a small amount of brickwork replacement may be required; doors and windows stick; service pipes may fracture; and weather-tightness is often impaired.	5 to 15 mm or a number of cracks > 3 mm	50 to 80 mm	1/175 to 1/120
Severe	Severe damage includes large cracks requiring extensive repair work involving breaking out and replacing sections of walls (especially over doors and windows); distorted windows and door frames; noticeably sloping floors; leaning or bulging walls; some loss of bearing in beams; and disrupted service pipes.	15 to 25 mm but also depends on number of cracks	80 to 130 mm	1/120 to 1/70
Very severe	Very severe damage often requires a major repair job involving partial or complete rebuilding; beams lose bearing; walls lean and require shoring; windows are broken with distortion; and there is damage of structural instability.	Usually > 25 mm but also depends on number of cracks	> 130 mm	> 1 / 70

**Table 8-5 Adopted settlement and differential settlement limits for failure severity or rehabilitation work category**

Failure severity / rehabilitation category	Limits	
	Settlement	Differential settlement
No Damage / No Rehabilitation	25 mm	0.025 m/m
Minor	60 mm	0.006 m/m
Major	100 mm	0.010 m/m
Demolish and Rebuild	130 mm	0.013 m/m

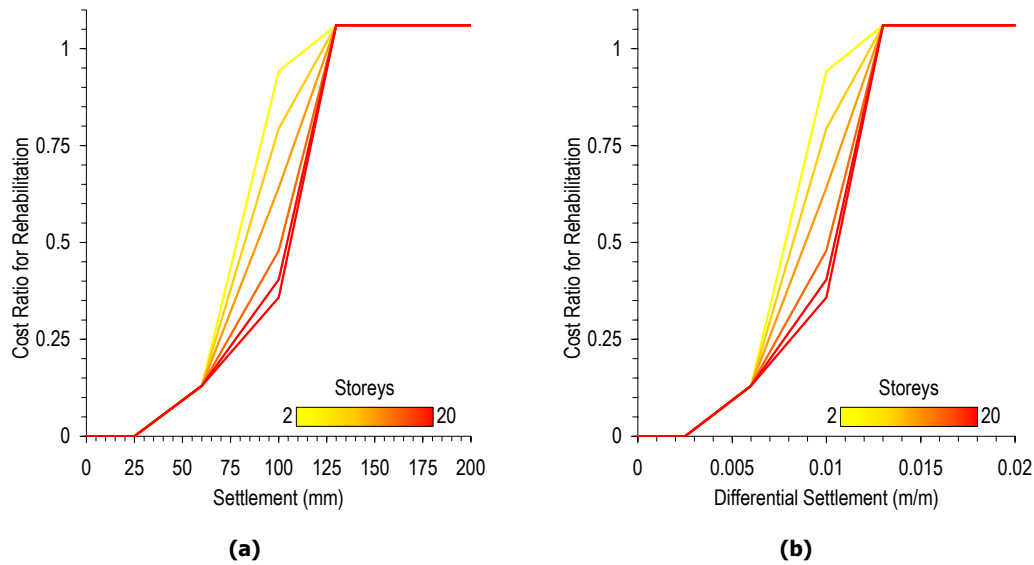


**Figure 8-4 Rehabilitation cost ratio for buildings of varying numbers of storeys undergoing increasing (a) total and (b) differential settlement**

### 8.3 EFFECT OF SITE INVESTIGATION SCOPE ON THE TOTAL FOUNDATION COST

Most of the results presented to date have indicated that the conservatism of a foundation design is significantly reduced as the sampling effort increases. A reduction in conservatism leads to a smaller footing and therefore, a cheaper solution. However, such a reduction in over-design was shown in Chapter 7 (§7.2), to be balanced by an increasing probability of under-design, which is related to a probability of failure. Therefore, to measure the impact of increased sampling, or the use of different reduction techniques, test types and settlement methods, on the total cost of a foundation design, an analysis incorporating costs associated with failure is undertaken. This form of analysis examines the degree of financial risk associated with a design that is based on the results of a site investigation (SI design). However, it should be noted at this stage, that risks associated with human loss or injury, or other indirect financial losses, are not included in the results that follow, since such costs are extremely difficult to quantify.

As described in the previous section, costs associated with the site investigation, construction of the foundation and structure and failure are assigned to each design. The site investigation costs are based on the sampling rate and type of test, while the foundation construction cost is determined using the footing area and thickness. Failure costs are based on the rehabilitation cost ratio, as shown in Figure 8-4, where the ‘true’ total and differential settlements are obtained by analysing the SI design using the complete knowledge of the soil (CK). Two different types of analyses to represent complete knowledge are dis-

cussed here; the 3DFEA and the Schmertmann 2B-0.6 settlement method, which uses an influence region of elastic moduli.

Results are presented in terms of an expected or average total cost, which is averaged over 1,000 Monte Carlo realisations. Variables affecting the impact of increased sampling on the total cost of the design are also examined. In most cases, the cost of the site investigation is expressed in terms of a percentage of the construction cost. This is to allow comparisons between past research regarding site investigation expenditure (e.g. Clayton et al. 1982, National Research Council 1984, Peacock and Whyte 1988, Site Investigation Steering Group 1993, Jaksa 2000) and to also identify a possible constant percentage that can be applied for most site conditions.

### 8.3.1 Failure Analysis Using 3DFEA

Analyses presented in this section involve using 3DFEA and complete knowledge of the soil (CK) to estimate the ‘true’ settlement of a footing design, which is based on the results of a site investigation. The ‘true’ settlement is then used to attribute failure costs, so that the total cost of the design can be determined. In this section, the footing design considered is based on a 20 m × 20 m, 5-storey building with 9 columns that transfer loads from the structure to the foundation, as shown in Figure 8-5. Note that this analysis considers a 5-storey building, as compared to the 3-storey building investigated in previous chapters. A larger building is preferred as the construction and failure costs are larger, which allows a clearer identification of trends. As with previous analyses, columns are spaced evenly at 8 m intervals in both horizontal directions and the column loads are assumed to be representative of their tributary slab areas supporting a dead load of 3 kPa and a live load of 5 kPa per storey. No load factoring is incorporated into the analysis as is standard practice when designing for settlement (Fenton et al. 2005).

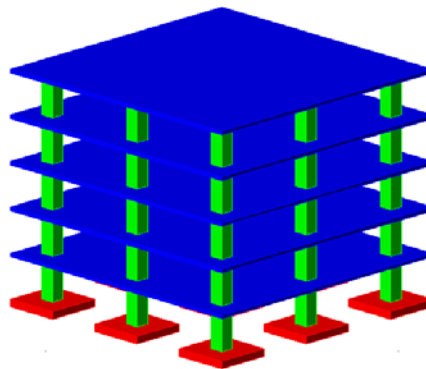


**Figure 8-5** Schematic of the 5-storey building with 9 columns transferring loads to the foundations

The soil is assumed to have a mean elastic modulus of 30,000 kPa and analyses are undertaken for soil COVs of 20%, 50% and 100%, and SOFs of 1, 4, 8 and 32 m. All soils are assumed to be isotropic, which is consistent with the results shown in Chapter 6 and Chapter 7 indicating that the degree of anisotropy had little effect on the design of the foundation. Instead, the size of the SOF in the horizontal and vertical directions independently affected the performance of the site investigation and the conservatism of the design, respectively.

In all cases presented in this section, the SI design is based on settlement estimates using the Schmertmann 2B-0.6 technique. Since 3DFEA is used to analyse the foundation design, the footing sizes are tied to the elements. Therefore, designs that do not meet the settlement criteria are increased by 1 m in one plan direction at a time. This process has been previously described in Chapter 3 (§3.5.1) and comparisons between a sizing increment of 1 m and 0.1 m have been discussed in Chapter 5 (§5.3).

The first series of results from this analysis are given in Figures 8-6 and 8-7, which illustrate the effect of increased site investigation expenditure on the construction, failure and total cost of the SI design for an increasing soil COV and SOF, respectively. Note the different scales on the vertical axis for failure costs. Neither the results shown in Figures 8-6 or 8-7 suggest that the total cost of the foundation is reduced for increased site investigation expenditure. In fact, only the construction cost appears to show a consistent trend for increased site investigation expenditure. In this case, the construction costs become larger as the site investigation expenditure increases. This is because the costs associated with the site investigation are included in the analysis. It is expected that the construction cost alone will decrease as the site investigation expenditure increases. This is due to the trends shown in Chapter 6 (§6.3), where the average total footing area was shown to decrease noticeably for an increased sampling effort. Comparisons between the effect of increased site investigation expenditure on the construction cost, both including and excluding the site investigation costs, are given in Figure 8-8 for the same soils investigated in Figures 8-6 and 8-7. Note the exaggerated scale in Figure 8-8, which clearly illustrates the trends due to increased site investigation expenditure.

Results presented in Figures 8-6 or 8-7 also indicate the cost of the optimal design. This is the construction cost of a foundation design that is based on the complete knowledge of the soil and 3DFEA. As such, no failure costs are attributed to the optimal design. In most cases, the construction and site investigation costs for the SI design are similar to that of

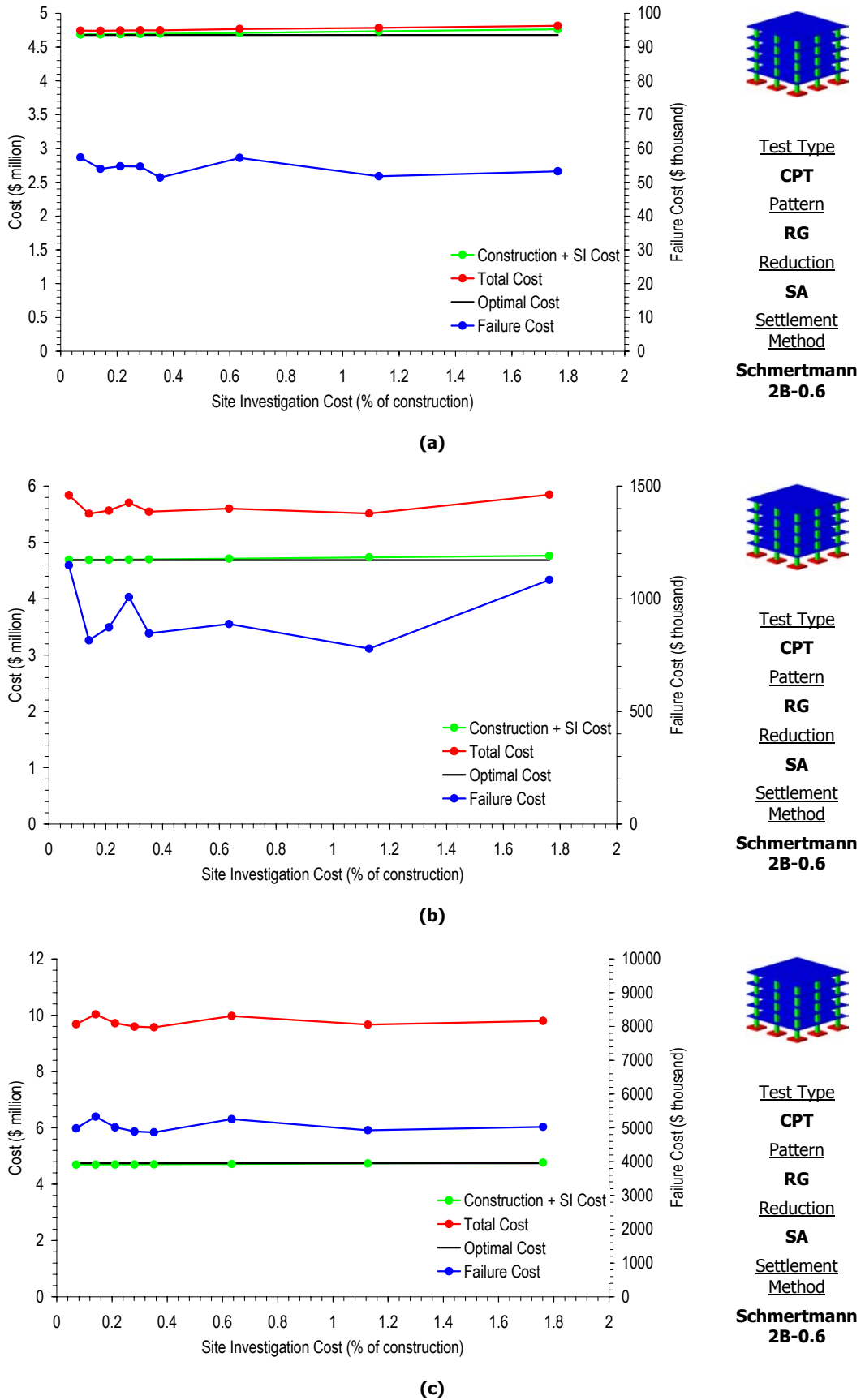


**Figure 8-6** Effect of increased site investigation expenditure on the construction, failure and total cost based on 3DFEA, for a soil SOF of 8 m and COV of (a) 20%, (b) 50% and (c) 100%

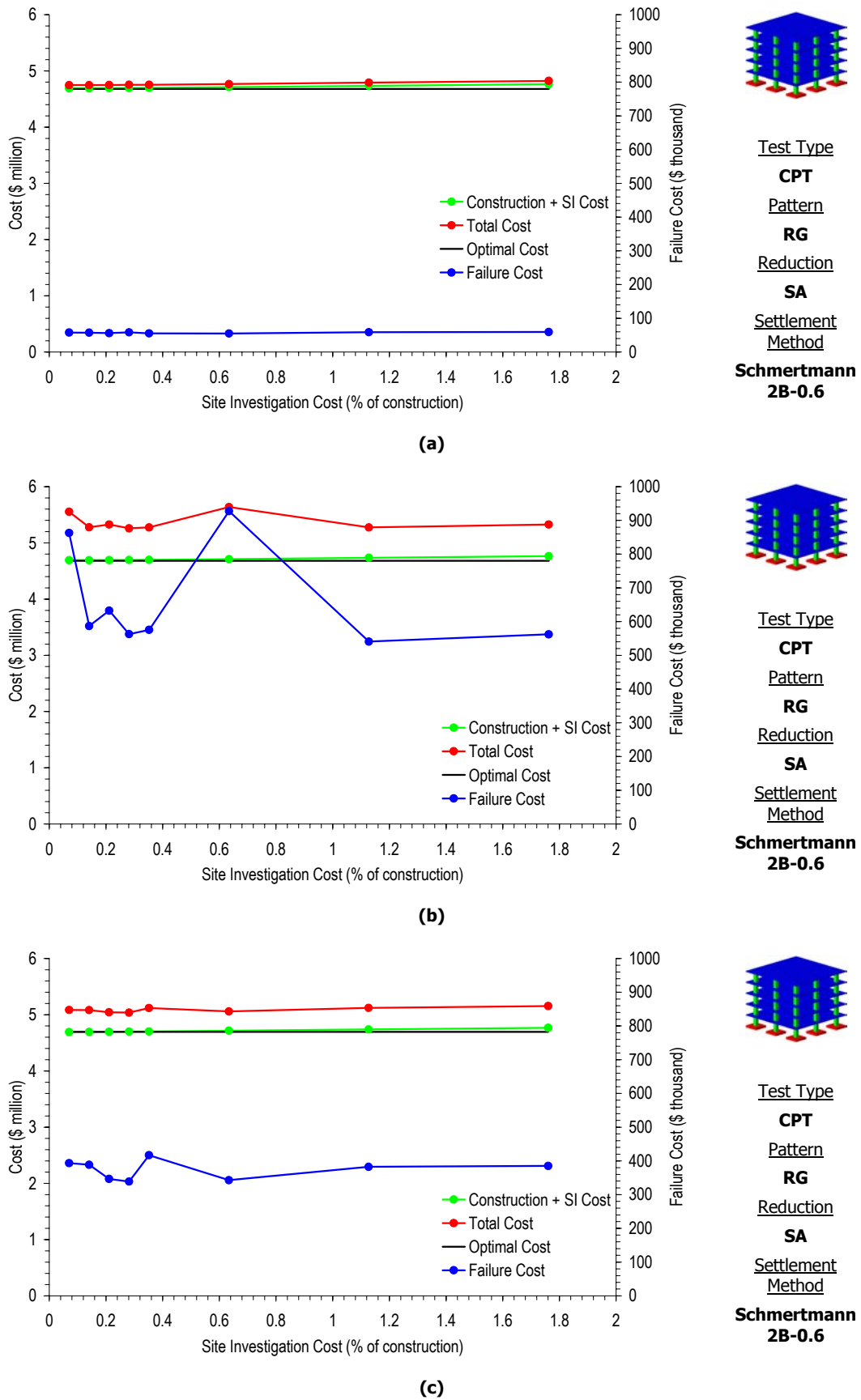
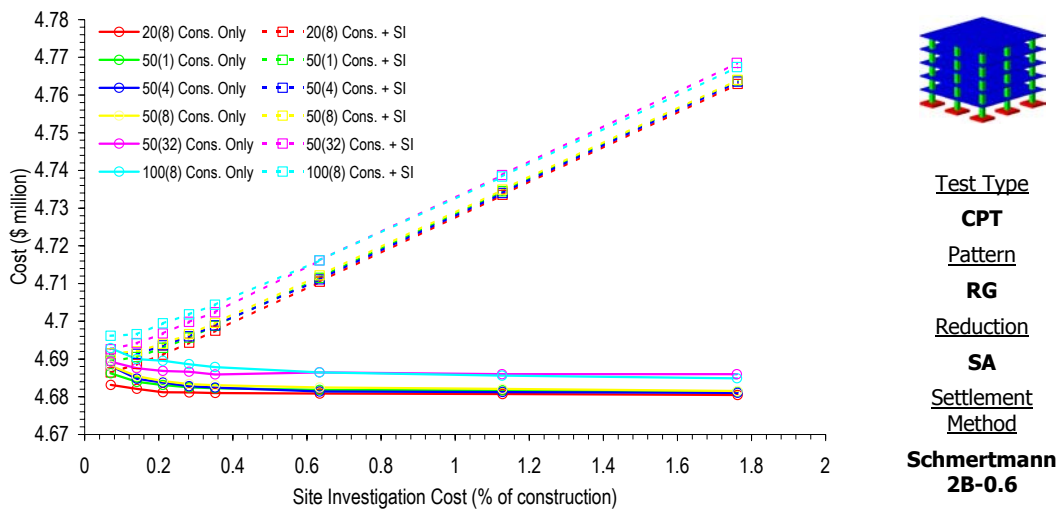


Figure 8-7 Effect of increased site investigation expenditure on the construction, failure and total cost based on 3DFEA, for a soil COV of 50% and SOF of (a) 1 m, (b) 4 m and (c) 32 m



the optimal design. However, the optimal design does not include any costs for a site investigation. Therefore, it appears that the SI design is reasonably smaller on average than the optimal design. This also causes the relatively high failure costs shown in Figure 8-6 or 8-7. However, the total cost of the design for soils with a low COV or SOF, shown in Figure 8-6(a) and 8-7(a), respectively, is not noticeably different from the optimal cost. This suggests that, for these soil conditions, the SI designs are reasonably accurate and the financial risk is low.



**Figure 8-8 Effect of increased site investigation expenditure on the construction cost of the design**

Although the results shown in Figures 8-6 and 8-7 do not show any general trend with increased sampling, the results in Figure 8-8 clearly indicate that the construction cost of the SI design reduces as the sampling effort increases. However, when the costs associated with the site investigation are included, this cost escalates for additional sampling. Therefore, the cost of the site investigation has a considerable impact on the project cost, which is defined as the cost of constructing the foundation and structure, as well as conducting the site investigation.

The absence of a general trend between the total cost of the design and the site investigation expenditure, shown in Figures 8-6 and 8-7, is unexpected and as such, warrants further investigation. Figure 8-9 illustrates the sample distributions of construction, failure and total costs, for three different sampling programs consisting of 1, 5 and 25 sample locations. Only a soil COV of 50% and SOF of 8 m is investigated in this analysis. These distributions show that there is little difference in failure costs for increased sampling. It was expected that the average and variability of the failure costs would reduce as the sam-

pling effort increased. However, the results shown in Figure 8-9 indicate no particular trend.

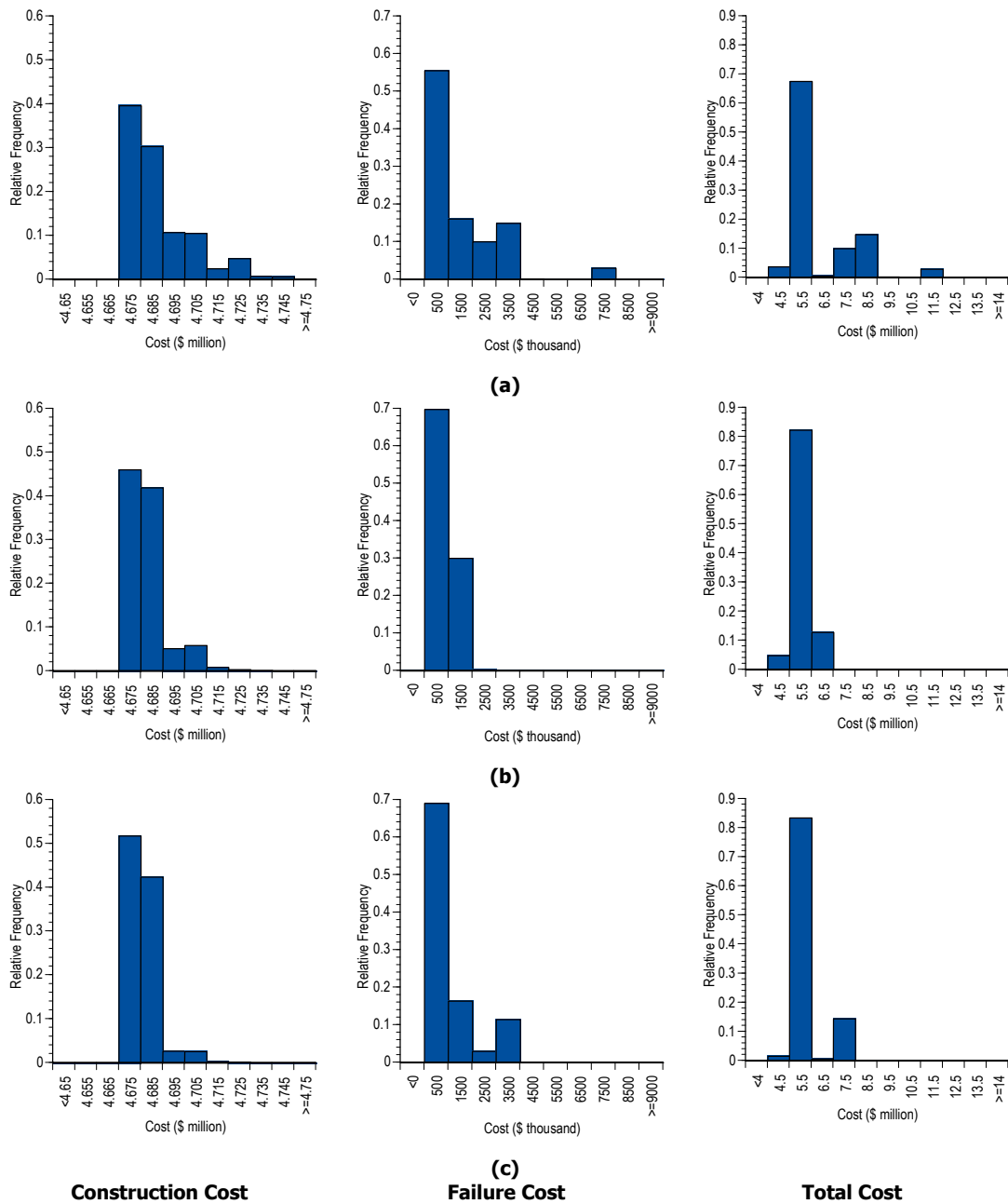


**Figure 8-9 Sample distributions of construction, failure and total costs for foundation designs based on (a) 1, (b) 5 and (c) 25 sample locations, for a soil COV of 50% and SOF of 8 m**

Since the costs associated with failure are based on the ‘true’ settlement of the foundation, which is analysed using 3DFEA and CK, sample distributions of the maximum ‘true’ settlement are also illustrated in Figure 8-10, for a soil COV of 50% and SOF of 8 m. These results indicate that the differences between the ‘true’ settlements for different sampling

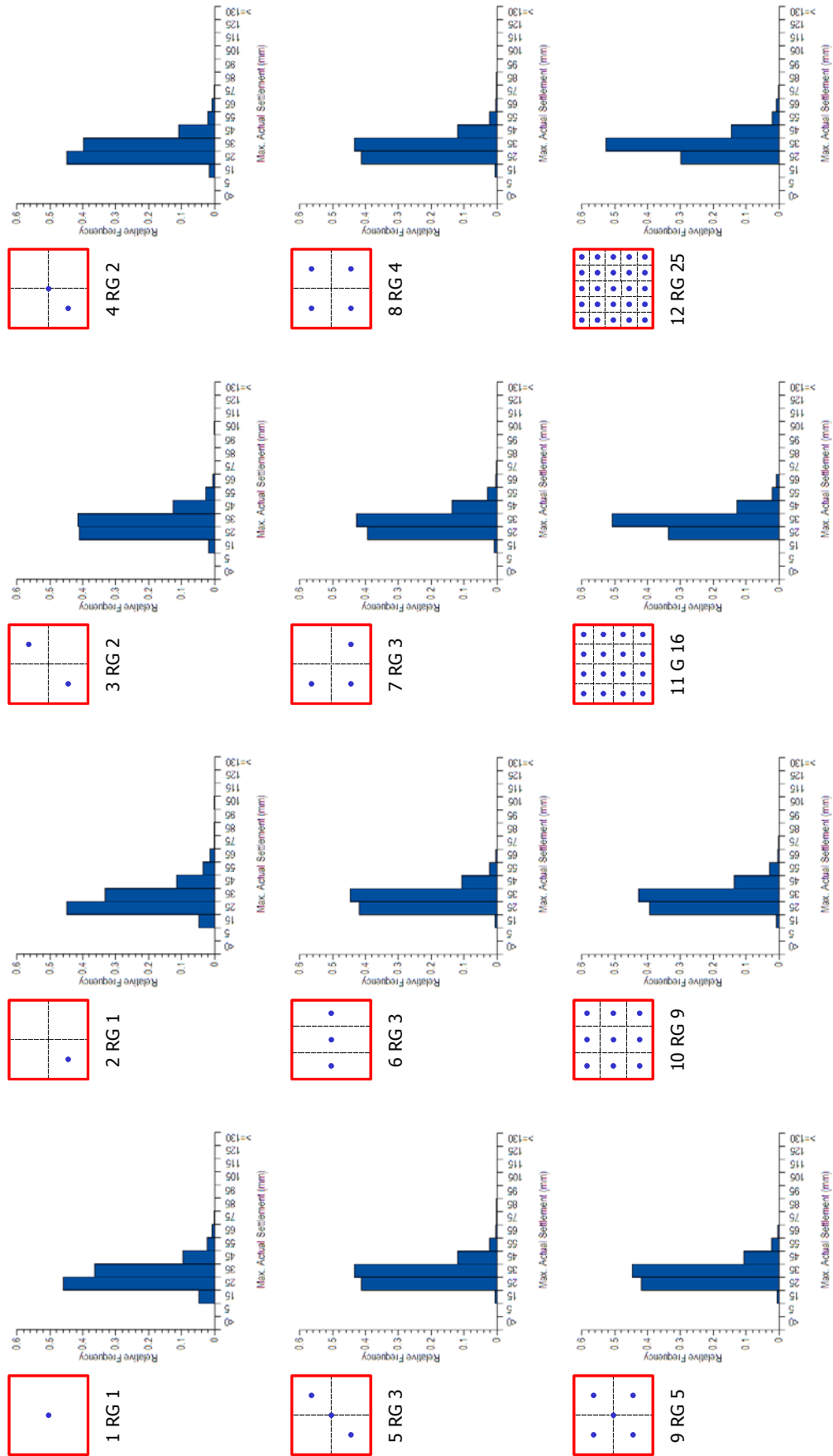


**Figure 8-10** Sample distribution of maximum settlements of the foundation design analysed using complete knowledge, for a soil COV of 50% and SOF of 16 m

efforts are almost negligible. Although this may be caused by a large bin size, the variability of the ‘true’ settlements also appears similar for different sampling efforts. This is unexpected, where the variability of the ‘true’ settlements with fewer sample locations is expected to be greater than that based on a higher sampling effort. In fact, the only apparent difference between the sample distributions is that the SI design based on less samples yields more ‘true’ settlements that are less than the design criterion of 25 mm (Figure 8-10). This is because the SI design with fewer samples has been shown in Chapter 6 (§6.3) to be conservative, where the average total footing area is larger than the optimal design, which is based on 3DFEA and CK.

An additional analysis is carried out to investigate the probability that ‘true’ settlements fall into the categories of; no failure, minor failure, major failure, and demolish and rebuild. These results are given in Figures 8-11(a) and (b) for the total and differential settlements, respectively. Such results indicate further reasons why there is an absence of a consistent trend in the total cost of the foundation. Figure 8-11(a) indicates that the number of ‘true’ settlements that occur between the limit of 25 mm, and the settlement that initiates minor rehabilitation (60 mm), increases as the sampling effort grows. This is consistent with the probability of under-design, shown in Chapter 7 (§7.2), for the same soil type and investigation program. However, the results shown in Figure 8-11(a) also suggest that none of the SI designs, based on a CPT, RG and SA, yield a ‘true’ settlement greater than 60 mm. In fact, the majority of designs yield a ‘true’ total settlement that is less than 25 mm, indicating that the SI design meets the design criteria reasonably well. However, the results shown in Figure 8-11(b) paint a very different picture. These results indicate that a large majority of SI designs yield a ‘true’ differential settlement that is greater than 0.0025 m/m and less than 0.006 m/m. This range corresponds to a minor rehabilitation category. However, the most pertinent observation made in Figure 8-11(b) is that the number of SI designs that yield a ‘true’ differential settlement between 0.0025 m/m and 0.006 m/m, remains relatively constant with increased sampling. This infers that the severity of failure does not reduce for an increased sampling effort. It should also be noted that the severity of failure is dependent on the largest total or differential settlement. Therefore, the results shown in Figure 8-11 suggest that the differential settlement typically controls the severity of failure where the design limit is exceeded on a more regular basis. This is to be expected for pad foundation systems.

It is also apparent that the probability of ‘true’ settlements falling in a failure category, does not decrease for an increased sampling effort. This is caused by the footing size restrictions imposed on the design to satisfy the use of 3DFEA. Such restrictions have been

discussed previously in Chapter 3 (§3.6.5) and infer that the footing size is increased by 1.0 m in one direction, every time the design criteria are exceeded. This is because the footing size is required to be a multiple of the element size of 0.5 m. Therefore, the possible footing sizes are: 1.5 × 1.5 m; 2.5 × 1.5 m; 2.5 × 2.5 m; 3.5 × 2.5 m; and so on. Such footing sizes relate to an increasing footing area of: 2.25 m<sup>2</sup>; 3.75 m<sup>2</sup>; 6.25 m<sup>2</sup>; 8.75 m<sup>2</sup>; and so on. Accordingly, the SI design does not necessarily target the design criteria of 25 mm maximum total settlement and 0.0025 m/m differential settlement. Instead, it yields a footing area with a much smaller total and differential settlement. Therefore, because the settlement of the designed footing is less than the target, the designs are already somewhat conservative.

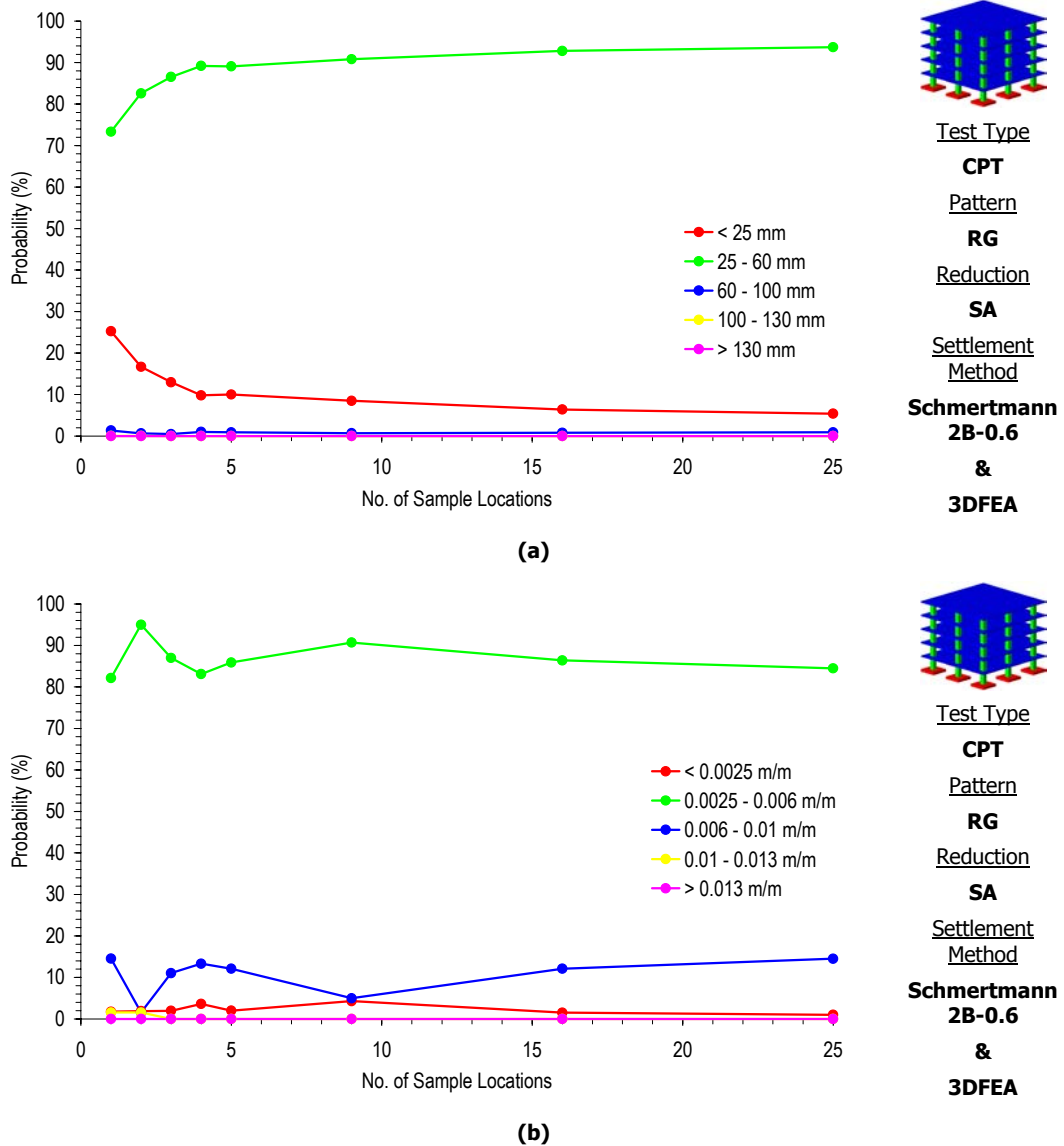


**Figure 8-11** Effect of increased sampling on the number of occurrences of 'true' (a) total and (b) differential settlements, based on 3DFEA using CK, for a soil COV of 50% and SOF of 16 m

Further evidence supporting the absence of a consistent trend between the total cost of the design and site investigation expenditure, is related to the minimum footing restriction imposed by the use of 3DFEA. Again, this has been discussed previously in Chapter 3 (§3.6.5.2) and essentially infers that the smallest possible footing in the analysis is 1.5 m × 1.5 m. This ensures that the footing consists of a suitable number of elements to reduce the effect of stress simulation errors. However, a minimum footing area also infers that an over-design condition is unlimited, but an under-design condition is limited. For example, if the SI design is based on a single sample location, which includes soil properties with high elastic moduli, the footing size is relatively small. However, the smallest size this footing can adopt is equal to the minimum footing size of 1.5 m × 1.5 m. On the other hand, a footing design based on a sample location with low elastic moduli can adopt almost any footing size. This is, however, restricted by the alternative foundation threshold discussed in Chapter 3 (§3.5.2). Therefore, it is not possible for the magnitude of an under-design, which controls the severity of failure, to be as large as the magnitude of an over-design. Such effects have been shown previously in Chapter 7 (§7.3), where the average design error was shown to be positive, but the average total footing area of the SI design was less than that of the optimal design.

Based on the discussions above, an analysis of the total cost of the design using 3DFEA appears to be heavily affected by the discretisation and the minimum footing restrictions imposed. Therefore, the results illustrating the effect of increasing site investigation expenditure on the total cost of the design, shown earlier in this section, are inconclusive. Without additional computing resources, the use of 3DFEA in this capacity has serious limitations. As a result, another method of analysing the foundation design using complete knowledge is adopted. This method is based on the analyses described in Chapter 5 (§5.2.3) and is discussed in the following section.

### **8.3.2 Failure Analysis Using Schmertmann 2B-0.6**

In this section, the costs associated with failure are assigned by analysing the SI design using the Schmertmann 2B-0.6 settlement prediction technique with an influence region of elastic moduli. Although this form of analysis does not strictly constitute complete knowledge of the soil, it has been shown in Chapter 5 (§5.2.3) to yield an average settlement error close to zero, when compared to 3DFEA and CK. Furthermore, the footing sizes are not required to be a multiple of the element size. Therefore, a much smaller sizing increment of 0.1 m is used. This increases the accuracy of the foundation design by closely targeting the settlement limits.

Before the Schmertmann 2B-0.6 settlement technique (Sch2B) can be used confidently with an influence region of elastic moduli, it is important to calibrate it to 3DFEA and CK. Therefore, a similar analysis to the one presented in Chapter 5 (§5.2.3) is undertaken. However, in this case, the object is to find a situation that yields a zero average settlement error. Since the results in Chapter 5 (§5.2.3) suggested that a geometric average of the moduli within the influence region preserved conservatism and rarely provided a zero average settlement error, the standard arithmetic average is used. It is also important to consider a number of footing sizes, because, in a design process, the footing size is iterated until it meets the criteria. As such, the results of this analysis are given in Figure 8-12 for a soil with a COV of 50% and varying SOF. An increasing soil COV is not considered as the results presented in Chapter 5 (§5.2.3) indicated that the COV had little impact on the optimal size of the region. The influence region size is expressed in terms of a width,  $b_{infrag}$ . Furthermore, the results in Figure 8-12 are based on an influence region width, which is normalised by the footing width,  $b$ .

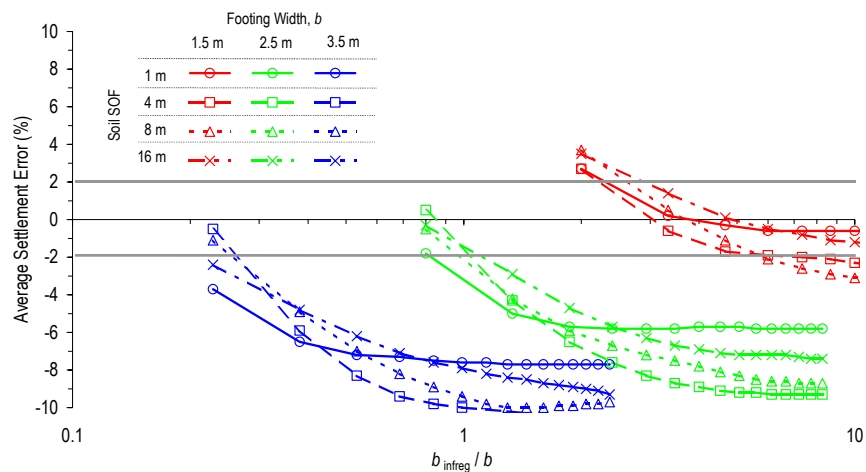


**Figure 8-12** Effect of increasing the width of the plan area of the influence region on the mean settlement error of a single footing for different site conditions and footing widths,  $b$ .

The grey lines in Figure 8-12 indicate results that have an average settlement error of  $\pm 2\%$ . Therefore, the results shown between these two lines indicate a settlement estimate that is within  $\pm 2\%$  of 3DFEA using CK. An error of  $\pm 2\%$  is considered adequate for the purposes of this research. Therefore, using results in Figure 8-12, when  $b = 1.5$  m, an influence region equal to 3 times the footing width is required to achieve a zero average settlement error. However, this reduces to 0.8 and 0.11 times the footing width when  $b$  is 2.5 m and 3.5 m, respectively. Furthermore, it is assumed that for footings larger than 3.5 m, an influence region size equivalent to  $0.11b$  is sufficient. However, it should be

noted that the element size remains 0.5 m. Therefore, the width of the influence region is rounded up to the nearest element width.

Since 3DFEA is no longer required in the analyses, the computational time is considerably reduced. With the inclusion of 3DFEA, the analysis of 1,000 Monte Carlo relationships required 2 weeks of computing time on a supercomputer (Hydra) with 8 CPUs. However, using the Schmertmann 2B-0.6 method and the influence region, this computational time is reduced to less than a days computing time, with 8 CPUs. As a result, it is possible to investigate the influence of several variables on the total cost. Such influences are described in the following sections.

### **8.3.3 Variables Impacting the Effect of Site Investigation Scope on the Total Foundation Cost**

Uncertainties associated with the soil variability, site investigation and settlement technique have all been shown previously to have an impact on the design of a foundation. Therefore, it is expected that each of these variables will also have an influence on the total cost of the design. As such, analyses are undertaken to examine the impact on total cost for each source of uncertainty, as well as other variables associated with the site investigation. This analysis uses the Schmertmann 2B-0.6 settlement technique with an influence region of elastic moduli to analyse the footings for the purpose of assigning failure costs. Similar to the analyses undertaken earlier, using 3DFEA and CK, the majority of results that follow are based on a foundation design for a 5-storey structure, with 9 pad footings [Figure 8-5]. Nevertheless, changes in building size are also examined.

#### **8.3.3.1 Soil Variability**

The soil COV and SOF has been shown throughout this document to have a marked impact on the average and variability of foundation design. Therefore, it is expected that an analysis dealing with the soil variability will show a similar affect on the total cost. As with previous analyses, the effect of soil variability is measured by varying the soil COV and SOF. In this case, soils with a COV of 20%, 50% and 100% are investigated, as well as soils with a SOF of 1, 4, 8 and 32 m. Results are given in Figures 8-13 and 8-14 for soils with an increasing COV and SOF, respectively. It should be noted that Figures 8-13 and 8-14 are based on the same conditions as Figures 8-6 and 8-7, where the SI design was analysed using 3DFEA. However, Figures 8-13 and 8-14, typically show a consistent trend, where the total cost reduces as the site investigation expenditure increases. In fact,



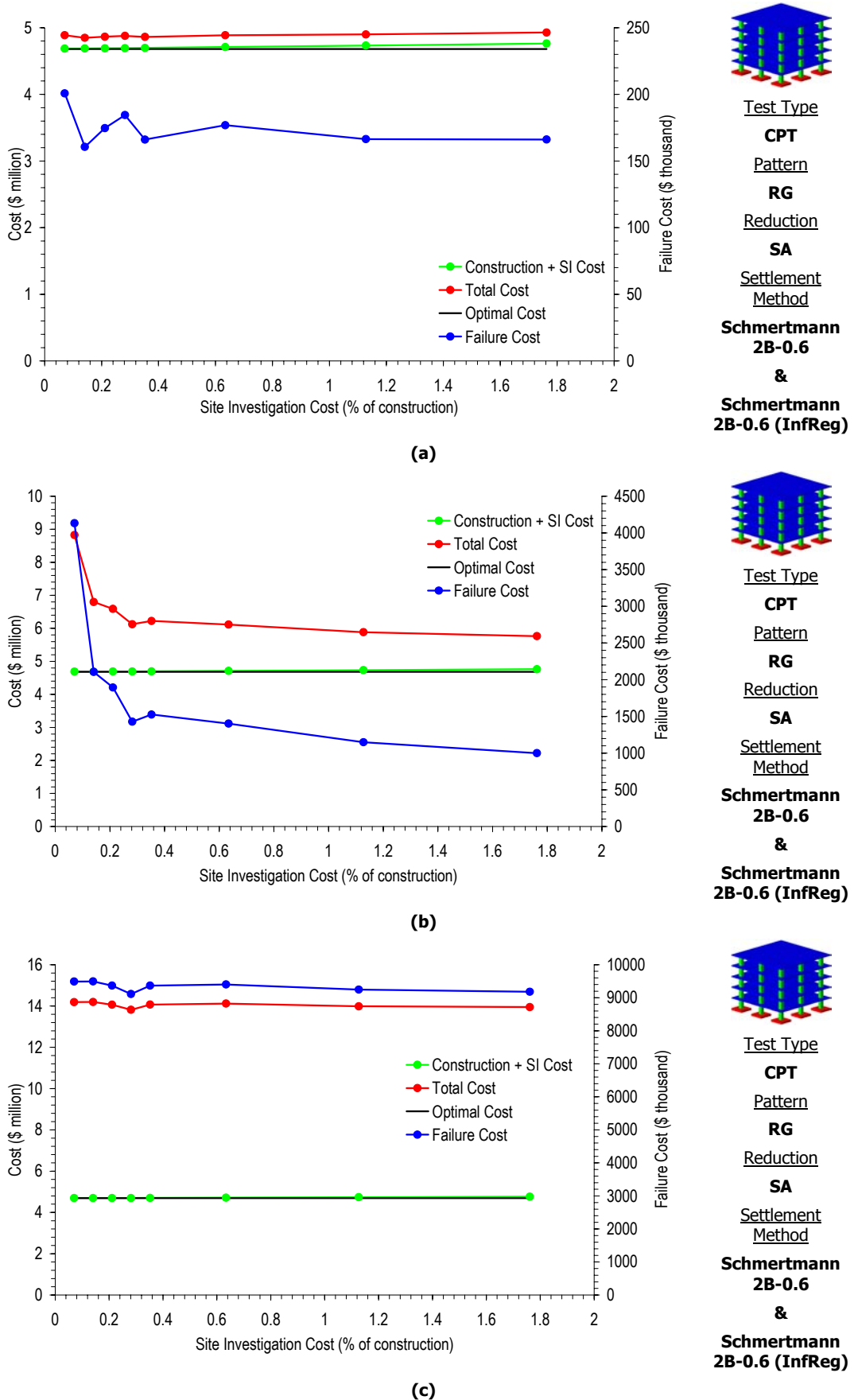
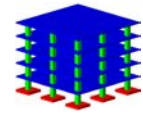
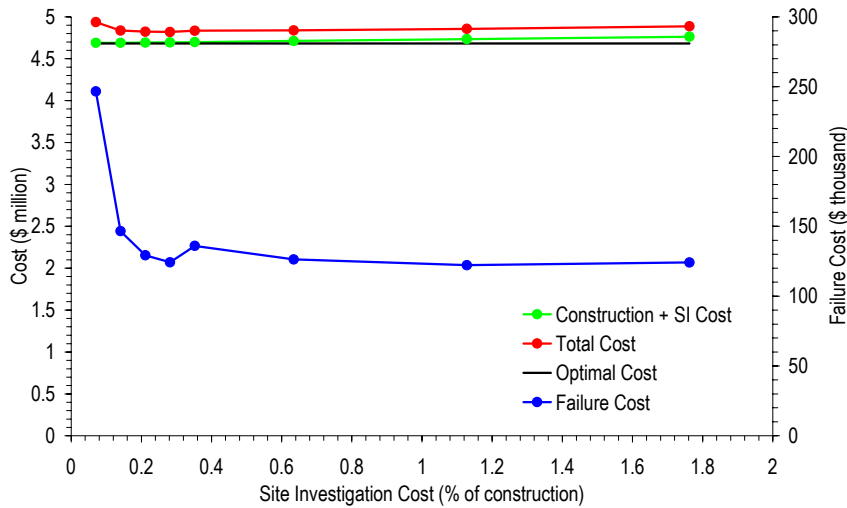


**Figure 8-13** Effect of increased site investigation expenditure on the construction, failure and total cost, based on an influence region analysis, for a soil SOF of 8 m and COV of (a) 20%, (b) 50% and (c) 100%



Test Type

CPT

Pattern

RG

Reduction

SA

Settlement

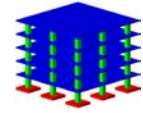
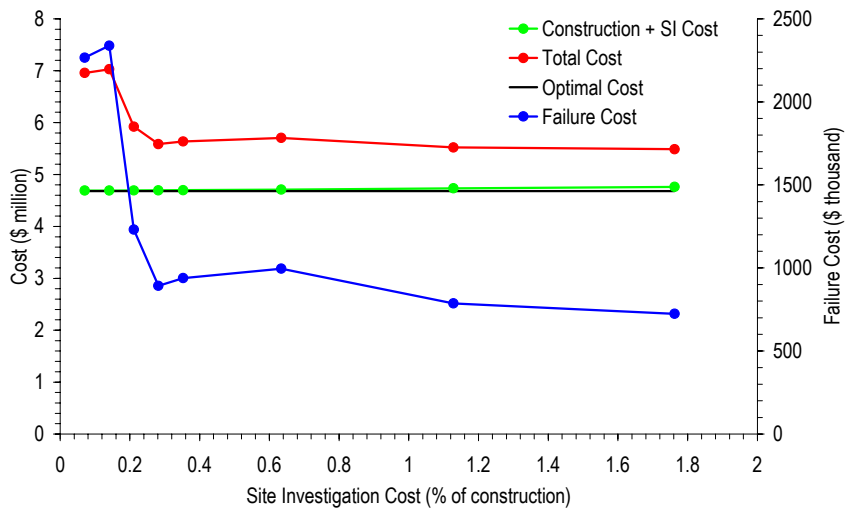
Method

Schmertmann  
2B-0.6

&

Schmertmann  
2B-0.6 (InfReg)

(a)



Test Type

CPT

Pattern

RG

Reduction

SA

Settlement

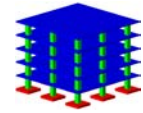
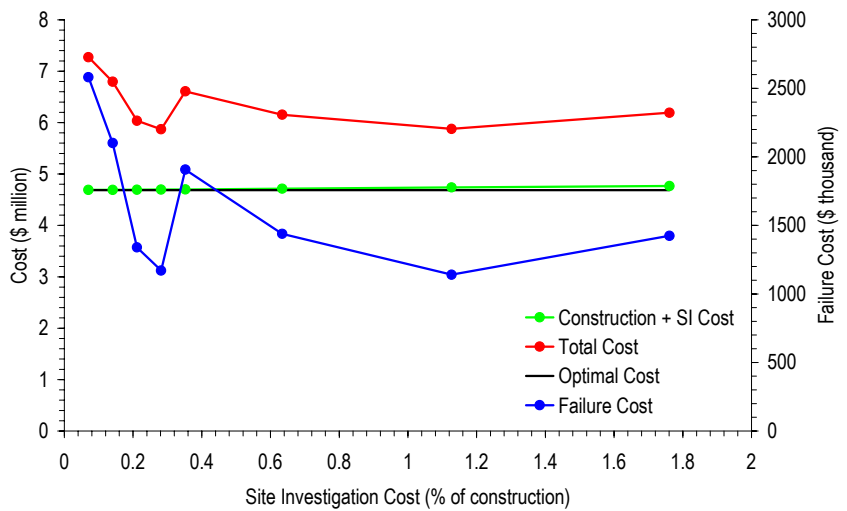
Method

Schmertmann  
2B-0.6

&

Schmertmann  
2B-0.6 (InfReg)

(b)



Test Type

CPT

Pattern

RG

Reduction

SA

Settlement

Method

Schmertmann  
2B-0.6

&

Schmertmann  
2B-0.6 (InfReg)

(c)

Figure 8-14 Effect of increased site investigation expenditure on the construction, failure and total cost, based on an influence region analysis, for a soil COV of 50% and SOF of (a) 1 m, (b) 4 m and (c) 32 m

several of the results indicate an optimal site investigation expenditure, which yields the least total cost. For example, a site investigation expenditure of 0.3% or 1.15% of the construction cost yields designs with the least total cost of approximately \$5.9 million, for a soil COV of 50% and SOF of 32 m [Figure 8-14(c)]. Compare this with the situation of a site investigation expenditure of 0.07%, where the total cost is \$7.4 million. This represents a financial saving of \$1.5 million or 20%. The increase in site investigation expenditure from 0.07% to 0.3% of the construction cost, relates to an additional expenditure of \$13,200, or an increase from 1 CPT sounding to 4.

The only site conditions that do not show an obvious reduction in total cost for increased site investigation expenditure are shown in Figure 8-13(a) and (c) for soils with a COV of 20% and 100%, respectively. In these cases, it appears that the total cost is constant for any degree of site investigation expenditure. Results shown later in this chapter demonstrate that this is a function of the SA reduction technique. The other techniques yield designs where the total cost reduces as the site investigation expenditure increases.

The results for a soil COV of 50% and a SOF of 32 m [Figure 8-14(c)] indicate that a site investigation expenditure of approximately 0.4% yields a total cost that is greater than when the site investigation expenditure is both higher and lower than 0.4%. This is due to the adopted sampling pattern, where the site investigation expenditure of 0.4% refers to an investigation with 5 sample locations. In this case, one sampling location occurs at the centre of the site. This appears to increase the total cost by increasing the costs associated with failure. A similar difference between investigations with 4 and 5 sampling locations was also evident with regard to the probability of under- and over-design, as shown in Chapter 7 (§7.2). In these results, however, the probability of under-design was noticeably less for the design based on the 5 sampling locations. As such, it appears that the number or degree of failures for the design based on 5 sample locations is greater than that for designs based on 5 or 9 sample locations.

It is obvious that the use of the influence region analysis provides a better representation of the results. This is because the footing size is not constrained by the element size. However, it should also be remembered that the influence region analysis is calibrated to 3DFEA settlement. Furthermore, uncertainties exist in both the calibration and 3DFEA. Therefore, all results and conclusions in this chapter are based on a method that has been calibrated to 3DFEA.

The results in Figures 8-13 and 8-14 also indicate that the total cost of the SI design is always greater than the cost of the optimal design. This is clearly understandable because any footing that is smaller than the optimal is considered to fail. However, in general, the construction cost of the SI design is not significantly different than the cost of the optimal design. This suggests that, on average, the footing sizes are similar. Hence, it is the variability of the SI design that causes the high probability of failure and, therefore, the high failure costs. However, when the soil COV is low [Figure 8-13(a)], the total cost of the SI design is close to the optimal, since the failure costs are low. This is because, for a low soil COV, the variability of the SI design is relatively small, as shown previously in Chapter 6 (Figure 6-27). Therefore, the reduction in failure cost, due to increasing site investigation expenditure, is caused by the diminishing design variability. However, the relative conservatisms in the design types should not be discounted. Both the design variability and conservatism has been shown in previous chapters to be affected by the site conditions, reduction techniques, test types and settlement predication methods. Discussions regarding the effect of reduction techniques, test types and prediction methods on the total cost, are reserved for later in this chapter.

A clearer indication of the impact of soil variability on the total cost of the SI design is presented in Figures 8-15(a) and (b), for an increasing soil COV and SOF, respectively. These results indicate that:

- The total cost of the SI design is higher for soils with a larger COV;
- Increased site investigation expenditure has a greater influence when the soil COV is 50%;
- Little benefit is evident for increased site investigation expenditure when the soil COV or SOF is low; and
- A worst case SOF is evident where the greatest benefit of increased expenditure occurs when the soil SOF is 8 m.

Although the aim of a site investigation is to reduce the risks associated with foundation failures, it is also worthwhile to investigate the effect of increased expenditure on the construction cost. This is because the construction cost indicates the initial outlay when the project is being constructed. Such results are shown in Figure 8-16 for a soil with a SOF of 8 m and increasing COV. These results illustrate the project costs, which include the costs associated with the construction of both the foundation and superstructure, as well as

the cost of the site investigation. Results for the construction costs alone mimic those shown in Chapter 6 (§6.3) for the average total footing area. However, when the site investigation expenditure is included, the construction costs are shown to increase noticeably for additional sampling. This infers that the savings expected from achieving a smaller footing design through increased sampling are outweighed by the expense of the additional sampling locations. In other words, increased sampling results in a more expensive foundation design. However, this is not the full story.

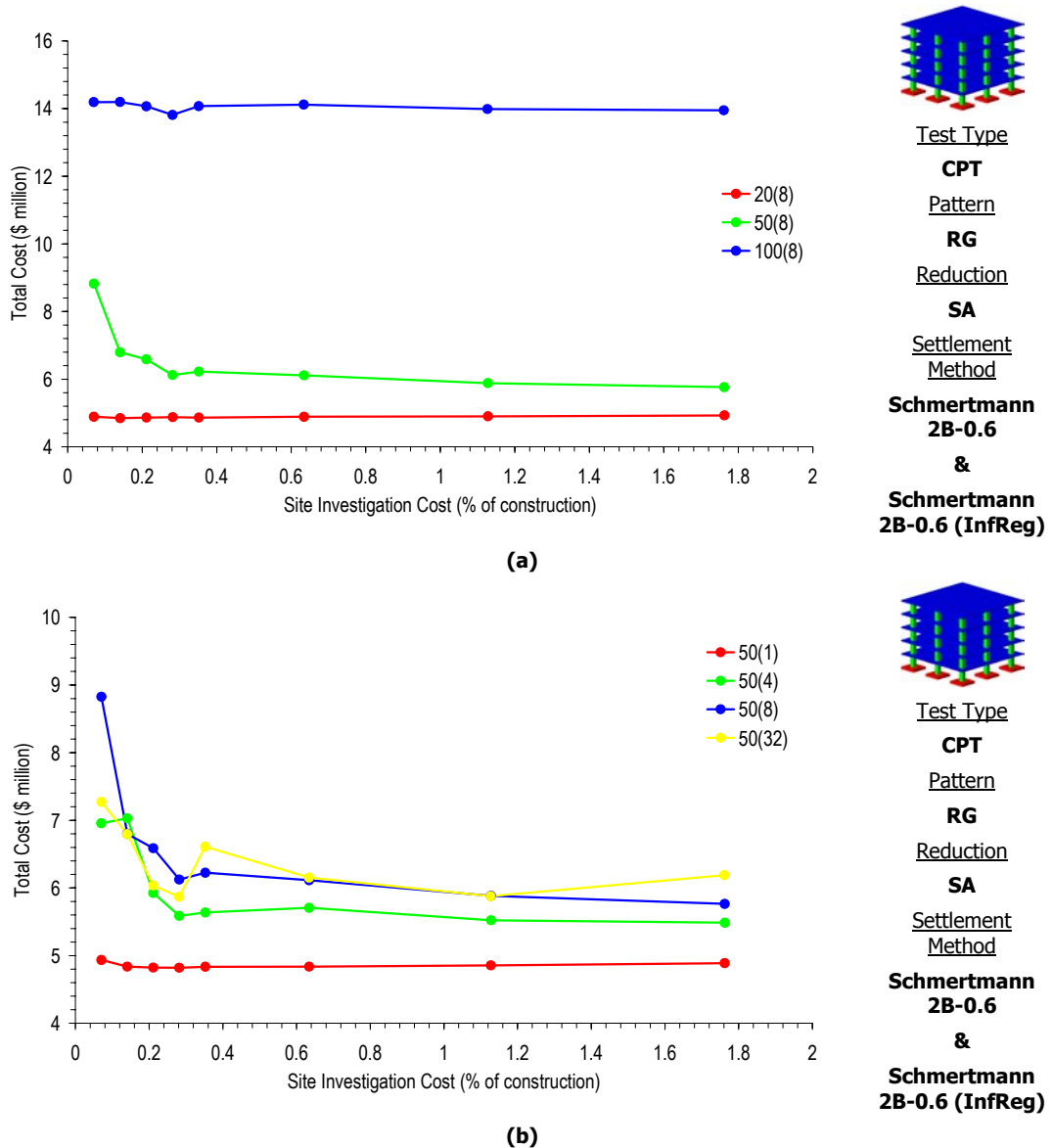


**Figure 8-15** Effect of increased site investigation expenditure on the total cost, based on an influence region analysis, for an increasing soil (a) COV (SOF of 8 m) and (b) SOF (COV of 50%)

By comparing the construction costs shown in Figure 8-16, with the total costs shown in Figure 8-15, it is apparent that a slightly conservative footing design yields a low total cost.

This is because the design guards against potential failures. Furthermore, because a foundation failure affects the entire building, and an over-design impacts only the size of the foundation, it is of greater benefit to avoid against a failure. Therefore, it appears that the costs associated with a foundation failure have the largest impact on the total cost. In fact, for a soil COV of 100% and SOF of 8 m [Figure 8-13(c)] the costs associated with foundation failure are upwards of \$8 million. This is approximately 50% of the total cost and approximately 180% of the project cost.

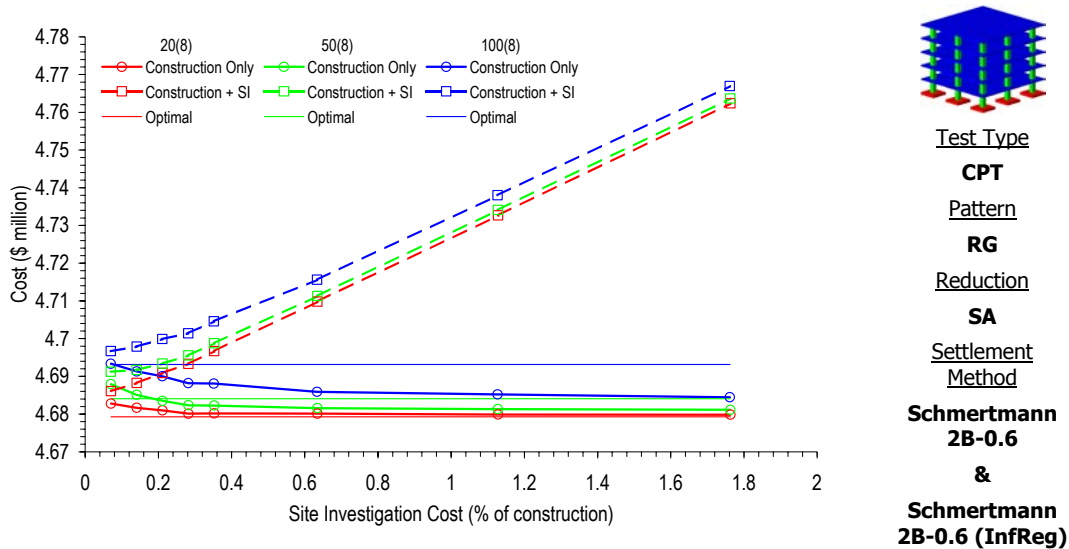


**Figure 8-16 Effect of increased site investigation expenditure on the construction cost including and excluding site investigation costs, for an increasing soil COV and SOF of 8 m**

### 8.3.3.2 Reduction Technique

The reduction techniques have been shown in previous chapters to have a marked impact on the conservatism of the foundation design and, since the results in the previous analysis indicated that a slightly conservative design appears preferable, it is worthwhile examining the influence of each of the reduction techniques. In this case, only a soil with a COV of 50% and SOF of 8 m is investigated. This is because it was shown in the previous section that the greatest impact of increased site investigation expenditure occurs for a soil with a COV of 50% and SOF of 8 m. However, results for other soil types are also given in Appendix E. Results of the analysis for the SA, GA, HA, ID and 1Q reduction techniques are given in Figure 8-17. The MN method is not examined here as its high degree of conservatism, which also increases as the sampling effort rises, yields very large and therefore, uneconomical footing designs. The I2 technique is also not shown in Figure 8-17 since its formulation is very similar to the ID. Furthermore, it has been shown previously that the

ID and I2 techniques yield very similar results and are both not recommended for use with a 9-pad foundation system (Chapter 7).

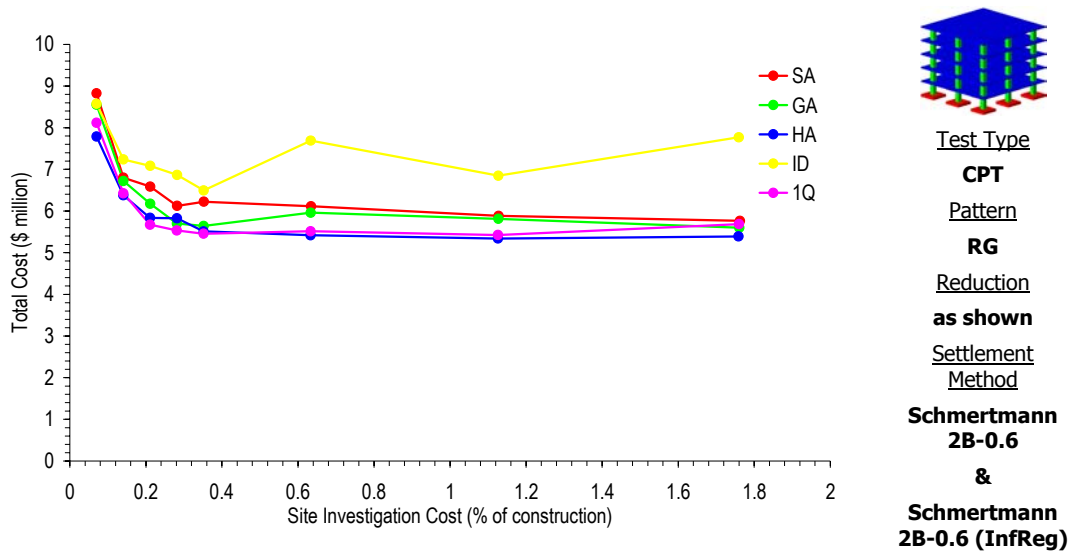


**Figure 8-17 Effect of increased site investigation expenditure with different reduction techniques on the total cost, based on an influence region analysis, for a soil COV of 50% and SOF of 8 m**

Results in Figure 8-17 suggest that:

- The HA and 1Q reduction techniques yield SI designs with the lowest total cost;
- Except for the ID method, the SA yields the highest total cost; and
- For all techniques, apart from the ID, the optimal site investigation expenditure, leading to the lowest total cost, is the same (approximately 0.35% of the construction cost).

These results provide different conclusions than those shown in Chapter 7 for the probabilities of under- and over design (§7.2) and the average design error (§7.3). Results in Chapter 7 suggested that the GA is the preferred technique. However, Figure 8-17 clearly indicates that either the 1Q or HA yield designs with lower total cost. This is because the 1Q and HA yield slightly more conservative solutions, which guard against potential failures. Such conservatism was shown in Chapter 6 (§6.3) for the average total footing area, but is also shown in Figure 8-18 for the construction costs associated with each reduction technique.

Results in Figure 8-18 indicate that the 1Q yields the highest project cost, when the site investigation expenditure is close to the optimal of 0.35%. On the other hand, the SA

yields a design with the least project cost. However, this is balanced by the high total cost shown in Figure 8-17. Therefore, the choice of reduction technique becomes a trade-off between achieving a low project cost, or a low total cost. Considering the difference between the projects costs at the optimal site investigation expenditure is only in the order of \$10,000, it seems of greater benefit to use the reduction technique that provides the lowest total cost.

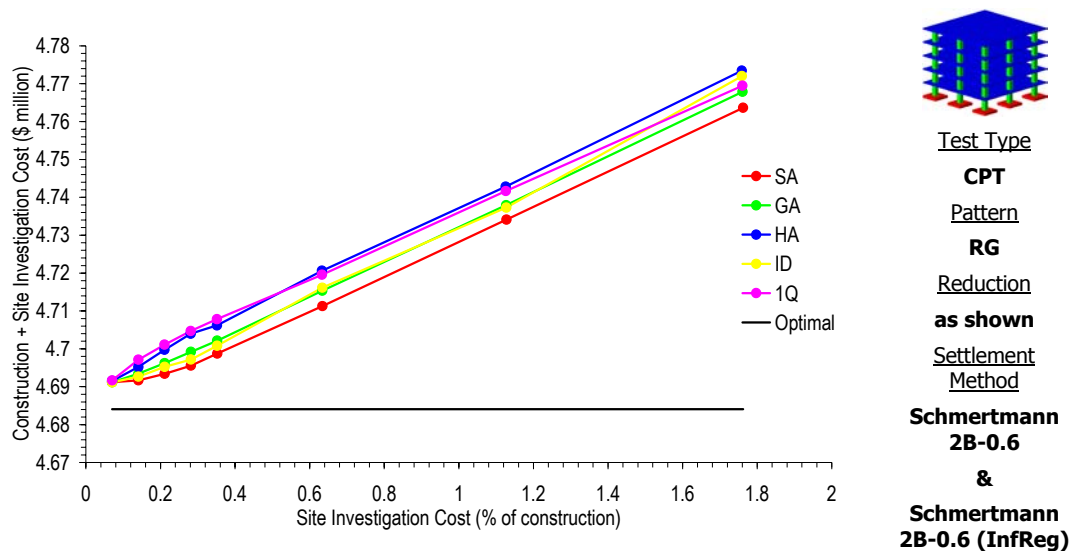


**Figure 8-18 Effect of increased site investigation expenditure with different reduction techniques on the construction cost, for a soil COV of 50% and SOF of 8 m**

**The 1Q reduction technique yields a design with the lowest total cost.**

### 8.3.3.3 Type of Soil Test

An analysis is also undertaken to investigate the impact of different test types on the total cost of the foundation. As similar to the reduction techniques, the test types have been shown previously (§6.3.3) to have an impact on the conservatism of the foundation design. However, until now, the relative cost of each test type has not been considered. Such costs were discussed earlier in this chapter (§8.2.1) and have a direct impact on the total cost of the design. Results for the different test types are given in Figure 8-19 for a soil COV of 50% and SOF of 8 m. As with previous analyses, results for other soil types are also provided in Appendix E.



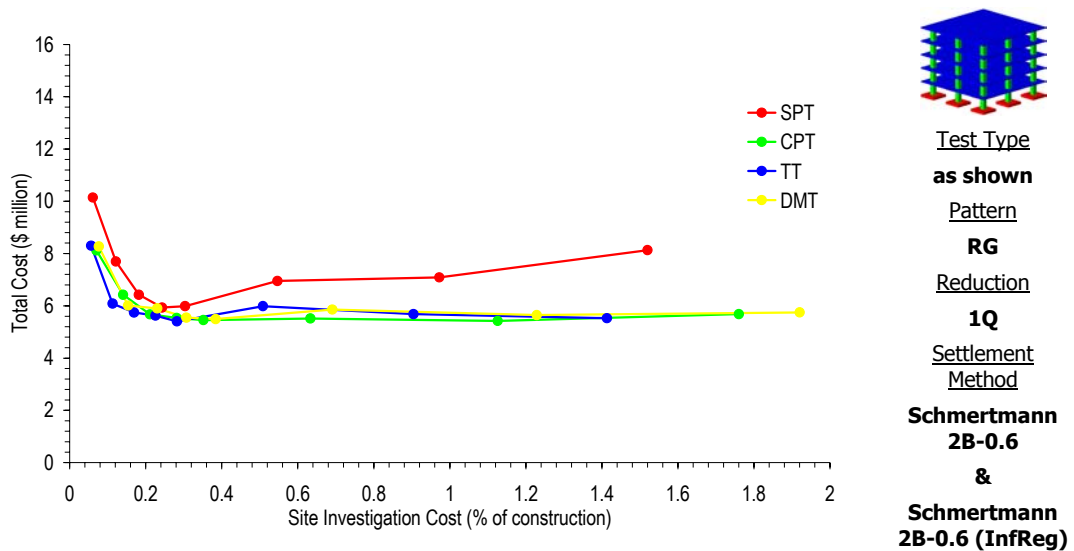


**Figure 8-19** Effect of increased site investigation expenditure with different test types on the total cost of the foundation, based on an influence region analysis, for a soil COV of 50% and SOF of 8 m

First, it is important to recognise that the different test types yield different site investigation expenditures, even with the same sampling patterns and number of sample locations. This is because the cost of the different test types varies in accordance with the discussions earlier in this chapter. As a comparison, the DMT yields the most expensive site investigation, closely followed by the CPT and SPT. The triaxial test (TT) yields the least expensive site investigation for the same number of sampling locations, but involves testing the least amount of soil. Although the TT provides a low cost site investigation, it does not necessarily result in a foundation design with the lowest total cost. In fact, the results shown in Figure 8-19 suggest that the CPT consistently provides a foundation design with the lowest total cost. Designs using the DMT appear to result in a total cost which is reasonably similar to that of the CPT and TT. However, the DMT is slightly more expensive than the CPT and TT (\$3,600 / sample location compared with \$3,300 and \$2,650, respectively), which imply that designs using the DMT are generally more expensive.

Designs based on the TT are shown not to have the same smooth relationship between site investigation expenditure and total cost as the other test types. For example, the results suggest that the total cost reduces as the site investigation expenditure increases to 0.24%. However, a further increase in expenditure to 0.28% increases the total cost. This does not occur for the CPT or DMT. This suggests that the results based on the TT are not as robust as these other test types. Hence, a small change in site investigation expense may cause a large change in total cost. This is primarily a function of the number of samples considered, where a TT uses only 2 elastic moduli per sample location and the CPT and DMT consider 60 and 30 properties per sample location, respectively. Therefore, an increase in

the number of sampling locations has a greater effect on the variability of the elastic moduli, when using the TT. It is also important to remember that the vertical sampling rate of the CPT is not representative of the test implementation. Therefore, it is expected that a further increase in vertical sampling rate would reduce the total cost. However, due to the constraints on the element size with regard to computational time, an analysis of this type is not considered.

**The CPT consistently yields the lowest total cost design.**

The results shown in Figure 8-19 also suggest that the SPT yields designs that have a noticeably greater total cost than the other test types. Although this may be related to the conservatism of the SPT in comparison to the other tests, it is more likely a function of the large uncertainties inherent with the SPT. Similar results regarding the variability of designs using the SPT have been shown in Chapter 6 (§6.4.3), where the COV of total footing area was much larger than the other test types. The designs based on the SPT are also shown to have a noticeable increase in total cost for a growing site investigation expense, after the optimal expenditure is reached.

#### 8.3.3.4 Settlement Prediction Technique

In keeping with the analyses in previous chapters, an examination of the use of different settlement prediction techniques on the total cost of the SI design is undertaken. In this case, the different methods are used to provide settlement estimates for the SI design. However, the influence region analysis is still based on the Schmertmann 2B-0.6 technique (Sch2B). Results of this analysis are, once again, provided for a soil COV of 50% and SOF of 8 m. However, using the conclusions from the previous section, the site investigation is based solely on the 1Q method and CPT. Results showing the impact of site investigation on the total cost are given in Figure 8-20, while the effect of increased knowledge on the project cost is shown in Figure 8-21. These results indicate that:

- The Perloff and Schmertmann Modified settlement techniques yield designs with the lowest total cost;
- The Newmark technique clearly yields the highest total cost;
- The optimal site investigation expenditure is reasonably similar for all settlement techniques; and

- Greater benefits for increased sampling are shown for techniques that yield a relatively high total cost.

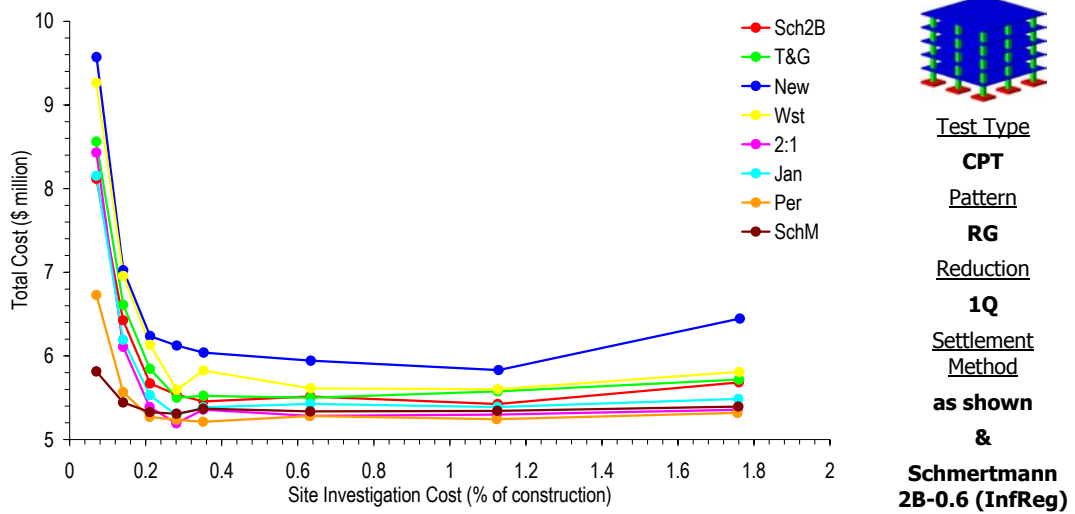


**Figure 8-20** Effect of increased site investigation expenditure with different settlement techniques on the total cost of the foundation, based on an influence region analysis, for a soil COV of 50% and SOF 8 m

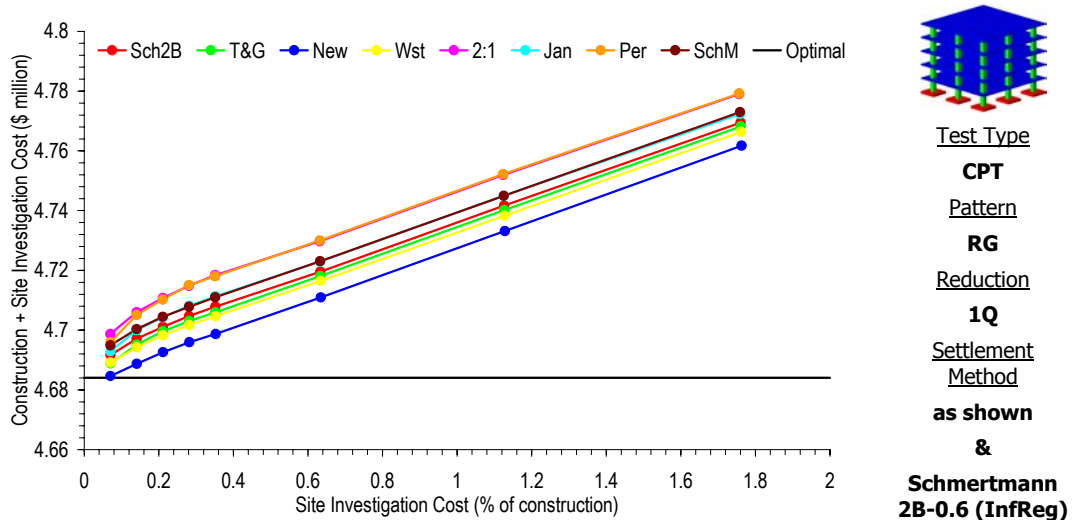


**Figure 8-21** Effect of increased site investigation expenditure with different settlement techniques on the total cost of the foundation, based on an influence region analysis, for a soil COV of 50% and SOF 8 m

As with the results for the reduction techniques, Figures 8-20 and 8-21 indicate that the settlement methods that yield designs with larger project costs (Figure 8-21) also yield low total costs (Figure 8-20). This reiterates that a conservative SI design is more beneficial in terms of total cost. It also creates a similar dilemma to that described for the reduction technique where the choice of a settlement relationship becomes a trade-off between outlay costs and the costs expected during the life of the structure. However, like the results

shown above, the difference in construction cost is heavily outweighed by the difference in total cost. Yet, it is important to remember that these results are based on expected or average costs. Therefore, these costs should only be considered for comparative purposes. This is due to several simplifications in the method including the use of a single layered, stationary soil (§3.3).

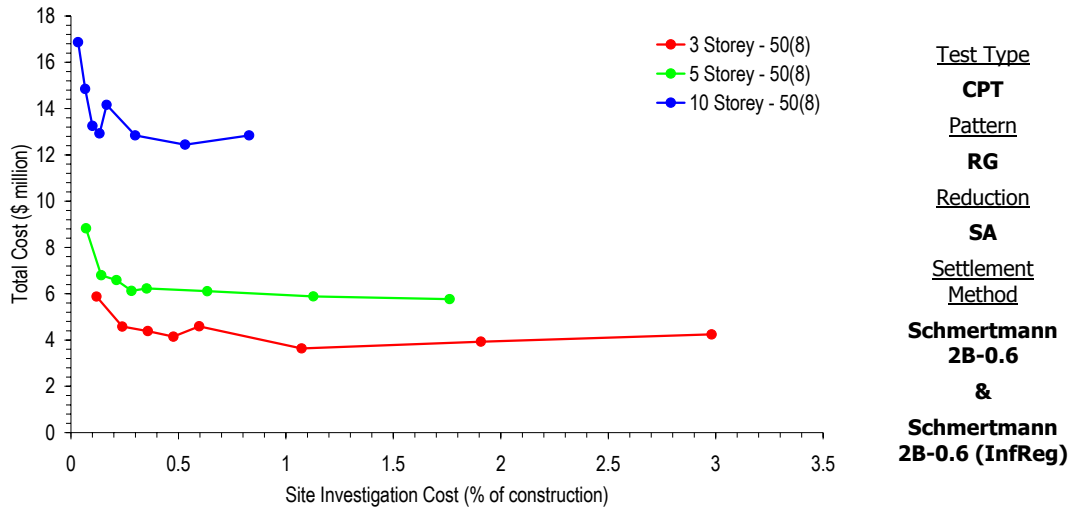
### 8.3.3.5 Building Heights

The optimal site investigation expenditure has been identified in the previous sections to be approximately 0.3% to 0.4% of the construction cost. However, this amount is based solely on a 20 m × 20 m, 5-storey building. As such, additional analyses are undertaken to investigate the impact of increased site investigation expenditure on the total cost of a SI design for buildings of varying height. In this case, buildings with 3-, 5- and 10-storeys are considered. Each building has a plan area of 20 m × 20 m, and a foundation system with 9-pad footings supporting a 5 kPa live load and 3 kPa dead load. The changing building height leads to varying footing loads as given in Table 8-6. Furthermore, different soils are also investigated for each building size. In this case, the analysis for the 3-storey structure is conducted for a soil with a mean elastic modulus of 10,000 kPa (10 MPa). The analyses for the 5- and 10-storey structures are based on a soil with a mean elastic modulus of 30,000 kPa (30 MPa), as similar with previous analyses in this chapter. Additional analyses examining the impact of using different mean elastic moduli on the total cost are discussed later.

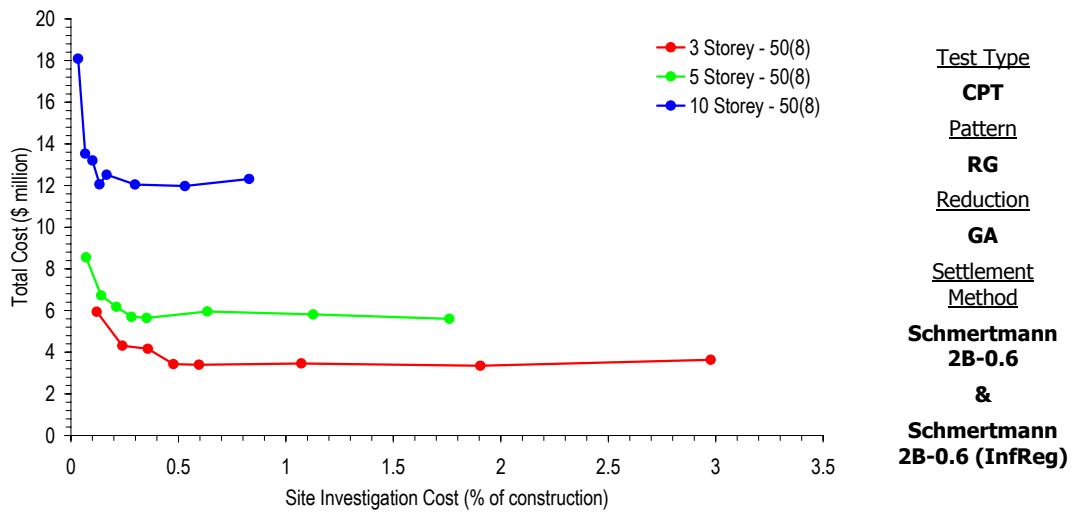
**Table 8-6 Pad footing loads for the three building sizes investigated**

Footing	Point Load		
	3 Storey	5 Storey	10 Storey
Corner	860 kN	1,433 kN	2,867 kN
Centre Edge	1,150 kN	1,917 kN	3,833 kN
Centre	1,540 kN	2,567 kN	5,133 kN

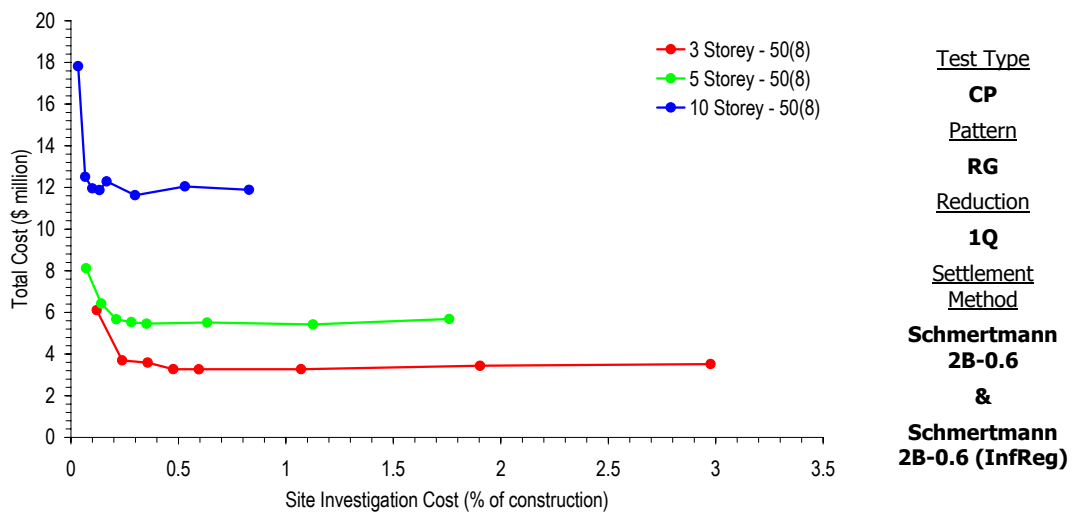
Since the reduction technique has been shown above to have the largest impact on the total cost of the design, the analysis for different building heights is conducted for a SI design that uses three different reduction methods. Results are given in Figure 8-22, where the SI design is based on the SA, GA and 1Q, respectively. In all cases, sampling locations are arranged using the RG, and the CPT test type is adopted. Furthermore, these results are based solely on a soil COV of 50% and SOF of 8 m.



(a)



(b)



(c)

Figure 8-22 Effect of increased site investigation expenditure using the (a) SA, (b) GA and (c) 1Q on the total cost of 3 different building sizes for a soil COV of 50% and SOF of 8 m

Results in Figure 8-22 demonstrate that:

- Increased site investigation expenditure benefits designs for all building heights, where the total cost is noticeably reduced;
- The optimal site investigation expenditure, as a percentage of the project cost, varies for different building heights. In this case, it reduces for an increasing building height;
- The reduction technique adopted does not favour one building size in particular; and
- The 1Q and GA generally yield a lower total cost than the SA.

The results in Figure 8-22 suggest that the optimal site investigation expenditure cannot be expressed in terms of a percentage of the project cost. Instead, the optimal site investigation expenditure is a smaller percentage when larger buildings are considered. This is despite the fact that research by others (e.g. Clayton et al. 1982, National Research Council 1984, Peacock and Whyte 1988, Site Investigation Steering Group 1993, Jaksa 2000) has documented expenditure in terms of a percentage of project cost. However, Littlejohn (1994) argued that site investigation expenditure should not be based on the project cost. His views are confirmed by the results in Figure 8-22. A clearer indication of the optimal site investigation is presented in Figure 8-23, which illustrates the impact of increased sampling, or site investigation expenditure, on the construction and failure costs of the three different building sizes. In this case, the site investigation expenditure is expressed in terms of a cost only, as well as the number of sampling locations. Such results indicate that the optimal site investigation occurs at the same sampling effort of approximately 4 locations. This corresponds to a site investigation cost of \$13,200 that, when expressed as a percentage of the construction cost, is equivalent to 0.48% for the 3-storey building, 0.35% for the 5-storey building, and 0.13% for the 10-storey building. As such, the optimal site investigation expenditure is influenced by the soil conditions and not the building height, in terms of number of storeys. In this case, an expenditure of \$13,200 yields the optimal characterisation for a 20 m × 20 m site area.

**The optimal cost of a site investigation is influenced by the site conditions and not the height of the building (in terms of number of storeys). Therefore, optimal site investigation expenditure should not be based on a percentage of the project cost.**

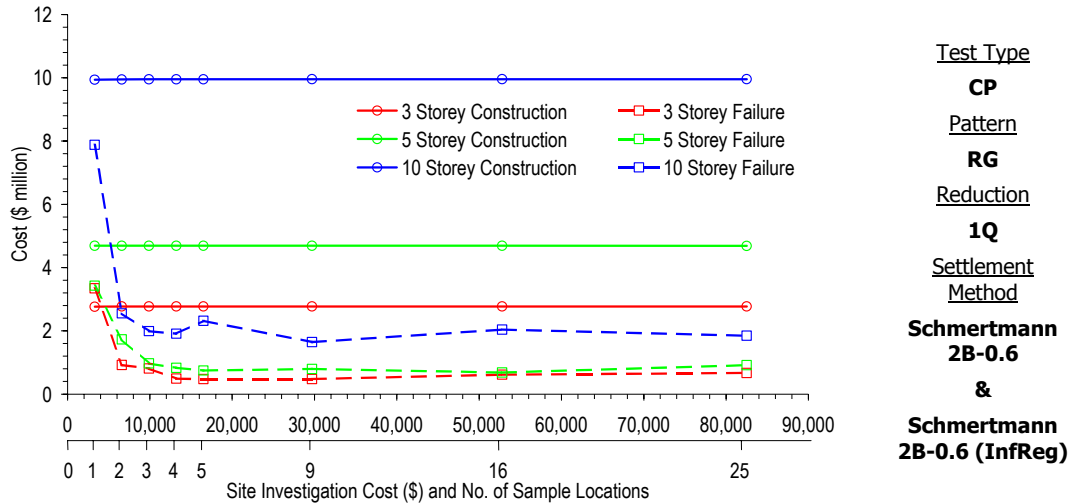


**Figure 8-23 Effect of increased site investigation expenditure on the construction and failure costs of 3 different building sizes, for a soil COV of 50% and SOF of 8 m**

The results in Figures 8-22 and 8-23 do indicate, however, that increased site investigation expenditure has a greater impact on taller buildings, or buildings with additional stories. This is because failure costs associated with a taller building are higher, and any reduction in failure cost will result in a larger decrease in total cost. This result is shown in Figure 8-23, where the failure costs associated with the 10-storey building are shown to reduce from about \$12 million for the least intensive site investigation, to about \$3 million for the optimal site investigation. This represents a saving of approximately \$9 million. Compare this to the expected savings for the 3-storey building that appear to be approximately \$3 million.

**The benefits of increased site investigation expenditure are greater for taller buildings, with additional stories, or buildings with a higher project cost.**

### 8.3.3.6 Site Area and Footing System

Although results in the previous section indicated that the building height, in terms of the number of stories, had little impact on the optimal sampling effort, such an analysis was based solely on a building with a plan size of 20 m × 20 m and 9-pad footings. Therefore, an additional analysis is undertaken to investigate the impact of increased site investigation expenditure on the size of the building. However, in this case, a much larger building with 5-storeys and a plan area of 50 m × 50 m is considered. Furthermore, the foundation system designed to support the structure consists of 25-pad footings separated by 10 m in each

plan direction. Accordingly, the site investigation size within which sampling occurs, is increased to 50 m × 50 m. Rather than using tributary areas to determine the footing loads, each footing is design to withstand an 8,000 kN force. To compensate for the increase in applied load, the mean elastic modulus is also increased to 60,000 kPa (60 MPa). This ensures that a sufficient number of valid pad footings are designed. A single soil with a COV of 50% and SOF of 8 m is examined.

The effects of increased site investigation expenditure on the total, construction and failure costs of the 25 pad foundation system for a SI design using the RG, 1Q and CPT are given in Figure 8-24(a), while the impact of using different reduction techniques is shown in Figure 8-24(b). Both figures are based on a SI design using the Schmertmann 2B-0.6 technique and an influence region analysis using the same prediction technique.

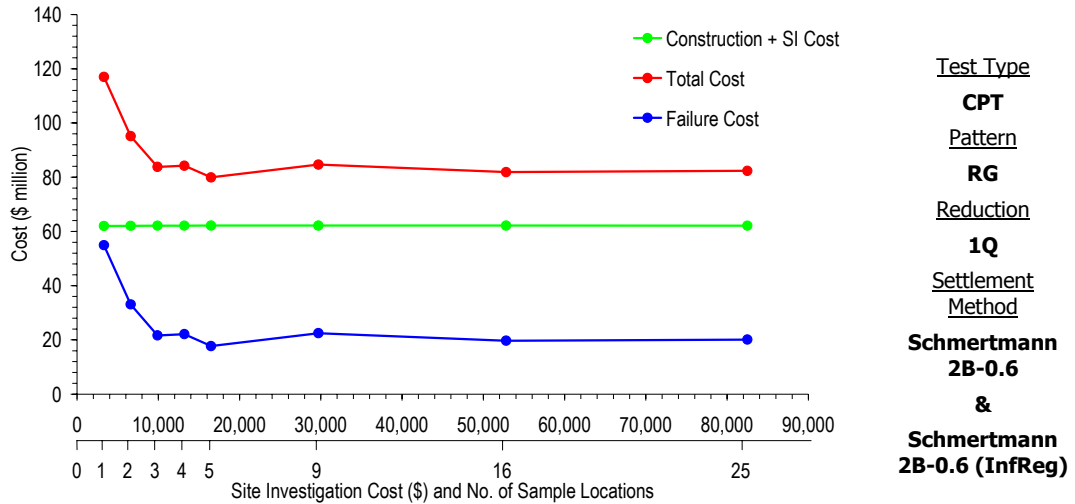
The results presented in Figure 8-24 indicate that:

- The optimal site investigation expenditure is approximately 0.24% of the construction cost. This corresponds to an expenditure of \$16,500, or 5 sampling locations;
- An increase in site investigation expenditure from \$3,300 (1 sampling location) to \$16,500 (5 sample locations) yields an expected total cost saving of approximately \$40 million; and
- The 1Q reduction technique appears, again, to yield the lowest total cost. However, the HA method also shows a low total cost, but for a larger site investigation expenditure.

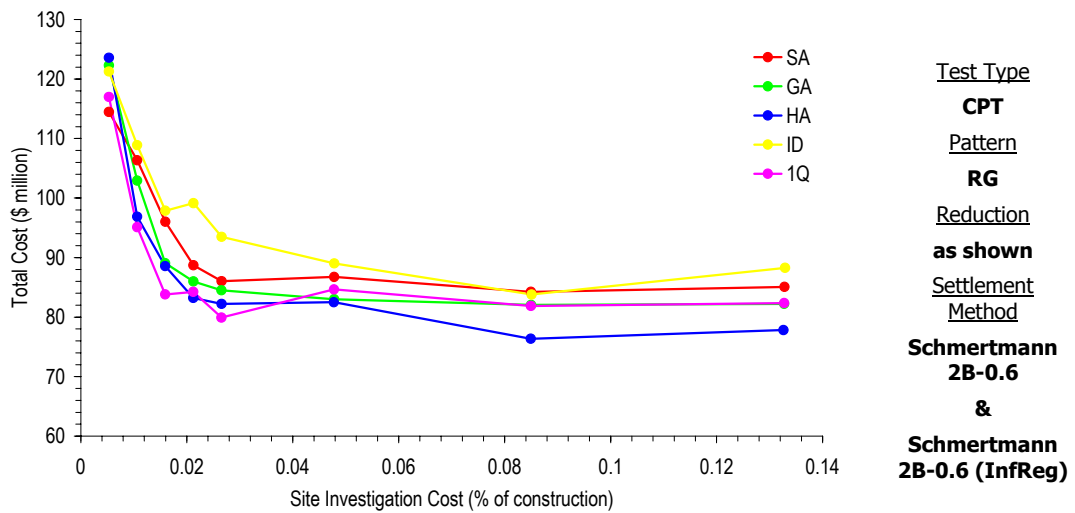
The 5 sampling locations required to yield the lowest total cost is in comparison to the 4 sampling locations required when the site investigation size was only 20 m × 20 m, as shown in previous section. Although one more location appears minor, it is important to remember that an additional sampling location with the CPT corresponds to 60 additional elastic moduli. This increase has a large impact on the apparent variability of the data and therefore, the foundation design, as discussed previously in Chapter 6 (§6.3 and §6.4).

**A site investigation consisting of 5 sample locations sufficiently characterises a site area of 50 m × 50 m, whereas 4 locations are sufficient for an area of 20 m × 20 m.**





(a)



(b)

**Figure 8-24 Effect of increased site investigation expenditure on the 25-pad system showing (a) total costs for different reduction techniques and (b) all costs using only the 1Q, for a soil COV of 50% and SOF of 8 m**

The large reduction in expected total cost for a seemingly small increase in site investigation expenditure is very encouraging. This infers that a more intensive sampling effort, which may lead to a slightly more conservative design, yields a design that has a very low expected failure cost and therefore, a low total cost.

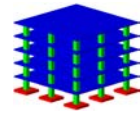
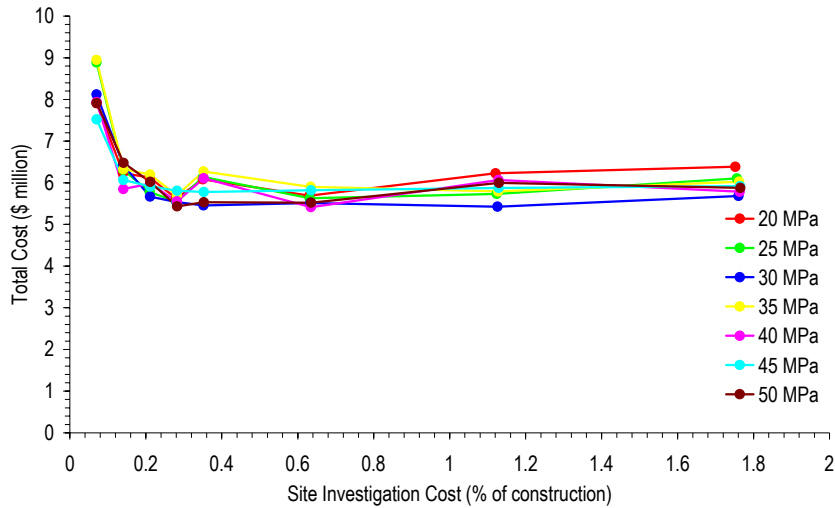
### 8.3.3.7 Mean Elastic Modulus

The final examination of variables affecting the total cost of the SI design, deals with the mean elastic modulus. In this case, the mean is varied between 20,000 kPa (20 MPa) and 50,000 kPa (50 MPa). This analysis considers only a 20 m × 20 m, 5-storey structure, with

a 20 m × 20 m site investigation plan area and a 9-pad foundation system. Furthermore, only soils with a COV of 50% and SOF of 8 m are examined. This is consistent with many of the results presented earlier in this chapter. Results are given in Figures 8-25(a), (b) and (c), for the total, construction and failure costs of the SI design, respectively. All SI designs are based on a site investigation using the RG, 1Q and CPT. The Schmertmann 2B-0.6 technique is used again for the SI design.

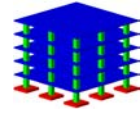
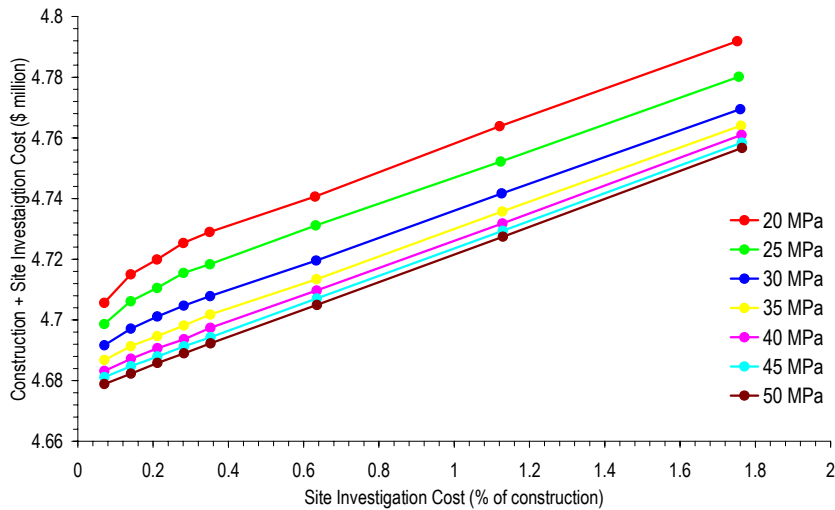
The results in Figure 8-25 show little difference between increased sampling in soils with increasing mean elastic modulus. In fact, the results indicate no general trend between an increasing mean elastic modulus and the total [Figure 8-25(a)] or failure [Figure 8-25(c)] cost. However, results in Figure 8-25(b) illustrate a clear increase in construction cost as the mean elastic modulus reduces. This is an expected result, as the reduction in the mean yields larger footing settlements and therefore, larger footings to meet the design criteria. However, in general, it appears that the mean elastic modulus has minimal influence on the effect of increased site investigation expenditure. This is because the implemented design always targets the design criterion that, in this case, is set to a maximum total settlement of 25 mm and a maximum differential settlement of 0.0025 m/m. Therefore, the design accommodates an increase or reduction in the mean elastic modulus by reducing or increasing the total footing area, respectively. However, it is neither possible, nor practical, to continually increase the total footing area, as discussed in Chapter 3 (§3.5.2). Instead, when the footings in the foundation system reach a nominated threshold, an alternative type would normally be sought. Although this analysis accommodates such a condition, it only records the occurrences of requiring an alternative foundation type. Therefore, the results do not account for the design of an alternative foundation type. However, an analysis investigating the probability that the design requires an alternative foundation is undertaken. The results of this analysis are given in Figure 8-26 for the same site conditions presented in Figure 8-25.

It is clear from these results that soils with a low mean elastic modulus show a higher probability of requiring an alternative foundation type. This is because the footing sizes are increased to meet the limits specified in the design criteria. However, for a soil with a mean elastic modulus of 20 MPa, approximately 30% of designs are considered too large for a pad footing system. This infers that an alternative foundation type is required. The results shown in Figure 8-26 also indicate that, for a soil with a mean elastic modulus of 20 MPa, a higher probability of requiring an alternative foundation type occurs when the site investigation expenditure is close to optimal. Therefore, it is also important to



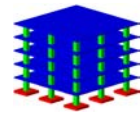
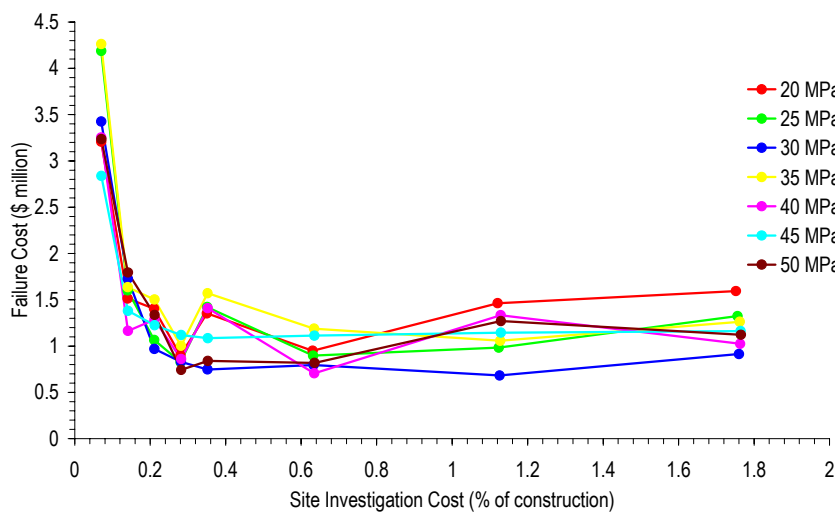
Test Type  
**CPT**  
 Pattern  
**RG**  
 Reduction  
**1Q**  
 Settlement Method  
**Schmertmann 2B-0.6**  
 &  
**Schmertmann 2B-0.6 (InfReg)**

(a)



Test Type  
**CPT**  
 Pattern  
**RG**  
 Reduction  
**1Q**  
 Settlement Method  
**Schmertmann 2B-0.6**  
 &  
**Schmertmann 2B-0.6 (InfReg)**

(b)



Test Type  
**CPT**  
 Pattern  
**RG**  
 Reduction  
**1Q**  
 Settlement Method  
**Schmertmann 2B-0.6**  
 &  
**Schmertmann 2B-0.6 (InfReg)**

(c)

**Figure 8-25 Effect of increased site investigation expenditure on the (a) total cost, (b) construction cost and (c) failure cost, for an increasing soil mean elastic modulus, a COV of 50% and SOF of 8 m**

consider the costs associated with an alternative foundation type. This would more accurately measure whether or not the mean elastic modulus influences the effect of increasing site investigation expenditure. However, the design and costing of an alternative foundation design is not considered here, as it is beyond the scope of this research but, instead, is recommended for future work.

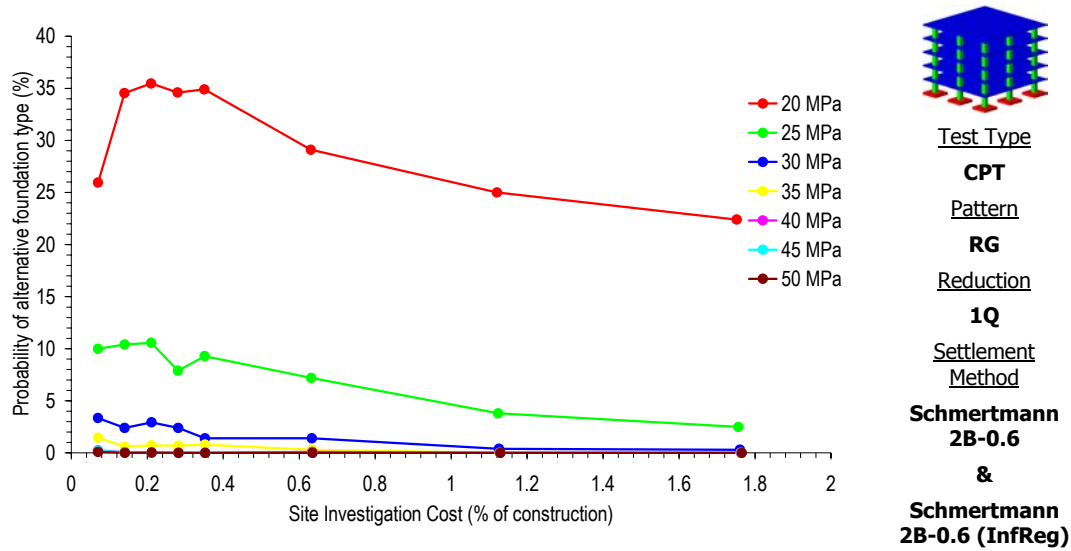


**Figure 8-26 Effect of increased site investigation expenditure on the probability of requiring an alternative foundation type, for a soil with an increasing mean elastic modulus, a COV of 50% and SOF of 8 m**

### 8.3.4 Sensitivity of Rehabilitation Limits on the Total Foundation Cost

The analyses regarding costs shown in this chapter have been based on the rehabilitation limits assumed in Table 8-5. However, these limits influence the degree of failure associated with the foundation design. Therefore, a sensitivity analysis investigating different rehabilitation category limits is conducted. This analysis is undertaken for the same 9-pad system considered throughout this chapter, which supports a 5-storey, 20 m × 20 m structure.

It is important to consider that, for this analysis, the original design limit of 25 mm total and 0.0025 m/m differential settlements remain unchanged. Instead, only the limits corresponding to the minor and major rehabilitation conditions and the limits associated with complete failure are varied. The ranges of limits investigated are shown in Table 8-7. Analyses are based solely on a SI design using the RG, 1Q, CPT and the Schmertmann 2B-0.6 method. To maintain consistency with the majority of results presented in the previous section, the mean elastic modulus is assumed to be 30,000 kPa (30 MPa) and the soil COV

and SOF are set to be 50% and 8 m, respectively. Results are given in Figures 8-27(a), (b) and (c), which illustrate the impact of increasing the limits to cause minor rehabilitation, major rehabilitation and complete failure, respectively. Although the limits associated with differential settlement are not presented, they are also increased in accordance with the ranges, given in Table 8-7.

**Table 8-7 Range of rehabilitation limits trailed in sensitivity analysis**  
Differential settlements in parenthesis (m/m)

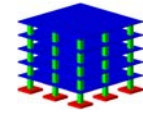
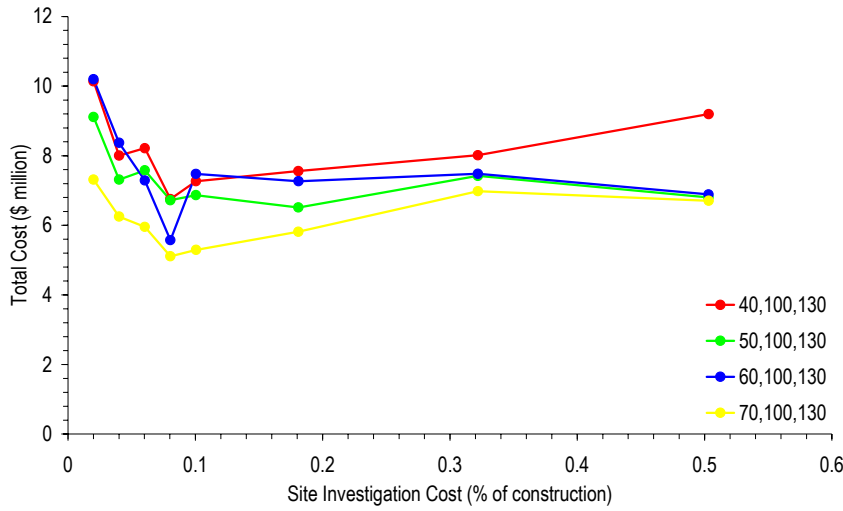
Rehabilitation Category	Original Limits (mm)	Limits Investigated (mm)
Minor	60	40, 50, 70
	(0.006)	(0.004), (0.005), (0.007)
Major	100	80, 90, 110
	(0.010)	(0.008), (0.009), (0.011)
Collapse	130	120,140,150
	(0.013)	(0.012), (0.014), (0.015)

Results in Figure 8-27 suggest that the rehabilitation limits have a minimal impact on the total cost of the foundation design and on the effect of increased site investigation expenditure. Although this is a unexpected result, it is also helpful, as it infers that the limits assumed earlier in this chapter can be applied to a wider range of conditions. However, even though Figure 8-27 suggests that the effect of changing the limits has little impact, the ranges investigated are not overly large. Therefore, further analysis beyond the scope of this research is required to identify the influence of different limits on the total cost of the foundation.

#### **8.4 OPTIMAL SITE INVESTIGATION STRATEGIES**

Results presented in this chapter, thus far, have identified the occurrence of an optimal site investigation that yields the design with the least total cost. This is an important result as it can be used to plan future site investigations. Therefore, this section contains a further treatment of the optimal site investigation and the sensitivity to changing site and building conditions.

In general, results in the previous sections have indicated that the 1Q reduction technique and the CPT consistently yield SI designs with the least total cost. As such, this combination is considered from this point forward as the optimal sampling strategy. However, it



Test Type

CPT

Pattern

RG

Reduction

1Q

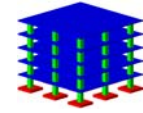
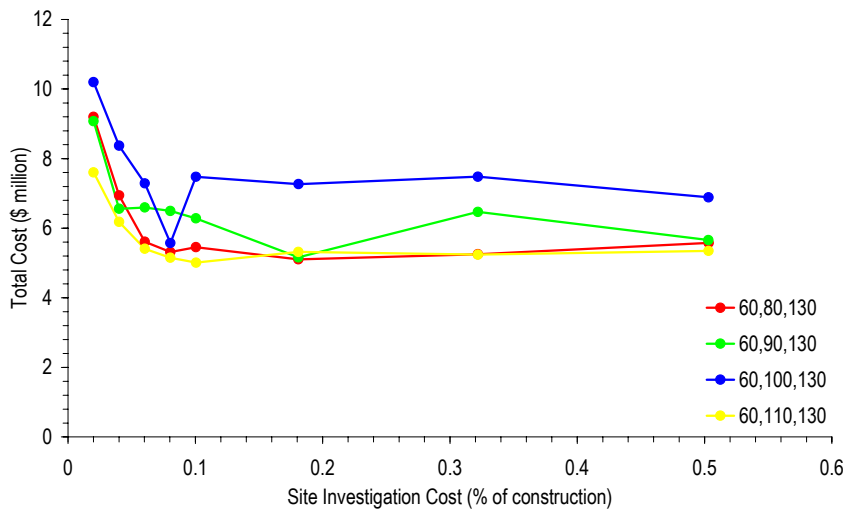
Settlement Method

Schmertmann 2B-0.6

&

Schmertmann 2B-0.6 (InfReg)

(a)



Test Type

CPT

Pattern

RG

Reduction

1Q

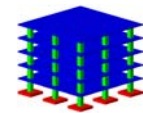
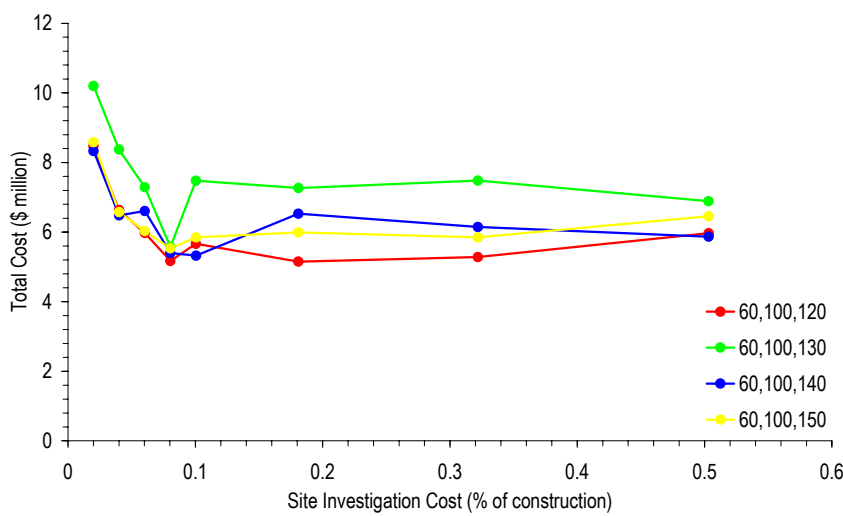
Settlement Method

Schmertmann 2B-0.6

&

Schmertmann 2B-0.6 (InfReg)

(b)



Test Type

CPT

Pattern

RG

Reduction

1Q

Settlement Method

Schmertmann 2B-0.6

&

Schmertmann 2B-0.6 (InfReg)

(c)

Figure 8-27 Effect of increased site investigation expenditure using the 1Q and the CPT, on the total cost, based on different rehabilitation limits, for a soil COV of 50% and SOF of 8 m

may not always be possible to use these methods, especially the test type. Therefore, results in this section examine the impact of using strategies other than the optimal. An investigation regarding different sampling patterns is not undertaken, as the results shown in previous chapters (Chapters 6 and 7) suggest that there is little difference between the RG and SR patterns. Furthermore, the RG pattern is the most common sampling arrangement (Ferguson 1992).

The first set of results indicates the sensitivity of the optimal sampling strategy to the site conditions or soil variability. These results are given in Figures 8-28(a) and (b) for increasing soil COV and SOF, respectively. In this case, the optimal site investigation expenditure,  $SI_{opt}$ , is approximately 0.35%. This is consistent for all site conditions investigated including soils with increasing COV [Figure 8-28(a)] and SOF [Figure 8-28(b)]. However, it should be noted that a site investigation expenditure greater than  $SI_{opt}$  leads to a greater total cost when the soil COV is 100% [Figure 8-28(a)]. Furthermore, a lower expenditure also yields the same total cost as the  $SI_{opt}$  when the soil COV or SOF is low. In other words,  $SI_{opt}$  is a worst case scenario and represents the maximum expenditure required to yield the least total cost. It is important to consider the relationship between increased site investigation expenditure and total cost for soils with different COVs and SOFs. From the results shown in Figure 8-28, the following conclusions are made:

- The optimal site investigation expenditure is a maximum at the worst case SOF;
- An investigation expenditure greater than the optimal will cause a higher total cost for soils with a high COV; and
- Increased sampling has little impact when the soil COV is low.

Using the above conclusions, and based on the results in Figure 8-28 a general rule is proposed, as shown in Figure 8-29, which indicates the impact of additional site investigation for soils with varying spatial statistics. The use of Figure 8-29 requires general knowledge regarding the soil COV and worst case SOF,  $\theta_{wc}$ . However, if there is insufficient knowledge regarding these variables, it is possible to use the maximum optimal site investigation expenditure,  $SI_{opt}^*$ . This corresponds to a soil COV of approximately 50% and SOF of 8 m, which has been shown earlier in this chapter to be a condition that is affected the greatest by increased sampling.

For the conditions presented in Figure 8-28, an  $SI_{opt}$  of 0.35% corresponds to the optimal sampling strategy of the RG, 1Q and CPT. However, results earlier in this chapter indi-

cated that for different reduction techniques and test types, the optimal expenditure was different. Therefore, an analysis is undertaken comparing the optimal site investigation expenditure for different reduction techniques and test types. Results illustrating these cost differences are given in Figure 8-30. Generally, these results indicate that:

- The ID and 1Q reduction techniques yield the lowest cost  $SI_{opt}$ ;
- The SPT yields a lower  $SI_{opt}$ , when the HA, ID or 1Q reduction techniques are used; and
- The cost of  $SI_{opt}$  using the CPT is consistent for all reduction techniques investigated.

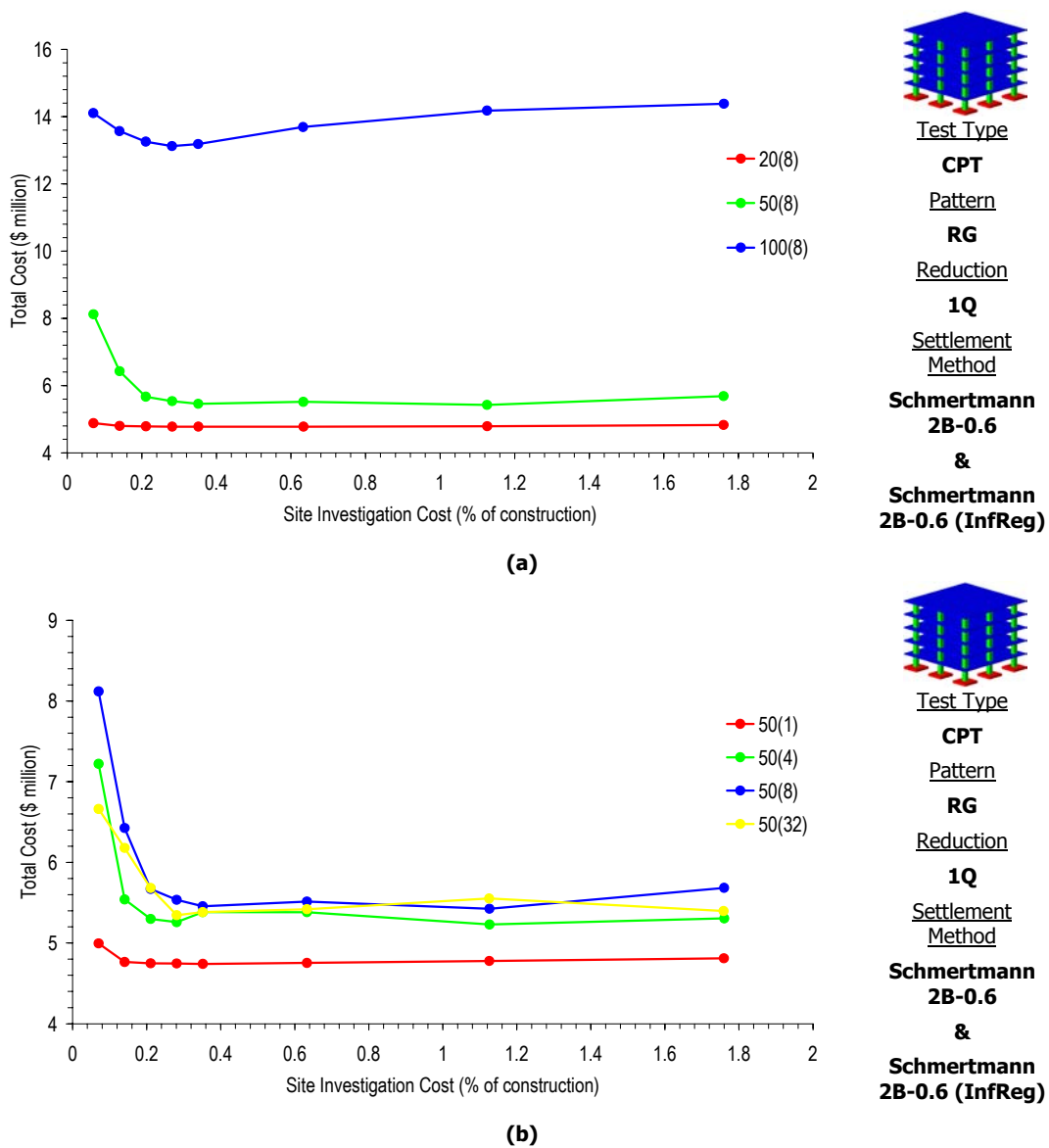
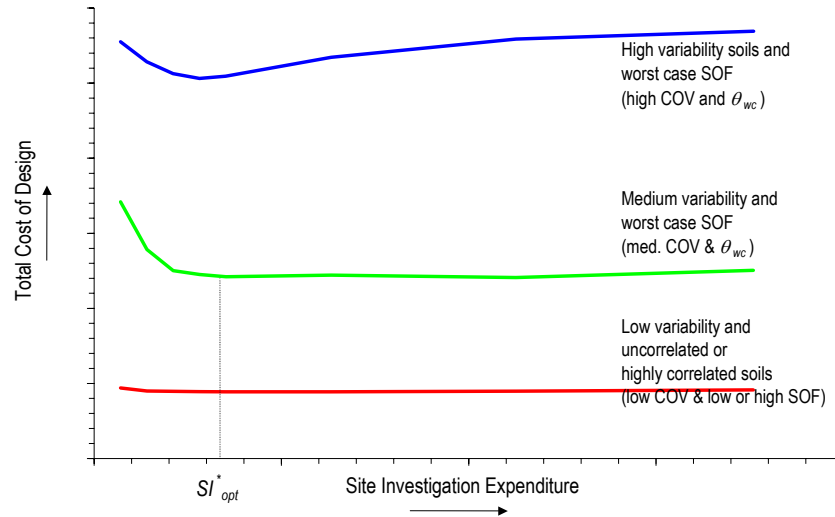
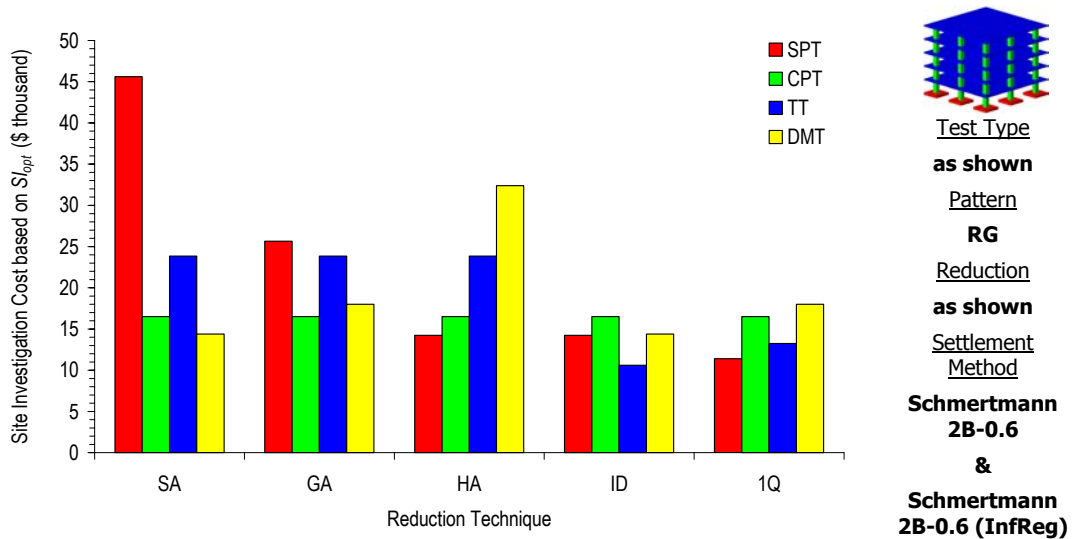


Figure 8-28 Effect of increased site investigation using the 1Q on the total cost, based on an influence region analysis, for an increasing soil (a) COV (SOF of 8 m) and (b) SOF (COV of 50%)





**Figure 8-29 Effect of increased site investigation expenditure on the total cost for changing soil variability**



**Figure 8-30 Cost of the optimal site investigation for different reduction techniques and test types, for a soil COV of 50% and SOF of 8 m**

Although the results presented in Figure 8-30 allow several conclusions regarding the optimal site investigation expenditure, it is important to also consider the resulting total cost of the design. This is because optimal site investigation expenditures for different reduction techniques and test types will result in varying total costs, as shown earlier in this chapter. As such, a further analysis is conducted to examine the total cost of the SI design based on the optimal site investigation expenditure for different reduction techniques and test types. These results are given in Figure 8-31 and suggest that:

- The ID yields very high total costs for all test types, even when the optimal site investigation expenditure is achieved. Therefore this technique is not recommended;
- The GA, HA and 1Q techniques yield the least total cost for most of the test types;
- There is little difference between the CPT, TT and DMT, for most of the reduction techniques; and
- The SPT should not be used in conjunction with the SA or GA reduction techniques.

Figure 8-30 suggests that, when using the SPT and the SA or GA reduction methods, a higher expense is required to achieve the optimal site investigation expenditure. Furthermore, the total cost of the SI design (Figure 8-31), is notably higher than most of the other tests and reduction techniques. Therefore, it is not recommended that the SPT be used with the SA or GA. Instead, the HA appears to provide a better combination where the optimal site investigation expenditure is achieved at a reasonable cost of \$15,000, and the total cost of the design is less than when the SA or GA is used.

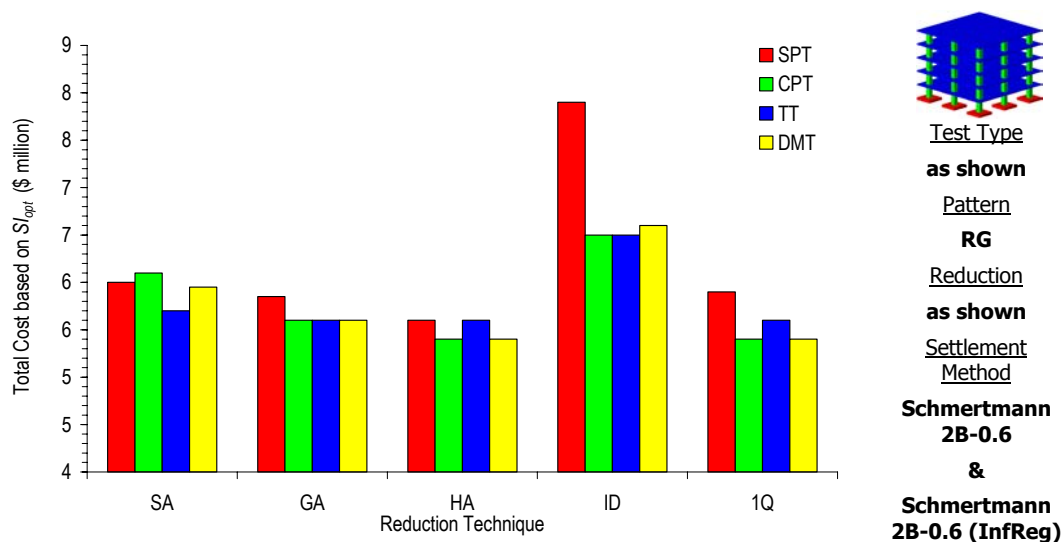


**Figure 8-31 Total costs results from the optimal site investigation for different reduction techniques and test types, for a soil COV of 50% and SOF of 8 m**

The CPT provides the most consistent result with all reduction techniques. In this case, the cost of the optimal site investigation is the same (Figure 8-30). Furthermore, the CPT also yields a relatively low total cost for most of the reduction techniques (Figure 8-30). With

either the 1Q or HA reduction techniques, the CPT yields the equal lowest total cost and is therefore, considered the optimal test type.

The TT yields reasonably low total costs (Figure 8-31). Yet, it appears that this test type requires additional expenditure to achieve the optimal site investigation (Figure 8-30). This is true for all reduction techniques, except the ID and 1Q. Although, the ID method has already been discounted as a viable technique. Therefore, it is recommended that the TT be used in conjunction with 1Q.

Finally the DMT yields similar results to the CPT. This is due to the similar measurement and transformation model error assumed, as discussed in previous chapters (§3.4.3, §6.2.3 and §7.4.2). However, Figure 8-30 suggests that the DMT, like the TT, requires additional expenditure to reach  $SI_{opt}$ . This is likely caused by the vertical sampling rate, where the SPT, TT and DMT yield discrete samples in the vertical direction, while the CPT yields a continuous vertical sample. Although in these analyses the CPT samples at only 0.5 m intervals (whereas in reality it may sample at less than 20 mm intervals), it still results in 3 times more samples than any other test investigated. As described earlier in this chapter and in Chapter 6 (§6.4.3), this has an impact on the variability of the soil data and therefore, the foundation design. However, the DMT with the 1Q, yields a total cost equivalent to the CPT and 1Q and a site investigation cost that is only \$2,500 more. Therefore, the DMT with the 1Q is the second favoured combination.

It is important to remember that the results in Figures 8-30 and 8-31 are based on the optimal site investigation expenditure. In most cases, this represents at least 4 or 5 sampling locations within a 20 m × 20 m plan area. Furthermore, it is also important to consider that this analysis considers only a single homogeneous layer of soil. In reality, soils consist of many defects and layers, which all require detailed investigation. Therefore, the recommendations made here should be considered as the minimum site investigation expenditure or scope. However, based on the analyses conducted and the results shown in this section, the following recommendations regarding a site investigation are made:

- The CPT is the best performing test and yields a reasonably low total cost for most reduction techniques. However, it performs best with the 1Q;
- The SA and GA reduction methods should be avoided when using the SPT. Instead, the HA should be used;

- The ID technique is not suited to characterising a soil for the purpose of a foundation design. Although the optimal site investigation with the ID occurs at a low cost, the total cost of the design is high; and
- The CPT, DMT and TT all perform best with the 1Q. Therefore, the 1Q reduction technique is considered the optimal method.

Furthermore, a summary of the impacts of changing site conditions and the use of different reduction techniques and test types is given in Table 8-8. This table indicates only whether the expected optimal site investigation, construction or total cost will increase, decrease or stay the same. However, Table 8-8 will give assistance to practitioners when planning site investigations and making decisions regarding which reduction technique or test type to use.

**Table 8-8 Effect of site conditions and site investigation variables on costs**

	Influence on Cost		
	Optimal Site Investigation	Construction	Total
<b>Soil Variability:</b>			
Increasing Soil COV	—	↑	↑
Increasing Soil SOF (< worst case)	↑	↑	↑
Increasing Soil SOF (> worst case)	↓	↑	—
<b>Project Size:</b>			
Increasing building height (no. of stories)	—	↑	↑
Increasing site size	↑	↑	↑
<b>Reduction Techniques</b> (as different from optimal – 1Q):			
Standard Arithmetica Average (SA)	↑	↓	↑
Geometric Average (GA)	↑	↓	—
Harmonic Average (HA)	↑	—	—
Inversed Distance Weighted (ID)	↓	↓	↑
1 <sup>st</sup> Quartile (1Q)	—	—	—
<b>Test Types</b> (compared with optimal – CPT):			
Standard Penetration Test (SPT)	↓	↑	↑
Cone Penetration Test (CPT)	—	—	—
Triaxial Test (TT)	↓	—	↑
Dilatometer Test (DMT)	↑	↑	—
— - remains relatively similar; ↑ - increases; ↓ - decreases			

It is important to note that these recommendations are only applicable to the general conditions investigated, i.e. a 50 m × 50 m site, 20 m × 20 m site investigation area and a single homogeneous layer of soil. Results presented previously in this chapter indicated that a

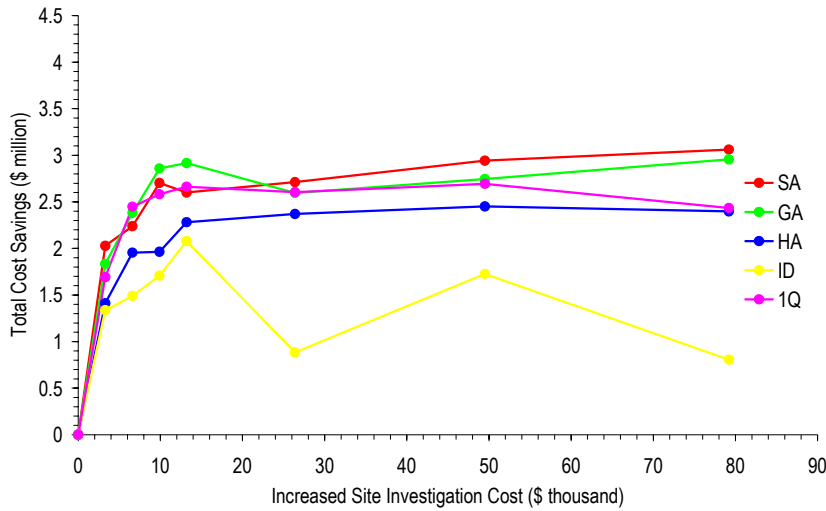
site investigation size of 50 m × 50 m required an additional sampling location to achieve the optimal site investigation. However, the same results indicated in general, that recommendations regarding the reduction method and test type are similar. As such, it is expected that the recommendations above are suited to site investigations of any size.

## **8.5 EXPECTED SAVINGS FROM INCREASED SITE INVESTIGATION**

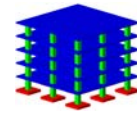
As discussed earlier in this chapter, increased site investigation expenditure through additional sampling, yields significant savings in the expected failure and total costs. Therefore, it is considered worthwhile to investigate the expected savings based on increased site investigation expenditure. As such, this section describes an analysis to quantify expected savings based on several different site and site investigation conditions. All analyses are based on the design of the same 9-pad foundation system, as presented earlier in this chapter (§8.3), where the foundation supports a 5-storey 20 m × 20 m building, with a 5 kPa live load and 3 kPa dead load.

Cost savings are examined with respect to the use of different reduction techniques, test types and settlement prediction methods. In all cases, the RG sampling pattern is used, while the site investigation plan is assumed to be 20 m × 20 m. Cost savings are calculated by comparing the total cost of an SI design considering more than 1 sampling location, with the total cost based on a single location. Therefore, a positive cost saving infers that increased sampling, over 1 sampling location is beneficial. Results are given in Figures 8-32(a), (b) and (c), for different reduction techniques, test types and settlement prediction methods, respectively. In these results, the site investigation expenditure is expressed as a cost rather than the percentage of project cost, as was used earlier in the chapter.

The maximum savings for the different reduction techniques, test types and settlement prediction techniques all occur at the same increased site investigation expenditure of approximately \$10,000. This corresponds to the optimal site investigation expenditure, as discussed in the previous section. Furthermore, the relationship between increased site investigation expenditure and cost savings appear similar for the different reduction methods, test types and settlement techniques. This infers that the main contributor to savings is additional sampling, which causes the increase in site investigation cost. However, the different reduction techniques, test types and settlement techniques respond differently to increased sampling and as such, the following conclusions from Figure 8-32 are made:



(a)



Test Type

**CPT**

Pattern

**RG**

Reduction

**as shown**

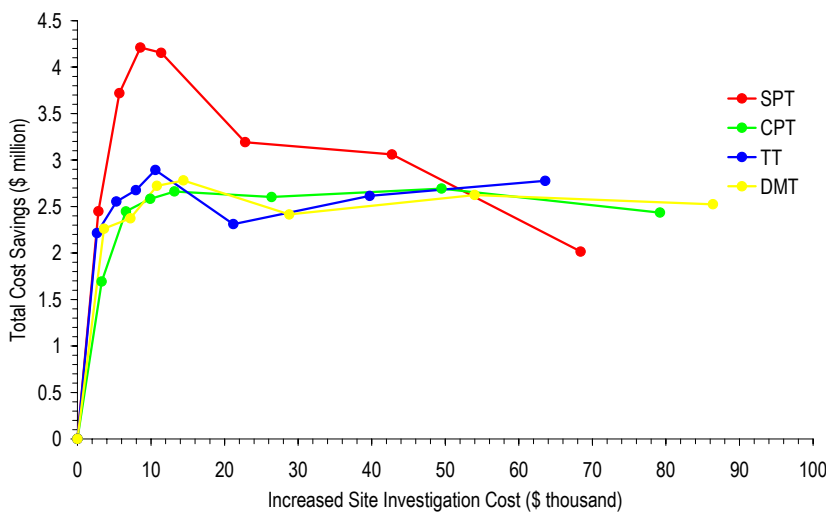
Settlement

Method

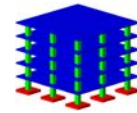
**Schmertmann  
2B-0.6**

**&**

**Schmertmann  
2B-0.6 (InfReg)**



(b)



Test Type

**as shown**

Pattern

**RG**

Reduction

**1Q**

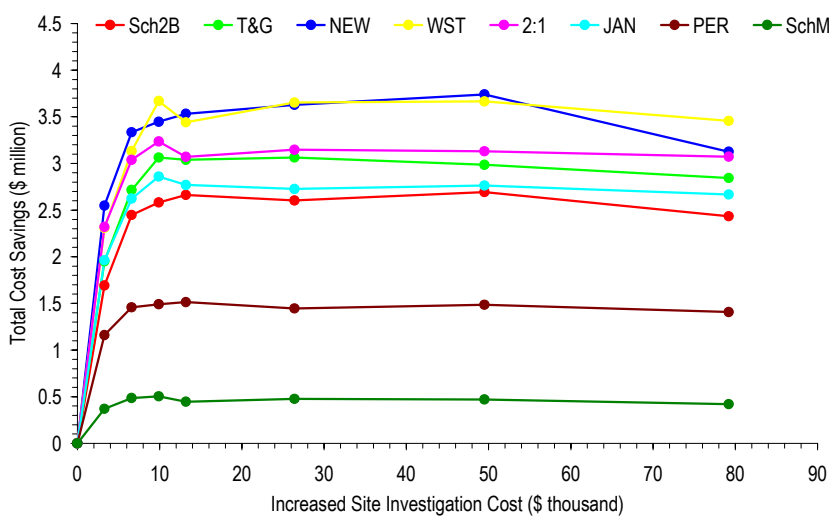
Settlement

Method

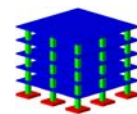
**Schmertmann  
2B-0.6**

**&**

**Schmertmann  
2B-0.6 (InfReg)**



(c)



Test Type

**CPT**

Pattern

**RG**

Reduction

**1Q**

Settlement

Method

**as shown**

**&**

**Schmertmann  
2B-0.6 (InfReg)**

Figure 8-32 Total cost savings for an increased site investigation cost using different test types, for a soil SOF of 8 m and COV of (a) 20%, (b) 50% and (c) 100%

- The SPT shows the greatest total cost saving for an increased site investigation expenditure of \$10,000. However, the benefits quickly reduce as the expenditure increases;
- The Newmark and Westergaard settlement techniques yield the greatest savings of about \$3.5 million, for an increased expenditure of \$10,000;

The reduction technique, test type and settlement techniques that yield the largest cost savings have also been shown to give designs with the highest total cost (Figure 8-20). Therefore, the high cost savings shown in Figure 8-32 for the SPT, Newmark and Westergaard settlement techniques are only due to their initial high total cost. Furthermore, the reduction techniques, test types and settlement techniques that were shown to yield the lowest total cost in Figure 8-20, indicate relatively small savings in Figure 8-32. As such, increased sampling is more important for the methods that yield high total costs. This includes the SPT as well as the Newmark and Westergaard settlement techniques.

## **8.6 SUMMARY**

---

It is important to note that the results presented in this chapter have dealt only with the expense of a site investigation with regard to characterising the site for settlement analysis. In reality, information regarding the stratigraphy and geology of the site would also be required, which therefore adds to the costs of the site investigation. Accordingly, the site investigation expenditures shown in this chapter should be regarded as a minimum cost.

The results presented in this chapter have provided strong evidence to justify increased site investigation expenditure. It has been shown that, in general, increased site investigation expenditure decreases the total cost, or financial risk, of the resulting design. Furthermore, the results have also indicated the existence of an optimal site investigation expenditure, which yields a design with the lowest financial risk. However, the optimal site investigation expenditure was shown to be uncorrelated to the project cost. Instead, the site investigation cost should be based on the site conditions and the type of investigation. For the 20 m × 20 m investigation plan area, 4 sampling locations were shown to yield a design with the lowest total cost. This investigation involved the 1Q reduction technique and CPT. The cost of this investigation corresponded to 0.48%, 0.35% and 0.13% of the project cost for the 3-, 5- and 10- storey buildings, respectively.

It was also observed in this chapter that, although an increasing soil COV provided a higher total cost, a soil with a COV of 50% was found to require the most expensive optimal site investigation. Furthermore, a soil with the worst case SOF of 8 m was also shown to require the highest optimal site investigation cost. As such, a maximum site investigation expenditure was identified which can be used for all soil COVs and SOFs.

Although the 1Q reduction technique and the CPT were identified as the preferred techniques, analyses also indicated the influence of using different methods. In some cases, the use of different reduction techniques or test types provided designs with lower project costs. However, in all cases, the CPT and 1Q provided designs with the lowest total cost.

Since all conclusions and recommendations made in this chapter are based on general soil conditions, it is important to verify that the same conclusions hold for more specific analyses. As such, the results in the following chapter investigate the strength of the conclusions in this chapter, using 3 specific sites where the spatial variability of the soil is known.



## Chapter 9 ANALYSIS USING SPECIFIC SOIL DATA

### 9.1 INTRODUCTION

---

The assessment of risk and reliability of a foundation design based on a site investigation has been based, in previous chapters, on generic site conditions where the variability of the soil was defined by the COV and SOF. This is because it is rare that the spatial variability of a soil is known with any degree of confidence. However, there are examples of large sampling efforts at specific sites, which have enabled the evaluation of statistical parameters including the mean, variance (coefficient of variation) and scale of fluctuation (correlation distance).

In this chapter, three specific soil sites are identified that provide adequate knowledge of the soil spatial variability. Using this knowledge, it is possible to employ the methodology discussed in Chapter 3 to quantify the relative benefit of increased site investigation expenditure. This analysis is conducted to confirm the conclusions made in Chapter 8, where soils with generic variability were investigated.

The analyses presented in this chapter are based on the footing design for a 9-pad foundation system similar to the bulk of analyses in Chapter 8. However, in this case, the foundation is designed to support a 3-storey structure, with a 5 kPa live load and 3 kPa dead load, as shown in Figure 9-1. This leads to the corner, centre and other footings having to support loads of 860 kN, 1540 kN and 1150 kN, respectively. A 3-storey structure is used in this analysis because the three sites examined have a low mean elastic modulus. Therefore, the footing loads are reduced to ensure that a sufficient number of valid pad footings are designed.

As with the majority of analyses in Chapter 8, the site investigation is constrained within a 20 m × 20 m plan area. Furthermore, all costs associated with the site investigation, con-

struction and failure are consistent with those used in Chapter 8. Settlement limits to cause minor, major refurbishment and complete reconstruction are assumed to be 60 mm, 100 mm and 130 mm, respectively. The corresponding differential settlement limits for minor, major refurbishment and complete reconstruction are assumed to be 0.006 m/m, 0.01 m/m and 0.013 m/m, respectively. These are also consistent with those adopted for analyses in Chapter 8. Finally, the settlement limits adopted to yield the foundation design are consistent with the limits used for all previous analyses. These are a maximum total settlement of 25 mm and a maximum differential settlement of 0.0025 m/m.

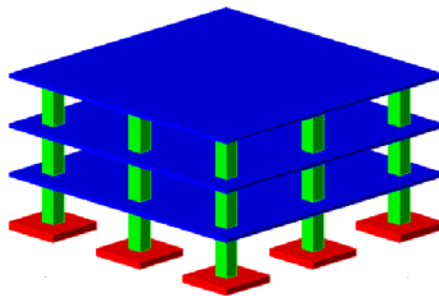


**Figure 9-1 Schematic of the 3-storey building with 9 columns transferring loads to the foundations**

The analysis of the design based on the site investigation information (SI) is conducted using the Schmertmann 2B-0.6 settlement technique with an influence region of elastic moduli, as discussed in Chapter 8 (§8.3.2). This allows a smaller sizing increment, where footings are increased in size by 0.1 m in one direction when their settlement exceeds the imposed limits.

## **9.2 SITE 1: STIFF OVER-CONSOLIDATED CLAY**

The first soil type investigated is based on a site located in the South Parklands of Adelaide in South Australia. The deposit consists of a stiff over-consolidated clay known as Keswick clay. Jaksa (1995) conducted 222 CPT samples at the South Parklands site to quantify the variability of the soil using geostatistics and random field theory. The sample program used by Jaksa (1995) is given in Figure 9-2 and the results of the data analysis are summarised in Table 9-1.

The statistical values shown in Table 9-1 are based on the cone tip resistance,  $q_c$ , results of the 222 CPT tests. Jaksa (1995) estimated that the clay had a maximum depth of 7 m. Therefore, an assumed site size of 50 m  $\times$  50 m with a depth of 7 m is adopted for the analysis to represent this site. The results shown in Table 9-1 indicate a  $q_c$  mean of

3.0 MPa, a COV of 59% and a vertical and horizontal SOF of 0.15 m and 1.5 m, respectively. While the COV and SOF values are assumed to be the same for the elastic modulus of the soil, it is necessary to estimate the elastic modulus mean using a correlation between  $q_c$  and elastic modulus,  $E$ . The following relationship is used:

$$E = 3q_c \tag{9.1}$$

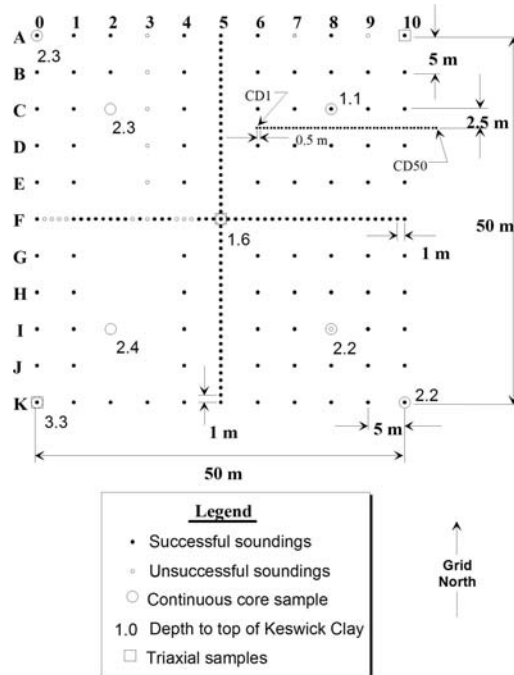


**Figure 9-2** Field testing layout for the Site 1  
After Jaksa (1995)

**Table 9-1** Summary of results from the South Parklands site  
Adapted from Jaksa (1995)

Mean (MPa)	COV (%)	Average Scale of Fluctuation (m)	
		Vertical	Horizontal
3.0	59	0.15	1.5

The correlation in Equation (9.1) is a compromise of two correlation models proposed by Craig (1997) for a square and rectangular footings. As such, a mean elastic modulus of 9.0 MPa (9,000 kPa) is adopted for this site.

The use of different sampling patterns was not investigated in Chapter 8, since the results in both Chapters 6 and 7 suggested that there was little difference between the regular grid (RG), stratified random (SR) and simple random (SR) arrangements. As such, the influence of sampling pattern is not considered here. Instead, all analyses presented in this chapter are based on a regular grid (RG) sampling pattern. According to Ferguson (1992) the RG is the most common pattern and, together with the herringbone, yields the optimal solution. However, different reduction techniques were shown in previous chapters to have a marked impact on the foundation design, as well as on the effects of increased sampling. Therefore, an analysis using the soil variability for Site 1 is conducted examining the use of different reduction techniques. Results of this analysis are given in Figure 9-3. All results for this site are based on the use of the CPT, because the CPT was used to initially characterise the variability of the soil (Jaksa 1995).

In general, the trends shown in Figure 9-3 confirm the conclusions drawn in Chapter 8, regarding the reduction technique. In this case, the 1Q method appears to yield the lowest total cost when the site investigation expenditure is approximately 0.11% of the project cost. This expenditure corresponds to 4 sampling locations, which is consistent with the conclusions drawn in Chapter 8, for the same sized site investigation area (20 m × 20 m).

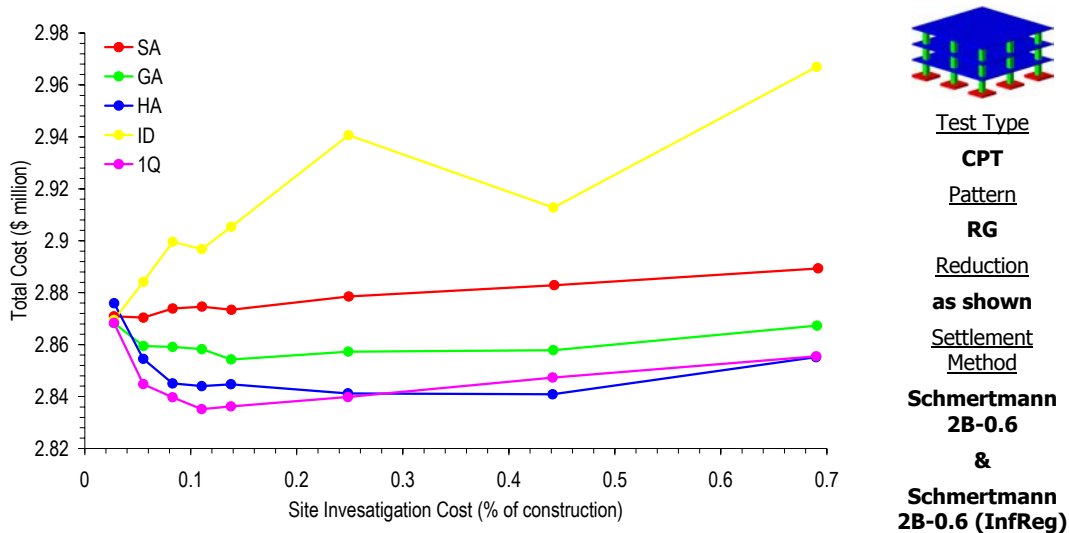


**Figure 9-3 Effect of increased site investigation expenditure on the total cost, using different reduction techniques, for Site 1**

Figure 9-3 clearly illustrates that the total cost increases when the optimal site investigation expenditure of 0.11% is exceeded. This is similar to the results shown in Figure 8-28(a) for a soil COV of 100% and SOF of 8 m. Therefore, Figure 9-3 provides additional evi-

dence that the total cost of the design increases after the optimal site investigation expenditure in soils with a high COV. In this case, the soil COV is 59%.

It should be noted that the site investigation expenditures shown in Figure 9-3 and for that matter throughout this chapter, are different to those illustrated in Chapter 8. This is because the assumed test costs are based on a linear metre rate, as shown in Table 8-1. Therefore, because the sizes of the site are different to those in Chapter 8, the test costs per sample location are also different. However, as shown in Figure 9-3 and discussed above, the optimal site investigation expenditure of 0.11% corresponds with 4 sampling locations, which is consistent with the results discussed in Chapter 8.

Analyses are also conducted to examine the influence of different settlement techniques on the total cost of the design. Such an analysis is based on a site investigation using the RG, 1Q and CPT. Results are given in Figure 9-4 and suggest that:

- Both Schmertmann techniques (Sch2B and SchM) yield designs with the lowest total cost;
- The Newmark technique bears the highest total cost; and
- The relationship between increased sampling and total cost is unaffected by the settlement techniques.

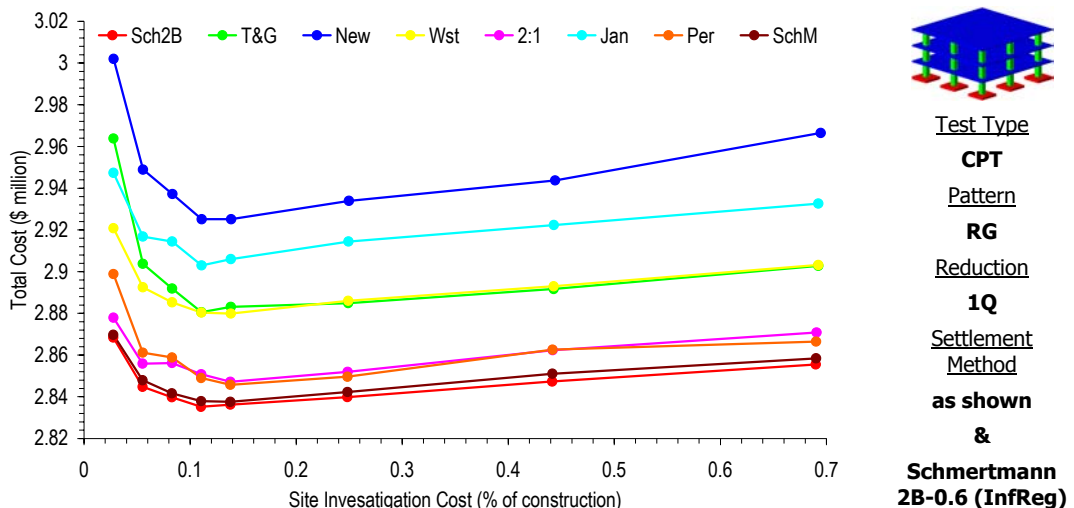
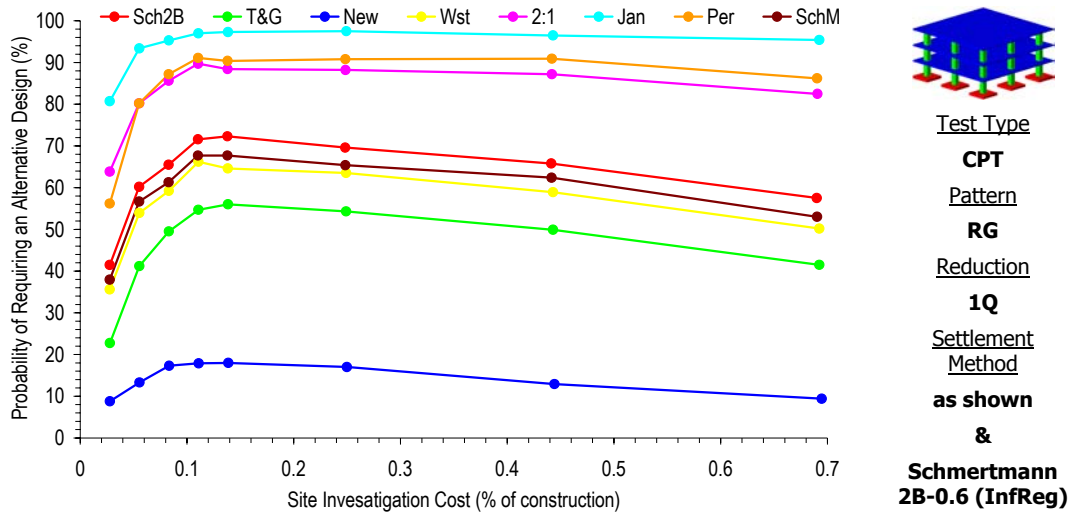


Figure 9-4 Effect of increased site investigation expenditure on the total cost, using different settlement prediction techniques, for Site 1

Two of the three conclusions above are consistent with the results presented in Chapter 8. First, the Newmark technique has been shown to yield design with very low conservatism (§5.3 and §6.3). This leads to a higher failure cost and therefore, a higher total cost, as shown in Figure 9-4 and previously in Figure 8-20. Second, in all past analyses, the use of different settlement techniques has been shown to have little impact on the effect of increased sampling. Instead, different techniques yield results with varying degrees of conservatism. However, the first conclusion listed above, which suggests that the Schmertmann 2B-0.6 method yields the lowest total design, contradicts the results presented in Chapter 8 (8-20). Furthermore, it is unusual to observe similar results for both the Schmertmann 2B-0.6 (Sch2B) and Modified technique (SchM).

In all of the analyses presented thus far, the Schmertmann 2B-0.6 method has yielded foundation designs with a smaller footing area than the Schmertmann Modified method. However, the cause of this discrepancy may have already been discussed in Chapter 5 (§5.2.1), where it was surmised that the conservatism of the Schmertmann Modified method is influenced by the size of the footing. Therefore, since the Schmertmann 2B-0.6 technique is similar to the Schmertmann Modified method in formulation, the Schmertmann 2B-0.6 technique would also be affected by footing size. Furthermore, considering the loads and site conditions analysed in this section are sufficiently different than those in Chapter 8, it is not unreasonable to suggest that this may be the cause. However, there is also another possibility. Since the analysis in this section is based on the measured properties of the soil, it has not been possible to condition the mean elastic modulus to enable a sufficient number of valid pad footing designs. As such, an analysis examining the probability of requiring an alternative foundation type is also undertaken. These results are given in Figure 9-5 for the different settlement prediction techniques.

Results in Figure 9-5 clearly indicate that a high proportion of designs were not able to meet the criteria as a pad foundation. As such, the results show a high probability of requiring an alternative type. Furthermore, the relative results, between settlement techniques are different to those in Figure 9-5. One would expect that a low total cost, which reflects a conservative design to avoid failures, would also yield a high probability of requiring an alternative design. However, there is no obvious relationship between the relative results in Figures 9-4 and 9-5. Therefore, it appears that the high probability of requiring an alternative design, due to the low mean elastic modulus, has an influence on the total cost, as shown in Figure 9-4.



**Figure 9-5** Effect of increased site investigation expenditure on the probability of requiring an alternative foundation design, using different settlement prediction techniques, for Site 1

A further analysis for Site 1 is also undertaken to examine the impact of additional site investigation expenditure on the project cost of the SI design. Such an analysis is conducted only for the different settlement techniques, with a site investigation consisting of the RG, 1Q and CPT. Results illustrating the project cost, which includes the cost of the site investigation and construction, are shown in Figure 9-6. Also included in these results is the construction cost of the optimal design, which is based on the Schmertmann 2B-0.6 technique and an influence region of elastic moduli.

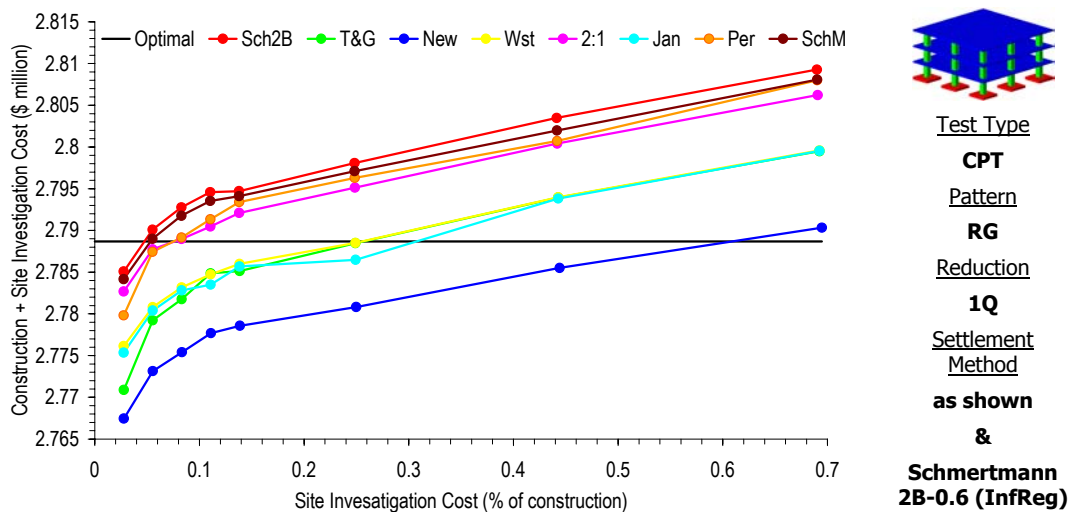


**Figure 9-6** Effect of increased site investigation expenditure on the construction cost, using different settlement prediction techniques, for Site 1

The results in Figure 9-6 provide a mirror image of those presented in Figure 9-4 for the total cost of the design. This suggests that the costs associated with failure have a notable impact on the total cost, which is consistent with the conclusions drawn in Chapter 8. Furthermore, comparisons between the results in Figures 9-4 and 9-6 suggest that a conservative foundation design yields a lower total cost. Again this is same as the trends observed in Chapter 8. Therefore, based on the results presented in this section, the major conclusions discussed in Chapter 8 are valid for Site 1. The only notable difference between results in this section, and those presented in Chapter 8, relate to the total cost of the Schmertmann 2B-0.6 technique. However, it appears the results presented here may be affected by a high probability of requiring an alternative design.

### 9.3 SITE 2: SAND SITE AT THE TEXAS A&M NGES

The sand site at the Texas A&M University consists of three layers of sand with silty sand for the first 4 m, overlying a 4 m layer of clean sand and a 4.5 m layer of clayey sand (Akkaya and Vanmarcke 2003). These first three layers overlie a hard clay layer of approximately 5.5 m, before bedrock. Although the effects of layering have not been considered in this analysis, the statistical properties resulting from the entire depth are considered sufficient to characterise this particular site.

The variability of the soil at the Texas A&M University sand site has been quantified by Akkaya and Vanmarcke (2003) using 22 CPTs, performed previously by Simon and Briaud (1996) and Tumay (1998). The results of their analysis are shown in Table 9-2 displaying the mean, COV and the vertical SOF of the cone tip resistance. The results shown in Table 9-2 are averaged values.

**Table 9-2 Average statistical values of the cone tip resistance for each layer and overall depth at the Texas A&M University "Sand Site"**  
Adapted from Akkaya and Vanmarcke (2003)

	Depth (m)	Mean (kPa)	COV (%)	SOF - vert (m)
Layer 1	0 – 4	6667	55	1.75
Layer 2	4 – 8	8814	35	1.64
Layer 3	8 - 12.5	9357	50	2.49
Layer 4	12.5 - 18	8764	22	0.85
Overall	0 – 18	8400	50	3.25



The 22 CPTs were conducted at a site with a plan area of 22,500 m<sup>2</sup>. Although such a sampling rate does not appear to be adequate to analyse the horizontal spatial variability, Akkaya and Vanmarcke (2003) still estimated the horizontal SOF to range between 2 m and 25 m. Based on the results shown in Table 9-2, the analysis adopted to represent this site includes a plan size of 50 m × 50 m, with a depth of 18 m, and an elastic modulus mean of 8,400 kPa, COV of 50%, plus horizontal and vertical SOFs of 13.5 m and 3.25 m, respectively. As similar with the analysis for Site 1, the CPT is only considered in the results that follow for Site 2. This is because Simon and Briaud (1996) initially used the CPT to characterise the variability of the site.

Analyses are conducted to investigate the influence of different reduction techniques on the total cost of the SI design. The results are given in Figure 9-7. The relationship between increased site investigation expenditure and total cost for different reduction techniques appears more erratic than the results shown previously for Site 1, and in Chapter 8. Furthermore, it is difficult to clearly distinguish the preferred technique. However, it does appear that the HA and 1Q are once again, the methods that provide the lowest total cost. This is consistent with results for Site 1 and the general conditions discussed in Chapter 8. However, the erratic relationship between increased expenditure and total cost warrants further investigation. Hence, an analysis examining the impact of additional expenditure on the probability of requiring an alternative foundation type is conducted. The results of this analysis are illustrated in Figure 9-8 and clearly indicate that a high proportion of solutions require an alternative design. This suggests that, as for Site 1, the mean elastic modulus of 8,400 kPa is, in general, too small for a pad foundation. However, because the design of an alternative foundation type is not considered, the results presented will suffice.

An examination of the impact of settlement prediction techniques on the total cost for Site 2 is also conducted. In this case, the site investigation is assumed to use the RG, 1Q and CPT. Results showing the effect of increased site investigation expenditure on the total cost for different settlement techniques is given in Figure 9-9, while the influence of increased expenditure on the probability of requiring an alternative design is also shown in Figure 9-10.

Results in Figure 9-9 indicate that the 2:1 method yields the lowest total cost. However, this is balanced by the results in Figure 9-10, where the 2:1 method is also shown to yield the highest probability of requiring an alternative foundation type. These results are very similar to those shown in Chapter 8 (Figure 8-20), suggesting that the general conditions

are also applicable to this specific site condition. Furthermore, the consistency between the results shown in Figures 9-9 and 8-20 also indicates that the mean elastic modulus has little impact on the effect of increased site investigation expenditure. This was also observed in Chapter 8 (§8.3.3.7).

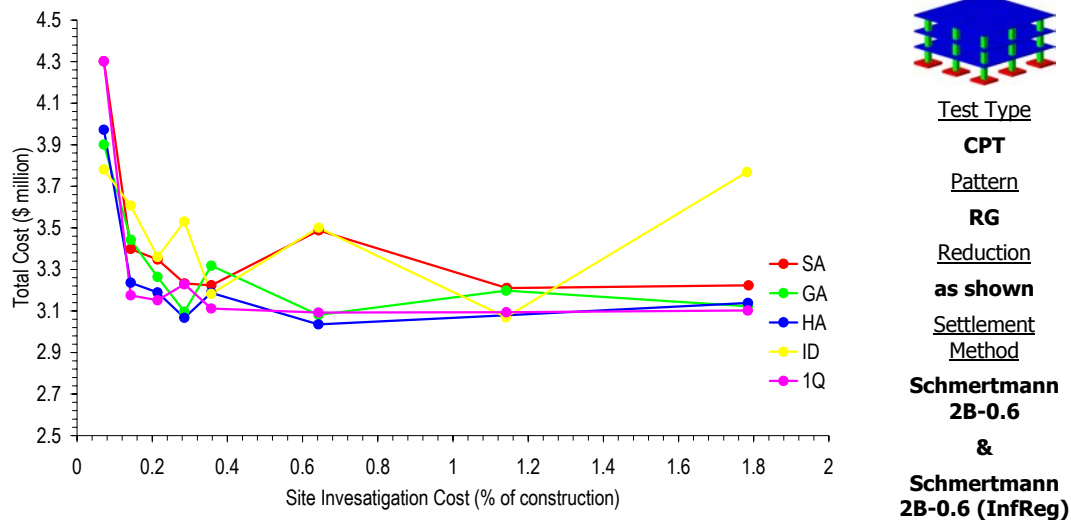


**Figure 9-7** Effect of increased site investigation expenditure on the total cost, using different reduction techniques, for Site 2

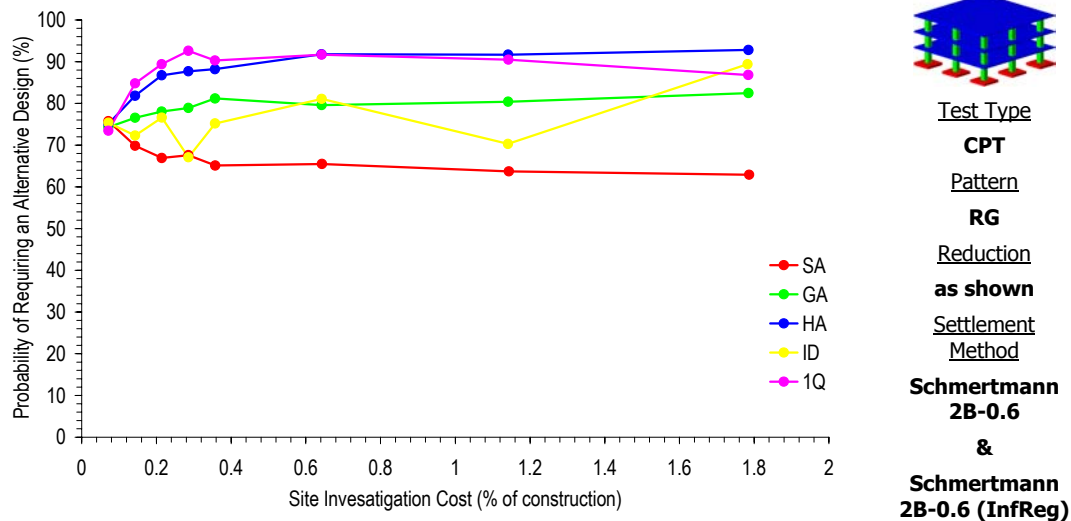


**Figure 9-8** Effect of increased site investigation expenditure on the probability of requiring an alternative foundation design, using different reduction techniques, for Site 2

Figure 9-9 indicates that the expected savings for a 0.1% increase in site investigation expenditure are approximately \$1.5 million for the Newmark method and \$250,000 for the Perloff. Therefore, it is apparent that increased investigation expenditure has a greater benefit for techniques that yield high total costs. Again, this was observed in Chapter 8.

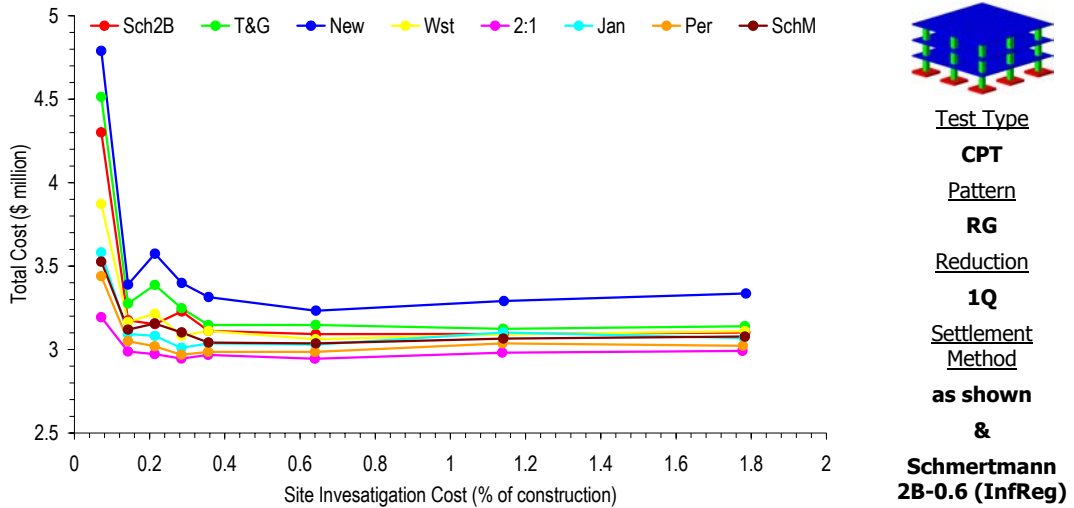


**Figure 9-9** Effect of increased site investigation expenditure on the total cost, using different settlement prediction techniques, for Site 2

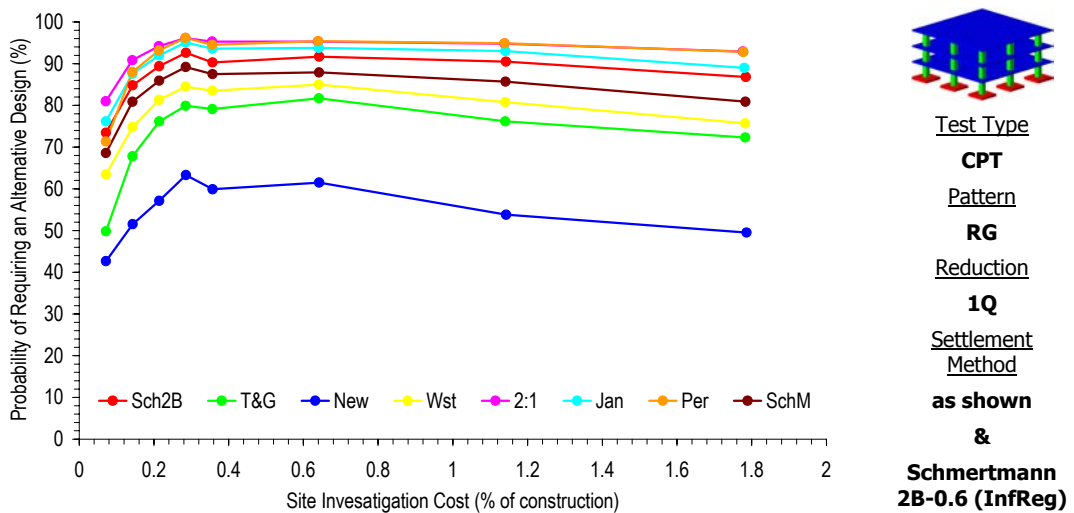


**Figure 9-10** Effect of increased site investigation expenditure on the probability of requiring an alternative foundation design, using different settlement prediction techniques, for Site 2

The high probability of requiring an alternative foundation type, shown in Figure 9-10, is similar to that shown for Site 1. However, in this case, all the settlement methods yield a relatively high probability. In fact, only the Newmark method with a single sample location yields a probability less than 50%. Furthermore, the 2:1 technique shows a greater than 80% probability of requiring an alternative foundation type, for all sampling efforts investigated. This infers that each result is based on less than 200 out of the 1,000 Monte Carlo realisations. Such a small proportion of results have an impact on the robustness of the analysis and leads to erratic relationships, as shown above in Figure 9-7.

## 9.4 SITE 3: VARVED CLAY

The final soil deposit investigated is based on a deep deposit of varved clay, located in New Liskeard, Ontario, Canada. Lacasse and Ladd (1973) investigated the circumstances of an embankment failure in 1963, which yielded sufficient investigation data for a complete statistical analysis. Soil properties used in the analysis were obtained using the vane shear test (VST). Results were summarised by Vanmarcke (1977b), in the form of soil shear strength. However, it is assumed for the purposes of this analysis that the variability and correlation of the shear strength is similar to that of the elastic modulus. A summary of the statistical properties of the varved clay is given in Table 9-3. Information regarding the depth of the deposit is limited. Therefore, an approximated depth of 15 m is assumed. Consequently, the analysis is conducted for a site with a plan size of 50 m × 50 m and a depth of 15 m.

**Table 9-3 Statistical properties of the varved clay site in New Liskeard, Canada**

Mean (kPa)	COV (%)	Scale of Fluctuation (m)	
		Vertical	Horizontal
?	32	5	46

Although it is reasonable to suggest that the variability of the elastic modulus,  $E$ , is similar to that of the undrained shear strength,  $s_u$ , it is not feasible to use the mean shear strength as the mean elastic modulus. Hence, a relationship between the shear strength and elastic modulus for clays is used (Bowles 1997), as given by:

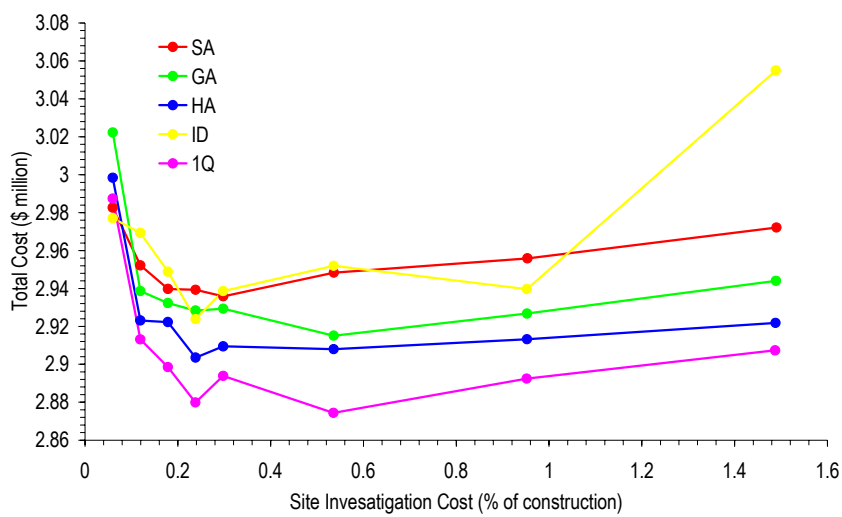
$$E = 300s_u \quad (9.2)$$

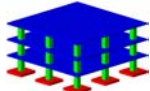
This results in a mean elastic modulus of 9,000 kPa, using an undrained shear strength that is assumed to be 30 kPa. Coincidentally, this is the same mean elastic modulus used for Site 1. However, the soil COV and SOF for this site are sufficiently different to warrant a full investigation.

The first set of analyses, as with the previous two sites, considers the impact of using different reduction techniques on the total cost of the design. Furthermore, an analysis is also conducted to examine the influence of using different types of soil tests. This form of analysis is undertaken because the VST, which was used initially to characterise the variability of the site, is not considered in the methodology described in Chapter 3. Therefore,

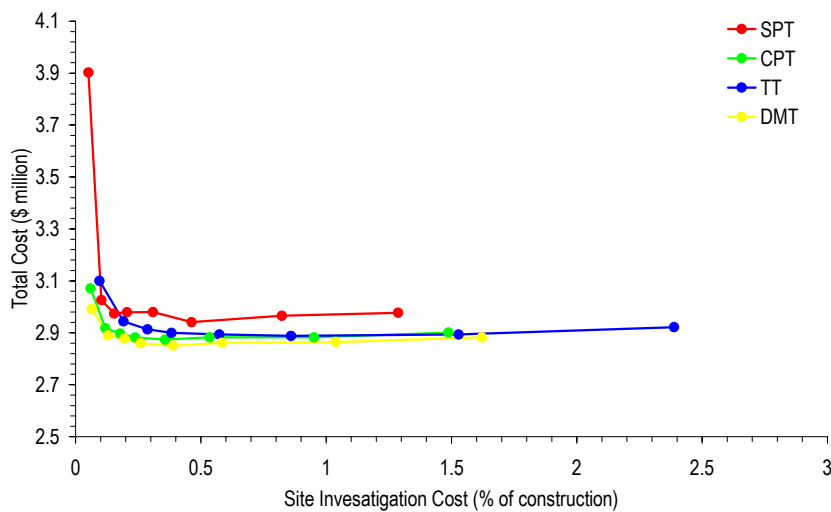
it is important to remember that the results that follow are based on a different test type than the one used to characterise the spatial variability.

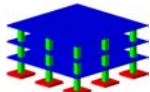
Results are shown in Figures 9-11(a) and (b) for the reduction technique and test type, respectively. In this case, the 1Q reduction technique [Figure 9-11(a)] and the DMT [Figure 9-11(b)] appear to yield the lowest total cost. These results are consistent with analyses presented earlier in this chapter and throughout Chapter 8, even though earlier results indicated that the CPT provided the lowest total cost. However, a closer examination of Figure 9-11(b) suggests there is little different between the CPT and DMT. Therefore, either test is suitable to yield a low total cost. It should also be remembered that neither test was used initially to characterise the variability of the soil.



  
Test Type  
**CPT**  
Pattern  
**RG**  
Reduction  
**as shown**  
Settlement  
Method  
**Schmertmann**  
**2B-0.6**  
**&**  
**Schmertmann**  
**2B-0.6 (InfReg)**

(a)



  
Test Type  
**as shown**  
Pattern  
**RG**  
Reduction  
**1Q**  
Settlement  
Method  
**Schmertmann**  
**2B-0.6**  
**&**  
**Schmertmann**  
**2B-0.6 (InfReg)**

(b)

**Figure 9-11 Effect of increased site investigation expenditure on the total cost, using different (a) reduction techniques and (b) test types, for Site 3**

The final analysis dealing with Site 3 involves the examination of different settlement techniques and their influence on the effect of increased site investigation expenditure. These results are given in Figure 9-12 and indicate that:

- The 2:1 and Perloff technique yield the lowest total cost;
- The Newmark provides the highest total cost; and
- There is little different between settlement techniques, with regard to the effect of increased expenditure on the total cost.

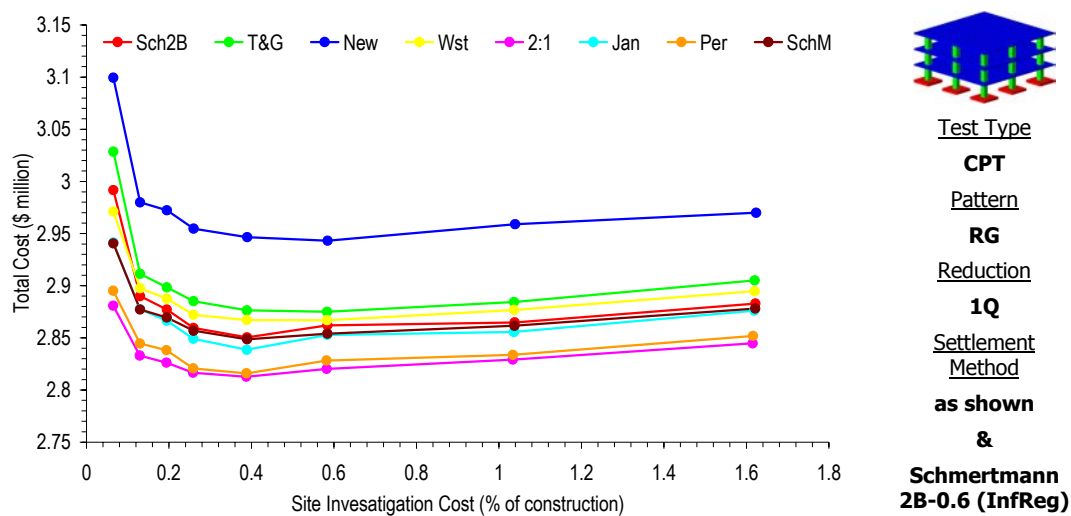


**Figure 9-12 Effect of increased site investigation expenditure on the total cost, using different settlement prediction techniques, for Site 3**

The results in Figure 9-12 show similar relative conservatisms for the settlement techniques as those shown in Figure 9-9 for Site 2. In fact, the order of settlement techniques that provide the lowest to highest total cost is the same. This infers that the settlement technique has little influence on the impact of additional site investigation expenditure. A similar conclusion has been made previously in Chapter 8 (§8.3.3.4) for general site conditions. However, the results in Figures 9-9 and 9-12 suggest that the 2:1 provides the lowest total cost. This was not observed in Chapter 8 (Figure 8-20) where the Perloff and Schmertmann Modified technique offered the lowest cost. However, as discussed for Site 2, the results for Site 3 are most likely influenced by a high probability of requiring an alternative foundation design type. As such, an examination of such probabilities is undertaken. These results are given in Figure 9-13 and clearly indicate that the settlement techniques that show a low total cost in Figure 9-12, also yield a high probability of requiring an alternative design type.

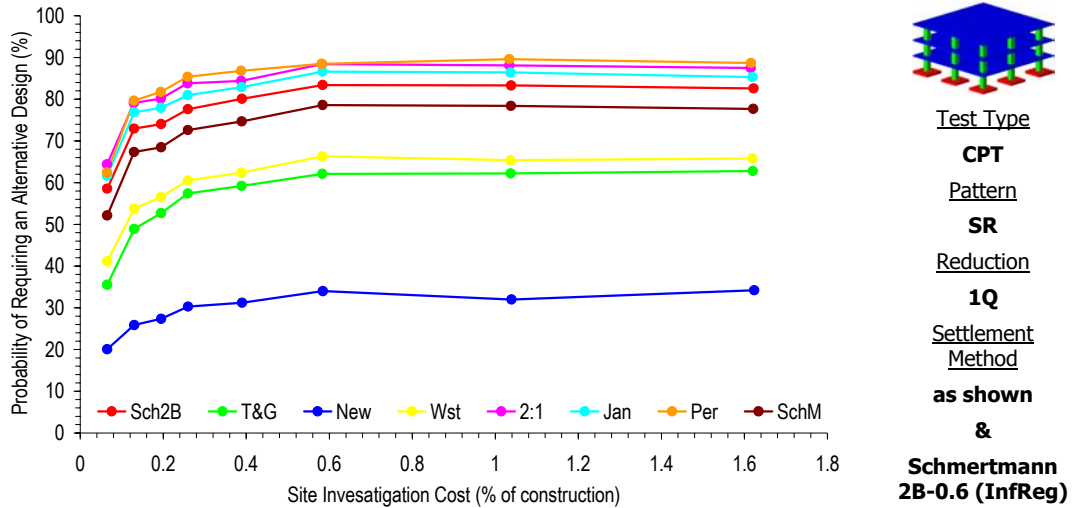


**Figure 9-13 Effect of increased site investigation expenditure on the probability of requiring an alternative foundation design, using different settlement prediction techniques, for Site 3**

The benefits of increased site investigation expenditure for Site 3 are also not as large as for Site 2. In fact, a cost saving of only \$150,000 is expected for the settlement methods that yield a high total cost, while for the other techniques a saving of less than \$100,000 is estimated. This is because the CPT was shown to yield similar total costs for increased site investigation expenditure [Figure 9-11(b)]. However, if the SPT is used, the expected savings are in the order of \$1 million.

Considering that the results for Site 3 (Figure 9-12) suggest differing degrees of conservatism for the settlement techniques than those for Site 1 (Figure 9-4), it is also worthwhile to analyse the use of these techniques on the project cost. The results of this analysis are illustrated in Figure 9-14 and indicate that the 2:1 and Perloff methods, which were shown in Figure 9-12 to yield the lowest total cost, also yield high project costs. As such, a higher initial cost is required to target a design with the lowest total cost. This conclusion is consistent with the results presented in Chapter 8 and intimates that the recommendations made for the general site conditions are also valid for specific cases.

## 9.5 SUMMARY

The analysis presented in this chapter illustrated the effect of increased site investigation expenditure on the total cost of a foundation design for three soil sites, where the spatial variability was known in detail. The aim of this analysis was to validate the conclusions and recommendations discussed in Chapter 8 for general site conditions. In most cases, such conclusions were confirmed, where the reduction technique required to provide a

design with the lowest total cost, was shown to be the same as in Chapter 8. Therefore, the conclusions made in Chapter 8 regarding the optimal site investigation expenditure and, for that matter, the optimal sampling strategy, are also valid for specific sites. Furthermore, the use of different reduction techniques was shown to have a similar impact on the results.

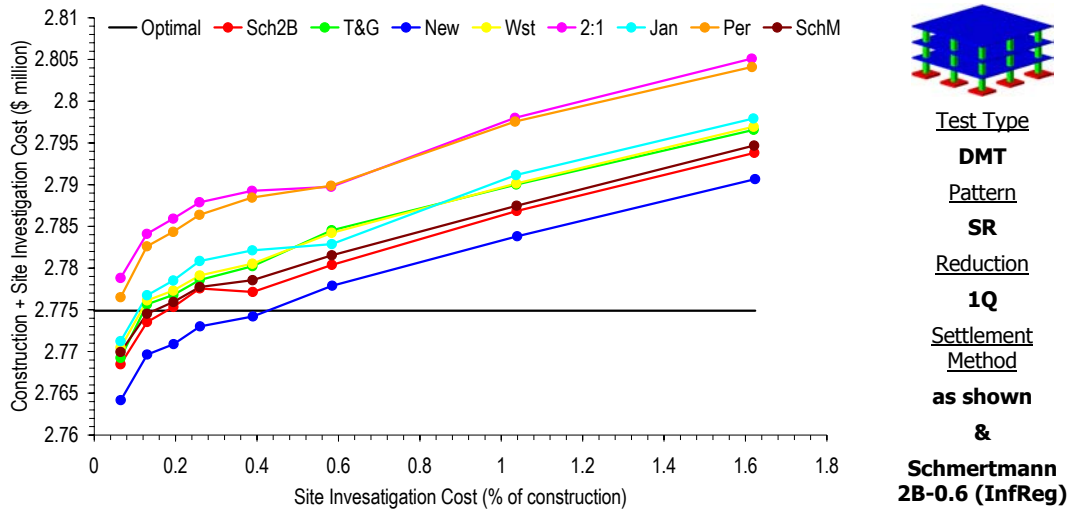


**Figure 9-14 Effect of increased site investigation expenditure on the construction cost, using different settlement prediction relationships, for Site 3**

The use of different settlement prediction techniques provided the sole discrepancies between conclusions in this chapter and Chapter 8. However, further analysis identified that results in this chapter were influenced by a high probability of requiring an alternative foundation design type. This issue was not observed in Chapter 8 because the mean elastic modulus was conditioned to ensure that a sufficient number of valid pad footings were possible.

Results also clearly illustrated the effect of increased site investigation expenditure. In all cases, an increase in expenditure led to a reduction in total cost, until the optimal site investigation was achieved. However, it was also shown that a similar increase in site investigation expenditure resulted in an escalating project cost. Therefore, the designs showing the lowest total cost also require an additional initial cost. This decision becomes one for the client or the owner of the project.



## **Chapter 10 SUMMARY AND RECOMMENDATIONS**

### **10.1 INTRODUCTION**

---

The previous nine chapters have discussed the development and results of a methodology to quantify the risk and reliability of a site investigation with respect to a pad foundation design for settlement. Many outcomes have been made throughout this research, most of which pertain to the site investigation phase of a foundation design. The more pertinent outcomes are noted in this chapter in the form of a summary of the research. Also included in this chapter is a discussion regarding the limitations and future directions of this type of work.

### **10.2 SUMMARY**

---

The importance of a site investigation on the financial and safety aspects of a design were outlined in Chapter 1. It was also observed that little quantitative research has been dedicated to the effectiveness of such investigations.

In Chapter 2, current foundation design practices were examined, with an emphasis on the design of shallow foundations. The uncertainties associated with such a design were also discussed, where it was shown that the uncertainties due to soil variability, sampling, measurement and transformation model errors, all have an influence on design. Furthermore, it was also demonstrated that several of these sources of uncertainty have received little attention in the past and hence, detailed research has been rare. The manner by which geotechnical engineers deal with the uncertainties in a foundation design was also discussed, where two methods are common: the traditional factor of safety approach and probabilistic techniques. The traditional factor of safety approach was observed to be more common. However, several authors recommended that probabilistic methods allow the rational treatment of uncertainties.

The methodology adopted to quantify the risks associated with a site investigation was described in Chapter 3, where the individual components of the foundation design process were detailed. The adopted methodology involved simulating a soil using local average subdivision (LAS), conforming to random field theory. The foundation design was assumed to consist of a simulated site investigation and a pad design for settlement. The scope of the site investigation was characterised by:

- The number of sample locations at the site;
- The pattern in which the sample locations were arranged;
- The test type adopted to estimate the elastic moduli; and
- The technique used to combine or reduce the results from multiple sample locations into a single vertical sample of elastic modulus values.

Methods adopted to include the uncertainties due to measurement and transformation model errors for each test type, were also described in Chapter 3, as well as the implementation of the settlement prediction techniques. Finally, the implementation of the Monte Carlo analysis to deal with the uncertainties in the foundation design was discussed, where it was determined that 1,000 realisations were sufficient to yield a stable footing design.

As with any simulation method, it was essential to verify that the results were both accurate and suitable. Such verification measures were discussed in Chapter 4 and included ensuring that:

- The generation of the simulated soil conformed to the target distribution and correlation structure;
- The settlement prediction techniques contained within the simulation method provided the same settlement estimates as theoretical calculations; and
- The use of the Monte Carlo analysis with 1,000 realisations yielded average and COV of settlement estimates that conformed to a theoretical evaluation using a second order Taylor series approximation and local averaging theory.

A worst case SOF of 8 m was also identified in Chapter 4, where the sample standard deviation of the simulated soil was the highest. Such a worst case SOF was determined to be

a function of the element size of 0.5 m. As such, the worst case SOF was used for the majority of analyses to present a conservative solution.

In Chapter 5, settlement analyses and foundations design were investigated, based on the use of different settlement prediction techniques. Although the results did not deal with site investigations, it was considered necessary to investigate the impacts of different prediction techniques on the settlement and design of a foundation. Therefore, the analyses in Chapter 5 were based on complete knowledge of the soil. In general, the settlement estimates for a footing of known size were shown to be influenced by the soil COV and SOF. More specifically:

- Footing settlement increased as the soil COV increased. Therefore, larger settlements occur on higher variability soils; and
- Soils that show a greater correlation (higher SOF) yield more variable settlement estimates.

The use of different settlement prediction techniques was shown to have little influence on settlement estimates for changing soil variability. Instead, the relative conservatism of each settlement method were preserved for different site conditions. Such conservatisms indicated that:

- The Perloff and Schmertmann Modified methods provide larger settlement estimates than the other techniques; and
- The Schmertmann 2B-0.6 and Janbu methods provide settlement estimates that are closest to 3DFEA.

The manner in which complete knowledge was assumed for the settlement estimates was shown to have a considerable impact. As such, the use of an influence region was considered, where soil properties within this region were used to characterise the soil variability. The influence region was also identified as having applications when planning site investigations. In this case, the size of the optimal influence region indicates whether soil properties obtained from a sampling location, should be included in the analysis. This is shown in Figure 10-1, where the sampled properties within the optimal influence region (SL2, SL3 and SL4) should be considered and properties outside the optimal influence region (SL1, SL5 and SL6) should be ignored.

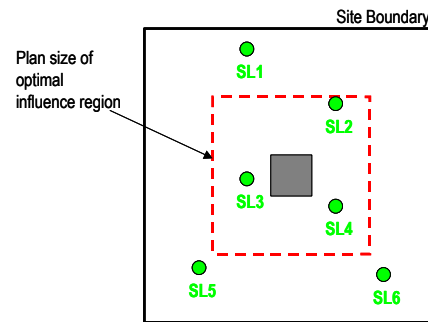


**Figure 10-1 Using an influence region to determine which soil properties should be considered**

The size of the optimal influence region was shown to be affected by the type of averaging used to combine properties and the soil SOF. However, based on the worst case SOF of 8 m, which was shown in Chapter 4 to yield the highest sample variability in the soil, the following recommendations were made:

- An influence region with a plan size of 6 times the footing area, when using the geometric average; and
- An influence region with a plan size greater than 21 times the footing area, when using a standard arithmetic average.

When the settlement prediction techniques were used in a design process, the relative conservatism was consistent with the settlement analysis. However, comparisons between designs using the settlement techniques and a single vertical sample of elastic moduli were shown to be affected less by the soil COV than the footing designs based on 3DFEA and complete knowledge of the soil.

In Chapter 6, the effects of using a site investigation were included into the analysis, where the impact of increased sampling on design parameters and the resulting foundation design was examined. In general, it was shown that an increased sampling effort led to a reduction in the average total footing area, suggesting a reduced conservatism. Furthermore, increased sampling was also shown in most cases, to reduce the variability of foundation design. This infers that additional sampling leads to a more robust design.

The use of different reduction techniques was shown to have a definitive impact on the effect of increased sampling. Specifically, the reduction method based on selecting the minimum value, MN, was shown to yield opposing trends for increased sampling compared with the other techniques. In this case, additional sampling led to a larger footing

design, which was also more variable. Furthermore, the weighting techniques (ID and I2) were shown to yield an erratic relationship between increased sampling and foundation design. This was caused by the occurrence of a sampling location coinciding with the footing. Specific conclusions regarding the use of different reduction techniques on the foundation design include:

- The MN reduction technique is not recommended, especially when the site investigation consists of multiple sampling locations;
- The ID and I2 methods should be avoided when a sampling location coincides with the footing. Furthermore, results from all sampling locations should be considered if the ID and I2 techniques are used; and
- The SA yields the smallest design with the lowest variability.

The types of soil tests were also shown to have an influence on the effect of increased sampling. In this case, the test types with higher measurement and transformation model errors were shown to yield larger footing designs. Furthermore, the differences between test types were shown to be affected by increased sampling, where the measurement errors were shown to average out for increased sampling. Therefore, the following conclusions regarding test types were made:

- Types of soil tests with high measurement errors should not be considered with a small sampling effort;
- Test types with small transformation model errors are preferred. In this case, a high sampling effort leads to a small testing error, even if the associated measurement errors are large.

It was observed that the use of different sampling patterns had little influence on the impact of increased sampling. Furthermore, it was evident that different sampling rates (expressed in terms of the number of samples per square metre area) that involved the same sampling effort had no impact on the design. As such:

- The number of samples has the greatest impact on the design of a foundation; and
- Sampling rates (samples per square metre area) should not be used.

Chapter 7 dealt with the effects of increased sampling on the design of a foundation in a probabilistic framework. In this case, the probabilities of under- and over-design were determined, as well as the probability of obtaining an optimal design and requiring an alternative foundation type. Under- and over-design conditions were assumed to occur when the design based on the data from a site investigation, provided either a smaller or larger footing, respectively, than the one based on 3DFEA and complete knowledge of the soil. In this case, additional sampling was shown to increase the probability of under-design, but decrease the probability of over-design. This was caused by the reduction in conservatism, due to additional sampling. The use of different reduction techniques was shown again to have an influence on the effect of increased sampling. In general, the results of the analysis were consistent with those in Chapter 6, where the techniques that caused the largest average total footing area were shown to yield high probabilities of over-design and low probabilities of under-design. More specific conclusions regarding the probabilities were identified as:

- A highly variable soil yields a site investigation design with a higher probability of under-design;
- The probability of over-design is similar for soils of any variability;
- Increased sampling has a greater impact on the probability of over-design;
- The SA reduction technique yields the highest probability of under-design and the lowest probability of over-design;
- Excluding the MN, the effect of increased sampling is the greatest when using the SA; and
- Differences between the types of soil tests are exaggerated for the probability of over-design.

An additional measure of the performance was discussed in Chapter 7. The design error illustrated the magnitude of under- or over-design, by normalising the difference between the footing areas from the two design types (SI and CK). In general, the design error was shown to reduce for an increased sampling effort. This inferred that it was controlled by an over-design condition. Furthermore, because negative design errors were also possible, several new conclusions were made regarding the suitability of different reduction techniques and test types. In summary these were:

- The GA and 1Q reduction techniques yield a design with a small positive design error for intensive sampling efforts;
- The SA yields a negative design error when more than 5 sampling locations are considered; and
- The SPT yields a small positive average design error when the sampling effort is high and the SA reduction technique is used.

However, the preferred combination of reduction method and test type, based on the average design error, was the GA, with either the CPT or DMT.

Further analyses in Chapter 7 quantified the average design error associated with using information from a sample location that did not coincide with the footing. In the case of a single footing, the average design error was shown to increase noticeably as the distance separating the sample and footing became larger. However, the average design error was shown to asymptote to a maximum at a separation distance that was influenced by the soil SOF. However, for a foundation system consisting of multiple pad footings, it was shown to be of greater benefit to sample at one of the footing locations. This does not necessarily infer sampling at the centre of the foundation system, especially when a footing is not located at the centre. Conclusions from this analysis were:

- Sample as close to any footing in the foundation system, preferably the one with the greatest applied load;
- For a single pad footing and a soil SOF of 16 m, a sampling location 5 m closer to the footing (from an original separation distance of 10 m), yields 50% less design error.

The final analysis in Chapter 7 dealt with the impact of measurement errors on the average design error. In this case it was shown that an increase in the bias and random components of measurement uncertainty have a similar impact on the average design error. Furthermore, it was observed that there is little impact on the design error for a vertical sampling rate of either 0.5 m or 1.5 m. However, for the triaxial test, an increase in sampling rate from 30 m to 15 m was shown to have a notable effect.

In Chapter 8, the risk associated with a site investigation was evaluated by including the costs associated with the site investigation, construction of the foundation and building,

and potential foundation failures. The costs associated with foundation failures were estimated by determining the probability and degree of failure for the designs based on the site investigation data. This was achieved by analysing such designs using 3DFEA with complete knowledge of the soil. However, it was found that the constraints associated with footing size had a marked influence on the results. Consequently, an alternative analysis, involving the Schmertmann 2B-0.6 settlement relationship and an influence region of elastic moduli (as used in Chapter 5), was adopted to estimate the probability and degree of failure.

Analyses in Chapter 8 identified that increased site investigation reduces the total cost of the design. However, this was balanced by a higher construction cost. Therefore, it was concluded that slightly conservative designs lead to a more economical solution. It was also found that the optimal site investigation expenditure, which provided the lowest total cost design, was not tied to the project cost. Therefore, the budget for a site investigation should not be based on a percentage of the project cost. Instead, the optimal site investigation expenditure was defined by the amount and type of sampling required for the site area and conditions. As such, the following conclusions were identified:

- The optimal site investigation costs is independent of building height (number of storeys). This infers that the budget for a site investigation should not be based on a percentage of the project cost;
- The highest optimal site investigation expenditure occurs when the soil COV is 50%. More variable soils do not require additional expenditure. However, the same expenditure on less variable soils also yields the lowest total cost.
- The optimal site investigation for a 20 m × 20 m site investigation area was shown to consist of 4 sampling locations using the CPT and the 1Q reduction technique. An additional sampling location was required when the site investigation area increased to 50 m × 50 m; and
- Reduction techniques and test types other than the CPT and 1Q may yield lower cost optimal site investigations, but the total cost of the design is higher.

A simplification of the relationship between increased site investigation and total cost for changing soil variability was also developed. This is shown in Figure 10-2 and separates the soil conditions into three separate categories:



- Highly variable soils with a worst case SOF;
- Medium variable soils with worst case SOF; and
- Low variable soils with low or high SOF.

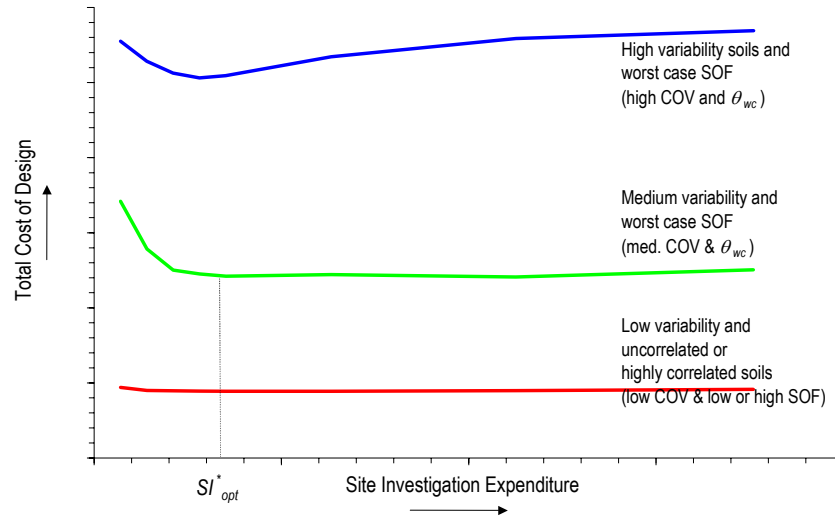


**Figure 10-2 General relationship between increased site investigation expenditure and total cost for different soil conditions**

In this case, the worst case SOF,  $\theta_{wc}$ , can be viewed as a conservative solution and should be adopted if there is limited knowledge of the soil SOF. However, it should also be remembered that the optimal site investigation expenditure,  $SI_{opt}^*$ , identified in these analyses should be considered the minimum, due to the assumption of a single layered stationary, or homogeneous, soil deposit.

To complement Figure 10-2, indications of the impact of different site conditions and site investigation variables on the cost of the optimal site investigation, project and total, are given in Table 10-1. These indicators demonstrate whether the soil variability, project size, reduction technique or test type, either increase, decrease or do nothing to the costs. In the case of the reduction technique and test types, the cost indicators are relative to the use of the 1Q and CPT, respectively. It is expected that practitioners may use this table when planning site investigations.

Several sensitivity analyses were also conducted in Chapter 8, where the impact of using different rehabilitation settlement limits and mean elastic moduli were examined. However, in all cases it appeared that the optimal site investigation involved the 1Q reduction technique and the CPT.

**Table 10-1 Effect of site conditions and site investigation variables on costs**

	Influence on Cost		
	Optimal Site Investigation	Construction	Total
<b>Soil Variability:</b>			
Increasing Soil COV	—	↑	↑
Increasing Soil SOF (< worst case)	↑	↑	↑
Increasing Soil SOF (> worst case)	↓	↑	—
<b>Project Size:</b>			
Increasing building height (no. of stories)	—	↑	↑
Increasing site size	↑	↑	↑
<b>Reduction Techniques</b> (as different from optimal – 1Q):			
Standard Arithmetica Average (SA)	↑	↓	↑
Geometric Average (GA)	↑	↓	—
Harmonic Average (HA)	↑	—	—
Inversed Distance Weighted (ID)	↓	↓	↑
1 <sup>st</sup> Quartile (1Q)	—	—	—
<b>Test Types</b> (compared with optimal – CPT):			
Standard Penetration Test (SPT)	↓	↑	↑
Cone Penetration Test (CPT)	—	—	—
Triaxial Test (TT)	↓	—	↑
Dilatometer Test (DMT)	↑	↑	—

Cost savings for increased site investigation expenditure were also identified in Chapter 8. In some cases, the expected costs savings for an increased site investigation expenditure of \$10,000 was observed to be nearly \$4 million. However, it was the reduction methods and test types that yielded the highest total cost, which were also shown to have the largest expected saving. Nevertheless, the expected cost savings for all reduction techniques and test types clearly outweighed the extra expenditure by two orders of magnitude.

Finally, the analyses in Chapter 9 used the known spatial statistics of three soil sites to verify the conclusions made in Chapter 8 regarding the optimal site investigation and the impact of increased sampling. Analyses for all three sites confirmed that the conclusions based on general site conditions made in Chapter 8 were applicable. However, the results also indicated that all three sites had a high probability of requiring an alternative foundation design type (other than a pad footing). This was caused by the low mean elastic modulus. As such, several of the results were not as conclusive as those presented in Chapter 8.

---

## 10.3 LIMITATIONS AND RESTRICTIONS

---

As with any simulation method, several simplifications and assumptions have been necessary to achieve manageable computational effort and suitable accuracy of results. Furthermore, the sheer number of variables affecting a geotechnical design meant that only few could be considered. The major limitations imposed on this research are categorized into factors that effect the soil simulation, site investigation and foundation design phases of this research. The following provides a detailed description of these limitations.

### 10.3.1 Soil Simulation

The largest simplification in the analysis presented relates to the assumption of a single layered homogeneous soil deposit. In reality, soil deposits consist of several layers or defects that can have large influence on the foundation. Furthermore, soil properties often show mean trends, especially with depth. All these factors add to the complexity of the soil, and therefore, require additional investigation for characterisation. As such, the conclusions made throughout this research regarding the optimal site investigation should be regarded as a minimum. It is expected that, to adequately characterise soils that are either multi-layered, include defects or show mean trends, a site investigation with a larger scope is required. Therefore, it is recommended that these factors be investigated in future research, as described in the following section.

The soil simulation is based on a numerical process that aims to provide properties that are equivalent to those in situ. However, the first issue that arises with this process is related to the limited knowledge of the spatial variability of a soil deposit. This is because statistical modelling of soils has only been in fashion for the last 30 years. Furthermore, considerable sampling is required to adequately characterise the soil. Such sampling is typically beyond the scope of most projects as the associated costs are prohibitive. Second, the common types of geotechnical tests that have been used to characterise soil variability are prone to considerable errors. Such errors have been discussed earlier. Although methods have been developed to quantify these errors, there is still doubt regarding the actual variability of soil properties.

The use of Local Average Subdivision (LAS), which conforms to random field theory, is also an assumption that warrants discussion. It was shown earlier that LAS yields a three-dimensional random field, which has maximum sample variability when the scale of fluctuation is a multiple of the element size. This is due to variance reduction in random

fields, which is commonly understood. However, the maximum sample variance that occurs at a specific scale of fluctuation, which has been called the worst case SOF in this research, may not necessarily be a phenomenon that exists in real soil deposits. Instead, this worst case SOF provides the most conservative solution for modelling. Therefore, it should not be expected that soil deposits have a worst case SOF. However, it should be remembered that variance reduction is caused by local averaging and, in most cases, all measurements are observed as averages. For example, consider the cone tip resistance of a CPT, which is an average of the resistance for the soil within the affected volume. Nevertheless, most of the results presented have been based on the analyses undertaken for soils with the worst case SOF, which intimates the highest variability in soil properties.

### **10.3.2 Simulated Site Investigation**

The simulated site investigation phase adopted in this research has also required several simplifications. First, the comparative vertical sampling rates of the CPT has been restricted to 0.5 m, which is considerably larger than the expected sampling rate of less than 20 mm. This has meant that the CPT only samples 3 times as many properties as the SPT and DMT. In reality, the CPT would yield many more data, which would have an impact on the foundation design. Second, the data sampled in the simulated site investigation are those taken directly from the generated field. These properties are influenced by local averaging, as discussed above. However, it was also described above that the measurements obtained by the common types of geotechnical tests could also be considered as averages of the soil response within a region. Therefore, the use of the data sampled directly from the generated field is expected to have little influence on the representativeness of the method. Third, the assumption of measurement and transformation model error for each of the test types was based on limited literature. Although a sensitivity analysis of the measurement errors for each test was discussed (§7.4.2), the bulk of the results were based on an assumed magnitude and type of uncertainty. However, all efforts were made to ensure that the comparative errors assumed for each type of test were consistent with the literature. Therefore, the SPT was considered the test type with the highest error or degree of uncertainty, while the TT was assumed to have a low transformation model error, as it is able to estimate the elastic modulus directly, albeit in the laboratory. Finally, because this research has considered only the serviceability design of a foundation, the ability of test types to provide other relevant properties has not been considered. However, it is recognised that the tests examined provide additional information that can be used for stability design or the classification of soils.

Additional to the assumptions made regarding the type of soil tests, the site investigation plans in this research have been based solely on sampling patterns like the regular grid, stratified random and simple random. However, it is common that practitioners plan sampling locations to test specific parts of a site, which may be known to be regions of interest prior to the investigation. This has not been accounted for in this research. Furthermore, site investigations are typically phased, where a small scope investigation is followed by a larger scale investigation. No consideration has been made for such phasing of investigations in this research. However, the use of phased investigations and strategic placement of sampling locations is suggested for future work, as discussed later. Finally, all site investigation plans in this research have involved the same type of soil test. However, it is common that combinations of test types are used in any one investigation. Again, an examination of these factors is recommended for future research, as described later in this chapter.

### 10.3.3 Foundation Design

All settlement predictions made in this research have been based on the assumption of linear elastic deformations. However, the stress-strain relationship in soil is highly non-linear. Furthermore, only the serviceability design of a foundation has been considered. This has limited the analysis to investigate only the settlements of footings. Therefore, it is proposed that the bearing capacity of a foundation design also be examined. This is expected to have a considerable impact on the results, as discussed later.

The significance of the element size assumption, as discussed above, should be further re-emphasised. This is because this assumption also had a considerable influence on the design of the foundation when 3DFEA was used. In this case, foundation size was tied to the element size. Furthermore, to minimise stress modelling errors, a minimum footing size constraint was introduced. This meant that the smallest footing that could be designed was  $1.5 \text{ m} \times 1.5 \text{ m}$ . As a result, 3DFEA was found to be unsuitable for analysing foundation designs to assign failure costs and an alternative method that accounted for the complete knowledge of the soil was employed. However, it was observed that when 3DFEA was not used, and the element size had little impact on the design, the effect of increased sampling was similar. Therefore, it is expected that the use of a coarse element size influences only the designed footing size and not the impact of increased sampling.

Several assumptions have also been made regarding the inclusion of costs related to the site investigation, construction of the building and foundation, and the costs associated

with failure. Again, the method adopted has been considered suitable for the purposes of this research. However, a more detailed description of costs is recommended for future research.

Finally, this research has only considered the design of a pad foundation. In reality, engineering practitioners decide between different foundation types including pads, strips, rafts or piles. It is expected that, in some cases, the data from a site investigation will require a different foundation type than that required when the complete knowledge of the soil is considered. These situations are expected to have a considerable impact on the results of the analysis and the performance of a site investigation. Therefore, it is recommended that additional research including the design of other types of foundation be explored. More details regarding recommended future work are discussed in the next section.

## **10.4 FUTURE DIRECTIONS OF RESEARCH**

---

This research is considered the first phase of measuring the impact of site investigations on the design of foundations. Additional variables and factors need to be incorporated into the analysis to identify the optimal site investigation strategy. Furthermore, several assumptions that were considered necessary for this research were also identified in the previous section. Some of these have a greater impact on the results than others. As such, it is considered of great benefit to refine the method to minimise the impact of such assumptions. Accordingly, the discussion that follows details recommended work that will minimise the impact of several assumptions and further the research toward the identification of the effect of site investigations on the design of foundations.

### **10.4.1 Analysis Using More Complex Soil Models**

The assumption of a single layered homogeneous soil is considered to have the greatest impact on the results presented. This is because soils are typically multi-layered, and possess defects, or inconsistencies, where the data are considerably different from those surrounding. Therefore, it is highly recommended that the analyses presented in this research be extended to examine the impact of site investigations on the design of a foundation for soils with multiple layers or other defects. It is expected that such analyses will indicate that a considerably larger site investigation scope is required to adequately characterise the soil. This is because additional information regarding the site geology is required. Furthermore, it is also expected that the arrangement of sampling locations will have a greater

influence on the design. This is because soil layers are not typically horizontal and the sampling location will influence the knowledge regarding the site geology.

Additional to the use of layered media, it is also recommended to investigate the impact of site investigations on the design of a foundation for other site conditions. For example, the design is expected to be different for an over-consolidated soil compared to a normally consolidated soil. Again, it is expected that a larger scope site investigation, than the one identified in previous chapters, would be required to adequately characterise these types of soil.

#### **10.4.2 Incorporating the Bearing Capacity of a Foundation**

Although it was stated that the differential settlement of a foundation is the primary cause of structural distress, it is considered important that the results presented in this thesis be examined when the foundation is designed for bearing capacity. It is also likely that the adequate characterisation of a soil for a bearing capacity design will require a different site investigation plan. This is because stresses are concentrated below the footing and soil properties located a distance away from the footing are less likely to have an impact. Furthermore, the low strength regions of soil heavily influence the bearing capacity of a foundation. Therefore, it is expected that reduction techniques that yield slightly conservative soil data, and are low strength dominated (i.e. the geometric and harmonic averages), will yield better designs.

#### **10.4.3 Investigating the Design of Other Types of Foundation Systems**

It was briefly discussed earlier in this chapter that it is highly recommended that this research be extended to include the design of other foundation systems. This is because it is anticipated that the required site investigation for a pad foundation design will be different to that required for a raft or pile foundation. Furthermore, it is also expected that, in some cases, the results from a site investigation will necessitate the design of a different type of foundation system than that required when the complete knowledge of the soil is considered. These situations will have a considerable influence on the total cost of the design, where a pile foundation is typically more expensive than a raft or pad foundation. However, this form of analysis is also expected to have an influence on the required scope of the investigation, as pile foundations need information about the soil at greater depths. Therefore, it is also recommended that future research be considered to examine the impact of site investigation on the design of raft and pile foundations separately. This type of

analysis would be similar to that described earlier, where the design of a foundation based on information from a site investigation is compared to an optimal design that utilises the complete knowledge of the soil. However, pile and raft foundation design methods are not typically as straightforward as those for pad foundations. As such, it is expected that an analysis dealing with the design of pile and raft foundations will require additional computational effort, unless a method to calibrate the design utilising complete knowledge can be found, as similar to that described in Chapter 8 (§8.3.2).

#### **10.4.4 Analysing More Complex Site Investigation Strategies**

Site characterisation and investigation activities vary from site to site, dependent on the availability of prior information and the conditions of the proposed project. Since only relatively simple site investigation strategies have been explored in this research, it is highly recommended that future research be directed towards quantifying the impact of more complex investigations. This may include phased site investigations, where initial sampling or testing is followed by a more extensive investigation that uses results from the initial effort. It is also recommended that future research investigate the use of sampling plans that involve more than one type of test. For example, it is typical that site investigation plans may involve, say, 3 CPTs and 2 SPTs. Therefore, the results from each type are combined with the aim of better characterising the soil.

It is expected that more complex site investigation strategies will have a considerable influence on the required scope to minimise the total cost. In some cases, phasing the investigation or using multiple types of tests will reduce the cost of the optimal strategy. However, it is also anticipated that increasing complexity will yield more expensive site investigations that are unnecessary, especially for small sites with simple geology like those discussed in this research. Therefore, any future research dealing with the use of more complex investigation strategies should be explored in conjunction with analyses on multi-layered soils, or soils with defects and inconsistencies.

#### **10.4.5 Refining the Element Size**

Many of the limitations associated with this research have related to the assumed element size of  $0.5 \text{ m} \times 0.5 \text{ m} \times 0.5 \text{ m}$ . Such a coarse element size was necessary to keep computational times for 3DFEA to manageable proportions. However, as described earlier in this chapter, the use of such an element size meant that a minimum footing size of  $2.25 \text{ m}^2$  ( $1.5 \text{ m} \times 1.5 \text{ m}$ ) and a 1 m sizing increment was required. Although the use of a 0.5 m



element size appeared to have little influence on the effects of increased sampling, it is recommended that future analyses investigate the use of a smaller element size to improve the resolution of the designed footing areas. There are also several alternative ways to reduce the element size without necessarily increasing the computational time. One may be to explore the use of a finite element mesh with variable element sizes. This is common in finite element modelling where the elements located closer to the footing are smaller than those further away. However, the use of a variable element size must be carefully implemented in a design situation, where the footing size is continually changing.

Another method of reducing the impact of element size on the analysis is to calibrate the design using 3DFEA and complete knowledge of the soil with another design method that does not require the footing size to be a function of the element size. This process was described in Chapter 8 (§8.3.2). However, it is recommended that additional research be conducted to explore such calibrations for a wider range of site and footing conditions.

Although the element size constraint imposed a minimum footing size and a 1 m sizing increment, it appeared to have little influence on the impact of additional sampling. Therefore, it is not expected that future research involving a smaller element size will change the conclusions regarding the effect of increased site investigation expenditure. However, it is expected that such results will provide a more accurate representation of the actual costs associated with a design based on information from a site investigation.

#### **10.4.6 Other Recommended Research**

It is recommended that future research explore the use of reliability-based foundation design, where the size of the footing is determined by minimising the expected probability of failure. It is anticipated that using a reliability-based foundation will have an impact on the total cost of the foundation design, while only having minimal influence on the effect of increased site investigation expenditure. However, reliability-based design methods accommodate the variability of the sampled data, and will, therefore have an influence on the robustness of the design. As such, the use of reliability-based design methods is recommended for future research.

Finally, it is suggested that future research should also examine comparisons between numerically based analysis tools, like 3DFEA, and common design methods, where both use the information from a site investigation. It is anticipated that, although providing an excellent representation of the soil response, the numerical based tools are still heavily influ-

enced by the accuracy of the input information. Therefore, such increase in accuracy may not be worth the additional effort or computational time. This form of research is considered beneficial as it will demonstrate whether practitioners need to adopt numerically based methods when there is only limited information regarding the site.

## 10.5 CONCLUSION AND RECOMMENDATIONS

---

Although it is well recognised that increased sampling is beneficial, the results presented in this thesis allow practitioners to optimise the benefits of increased sampling by using different reduction techniques and test types, while also having reasonable knowledge regarding the level of uncertainty in the design. Results have also confirmed that a slightly conservative foundation design yields a better long-term solution. However, the benefits of additional sampling are caused primarily by the increased confidence or robustness of the design.

In conclusion, the following recommendations will assist engineering practitioners with the planning of site investigations and the design of foundations based on the results from a site investigation.

- Design slightly conservative foundations to avoid the possibility of failures;
- Undertake increased sampling or site investigation expenditure on more variable soils;
- Avoid using the SA, GA or 1Q reduction techniques with the SPT. Instead use the HA method;
- Avoid the MN, ID and I2 reduction techniques. If the ID or I2 techniques are used, ensure that results from all sampling locations are considered;
- Use the 1Q reduction technique with the CPT or DMT;
- Consider the required number of sampling locations, rather than a sampling rate; and
- Base the site investigation expenditure on the site conditions and NOT the project cost. As a guide, additional sampling is required when the soil variability is high and the plan size of the building is large. In this research, 4 sampling locations were observed to be sufficient for a 20 m × 20 m plan area; yet 5 locations were required for a 50 m × 50 m area.

## REFERENCES

**AUSTROADS. (1992).** "HB 77 Austroads Bridge Design Code."

**Australian Standards. (1993).** "AS1726 Geotechnical Site Investigations."

**Australian Standards. (2004).** "AS 5100 Bridge Design."

**Akkaya A, and Vanmarcke E. (2003).** *Estimation of Spatial Correlation of Soil Parameters Based on Data from the Texas A&M University NGES*, American Society of Civil Engineers, Virginia, USA.

**Baecher G B. (1979).** "Analysing exploration strategies." *Site Characterisation and Exploration*, Northwest University, Illinois, USA, pp. 220-246.

**Baecher G B. (1982).** "Statistical methods in site characterization." *Updating Subsurface Samplings of Soils and Rocks and their In-Situ Testing*, Santa Barbara, USA, pp. 463-492.

**Baecher G B. (1986).** "Geotechnical error analysis." 1105, Transport Research Rec.

**Baecher G B, and Christian J T. (2003).** *Reliability and Statistics in Geotechnical Engineering*, John Wiley & Sons Ltd., Chichester, England.

**Baecher G B, and Ingra T S. (1981).** "Stochastic FEM in settlement prediction." *Journal of the Geotechnical Engineering Division*, 107(4), pp. 449-463.

**Baecher G B, Pate M E, and de Neufville R. (1980).** "Risk of Dam Failure in Benefit-Cost Analysis." *Water Resources Research*, 16(3), pp. 449-456.

**Banerjee P K, and Davies T G. (1977).** "Analysis of pile groups embedded in Gibson soil." *Ninth International Conference on Soil Mechanics and Foundation Engineering*, pp. 381-386.

**Becker D E. (2001).** "Site Characterization." *Geotechnical and Geoenvironmental Engineering Handbook*, R Rowe, ed., Kluwer Academic Publishers, Boston, USA, pp. 69-106.

**Bell R M, Giddon A, and Parry G D R. (1983).** "Sampling strategy and data interpretation for site investigation of contaminated land." *Reclamation of Former Iron and Steel Works Sites*, Durham and Cumbria County Councils, Durham, England.

**Benjamin J R, and Cornell C A. (1970).** *Probability, Statistics, and Decision for Civil Engineers*, McGraw-Hill, New York, USA.

**Bjerrum L. (1963).** "Allowable Settlements of Structures." *Proceedings of European Conference on Soil Mechanics and Foundation Engineering*, Wiesbaden, Germany, pp. 135-137.

**Bolton M D. (1989).** "Development of Codes of Practice for Design." *12th International Conference on Soil Mechanics and Foundation Engineering*, Rio de Janeiro, Brazil, pp. 2073-2076.

**Booker J R, Carter J P, Small J C, Brown P T, and Poulos H G. (1989).** "Some Recent Applications of Numerical Methods to Geotechnical Analysis." Research Report 598, University of Sydney, Sydney, Australia.

**Booker J R, and Small J C. (1983).** "The analysis of liquid storage tanks on deep elastic foundations." *International Journal for Numerical and Analytical Methods in Geomechanics*, 7, pp. 187-207.

**Boone S J. (2004).** "Evaluating Damage to Buildings from Settlement and Construction-Induced Movement." *The International Conference on Structural and Foundation Failures*, Singapore, pp. 612-623.

**Bowerman B L, and O'Connell R T. (1979).** *Forecasting and Time Series*, Duxbury Press, Massachusetts, USA.

**Bowles J E. (1997).** *Foundation Analysis and Design*, McGraw-Hill, Singapore.

**Brejda J J, Moorman T B, Smith J L, Karlen D L, Allan D L, and Dao T H. (2000).** "Distribution and Variability of Surface Soil Properties at a Regional Scale." *Soil Science Society of America Journal*, 64, pp. 974-982.

**Bridges E M. (1987).** *Surveying Derelict Land*, Oxford University Press, Oxford, England.

- British Standards Institution. (1988).** "Code of practice for the identification of potentially contaminated land and its investigation." Draft for Development 175.
- Brockwell P J, and Davis R A. (1987).** *Time Series: Theory and Methods*, Springer-Verlag, New York, USA.
- Burd H J, and Frydman S. (1997).** "Bearing capacity of plane-strain footings on layered soils." *Canadian Geotechnical Journal*, 34(2), pp. 241-253.
- Burland J B. (1973).** "Shaft friction of piles in clay, A simple fundamental approach." *Ground Engineering*, 6(1), pp. 30-42.
- Butterfield R, and Banerjee P K. (1971).** "The elastic analysis of compressible piles and pile groups." *Geotechnique*, 21(1), pp. 43-60.
- Carpenter L. (1980).** "Computer Rendering of Fractal Curves and Surfaces." SIGGRAPH, Association for Computing Machinery, Seattle, Washington, USA.
- Chatfield C. (1975).** *The Analysis of Time Series: Theory and Practice*, Chapman and Hall, London, England.
- Chen W, and McCarron W. (1991).** "Bearing Capacity of Shallow Foundations." *Foundation Engineering Handbook*, H Fang, ed., Van Nostrand Reinhold, New York, USA, pp. 144-165.
- Chen W F. (1975).** *Limit Analysis and Soil Plasticity*, Elsevier, Amsterdam, Netherlands.
- Christian J T, and Carrier III W D. (1978).** "Janbu, Bjerrum and Kjaernsli's chart reinterpreted." *Canadian Geotechnical Journal*, 15, pp. 123-128.
- Christian J T, Ladd C C, and Baecher G B. (1994).** "Reliability Applied to Slope Stability Analysis." *Journal of Geotechnical Engineering*, 120(12), pp. 2180-2207.
- Clarke I. (1979).** *Practical Geostatistics*, Applied Science Publishers, London, England.
- Clayton C R I. (2001).** "Managing geotechnical risk: time for change?" *Geotechnical Engineering*, 149(1), pp. 3-11.
- Clayton C R I, Simons N E, and Matthews M C. (1982).** *Site Investigation*, Granada Publishing, London, England.
- Cochran W G. (1977).** *Sampling Techniques*, John Wiley & Sons, New York, USA.

**Compaq Computer Corporation. (2000).** Compaq Visual FORTRAN Standard Edition 6.6.A.

**Cook R D, Malkus D S, and Plesha M E. (1989).** *Concepts and Applications of Finite Element Analysis*, John Wiley and Sons Inc, Toronto, Canada.

**Craig R F. (1997).** *Soil Mechanics*, E & FN Spon, London, England.

**Cressie N A C. (1993).** *Statistics for Spatial Data*, John Wiley & Sons, Inc, New York, USA.

**D'Agostino R B, and Stephens M A. (1986).** *Goodness-Of-Fit Techniques*, Marcel Dekker Inc., New York, USA.

**D'Appolonia D J. (1968).** "Settlement of Spread Footings on Sand." *Journal of Soil Mechanics and Foundations Division, ASCE*, 94(SM 3), pp. 753-760.

**Davisson M T, and Salley J R. (1972).** "Settlement Histories of Four Large Tanks on Sand." *5th PSC, ASCE*, 1(2), pp. 981-996.

**Day R. (1999).** *Forensic Geotechnical and Foundation Engineering*, McGraw-Hill Companies Inc, USA.

**DeGroot M H. (1986).** *Probability and Statistics*, Addison-Wesley Publishing Company, Reading, USA.

**Department of the Environment. (1988).** "Problems arising with the redevelopment of gas works sites and similar sites." HMSO, 2nd ed., London, England.

**Department of the Environment / National Water Council. (1986).** "The sampling and initial preparation of sewage and waterworks' sludges, soils, sediments, plant materials and contaminated wildlife prior to analysis." 2nd ed., London, England.

**Desai C S, and Abel J F. (1972).** *Introduction to the Finite Element Method*, Van Nostrand Reinhold, New York, USA.

**Deutsch C V, and Journel A G. (1992).** *GSLIB: Geostatistical Software Library and User's Guide*, Oxford University Press, USA.

**Djoenaidi W J. (1985).** "A compendium of soil properties and correlations," Masters, University of Sydney, Sydney, Australia.

- Duncan J M. (1999).** "The use of back analysis to reduce slope failure risk: The Seventh Annual Arthur Casagrande Memorial Lecture." *Civil Engineering Practice, Journal of the Boston Society of Civil Engineers*, 14(1), pp. 75-91.
- Duncan J M, and D'Orazio T B. (1984).** "Stability of Steel Storage Tanks." *Journal of Geotechnical Engineering*, 110(9), pp. 1219-1238.
- Ergatoudis J, Irons B M, and Zienkiewicz O C. (1968).** "Three Dimensional Analysis of Arch Dams and Their Foundations." Research C/R/74/67, University of Wales, Swansea, Wales.
- Fang H Y. (1991).** *Foundation Engineering Handbook*, Van Nostrand Reinhold, New York, USA.
- Fellenius B H. (1991).** "Pile Foundations." *Foundation Engineering Handbook*, H Fang, ed., Van Nostrand Reinhold, New York, USA, pp. 923.
- Fenton G, Paice G, and Griffiths D. (1996).** "Probabilistic Analysis of Foundation Settlement." *ASCE Uncertainty '96 Conference*, Madison, Wisconsin, USA, pp. 651-665.
- Fenton G A. (1990).** "Simulation and Analysis of Random Fields," PhD, Princeton University, New Jersey, USA.
- Fenton G A. (1994).** "Error Evaluation of Three Random Field Generators." *Journal of Engineering Mechanics*, 120(12), pp. 2487-2497.
- Fenton G A. (1996).** "Probabilistic Methods in Geotechnical Engineering." ASCE GeoLogan 1997 Conference - Workshop, Logan, Utah, USA.
- Fenton G A. (1999).** "Random Field Modelling of CPT Data." *Journal of Geotechnical and Geoenvironmental Engineering*, 125(6), pp. 486-498.
- Fenton G A. (2002).** "Risk Assessment & Management." Course Notes EMGM4675/6675, Dalhousie University, Canada.
- Fenton G A, and Griffiths D V. (2002).** "Probabilistic Foundation Settlement on Spatially Random Soil." *Journal of Geotechnical and Geoenvironmental Engineering*, 128(5), pp. 381-390.

**Fenton G A, and Griffiths D V. (2005).** "Three-dimensional probabilistic foundation settlement." *Journal of Geotechnical and Geoenvironmental Engineering*, 131(2), pp. 232-239.

**Fenton G A, Griffiths D V, and Cavers W. (2005).** "Resistance factors for settlement design." *Canadian Geotechnical Journal*, 42(6), pp. 1422-1436.

**Fenton G A, and Vanmarcke E. (2003).** "Random Field Characterization of NGES Data." Probabilistic Site Characterization at the National Geotechnical Experimentation Sites - GSP 121, E Vanmarcke and G A Fenton, eds., American Society of Civil Engineers, Virginia, USA, pp. 61-78.

**Fenton G A, and Vanmarcke E H. (1990).** "Simulation of Random Fields via Local Average Subdivision." *Journal of Engineering Mechanics*, 116(8), pp. 1733-1749.

**Fenton G A, Zhou H, Jaksa M B, and Griffiths D V. (2003).** "Reliability analysis of a strip footing designed against settlement." *9th International Conference of Applications of Statistics and Probability in Civil Engineering*, San Francisco, USA, pp. 1271-1277.

**Ferguson C C. (1992).** "The Statistical Basis for Spatial Sampling of Contaminated Land." *Ground Engineering*, 25(6), pp. 34-38.

**Filippas O B, Kulhawy F H, and Grigoriu M D. (1988).** "Reliability-Based Foundation Design for Transmission Line Structures: Uncertainties in Soil Property Measurement." Research Report 1493-3 EL-5507, Vol. 3, Cornell University / Electric Power Research Institute, Palo Alto, California, USA.

**Fischer J A. (1972).** "Settlement of a Large Mat on Sand." *5th PSC, ASCE*, 1(2), pp. 997-1018.

**Fournier A, Fussell D, and Carpenter L. (1982).** "Computer Rendering of Stochastic Models." *Communications of the Association for Computing Machinery*, 25, pp. 371-384.

**Fraser R A, and Wardle L J. (1976).** "Numerical analysis of rectangular rafts on layered foundations." *Geotechnique*, 26(4), pp. 613-630.

**Freudenthal A M. (1951).** "Planning and interpretation of fatigue tests." Symposium on Statistical Aspects of Fatigue, ASTM Special Technical Publication No. 121.

**Freudenthal A M, Garrelts J M, and Shinozuka M. (1966).** "The analysis of structural safety." *Journal of the Structural Division*, 92(ST1), pp. 267-325.



- Freudenthal A M, and Gumbel E J. (1956).** "Physical and statistical aspects of fatigue." *Advances in Applied Mechanics*, 4, pp. 117-159.
- Goble G. (1999).** "Geotechnical related development and implementation of load and resistance factor design (LRFD) methods." NCHRP Synthesis 276, Transportation Research Board, Washington, USA.
- Griffiths D V. (1982).** "Computation of bearing capacity on layered soils." *4th International Conference on Numerical Methods in Geomechanics*, Edmonton, Canada, pp. 163-170.
- Griffiths D V, and Fenton G A. (2000).** "Influence of Soil Strength Heterogeneity on the Stability of an Undrained Clay Slope by Finite Elements." *ASCE Geotechnical Specialty Publication No 101*, GeoDenver 2000 Symposium, pp. 184-193.
- Griffiths D V, Fenton G A, and Manoharan N. (2002a).** "Bearing Capacity of Rough Rigid Strip Footing on Cohesive Soil: Probabilistic Study." *Journal of Geotechnical and Geoenvironmental Engineering*, 128(9), pp. 743-755.
- Griffiths D V, Fenton G A, and Tveten D E. (2002b).** "Probabilistic Geotechnical Analysis: How difficult does it need to be?" *Probabilistics in Geotechnics - Technical and Economic Risk Estimation*, Graz, Austria, pp. 3-20.
- Griffiths D V, and Smith I M. (1991).** *Numerical Methods for Engineers*, Blackwell, Oxford, England.
- Guan X L, and Melchers R E. (2000).** "A comparison of some FOSM and Monte Carlo results." *8th International Conference on Applications of Statistics and Probability in Civil Engineering (ICASP8)*, Sydney, Australia, pp. 65-71.
- Halim I S, and Tang W H. (1993).** "Site Exploration Strategy for Geologic Anomaly Characterisation." *Journal of Geotechnical Engineering*, 119(2), pp. 195-213.
- Hamilton J D. (1994).** *Time Series Analysis*, Princeton University Press, New Jersey, USA.
- Hansen J B. (1961).** "A General Formula for Bearing Capacity." *Danish Geotechnical Institute, Bulletin No. 11*, pp. 46.

**Hansen J B. (1965).** "Philosophy of Foundation Design: Design Criteria, Safety Factors and Settlement Limits." *Symposium on Bearing Capacity & Settlement of Foundations*, Duke University, Durham, USA, pp. 1-13.

**Hansen J B. (1970).** "A Revised and Extended Formula for Bearing Capacity." *Danish Geotechnical Institute, Bulletin No. 28*, pp. 21 (successor to Bulletin No. 11).

**Harr M E. (1966).** *Foundations of Theoretical Soil Mechanics*, McGraw Hill, New York, USA.

**Harr M E. (1987).** *Reliability-Based Design in Geotechnical Engineering*, McGraw-Hill, New York, USA.

**Harr M E. (1989).** "Probabilistic estimates for multivariate analyses." *Applied Mathematical Modelling*, 13(5), pp. 313-318.

**Hoeksema R J, and Kitanidis P K. (1985).** "Analysis of the spatial structure of properties of selected aquifers." *Water Resources Research*, 21(4), pp. 563-572.

**Hohn M E. (1988).** *Geostatistics and Petroleum Geology*, Van Nostrand Reinhold, New York, USA.

**Holtz R D. (1991).** "Stress Distribution and Settlement of Shallow Foundations." *Foundation Engineering Handbook*, H Y Fang, ed., Van Nostrand Reinhold, New York, USA, pp. 166-223.

**Holtz R D, and Kovacs W D. (1981).** *An Introduction to Geotechnical Engineering*, Prentice Hall, New Jersey, USA.

**Hrennikoff A R. (1941).** "Solution of the Problems in Elasticity by the Framework Method." *Journal of Applied Mechanics*, 8(4), pp. A169-A175.

**Institute of Civil Engineers. (1991).** *Inadequate Site Investigation*, Thomas-Telford, London, England.

**Intel Corporation. (2004).** Intel(R) FORTRAN Compiler for 32-bit applications Version 7.1.

**Interdepartmental Committee for the Redevelopment of Contaminated Land. (1987).** "Guidance on the assessment and redevelopment of contaminated land." *2nd ed.*, Guidance note 59/83.

- Jaksa M B. (1995).** "The Influence of Spatial Variability on the Geotechnical Design Properties of a Stiff, Overconsolidated Clay," PhD, The University of Adelaide, Adelaide.
- Jaksa M B. (2000).** "Geotechnical Risk and Inadequate Site Investigations: A Case Study." *Australian Geomechanics*, 35(2), pp. 39-46.
- Jaksa M B. (2004).** "Geotechnical Engineering and Design III." Course Notes, The University of Adelaide, South Australia.
- Jaksa M B, Brooker P I, and Kaggwa W S. (1997).** "Inaccuracies associated with estimating random measurement errors." *Journal of Geotechnical and Geoenvironmental Engineering*, 123(5), pp. 393-401.
- Jaksa M B, and Fenton G A. (2002).** "Assessment of Fractal Behaviour of Soils." *Probabilistics in Geotechnics - Technical and Economic Risk Estimation*, Graz, Austria, pp. 47-54.
- Jaksa M B, Goldsworthy J S, Fenton G A, Kaggwa W S, Griffiths D V, Kuo Y L, and Poulos H G. (2005).** "Towards Reliable and Effective Site Investigations." *Geotechnique*, 55(2), pp. 109-121.
- Jaksa M B, Kaggwa W S, and Brooker P I. (1993).** "Geostatistical modelling of the undrained shear strength of a stiff overconsolidated clay." *Proceedings of Conference on Probabilistic Methods in Geotechnical Engineering*, Canberra, Australia, pp. 185-194.
- Jaksa M B, Kaggwa W S, Fenton G A, and Poulos H G. (2003).** "A framework for quantifying the reliability of geotechnical investigations." *9th International Conference on the Application of Statistics and Probability in Civil Engineering*, San Francisco, USA, pp. 1285-1291.
- Janbu N, Bjerrum L, and Kjaernsli B. (1956).** "Veiledning ved losning av fundamenteringsoppgaver." Norwegian Geotechnical Institute Publication 16, Oslo, Norway, pp. 30-32.
- Jardine R J, Potts D M, Fourie A B, and Burland J B. (1986).** "Studies of the influence of non-linear stress-strain characteristics in soil-structure interaction." *Geotechnique*, 36(3), pp. 377-396.
- Jennings A, and McKeown J. (1992).** *Matrix Computation for Engineers and Scientists*, John Wiley, London, England.

**Johannessen I J, and Bjerrum L. (1965).** "Measurement of the compression of a steel pile to rock due to settlement of the surrounding clay." *6th International Conference on Soil Mechanics and Foundation Engineering*, Montreal, Canada, pp. 261-264.

**Journel A G, and Huijbregts C J. (1978).** *Mining Geostatistics*, Academic Press, London, England.

**Kantey B. (1965).** "Shallow Foundations and Pavements." *6th International Conference on Structural Mechanics and Foundation Engineering*, pp. 453-455.

**Kay J N, and Cavagnaro R L. (1982).** "Settlement of Raft Foundations." Research R42, The University of Adelaide, Adelaide, Australia.

**Kraft L M, Ray R P, and Kagawa T. (1981).** "Theoretical t-z curves." *Journal of Geotechnical Engineering Division*, 107(11), pp. 1543-1561.

**Krige D G. (1951).** "A Statistical Approach to Some Mine Valuations and Allied Problems at the Witwatersrand," unpublished Master's Thesis, University of Witwatersrand.

**Kulatilake P H S W, and Um J. (2003).** "Spatial Variation of Cone Tip Resistance for the Clay Site at Texas A&M University." Probabilistic Site Characterization at the National Geotechnical Experimentation Sites - GSP 121, E Vanmarcke and G A Fenton, eds., American Society of Civil Engineers, Virginia, USA, pp. 41-60.

**Kulhawy F H. (1984).** "ASCE drilled shaft standard: University perspective." Analysis and Design of Pile Foundations, ASCE, New York, USA, pp. 390-395.

**Kulhawy F H. (1992).** "On Evaluation of Static Soil Properties." Stability & Performance of Slopes & Embankments II (GSP 31), R B Seed and R W Boulanger, eds., ASCE, New York, USA, pp. 95-115.

**Kulhawy F H, Birgisson B, and Grigoriu M D. (1992).** "Reliability-Based Foundation Design for Transmission Line Structures: Transformation Models for In-Situ Tests." Research Project 1493-4 EL-5507, Vol. 4, Cornell University / Electric Power Research Institute, Palo Alto, California, USA.

**Kulhawy F H, and Mayne P W. (1990).** "Manual on estimating soil properties for foundation design." EL-6800, Electric Power Research Institute, Palo Alto, California, USA.

- Kulhawy F H, and Phoon K K. (1993).** "Drilled shaft side resistance in clay soil to rock." *Proceedings Conference on Design and Performance of Deep Foundations: Piles and Piers in Soil and Soft Rock*, Reston, USA, pp. 172-183.
- Kulhawy F H, and Phoon K K. (2002).** "Observations on Geotechnical Reliability-Based Design Development in North America." *International Workshop on Foundation Design Codes and Soil Investigations in view of International Harmonisation and Performance Based Designs*, pp. 31-48.
- Lacasse S, and Ladd C C. (1973).** "Behavior of Embankments on New Liskeard Varved Clay." Department of Civil Engineering Research Report R72-16, Massachusetts Institute of Technology, Cambridge, Massachusetts, USA.
- Lee I K, White W, and Ingles O G. (1983).** *Geotechnical Engineering*, Pittman Publishing Inc, Massachusetts, USA.
- Li K S, and White W. (1987).** "Probabilistic Characterisation of Soil Profiles." Research Report No. 19, Australian Defence Force Academy, University of New South Wales, Canberra, ACT, Australia.
- Littlejohn G S, Cole K W, and Mellors T W. (1994).** "Without Site Investigation Ground is a Hazard." *Proceedings of the Institution on Engineers*, 102, pp. 72-78.
- Lord D W. (1987).** "Appropriate site investigations." *Reclaiming Contaminated Land*, T Cairney, ed., Blackie, Glasgow, Scotland, pp. 62-113.
- Lowe III J, and Zaccheo P F. (1991).** "Subsurface Exploration and Sampling." *Foundation Engineering Handbook*, H Fang, ed., Chapman Hall, New York, USA, pp. 1-71.
- Lumb P. (1966).** "The variability of natural soils." *Canadian Geotechnical Journal*, 3(2), pp. 74-97.
- Lumb P. (1970).** "Safety Factors and the Probability Distribution of Soil Strength." *Canadian Geotechnical Journal*, 7(3), pp. 225-242.
- Lumb P. (1974).** "Application of Statistics in Soil Mechanics." *Soil Mechanics - New Horizons*, I Lee, ed., Butterworth and Co (Publishers), London, England, pp. 44-111.
- Lunne T, Eidsmoen T, Gillespie D, and Howland J D. (1986).** "Laboratory and Field Evaluation of Cone Penetrometers." *Use of Insitu Tests in Geotechnical Engineering*, ASCE, ed., GSP No 6, Blacksburg, pp. 714-729.

**Lyamin A V, and Sloan S W. (2002a).** "Lower bound limit analysis using non-linear programming." *International Journal for Numerical Methods in Engineering*, 55, pp. 573-611.

**Lyamin A V, and Sloan S W. (2002b).** "Upper bound limit analysis using linear finite elements and nonlinear programming." *International Journal for Numerical and Analytical Methods in Geomechanics*, 26, pp. 181-216.

**MacDonald D H, and Skempton A W. (1955).** "A Survey of Comparisons between Calculated and Observed Settlements of Structures on Clay." *Conference on Correlation of Calculated and Observed Stresses and Displacements*, London, England, pp. 318-337.

**Marchetti S. (1980).** "In situ tests by flat dilatometer." *Journal of Geotechnical Engineering*, 106(3), pp. 299-321.

**Marchetti S, and Crapps D K. (1981).** "Flat Dilatometer Manual." Gainesville, Florida, USA.

**Matheron G. (1963).** "Principles of Geostatistics." *Economic Geology*, 58, pp. 1246-1266.

**Matheron G. (1965).** *Les Variables Regionalisees et leur Estimation*, Masson et Cie, Paris, France.

**Matheron G. (1971).** *The Theory of Regionalized Variables and Its Applications - Spatial Variabilities of Soil and Landforms*, Les Cahiers du Centre de Morphologie Mathematique 8, Fontainebleau.

**Mayne P W, and Poulos H G. (1999).** "Approximate Displacement Influence Factors for Elastic Shallow Foundations." *Journal of Geotechnical and Geoenvironmental Engineering*, 125(6), pp. 453-460.

**McBratney A B, Webster R, and Burgess T M. (1981).** "The design of optimal sampling schemes for local estimation and mapping of regionalized variables - I." *Computers and Geosciences*, 7, pp. 331-334.

**Meyerhof G G. (1951).** "The Ultimate Bearing Capacity of Foundations." *Geotechnique*, 2(4), pp. 301-332.

**Meyerhof G G. (1956).** "Penetration Tests and Bearing Capacity of Cohesionless Soils." *Journal of the Soil Mechanics and Foundations Division*, 82(SM1), pp. 1-19.

- Meyerhof G G. (1963).** "Some Recent Research on the Bearing Capacity of Foundations." *Canadian Geotechnical Journal*, 1(1), pp. 16-26.
- Meyerhof G G. (1974).** "General Report: Outside Europe." *1st European Symposium on Penetration Testing*, Stockholm, Sweden, pp. 40-48.
- Meyerhof G G. (1984).** "Safety Factors & Limit States Analysis in Geotechnical Engineering." *Canadian Geotechnical Journal*, 21(1), pp. 1-7.
- Moh Z C. (2004).** "Site Investigation and Geotechnical Failures." *The International Conference on Structural and Foundation Failures*, Singapore, pp. 58-71.
- Mortensen D. (1993).** "Safety Requirements for Foundation Structures Determined by Economical Considerations." *International Symposium on Limit State Design in Geotechnical Engineering*, Copenhagen, Denmark, pp. 683-686.
- National Research Council. (1984).** "Geotechnical Site Investigations for Underground Projects." US National Committee on Tunnelling Technology Vol. 1, National Academy Press, Washington, USA.
- Newmark N M. (1935).** "Simplified Computation of Vertical Pressures in Elastic Foundations." Circular No. 24, University of Illinois Engineering Experiment Station, Urbana, Illinois, USA.
- Olea R A. (1984).** "Sampling design optimization for spatial functions." *Journal of the International Association for Mathematical Geology*, 16, pp. 369-392.
- Orchant C J, Kulhawy F H, and Trautmann C H. (1988).** "Reliability-Based Foundation Design for Transmission Line Structures: Critical Evaluation of In-Situ Test Methods." Research Report 1493-2 EL-5507, Vol. 2, Cornell University / Electric Power Research Institute, Palo Alto, California, USA.
- Osterberg J O. (1989).** "Necessary Redundancy in Geotechnical Engineering." *Journal of Geotechnical Engineering*, 115(11), pp. 1513-1531.
- Parsons R L, and Frost J D. (2002).** "Evaluating Site Investigation Quality using GIS and Geostatistics." *Journal of Geotechnical and Geoenvironmental Engineering*, 128(6), pp. 451-461.
- Peacock W S, and Whyte I L. (1988).** "Site investigation practice." *Proceedings of the Institution of Civil Engineers Municipal Engineers*, 5, pp. 235-245.

- Perloff W H. (1975).** "Pressure distribution and settlement." *Foundation Engineering Handbook*, H Winterkorn and H Fang, eds., Van Nostrand Reinhold, New York, USA, pp. 148-196.
- Phoon K K, and Kulhawy F H. (1999a).** "Characterization of geotechnical variability." *Canadian Geotechnical Journal*, 36(4), pp. 612-624.
- Phoon K K, and Kulhawy F H. (1999b).** "Evaluation of geotechnical property variability." *Canadian Geotechnical Journal*, 36(4), pp. 625-639.
- Phoon K K, Kulhawy F H, and Grigoriu M D. (1995).** "Reliability Based Design of Foundations for Transmission Line Structures," PhD, Cornell University, Ithaca.
- Polshin D E, and Tokar R A. (1957).** "Maximum Allowable Non-Uniform Settlement of Structure." *4th International Conference on Structural Mechanics and Foundation Engineering*, pp. 402-405.
- Polyhedron Software. (2004).** <http://www.polyhedron.co.uk>
- Poulos H G. (1993).** "Settlement of bored pile groups." *BAP II*, pp. 103-117.
- Poulos H G. (2001).** "Pile Foundations." *Geotechnical and Geoenvironmental Engineering Handbook*, R Rowe, ed., Kluwer Academic Publishers, Boston, USA, pp. 261-304.
- Poulos H G, and Davis E H. (1980).** *Pile Foundation Analysis and Design*, Wiley, New York, USA.
- Randolph M F. (1994).** "Design methods for pile groups and piled rafts." *13th International Conference Soil Mechanics and Foundations Engineering*, pp. 61-82.
- Rawlinsons. (2004).** *Australian Construction Handbook 2004*, Rawlhouse Publishing Pty. Ltd., Perth, Australia.
- Riedel W. (1927).** "Beitrage zur Losung des ebenen Problems eines elastischen Korpers mittels der Airyschen Spannungsfunktion." *Zeitschrift fur Angewandte Mathematik und Mechanik*, 7(3), pp. 169-188.
- Righetti G, and Harrop Williams K. (1988).** "Finite Element Analysis of Random Soil Media." *Journal of Geotechnical Engineering*, 114(1), pp. 59-74.
- Rosenblueth E. (1975).** "Point estimates for probability methods." *Proceedings, National Academy of Science*, 72(10), pp. 3812-3814.



- Schmertmann J H. (1970).** "Static Cone to Compute Static Settlement Over Sand." *Journal of the Soil Mechanics and Foundations Division*, 96(SM3), pp. 1011-1043.
- Schmertmann J H, Hartmann J P, and Brown P R. (1978).** "Improved Strain Influence Factor Diagrams." *Journal of the Geotechnical Engineering Division*, 104(GT8), pp. 1131-1135.
- Seycek J. (1991).** "Settlement calculation limited to actual deformation zone." *10th European Conference on Soil Mechanics and Foundation Engineering*, Florence, Italy, pp. 543-548.
- Simon P A, and Briaud J L. (1996).** "The National Geotechnical Experimentation Sites at Texas A&M University: Clay and Sand Soil Data in Electronic Form." NGES-TAMU 006, Texas A&M University, Civil Engineering, USA.
- Simpson B, Pappin J W, and Croft D D. (1981).** "An Approach to Limit State Calculations in Geotechnics." *Ground Engineering*, 14(6), pp. 21-28.
- Site Investigation Steering Group. (1993).** *Site investigation in construction*, Thomas Telford Services Ltd., London, England.
- Small J C. (2001).** "Shallow Foundations." *Geotechnical and Geoenvironmental Engineering Handbook*, R Rowe, ed., Kluwer Academic Publishers, Boston, USA, pp. 223-260.
- Smith I M, and Griffiths D V. (2004).** *Programming the Finite Element Method*, John Wiley & Sons Ltd, West Sussex, England.
- Smith M A, and Ellis A C. (1986).** "An investigation into methods used to assess gas works sites for reclamation." *Reclamation and Revegetation Research*, 4, pp. 183-209.
- Snedecor G W, and Cochran W G. (1980).** *Statistical Methods*, The Iowa State University Press, Ames, USA.
- Snir M, Otto S W, Huss-Lederman S, Walker D W, and Dongarra J. (1996).** *MPI: The Complete Reference*, The MIT Press, Cambridge, USA.
- Sokolovskii V V. (1965).** *Statics of Granular Material*, Pergamon Press, New York, USA.
- Souliè M, Montes P, and Silvestri V. (1990).** "Modelling spatial variability of soil properties." *Canadian Geotechnical Journal*, 27, pp. 617-630.

**Sowers G F. (1962).** "Shallow Foundations." Foundation Engineering, G A Leonards, ed., McGraw Hill, New York, USA, pp.

**Spry M J, Kulhawy F H, and Grigoriu M D. (1988).** "Reliability-Based Foundation Design for Transmission Line Structures: Geotechnical Site Characterization Strategy." Research Report 1493-1 EL-5507, Vol. 1, Cornell University / Electric Power Research Institute, Palo Alto, California, USA.

**Stas C V, and Kulhawy F H. (1984).** "Critical Evaluation of Design Methods for Foundations under Axial Uplift and Compression Loading." EL-3771, Electric Power Research Institute, Cornell University, USA.

**Sudicky E A. (1986).** "A natural gradient experiment on solute transport in a sand aquifer: Spatial variability of hydraulic conductivity and its role in the dispersion process." *Water Resources Research*, 22(13), pp. 2069-2083.

**Swiger W F. (1974).** "Evaluation of Soil Moduli." *6th ASCE Specialty Conference on Analysis and Design in Geotechnical Engineering*, Austin, USA, pp. 79-92.

**Tabba M M, and Yong R N. (1981).** "Mapping and Predicting Soil Properties: Theory." *Journal of Engineering Mechanics*, 107(EM5), pp. 773-793.

**Taylor D W. (1948).** *Fundamentals of Soil Mechanics*, John Wiley and Sons Inc., New York, USA.

**Temple M W B, and Stukhart G. (1987).** "Cost Effectiveness of Geotechnical Investigations." *Journal of Management in Engineering*, 3(1), pp. 8-19.

**Terzaghi K. (1943).** *Theoretical Soil Mechanics*, John Wiley and Sons Inc., New York, USA.

**Terzaghi K, and Peck R B. (1967).** *Soil Mechanics in Engineering Practice*, John Wiley, New York, USA.

**Terzaghi K, and Peck R B. (1968).** *Soil Mechanics in Engineering Practice*, John Wiley and Sons, New York, USA.

**Thompson S K. (2002).** *Sampling*, John Wiley & Sons, New York, USA.

**Timoshenko S, and Goodier J N. (1951).** *Theory of Elasticity*, McGraw-Hill, New York, USA.

- Tomlinson M J. (1971).** "Some Effects of Pile Driving on Skin Friction." *Conference on Behaviour of Piles*, London, England, pp. 107-114.
- Tomlinson M J. (1986).** *Foundation Design and Construction*, Longman, Harlow, England.
- Trochanis A M, Bielak J, and Christiano P. (1991).** "Three-dimensional non-linear study of piles." *Journal of Geotechnical Engineering*, 117(3), pp. 429-447.
- Tsai Y C, and Frost J D. (1999).** "Using geographic information system and knowledge base system technology for real-time planning of site characterization activities." *Canadian Geotechnical Journal*, 36(2), pp. 300-312.
- Tschebotarioff G P. (1973).** *Foundations, Retaining and Earth Structures*, McGraw-Hill, New York, USA.
- Tumay M T. (1998).** "In Situ Testing at the National Geotechnical Experimentation Sites (Phase 2)." Federal Highway Administration Contract No. DTFH61-97-P-00161, Louisiana Transportation Research Centre, Louisiana State University, Baton Rouge, USA.
- United States Army Corp of Engineers. (1990).** "Settlement Analysis." Engineering and Design, Washington DC, USA.
- Vanmarcke E H. (1977a).** "Probabilistic Modeling of Soil Profiles." *Journal of the Geotechnical Engineering Division*, 103(GT11), pp. 1227-1246.
- Vanmarcke E H. (1977b).** "Reliability of Earth Slopes." *Journal of the Geotechnical Engineering Division*, 103(GT11), pp. 1247-1265.
- Vanmarcke E H. (1982).** "Developments in Random Field Modelling." *Nuclear Engineering and Design*, 71(3), pp. 325-327.
- Vanmarcke E H. (1983).** *Random Fields: Analysis and Synthesis*, The MIT Press, Cambridge, Massachusetts, USA.
- Vanmarcke E H, Shinozuka M, Nakagiri S, Schueller G I, and Grigoriu M D. (1986).** "Random Fields and Stochastic Finite Elements." *Structural Safety*, 3, pp. 143-166.
- Vesic A S. (1973).** "Analysis of Ultimate Loads of Shallow Foundations." *Journal of the Soil Mechanics and Foundations Division*, 99(SM1), pp. 45-73.
- Vick S G. (1992).** "Risk in Geotechnical Practice." *Geotechnical News*, 10(1), pp. 55-57.

**Vijayvergiya V N, and Focht Jnr. J A. (1972).** "A New Way to Predict Capacity of Piles in Clay." OTC Paper 1718, 4th Offshore Technology Conference, Houston, USA.

**Voss R. (1984).** "Random Fractal Forgeries - From Mountains to Music." *Science and Uncertainty*, Science Reviews Ltd., Middlesex, England, pp. 69-85.

**Wahls H. (1981).** "Tolerable Settlements of Buildings." *Journal of the Geotechnical Engineering Division*, 107(ET11), pp. 1489-1504.

**Warner R F, Rangan B V, Hall A S, and Faulkes K A. (1998).** *Concrete Structures*, Addison Wesley Longman Pty. Ltd., South Melbourne, Australia.

**Waterhouse P S. (1980).** "The sampling and analysis of polluted sites." *Reclamation of Contaminated Land*, Society of Chemical Industry, Eastbourne, England.

**Webb D L, and Milvill A L. (1971).** "Discussion: Static Cone to Compute Static Settlement over Sand." *Journal of Soil Mechanics and Foundations Division, ASCE*, 97(SM 3), pp. 587-589.

**Wennerstrand J. (1979).** "Comparison of predicted settlements for a fine sand." *Design Parameters in Geotechnical Engineering*, Brighton, England, pp. 295-298.

**Westergaard H M. (1938).** "A Problem of Elasticity Suggested by a Problem in Soil Mechanics: Soft Material Reinforced by Numerous Strong Horizontal Sheets." Contributions to the Mechanics of Solids - Stephen Timoshenko 60th Anniversary Volume, Macmillan, New York, USA.

**Whitman R V. (1984).** "Evaluating Calculated Risk in Geotechnical Engineering." *Journal of Geotechnical Engineering*, 110(2), pp. 145-188.

**Whitman R V. (2000).** "Organising and Evaluating Uncertainty in Geotechnical Engineering." *Journal of Geotechnical and Geoenvironmental Engineering*, 126(7), pp. 583-593.

**Whyte I L. (1995).** "The Financial Benefit from Site Investigation Strategy." *Ground Engineering*, 10, pp. 33-36.

**Wieghardt K. (1906).** "Über einen Grenzübergang der Elastizitätslehre und seine Anwendung auf sie Statik hochgradig statisch unbestimmter Fachwerke." *Verhandlungen des Vereins z. Beförderung des Gewerbefleißes, Abhandlungen*, 85, pp. 139-176.

**Wiesner T. (1999).** "Site Characterisation." *Australian Geomechanics*, 34(4), pp. 41-57.

**Wolff T F. (1996).** "Probabilistic slope stability in theory and practice." *Uncertainty in the Geologic Environment*, ASCE, Madison, USA, pp. 419-433.

**Wu T H, Kjekstad O, Lee I, and Lacasse S. (1989).** "Reliability analysis of foundation stability for gravity platforms in the North Sea." *Canadian Geotechnical Journal*, 26, pp. 359-368.

**Yfantis E A, Flatman G T, and Behar J V. (1987).** "Efficiency of kriging estimation for square, triangular and hexagonal grids." *Mathematical Geology*, 19, pp. 183-205.



## **APPENDICES**





## **Appendix A Settlement Analysis**

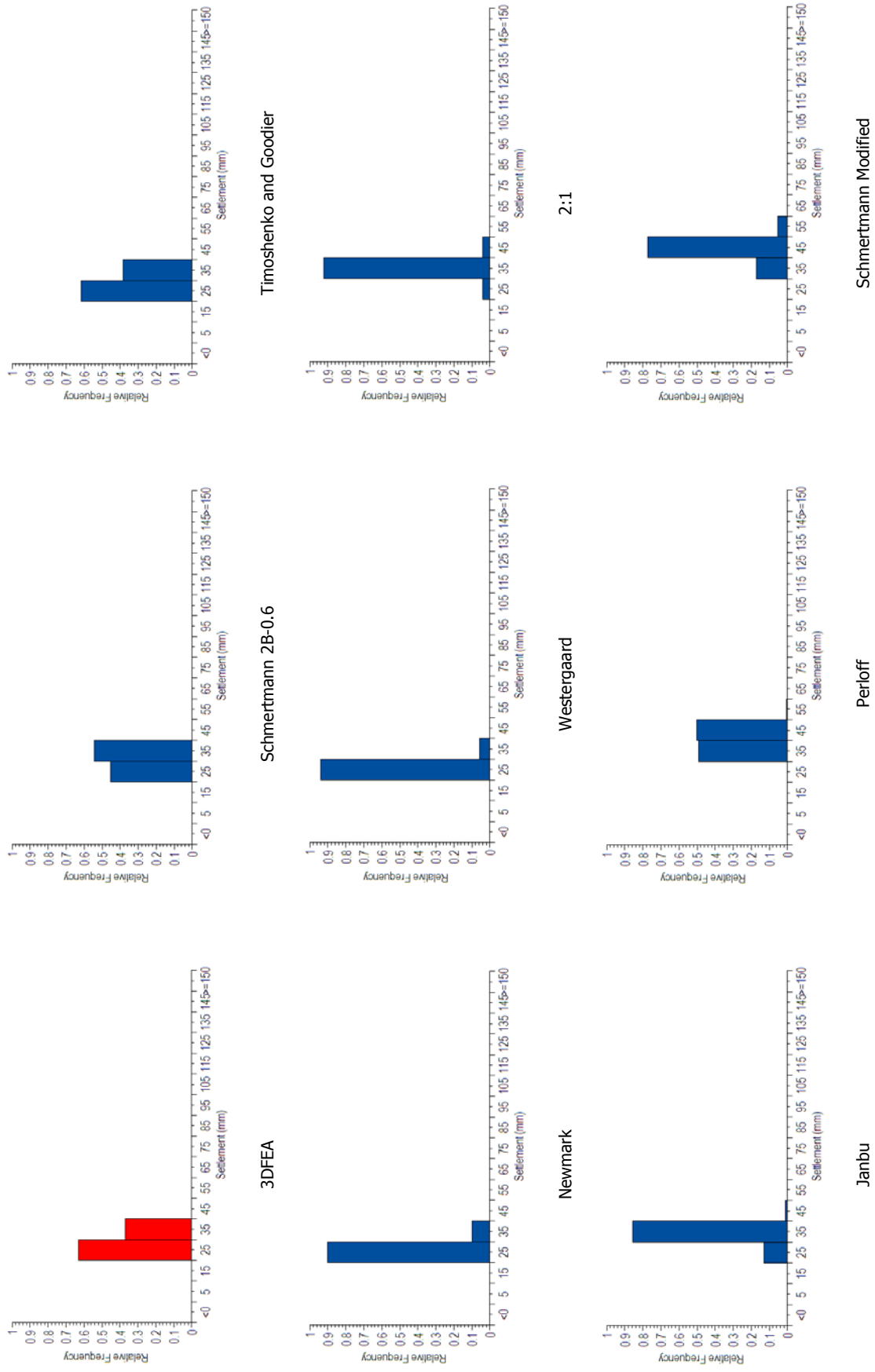


**Figure A-1** Settlement distributions of different settlement prediction techniques for a soil with a COV of 10% and SOF of 8 m

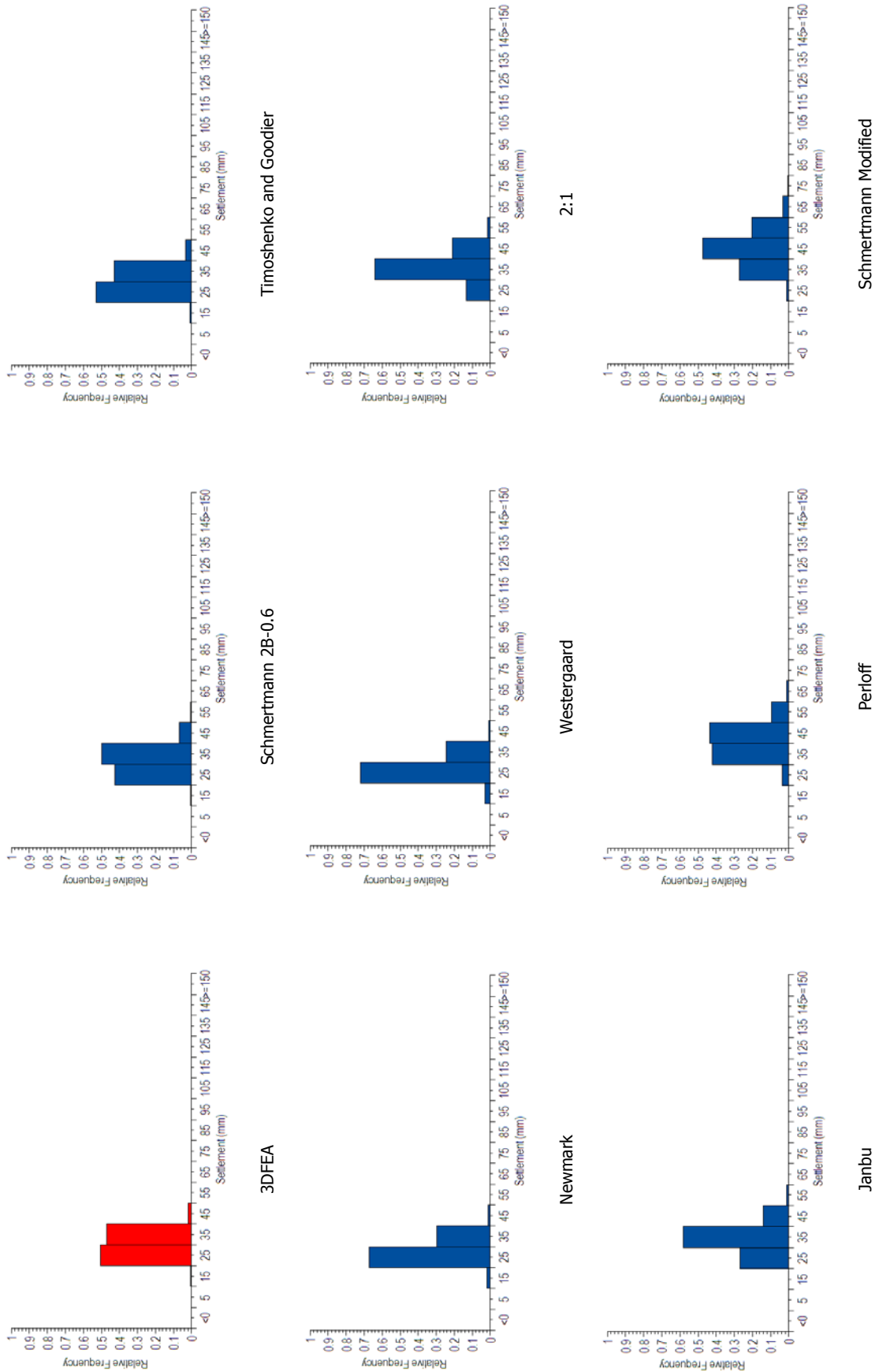


**Figure A-2 Settlement distributions of different settlement prediction techniques for a soil with a COV of 20% and SOF of 8 m**

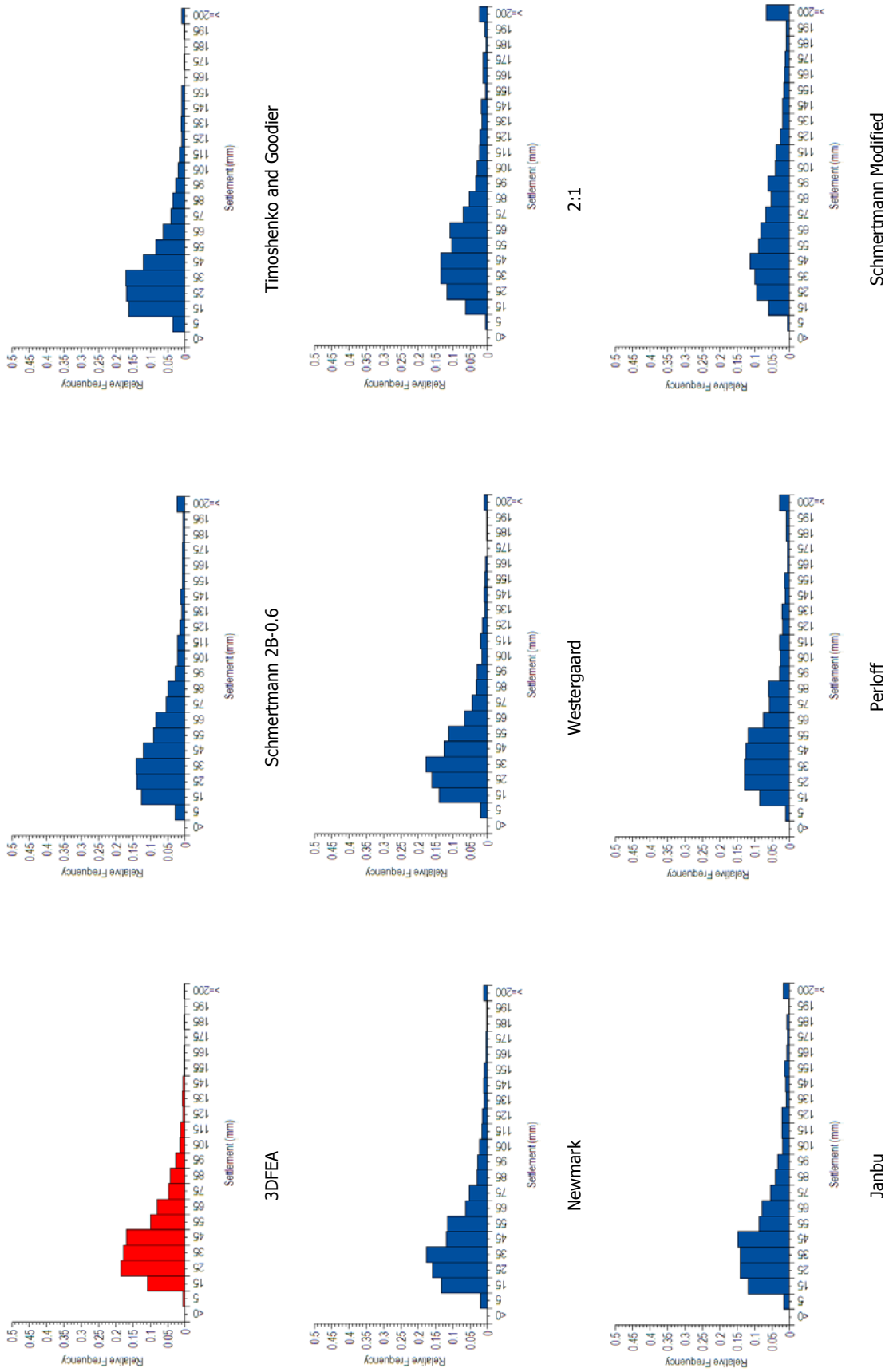


Figure A-3 Settlement distributions of different settlement prediction techniques for a soil with a COV of 100% and SOF of 8 m

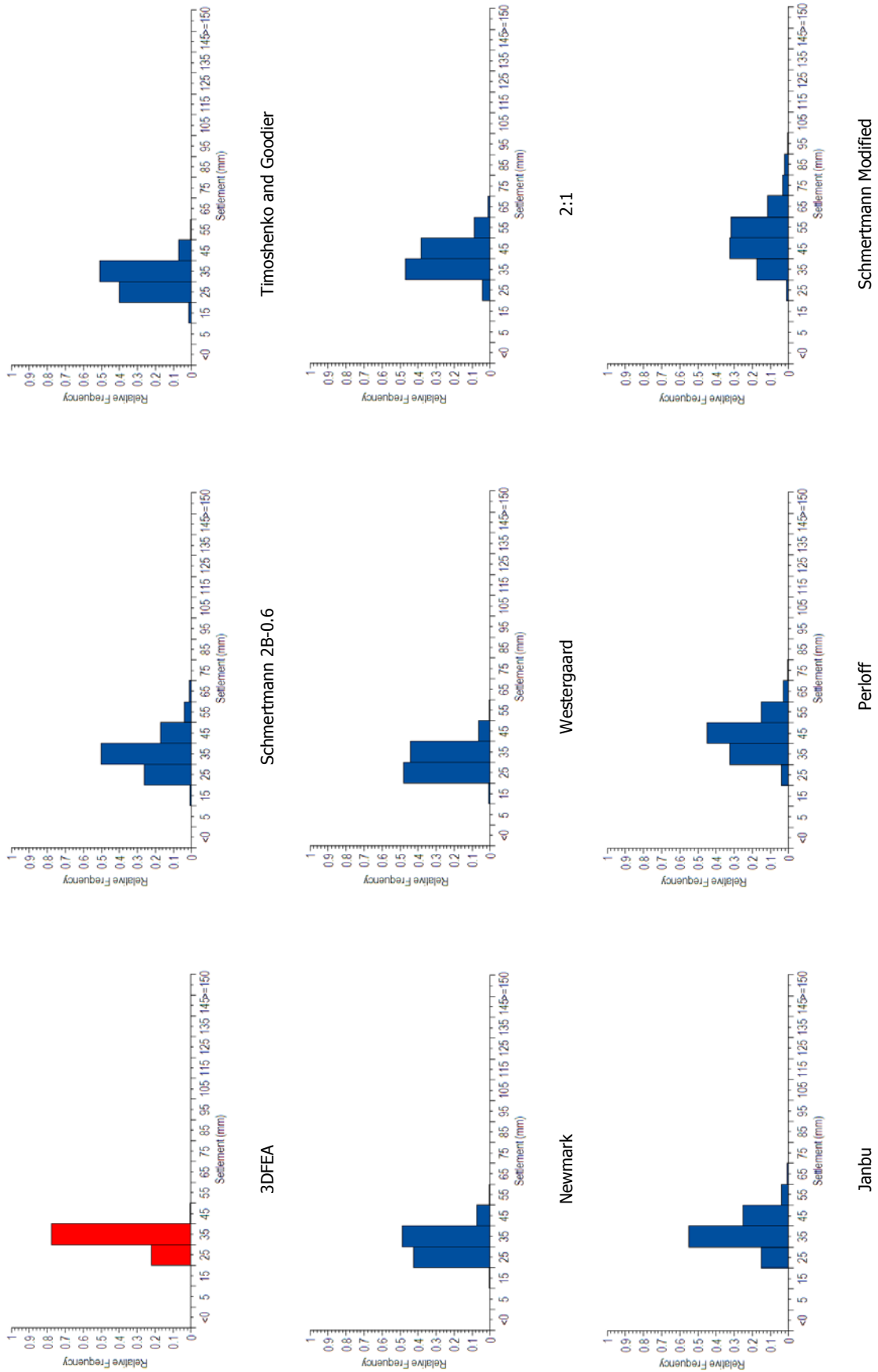
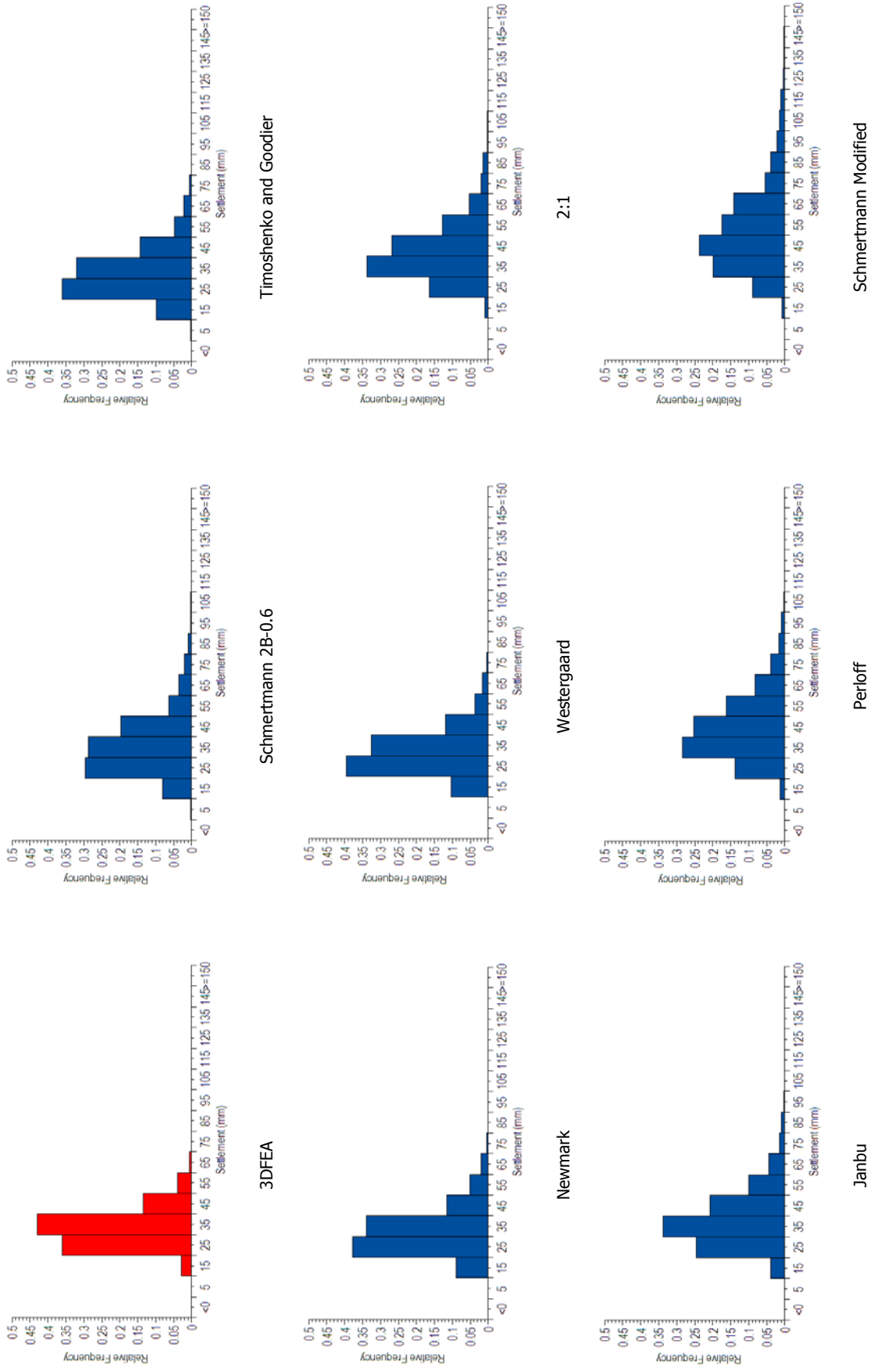


Figure A-4 Settlement distributions of different settlement prediction techniques for a soil with a COV of 50% and SOF of 1 m



**Figure A-5** Settlement distributions of different settlement prediction techniques for a soil with a COV of 50% and SOF of 4 m

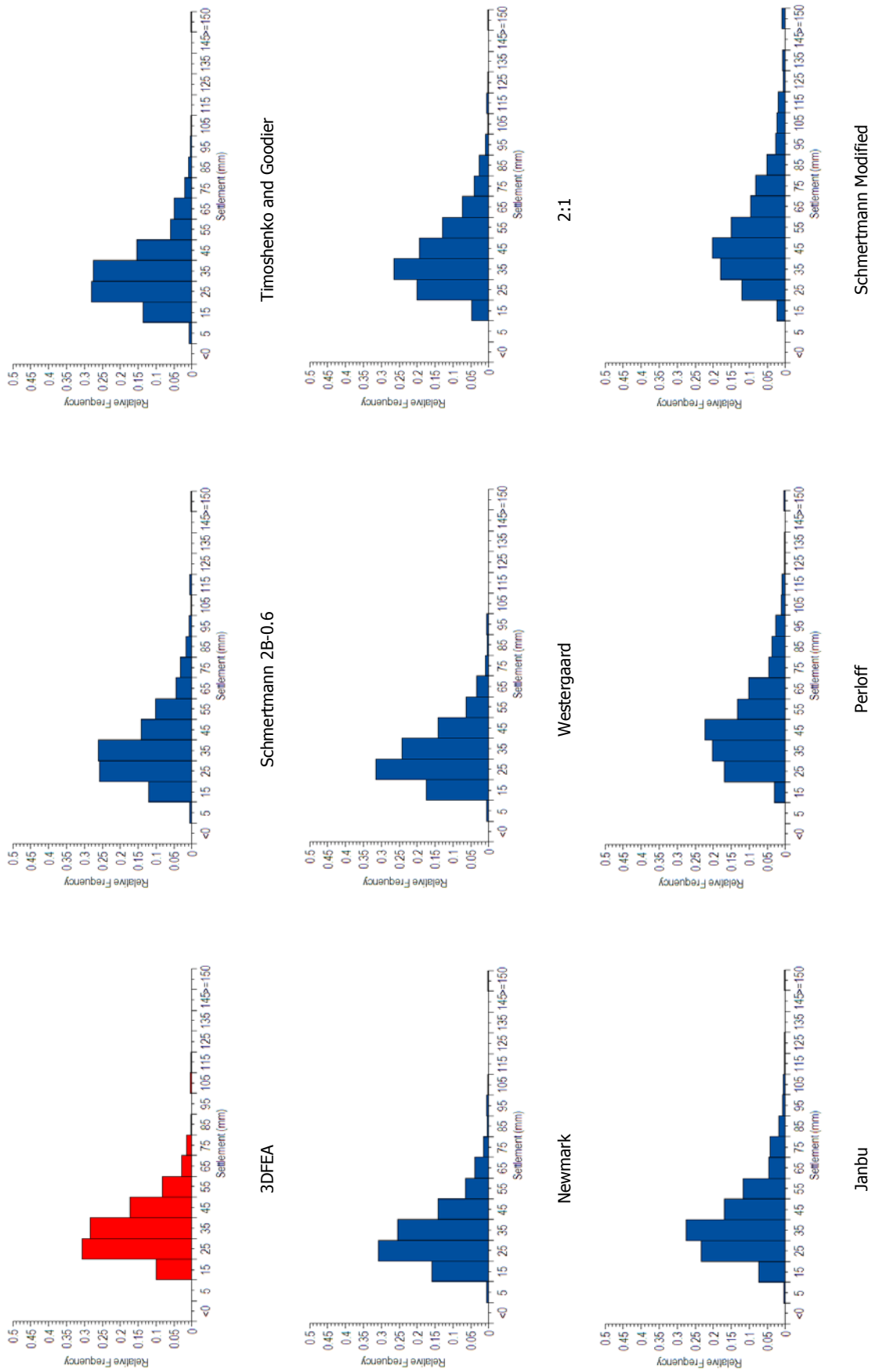
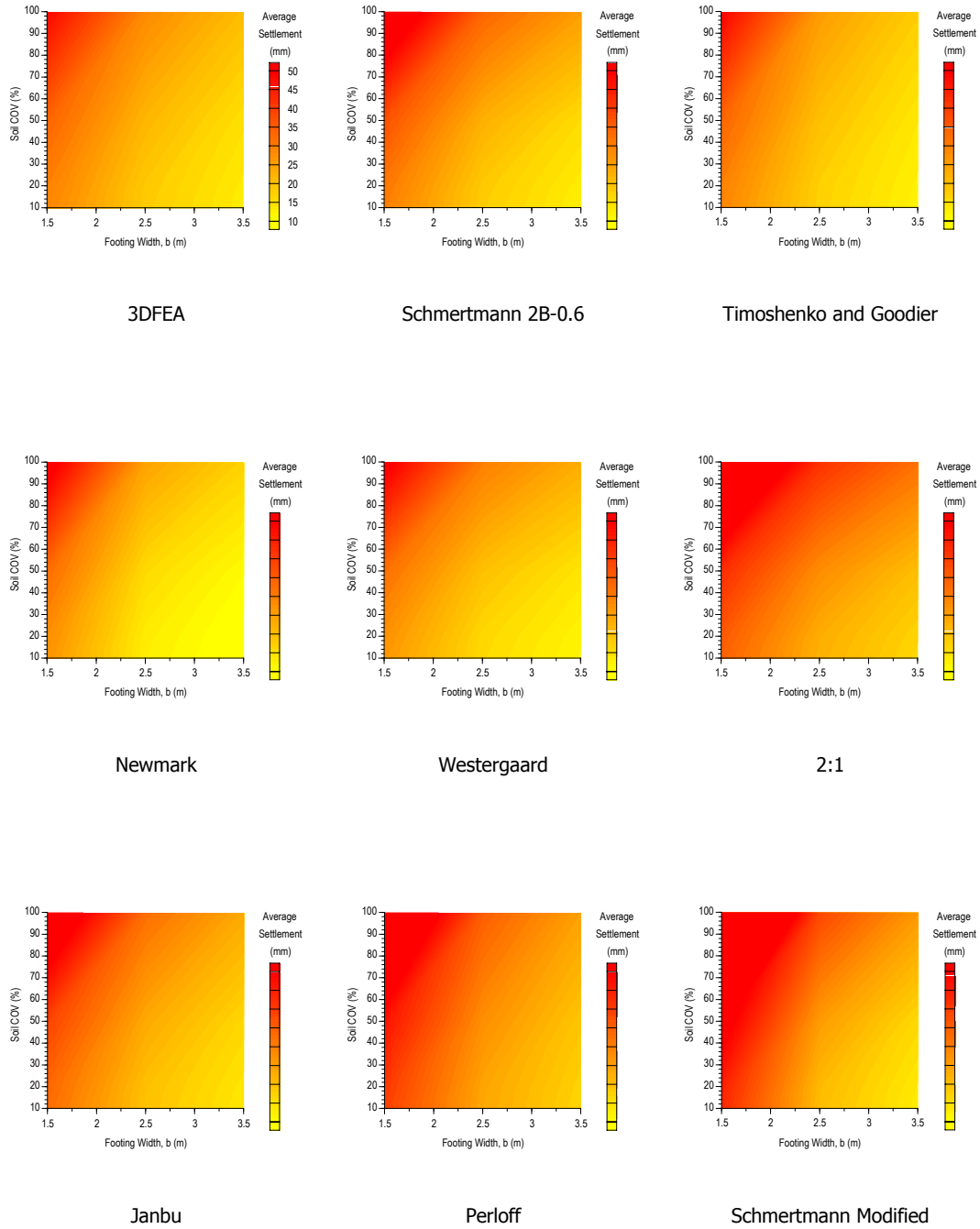
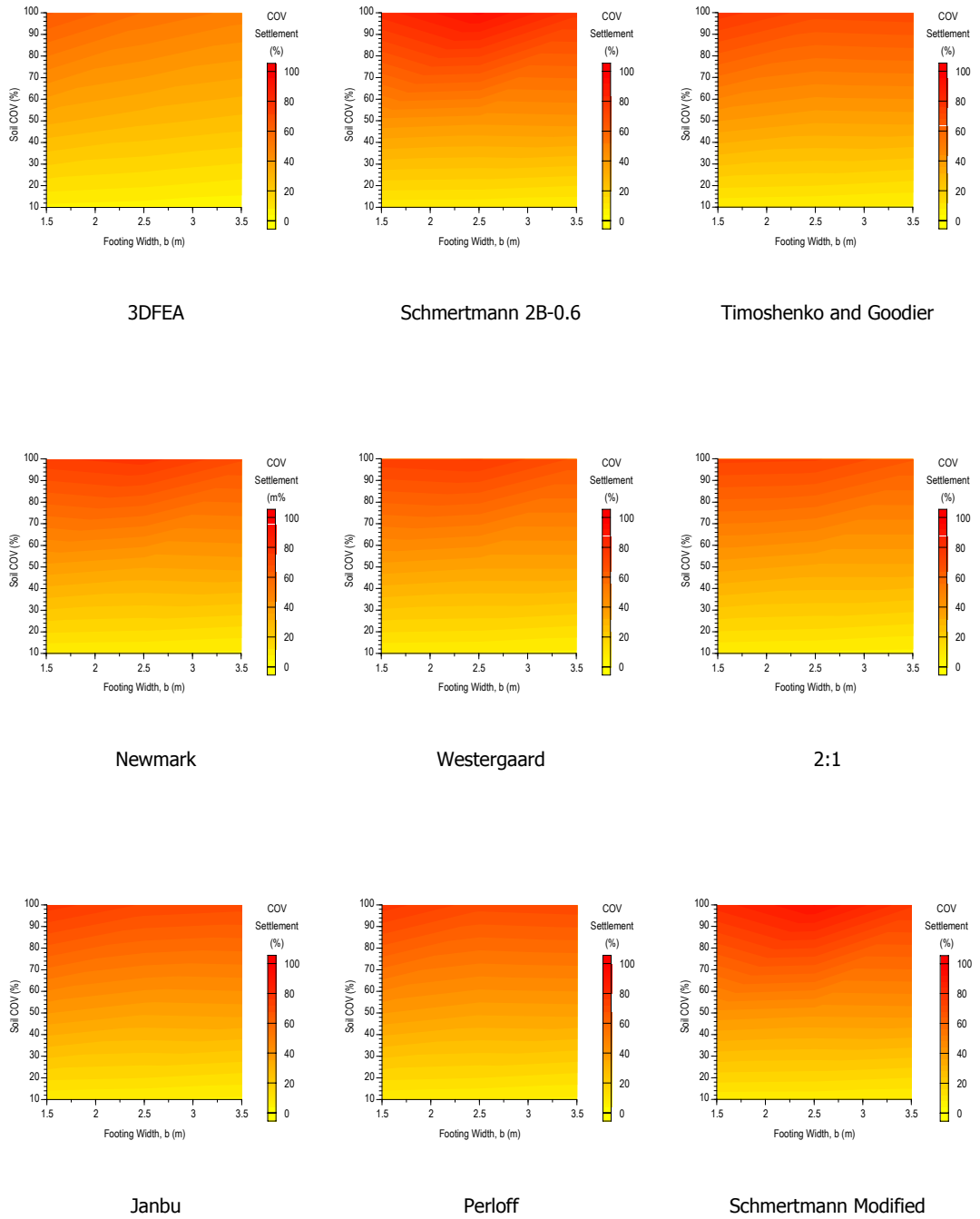


Figure A-6 Settlement distributions of different settlement prediction techniques for a soil with a COV of 50% and SOF of 16 m



**Figure A-7 Effect of increasing the soil COV (SOF of 8 m) on the average settlement of a single pad footing using different prediction techniques**





**Figure A-8 Effect of increasing the soil COV (SOF of 8 m) on the settlement COV of a single pad footing using different prediction techniques**

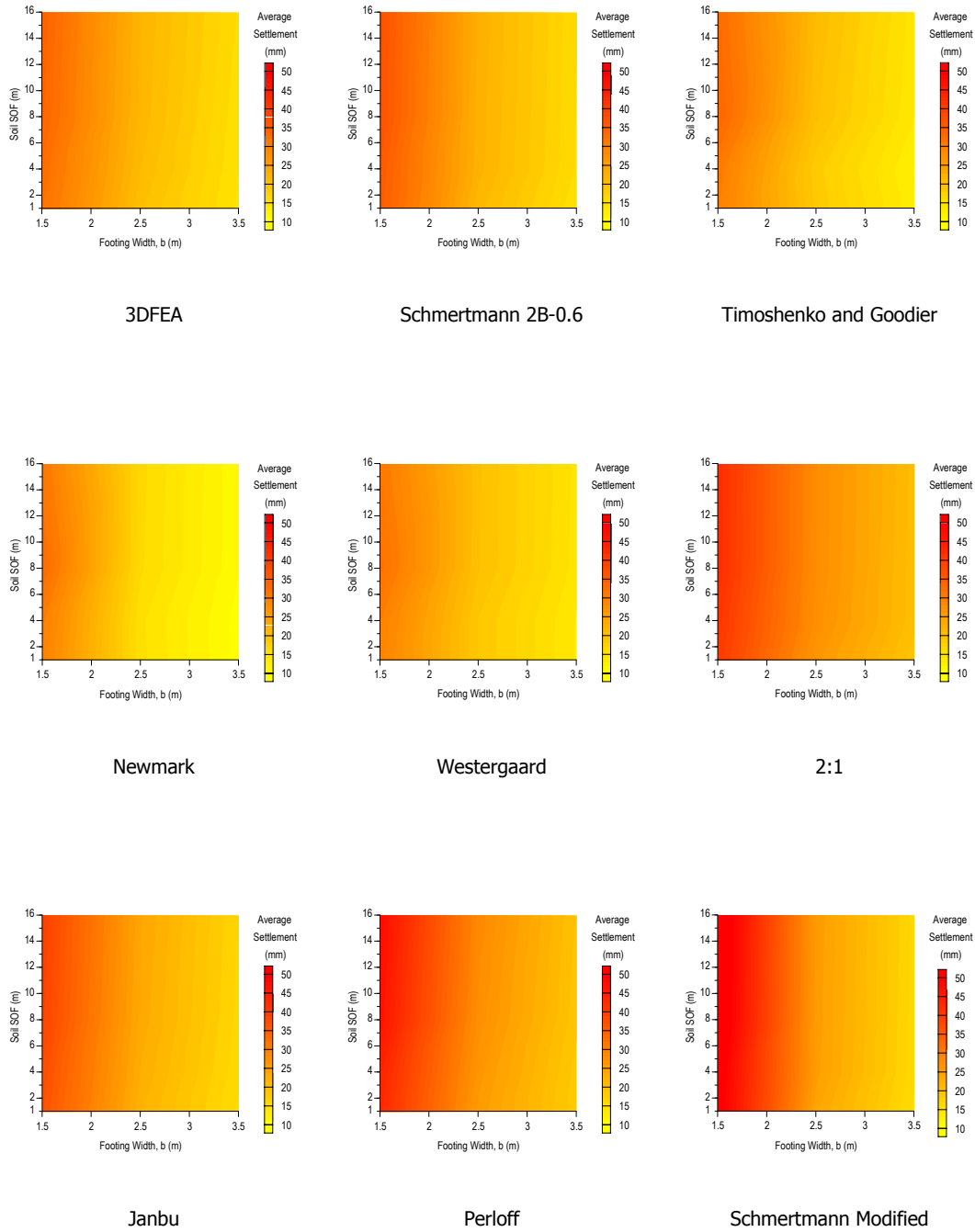


**Figure A-9 Effect of increasing the soil SOF (COV of 50%) on the average settlement of a single pad footing using different prediction techniques**

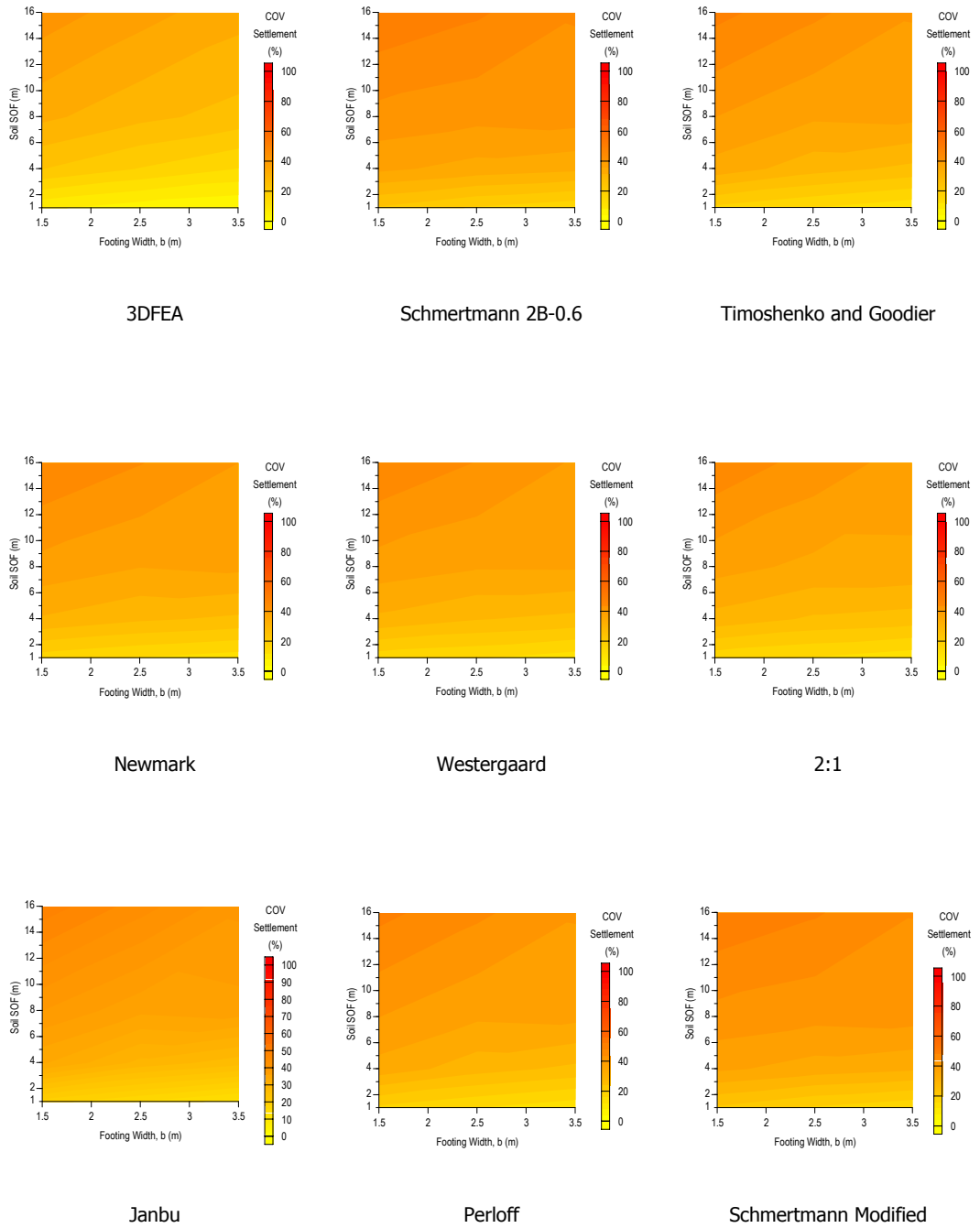


**Figure A-10 Effect of increasing the soil SOF (COV of 50%) on the settlement COV of a single pad footing using different prediction techniques**



## **Appendix B Average and Variance of Foundation Design Results**

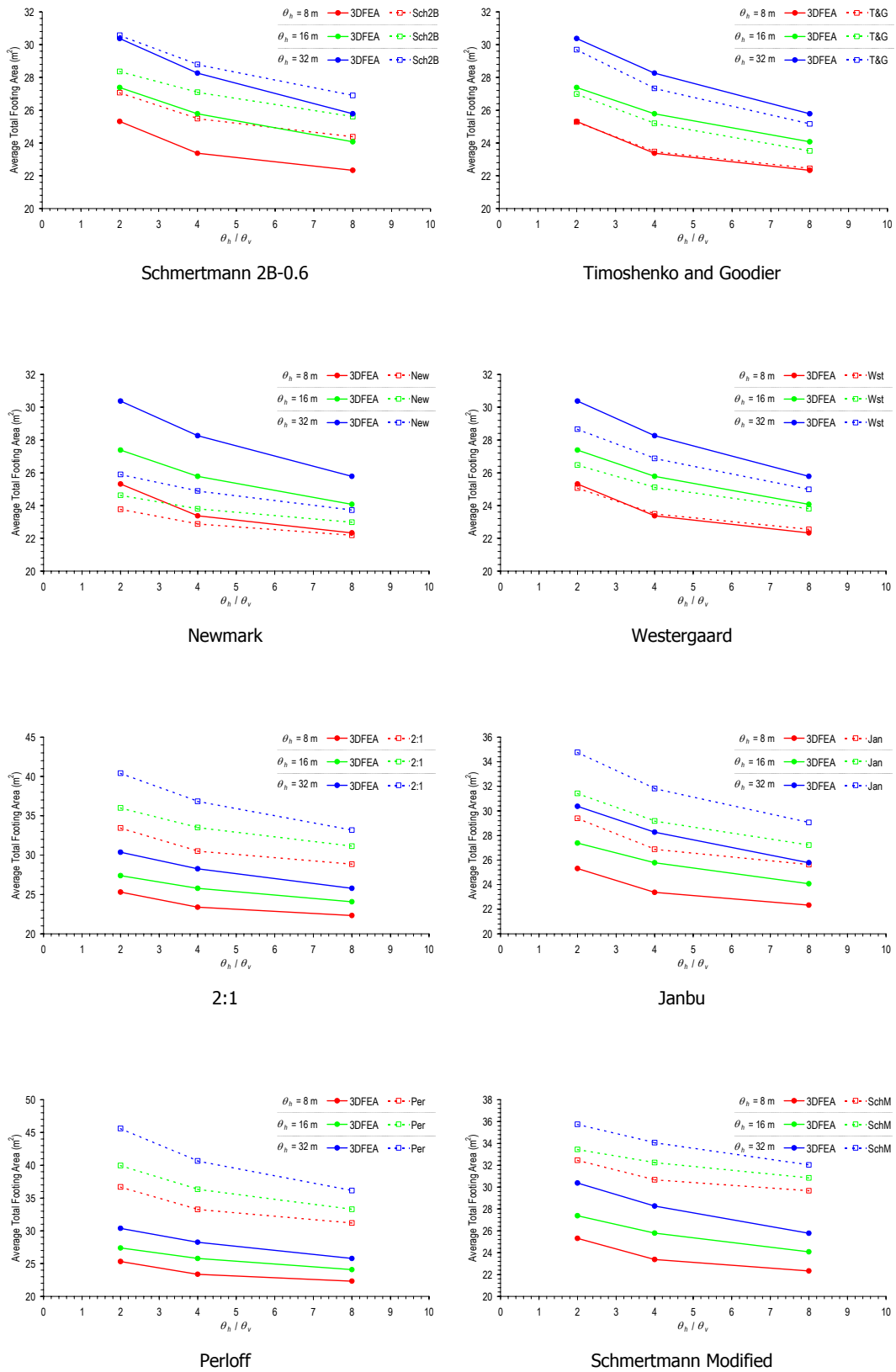
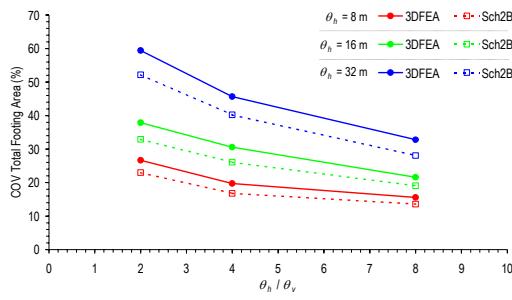
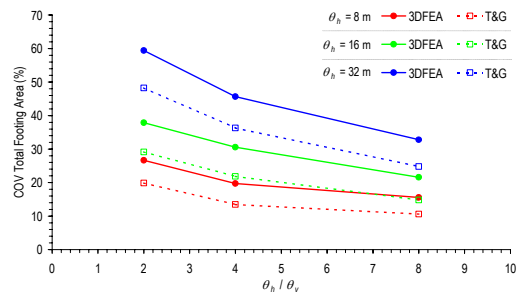


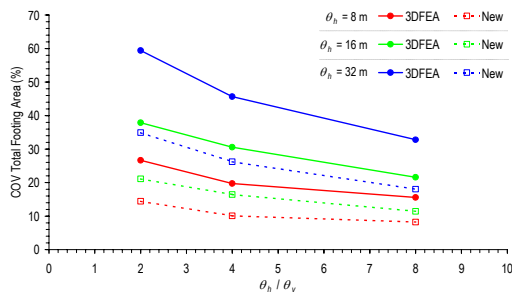
**Figure B-1 Effect of increasing the horizontal to vertical SOF ratio (COV of 50%) on the average total footing area, of the 9-pad system, designed using 3DFEA and different prediction techniques**



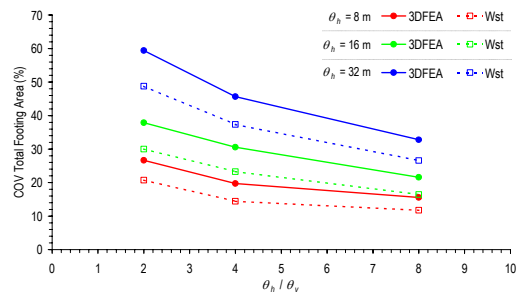
Schmertmann 2B-0.6



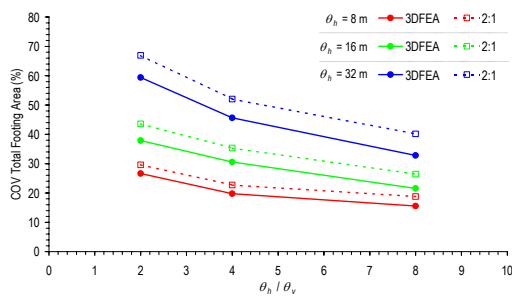
Timoshenko and Goodier



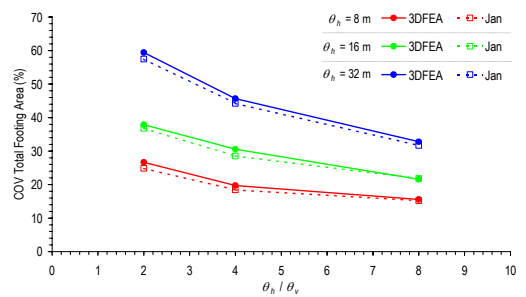
Newmark



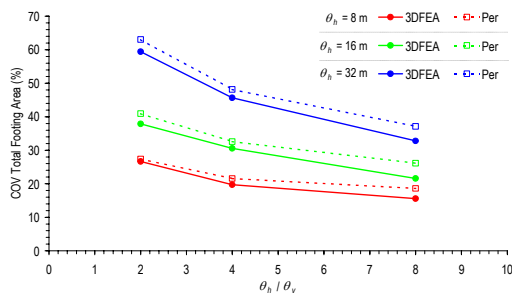
Westergaard



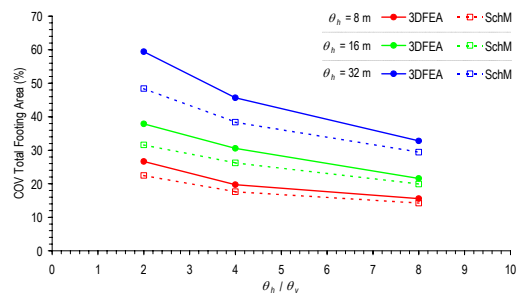
2:1



Janbu



Perloff



Schmertmann Modified

Figure B-2 Effect of increasing the horizontal to vertical SOF ratio (COV of 50%) on the COV of total footing area, of the 9-pad system, designed using 3DFEA and different prediction techniques

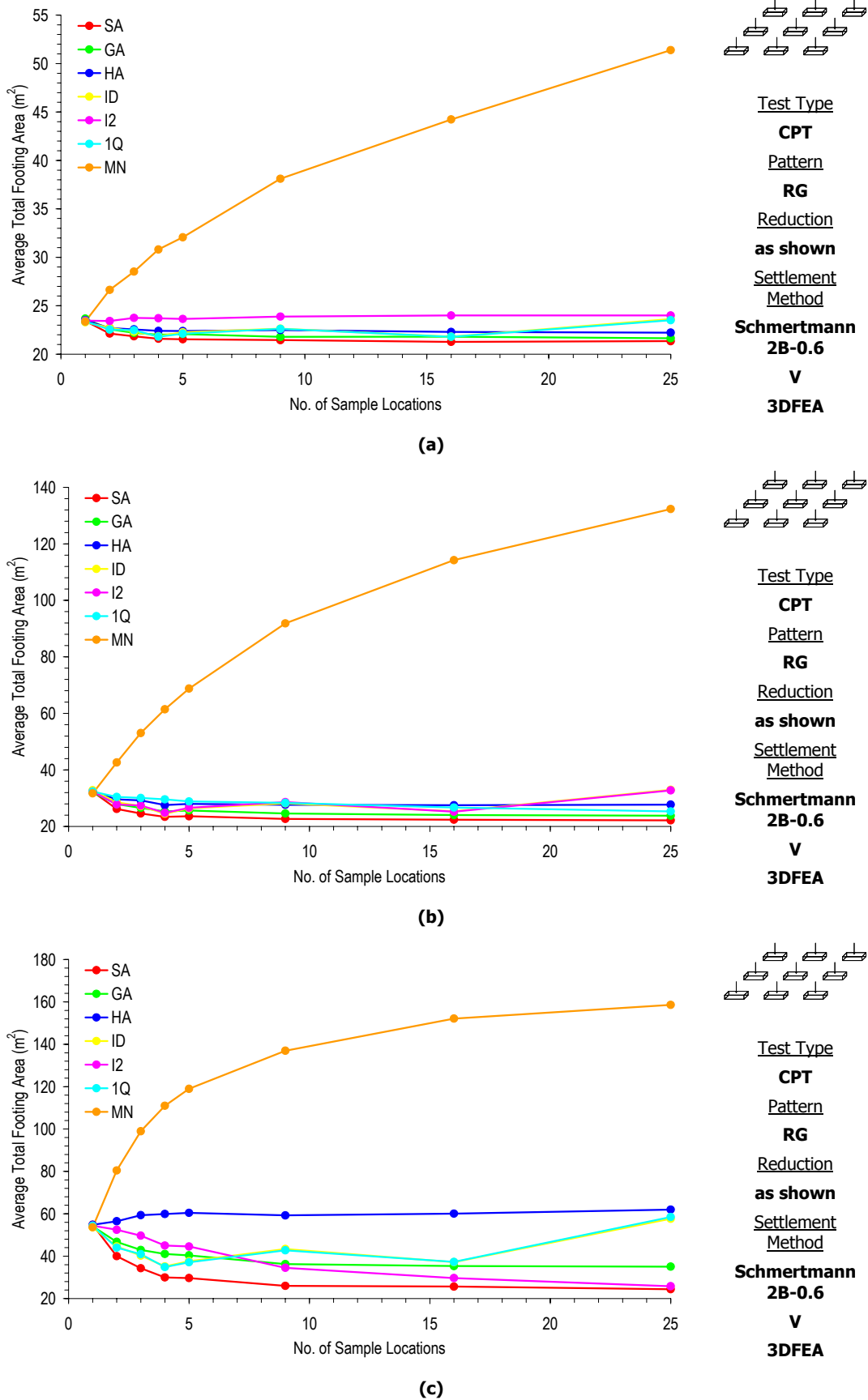
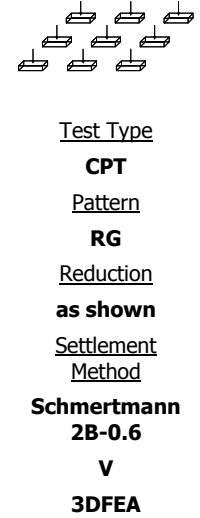
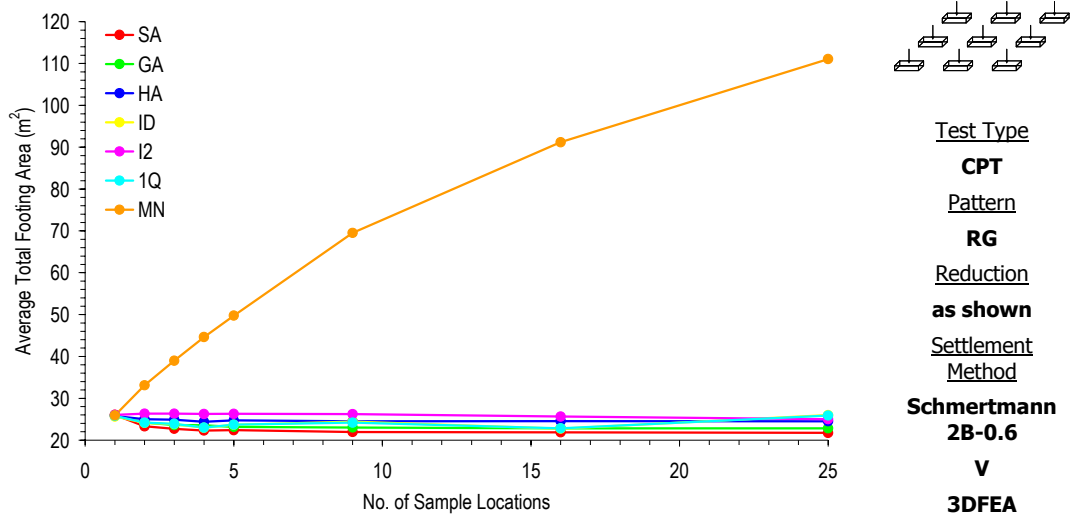
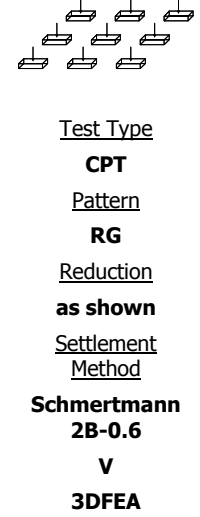
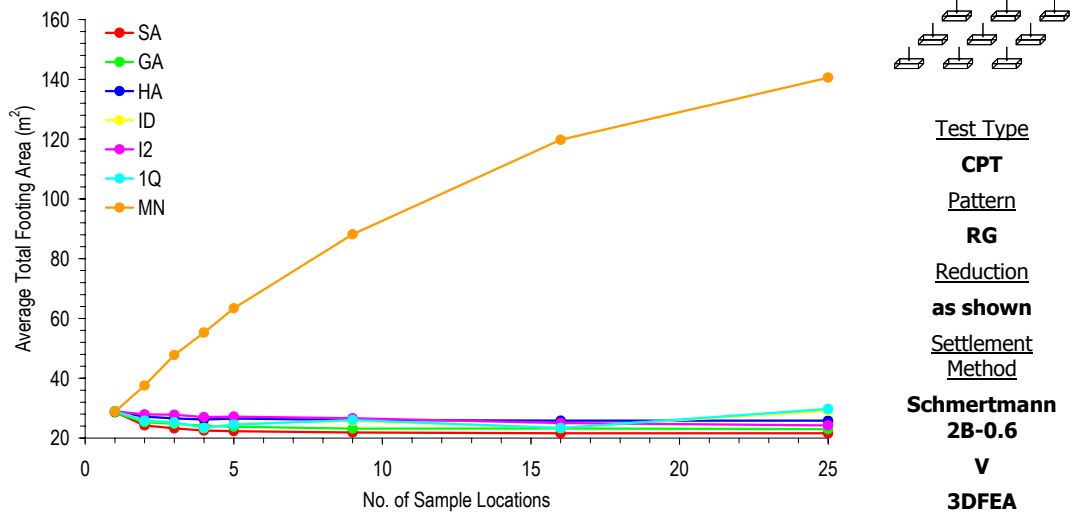


Figure B-3 Effect of increased sampling using different reduction techniques on the average total footing area, for a soil SOF of 8 m and COV of (a) 20%, (b) 50% and (c) 100%

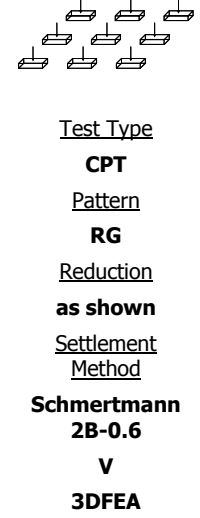
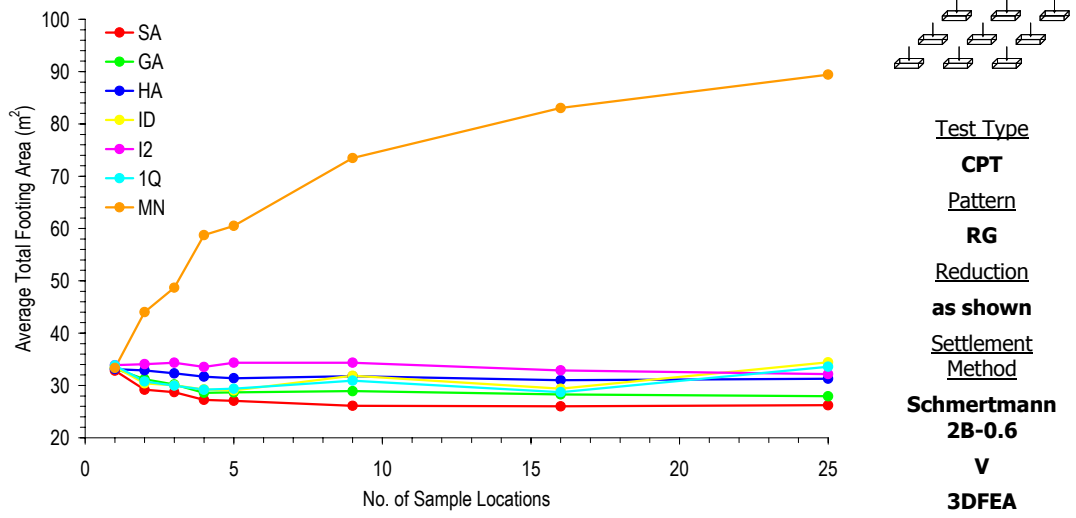




(a)

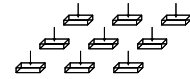
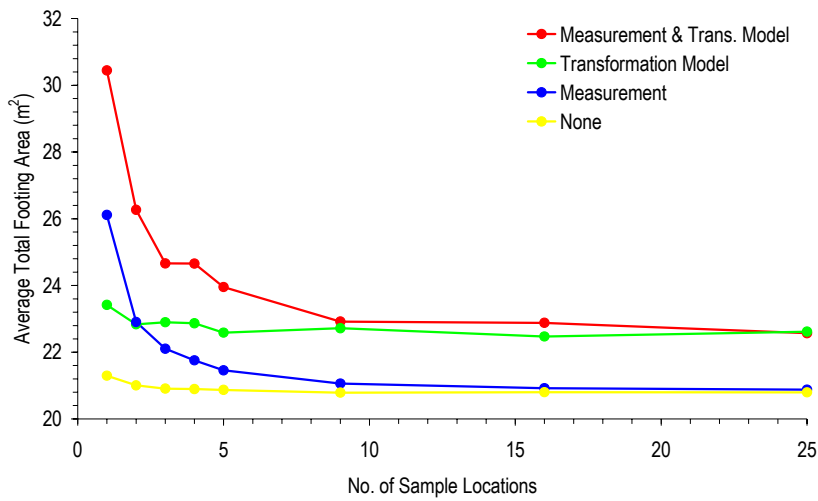


(b)



(c)

**Figure B-4** Effect of increased sampling using different reduction techniques on the average total footing area, for a soil COV of 50% and SOF of (a) 1 m, (b) 4 m and (c) 32 m



Test Type

SPT

Pattern

RG

Reduction

SA

Settlement

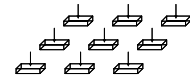
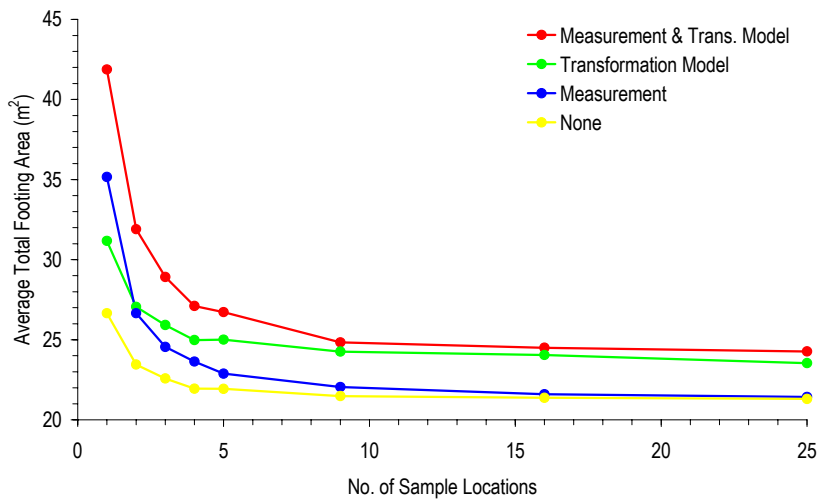
Method

Schmertmann  
2B-0.6

V

3DFEA

(a)



Test Type

SPT

Pattern

RG

Reduction

SA

Settlement

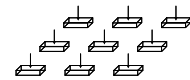
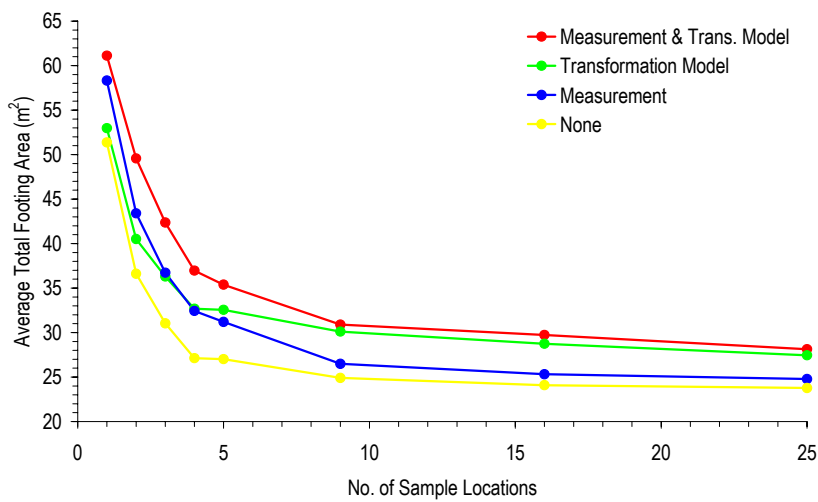
Method

Schmertmann  
2B-0.6

V

3DFEA

(b)



Test Type

SPT

Pattern

RG

Reduction

SA

Settlement

Method

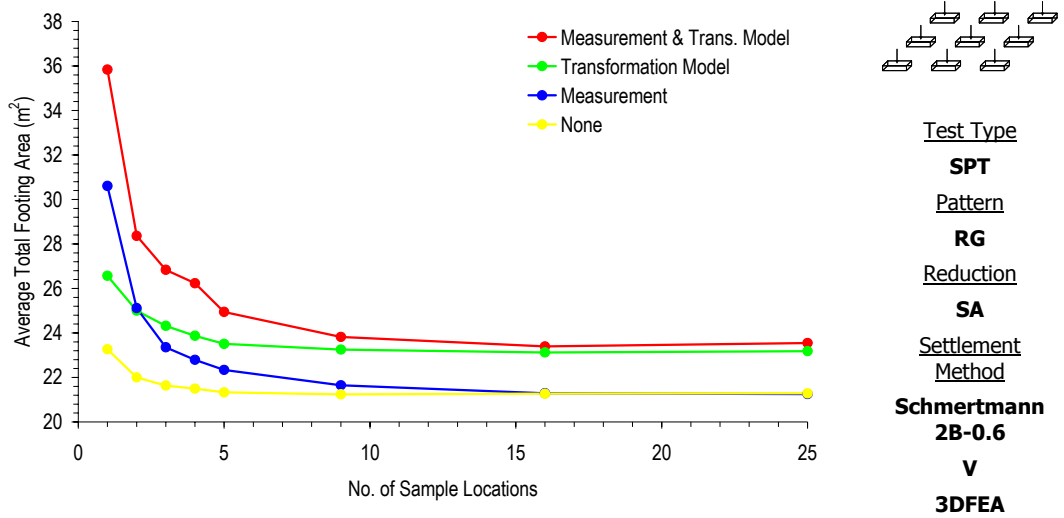
Schmertmann  
2B-0.6

V

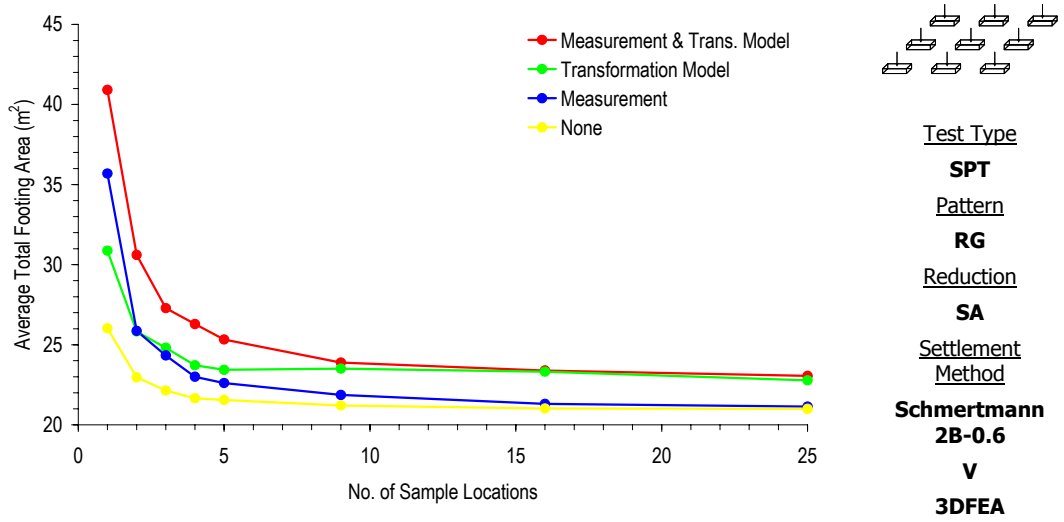
3DFEA

(c)

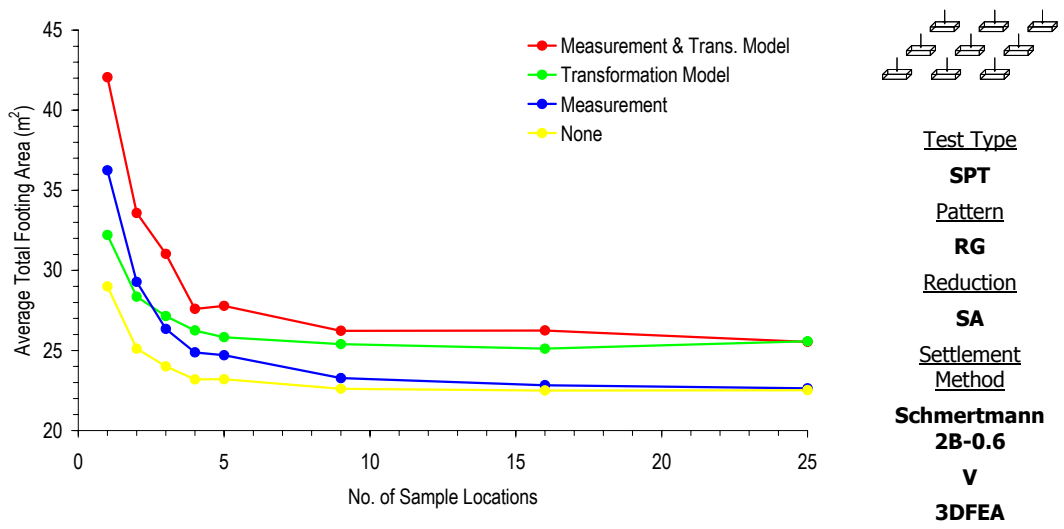
**Figure B-5 Effect of increased sampling and the inclusion of measurement and transformation model errors of the SPT on the average total footing area, for a soil SOF of 8 m and COV of (a) 20%, (b) 50% and (c) 100%**



(a)

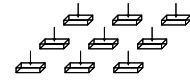
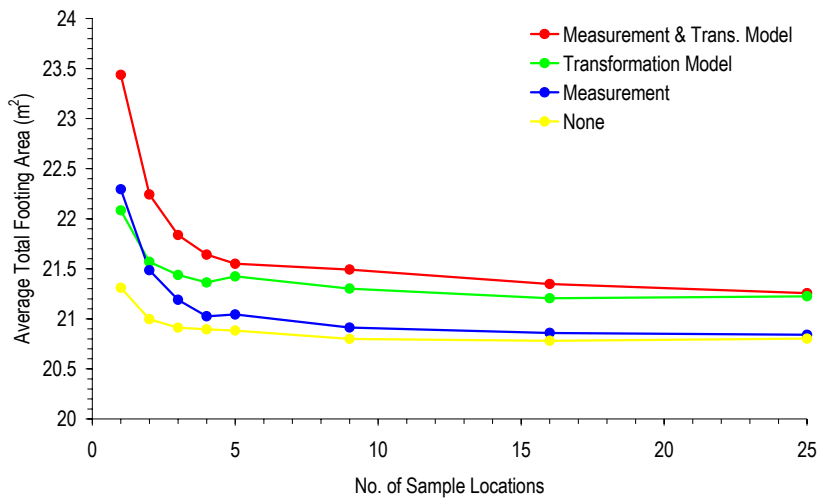


(b)



(c)

**Figure B-6 Effect of increased sampling and the inclusion of measurement and transformation model errors of the SPT on the average total footing area, for a soil COV of 50% and SOF of (a) 1 m, (b) 4 m and (c) 16 m**



Test Type

CPT

Pattern

RG

Reduction

SA

Settlement

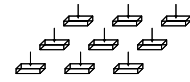
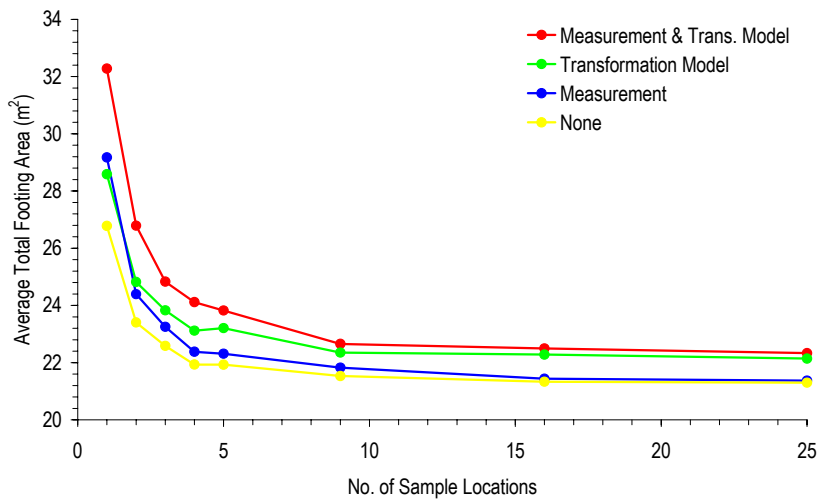
Method

Schmertmann  
2B-0.6

V

3DFEA

(a)



Test Type

CPT

Pattern

RG

Reduction

SA

Settlement

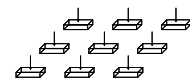
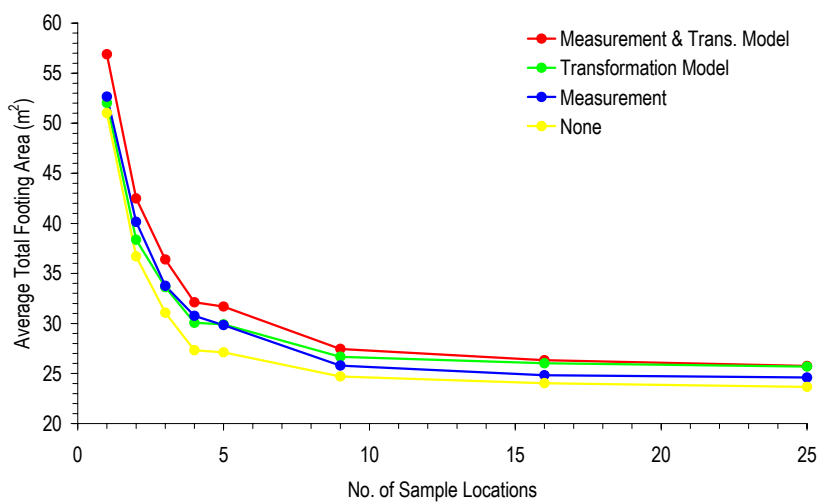
Method

Schmertmann  
2B-0.6

V

3DFEA

(b)



Test Type

CPT

Pattern

RG

Reduction

SA

Settlement

Method

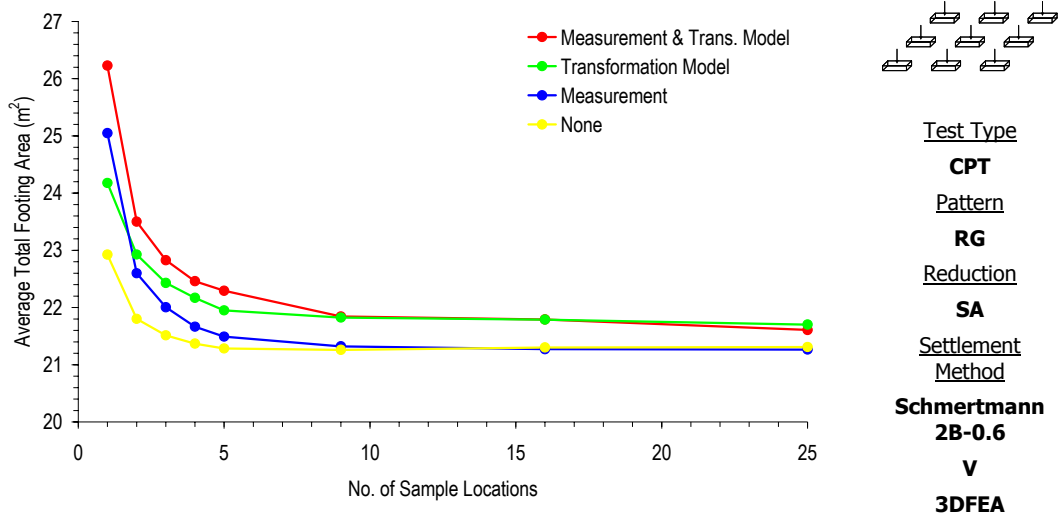
Schmertmann  
2B-0.6

V

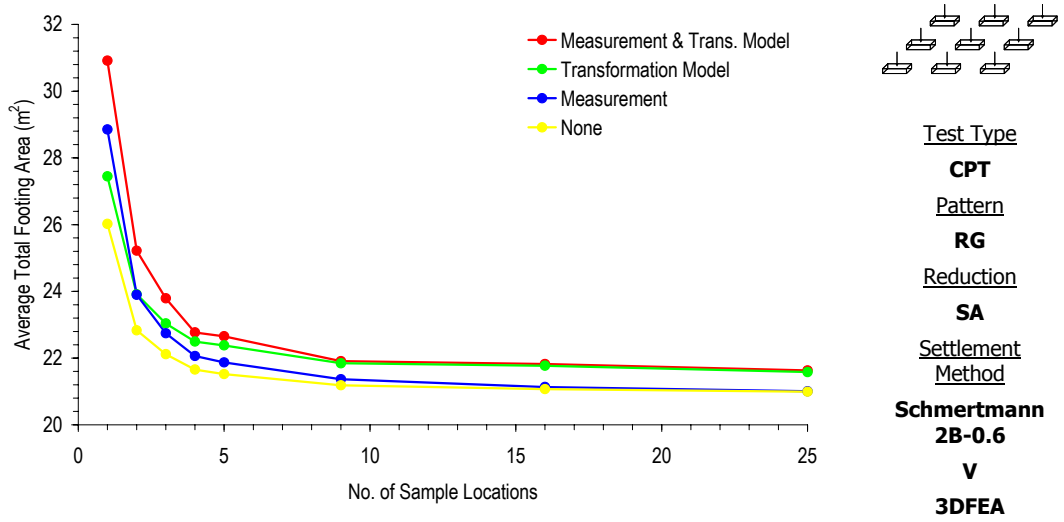
3DFEA

(c)

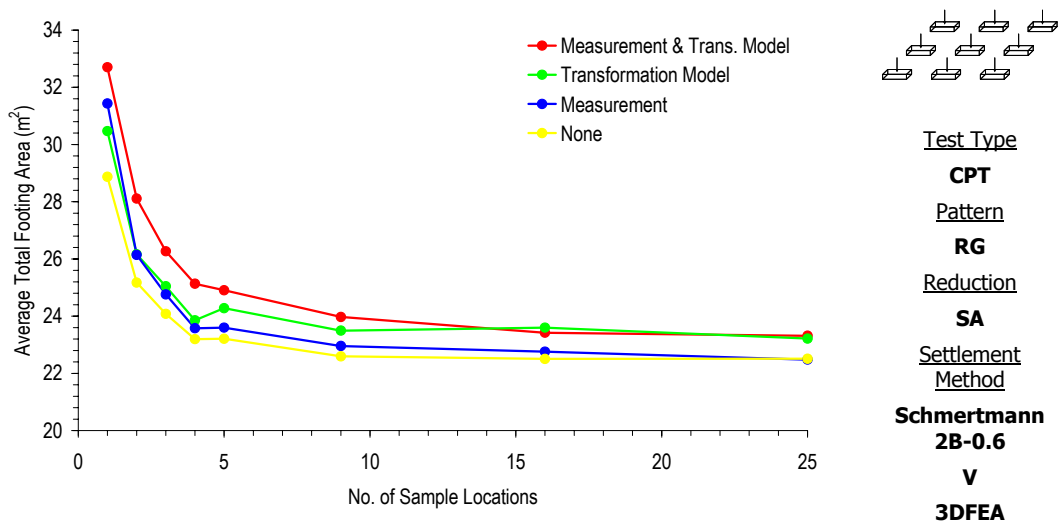
**Figure B-7 Effect of increased sampling and the inclusion of measurement and transformation model errors of the CPT on the average total footing area, for a soil SOF of 8 m and COV of (a) 20%, (b) 50% and (c) 100%**



(a)

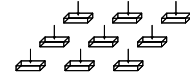
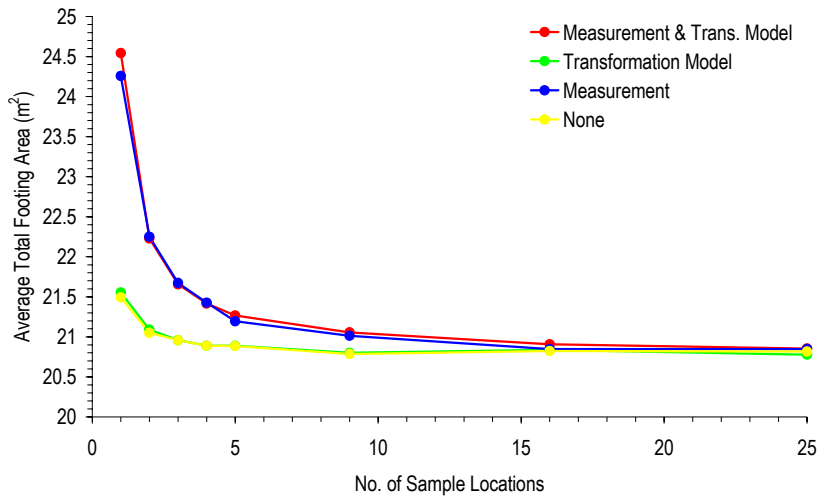


(b)



(c)

**Figure B-8 Effect of increased sampling and the inclusion of measurement and transformation model errors of the CPT on the average total footing area, for a soil COV of 50% and SOF of (a) 1 m, (b) 4 m and (c) 16 m**



Test Type

TT

Pattern

RG

Reduction

SA

Settlement

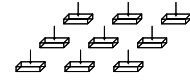
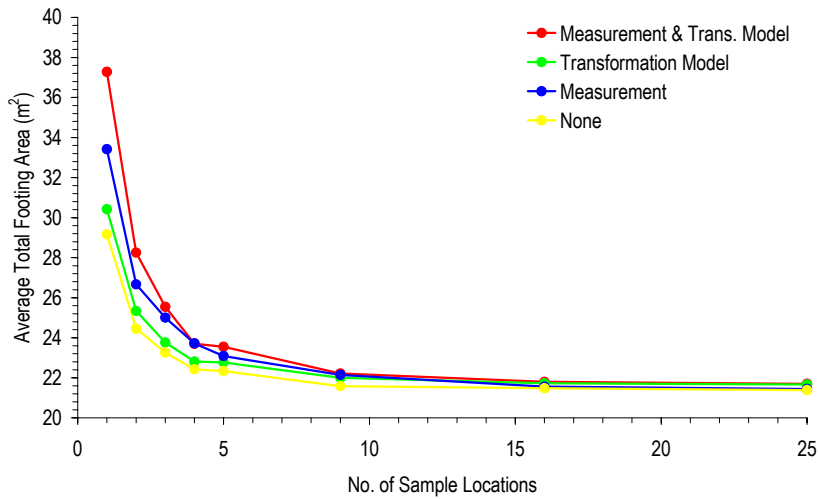
Method

Schmertmann  
2B-0.6

V

3DFEA

(a)



Test Type

TT

Pattern

RG

Reduction

SA

Settlement

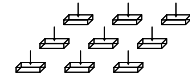
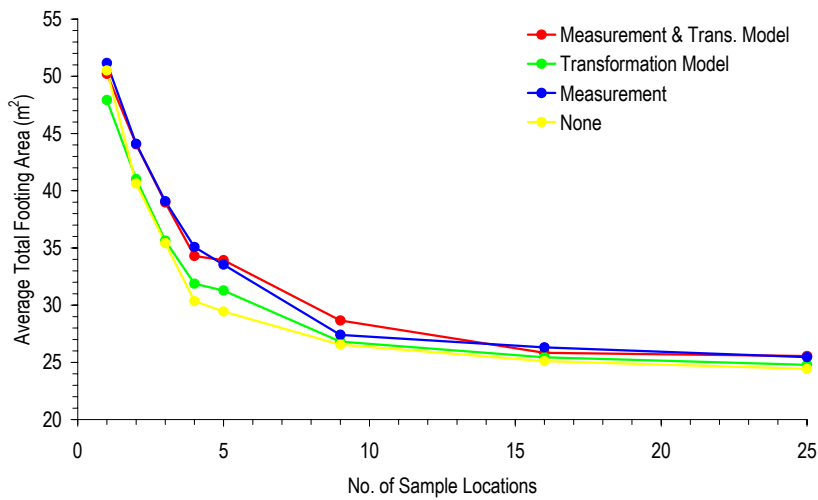
Method

Schmertmann  
2B-0.6

V

3DFEA

(b)



Test Type

TT

Pattern

RG

Reduction

SA

Settlement

Method

Schmertmann  
2B-0.6

V

3DFEA

(c)

**Figure B-9** Effect of increased sampling and the inclusion of measurement and transformation model errors of the TT on the average total footing area, for a soil SOF of 8 m and COV of (a) 20%, (b) 50% and (c) 100%

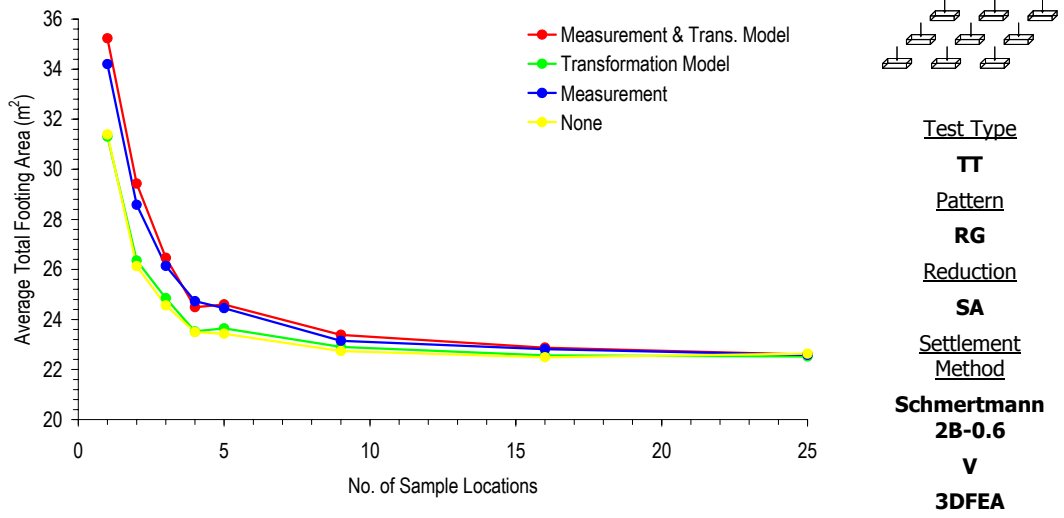
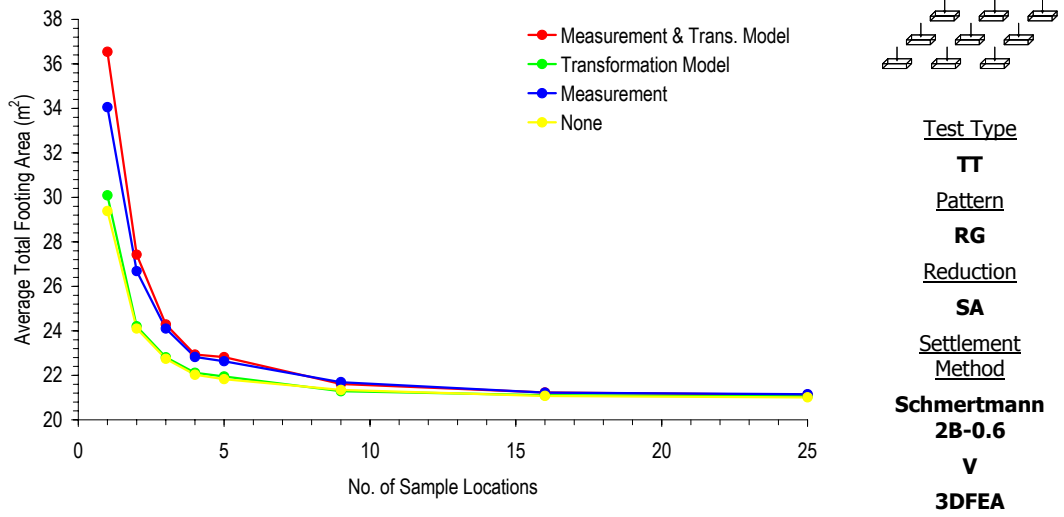
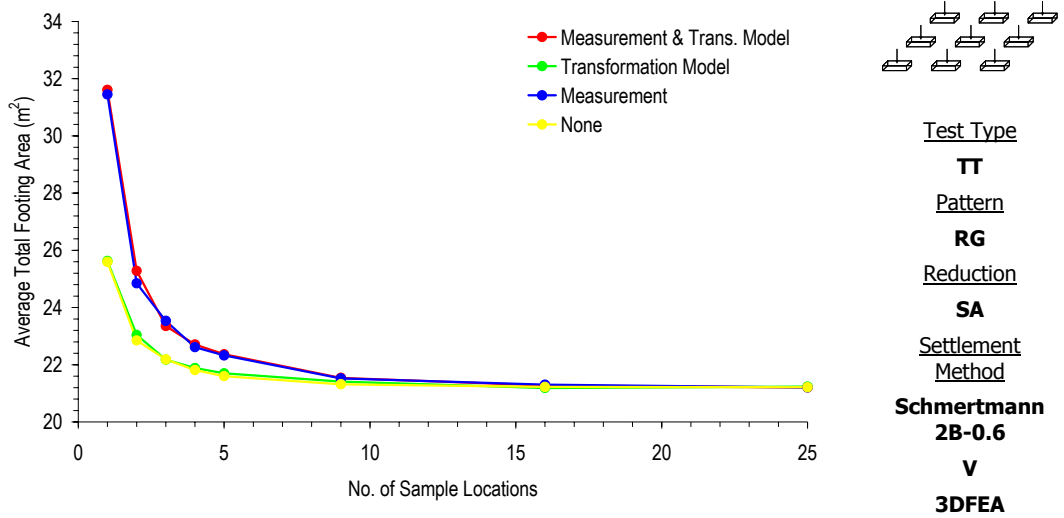
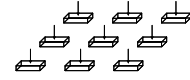
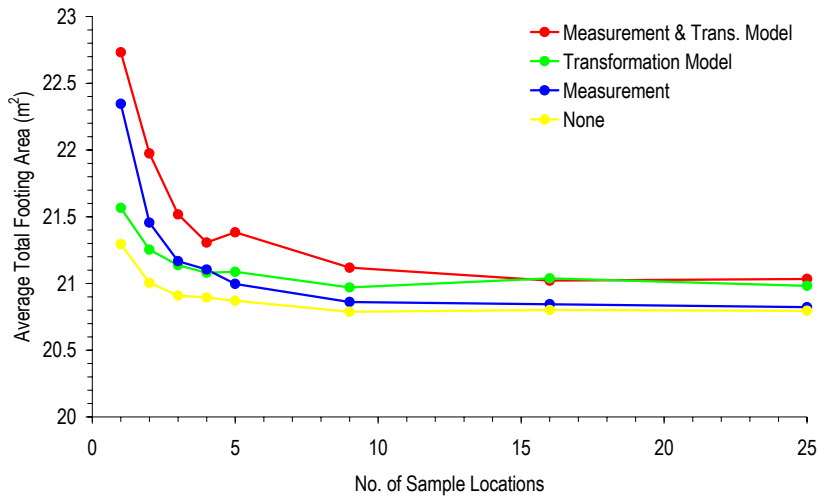


**Figure B-10 Effect of increased sampling and the inclusion of measurement and transformation model errors of the TT on the average total footing area, for a soil COV of 50% and SOF of (a) 1 m, (b) 4 m and (c) 16 m**



Test Type

**DMT**

Pattern

**RG**

Reduction

**SA**

Settlement

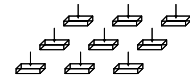
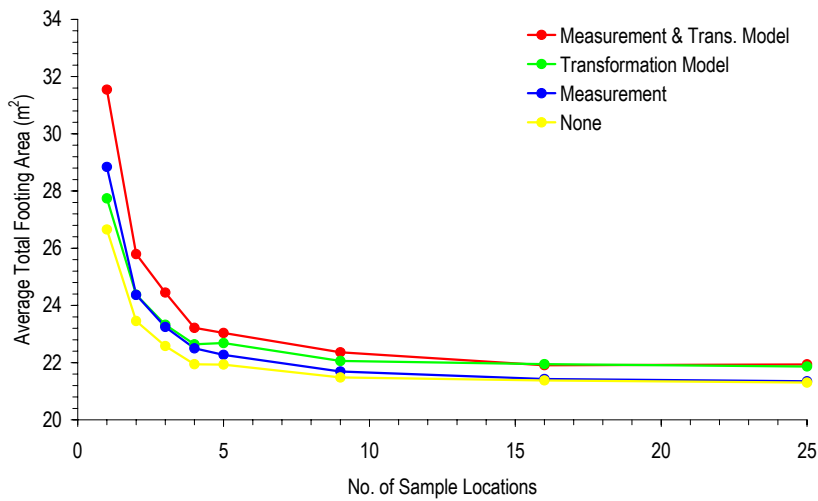
Method

**Schmertmann  
2B-0.6**

**V**

**3DFEA**

(a)



Test Type

**DMT**

Pattern

**RG**

Reduction

**SA**

Settlement

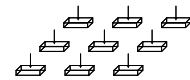
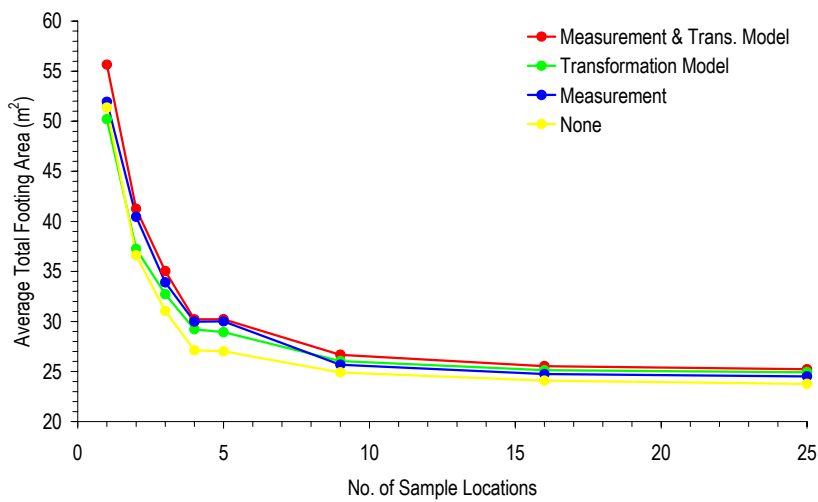
Method

**Schmertmann  
2B-0.6**

**V**

**3DFEA**

(b)



Test Type

**DMT**

Pattern

**RG**

Reduction

**SA**

Settlement

Method

**Schmertmann  
2B-0.6**

**V**

**3DFEA**

(c)

**Figure B-11 Effect of increased sampling and the inclusion of measurement and transformation model errors of the DMT on the average total footing area, for a soil SOF of 8 m and COV of (a) 20%, (b) 50% and (c) 100%**



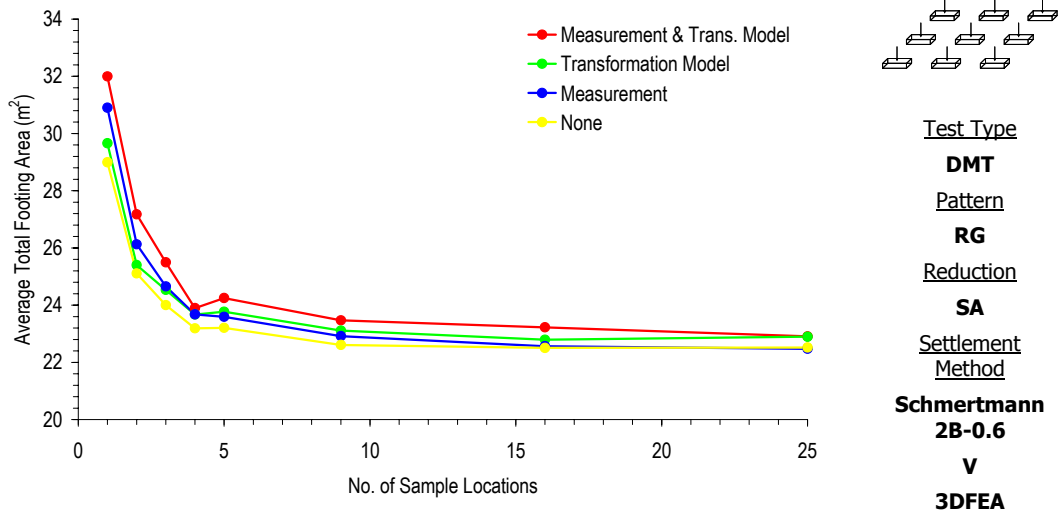
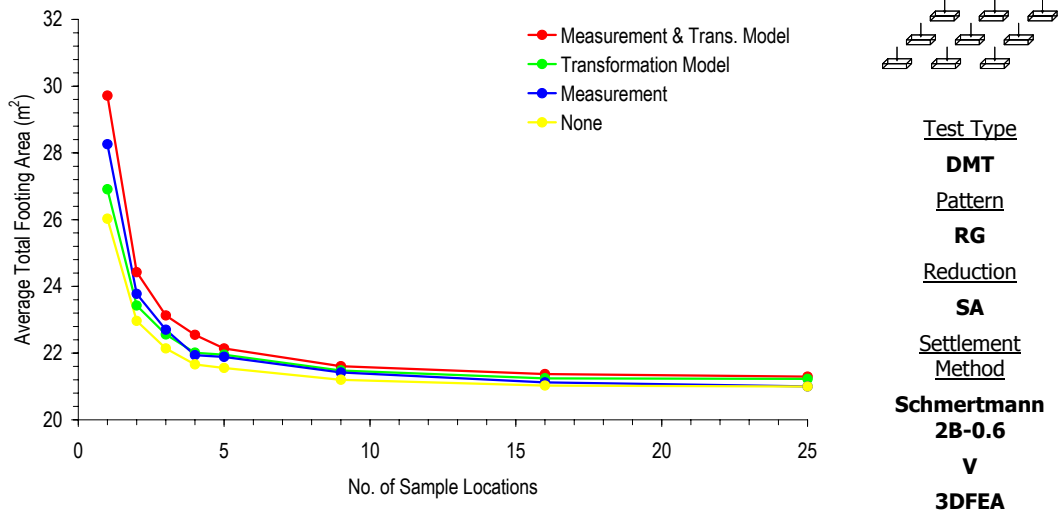
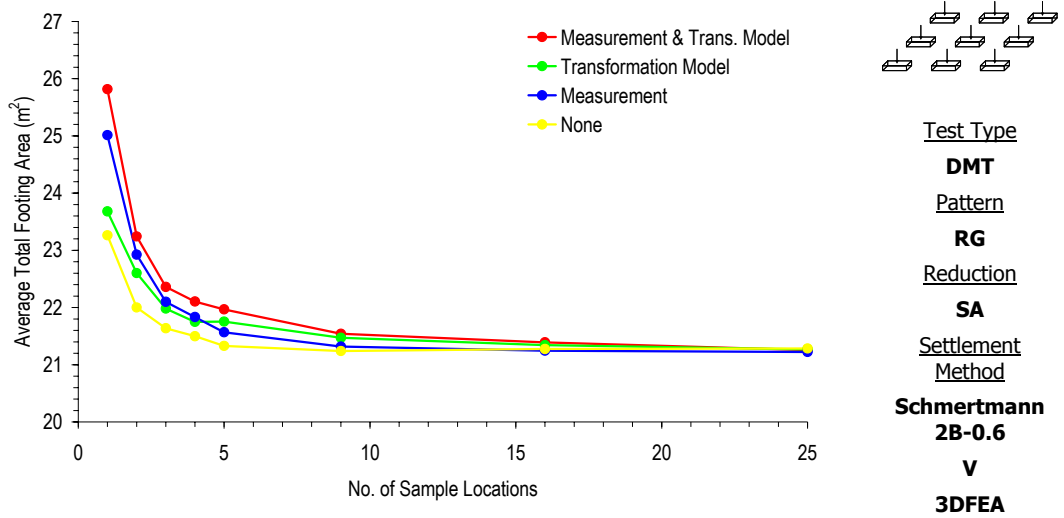
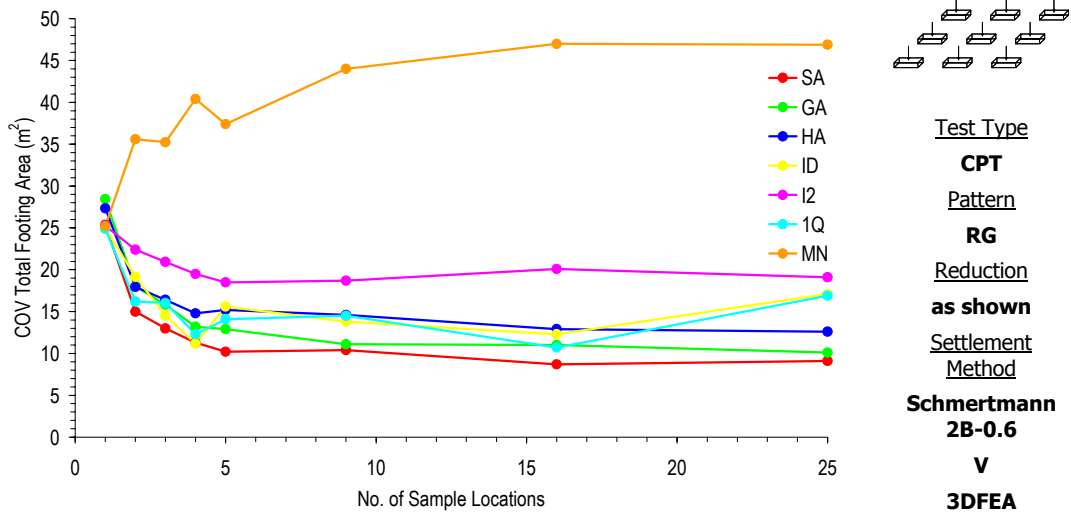
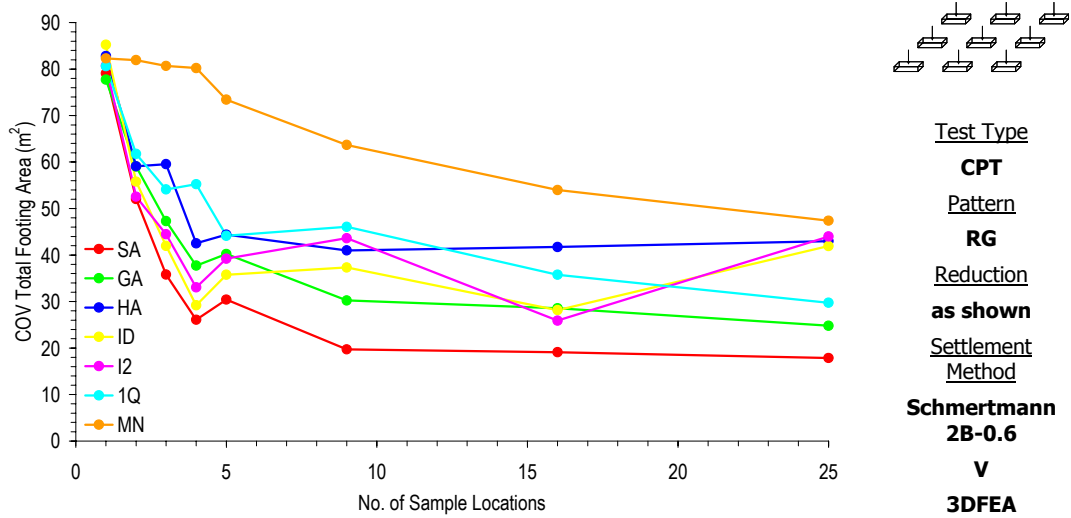


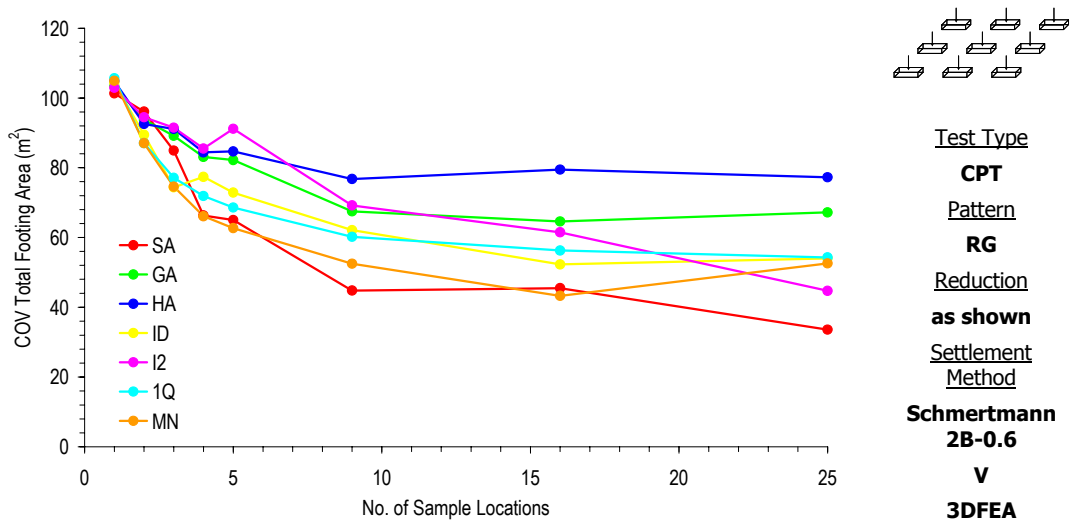
**Figure B-12 Effect of increased sampling and the inclusion of measurement and transformation model errors of the DMT on the average total footing area, for a soil COV of 50% and SOF of (a) 1 m, (b) 4 m and (c) 16 m**



(a)



(b)



(c)

Figure B-13 Effect of increased sampling using different reduction techniques on the COV of total footing area, for a soil SOF of 8 m and COV of (a) 20%, (b) 50% and (c) 100%

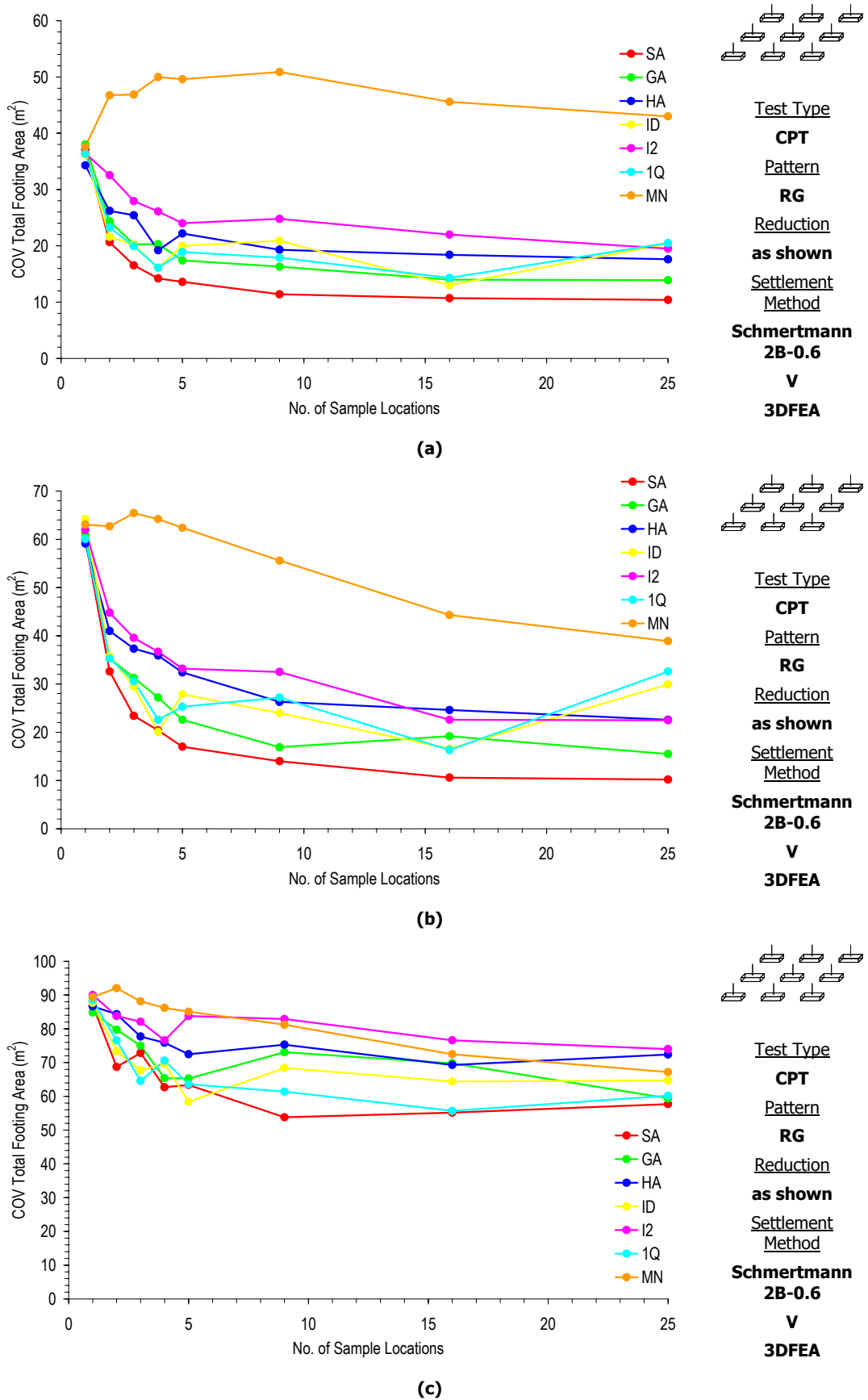
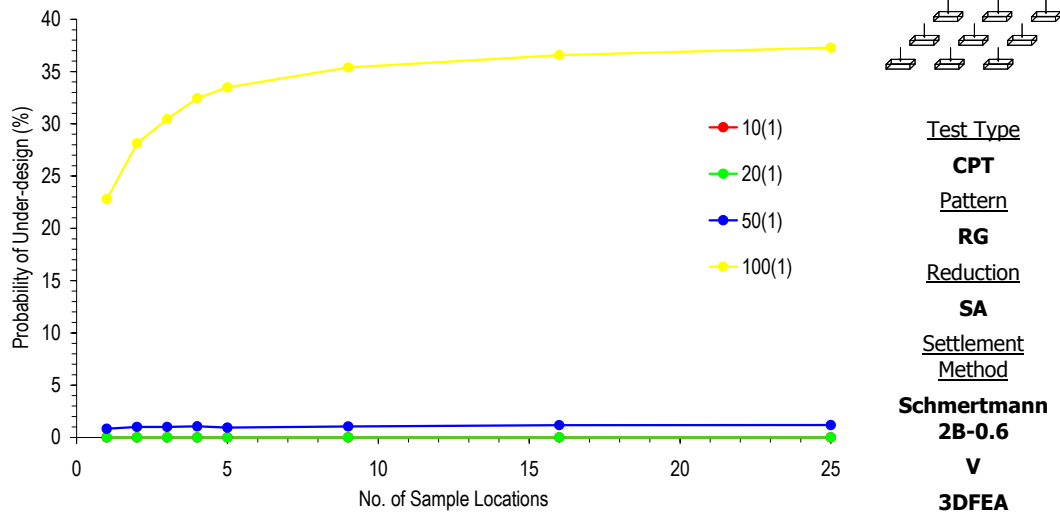


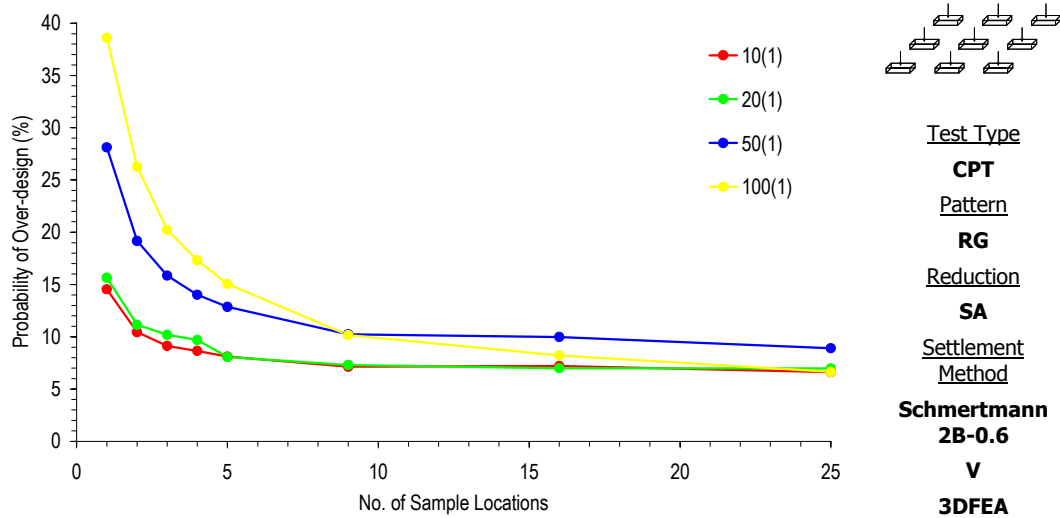
Figure B-14 Effect of increased sampling using different reduction techniques on the COV of total footing area, for a soil COV of 50% and SOF of (a) 1 m, (b) 4 m and (c) 32 m



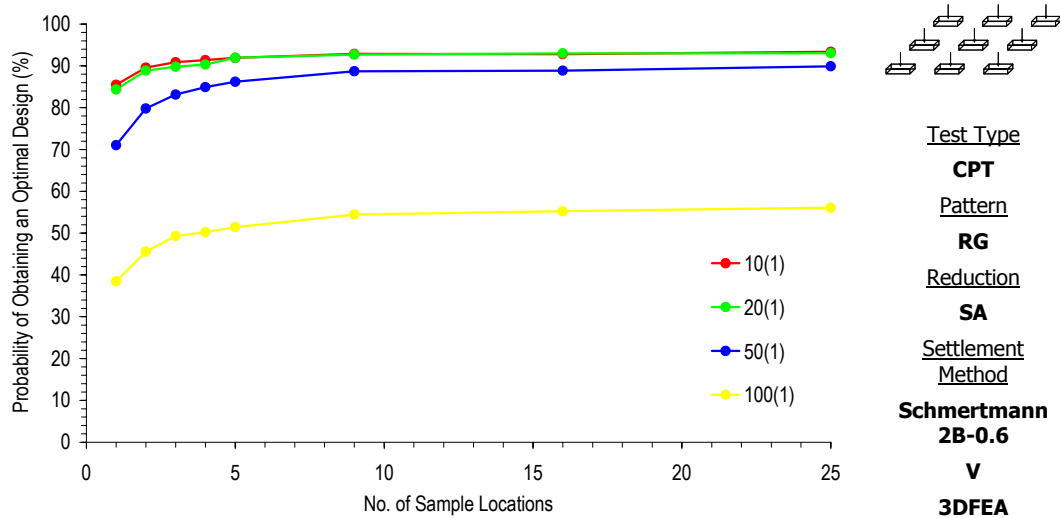
## **Appendix C Probabilities of Under- and Over-design and Probabilities of Obtaining an Optimal Design**



(a)

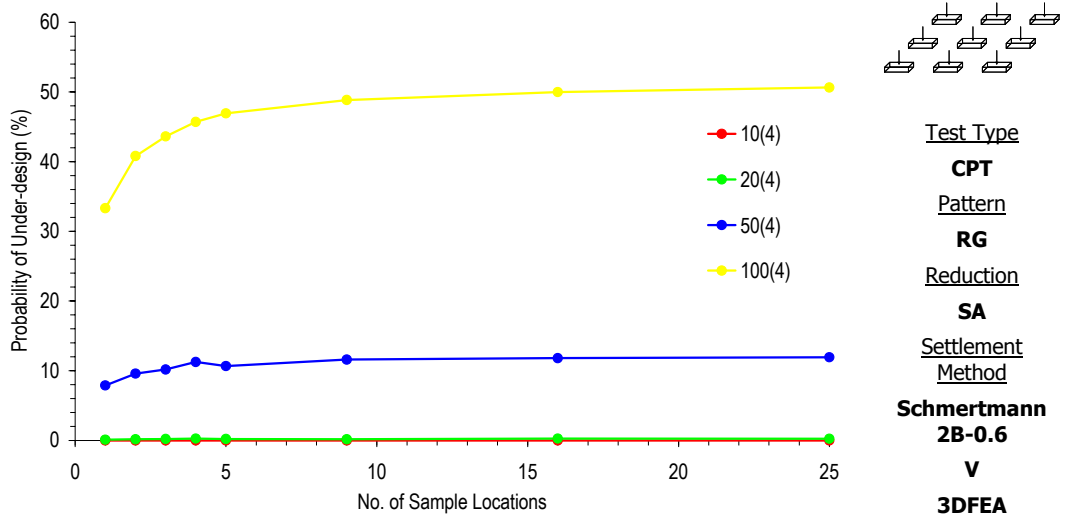


(b)

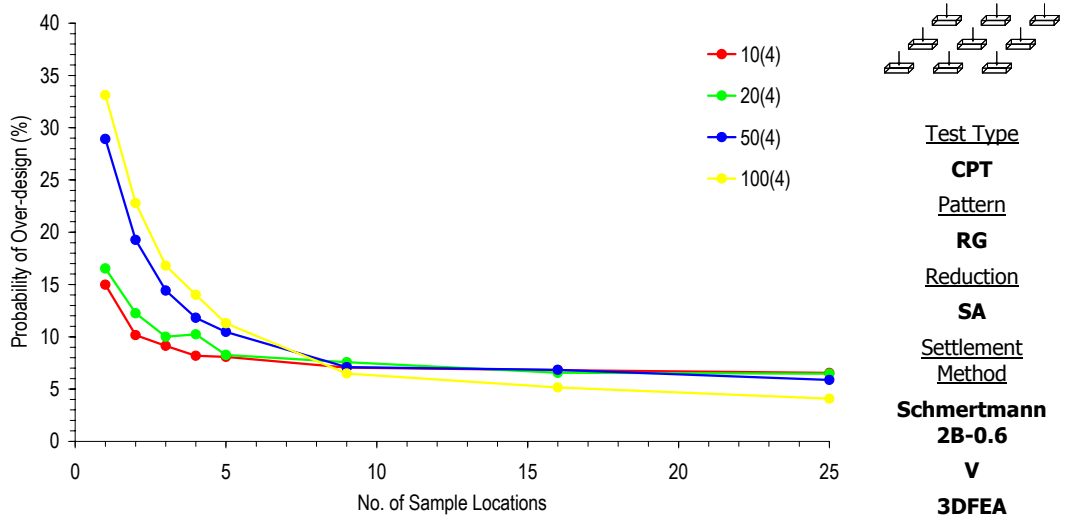


(c)

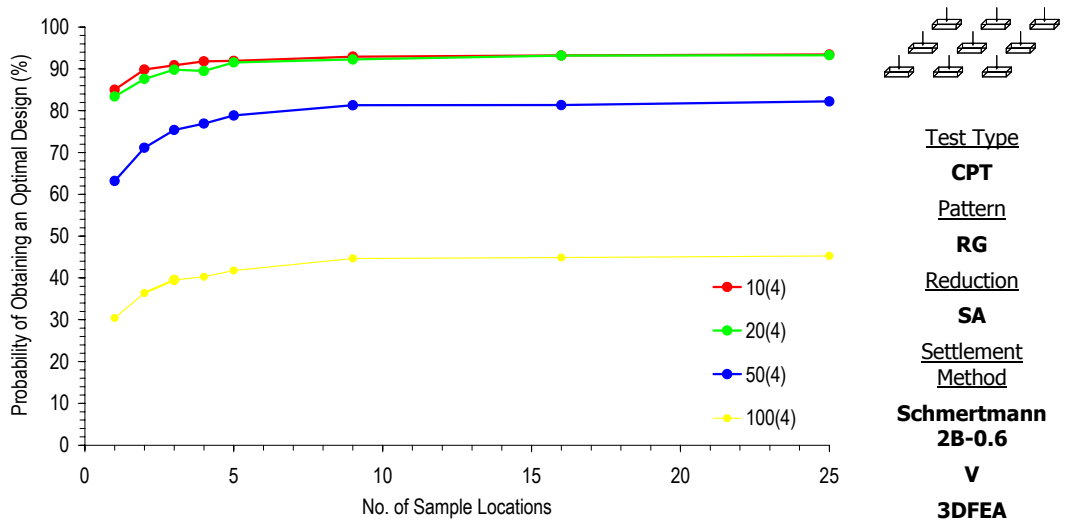
Figure C-1 Effect of increased sampling on the probability of (a) under- and (b) over-design and (c) the probability of obtaining an optimal design, for a soil SOF of 1 m and varying COV



(a)



(b)



(c)

Figure C-2 Effect of increased sampling on the probability of (a) under- and (b) over-design and (c) the probability of obtaining an optimal design, for a soil SOF of 4 m and varying COV

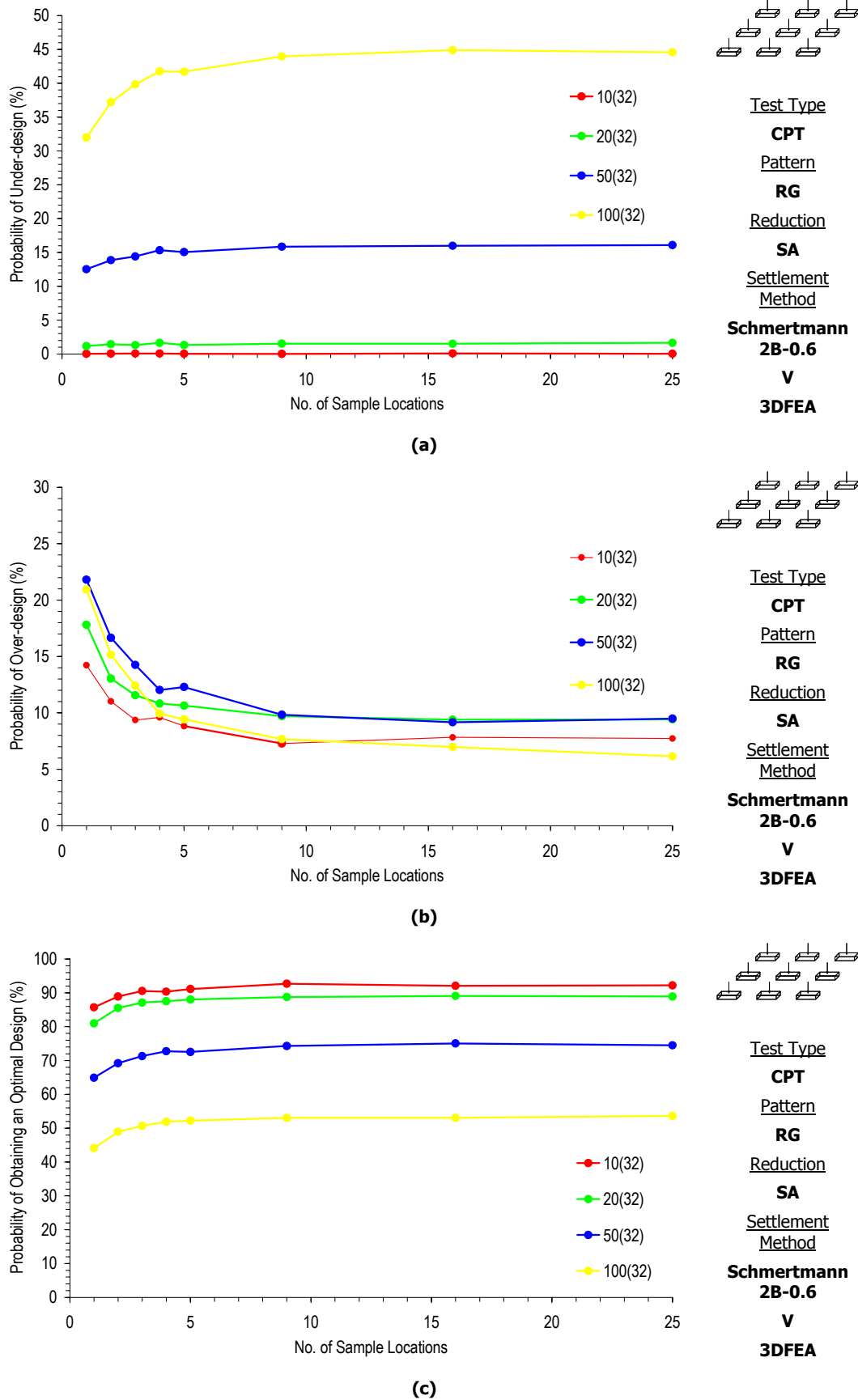


Figure C-3 Effect of increased sampling on the probability of (a) under- and (b) over-design and (c) the probability of obtaining an optimal design, for a soil SOF of 32 m and varying COV



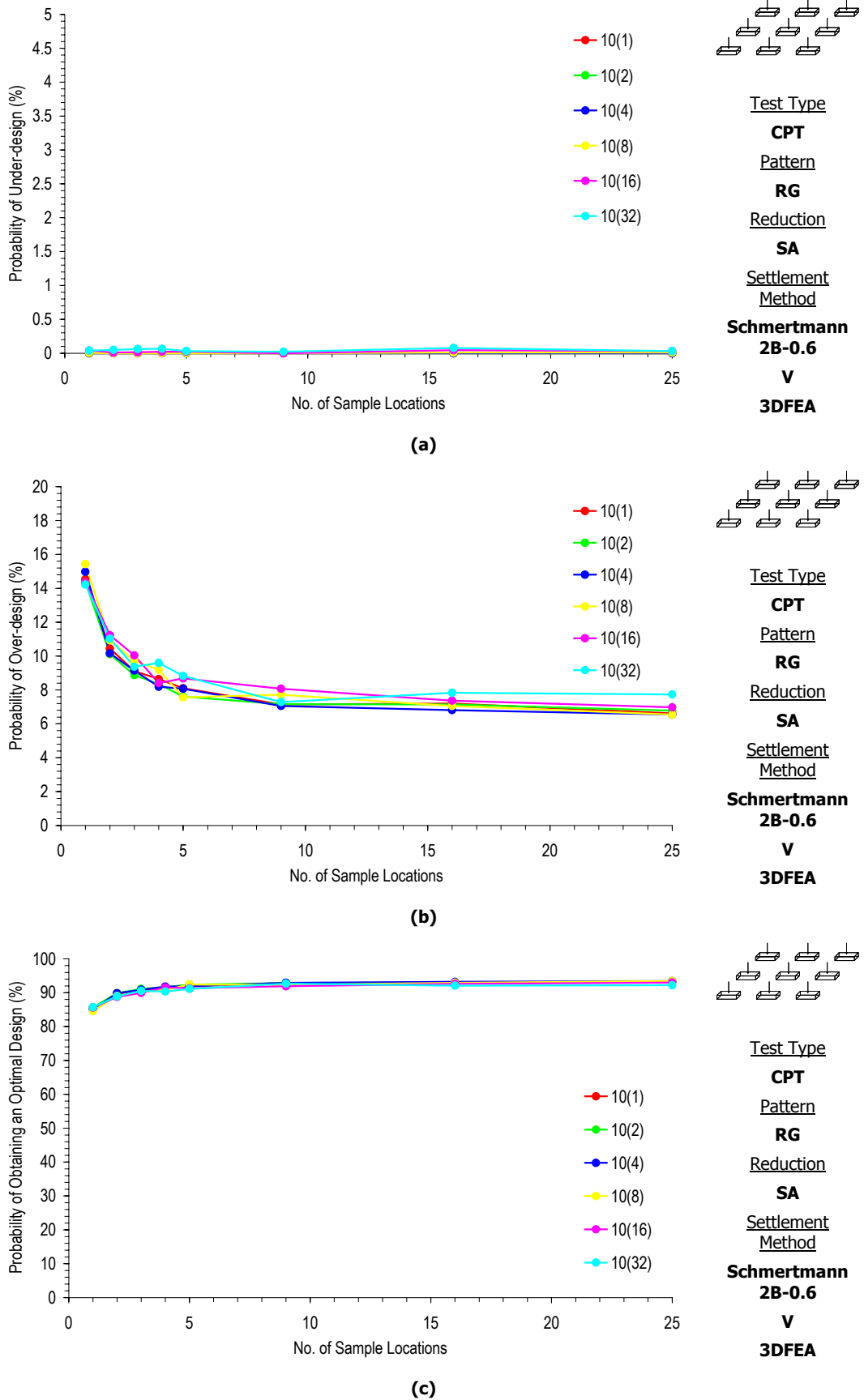


Figure C-4 Effect of increased sampling on the probability of (a) under- and (b) over-design and (c) the probability of obtaining an optimal design, for a soil COV of 10% and varying SOF

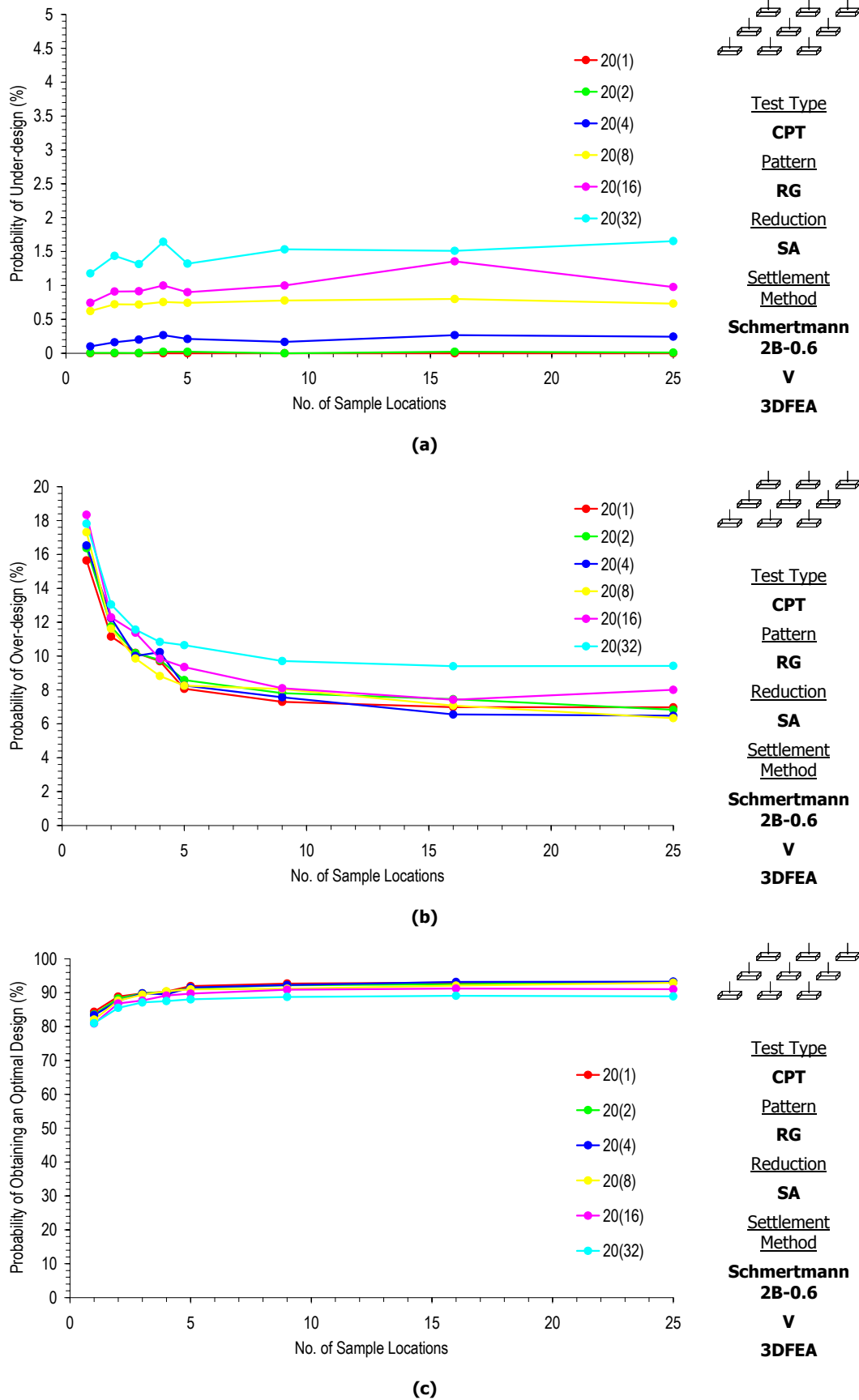


Figure C-5 Effect of increased sampling on the probability of (a) under- and (b) over-design and (c) the probability of obtaining an optimal design, for a soil COV of 20% and varying SOF

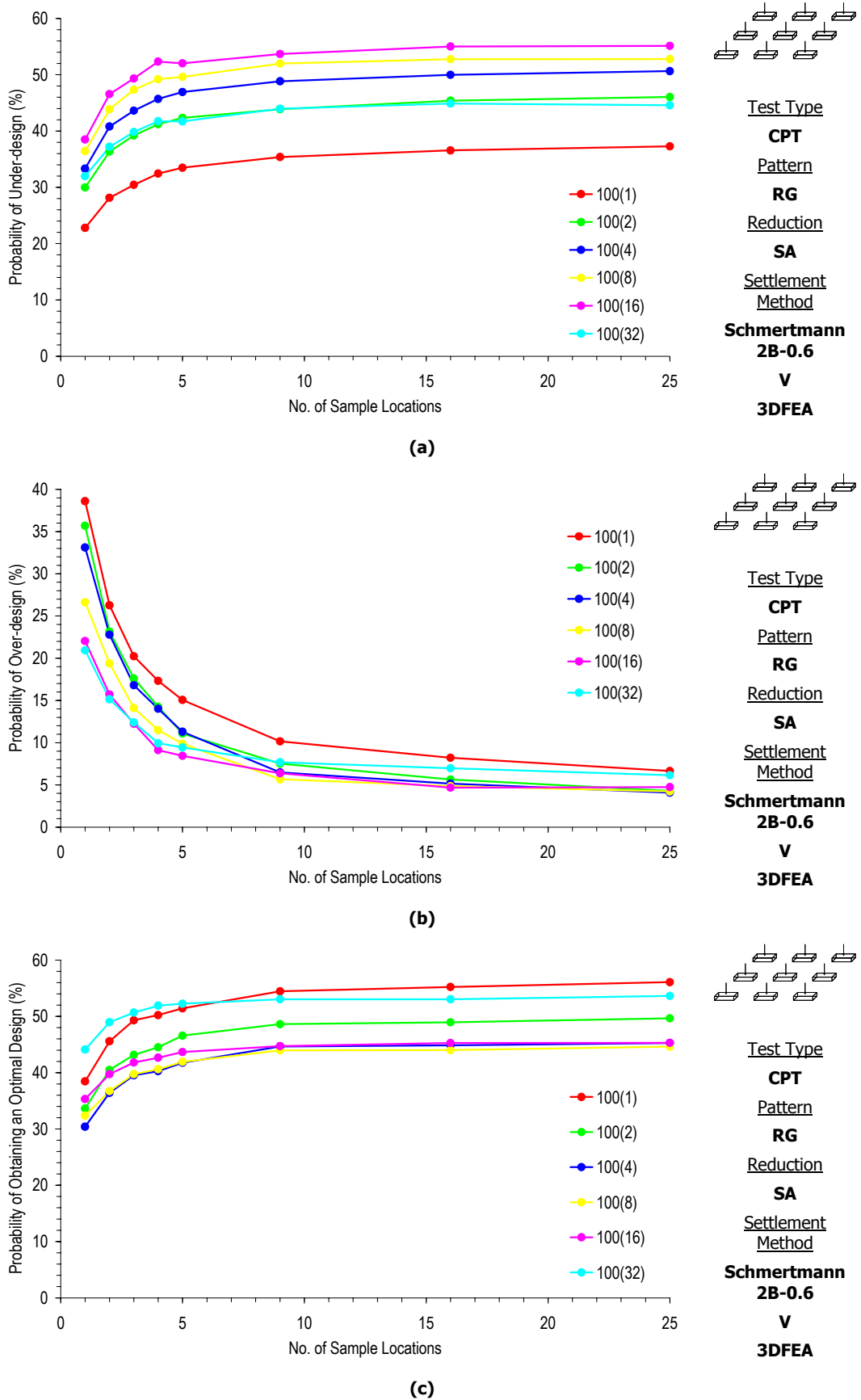
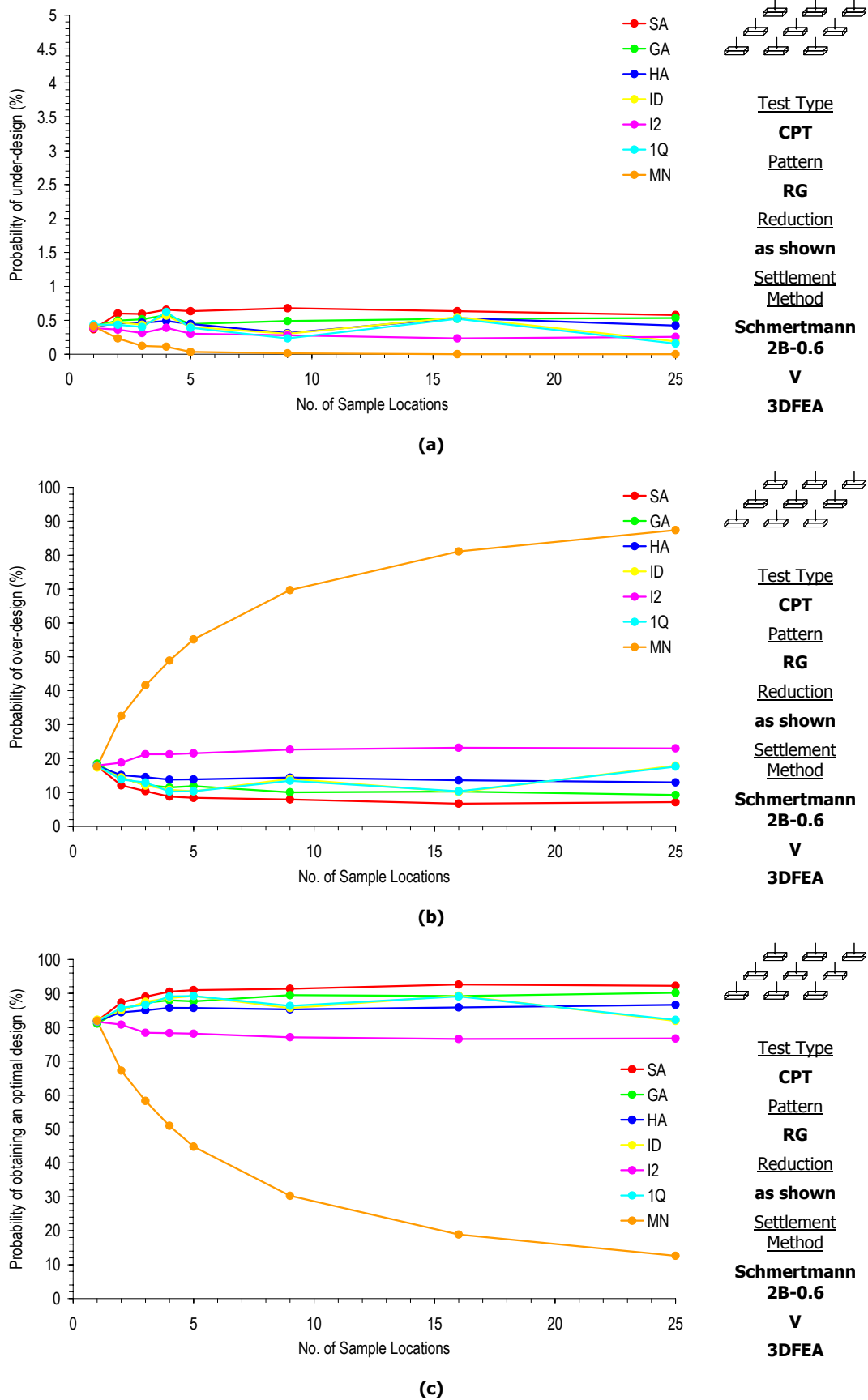
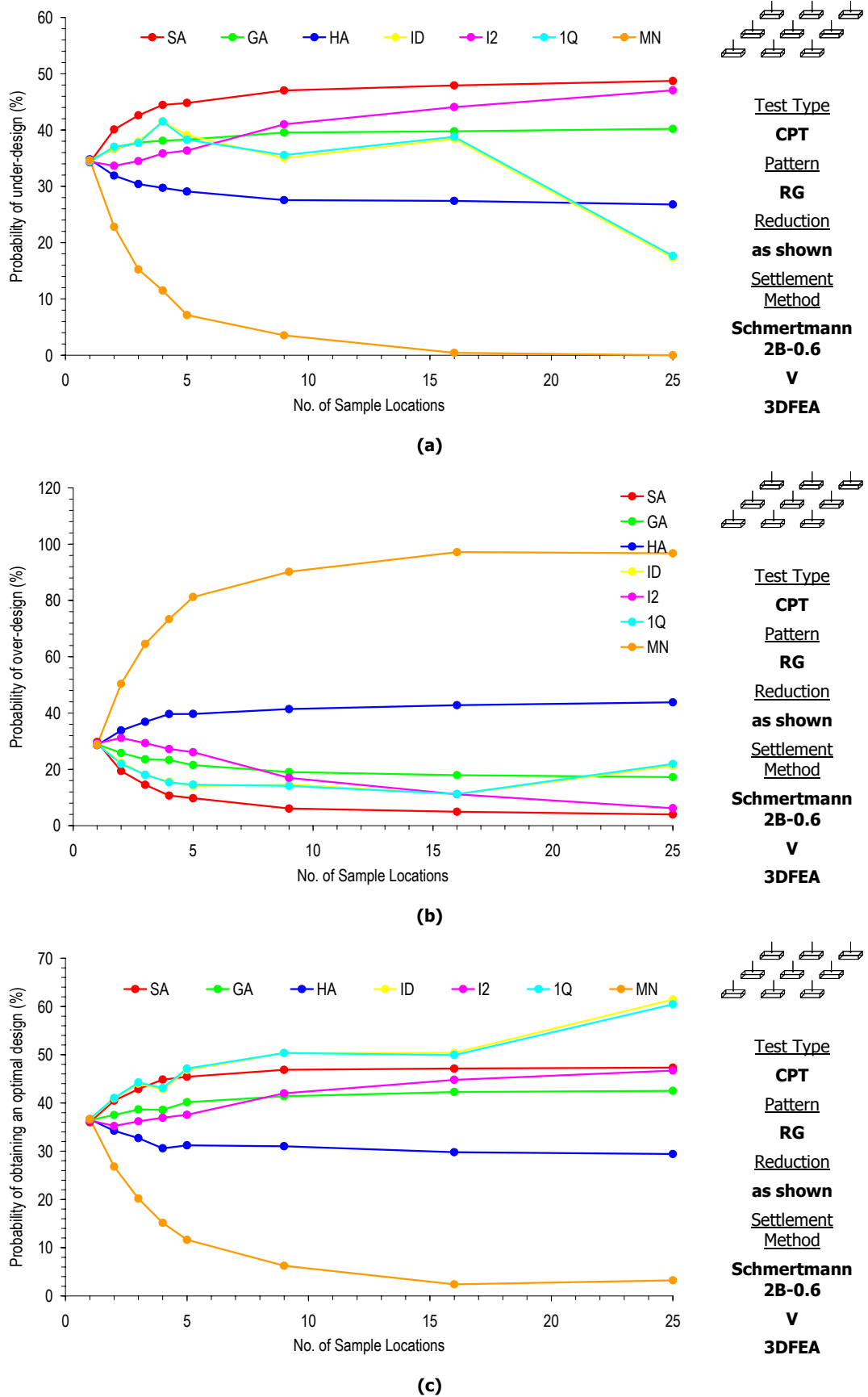


Figure C-6 Effect of increased sampling on the probability of (a) under- and (b) over-design and (c) the probability of obtaining an optimal design, for a soil COV of 100% and varying SOF



**Figure C-7** Effect of increased sampling with different reduction techniques on the probability of (a) under- and (b) over-design and (c) the probability of obtaining an optimal design, for a soil COV of 20% and SOF of 8 m



**Figure C-8 Effect of increased sampling with different reduction techniques on the probability of (a) under- and (b) over-design and (c) the probability of obtaining an optimal design, for a soil COV of 100% and SOF of 8 m**

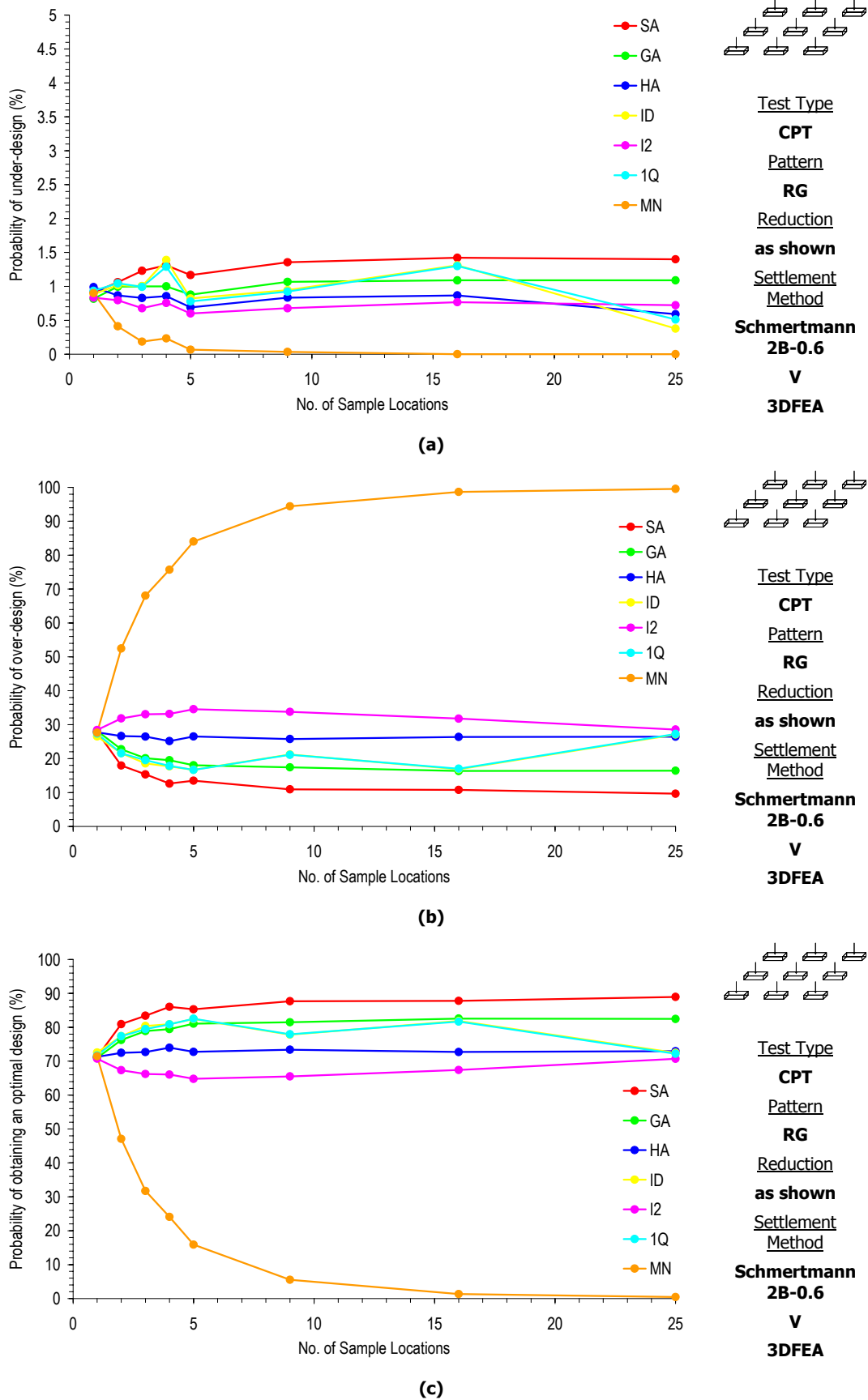


**Figure C-9** Effect of increased sampling with different reduction techniques on the probability of (a) under- and (b) over-design and (c) the probability of obtaining an optimal design, for a soil COV of 50% and SOF of 1 m

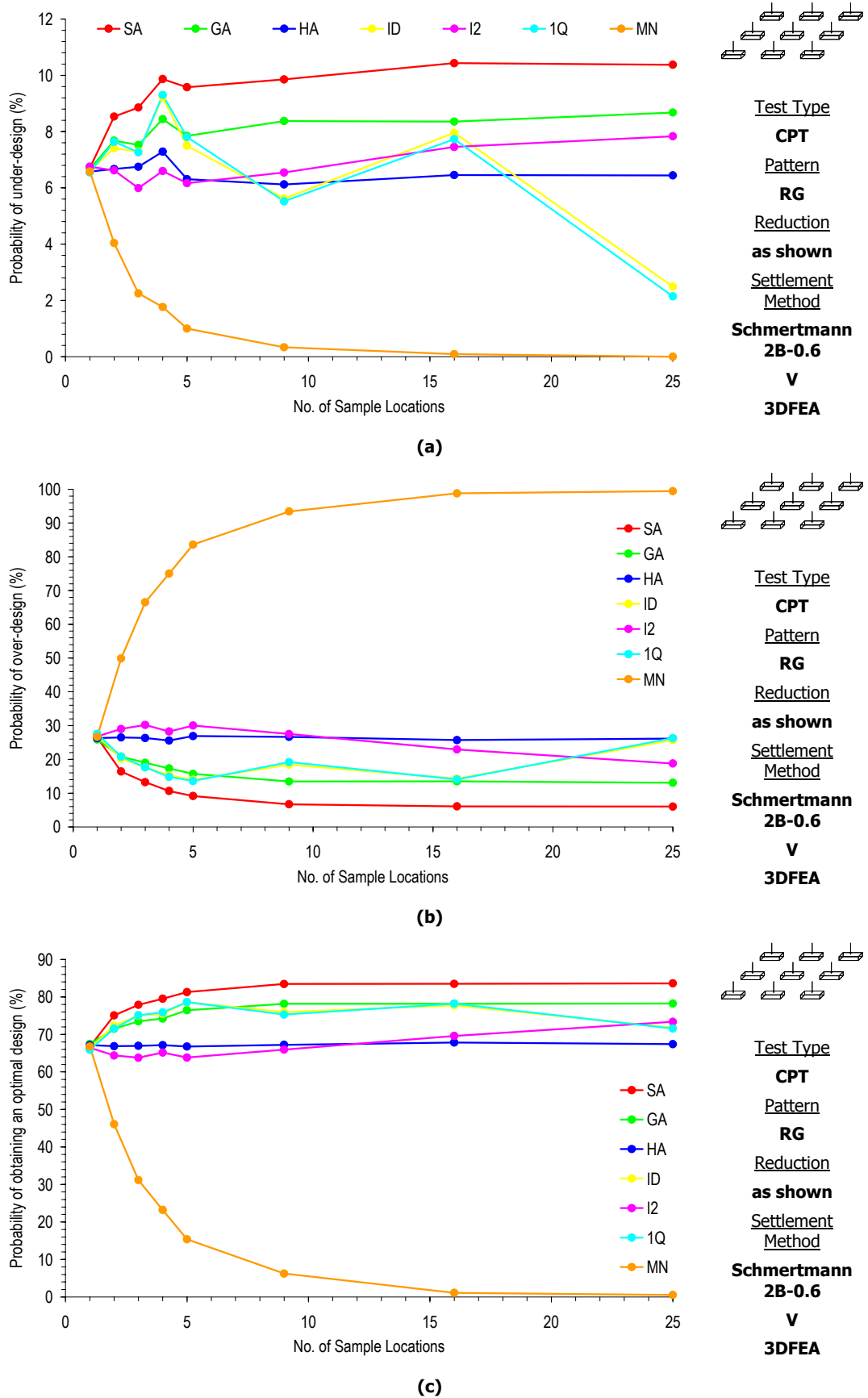


**Figure C-10 Effect of increased sampling with different reduction techniques on the probability of (a) under- and (b) over-design and (c) the probability of obtaining an optimal design, for a soil COV of 50% and SOF of 4 m**

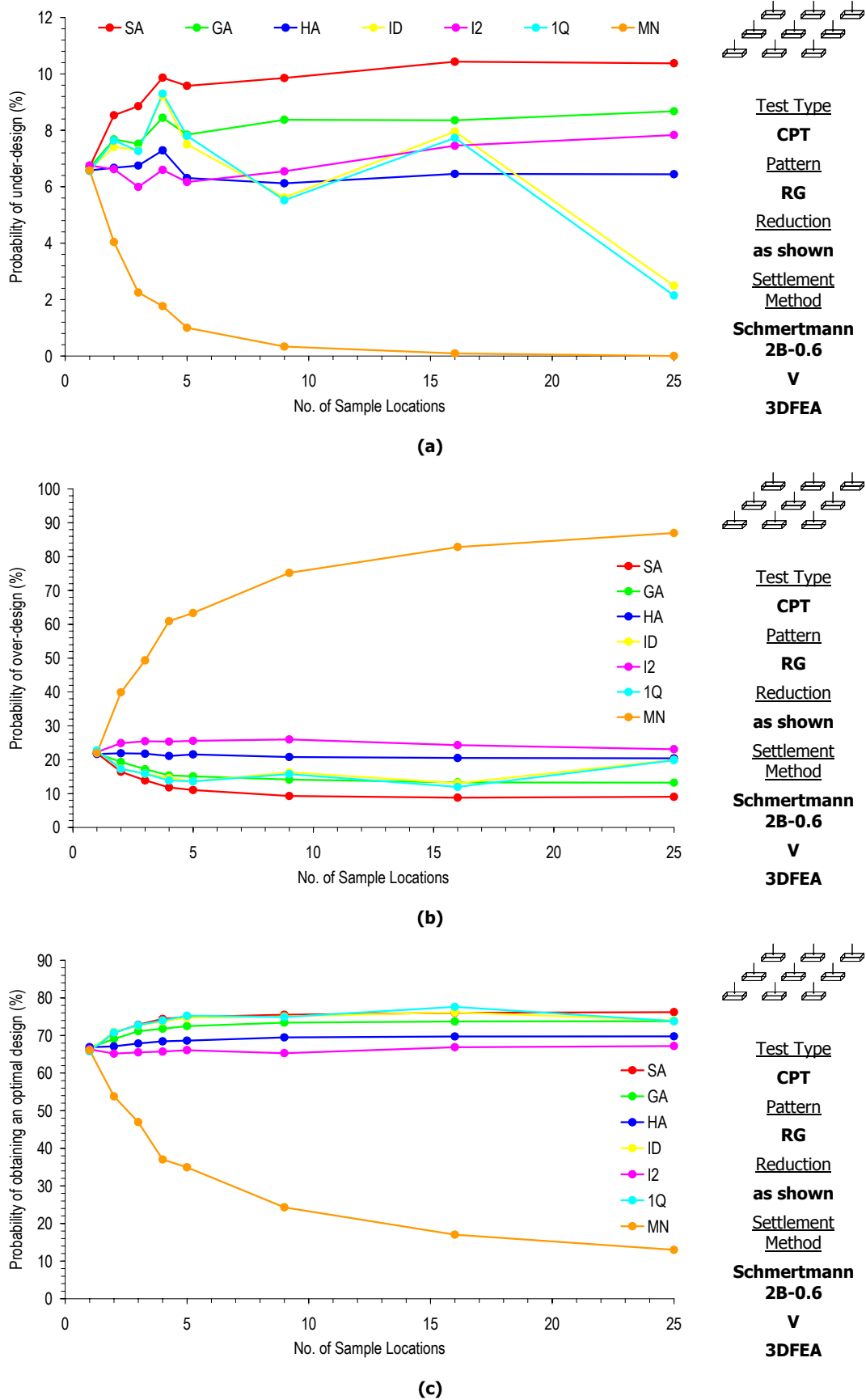
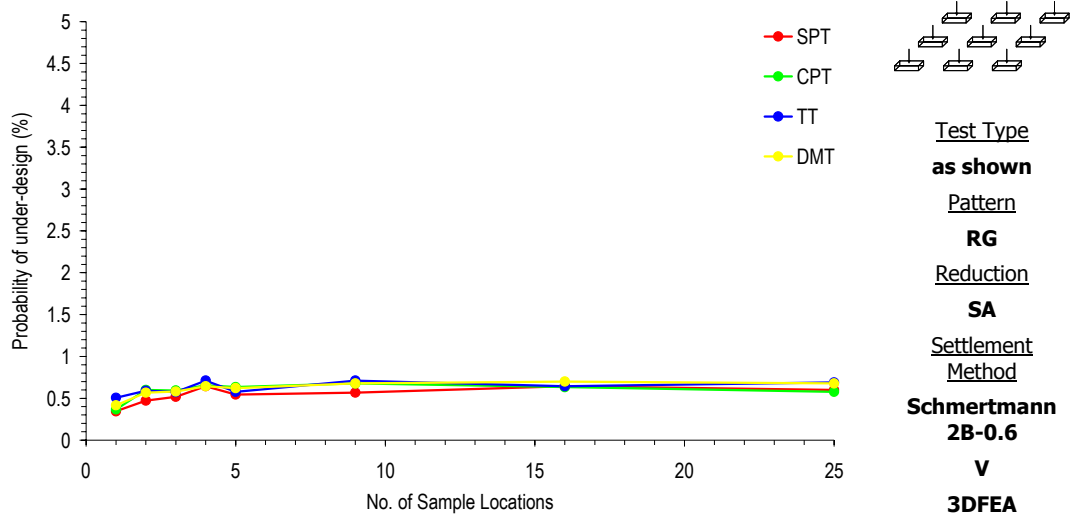
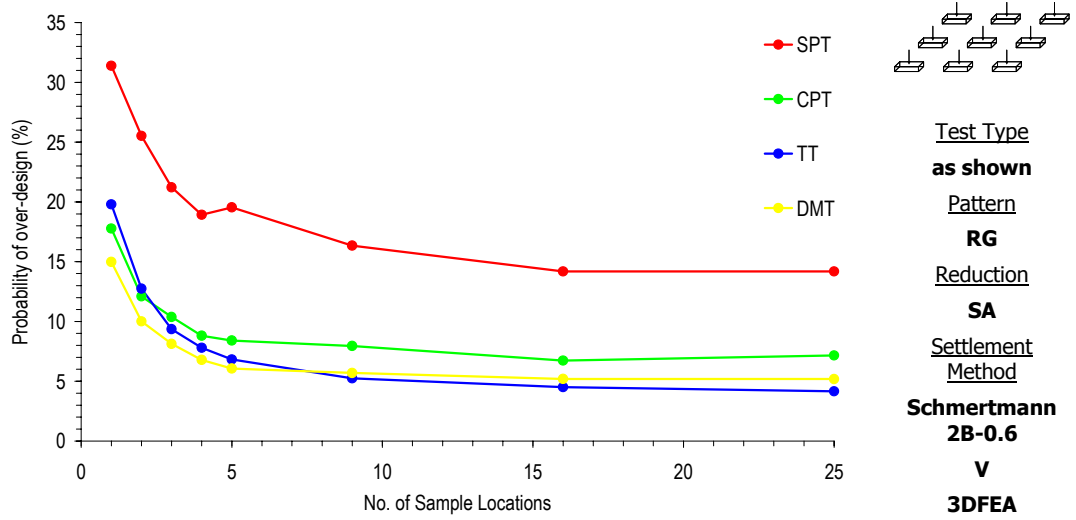


**Figure C-11** Effect of increased sampling with different reduction techniques on the probability of (a) under- and (b) over-design and (c) the probability of obtaining an optimal design, for a soil COV of 50% and SOF of 32 m

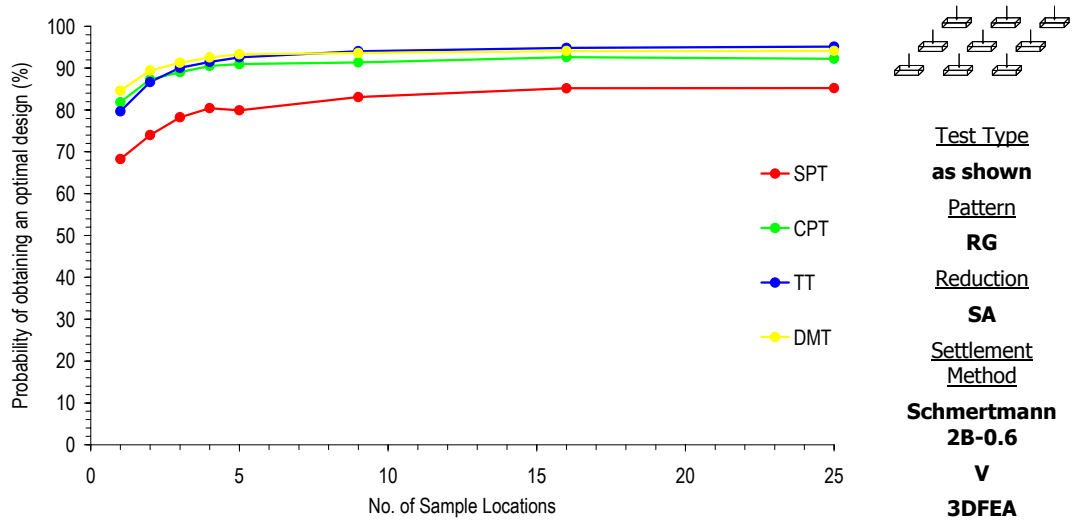




(a)



(b)



(c)

**Figure C-12 Effect of increased sampling with different test types on the probability of (a) under- and (b) over-design and (c) the probability of obtaining an optimal design, for a soil COV of 20% and SOF of 8 m**

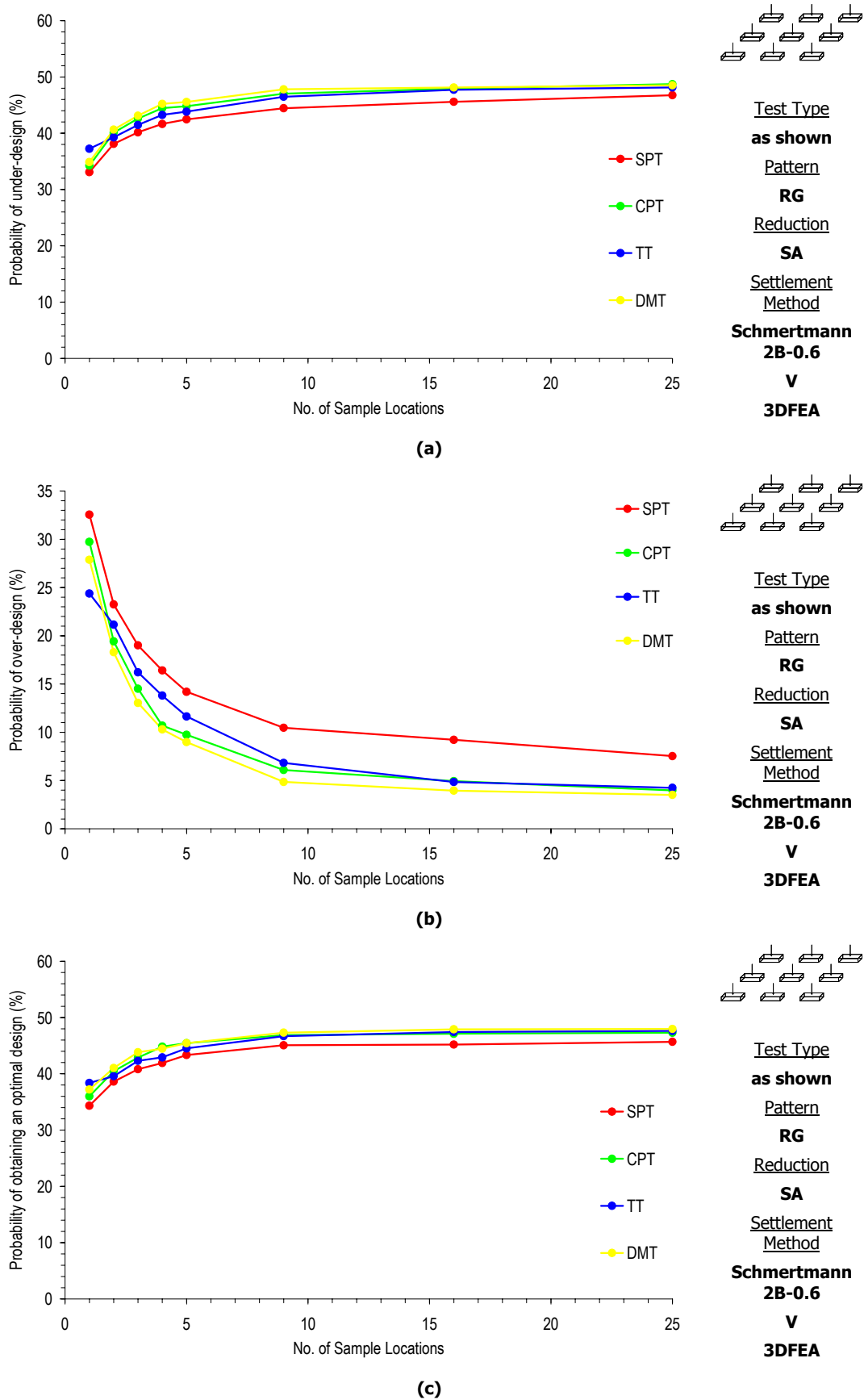
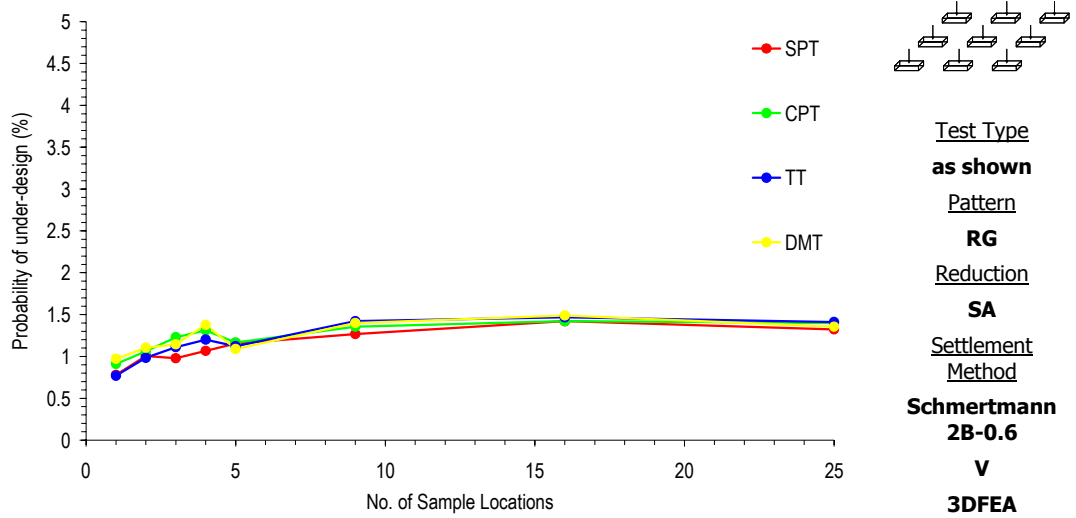
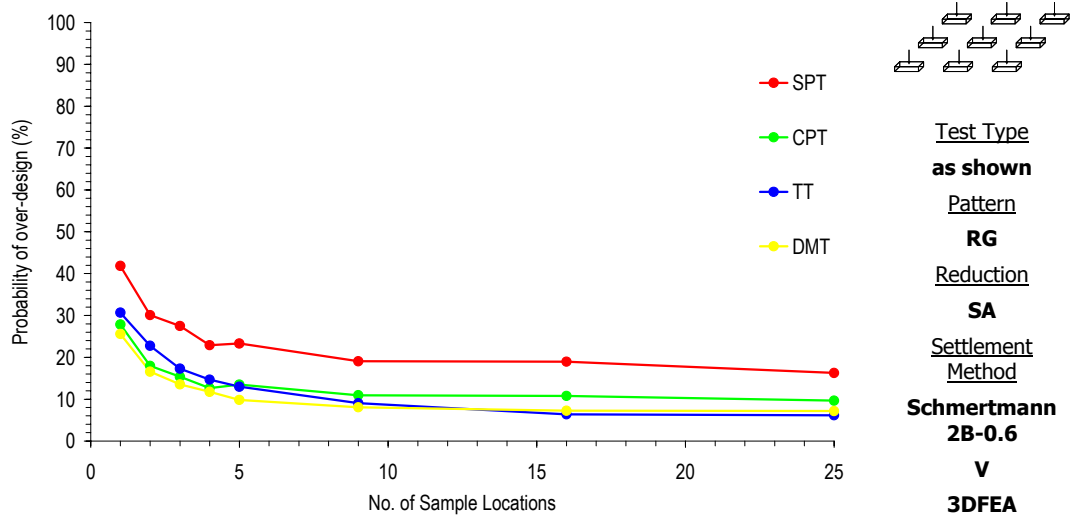


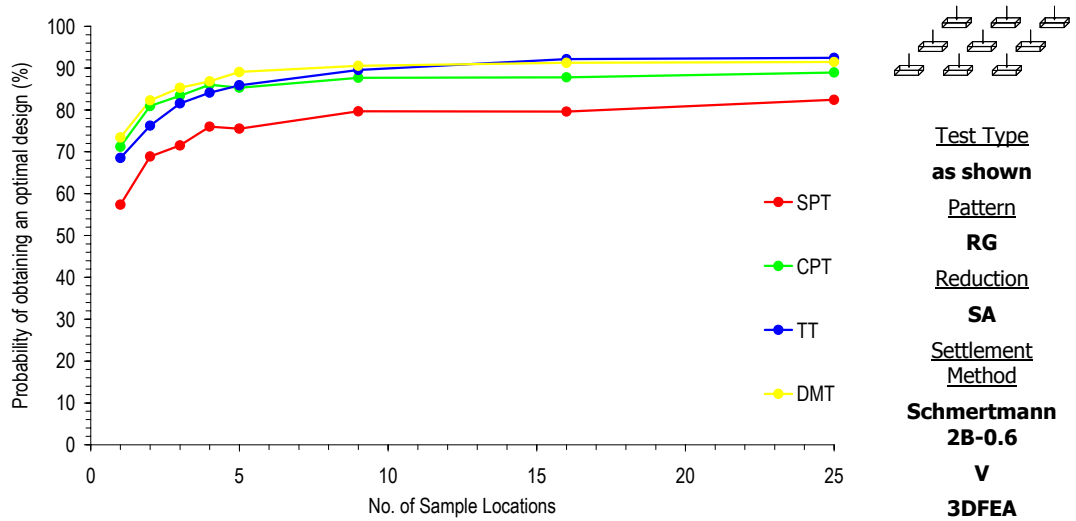
Figure C-13 Effect of increased sampling with different test types on the probability of (a) under- and (b) over-design and (c) the probability of obtaining an optimal design, for a soil COV of 100% and SOF of 8 m



(a)

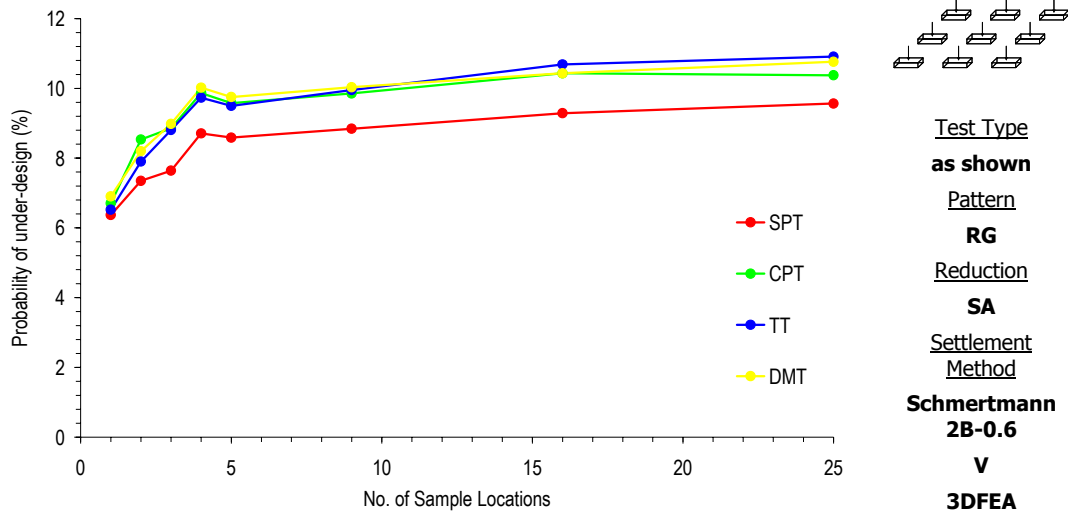


(b)

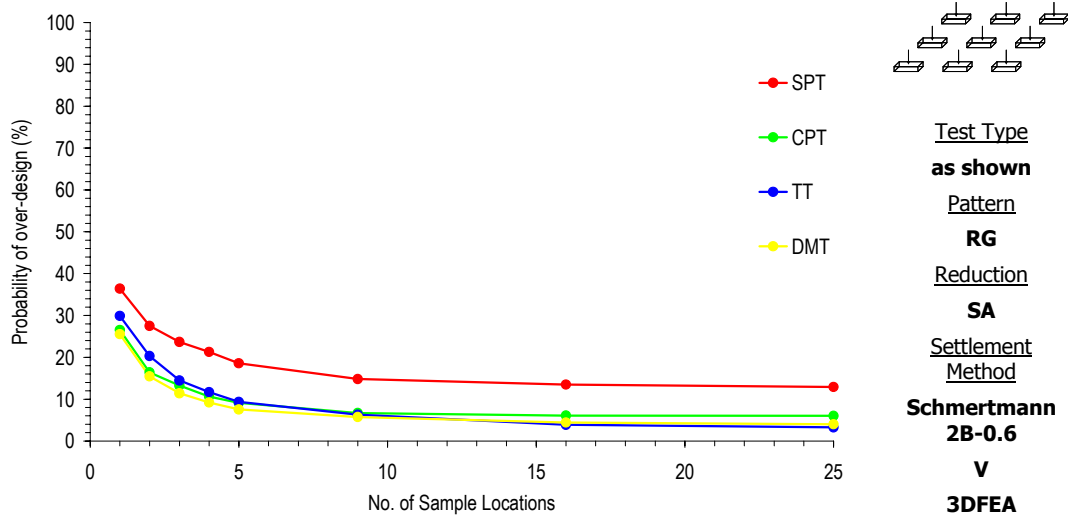


(c)

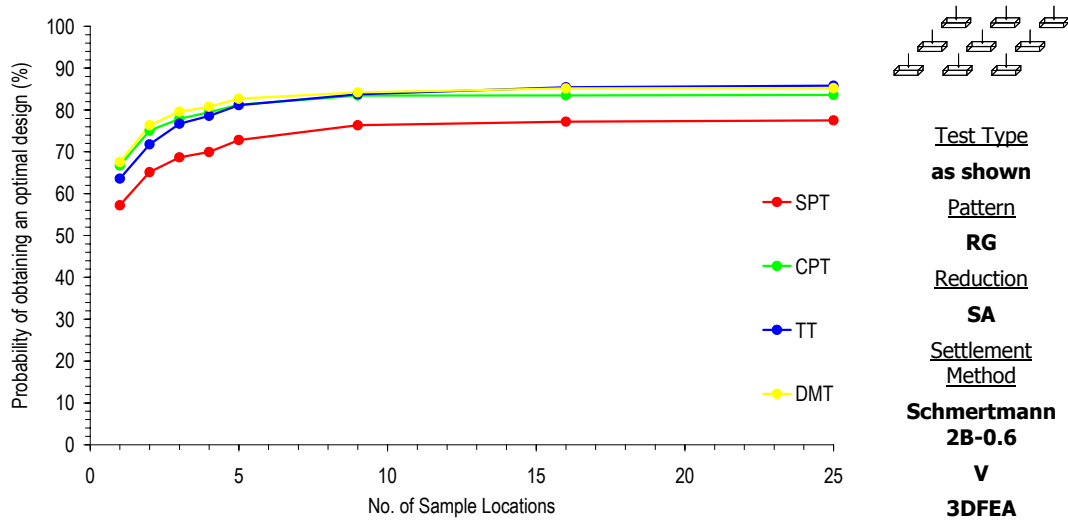
**Figure C-14 Effect of increased sampling with different test types on the probability of (a) under- and (b) over-design and (c) the probability of obtaining an optimal design, for a soil with a COV of 50% and a SOF of 1 m**



(a)

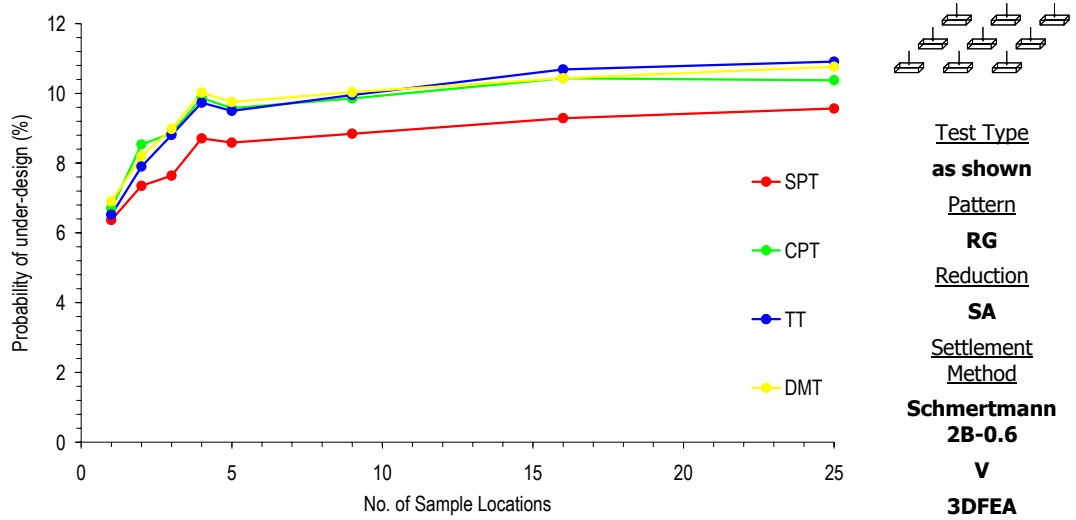


(b)

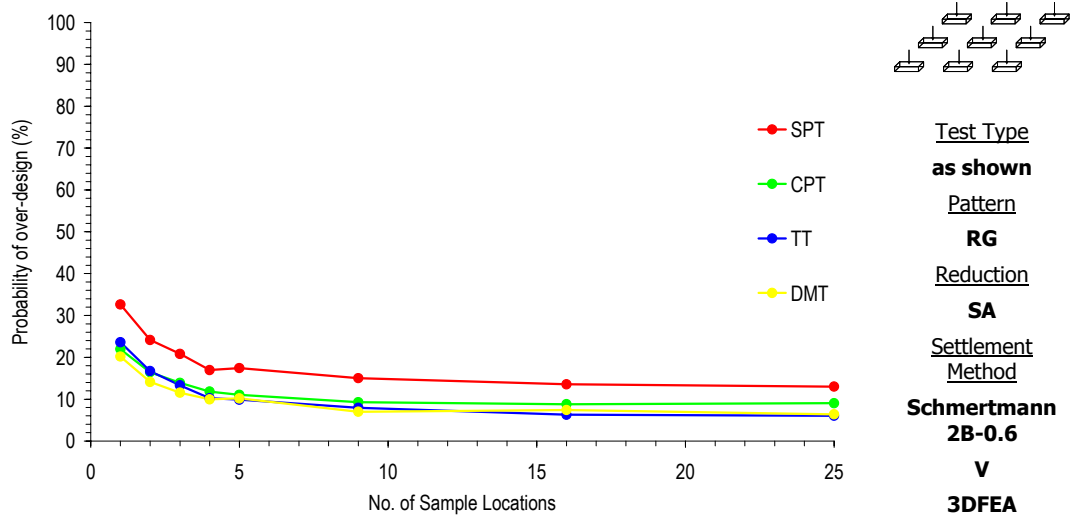


(c)

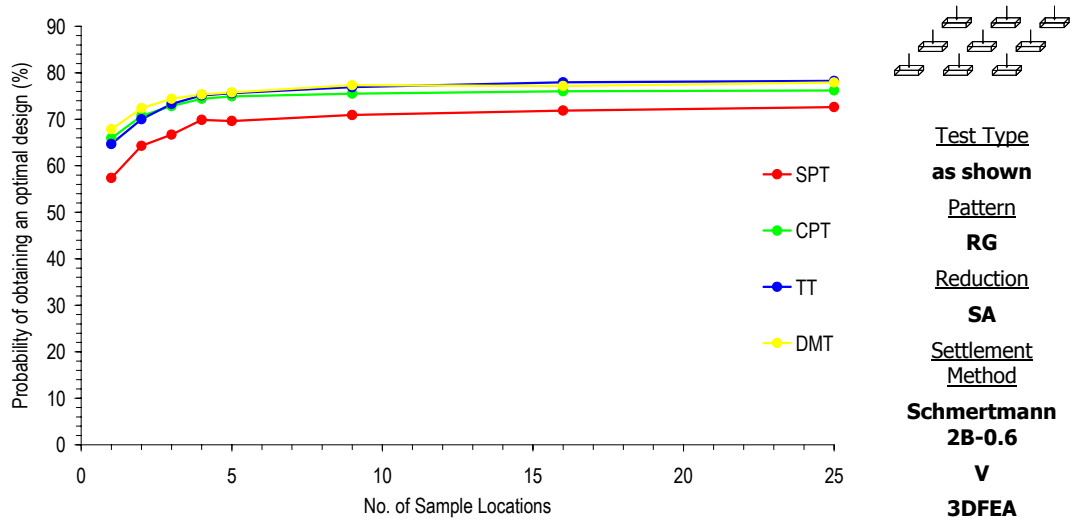
Figure C-15 Effect of increased sampling with different test types on the probability of (a) under- and (b) over-design and (c) the probability of obtaining an optimal design, for a soil COV of 50% and SOF of 4 m



(a)



(b)



(c)

**Figure C-16 Effect of increased sampling with different test types on the probability of (a) under- and (b) over-design and (c) the probability of obtaining an optimal design, for a soil COV of 50% and SOF of 32 m**

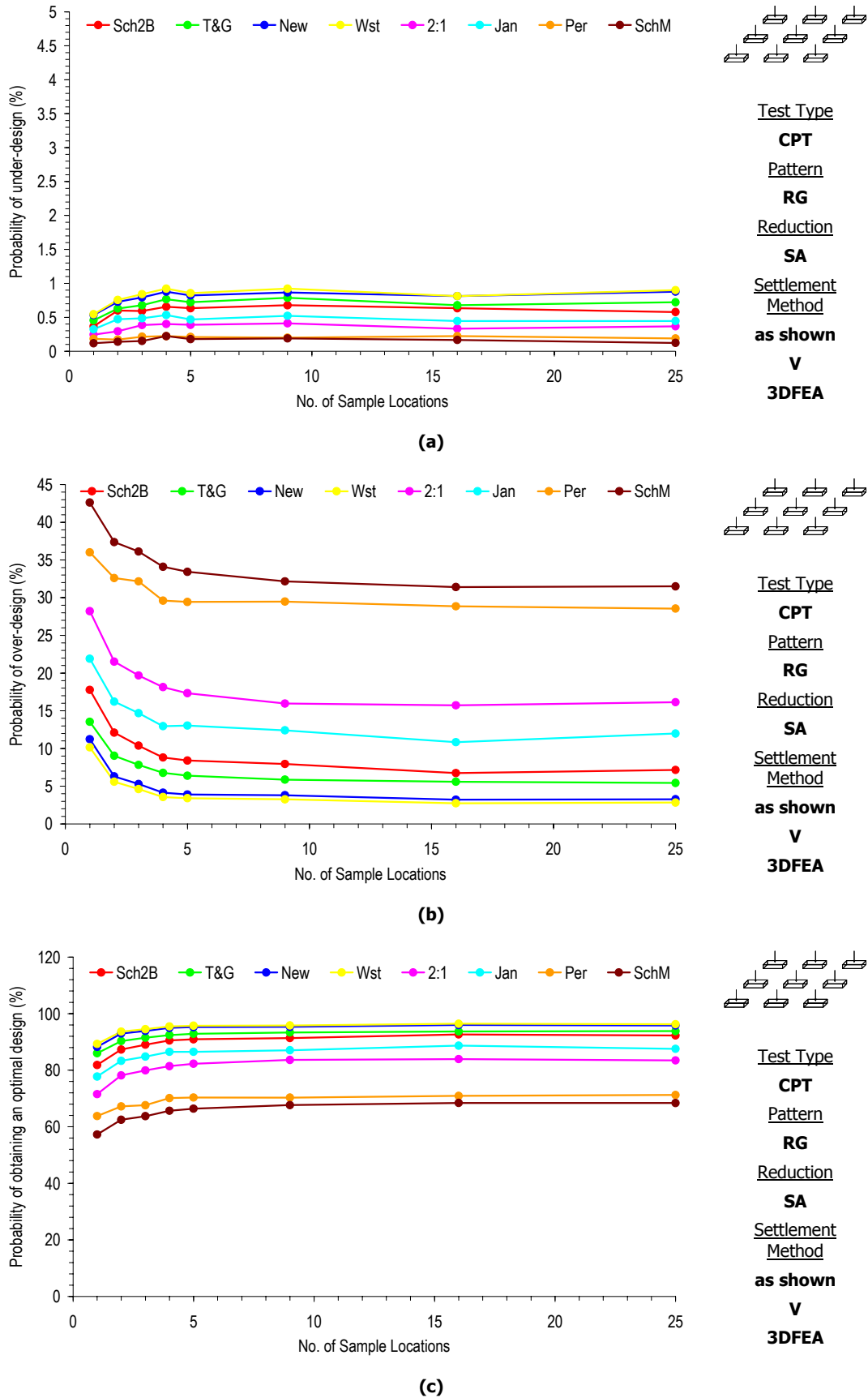


**Figure C-17 Effect of increased sampling and different prediction techniques on the probability of (a) under- and (b) over-design and (c) the probability of obtaining an optimal design, for a soil COV of 20% and SOF of 8 m**

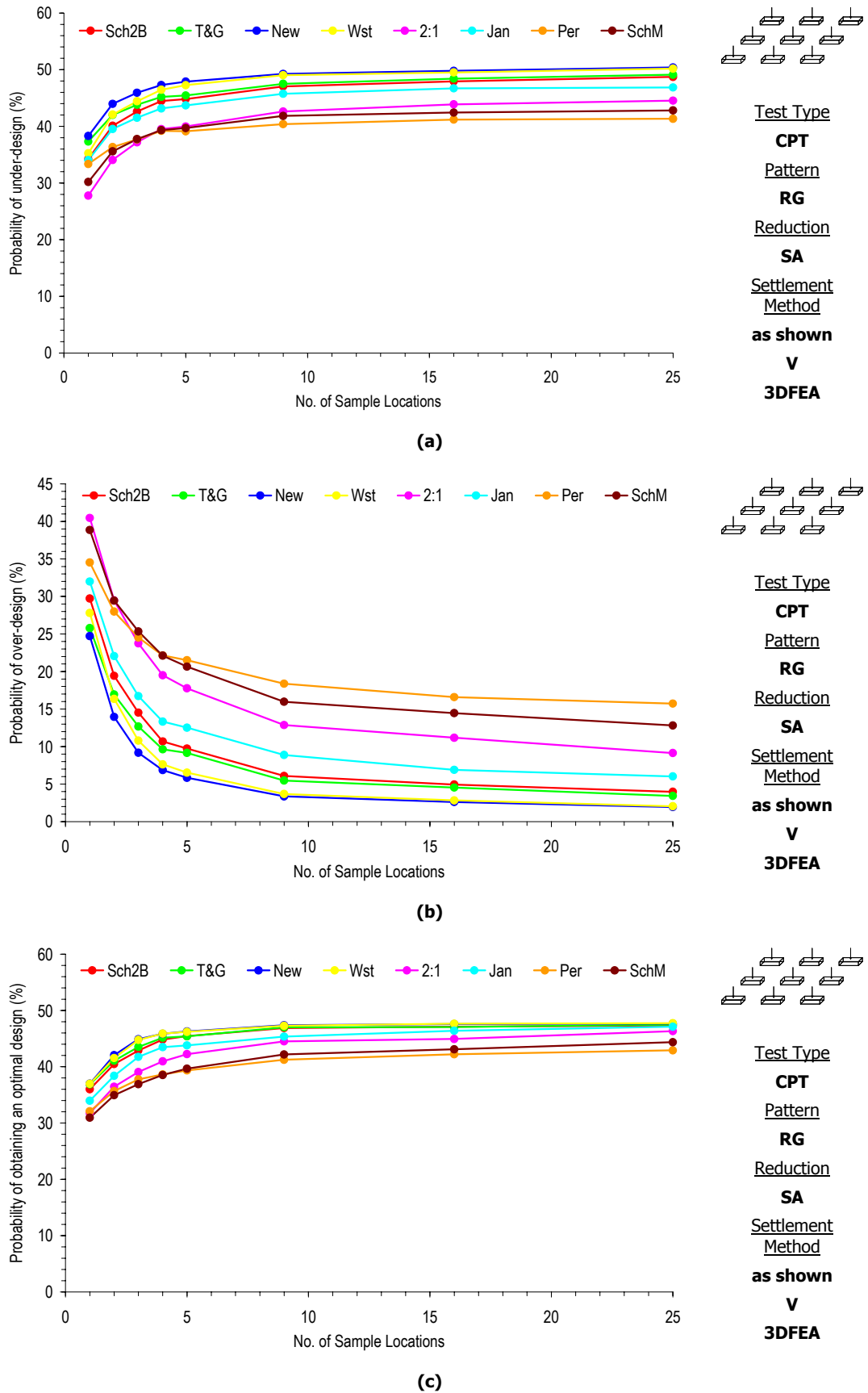


**Figure C-18** Effect of increased sampling and different prediction techniques on the probability of (a) under- and (b) over-design and (c) the probability of obtaining an optimal design, for a soil COV of 100% and SOF of 8 m

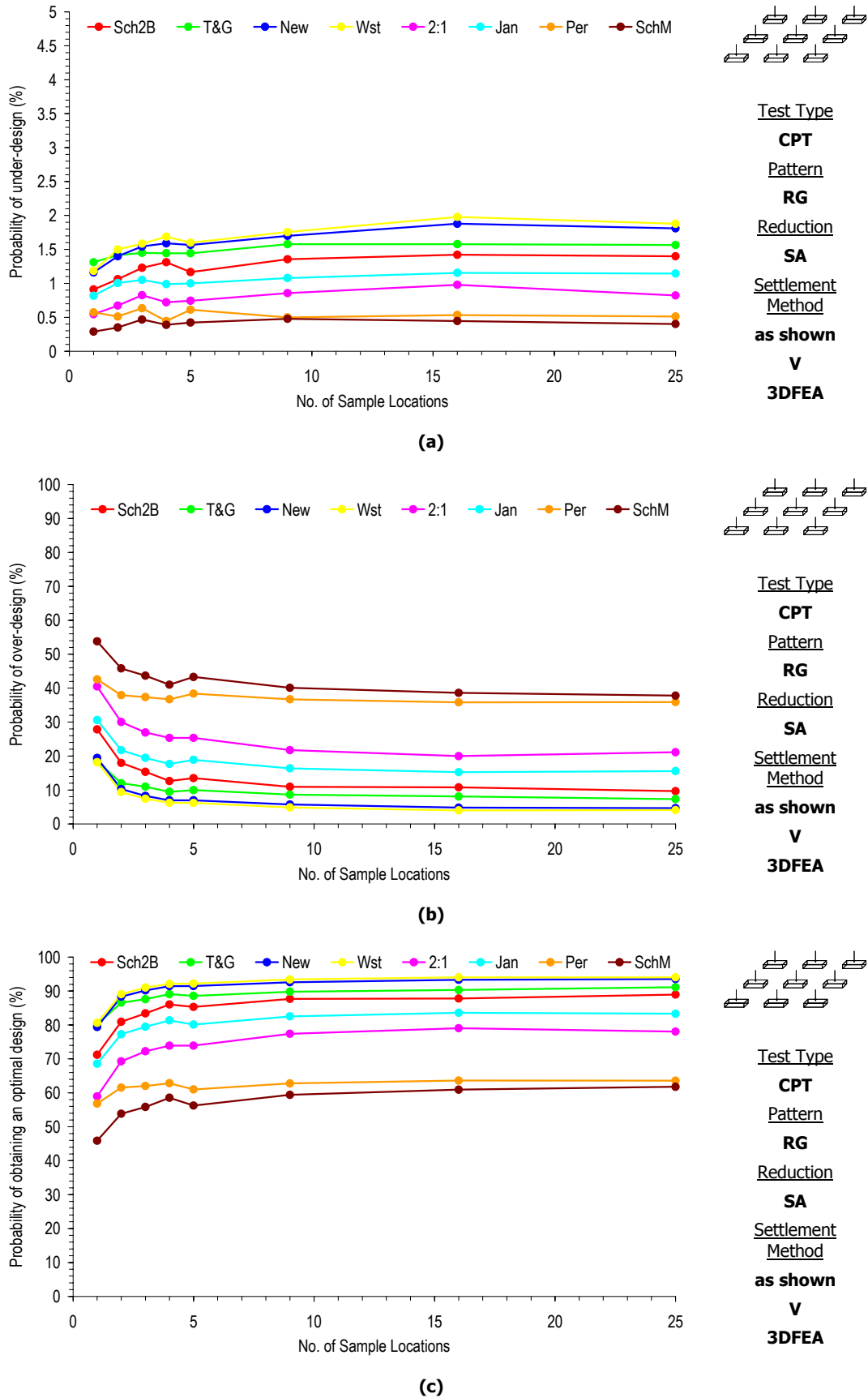


**Figure C-19** Effect of increased sampling and different prediction techniques on the probability of (a) under- and (b) over-design and (c) the probability of obtaining an optimal design, for a soil COV of 50% and SOF of 1 m



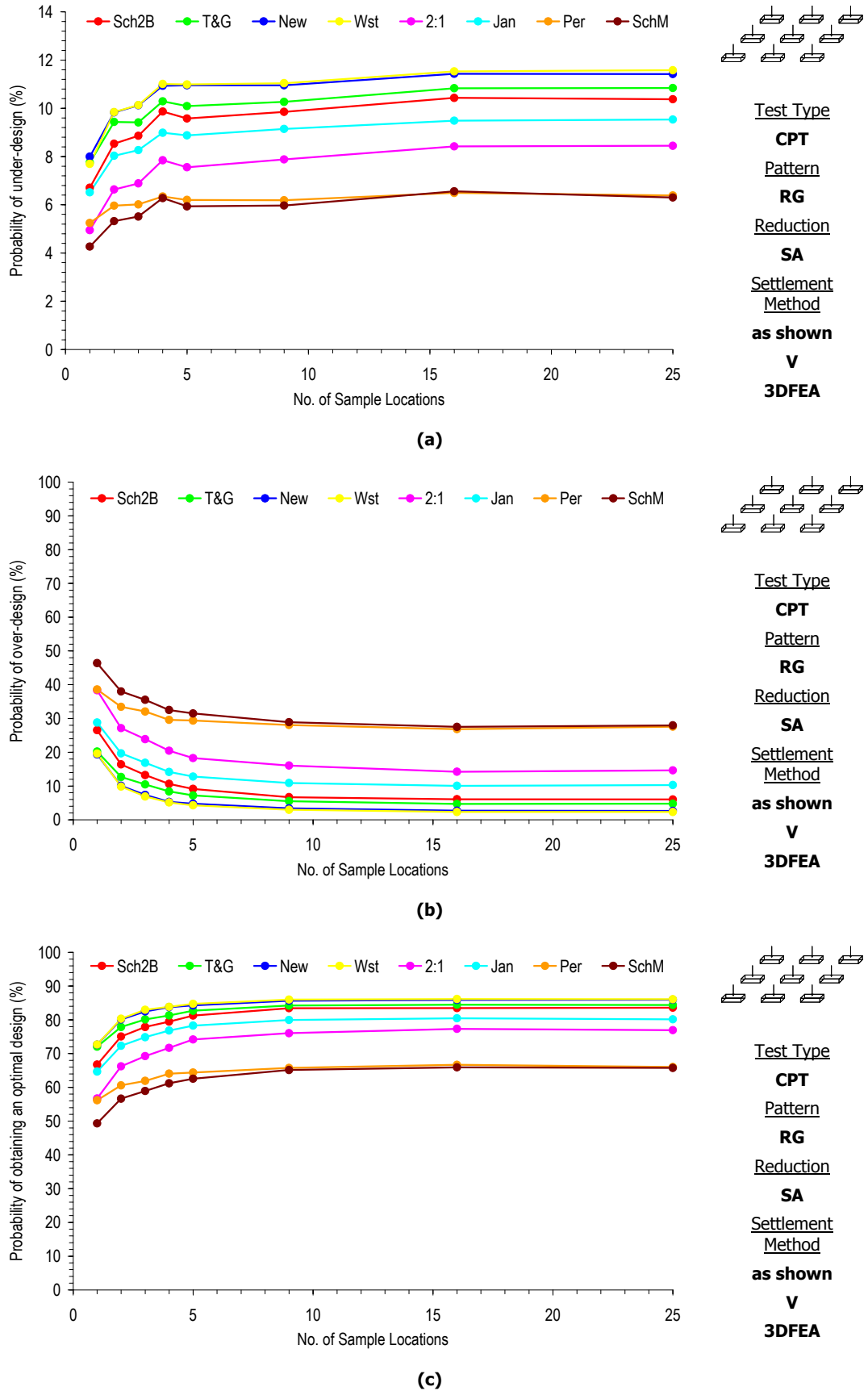


**Figure C-20 Effect of increased sampling and different prediction techniques on the probability of (a) under- and (b) over-design and (c) the probability of obtaining an optimal design, for a soil COV of 50% and SOF of 4 m**

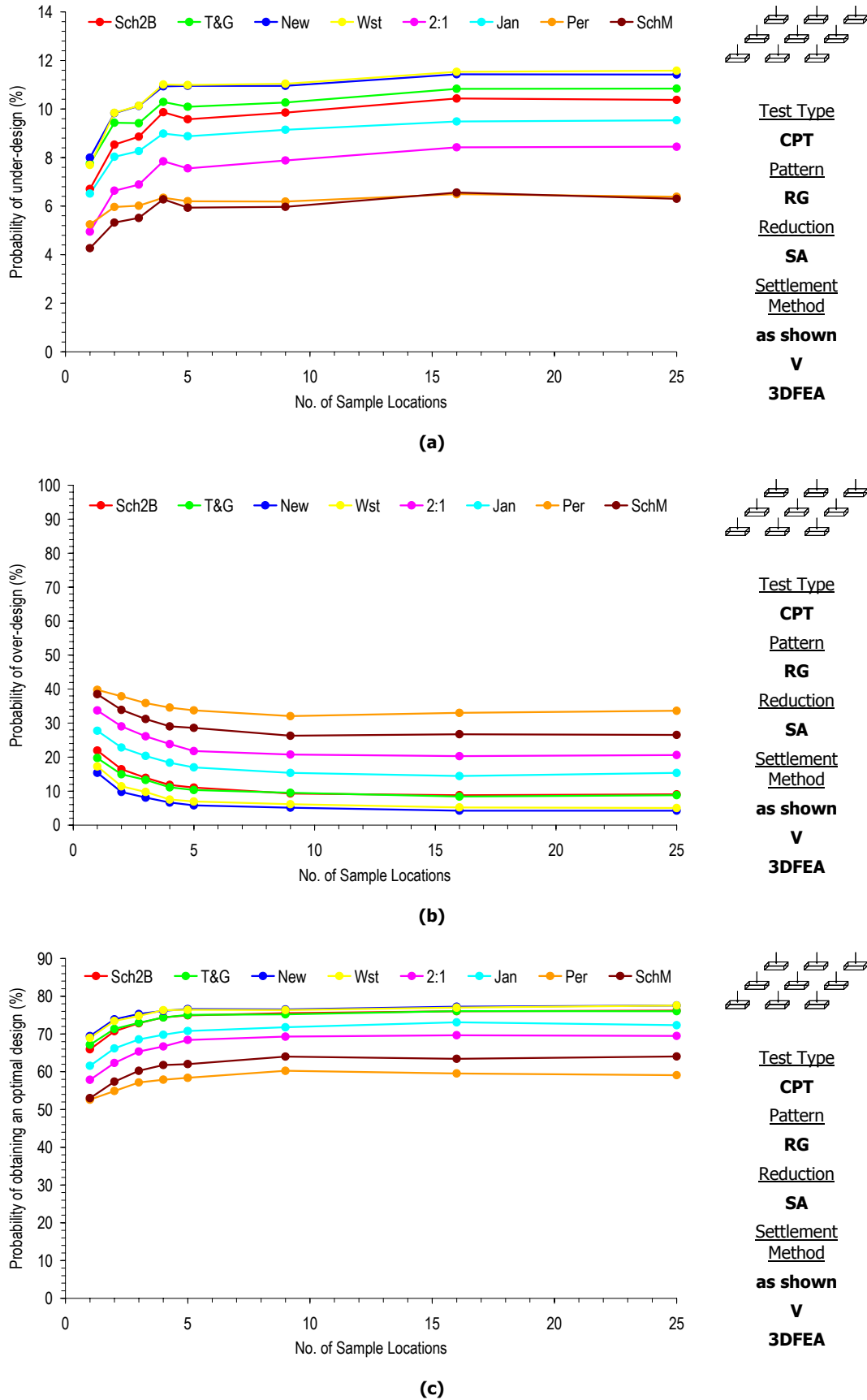


**Figure C-21** Effect of increased sampling and different prediction techniques on the probability of (a) under- and (b) over-design and (c) the probability of obtaining an optimal design, for a soil COV of 50% and SOF of 32 m

## **Appendix D Average Design Error**

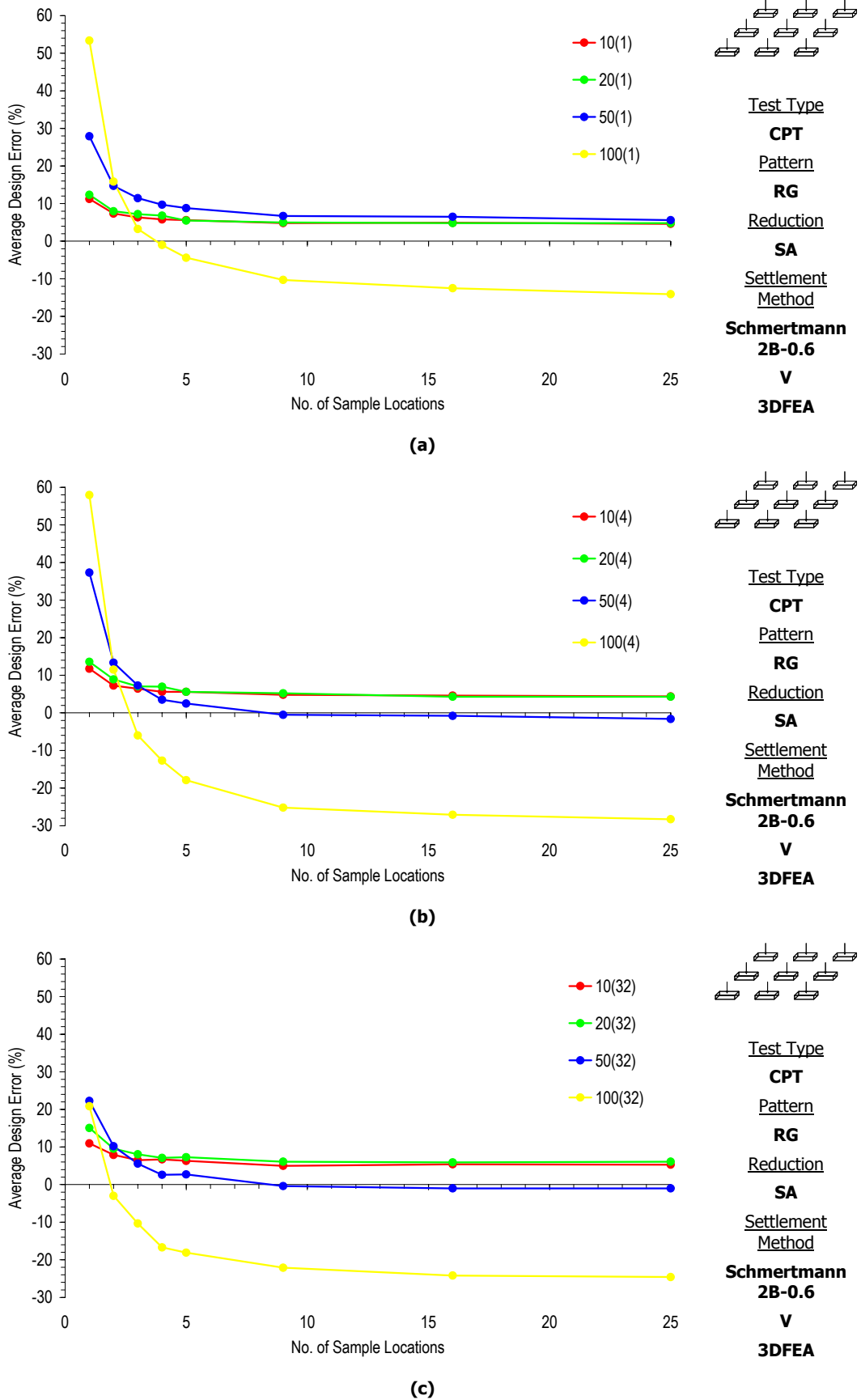
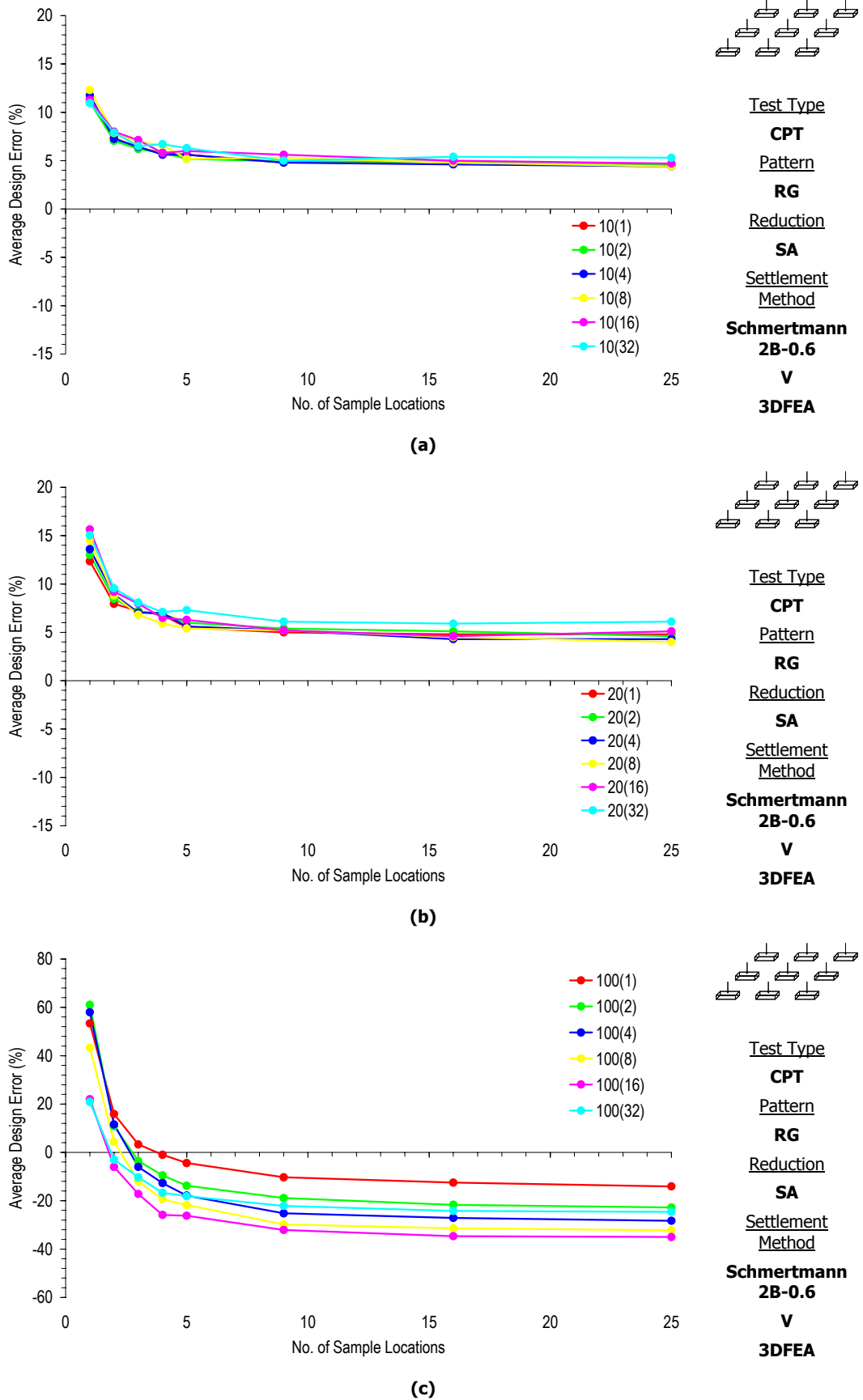


Figure D-1 Effect of increased sampling on the average design error for a soil with an increasing COV and a SOF of (a) 1 m, (b) 4 m and (c) 32 m



**Figure D-2 Effect of increased sampling on the average design error for a soil with an increasing SOF and a COV of (a) 10%, (b) 20% and (c) 100%**

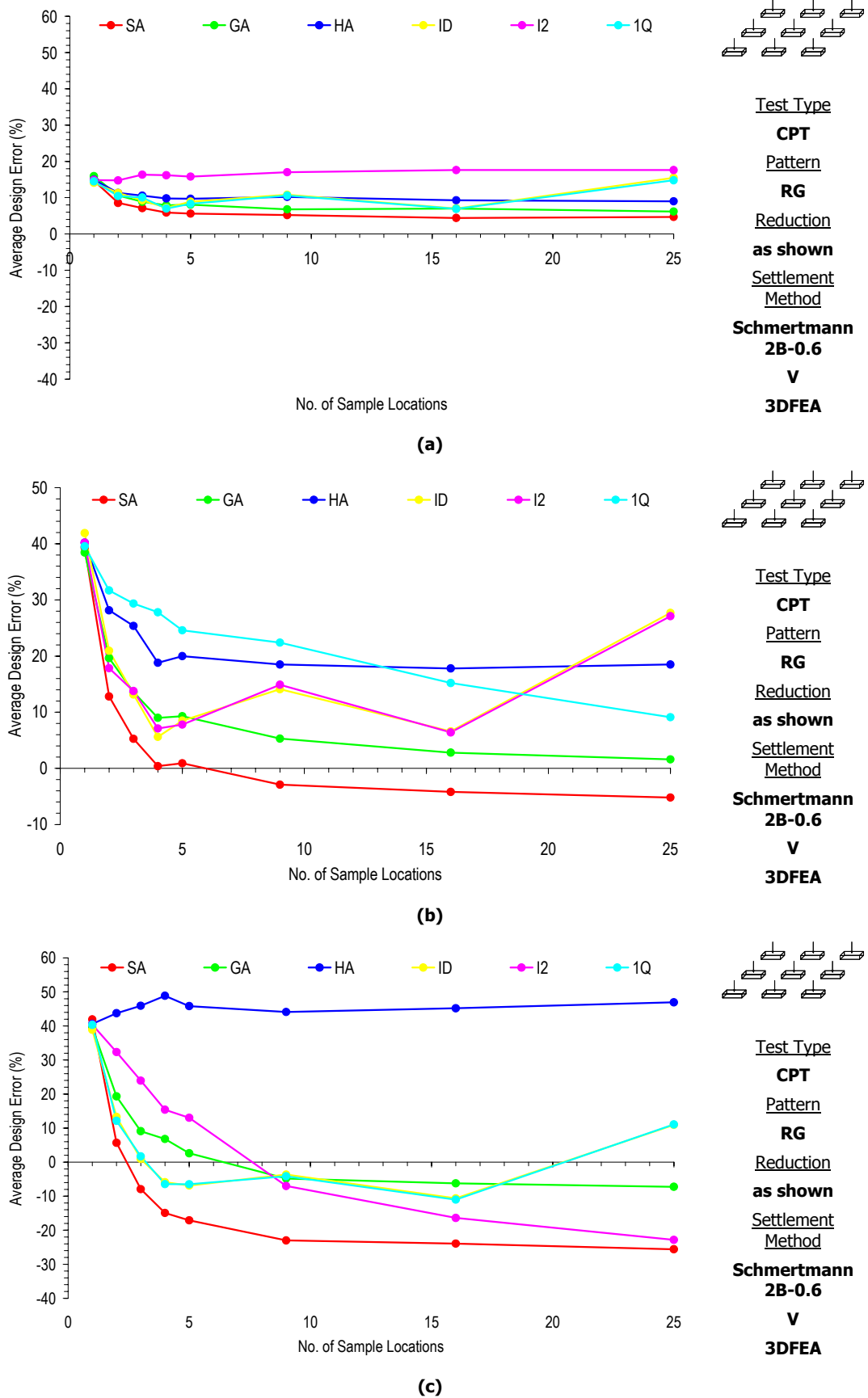
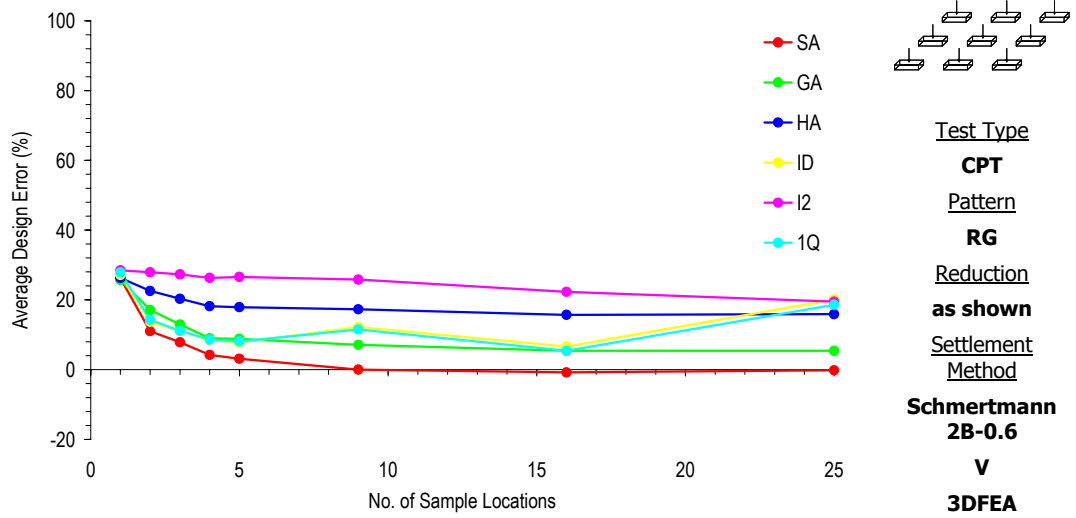
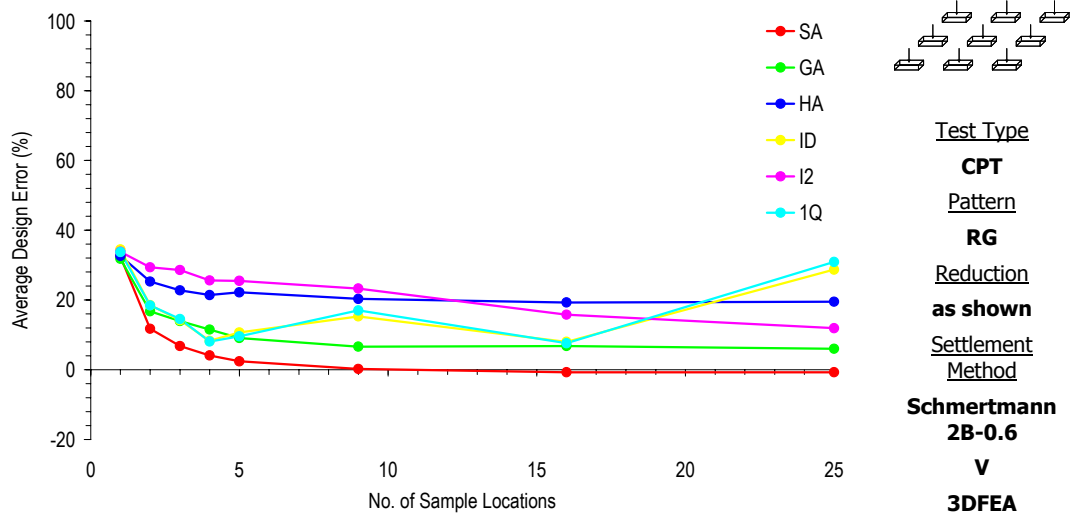
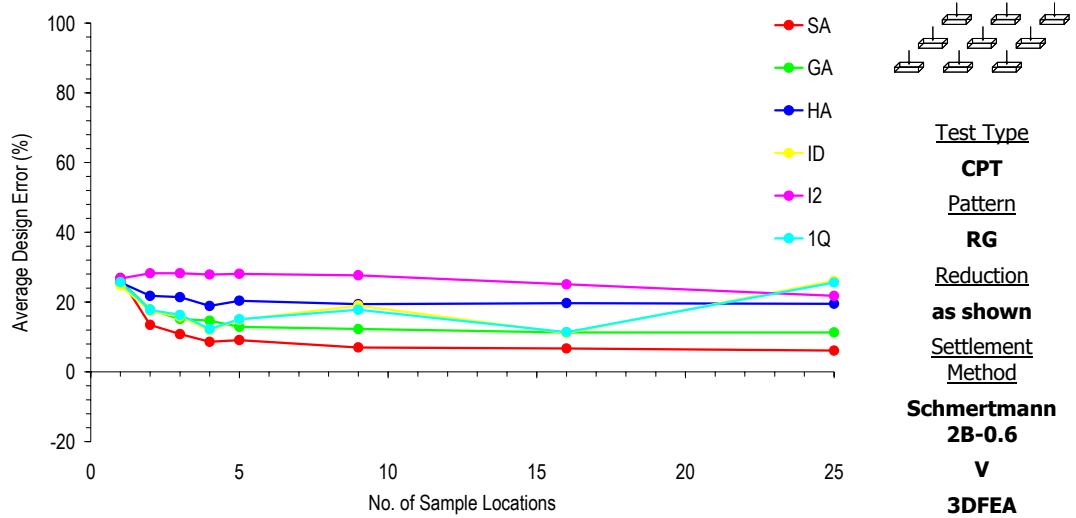


Figure D-3 Effect of increased sampling with different reduction techniques on the average design error for a soil SOF of 8 m and a COV of (a) 10%, (b) 20% and (c) 100%



**Figure D-4** Effect of increased sampling with different reduction techniques on the average design error for a soil with a COV of 50% and a SOF of (a) 1 m, (b) 4 m and (c) 32 m

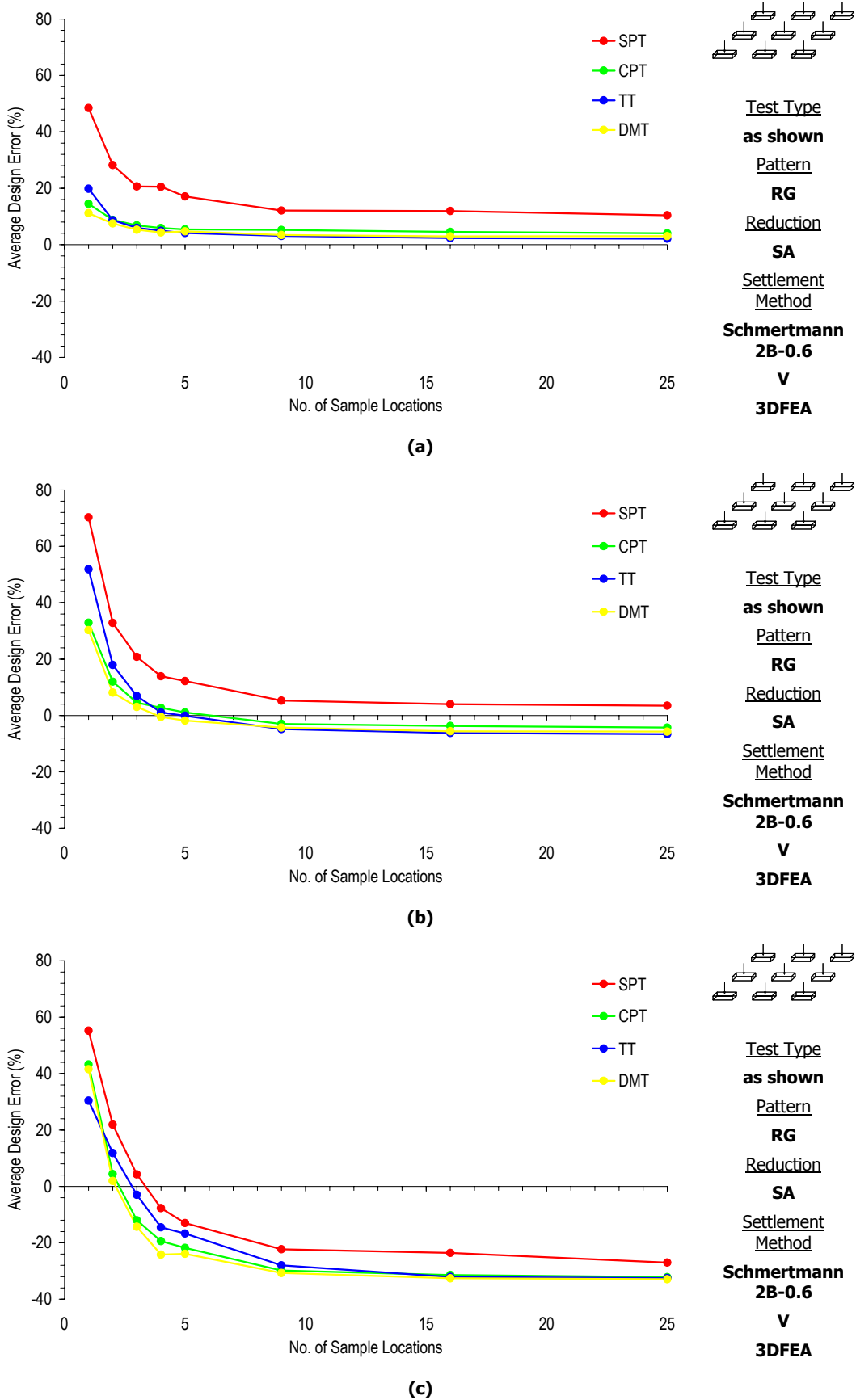
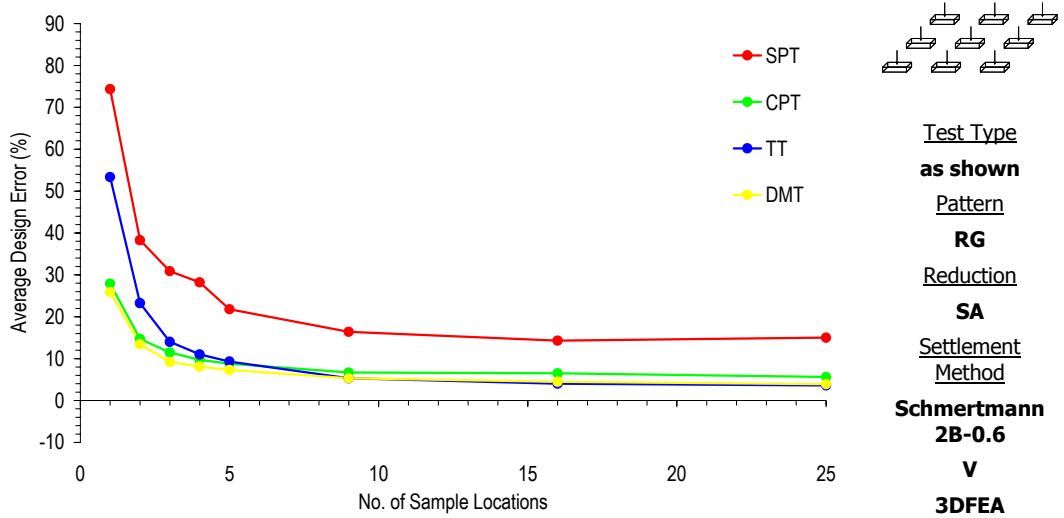
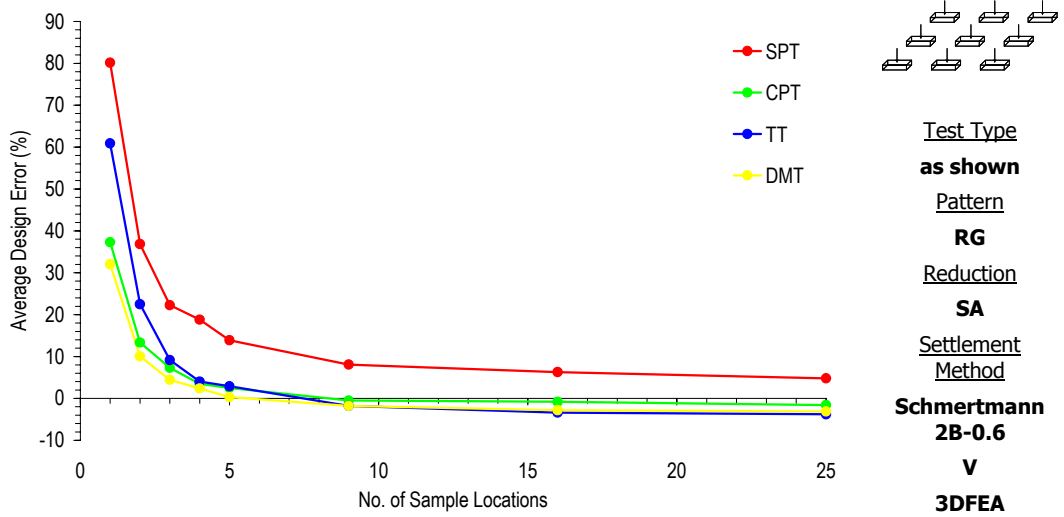


Figure D-5 Effect of increased sampling with different test types and the SA on the average design error for a soil with a SOF of 8 m and a COV of (a) 10%, (b) 20% and (c) 100%

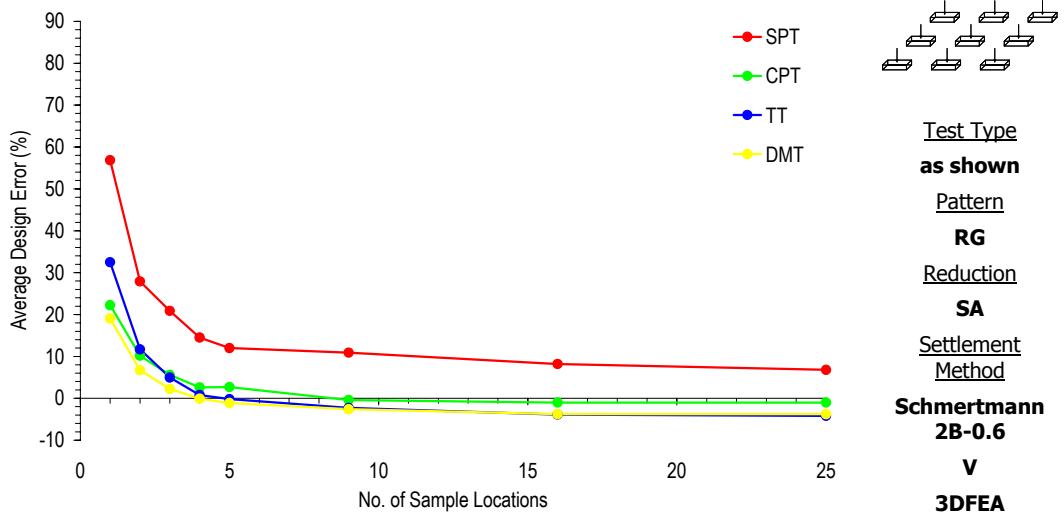




(a)

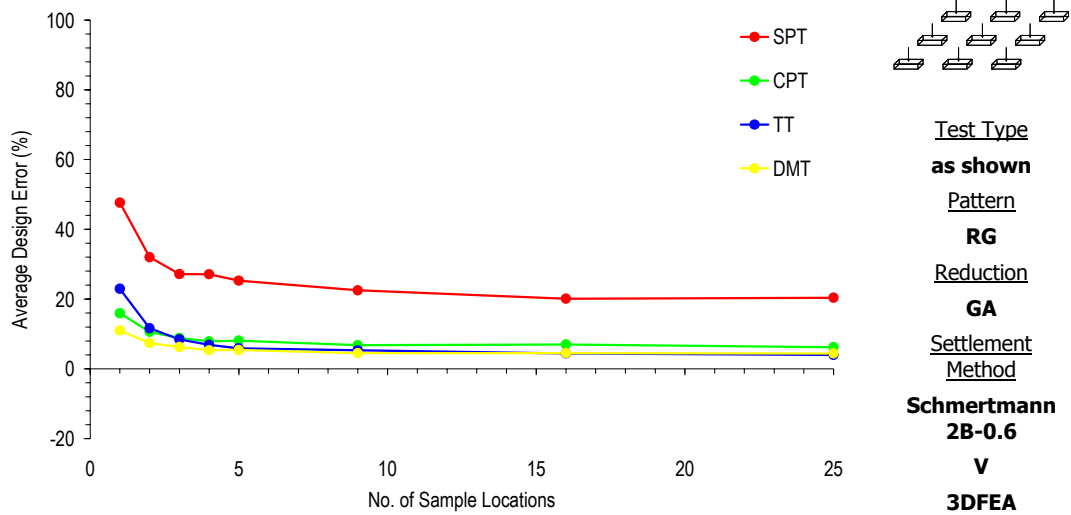


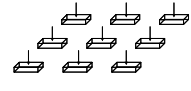
(b)



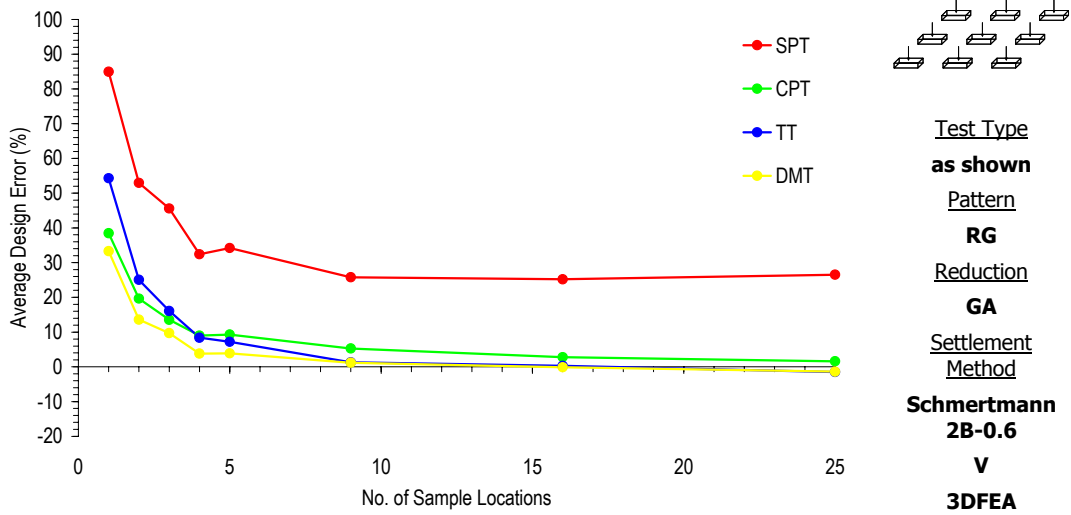
(c)

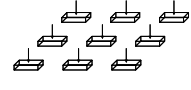
**Figure D-6** Effect of increased sampling with different test types and the SA on the average design error for a soil with a COV of 50% and a COV of (a) 1 m, (b) 4 m and (c) 32 m



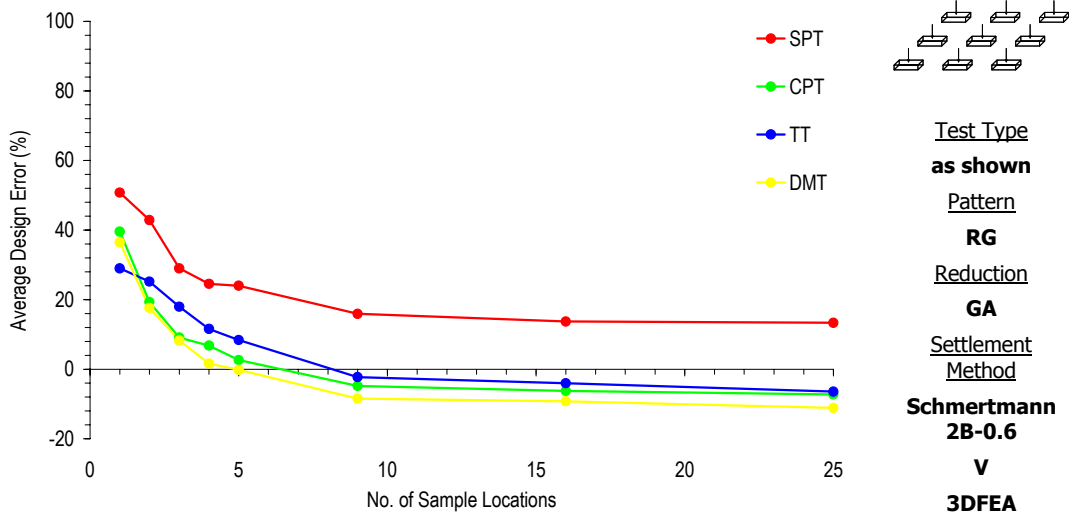
  
 Test Type  
**as shown**  
 Pattern  
**RG**  
 Reduction  
**GA**  
 Settlement Method  
**Schmertmann 2B-0.6**  
**V**  
**3DFEA**

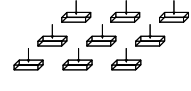
(a)



  
 Test Type  
**as shown**  
 Pattern  
**RG**  
 Reduction  
**GA**  
 Settlement Method  
**Schmertmann 2B-0.6**  
**V**  
**3DFEA**

(b)



  
 Test Type  
**as shown**  
 Pattern  
**RG**  
 Reduction  
**GA**  
 Settlement Method  
**Schmertmann 2B-0.6**  
**V**  
**3DFEA**

(c)

**Figure D-7 Effect of increased sampling with different test types and the GA on the average design error for a soil with a SOF of 8 m and a COV of (a) 10%, (b) 20% and (c) 100%**

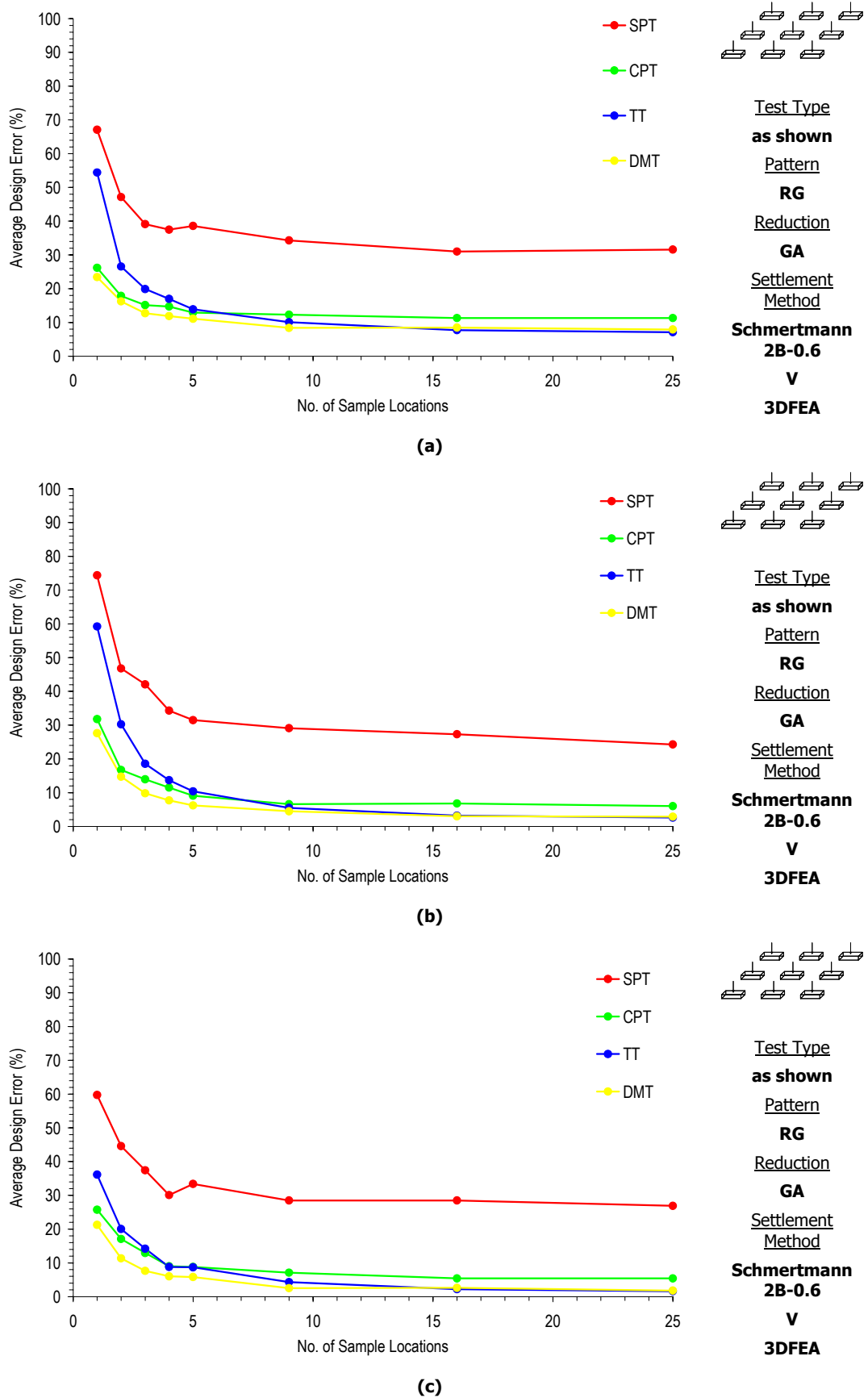


Figure D-8 Effect of increased sampling with different test types and the GA on the average design error for a soil with a COV of 50% and a COV of (a) 1 m, (b) 4 m and (c) 32 m

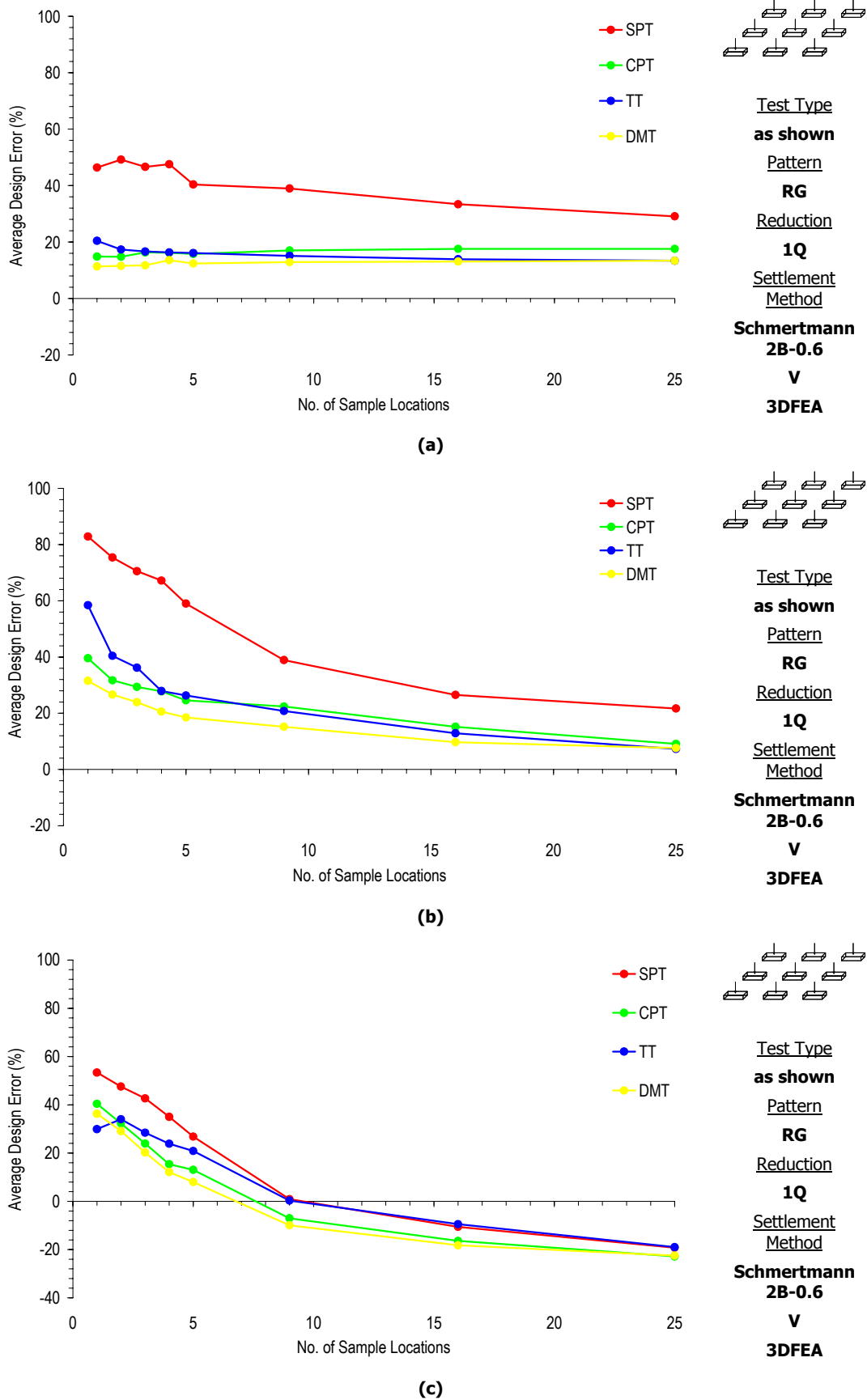


Figure D-9 Effect of increased sampling with different test types and the 1Q on the average design error for a soil with a SOF of 8 m and a COV of (a) 10%, (b) 20% and (c) 100%

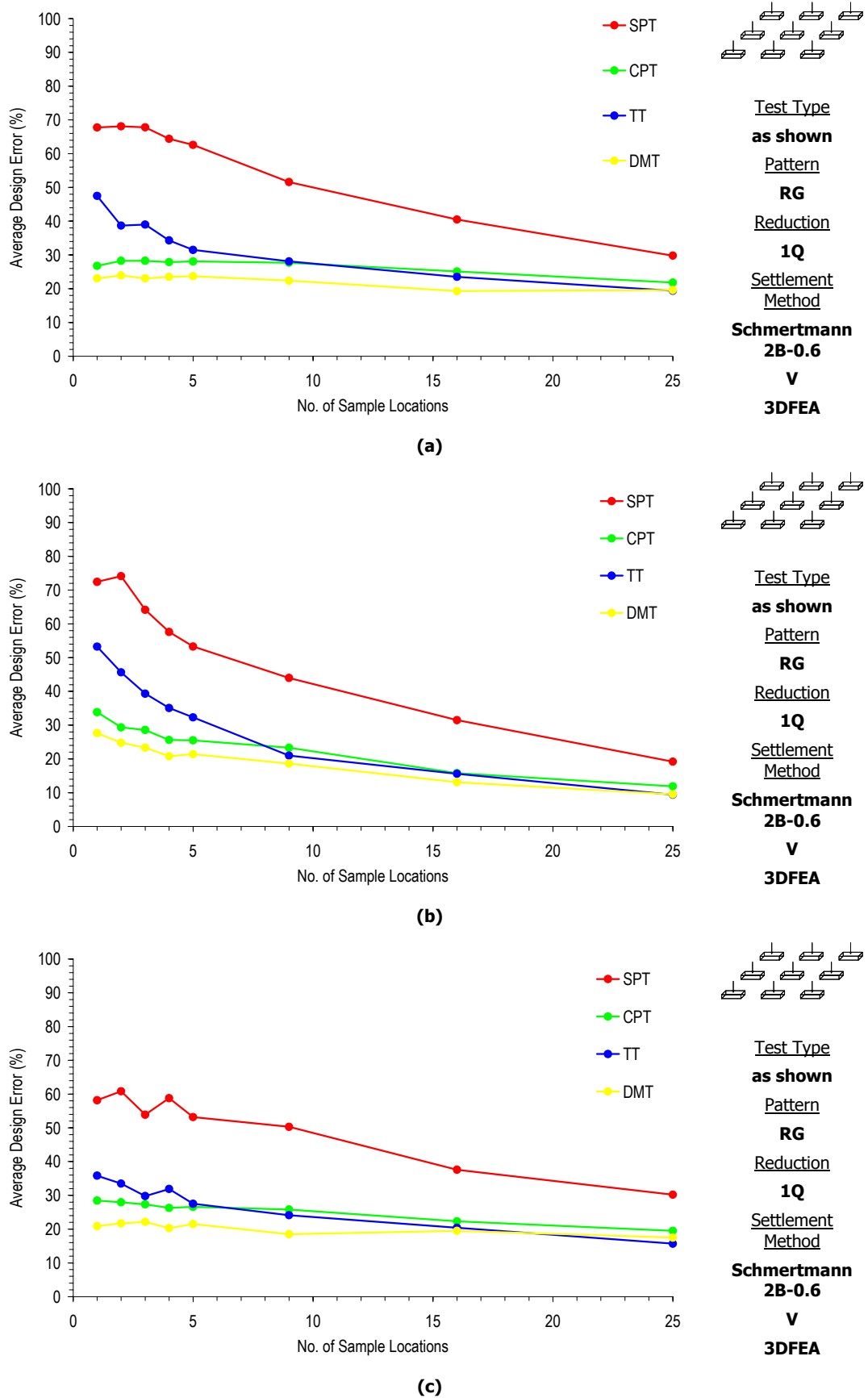


Figure D-10 Effect of increased sampling with different test types and the 1Q on the average design error for a soil with a COV of 50% and a COV of (a) 1 m, (b) 4 m and (c) 32 m

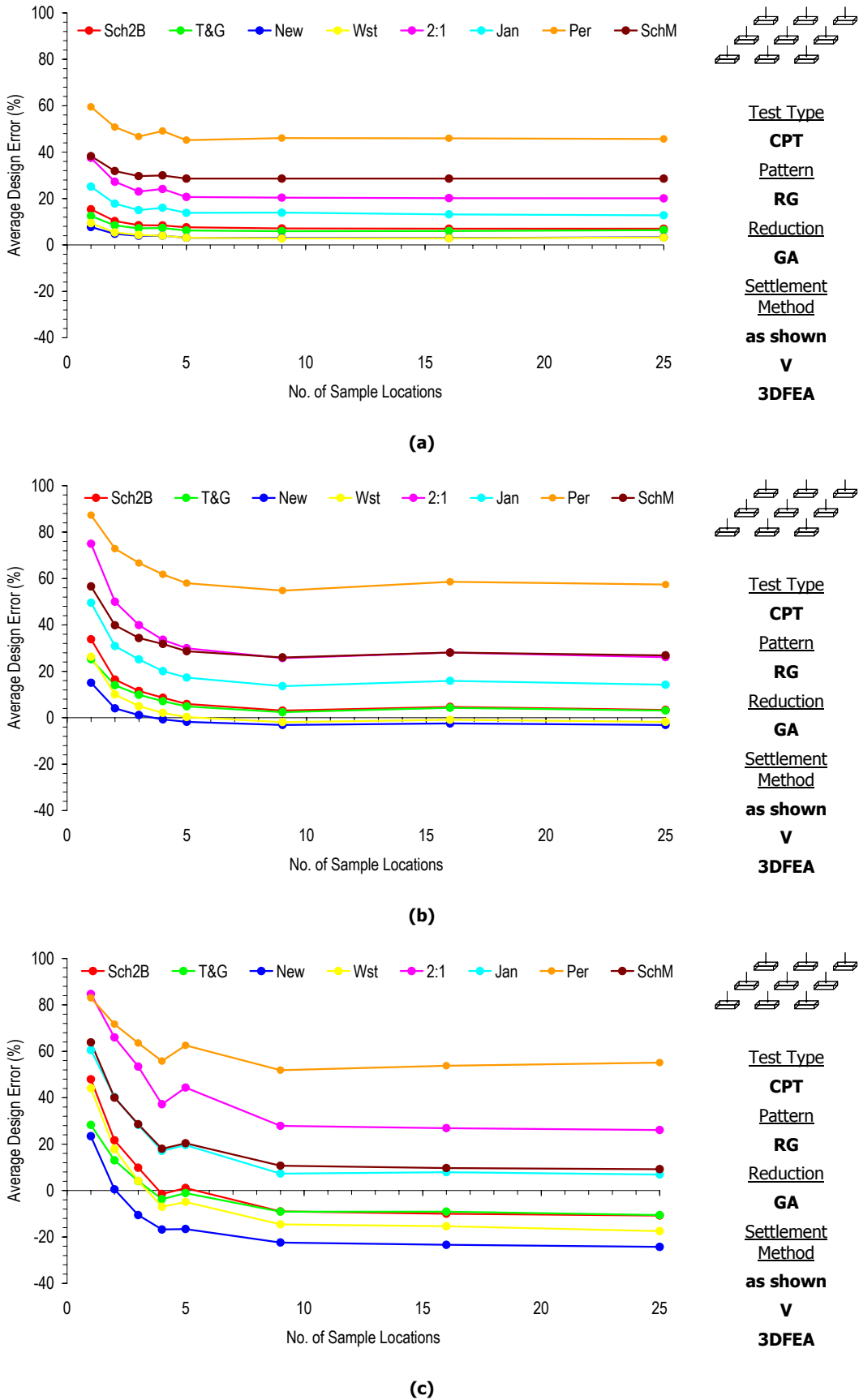
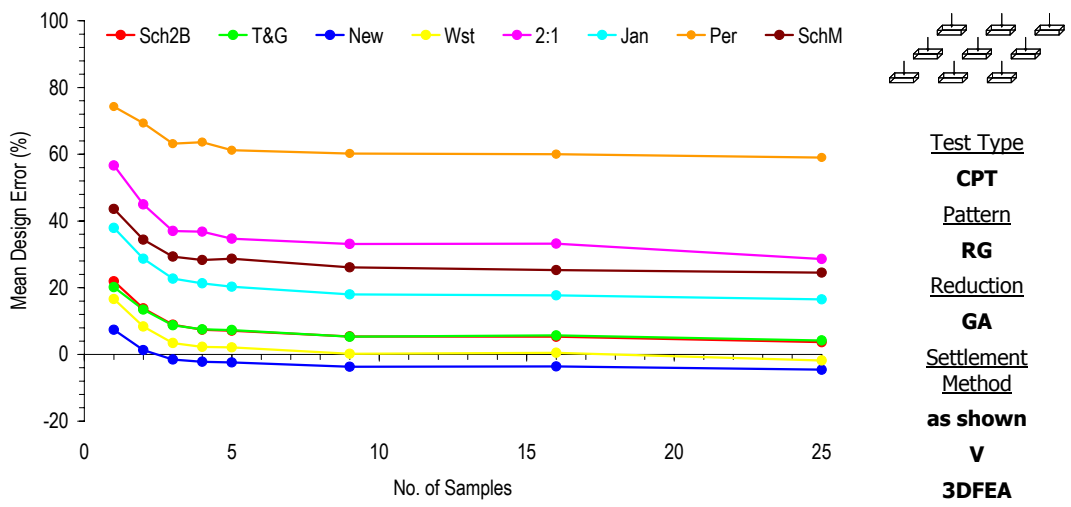
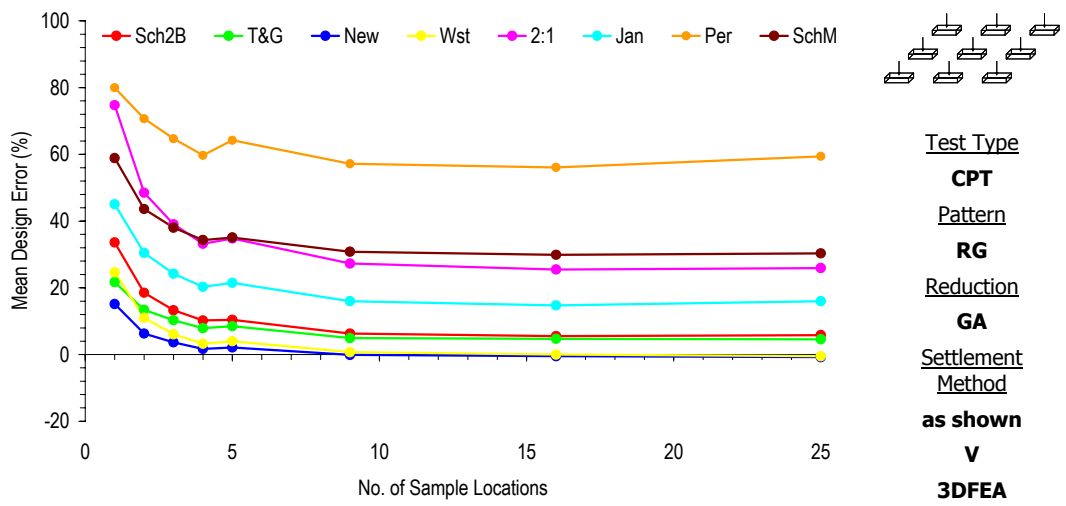
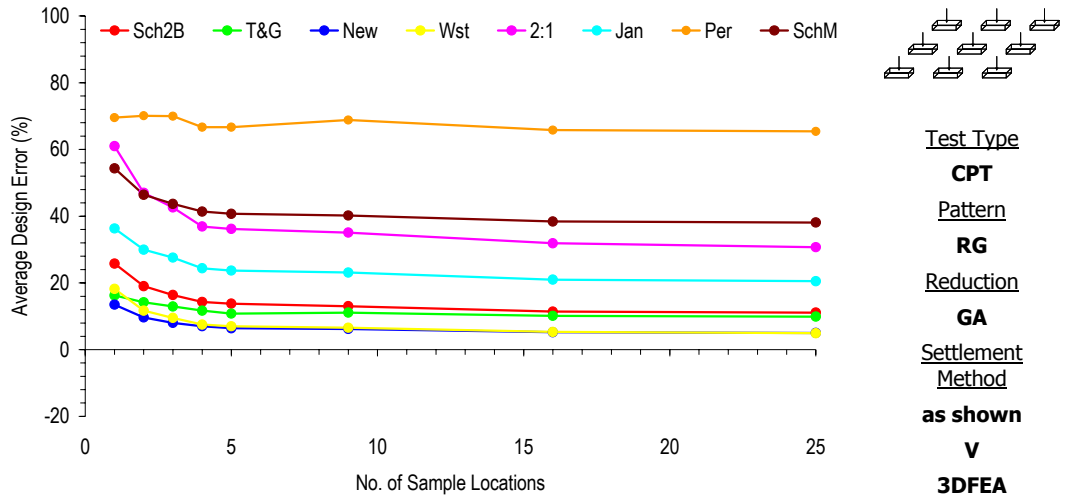
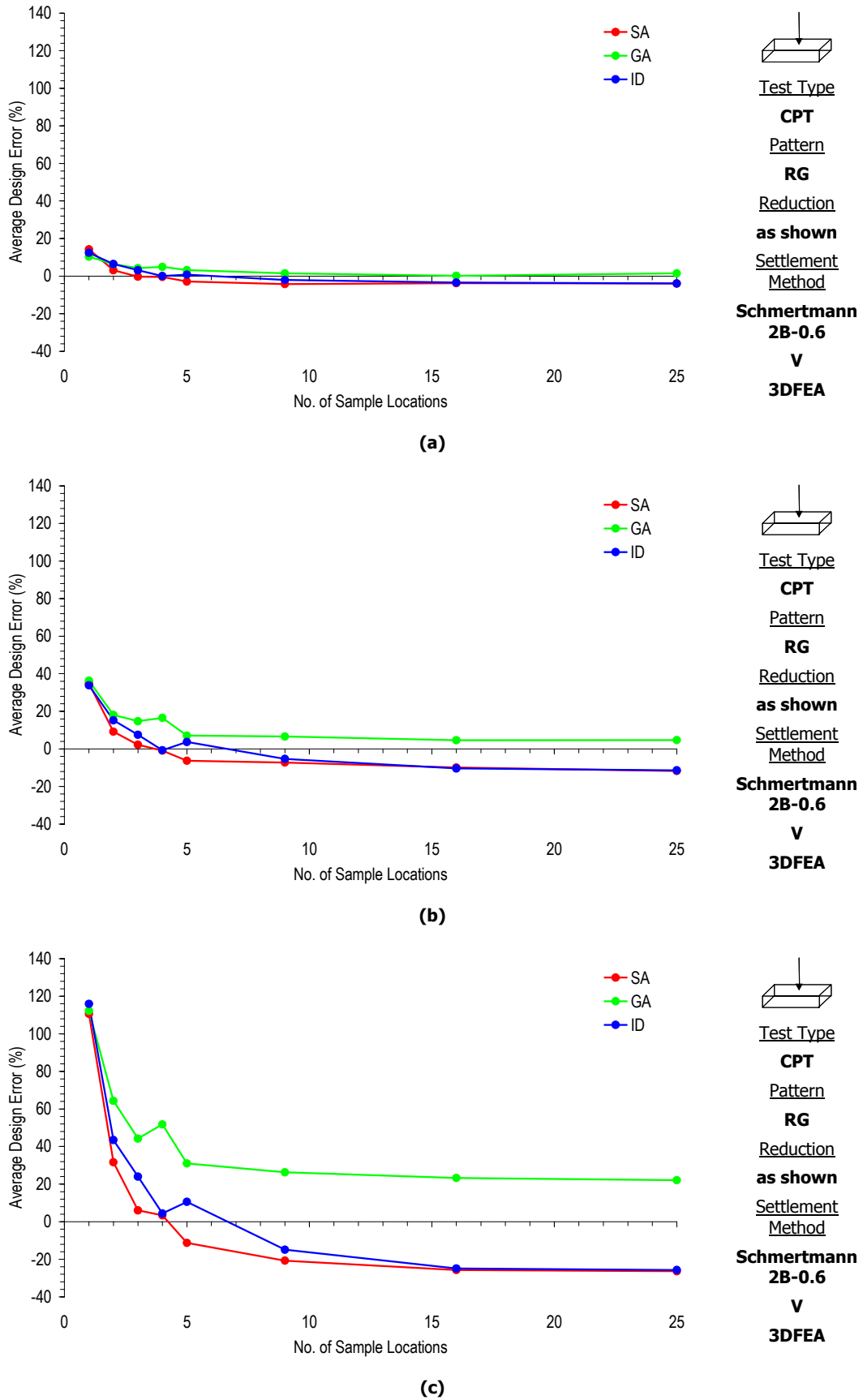


Figure D-11 Effect of increased sampling using the GA and different settlement prediction techniques on the average design error, for a soil SOF of 8 m and COV of (a) 20%, (b) 50% and (c) 100%

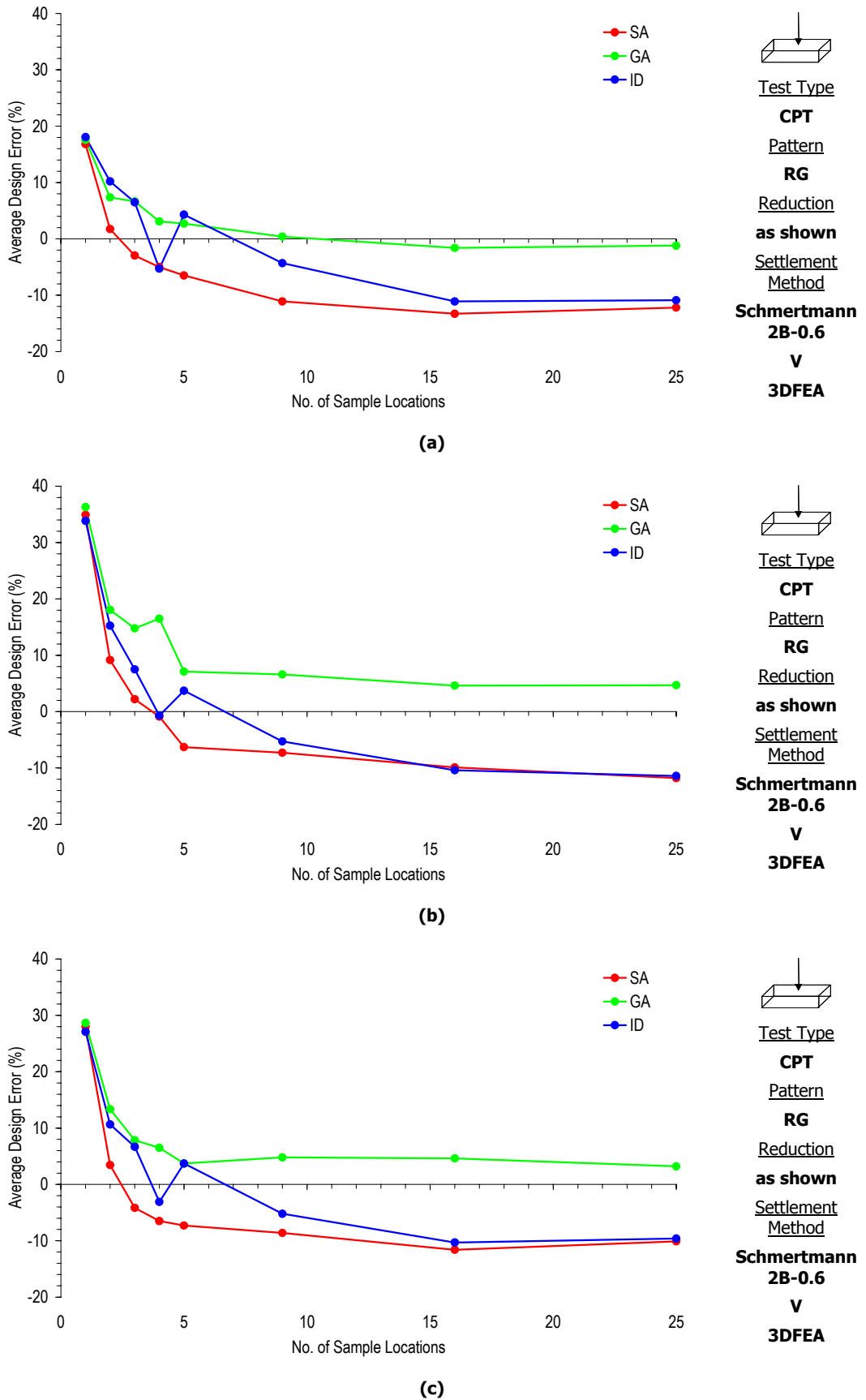


**Figure D-12 Effect of increased sampling using the GA and different settlement prediction techniques on the average design error, for a soil COV of 50% and SOF of (a) 1 m, (b) 4 m and (c) 32 m**



**Figure D-13 Effect of increased sampling with different reduction techniques on the average design error of the single pad foundation system, for a soil SOF of 4 m and COV of (a) 20%, (b) 50% and (c) 100%**

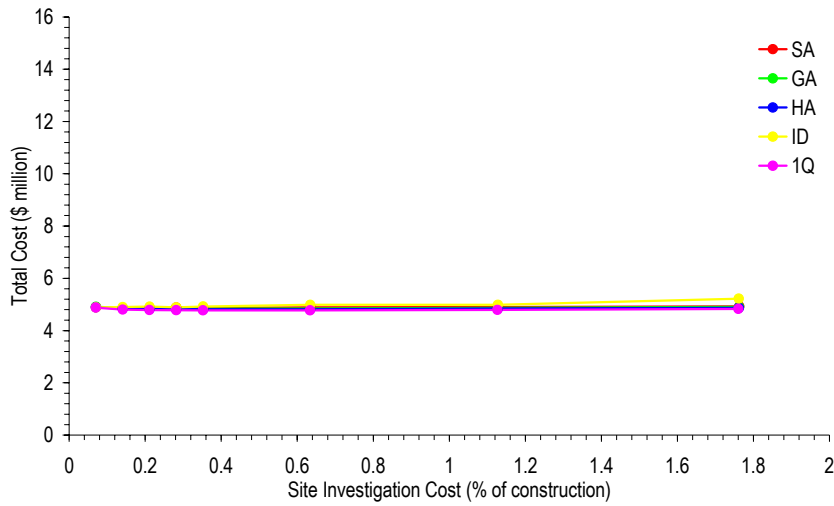
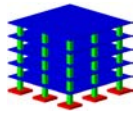




**Figure D-14** Effect of increased sampling with different reduction techniques on the average design error of the single pad foundation system, for a soil COV of 50% and SOF of (a) 1 m, (b) 4 m and (c) 16 m

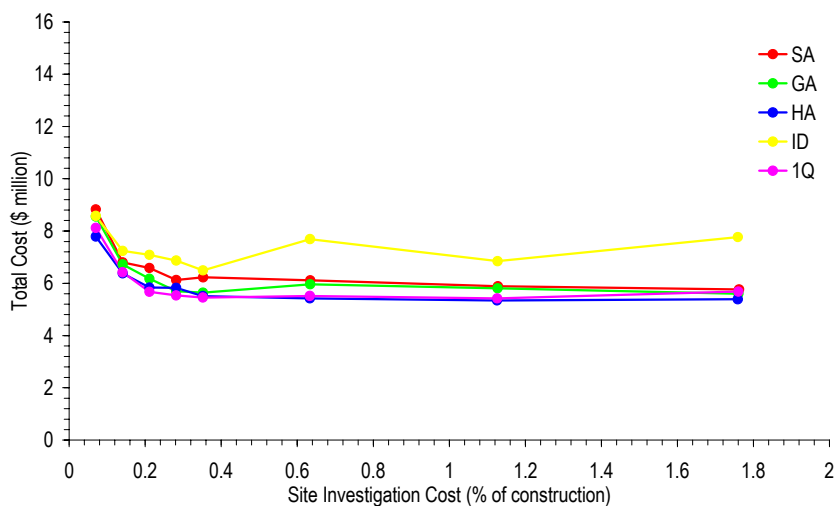
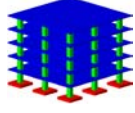


## **Appendix E   Foundation Design Costs**

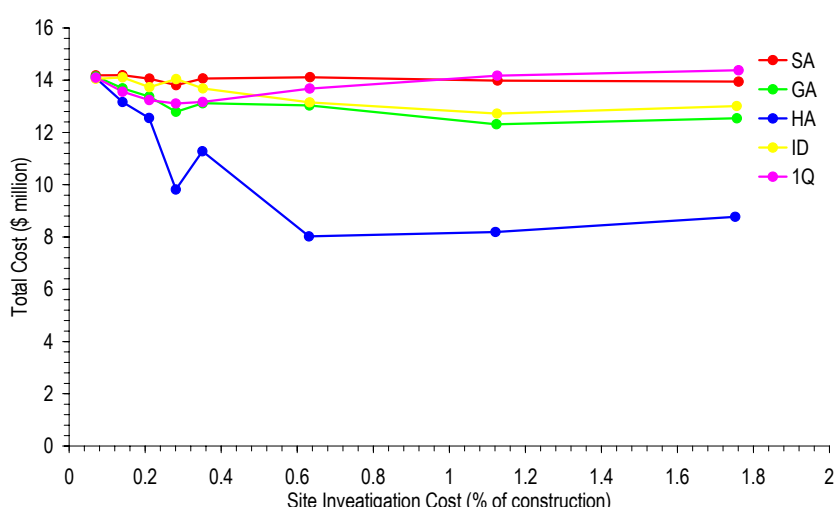
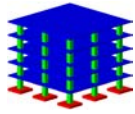
Test Type  
**CPT**  
 Pattern  
**RG**  
 Reduction  
**as shown**  
 Settlement Method  
**Schmertmann 2B-0.6**  
 &  
**Schmertmann 2B-0.6 (InfReg)**

(a)

Test Type  
**CPT**  
 Pattern  
**RG**  
 Reduction  
**as shown**  
 Settlement Method  
**Schmertmann 2B-0.6**  
 &  
**Schmertmann 2B-0.6 (InfReg)**

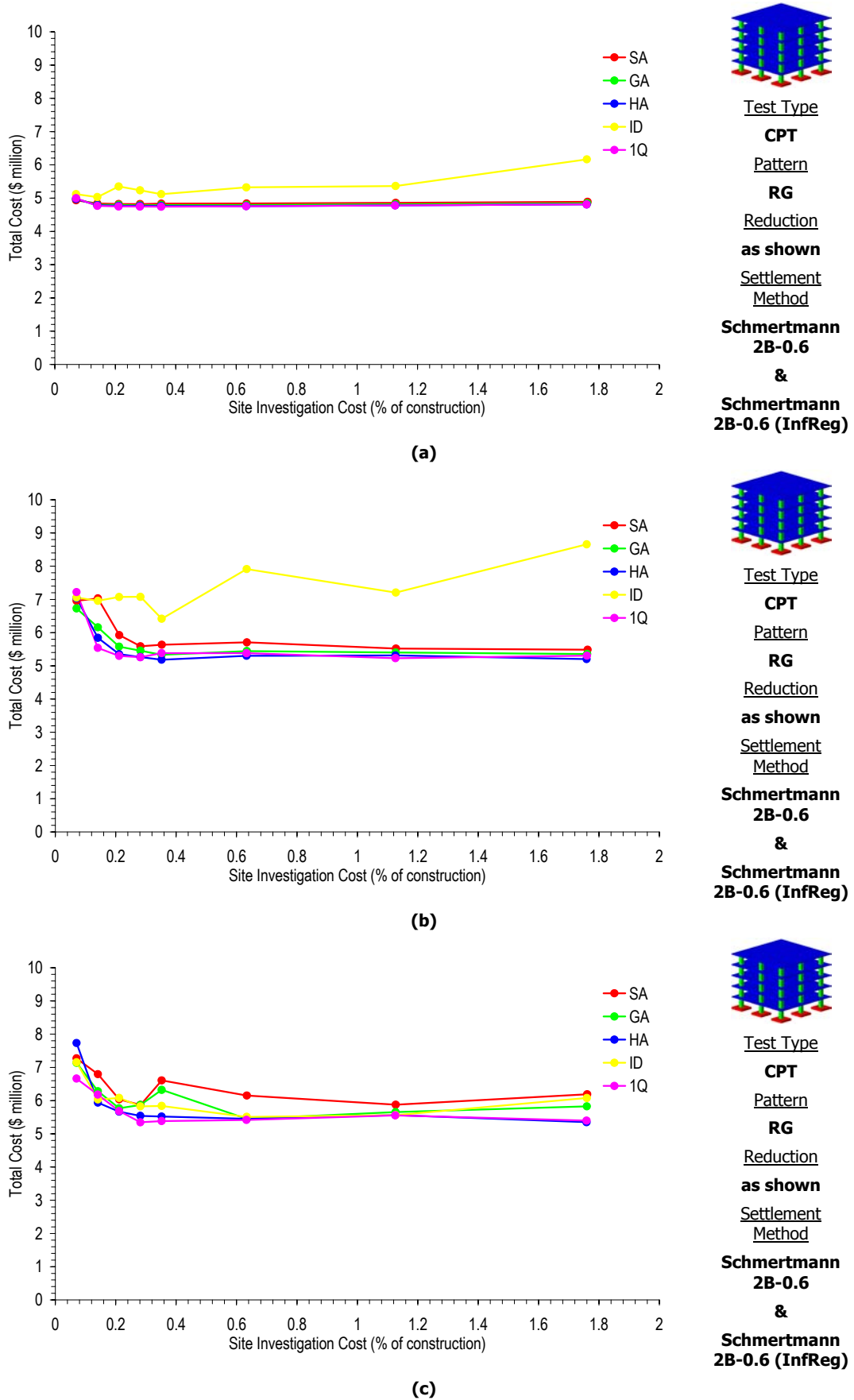
(b)

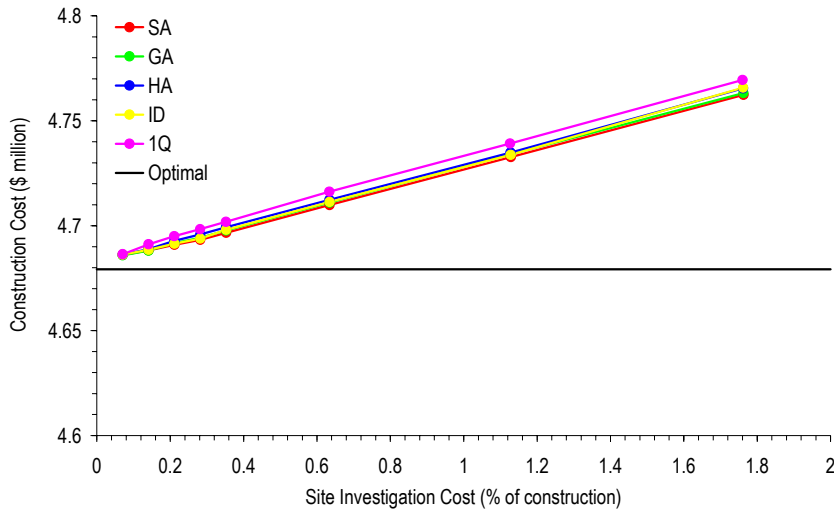
Test Type  
**CPT**  
 Pattern  
**RG**  
 Reduction  
**as shown**  
 Settlement Method  
**Schmertmann 2B-0.6**  
 &  
**Schmertmann 2B-0.6 (InfReg)**

(c)

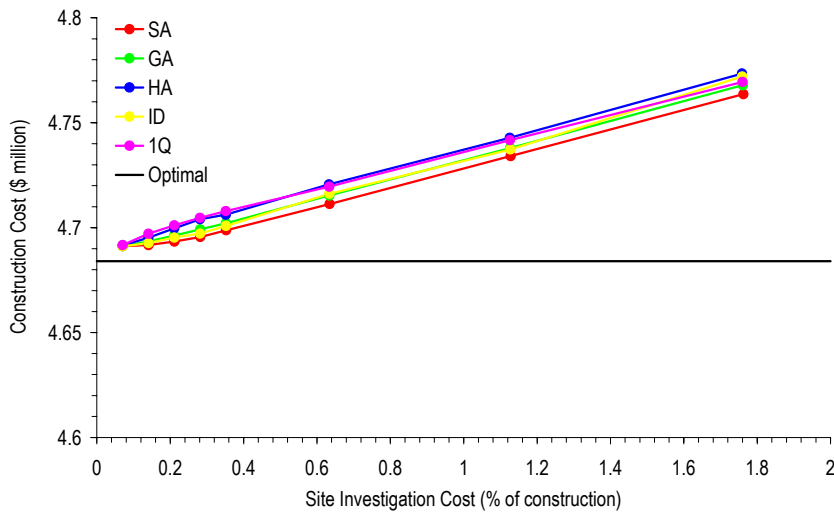
**Figure E-1 Effect of increased site investigation expenditure with different reduction techniques on the total cost, based on an influence region analysis, for a soil SOF of 8 m and COV of (a) 20%, (b) 50% and (c) 100%**



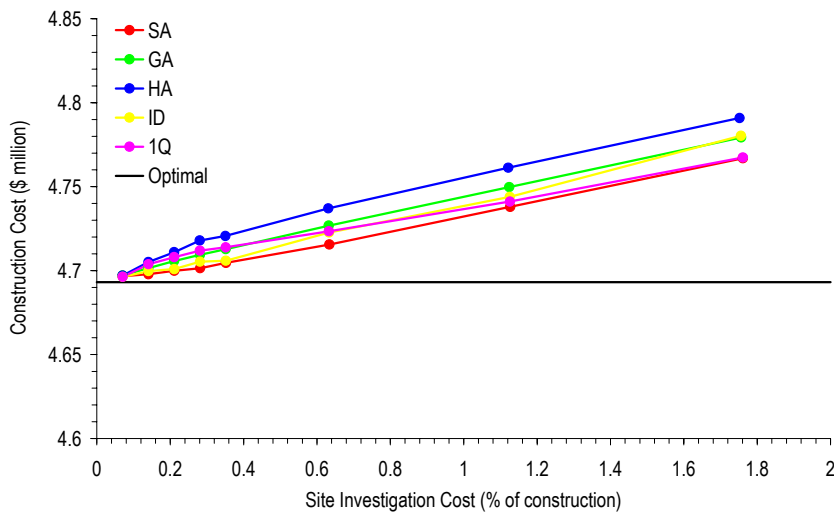
**Figure E-2 Effect of increased site investigation expenditure with different reduction techniques on the total cost, based on an influence region analysis, for a soil COV of 50% and SOF of (a) 1 m, (b) 4 m and (c) 32 m**



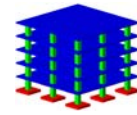
(a)



(b)



(c)



Test Type

CPT

Pattern

RG

Reduction

as shown

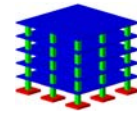
Settlement

Method

Schmertmann  
2B-0.6

&

Schmertmann  
2B-0.6 (InfReg)



Test Type

CPT

Pattern

RG

Reduction

as shown

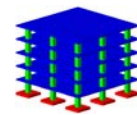
Settlement

Method

Schmertmann  
2B-0.6

&

Schmertmann  
2B-0.6 (InfReg)



Test Type

CPT

Pattern

RG

Reduction

as shown

Settlement

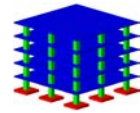
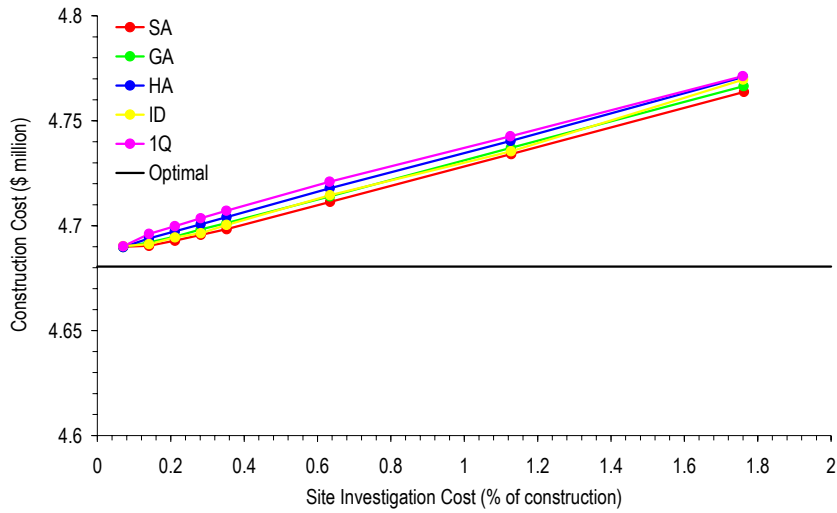
Method

Schmertmann  
2B-0.6

&

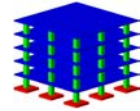
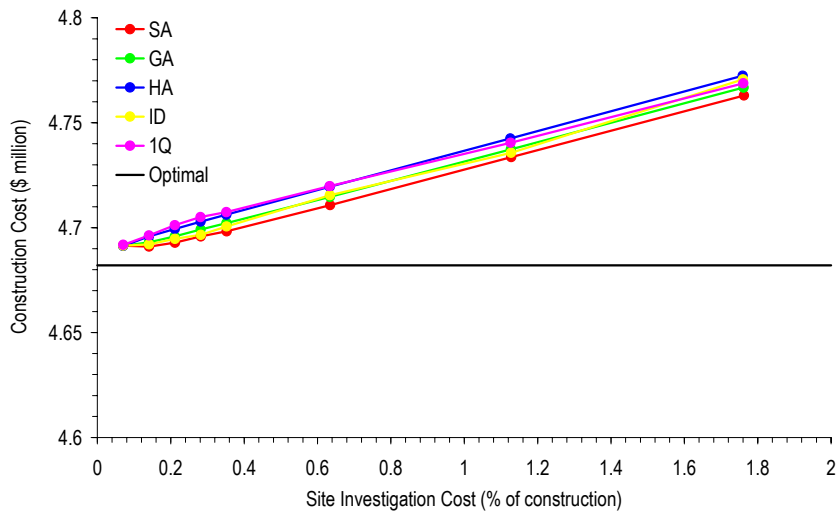
Schmertmann  
2B-0.6 (InfReg)

Figure E-3 Effect of increased site investigation expenditure with different reduction techniques on the construction cost, for a soil SOF of 8 m and COV of (a) 20%, (b) 50% and (c) 100%



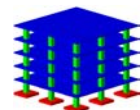
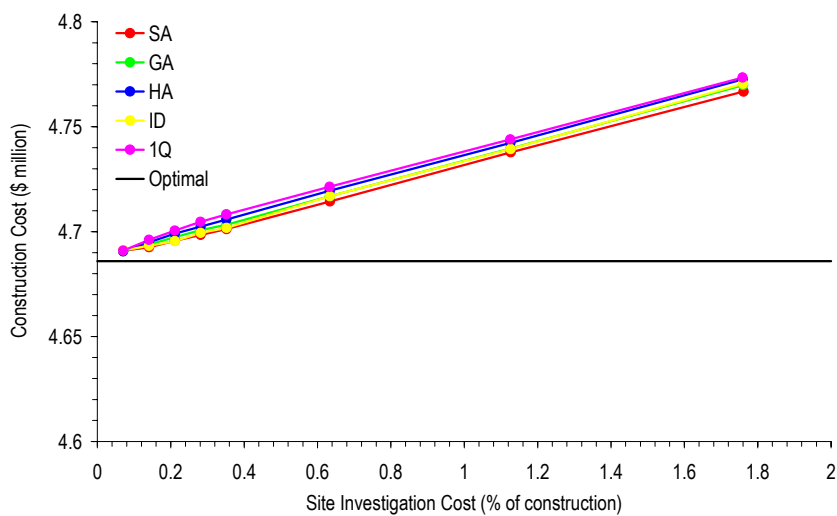
Test Type  
**CPT**  
 Pattern  
**RG**  
 Reduction  
**as shown**  
 Settlement  
 Method  
**Schmertmann  
 2B-0.6**  
 &  
**Schmertmann  
 2B-0.6 (InfReg)**

(a)



Test Type  
**CPT**  
 Pattern  
**RG**  
 Reduction  
**as shown**  
 Settlement  
 Method  
**Schmertmann  
 2B-0.6**  
 &  
**Schmertmann  
 2B-0.6 (InfReg)**

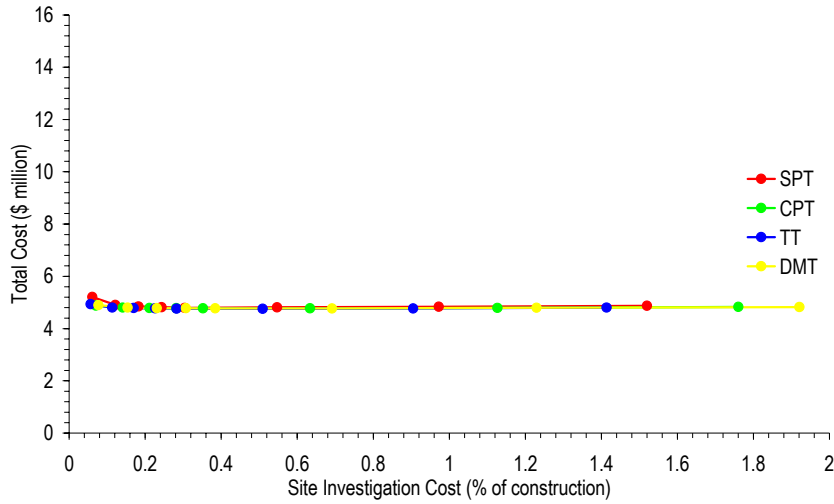
(b)



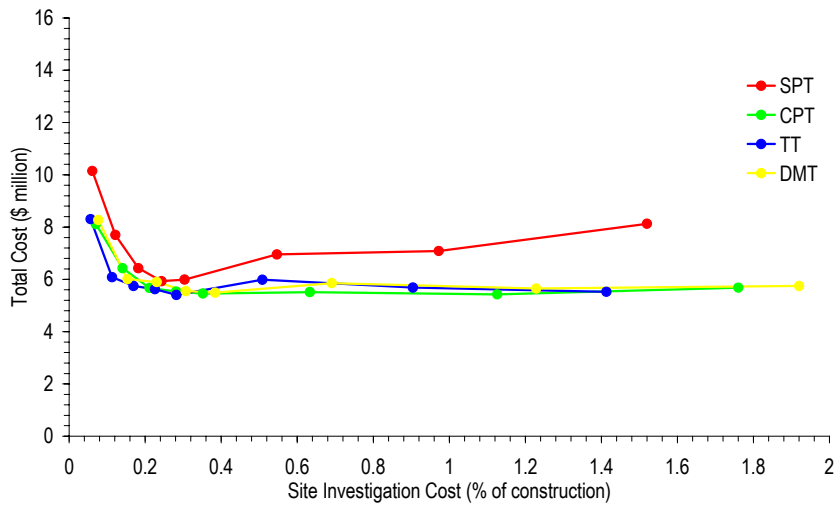
Test Type  
**CPT**  
 Pattern  
**RG**  
 Reduction  
**as shown**  
 Settlement  
 Method  
**Schmertmann  
 2B-0.6**  
 &  
**Schmertmann  
 2B-0.6 (InfReg)**

(c)

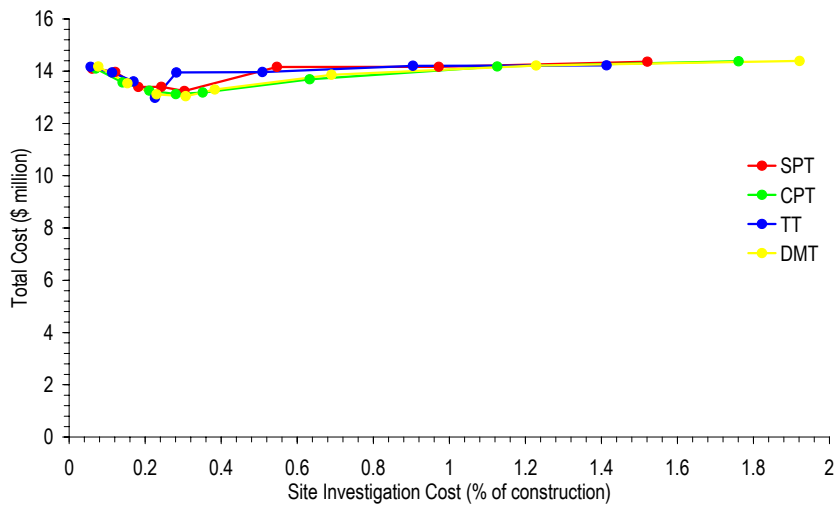
**Figure E-4 Effect of increased site investigation expenditure with different reduction techniques on the construction cost, for a soil COV of 50% and SOF of (a) 1 m, (b) 4 m and (c) 32 m**



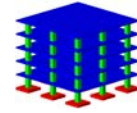
(a)



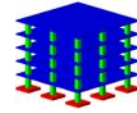
(b)



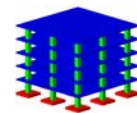
(c)



Test Type  
as shown  
Pattern  
RG  
Reduction  
1Q  
Settlement  
Method  
Schmertmann  
2B-0.6  
&  
Schmertmann  
2B-0.6 (InfReg)



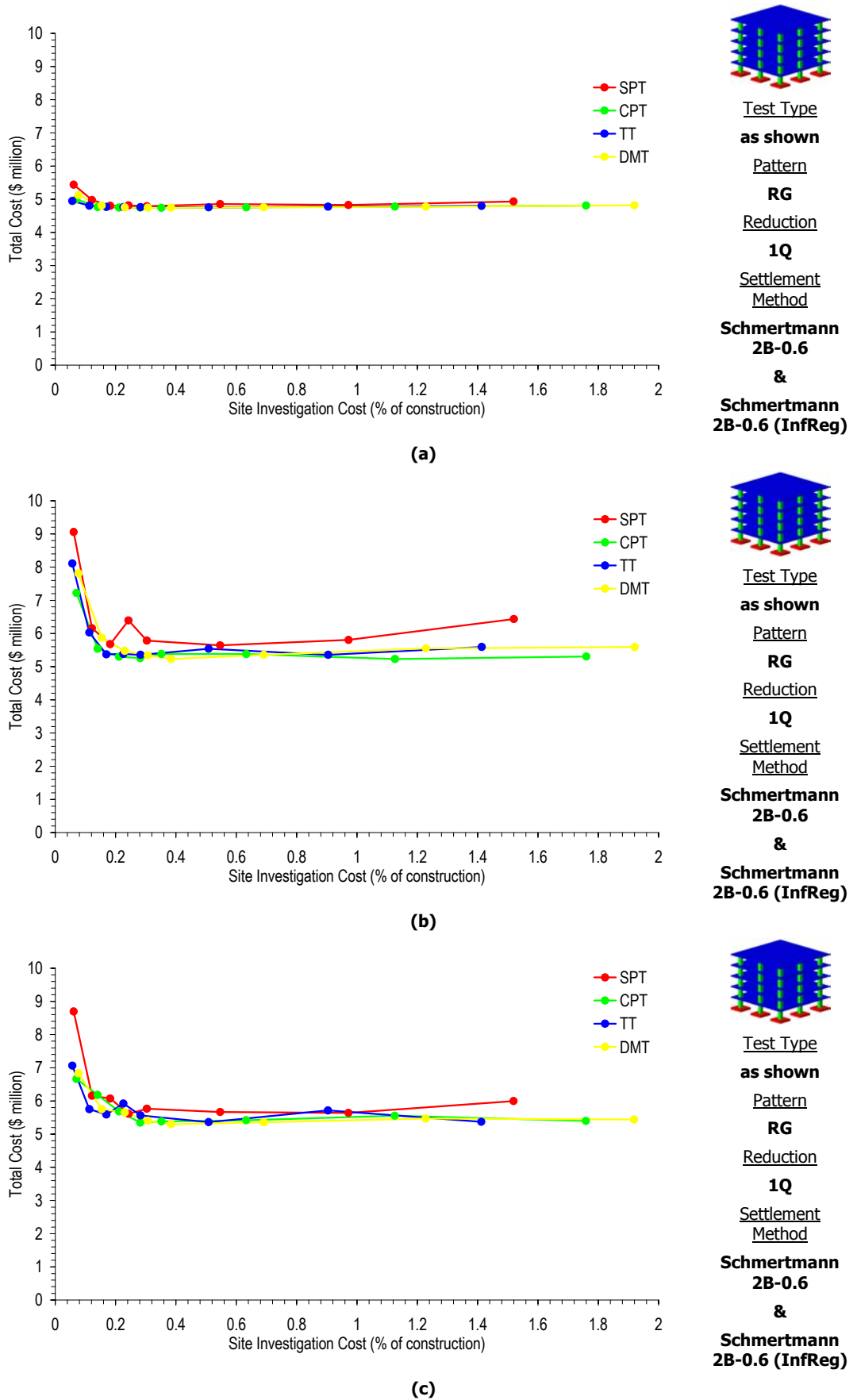
Test Type  
as shown  
Pattern  
RG  
Reduction  
1Q  
Settlement  
Method  
Schmertmann  
2B-0.6  
&  
Schmertmann  
2B-0.6 (InfReg)



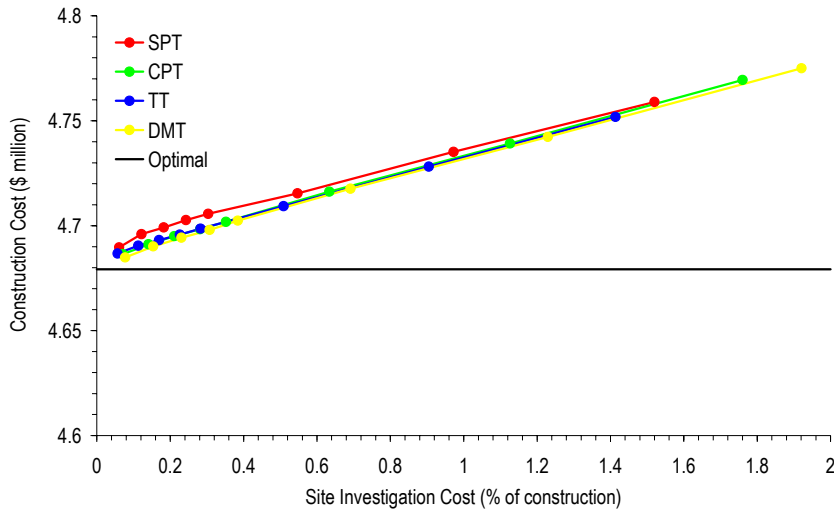
Test Type  
as shown  
Pattern  
RG  
Reduction  
1Q  
Settlement  
Method  
Schmertmann  
2B-0.6  
&  
Schmertmann  
2B-0.6 (InfReg)

Figure E-5 Effect of increased site investigation expenditure with different test types on the total cost, based on an influence region analysis, for a soil SOF of 8 m and COV of (a) 20%, (b) 50% and (c) 100%

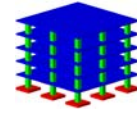




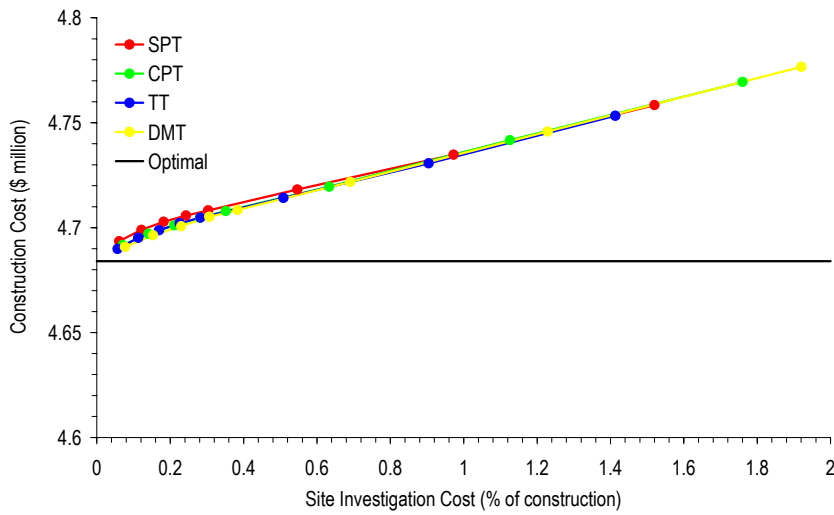
**Figure E-6** Effect of increased site investigation expenditure with different test types on the total cost, based on an influence region analysis, for a soil COV of 50% and SOF of (a) 1 m, (b) 4 m and (c) 32 m



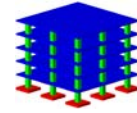
(a)



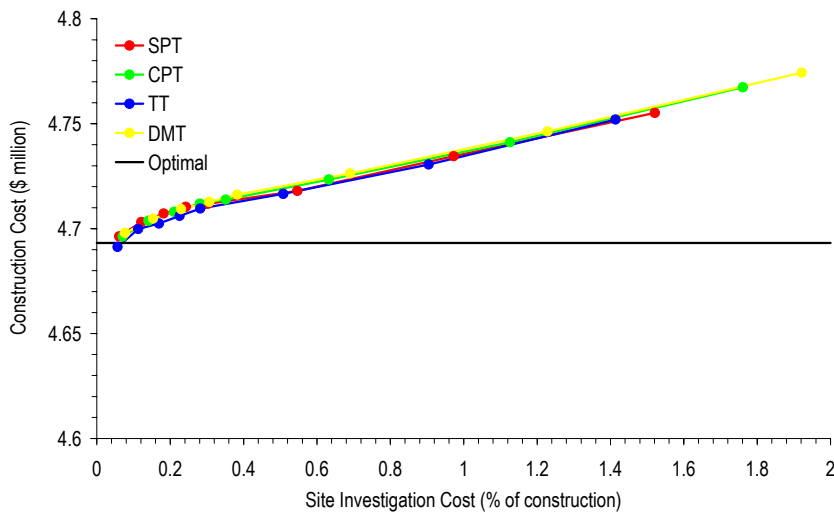
Test Type  
as shown  
Pattern  
RG  
Reduction  
1Q  
Settlement  
Method  
Schmertmann  
2B-0.6  
&  
Schmertmann  
2B-0.6 (InfReg)



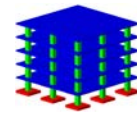
(b)



Test Type  
as shown  
Pattern  
RG  
Reduction  
1Q  
Settlement  
Method  
Schmertmann  
2B-0.6  
&  
Schmertmann  
2B-0.6 (InfReg)

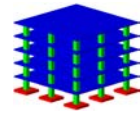
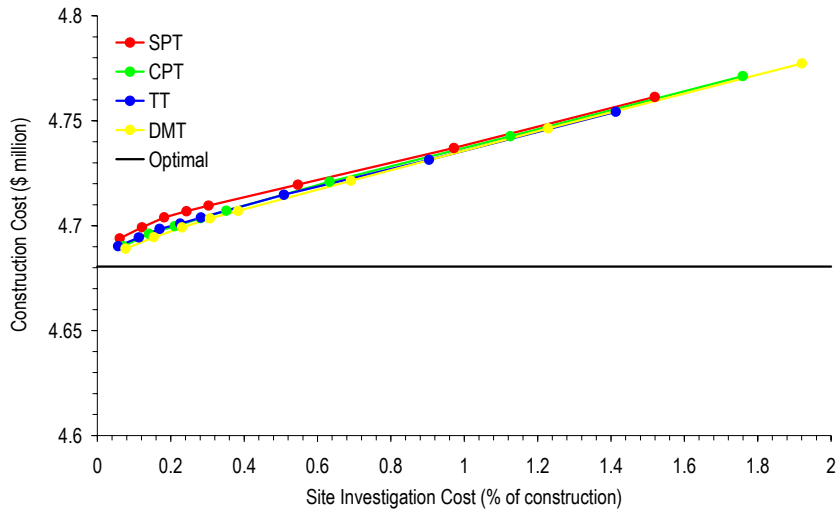


(c)



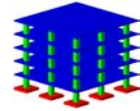
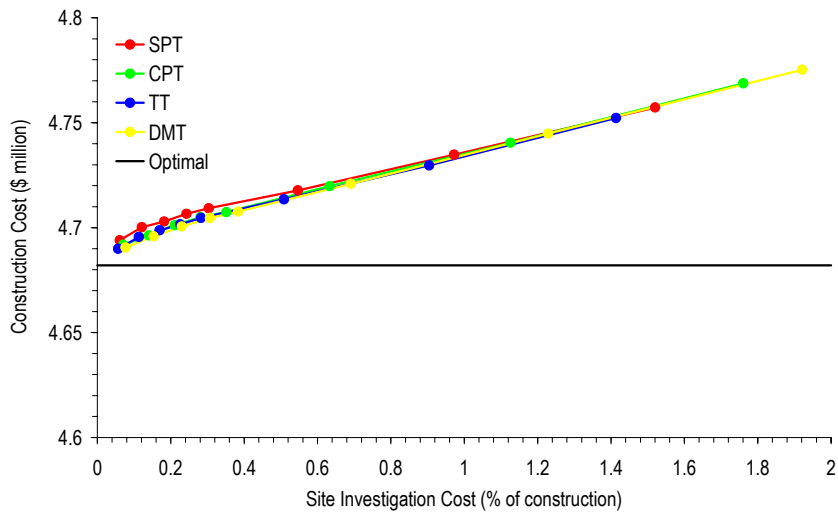
Test Type  
as shown  
Pattern  
RG  
Reduction  
1Q  
Settlement  
Method  
Schmertmann  
2B-0.6  
&  
Schmertmann  
2B-0.6 (InfReg)

Figure E-7 Effect of increased site investigation expenditure with different test types on the construction cost, for a soil SOF of 8 m and COV of (a) 20%, (b) 50% and (c) 100%



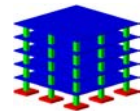
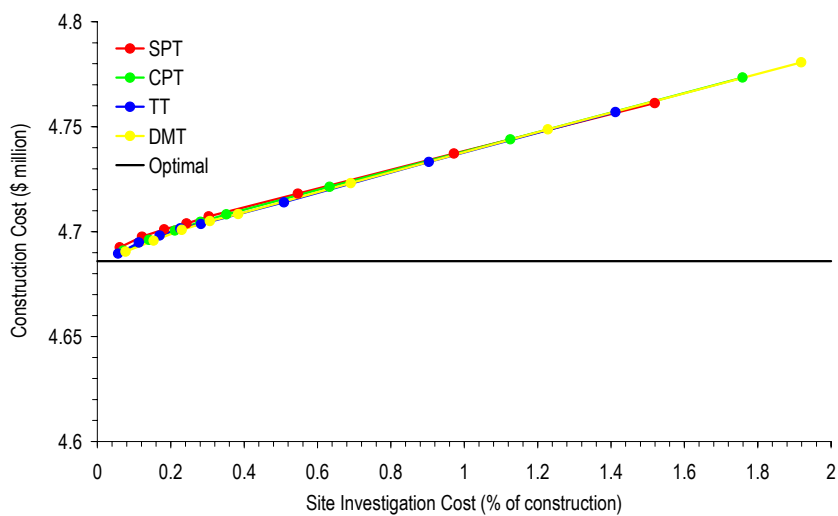
Test Type  
as shown  
Pattern  
RG  
Reduction  
1Q  
Settlement  
Method  
Schmertmann  
2B-0.6  
&  
Schmertmann  
2B-0.6 (InfReg)

(a)



Test Type  
as shown  
Pattern  
RG  
Reduction  
1Q  
Settlement  
Method  
Schmertmann  
2B-0.6  
&  
Schmertmann  
2B-0.6 (InfReg)

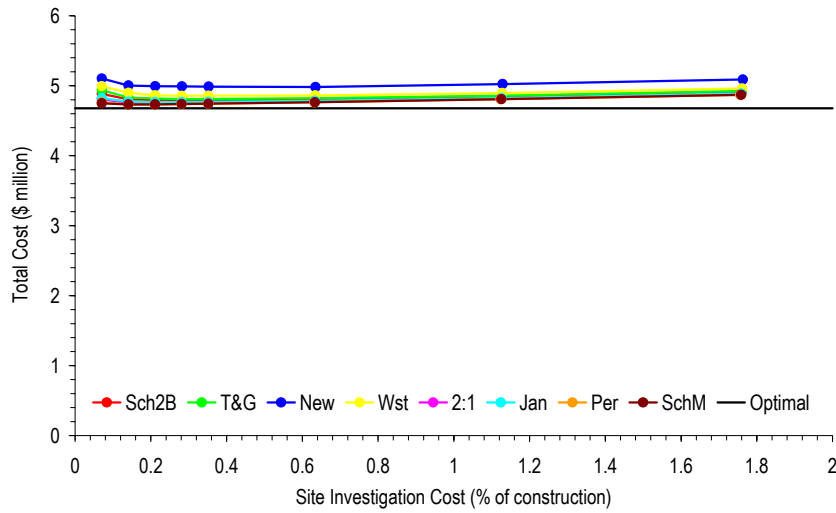
(b)



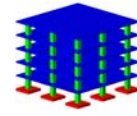
Test Type  
as shown  
Pattern  
RG  
Reduction  
1Q  
Settlement  
Method  
Schmertmann  
2B-0.6  
&  
Schmertmann  
2B-0.6 (InfReg)

(c)

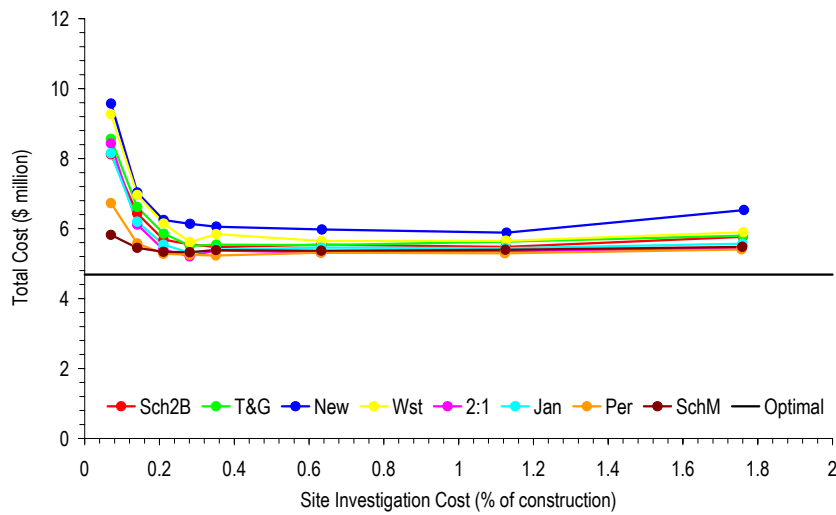
**Figure E-8** Effect of increased site investigation expenditure with different test types on the construction cost, for a soil COV of 50% and SOF of (a) 1 m, (b) 4 m and (c) 32 m



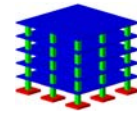
(a)



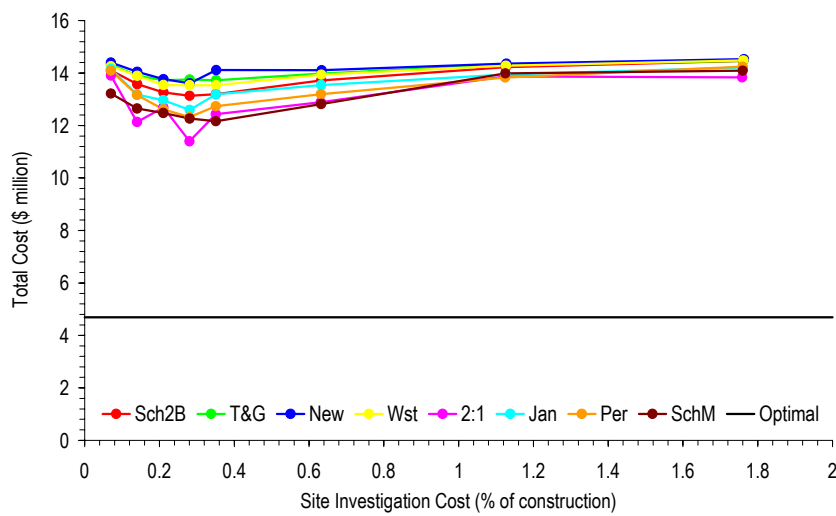
Test Type  
**CPT**  
 Pattern  
**RG**  
 Reduction  
**1Q**  
 Settlement Method  
**as shown**  
 &  
**Schmertmann 2B-0.6 (InfReg)**



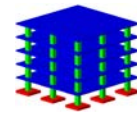
(b)



Test Type  
**CPT**  
 Pattern  
**RG**  
 Reduction  
**1Q**  
 Settlement Method  
**as shown**  
 &  
**Schmertmann 2B-0.6 (InfReg)**

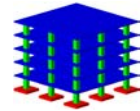
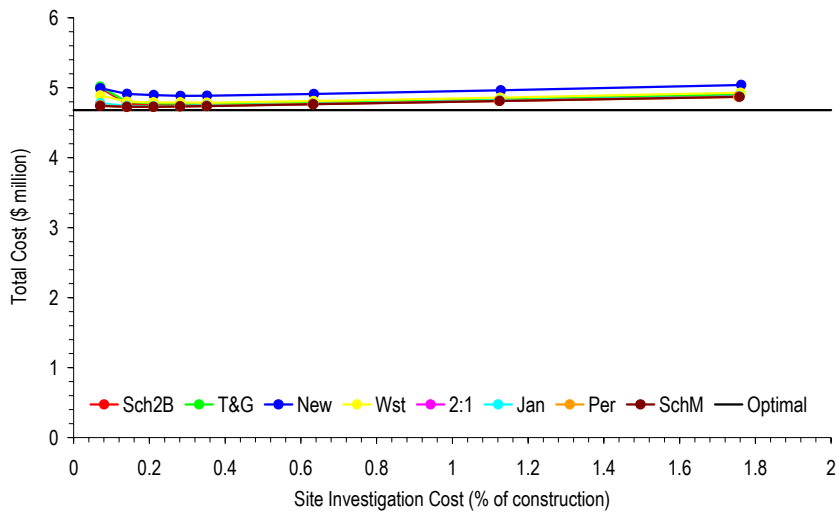


(c)



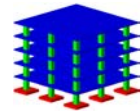
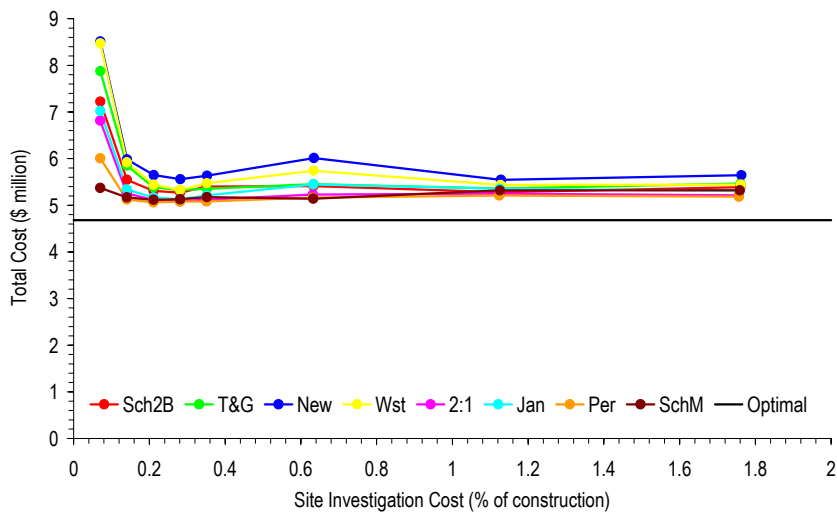
Test Type  
**CPT**  
 Pattern  
**RG**  
 Reduction  
**1Q**  
 Settlement Method  
**as shown**  
 &  
**Schmertmann 2B-0.6 (InfReg)**

**Figure E-9 Effect of increased site investigation expenditure with different settlement prediction techniques on the total cost, based on an influence region analysis, for a soil SOF of 8 m and COV of (a) 20%, (b) 50% and (c) 100%**



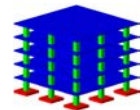
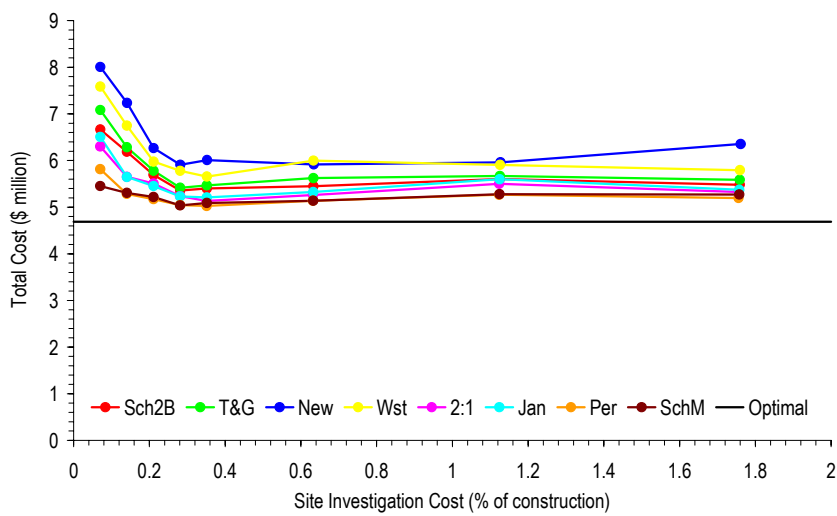
Test Type  
**CPT**  
 Pattern  
**RG**  
 Reduction  
**1Q**  
 Settlement Method  
as shown  
 &  
**Schmertmann 2B-0.6 (InfReg)**

(a)



Test Type  
**CPT**  
 Pattern  
**RG**  
 Reduction  
**1Q**  
 Settlement Method  
as shown  
 &  
**Schmertmann 2B-0.6 (InfReg)**

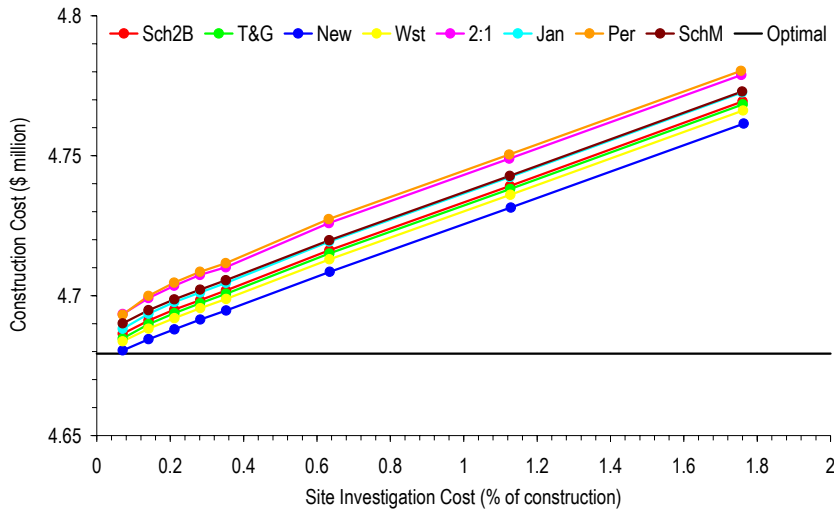
(b)



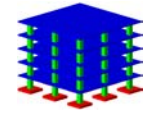
Test Type  
**CPT**  
 Pattern  
**RG**  
 Reduction  
**1Q**  
 Settlement Method  
as shown  
 &  
**Schmertmann 2B-0.6 (InfReg)**

(c)

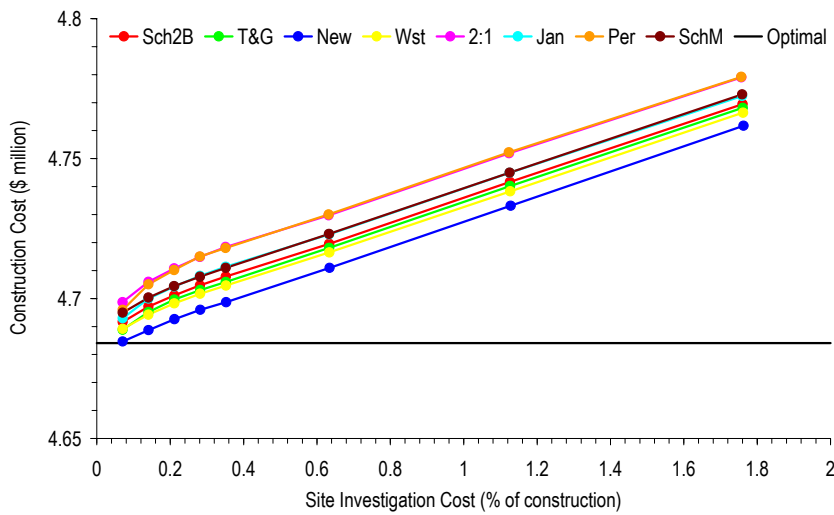
**Figure E-10 Effect of increased site investigation expenditure with different settlement prediction techniques on the total cost, based on an influence region analysis, for a soil COV of 50% and SOF of (a) 1 m, (b) 4 m and (c) 32 m**



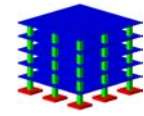
(a)



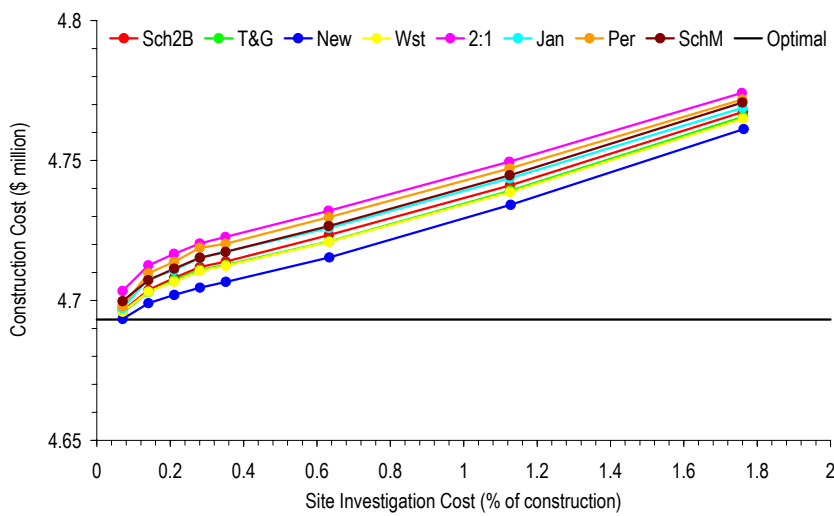
Test Type  
**CPT**  
 Pattern  
**RG**  
 Reduction  
**1Q**  
 Settlement Method  
**as shown**  
 &  
**Schmertmann 2B-0.6 (InfReg)**



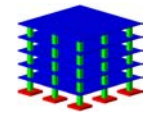
(b)



Test Type  
**CPT**  
 Pattern  
**RG**  
 Reduction  
**1Q**  
 Settlement Method  
**as shown**  
 &  
**Schmertmann 2B-0.6 (InfReg)**

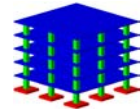
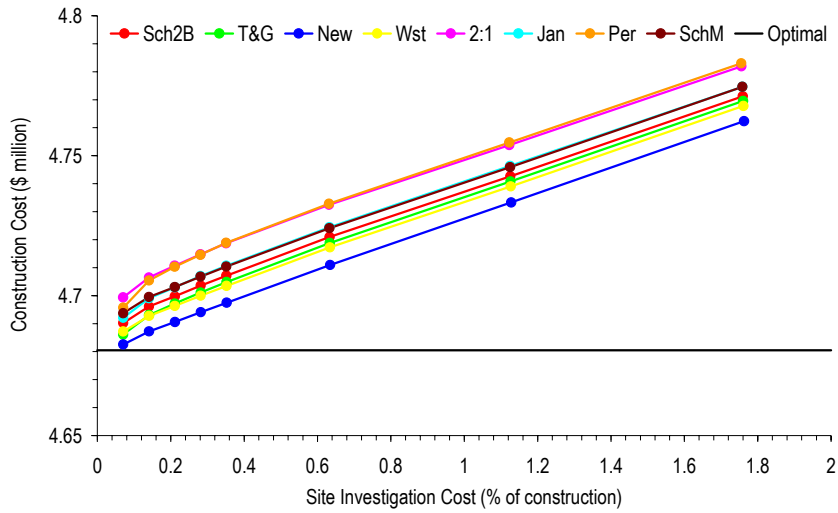


(c)



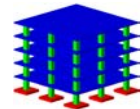
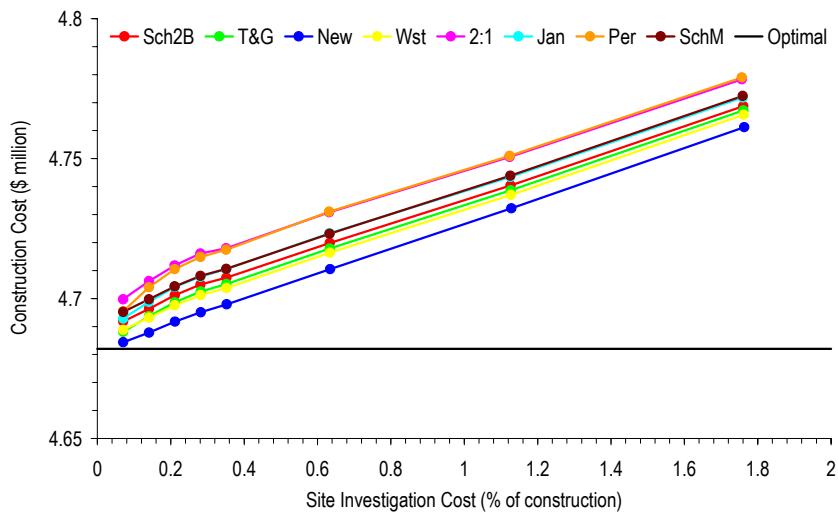
Test Type  
**CPT**  
 Pattern  
**RG**  
 Reduction  
**1Q**  
 Settlement Method  
**as shown**  
 &  
**Schmertmann 2B-0.6 (InfReg)**

**Figure E-11 Effect of increased site investigation expenditure with different settlement prediction techniques on the construction cost, for a soil SOF of 8 m and COV of (a) 20%, (b) 50% and (c) 100%**



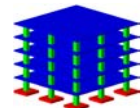
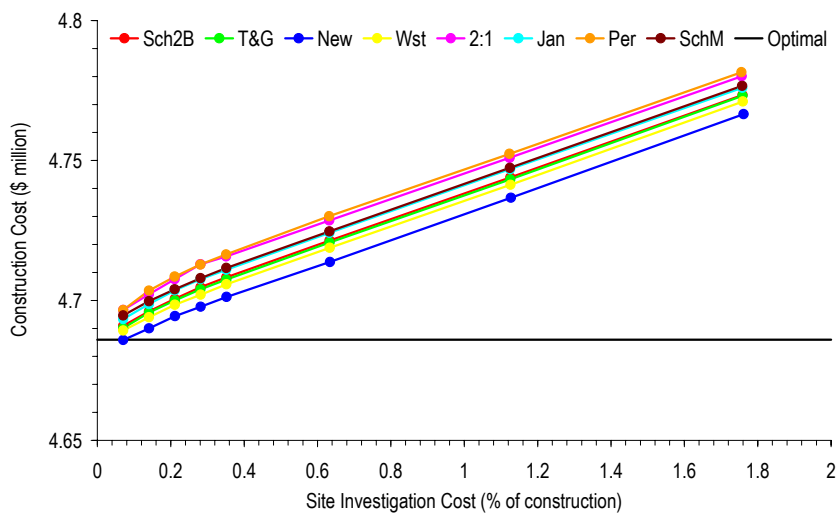
Test Type  
**CPT**  
 Pattern  
**RG**  
 Reduction  
**1Q**  
 Settlement Method  
**as shown**  
 &  
**Schmertmann 2B-0.6 (InfReg)**

(a)



Test Type  
**CPT**  
 Pattern  
**RG**  
 Reduction  
**1Q**  
 Settlement Method  
**as shown**  
 &  
**Schmertmann 2B-0.6 (InfReg)**

(b)



Test Type  
**CPT**  
 Pattern  
**RG**  
 Reduction  
**1Q**  
 Settlement Method  
**as shown**  
 &  
**Schmertmann 2B-0.6 (InfReg)**

(c)

**Figure E-12 Effect of increased site investigation expenditure with different settlement prediction techniques on the construction cost, for a soil COV of 50% and SOF of (a) 1 m, (b) 4 m and (c) 32 m**





## ADDENDUM

### CHAPTER 1 – INTRODUCTION

---

No changes.

### CHAPTER 2 – LITERATURE REVIEW

---

**Page 17, Paragraph 1, add between Sentence 2 and 3:**

Eq (2.5) is the common idealisation of the strain equation which, in actual fact, includes a radial strain component. However, for most foundation design applications, the strain estimate considers only the vertical component and, as such, will be adopted in this research.

**Page 29, add after Paragraph 4:**

The main reason for detrending data is to obtain a set of properties that are largely spatially independent (Fenton 199b). This is because classic statistical methods require independent and identically distributed data. The detrending process typically involves using regression analysis to fit a low-order polynomial (Jaksa et al. 1997) to the data set and removing it from the property value to leave a random residual,  $w(z)$ . However, Phoon et al. (2003) comments that detrending is not unique, and different procedures will result in different random residuals. As discussed earlier, Fenton (1999) warns that a trend should only be removed if it has physical meaning. Furthermore, Fenton (1999b) also warns that trends should be investigated with caution, because they could be a part of a larger process.

Phoon et al. (2003) suggests that the success of the detrending process can be measured by comparing the results of a statistical analysis on the random residual after a trend with an increasingly higher order polynomial is removed from the data. However, Fenton (1999) found that an apparent trend in a set of cone penetration test (CPT) data had little significance to the resulting statistical analysis. Therefore, Fenton (1999) did not remove

the trend which would have resulted in a different mean, variability and correlation structure.

Although past research has demonstrated that it is important to attain a statistically homogeneous data set for a meaningful statistical analysis, care must be taken when detrending data, because the apparent trend may be a part of a much larger process that is not captured in a finite sample data set.

**Page 31, Paragraph 2, Sentence 1:**

The correlation between two properties is bounded by -1 and 1, where  $\rho_\tau = \pm 1$  relates to the observations being perfectly correlated (either positively or negatively) and  $\rho_\tau = 0$  relates to the observations being completely unrelated or purely random, provided that the observations [X and Y in Equation (2.19)] are not functionally related (Vanmarcke 1977a).

---

**CHAPTER 3 – METHODOLOGY DEVELOPMENT**

---

**Page 62, Paragraph 1, Sentence 1:**

As LAS appears to generate random fields considerably faster than the Turning Bands Method, and does not suffer from a symmetric covariance structure (Fenton 2002), like the Fast Fourier Transformation, it is adopted for this research.

**Page 65, Equation 3.3, replace with:**

$$\sigma_{\ln x} = \sqrt{\ln\left(1 + \frac{\sigma_x^2}{\mu_x^2}\right)} \quad (3.3)$$

**Page 66, Paragraph 1, add at end:**

It should also be recognised that the SOF used throughout this research is the SOF of the underlying Gaussian random field, and not the SOF of the lognormal random field.

**Page 73, Paragraph 3, add after Sentence 2:**

It should also be recognised that the reduction techniques only average properties in the same horizontal plane. In other words, the reduction techniques do not combine elastic moduli at different depths.

**Page 74, Paragraph 2, add at end:**

Furthermore, the DMT can also be undertaken at smaller than 1.5 m depth intervals. However, it is rare that 30 DMT tests are taken in one borehole or sampling location, and the DMT is typically more discrete than the CPT. Therefore, for the purposes of this research, a vertical sampling rate of 1.5 m for the DMT is adopted.

**Page 99, Paragraph 1, delete Sentence 1.****Page 99, Paragraph 2, Sentence 2:**

The analysis to investigate the convergence of the Monte Carlo analysis is based on a foundation system consisting of 9-pad footings, as shown in Figure 3-30, centred on a 50 m × 50 m site with a 30 m deep soil layer.

**CHAPTER 4 – VERIFICATION OF METHODOLOGY****Page 110, Paragraph 4, add at end:**

However, it should also be recognised that the Chi-square goodness-of-fit test is based on independent samples, and as the SOF increases, the soil properties become more correlated and less independent. Therefore, the Chi-square test is less applicable when the SOF is large.

**Page 136, Paragraph 3, Sentence 2:**

Since the elastic modulus,  $E_i$ , is stochastic and represented by a lognormal random variable, the settlement can also be expressed in terms of a lognormal stochastic variable.

**Page 137, Equation 4.11, replace with:**

$$\text{Cov}[S_1, S_2] = \left( \frac{1 + \text{COV}_E^2}{\mu_E} \right)^2 \left[ \sum_{i=1}^n \sum_{j=1}^n C_i^{1**} C_j^{2**} (1 + \text{COV}_E^2)^{\rho_{ij}} - \sum_{i=1}^n C_i^{1**} \sum_{j=1}^n C_j^{2**} \right] \quad (4.11)$$

## CHAPTER 5 – EFFECT OF DIFFERENTIAL SETTLEMENT TECHNIQUES ON THE DESIGN AND ANALYSIS OF A PAD FOUNDATION

---

**Page 158, add between Paragraphs 1 and 2:**

The results shown in Figures 5-8 and 5-9 suggest that the variability of settlement estimates using 3DFEA is typically smaller than that from the other prediction models. This fact is evident because the distributions for 3DFEA settlement are narrower than the others. The 3DFEA settlement estimates are less variable because they make use of every soil property in the field, whereas the other prediction models only use a sample of elastic moduli to yield a settlement. Therefore, increased averaging occurs in 3DFEA settlement estimates, and therefore, the results are less variable. This explanation is also valid for comparisons between the other settlement prediction models. Comparisons between the variability are also influenced by the degree of conservatism in the model. It is shown later that more conservative prediction techniques, such as the Schmertmann Modified, yield more variable results. This is because the settlement estimates are closely linked to a lognormal distribution, and the variance and mean are related.

**Page 162, add between Paragraphs 3 and 4:**

Equation (5.7) assumes that the settlement estimates given by 3DFEA and the other techniques are independent. Therefore, the probabilities given in Table 5-3 also assume that the settlement estimates are independent. In actual fact, the settlement estimates will have some correlation because the same elastic moduli have been used in predicting the settlement. However, to keep this form of analysis relatively straightforward, the settlement estimates are assumed to be independent. The numerical analysis described later in this chapter, where footing settlement is determined as part of a Monte Carlo simulation incorporates the correlation between 3DFEA settlements and those from the other prediction techniques.

**Page 188, add after Paragraph 3:**

It should also be noted that the probabilities of under- and over-design, shown in Figures 5-30(a) and (b) respectively, do not add to unity for the same soil SOF and COV combination. This is because there is also a probability that the design based on 3DFEA and Schmertmann 2B-0.6 settlement prediction techniques will be equal. This is the case of the Schmertmann method yielding an optimal design, as is discussed later. It is also introduced, in later chapters, that the probability of obtaining an optimal design is

relatively high because of the discretisation in footing size to keep 3DFEA computational times manageable.

---

## **CHAPTER 6 – EFFECT OF SITE INVESTIGATIONS ON DESIGN PARAMETERS AND THE DESIGN OF A PAD FOUNDATION**

---

**Page 198, Paragraph 3, Sentence 2:**

A sampling location includes all elastic moduli in a vertical sample, leading to 60 values spaced at 0.5 m intervals.

**Page 198, Paragraph 3, add between Sentence 5 and 6:**

In all cases, the target mean of the random field is set to be 10,000 kPa.

**Page 204, Paragraph 2, Sentence 10, replace:**

This is further discussed later in this section.

*with*

Although this may seem counterintuitive, the average design parameter is influenced by the variability of the sampled elastic modulus values. For example, in the limiting case when only a single elastic modulus is sampled, the variance in the sample is zero. However, when additional samples are taken, the variability increases and tends toward the target variance. The increase in average design parameter is further influenced by the lognormal distribution, where a higher variance results in an increasing mean. Therefore, the results in Figure 6-4, which show that the parameter variability increases as the sampling effort grows, also causes a larger average design parameter.

**Page 209, Paragraph 1, add at end:**

However, in this case, the ID and I2 methods yield identical results. Therefore, the ID result is not shown in Figures 6-8 and 6-9.

**Page 219, add between Paragraphs 3 and 4:**

The recommendation of an absolute number of sampling locations over a sampling rate may at first seem counterintuitive; however, the influence of property variability must be carefully considered. It seems from the results shown in Figures 6-15 and 6-16 that 5 sampling locations yields the best answer. This is most likely because adequate averaging between soil properties occurs with this number of sampling locations, and the property variability is, as a result, low. However, if the site size is reduced a sampling rate yields a recommendation for fewer sampling locations, which results in less property averaging.

Therefore, the property variability is high, and the error in the design is large. On the other hand, if the site is larger, a sampling rate infers a greater number of sampling locations, which may be redundant and has little influence on the accuracy of the design.

Hence, it follows that sampling methods that retain more information per sampling location achieve more accurate designs with fewer sampling locations. For example, the cone penetration test (CPT), which is a relatively continuous sampling method, requires fewer sampling locations to achieve an equally accurate design, than the standard penetration test (SPT). This type of analysis is discussed later, yet, in this research, the CPT is modelled to attain only 3 times as many samples as the SPT (§3.4.3). It should also be remembered that different test types are also influenced by their own inherent errors, as discussed earlier in Chapter 2 (§2.3.4), which have a considerable impact on the accuracy of the design. The influence of such inherent testing errors is also discussed later.

Although the results shown in Figures 6-15 and 6-16 suggest the use of an absolute number of sampling locations is preferred, it is important to remember that this analysis is based on a single-layered soil deposit that is statistically homogeneous. Additional sampling is always recommended for soil deposits with multiple layers and geological anomalies.

## **CHAPTER 7 – RELIABILITY ASSESSMENT OF A SITE INVESTIGATION IN TERMS OF FOUNDATION DESIGN**

---

### **Page 290, Paragraph 1, add at end:**

Figure 7-24 shows that the average design error is low when the soil SOF is small. This same phenomenon was shown in Figure 7-23(a) where the average design error was relatively small when a sample location was positioned around the site. The average design error is relatively low when the soil SOF is small because of two reasons. Firstly, the apparent variability of the soil properties is less when the soil SOF is small, as shown in Chapter 4 (§4.2.1). Secondly, and more importantly, considerable local averaging occurs when the soil SOF is small. Therefore, the variability of the sampled properties used in the footing design is less and, as a result, the average design error is low. In the limiting case, where the soil SOF approaches zero, soil properties at 0.5 m spacings will be the same because of local averaging. In this case, the average design error is zero.

## **CHAPTER 8 – RISK ASSESSMENT OF A SITE INVESTIGATION IN TERMS OF FOUNDATION DESIGN**

---

### **Page 310, Paragraph 3, Sentence 2:**

Figures 8-6 and 8-7, as well as other figures in Chapter 8, the terminology of “failure cost”, or “cost”, is used for the vertical axis label. These costs are, in fact, expected costs and reflect the average calculated over 1000 Monte Carlo realizations. Also note the different scales on the vertical axis for total and failure costs.

### **Page 347, Paragraph 4, Sentence 3:**

Furthermore, it is also important to consider that this analysis considers only a single, statistically homogeneous layer of soil.

## **CHAPTER 9 – ANALYSIS USING SPECIFIC SOIL DATA**

---

No changes.

## **CHAPTER 10 – SUMMARY AND RECOMMENDATIONS**

---

No changes.

## **REFERENCES**

---

**Fenton G A. (1999b).** "Estimation for Stochastic Soil Models." *Journal of Geotechnical and Geoenvironmental Engineering*, 125(6), pp. 470-485.

**Phoon K K, Quek S T and An P. (2003).** "Identification of Statistically Homogeneous Soil Layers Using Modified Bartlett Statistics." *Journal of Geotechnical and Geoenvironmental Engineering*, 129(7), pp. 649-659.